Biomedical Visualization 2

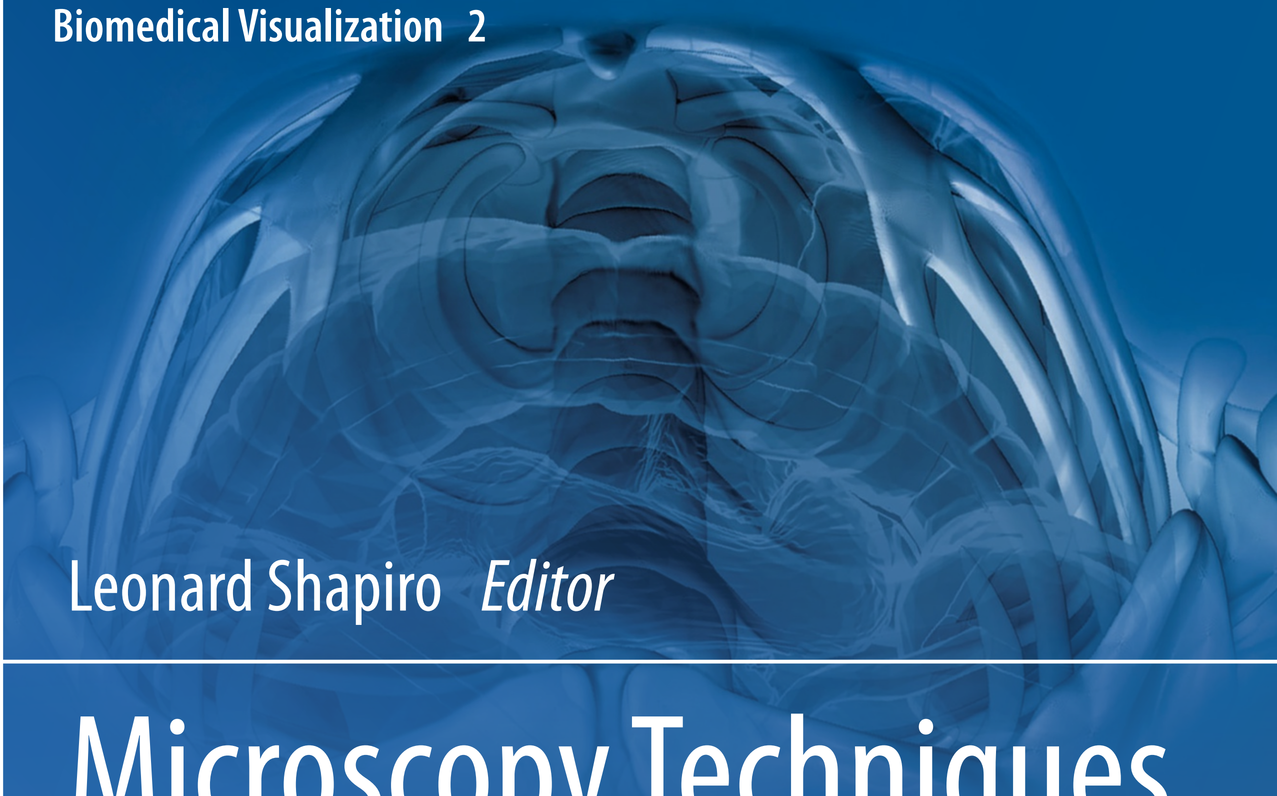

Leonard Shapiro *Editor*

Microscopy Techniques for Biomedical Education and Healthcare Practice

Principles in Light, Fluorescence, Super-Resolution and Digital Microscopy, and Medical Imaging

Springer

Biomedical Visualization

Volume 2

Series Editor

Paul M. Rea, Anatomy Facility, School of Medicine, Dentistry and Nursing, College of Medical, Veterinary and Life Sciences, University of Glasgow, Glasgow, UK

The Biomedical Visualization book series invites contributions related to visualization and imaging in the biomedical sciences and related fields such as medicine, dentistry, veterinary surgery, informatics, and the allied health professions.

This can encompass work in image analysis, workflow methodologies, photogrammetry in science, animations, digital reconstructions and applications, big data and visualizations, educational methodologies, usability and evaluations, augmented and virtual reality, and 3D and 4D technologies, including 3D printing, as well as informatics, e-tutorials, MOOCs, HCI and public engagement. It can be from macroscopic to microscopic but show how we can view data and information related to the biomedical field in a much more accessible, innovative and engaging way using technology.

This series is intended for researchers, clinicians, students, and teaching staff in biomedical and medical schools who use and develop visualization and imaging techniques in medical education, patient care, and biomedical and medical research.

Leonard Shapiro
Editor

Microscopy Techniques for Biomedical Education and Healthcare Practice

Principles in Light, Fluorescence, Super-Resolution and Digital Microscopy, and Medical Imaging

Springer

Editor
Leonard Shapiro
Department of Human Biology
University of Cape Town
Cape Town, South Africa

ISSN 2731-6130 ISSN 2731-6149 (electronic)
Biomedical Visualization
ISBN 978-3-031-36849-3 ISBN 978-3-031-36850-9 (eBook)
https://doi.org/10.1007/978-3-031-36850-9

© The Editor(s) (if applicable) and The Author(s), under exclusive license to Springer Nature Switzerland AG 2023
This work is subject to copyright. All rights are solely and exclusively licensed by the Publisher, whether the whole or part of the material is concerned, specifically the rights of translation, reprinting, reuse of illustrations, recitation, broadcasting, reproduction on microfilms or in any other physical way, and transmission or information storage and retrieval, electronic adaptation, computer software, or by similar or dissimilar methodology now known or hereafter developed.
The use of general descriptive names, registered names, trademarks, service marks, etc. in this publication does not imply, even in the absence of a specific statement, that such names are exempt from the relevant protective laws and regulations and therefore free for general use.
The publisher, the authors, and the editors are safe to assume that the advice and information in this book are believed to be true and accurate at the date of publication. Neither the publisher nor the authors or the editors give a warranty, expressed or implied, with respect to the material contained herein or for any errors or omissions that may have been made. The publisher remains neutral with regard to jurisdictional claims in published maps and institutional affiliations.

Cover Illustration: Catherine MacRobbie

This Springer imprint is published by the registered company Springer Nature Switzerland AG
The registered company address is: Gewerbestrasse 11, 6330 Cham, Switzerland

Paper in this product is recyclable.

Preface

What has been the effect of the shift in power from conventional to digital to virtual microscopy? What instruments do we use to visualize the microscopic? How do we account for our personal interpretation of what we are seeing at a microscopic level? What are the benefits of visualizing structures at a microscopic level from the perspective of research and practical applications? What are the advantages of studying genes at an ultra-microscopic level? These questions and others are explored in a diverse and yet related variety of chapters, written by experts in their specialized areas of microscopy. We begin our book with a thought-provoking chapter on the psychology of perception and how this affects our understanding of cells and tissue. Thereafter, chapters follow that include morphometric image analysis and its applications in biomedicine using different modes of microscopy, the development of fluorescence methods and technologies that make biomedical imaging more accessible and engaging, and particle tracking techniques with applications in biomedical research and nanomedicine.

In the second part of this book, chapters on education in anatomy and cell biology cover the history of anatomical models and their use in educational settings, 3D printing of functional human anatomical models that can be created using readily available resources, the use of biomedical imaging in visuospatial teaching of anatomy, the novel use of ultrasound in anatomy education and clinical practice, and skill acquisition for education in histology.

Cape Town, South Africa Leonard Shapiro

Acknowledgement

My gratitude to each of the authors for their valuable contribution to this book, which will inform and inspire readers.

It is a pleasure to work with Series Editor Paul Rea and Editor at Springer Nature, Ina Stoeck. Thank you for your expertise, enthusiasm and support throughout the months of work that went into preparing the contents of this book for publication. My thanks to the Springer design and production team for their attention to detail and the efficiency with which they produced this book. You all made this journey a pleasure!

Contents

Part I Advances in Microscopy for Visualization, Education and Healthcare Practice

1 Visualizing the Invisible: Microscopy and How It Affects Our Understanding of Cells and Tissues 3
Felix Hutmacher, Ida S. Opstad, Fabian Hutmacher, and Florian Ströhl

2 Morphometric Image Analysis and its Applications in Biomedicine Using Different Microscopy Modes 25
Vesselina Merhar and Thajasvarie Naicker

3 The Shift in Power from Conventional to Digital and Virtual Microscopy 41
Shoohana Singh and Thajasvarie Naicker

4 How Visualizations Have Revolutionized Taxonomy: From Macroscopic, to Microscopic, to Genetic 55
Andrew J. Lunn, Isabelle C. Winder, and Vivien Shaw

5 Bright New World: Principles of Fluorescence and Applications in Spectroscopy and Microscopy 89
John G. Woodland

6 An Introduction to Particle Tracking Techniques with Applications in Biomedical Research 103
Sourav Bhattacharjee

7 An Exploration of the Practice of CT Modalities to Evaluate Anterior Cranial Deformities in Craniosynostosis 125
Anil Madaree, Vensuya Bisetty, Nivana Mohan, Courtney Barnes, and Lelika Lazarus

Part II Anatomical and Cell Biology Education

8 The Use of Biomedical Imaging in Visuospatial Teaching of Anatomy 145
Sashrika Pillay-Addinall, Nhlanhla L. Japhta, and Sabashnee Govender-Davies

9 Ultrasound Imaging for Musculoskeletal Research 179
Nkhensani Mogale

10 Skill Acquisition in Histology Education 199
Rachael Door

Editors and Contributors

About the Series Editor

Paul M. Rea Paul is Professor of Digital and Anatomical Education at the University of Glasgow. He is Director of Innovation, Engagement and Enterprise within the School of Medicine, Dentistry and Nursing. He is also a Senate Assessor for Student Conduct, Council Member on Senate and coordinates the day-to-day running of the Body Donor Program and is a Licensed Teacher of Anatomy, licensed by the Scottish Parliament.

He is qualified with a medical degree (MBChB), an MSc (by research) in craniofacial anatomy/surgery, a PhD in neuroscience, the Diploma in Forensic Medical Science (DipFMS), and an MEd with Merit (Learning and Teaching in Higher Education). He is a Senior Fellow of the Higher Education Academy, Fellow of the Institute of Medical Illustrators (MIMI) and a registered medical illustrator with the Academy for Healthcare Science.

Paul has published widely and presented at many national and international meetings, including invited talks. He has been the lead Editor for Biomedical Visualiz(s)ation over 15 published volumes and is the founding editor for this book series. This has resulted in almost over 110,000 downloads across these volumes, with contributions from over 450 different authors, across approximately 100 institutions from 23 countries across the globe. It has over 500 citations from these volumes. He is Associate Editor for the European Journal of Anatomy and has reviewed for 25 different journals/publishers. He is the Public Engagement and Outreach lead for anatomy coordinating collaborative projects with the Glasgow Science Centre, NHS and Royal College of Physicians and Surgeons of Glasgow. Paul is also a STEM ambassador and has visited numerous schools to undertake outreach work.

His research involves a long-standing strategic partnership with the School of Simulation and Visualisation, The Glasgow School of Art. This has led to multi-million-pound investment in creating world leading 3D digital datasets to be used in undergraduate and postgraduate teaching to enhance learning and assessment. This successful collaboration resulted in the creation of the world's first taught MSc Medical Visualisation and Human Anatomy combining anatomy and digital technologies, for which Paul was the Founding Director having managed this for 12 years. The Institute of Medical Illustrators also accredits this postgraduate degree. Paul has led college-wide, industry, multi-institutional and NHS research linked projects for students.

About the Editor

Leonard Shapiro Leonard is a visual artist affiliated with the Department of Human Biology at the University of Cape Town, South Africa. He has a keen interest in Anatomy Education and has developed a number of art-based exercises to address and improve students' three-dimensional (3D) spatial awareness and observation ability. His courses and workshops are in collaboration with lecturers who are actively engaged in improving education methodology in anatomy. These are offered to medical students and lecturers in South Africa and abroad. Leonard has developed a multi-sensory observation method that crucially employs the sense of touch (haptics) coupled with the simultaneous act of drawing. It is called the haptico-visual observation and drawing (HVOD) method. In anatomy education, the benefits of using the HVOD method include the enhanced observation of the 3D form of anatomical parts, the cognitive memorization of anatomical parts as a 3D mental picture, improved spatial orientation within the volume of the anatomy, and an ability to draw. Leonard has taught the HVOD method at the University of Cape Town (South Africa), Newcastle University (England), the University of British Columbia (Canada), Carnegie Mellon University (USA), the Gordon Museum of Pathology at King's College London (England), University College Cork (Ireland), and Weill Cornell Medical College (USA). Leonard contributes to the anatomy education discourse by presenting at anatomy conferences as well as via publications and articles. Leonard graduated in BSocSci and in BA Fine Art (Hons) from the University of Cape Town.

List of Contributors

Courtney Barnes Discipline of Clinical Anatomy, School of Laboratory Medicine and Medical Science, College of Health Sciences, University of KwaZulu-Natal, Durban, South Africa

Sourav Bhattacharjee School of Veterinary Medicine, University College Dublin, BelfieldDublin, Ireland

Vensuya Bisetty Discipline of Clinical Anatomy, School of Laboratory Medicine and Medical Science, College of Health Sciences, University of KwaZulu-Natal, Durban, South Africa

Rachael Door School of Medicine, Keele University, Staffordshire, UK

Sabashnee Govender-Davies Department of Anatomy and Histology, School of Medicine, Sefako Makgatho Health Sciences University, Ga-Rankuwa, South Africa

Fabian Hutmacher Human-Computer-Media Institute, Julius-Maximilians-University Würzburg, Würzburg, Germany

Felix Hutmacher Child and Youth Hospital, Kantonsspital Aarau AG, Aarau, Switzerland

Nhlanhla L. Japhta Department of Anatomy and Histology, School of Medicine, Sefako Makgatho Health Sciences University, Ga-Rankuwa, South Africa

Lelika Lazarus Discipline of Clinical Anatomy, School of Laboratory Medicine and Medical Science, College of Health Sciences, University of KwaZulu-Natal, Durban, South Africa

Andrew J. Lunn School of Natural Sciences, Bangor University, Bangor, UK

Anil Madaree Department of Plastic and Reconstructive Surgery, Inkosi Albert Luthuli Central Hospital, Durban, South Africa

Vesselina Merhar Department of Biology, Medical Genetics and Microbiology, Faculty of Medicine, University Prof. Dr. Assen Zlatarov, Burgas, Bulgaria

Nkhensani Mogale Department of Anatomy, School of Medicine, Faculty of Health Sciences, University of Pretoria, Pretoria, South Africa

Nivana Mohan Discipline of Clinical Anatomy, School of Laboratory Medicine and Medical Science, College of Health Sciences, University of KwaZulu-Natal, Durban, South Africa

Thajasvarie Naicker Optics and Imaging Centre, Doris Duke Medical Research Institute, College of Health Sciences, University of KwaZulu-Natal, Durban, South Africa

Ida S. Opstad Department of Physics and Technology, UiT The Arctic University of Norway, Tromsø, Norway

Sashrika Pillay-Addinall Department of Anatomy and Histology, School of Medicine, South Africa

Vivien Shaw Academic Visitor at Hull York Medical School, Faculty of Health Sciences, University of Hull, Hull, UK

Shoohana Singh Optics and Imaging Centre, Doris Duke Medical Research Institute, College of Health Sciences, University of KwaZulu-Natal, Durban, South Africa

Florian Ströhl Department of Physics and Technology, UiT The Arctic University of Norway, Tromsø, Norway

Isabelle C. Winder School of Natural Sciences, Bangor University, Bangor, UK

John G. Woodland Department of Chemistry and Holistic Drug Discovery and Development (H3D) Centre, University of Cape Town, Cape Town, South Africa
South African Medical Research Council Drug Discovery and Development Research Unit, Institute of Infectious Disease and Molecular Medicine, University of Cape Town, Cape Town, South Africa

Part I

Advances in Microscopy for Visualization, Education and Healthcare Practice

Visualizing the Invisible: Microscopy and How It Affects Our Understanding of Cells and Tissues

1

Felix Hutmacher, Ida S. Opstad, Fabian Hutmacher,
and Florian Ströhl

Abstract

Microscopy is constantly improving its capacities for depicting a world that is beyond the limitations of the human visual system and is therefore shaping and reshaping our understanding of cells and tissue and their functioning. This chapter presents a brief outline of the history of microscopy, discusses the application of these techniques in the medical field in relation to both medical education and clinical applications, and concludes with the latest super-resolution microscopy techniques. However, all microscopy techniques have their limitations—and sometimes one of these limitations is the operator. As such, this chapter concludes with a description of both the possibilities and limitations of automated image processing using artificial intelligence, as well as an outline of psychological and perceptual phenomena that play a key role when a human observer interprets pictures acquired with the aid of a microscope.

Keywords

Microscopy · Super-resolution microscopy · Medical education · Pathology · Artificial intelligence · Visual perception

1.1 Introduction

Since its invention around 400 years ago (Croft 2006), microscopy has allowed for the visualization and discovery of features previously invisible and therefore unknown to humankind. If we had not seen it, we would probably still not know that in fact all living creatures are either comprised of individual cells (like bacteria or amoebae) or a well-organized composition of many cells, as is the case in plants, humans, and other animals. Lesser known is that what we understand from our observations is also largely influenced by what we *expect* to see. For example, human sperm cells (first observed by Antonie van Leeuwenhoek in 1677) were—based on the religious and ideological convictions that people held at the time—often not viewed as single motile cells (which they are) but as tiny but complete human beings (Casetta 2020).

Are we still victims of similar misconceptions today and if so, how can we avoid them? To answer these questions, we will first review

---

Felix Hutmacher, Ida S. Opstad, Fabian Hutmacher and Florian Ströhl contributed equally to this chapter.

F. Hutmacher
Child and Youth Hospital, Kantonsspital Aarau AG, Aarau, Switzerland

I. S. Opstad · F. Ströhl (✉)
Department of Physics and Technology, UiT The Arctic University of Norway, Tromsø, Norway
e-mail: florian.strohl@uit.no

F. Hutmacher
Human-Computer-Media Institute, Julius-Maximilians-University Würzburg, Würzburg, Germany

© The Author(s), under exclusive license to Springer Nature Switzerland AG 2023
L. Shapiro (ed.), *Microscopy Techniques for Biomedical Education and Healthcare Practice*, Biomedical Visualization 2, https://doi.org/10.1007/978-3-031-36850-9_1

microscopy in the context of medicine and how it is introduced as a topic in (Western) medical education. We will continue with an overview of modern microscopy from the perspective of physics and highlight common implementations, their practical use cases and limitations. Equipped with this basic knowledge, we will consider microscopy images from a data science perspective and try to understand how multidimensional image data can be visualized and quantified using image processing tools and techniques that *limit* the influence of human perception. In the final section, we will consider the importance of visualization in the context of learning and how prior knowledge and assumptions affect our observations and conclusions.

1.2 Microscopy in Medical Research and Education

1.2.1 Old Textbook Knowledge Shapes our Understanding of Cellular Details

Living cells are highly dynamic, three-dimensional (3D) structures. This is apparent when viewing images generated by modern live-cell imaging techniques, but it may not be the impression students get from watching sessile, two-dimensional (2D) structures as typically depicted in the lecture theater. For example, Fig. 1.1a depicts a typical school book sketch of the constituents of an animal cell. The organelle number 9 is a mitochondrion as also shown in the electron micrograph in panel b. This is likely to be the way that most people think of mitochondria and try to sketch them. Panel c shows a mitochondrial network within *living* cells, imaged using fluorescence super-resolution microscopy. Interestingly, if the living mitochondria are repeatedly imaged under a number of relatively harsh conditions (e.g., using dye and intense light exposure), they will often become spherical, as in the electron micrograph (panels d–f). Hence, the grain-like shape of mitochondria that is typically depicted in textbooks might be nothing but an artifact resulting from the sample processing (and fixation) before electron microscopy image acquisition. Although electron microscopy has allowed for the discovery of details about the structural details inside cells in an unprecedented manner, the development of live-cell compatible high-resolution microscopy has in turn also changed the image and understanding of mitochondria for those who have access to this domain of knowledge.

As this example illustrates, technological development has the potential for extending the limits of human understanding, and this should be reflected in medical education. Improved microscopy imaging methods can expand the horizon of medical diagnosis and treatment, including determining success rates and treatment costs. For instance, modern immunomodulating cancer therapies highly depend on detecting the presence of specific molecular features on the surface of cells, a task that involves a dedicated sample treatment and successive observation in a specialized microscope. Note that there are a plethora of microscopy techniques, all different in the way they function. With this broad and ever-expanding repertoire of imaging technologies and visualization options, it is more relevant than ever to be aware of how an image was formed, how it was processed and what this means for our interpretation of the scientific or medical image data. However, interpreting an image is not only about the technical features that led to its creation, but also about the human recipient processing and interpreting the image. Visualizations can help us to discover new features previously invisible. On the other hand, the expectations can blind the observer to unexpected or unknown image features. This can be explained by contemporary psychological theories on (visual) learning and instruction, and will be covered in the last section of this chapter.

1.2.2 Finding Patterns in Biological Chaos: Histology as a Subject at Universities

In today’s medical school curricula, histology—or microscopic anatomy—plays a key role.

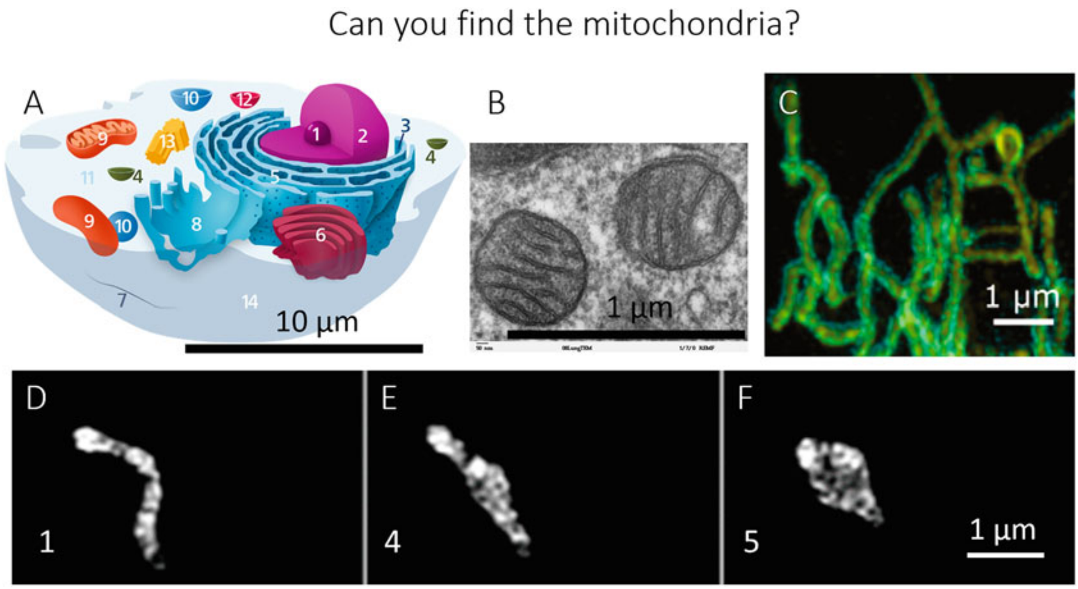

Fig. 1.1 Does how we learn to see mitochondria correspond to the reality in living cells? (**a**) typical sketch of cell organelles: 1 Nucleolus, 2 Nucleus, 3 Ribosome (dots as part of 5), 4 Vesicle, 5 Rough endoplasmic reticulum, 6 Golgi body, 7 Cytoskeleton, 8 Endoplasmic reticulum, 9 Mitochondrion, 10 Vacuole, 11 Cytosol, 12 Lysosome, 13 Centrosome, and 14 Cell membrane; (**b**) Transmission electron micrograph of mitochondria in lung tissue (Louisa Howard, public domain); (**c**) mitochondrial network imaged in living cells using fluorescence super-resolution microscopy; (**d**–**f**) super-resolution time-sequence of mitochondria labeled using a chemical (MitoTracker). The numbers in the lower left corners correspond to the image number in the time-sequence (video). The mitochondria change from thin and elongated to rounded (as in **b**) during the time-sequence, likely an effect of the toxicity of the dye in combination with repeated intense light exposure. (**c**–**f**) adapted from Opstad et al. (2018)

Learning about macroscopic anatomical features of the human body is the basis for understanding many diseases and surgical interventions. Histology provides the basis for later education in pathology as well as understanding the cellular processes leading to certain diseases.

At many universities, students have the opportunity to look at slides themselves, using standard light microscopes. They are usually encouraged to draw at least parts of what they see in the slides into a notebook or coursebook for a better understanding and memorization of the tissues they are examining. Oftentimes, students are also encouraged to look for certain typical features of cells (Chapman et al. 2020). However, this method of examining samples has its limitations. A typical example would be the microscopy of cells in the state of mitosis (i.e., cell division). Mitosis is usually described in textbooks as a sequence of consecutive steps that are clearly marked by certain cellular features. However, this method of looking at the process of mitosis in a histology class (by trying to find good examples of cells in a slide that clearly show features of one of the described steps) totally ignores the fact that mitosis is a continuous, biological process that never stops at certain stages but rather moves through them.

Furthermore, histological assessment is often focused on certain cellular features and potentially makes the observer ignore many of the other features that a slide might contain. In the case of mitosis, finding a cell in a certain state simply means that, by coincidence, the tissue was preserved at just the right moment, but the focus is taken away from the continuity of the process. This seems like trying to understand the movements of a galloping horse by a series of consecutive photographs. The photographs might explain and reveal certain features (just like the first pictures of a galloping horse put an end to the discussion whether the feet of a horse actually touch the ground when it is running), but to fully understand what you see, you need to be acutely aware of the fact that you are taking a static glimpse into an ever-changing process.

Students are also not always shown human tissue. In some cases, this is because slides of other species are available more easily and essentially show the same anatomical features. There are also cases, however, where probes of different species are used because they show anatomical features more clearly. For example, the human liver does not show its subdivision into lobula as clearly as the liver of a pig, which is why oftentimes, slides of pig liver are used to point out the anatomical features of liver more clearly (Lüllmann-Rauch and Asan 2019).

Another limitation of conventional microscopy as it is used in medical education has become even more marked with the introduction of virtual microscopy. When examining a slide under a microscope, the examiner can alter the focus of the microscope and therefore scan through the whole slide. This might seem irrelevant, but looking at an axon in a microscope, for example, differs a lot from looking at it as a picture or on a screen. By changing the microscope's focus, one becomes aware of the fact that an axon is a cylindrical object rather than a flat line, and one will also recognize that it does not move straight, but rather twists and turns its way through the tissue. This impression of three-dimensionality gets lost once the slide has been photographed.

Another relevant aspect students learn during histology class is getting used to artifacts. Slides may contain cuts, cracks, and holes, which are a result of the process of preservation: cutting and labeling the tissue can cause it to deteriorate, detach, shrink, or expand. Distinguishing between artifacts and actual anatomical features of interest might be possible by taking into account certain features such as the discontinuity of membranes, but in many cases it is only possible to discern the difference from experience.

All in all, one could say that histology, as it is often taught at universities, is focused on anatomical patterns and classifications of certain tissues (Chapman et al. 2020) based on a minimalistic dataset, whereas it lacks the dynamic nature of living cells, and sometimes even the three-dimensionality of tissue. Hence, it is a good approach for detecting irregularities in a pattern—highly relevant for pathologists—but not necessarily optimal for understanding biological systems such as the human body.

Assuming that we were completely free in our choice of imaging technology in the medical classroom, how could we best exploit this technology to effectively convey understanding of living systems and pathologies? As a first step to answer this question, the next part of our chapter will look at the way in which modern microscopes form magnified images and how different types of microscopes function. We will also point out their respective advantages and limitations, and highlight some applications in the medical context.

1.3 Simple Microscopy and Advanced Variants

This chapter focuses on *optical* microscopy techniques. It is possible to generate images of biological samples using something other than light (e.g., an electron beam and ultrasound waves), but this will not be covered here. Optical imaging techniques are broadly applied, often low-cost, and easy to use. As will become clear, there is no one-size-fits-all method, but every technique has its advantages and disadvantages.

1.3.1 The Microscope—An Optical Assembly to Magnify Small Things

Optical microscopy techniques use visible light, namely electromagnetic radiation in the visible wavelength range from 400 to 700 nanometers (nm, 10^{-9} m). A very important advantage of working with visible light is that humans can see it without using an additional detector (like a camera). It is furthermore relatively harmless compared to highly energetic gamma or X-ray radiation and there is a broad range of optical components available (e.g., lenses, filters, and lasers) which make it a highly versatile wavelength regime. A sketch of a simple modern microscope is shown in Fig. 1.2.

A magnified image of a sample is formed where a *wide* light cone from the sample plane is brought back together in a *thinner* cone. The magnification as a dimensionless number is the ratio of the apparent size and the true size of the object in the sample plane. In practice, it is usually sufficient to read off the magnification value printed on the objective lens.

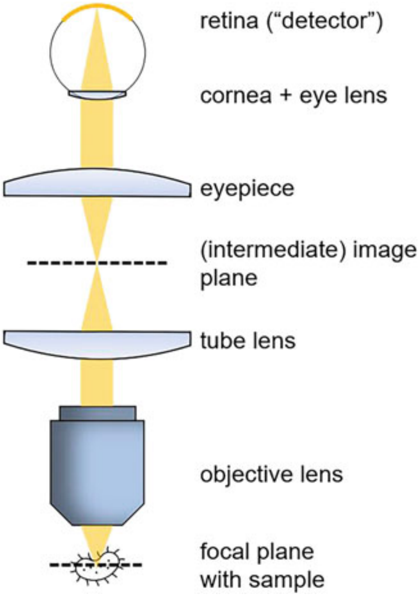

Fig. 1.2 A simple (modern) microscope in combination with an eyepiece and eye. From the sample to an observer's retina, light coming from the sample passes through several optical elements. First, the objective lens captures light in a wide cone (described by the objective's numerical aperture) and provides the main source of increased resolution. The magnification (as written on the objective) is actually only defined together with the second element, the tube lens. Magnification is the ratio of the focal lengths of both elements. In a digital microscope, the camera is placed in the focus of the tube lens in the image plane. Because human eyes have "bigger pixels" than cameras, a manual microscope has another magnification stage, basically another microscope. It consists of the eyepiece and the refractive part of the eye, namely cornea and eye lens

Humans have larger sensory units ("pixels") compared with cameras and require an additional magnification step, which is catered for through the eyepiece (i.e., the glass piece that an operator's eye is close to). Together with the operator's eye, this gives another 10–30x magnification, depending on the eyepiece used. However, magnification alone does not make for a good microscope. Resolution and contrast are two further very important attributes of a microscope that one should be aware of.

1.3.2 Sample Contrast Mechanisms

1.3.2.1 Brightfield, Labels, and Phase Contrast

In the previous section, we introduced magnification as an important prerequisite for visualizing certain sample or object details; an important prerequisite for a microscope, though insufficient on its own. If you spill coffee on a white shirt, it will be spectacularly visible under almost any lighting condition. If you spill coffee on a coffee-colored shirt, however, the stain will not be easily detectable unless the light falls from a particularly unfortunate angle.

This scenario is similar in the microscopic world. If the sample has intrinsic contrast in the form of strongly scattering or absorbing components, we might achieve sufficient contrast by illuminating the sample straight on. This is called brightfield microscopy (Fig. 1.3a). If instead the sample is nearly perfectly transparent, we need to tweak the illumination to see additional sample details, for instance, by using differential interference contrast (DIC; Fig. 1.3b) or colorful chemicals like hematoxylin and eosin (H&E) to artificially stain the sample (Fig. 1.3c). Other common optical methods to provide contrast are *darkfield* and *phase contrast microscopy*. In darkfield microscopy, only the light that strongly interacts with the sample (i.e., scattered light) will reach the camera and contribute to the image signal. In phase contrast microscopy (and DIC), various light wave paths are slightly altered

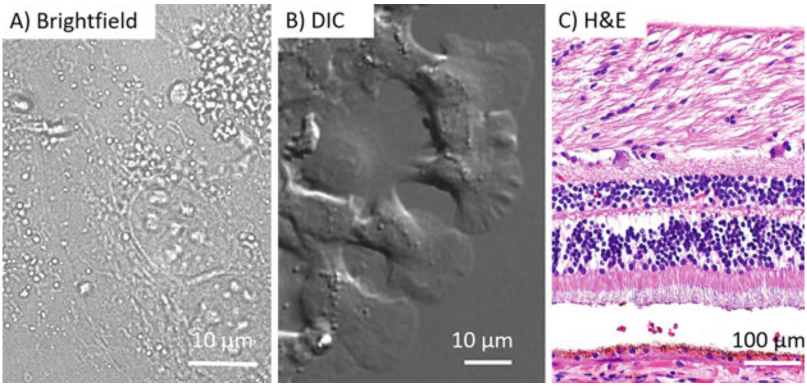

Fig. 1.3 (**a**) Brightfield image of rat cardiomyoblasts, (**b**) DIC image of salmon keratocytes and (**c**) a brightfield image of retina stained with H&E (approximate scale bar). H&E image by Librepath—Own work, CC BY-SA 3.0, https://commons.wikimedia.org/w/index.php?curid=45308378

using special optical elements, such that they will combine their wavefronts either constructively or destructively (in particular at cell/sample borders), resulting in image intensity variations which add image contrast to cellular details.

It is worth noting that these contrast methods do not provide quantitative intensity information. One can measure, for example, how long a muscle fiber is, but one cannot accurately measure sample features like mass, refractive index, or cell thickness using any of the above-mentioned techniques. Quantitative phase microscopy (QPM) provides such capabilities.

1.3.2.2 Quantitative Phase Microscopy

QPM can estimate the *phase delay* experienced by light waves traversing a specimen compared to the surrounding medium. Light travels as a wave and the physical property *refractive index* (of any transparent medium like light, glass, or water) indicates how fast it moves while traveling. Indeed, the refractive index can be defined as the factor by which light is delayed in a medium compared to that of the speed of light in a vacuum. Vacuum light speed is normally referred to as *the* speed of light (about 3 × 10^8 m/s). So QPM exploits the fact that light travels slightly slower in cells and various organelles as compared to a surrounding buffer. If the refractive index of a sample is known, one can quite accurately calculate the sample height (to an accuracy of about 1 nm), or vice versa, and obtain a dry-mass estimate: generally, the more massive a cell, the higher the phase delay.

When the refractive index is known, QPM is a 2.5 dimensional (2.5D) imaging technique as for each x and y point one obtains a height estimate. Importantly, it does not have the ability to distinguish between different features along the third (z-) dimension. This means that one cannot discern if two cells are on top of each other or if it is one large cell.

However, approaches exist to make QPM appear "three-dimensional" using tomography, viz. illuminating and measuring a sample from many different angles and using the data to reconstruct a "3D" image computationally. In that, QPM is the equivalent of a "stack" of brightfield images. Crucially, tomographic QPM is still missing *optical sectioning*, a key feature of real volumetric microscopy that allows one to distinguish features along the axial dimension. But before we can discuss 3D microscopy, we need to first understand some concepts about resolution and fluorescence. Let us begin with fluorescence: although we can achieve good contrast of some cellular features with QPM and see many dynamical processes taking place inside living cells, we do not necessarily know *exactly what* we are looking at. However, if our molecules of interest were tagged with a clearly identifiable *label*, this problem would be solved.

1.3.2.3 Fluorescence Microscopy

In the previous section, we have seen how different ways of illuminating the sample can be exploited to enhance the sample contrast for different cellular details. We also noted that we usually cannot be sure of what exactly we are looking at in terms of molecular specificity with the techniques described above. Fluorescence microscopy in its many variations is a tool that solves this issue, but as we will see, introduces other challenges and tradeoffs.

Fluorescence microscopy relies on fluorescent molecules. These can be naturally occurring in the sample, but the best fluorescent molecules for microscopy (called fluorophores, labels, dyes, or markers) are usually added to a sample during preparation for microscopy. Fluorescent molecules can be *conjugated to* an antibody (or other molecules) specifically targeting a particular protein/antigen in the sample. A similar or even better specificity can be achieved by genetically altering cultivated cells to produce a fluorescent protein attached to the cellular protein of interest. Many different labeling techniques as well as chemicals for adding contrast and specificity to cellular features exist (for an overview of this complex topic, see, e.g., Wiederschain 2011).

Fluorescence as described by physics, is a quantum mechanical phenomenon. If a fluorescent molecule like a fluorescent marker absorbs a photon, it gets energized and after a short period (usually in the order of nanoseconds) emits a new photon. Importantly, a small part of the absorbed photon's energy is kept by the molecule and thus the emitted photon has less energy. Photon energy is directly linked to photon wavelength, so this loss in energy causes a red-shift in wavelength. Crucially, this shift is big enough for specially engineered filters to separate the excitation light (used to illuminate the sample) from the emitted light (used to form the image). An example of the fluorescence excitation and emission spectra for the cellular marker MitoTracker Green FM is shown in Fig. 1.4. The appropriate choice of optical filters both for the excitation and for the emitted light is important to ensure that one only image the intended type of molecule. It is similarly important to collect as much signal as possible from this particular molecule, as fluorescence is a weak signal compared to illumination or ambient light. An optical filter allows selecting of certain wavelengths or polarizations while blocking others.

Autofluorescence in Pathology

Autofluorescence is often seen as a major problem in pathology. Many tissues are formalin-fixed, which causes strong sample autofluorescence. This is an issue, as modern pathological methods often not only require measuring the average expression of molecules in homogenized tissue but also their distribution within the sample while preserving its cellular and architectural features (Mansfield 2013). This can be very difficult once the weak *extrinsic* fluorescence signal is mixed with a varying level of autofluorescence. However, there are a number of applications that also exploit tissue autofluorescence.

Gastroenterologists use a technique called confocal laser endomicroscopy (CLE). In this technique, tissue is illuminated using a low-power focused laser. The intrinsic fluorescent signal emitted from the tissue is then measured and the spectrum enables the diagnosis of potentially dangerous tissue changes (ASGE Technology Committee 2014). CLE can also obtain images with good contrast of the mucosal layer of the gastrointestinal tract and can be used for surveillance and detection of diseases like *Barrett's esophagus* (Xiong et al. 2017), diagnosis of *indeterminate biliary strictures* and post-resection follow-up of lesions in the colon (ASGE Technology Committee 2014). Further development of the technique might lead to the possible differentiation of a multitude of gastrointestinal diseases. This could be useful in diseases like *ulcerative colitis* and gastric cancer, in which large areas of mucosa can be affected by areas of *dysplasia* that are not visible with techniques currently in use (Falk 2009). However, setting up such a micro-endoscopy system takes 5–10 min—which is a lot given the limited time a doctor has available for his or her patients. Despite its benefits, faster (and/or cheaper) alternative methods exist, and therefore CLE is still not in everyday clinical use (ASGE Technology Committee 2014).

To give but one more example, ophthalmologists rely on the autofluorescence of lipofuscin and other endogenous fluorophores

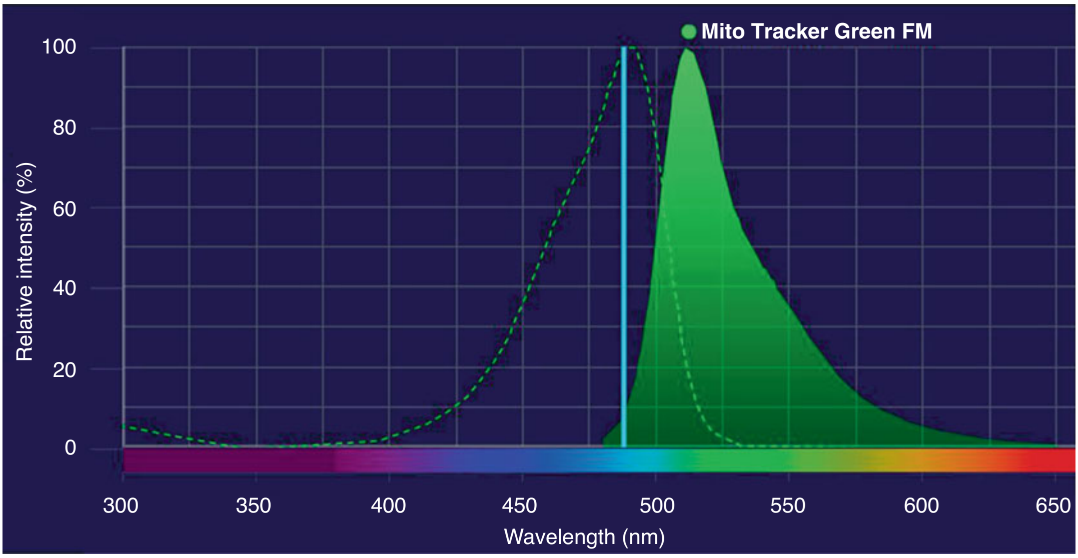

Fig. 1.4 Normalized excitation (dotted line) and emission (full line) spectra for the cellular probe MitoTracker Green FM using a 488-nm excitation wavelength (vertical blue line). Such spectra are very useful for choosing combinations of dyes, light sources, and filters for fluorescence microscopy experiments. The plot was made using Thermo Fisher Scientific's Fluorescence SpectraViewer

accumulated in retinal pigment epithelium (Nandakumar et al. 2012) for disease diagnostics in the eye of age-related macular degeneration, retinal dystrophies, and ocular tumors (Almeida et al. 2013). Other applications include the possible differentiation between *ad integrum* healed white matter lesions and non-affected tissue in multiple sclerosis (Morgan et al. 2020), and the possible use of near-infrared autofluorescence in thyroid surgery (Demarchi et al. 2021).

Applications of Fluorescence Microscopy in Medicine

The field of fluorescence microscopy has a much wider variety of clinical applications than the comparatively small field of autofluorescence. The World Health Organization recommends the use of fluorescence microscopy due to its ease of application and interpretability (World Health Organization 2005).

An important field of application is oncology, where fluorescence microscopy plays a key role. The specificity of this technique enables the differentiation of different cell surface molecules that would otherwise not be visible. In certain forms of leukemia and blood cancer, fluorescence microscopy can therefore help to screen for the presence of cells that look morphologically normal but still express pathological surface proteins—a state that is called "minimal disease" and would otherwise not be detectable. In addition, fluorescence microscopy is used to phenotype morphologically abnormal cells and therefore choose the correct targeted treatment (Higgins et al. 2008). Similarly, fluorescence microscopy is used in the diagnostics of breast cancer to screen for the expression of estrogen and progesterone receptors. This helps predict the response to certain targeted therapies (Ciocca and Elledge 2000; Anim et al. 2005). Fluorescence microscopy also comes into play once there is a tumor of unknown origin. In such situations, the labeling of certain tissue-specific markers by using antibodies and visualizing them with fluorescent secondary antibodies helps to determine the origin of the degenerated cells. Once successful, it is this exact determination that allows for starting treatment with a targeted therapy (Leong and Wright 1987).

Applications of fluorescence microscopy are also abundant outside of oncology, for instance, in infectiology. Viruses, for example, are challenging to observe due to their small size and subcellular localization. Yet, the common pathogens *cytomegalovirus* or *hepatitis B virus* (HBV) are reliably detectable using fluorescence microscopy, as it is possible to target virally expressed proteins specifically with selected antibodies. This also applies to common bacteria, like *Helicobacter pylori*, which are responsible for certain forms of gastritis. Sometimes, these bacteria cannot be detected using normal, non-fluorescent staining, even though there are suggestive pathological features in biopsies. In these situations, using antibodies against proteins of this organism enables detection of the bacteria in question (Leong et al. 2003).

1.3.3 Resolution and the Microscope's *Blurring Function*

The component in a microscope that determines its resolution is the objective lens. The main task of the microscope objective is to collect light from the sample as shown in Fig. 1.2. The wider the light cone the objective lens captures, the higher the image resolution that can be achieved. Resolution in this context describes how far apart two details can be in order to still be discernible as separate. An important prerequisite is that the camera (or detector) has correctly sized pixels with respect to the desired image resolution. If the pixels are too large, the magnification is too low. If the pixels are too small, the camera is *oversampling* and a lot of the magnification is *empty*. In itself, oversampling does not impact resolution, but it limits the observable sample area.

The more "angles of light" from the sample one can collect (given by the cone of the objective lens), the more information (i.e., higher resolution) can be present in the image. A single point in the sample will always look blurred after imaging through an aperture (like the objective) and is indeed a very good way to describe the performance of a microscope. It is called the microscope's *point spread function (PSF)* and it describes the image of a very small particle in the sample. As a consequence, the image of the sample is recorded as if drawn with a thick pencil (the pencil tip being the size of the PSF), smearing tiny details into each other such that they become indistinguishable if too close together. How close together two particles can be and still be seen as separate, defines the optical resolution. Conventionally, the best possible image resolution is given by the imaged wavelength divided by twice the numerical aperture of the objective (abbreviated NA and usually printed on the objective). Any optical technique that provides better resolution is part of the field of *super-resolution microscopy (SRM;* Kubitscheck 2017).

1.3.4 Super-Resolution Microscopy

Until now, we have only considered optical imaging techniques within the conventional resolution regime. This covers the details that can be seen after being painted with a "thick PSF pencil" as described above, typically >200 nm, depending on the objective lens and wavelength. Could it be possible for the microscope to start drawing sample details with a thinner brush than determined by the physical law of diffraction? Not directly, but there are several techniques that enable better resolution than dictated by the conventional limit. An example of what this means in practice is displayed in Fig. 1.5, where structured *illumination microscopy* (SIM) manages to resolve details of mitochondria that are unobservable in conventional microscopy. Collectively, the techniques surpassing the optical diffraction limit are called *super-resolution microscopy* (SRM) and they encompass a multitude of very different methods that each have their prime application regimes (for a detailed overview, see, e.g., Schermelleh et al. 2019).

There are a few biomedical applications where even a minor resolution increase can make a big analytical difference. One example is in visualizing the glomerular filtration barrier. The glomerular filtration barrier is a structure in the

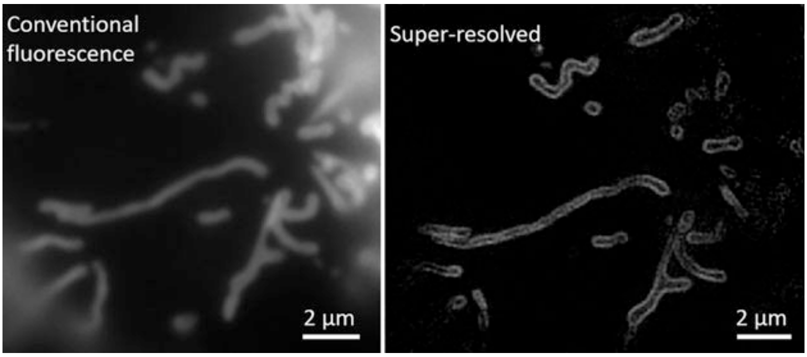

Fig. 1.5 Comparison of conventional fluorescence microscopy and a super-resolution SIM image. The images are of the mitochondrial outer membrane in living cells, labeled using genetically encoded fluorescent protein. The figure is modified from Opstad (2021)

kidney that helps to filter urine from the blood passing through the kidneys by building a barrier for substances that are supposed to stay inside the body and letting pass substances that are supposed to leave the body via the urinary tract. The glomerular filtration barrier is a subcellular structure that is not within the resolution of conventional light microscopy and therefore usually examined using electron microscopy. As the alteration of this filtration barrier plays an important role in many kidney diseases, it is a relevant research topic, for example, of diabetic kidney disease (Ricciardi and Gnudi 2021). The use of super-resolution microscopy techniques allows for an unprecedented visualization of immunogenic alterations in the filtration barrier, as antibodies are much better preserved than in electron microscopy (Wunderlich et al. 2021).

Depending on the particular application and sample, different trade-offs between imaging speed, area, and resolution must be made. Also, instrument cost and expertise availability can be important determinants of one's choice. In general, "there is no such thing as a free lunch" and a resolution increase is always paid for by reduced field of view, higher light exposure, and both longer preparation and imaging times. It is therefore important to understand what information is relevant to get from a sample before applying SRM. For example, cell migration studies or fluorescence intensity measurements are usually better performed using simpler, conventional microscopy, while resolving the internal structures of cell organelles usually requires SRM or electron microscopy. For applications where cellular structure and dynamics in three dimensions play an important role, techniques that deliver *depth information* within the resolution limit are often sufficient and preferable over SRM, both due to a lower light dose on the sample and often also reduced experimental cost and complexity. High light doses cause photobleaching and photodamage to the sample, so the illumination intensity should be kept at a minimum, especially when considering living samples (Laissue et al. 2017).

1.3.5 3D Microscopy

Representing a 2D image or a 2.5D height map is simple—this is the standard that our human vision is used to and is usually done using a grid with small picture elements called pixels. A real 3D scene, however, is difficult to visualize and also to imagine. If you look at a hilly landscape, you have a 2.5D image, but in full 3D you would also simultaneously "see" the different layers of rock, underground caves, etc. below the surface. A good work-around is to separate the 3D scene into 2D slices. In traditional histology, a block of tissue can be sliced into a multitude of thin elements called serial sections. When assembled in a computer, this allows for a dynamic exploration of the tissue. Fresh tissue is comparatively soft and cannot be cut into very thin sections, which necessitates that the 3D tissue under investigation is either frozen or embedded in a solid material like paraffin—neither is suitable to keep cells in the tissue alive.

1.3.5.1 Optical Sectioning

In living samples, it is therefore necessary to perform 3D microscopy with *optical* sectioning. In a widefield fluorescence microscope (a "normal" microscope), it is possible to "scroll" through the *z*-direction with the focus wheel. Turning the wheel moves the objective and with it the focal plane. While in a thin sample this enables focusing (i.e., finding the plane of maximum sharpness), in a thick sample there is no single sharp plane. It is rather that separate features of the sample come into focus while the blur from all other parts of the sample overlaps the image. This is called *out-of-focus light* and its removal or avoidance is referred to as *optical sectioning*. Only with sectioning it is possible to build up a proper 3D representation of the sample. See Fig. 1.6 for a visual explanation of the widefield microscope geometry, as compared with two methods that manage to provide optical sectioning: confocal microscopy and light-sheet microscopy.

1.3.5.2 Confocal

The gold standard in 3D fluorescence microscopy with optical sectioning is laser scanning confocal microscopy, often simply referred to as *confocal*. Its working principle is described by its name, so let us dissect it. To produce as small a spot as possible, illumination light needs to be coherent. Coherence is one of the properties that distinguish *laser* light from the light a lamp produces: coherent light means that the waves of individual wavelets of a laser beam move in phase with each other, that is, having their crests and troughs aligned in space and time. This enables focusing down to the diffraction limit. With this laser focus, one excites fluorescence in the focal plane. Fluorescence is, however, also excited in the cone the light takes toward the focus (and after it). If one places a pinhole in the image plane exactly conjugated to the location where the laser focus is, only the in-focus light passes, while almost all out-of-focus light is blocked. With this arrangement, one can record exactly the voxel (volume pixel) value of a sample at the chosen *XYZ* scan position of the laser focus. Scanning the stage thus allows to raster the entire volume. Such "stage-scanning" is usually very slow, so modern confocal microscopes often scan only the stage in Z (i.e., change the focus plane), while the laser spot itself is scanned with fast galvanometer mirrors that are hidden from the user inside the microscope.

As confocal light still excites all fluorophores in the sample volume during a single scan, it is often not considered ideal for live-cell microscopy and can quickly bleach fluorescence or even kill the sample due to the intense laser focus.

1.3.5.3 Light-Sheet Microscopy

An even faster and to-date the gentlest 3D microscopy method is light-sheet microscopy. Here, two objectives are used simultaneously. From the illumination objective, a sheet of light is launched into the sample to excite fluorophores in a single plane, while a second objective placed orthogonally captures the emitted signal in exactly that plane. Thus, out-of-focus light is avoided altogether, all illumination light results in usable in-focus fluorescence, and each focal plane is recorded at the speed of widefield microscopy (the speed of the camera capturing the entire image at once). The drawback of this technique is its two-objective design (see Fig. 1.6c), which obstructs many conventional sample mounting methods. Most sample preparation protocols are tailored for glass-bottom dishes or large microscopy slides, which are hard to combine with light-sheet microscope geometry. This has so far prevented widespread use of the technique.

In the near future, a new generation of light-sheet microscopy will become available that manages to pack both the light-sheet generating illumination objective and the detection objective into a single lens (often referred to as SOLS—single objective light-sheet) such that conventional sample mounting becomes possible in a similar vein as in confocal microscopy (Dunsby 2008; Sapoznik et al. 2020; Ströhl et al. 2022).

The ability to follow dynamics of living cells and even their internal structures is an exceptional window to understanding cellular function and morphology. How does one's impression and understanding of a mitochondrion change from

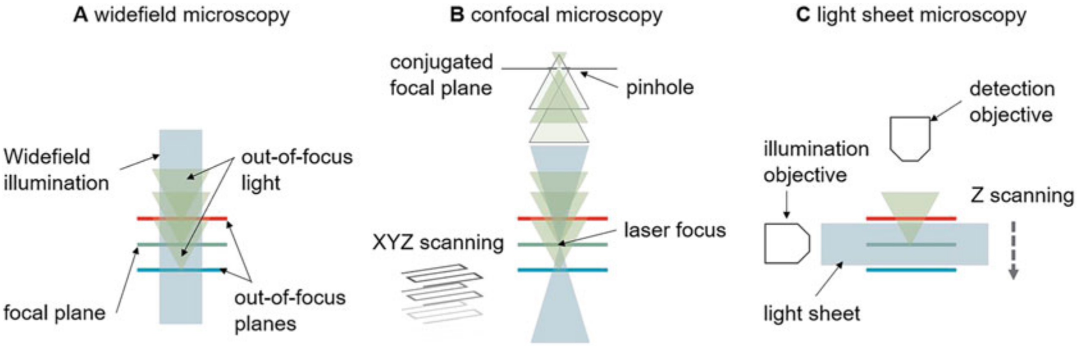

Fig. 1.6 (**a**) Out-of-focus light causes a substantial background haze in widefield microscopy, which renders the technique unsuitable for 3D imaging on its own. (**b**) In confocal microscopy, a single laser spot is scanned in XYZ through the sample. a reading is taken at each scan position and saved as voxel (volume pixel) value. Through a pinhole in a plane conjugated to the sample plane, only light from the focus can pass, while light excited by the path of the laser in other planes is largely blocked from reaching the (point-) detector. (**c**) In light-sheet microscopy, a laser beam is shaped into a thin sheet of light and launched through a secondary (illumination) objective into the sample. Thus, signal is only generated in the focal plane of the detection objective and out-of-focus light is largely avoided all together. Light-sheet microscopy can be much faster than confocal microscopy, as scanning is only required in the Z-direction

seeing only the electron micrograph in the introduction versus seeing it wiggling like a worm in 3D live-cell imaging? And how do we visualize and comprehend such information-dense multidimensional data?

1.4 Data Processing

In the previous sections, we have described many different ways of acquiring optical image data applicable to many sample types. Some of these techniques, like QPM or SIM, also inherently require computational post-processing to form a ready image. However, assuming we now have our images acquired and safely stored, how do we visualize and derive meaningful information from them? In this section, we will introduce some important concepts in bioimage visualization and processing. The concepts introduced are named according to functions in the open and popular image analysis toolkit ImageJ/Fiji (Schindelin et al. 2012), so that you can apply them yourself or with available open data (some even built-in in ImageJ/Fiji).

1.4.1 Visualization

1.4.1.1 Grayscale and Color Images

A digital image in its simplest form constitutes a 2D array of numbers, where each entry represents an intensity value. As such, in data storage we have—either from the camera directly or resulting from computational post-processing—a spatially organized set of numbers that need to be represented on the computer screen. That is usually done with the help of something called a *color map* or *Lookup Table* (LUT). The most basic one is *Grays*, where the color black represents zero intensity and the highest number (e.g., 255 for 8-bit images) is displayed as white. Between these intensities are 254 different shades of gray. Although this way of representing the image is called “grayscale,” one can choose any other LUT to represent one’s set of numbers that might make it easier (or at least more visually pleasing) to observe certain image features. Some common LUTs are displayed in Fig. 1.7 with an example intensity representation above.

However, colorful they may look, grayscale images do not necessarily have any color information pertaining to the sample, as the color only represents intensity information (usually

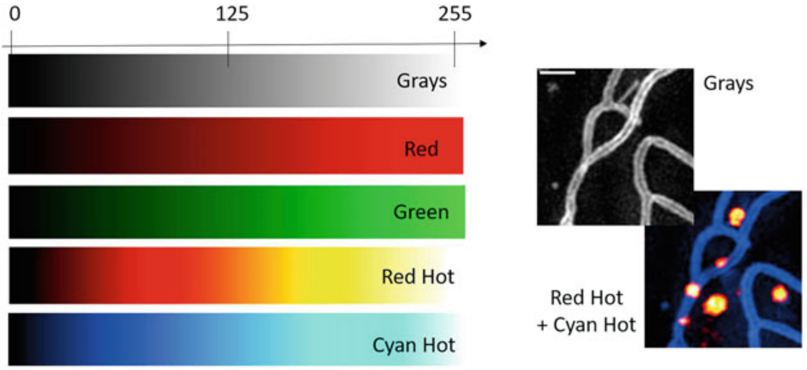

Fig. 1.7 On the left, you can see look-up tables (LUTs) with exemplary 8-bit pixel intensity assignments. The right side shows a grayscale image displayed with the LUT Grays, and an example of a two-channel image displayed with the LUTs Red Hot and Cyan Hot (combined and saved as an RGB single-layer image). The scale bar is 1 μm

proportional to how many photons hit the camera in certain locations). If an optical filter was used in front of the camera, for example, a green emission filter (letting through light of wavelength around 510 nm), the camera can count photons as it normally does, and we can store this image as the color green. If we do this for different colors, say for blue and red lights, we can put these three images together as one three-channel image and even overlay them as a multicolor image. Different LUTs can be used for different color channels and combined, as displayed in the bottom right of Fig. 1.7.

1.4.1.2 Volumetric and Video Microscopy Images

A standard PC screen is made for displaying 2D information such as an RGB image: patterns of different intensities with color information. However, what happens if we have additional dimensions to visualize, as in a volume or during a time-lapse? We can of course run through both the time-lapse and volume plane-wise and view one frame at a time (as z2–z14 in the left of Fig. 1.8), but it will lack the volumetric feel to it. To understand how a volumetric organelle, cell, or even whole organism develops over time, we need further visualization tools and "tricks."

In order to view how the imaged object is organized in the orthogonal dimension, one can—instead of viewing the data as *XY*-planes—"cut" the data along the *Z*-dimension, and reorganize (on the display) the viewed pixels as XZ or YZ. This is called *orthogonal view* and is illustrated in the red box of Fig. 1.8. From this, one can see how certain sample points relate to one another in the third spatial dimension, but the picture still lacks a volumetric impression. Aside from this, most of the sample is not seen at one axial cross-section, so one might feel like one is losing the overall view of the sample. The sample overview is often needed, because when just seeing a dot or a line, one cannot really tell if it is a biological structure at all. When looking at distributions of dots or lines around (e.g., a cell nucleus), one can understand something from the dots or lines. This is the overview that often goes lost when just looking at a single axial cross-section.

To receive a quick overview of the image volume simultaneously, a *z*-projection function can be used. An example of a *maximum intensity z*-projection is displayed in the blue box in Fig. 1.8. Here, only the voxel with the highest intensity along the *z*-direction is displayed. The main limitation of this simplified volumetric view is that one cannot determine if different cellular components are actually in the same location

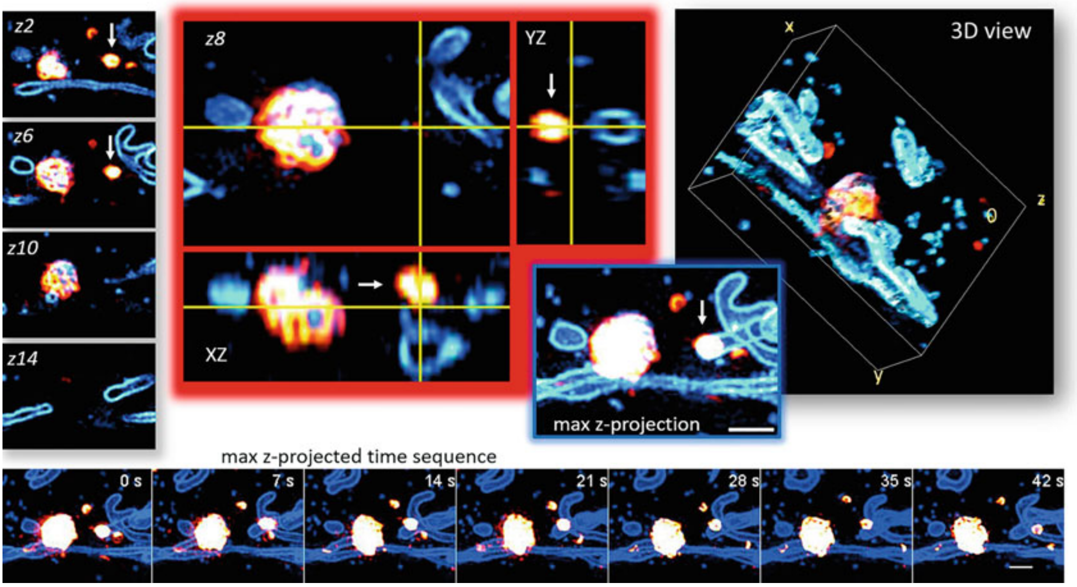

Fig. 1.8 Left column: four individual z-planes. Red box: orthogonal views. Blue box and bottom row: maximum intensity z-projection. The scale bars are 1 µm. Left: 3D rendering using the Fiji plugin 3D viewer. The figure shows 3D SIM images of mitochondria (cyan) and Lysosomes (red). The data used for this figure is openly available and further described in Opstad et al. (2022b)

(colocalized) or just in different *z*-planes. For example, the white arrows in Fig. 1.8 point at a lysosome that in the projected view looks like it could be inside a mitochondrion, but in reality is located above and actually not at all in contact with the mitochondrion, as is apparent from the orthogonal *XZ* view.

If one wishes to display a volumetric object from different angles and interactively rotate the image, one can use a 3D viewer that displays a projected image from different angles (an example using the Fiji plugin *3D viewer* is displayed on the right of Fig. 1.8).

Is there now anyway of adding yet another dimension to the image, such as time? The best solution here can often be to save the 2D or 3D rendered image as a motion picture. If a still image is desired, several time-points can be added in a figure next to each other (as in the bottom row of Fig. 1.8) or even added onto the same panel using color-encoded time information.

Which visualization technique to choose for different sets of image data clearly depends on what one wants to show with the image visualization. For the same multidimensional data, the most insightful visualization might be to use several display modes, each highlighting different object features. Unfortunately, the most common convention for display in biomedical (or other) textbooks appears to be simple 2D images without much information about how they were formed, processed, or—if any—what the different colors represent (Jambor et al. 2021).

1.4.2 Quantification

As we have seen in the previous sections, well-presented microscopy data can effectively convey morphological details and new understandings about cells and tissues. Sometimes, however, quantitative information is also desired and needed. So, how do we derive informative numbers from our images? This section outlines some important concepts for image quantification.

After finding a suitable software to display and process one's images, the first thing one needs to know is likely the *image pixel size*, or more accurately, how much area in the actual sample one pixel in the microscopy image represents. With the image dimensions in place, one can measure object features like size, volume, relative distances, or even image resolution, if the microscope performance is of interest. The relative intensity of different objects and labels might be relevant when some structures overlap (colocalization), and how fast objects are moving or changing over time.

The object has been mentioned many times so far, but how do we even define an object to be measured? To measure the area of an image object such as a cell or cellular organelle, we first need to clearly define what the object is. In microscopy images, there can be surprisingly many different solutions to this seemingly clear task, even for the same data. The main reason for this is the blurring of image details as compared with normal photography of larger objects. When the—in some way different intensity—values indicating the object are not sharply cut off but instead significantly blurred, the object area can be defined in many ways. Some examples of this are illustrated in Fig. 1.9, where three different possible segmentations of fluorescent mitochondria are shown. The *Huang* and *Otsu's methods* are *hard thresholding* algorithms based on the image intensity statistics (i.e., the image histogram, as shown on the right side of Fig. 1.9). The image object (or objects) can then be defined by the pixels with intensity values above the threshold determined by the algorithms. A hard threshold is simple and works well enough for some data and some applications. If on the other hand, one would like to measure and count the small vesicles surrounding the mitochondria (called mitochondria-derived vesicles), this segmentation procedure would not be accurate enough as in some places noise/artifacts would be counted as vesicles and in other places (in reality continuous) mitochondria appear broken up and would also be counted as small vesicles (in automated analysis).

The bottom row of Fig. 1.9 shows segmentation with the help of machine learning (Trainable Weka Segmentation; Arganda-Carreras et al. 2017) to better separate noise and image artifacts from mitochondria. As this simple form of machine learning uses individual pixels (and their neighboring pixels) as training points, one can obtain enough training data from a single image and apply the trained classifier to many more images—provided that the data is similar enough in whatever data aspect was learned by the program. A more advanced and sometimes controversial form of machine learning is *deep learning*. Compared to *shallow* or more conventional machine learning, deep learning requires large amounts of input data ("big data") and usually learns classification rules that remain hidden ("black box"). This certainly brings along many additional challenges, but the unprecedented performance of deep learning algorithms is being explored and exploited for many new applications (Goecks et al. 2020).

1.4.3 Machine Learning in Pathology

The term "big data" usually refers to the fact that there is a huge amount of information to be processed beyond the capacity of human analysis. When analyzing microscopy images, pathologists are often relying on defining areas of interest within a certain slide that they are examining; it is simply not possible—and also not helpful for the quality of the diagnosis—to examine *the whole slide* in detail.

However, examining the whole slide might actually reveal more detailed and helpful information—just like it is never possible to predict a popular vote exactly by merely asking a set of defined people for whom they voted. This is where artificial intelligence (AI) comes into play: diagnostic pathology is adopting the use of whole-slide digital imaging such that entire slides can be captured in high quality and taken into account for examination and diagnostics (Ibrahim et al. 2020). This novel approach to pathology

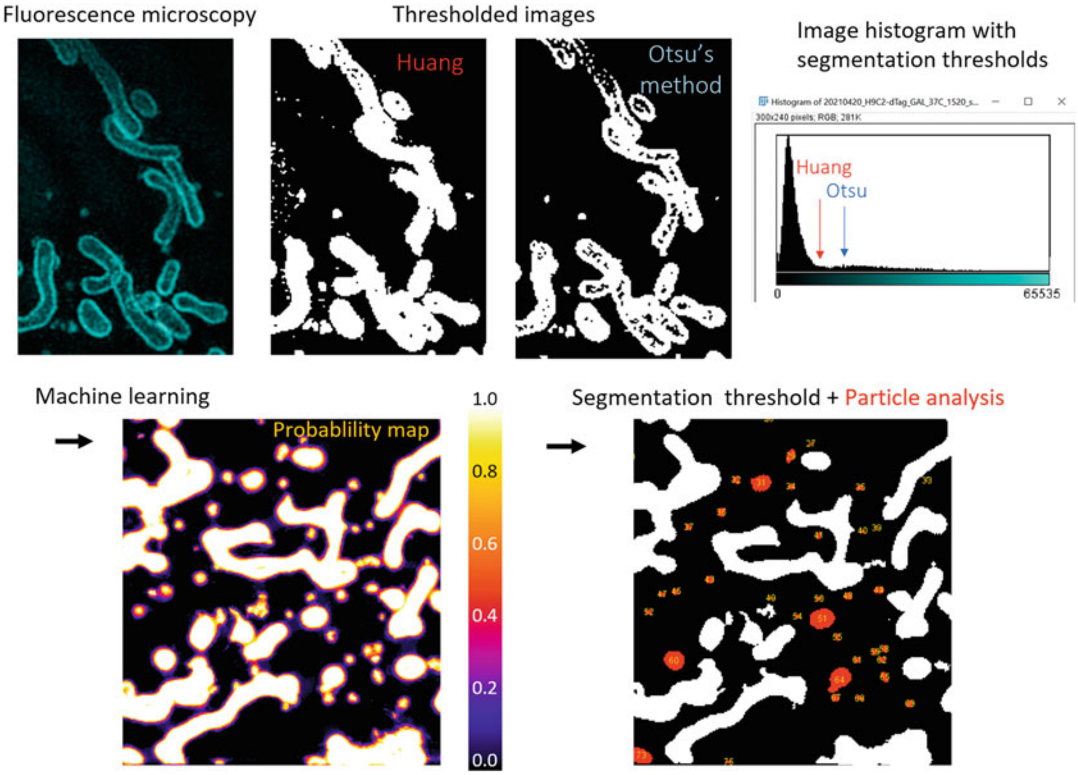
Fluorescence microscopy
Thresholded images
Huang
Otsu's method
Image histogram with segmentation thresholds
Histogram of 20210420_H9C2-dTag_GAL_37C_1520_s...
300x240 pixels; RGB; 281K
Huang
Otsu
0
65535
Machine learning
Probablility map
1.0
0.8
0.6
0.4
0.2
0.0
Segmentation threshold + Particle analysis

Fig. 1.9 Defining the object: different automated segmentation methods for fluorescence microscopy images. Upper row: hard thresholding methods. Lower row: Machine learning-based segmentation and subsequent thresholding and particle analysis. When the objects to be analyzed are clearly defined in a binary image (white/black), the image objects can be counted and measured automatically (the objects shown in red are counted and measured after excluding the other image features after their shape and size). The figure was adapted from Opstad et al. (2022a)

enables both remote analysis of large image data and the analysis supported by AI.

AI approaches have already been approved by the Food and Drug Administration (FDA) to support the rapid detection and diagnosis of cancerous tissue (Niazi et al. 2018; Dlamini et al. 2020). AI has been shown to achieve superior accuracy in primary cancer diagnosis, reduced errors, increased speed, and differentiation between benign and malignant tumors (Evans et al. 2018; Mukhopadhyay et al. 2018; Niazi et al. 2018). This reduces the time spent on each case and is therefore greatly beneficial for overall patient care. In the near future, these algorithms might also allow for the automated scanning of metastatic cancer cells (Liu et al. 2019).

Machine learning can also be used to identify new information variables. One such example is C-Path (Beck et al. 2011; Martin 2012), short for “Computational Pathologist.” This tool was developed in order to improve diagnosis and ameliorate prognosis for women suffering from breast cancer based on the automated analysis of tumor slides. C-Path focuses on identifying new features that were not part of the to-date scoring system used by pathologists based on automated image processing. From these new-found features, a model was developed to predict survival which proved to be superior to the expert opinion of community pathologists. It was especially impressive that C-Path scores were significantly associated with 5-year survival; their prediction was better than any established clinical or molecular factor (Deo 2015).

In this chapter, we have discussed how microscopy images are formed; how the data can be combined into colorful displays; and how its processing can reveal information that is not accessible to the human mind alone. It is now time to think about how these technological advancements can and should be used to effectively discover and teach students about cell and human function, and what their limitations and potentials are.

1.5 Synthesizing Microscopy, Visual Representation, and Learning

1.5.1 The Importance of Visualizations for Learning and Understanding

Common wisdom has it that "a picture is worth a thousand words." Although by far not all claims from everyday folk psychology stand up to scrutiny, this one does: Visualizations and visual displays can be tremendously helpful for learning and understanding. More specifically, visualizations have at least four functions (Levin et al. 1987): First, they provide a visual *representation* of ideas, concepts, or observations that can be described verbally within a text. Consequently, they also foster the *organization* and *interpretation* of new information, and ultimately enable the encoding and storage of the acquired knowledge in memory (*transformation*). In other words, including visualizations in teaching materials, poster presentations, or conference talks is not merely decorative and aesthetically appealing but plays a key role in knowledge transmission: Humans learn better from words and pictures than from words alone (so-called "multimedia principle"; Mayer 2002). Hence, it is unsurprising that educational researchers have put a great amount of effort into improving multimedia learning, for instance, by formulating a diverse set of design recommendations (cf. Mayer 2014).

However, creating helpful visualizations is far from trivial and comes with a number of challenges (for an overview, see Renkl and Scheiter 2017). Perhaps most importantly, learners do not always know how to make the best use of visualizations. This includes ignoring visualizations, focusing on salient features of a visualization that are in fact irrelevant for understanding, and a lack of integration between visual and textual information that prevents the formation of an accurate mental model. In short, learners need to have a variety of skills and domain knowledge in order to be able to make sense of visualizations and benefit from them in the learning process (for an exemplary application of these insights in the context of biochemistry, see Schönborn and Anderson 2010). For teachers, this also means that they should not expect visual displays to be self-explanatory. Quite the contrary, learners do not only *learn by using visualizations*—they also need to *learn how to use visualizations while learning*.

In that regard, super-resolution and other modern microscopy techniques seem to offer a whole lot of new opportunities for medical education: They depict structures of our body in unprecedented quality and clarity, and they even allow for real-time visualization of cellular processes. Generally speaking, one could state that this helped to shift our image of the living cell from being a factory for proteins only, to being more like a whole company with strong internal communication, defined and complex processes, layers of decision-making, and so on. Dynamizing our mental representations of cells can then, in a second step, also dynamize our thinking about them. For instance, knowing that DNA is surrounded by important structures regulating its activity led to the idea that the environment of a living being can actually leave its traces around the DNA. These changes are sometimes even inheritable, which seemed not very likely at the moment DNA was discovered as it was thought to be an unchangeable blueprint for the construction of proteins (Zhang et al. 2020).

However, one has to keep in mind that pictures that are created through the use of one of the many microscopy techniques presented in this chapter are pictures with a specific focus, ignoring much of the information contained in the slide. For instance, using fluorescence microscopy targeting specific surface proteins also means ignoring many other surface proteins and not depicting lots of cellular structures that are actually present. That is, learning how to use visualizations also entails learning about the conditions under which these visualizations have been obtained. In other words, the different microscopy techniques make certain aspects of reality visible to our experience and thereby—at least partially—constitute the phenomena under investigation (cf. Horne and Siemers 2023). Acknowledging this and acknowledging the limitations of the different techniques are indispensable preconditions for becoming a competent user of the respective techniques.

In essence, high-end microscopy techniques can be tremendously helpful tools for illustrating learning content as they have a strong ability to dynamize our mental representations. Further, the apparent advantages of super-resolution microscopy are not limited to education. Super-resolution microscopy techniques offer unique opportunities for researchers, too. For example, they were used extensively to study the behavior of the HI-Virus in human cells and therefore helped to better understand the process of viral infection in general (Saffarian 2021).

Despite these clear advantages, super-resolution microscopy is to-date not a technique that is commonly used outside of biomedical research. It does not play a key role in medical education or clinical practice. Why is this so? Medical education in both macroscopic and microscopic anatomy is based on the direct interaction of the learner with the matter—students learn to interpret slides while looking at them themselves through a microscope, or, as stated above, they *learn to use visual representations while learning*. Super-resolution microscopy does not allow a student that special form of interaction, as imaging with super-resolution microscopy techniques has to be achieved by a trained expert and often requires expensive and large machinery. Not knowing enough about the sample preparation also puts one at risk of being deceived by artifacts. With improving system design, falling costs, and a more user-friendly operation, this might change in the future.

This potential development is supported by electron microscopy, a similarly complex technique. It is both used in education and diagnosis, for example, in kidney diseases (Alvarado et al. 2021) and more recently, in research on COVID-19 soon after the outbreak of the pandemic (Mansy and AbouSamra 2022). Electron microscopy images are being used in medical education to illustrate structures that are not visible in normal light microscopy. Additionally, electron microscopy took a long period of time from its initial development to regular clinical application; the first electron microscope was built in 1931 by Ruska (Robinson 1986), however, it took until 1986 until he was awarded the Nobel Prize as the technique had proven to be reliable and helpful in everyday use. Super-resolution microscopy was developed in the 1990s and early 2000s and was awarded a Nobel prize in 2014 (Möckl et al. 2014), so it might be that it is only a matter of time until super-resolution microscopy (and other advanced variants) find their place outside of research and within clinical practice and education.

1.5.2 Seeing What we Want to See: Motivated Perception and the Downsides of Expertise

With the advent of a wider use of advanced microscopy, more accurate visualizations of life on the smallest scale become technically possible. But there is a potentially negative aspect to this; the use of visualizations might be constrained on an even more fundamental level. While a picture may be “worth a thousand words,” we are also prone to *seeing what we want to see*. This tendency, which has been termed *motivated perception* (Balcetis and Dunning 2006; Dunning and Balcetis 2013), describes the fact that our preferences and prior expectations shape what we perceive. In many cases, this is an adaptive feature of human information processing (Hohwy 2017): being able to make reliable predictions about our (visual) environment and forming expectations regarding certain recurring structures and patterns reduces cognitive load. It frees us from the necessity to constantly rebuild a representation of the world around us and enables us to focus on the unexpected elements in our environment that do not behave according to our predictions. However, if our top-down predictions become too dominant and inflexible, we run the risk of missing crucial features which do not conform to our mental models.

Paradoxically, such blinding top-down effects can sometimes be most pronounced among experts, viz. among the group of people that one might intuitively consider to be less biased compared to the average person. Why is that? To begin with, "being an expert entails using schemas, selective attention, chunking information, automaticity and more reliance on top-down information, all of which allows experts to perform quickly and efficiently" (Dror 2011). Experts use their knowledge and skills to decide where to look, what to focus on, and what to ignore. They know which patterns to expect (see, e.g., Chase and Simon 1973). At the same time, these very abilities may blind experts from perceiving what is *actually there*, especially when new and unexpected features emerge. That is to say that retaining the ability to *take a fresh look* not only at theory and data in general, but at visualizations and visual displays in particular, is key for making discoveries which deal—by definition—with the new and the unexpected (cf. von Wright 1992).

However, avoiding these potential pitfalls is not always possible. The late discovery of the first so-called giant virus in 2003 (Scola et al. 2003) might be one such case where top-down perception and expertise as described above, hindered researchers from making a discovery for a long time. Viruses were thought to be much smaller than bacteria by definition. For example, bacteria like *E. coli* usually measure 2000–6000 nanometers in length, whereas viruses like the HI-virus measure 100–120 nanometers in diameter. That is why viruses are usually not visible using a light microscope but require electron microscopy for detection. However, there are a large variety of viruses that are big enough to be seen in a conventional microscope and measure up to 400 nanometers in diameter but they were ignored, filtered out of the samples prior to examination (van Etten et al. 2010), or mistaken for bacteria (Abergel et al. 2015). However, *once* scientists realized that they were looking at something new, they started seeing a whole lot of so-called giant viruses. By now, over a hundred giant viruses have been discovered, which reveal fascinating and unexpected characteristics (Brandes and Linial 2019).

While we are not mistaking sperm cells for little humans anymore, as did many of Antonie van Leeuwenhoek's peers in the late seventeenth century, we can still expect to succumb to the same human errors. It is therefore exciting to see the advances of machine learning and perhaps the next generation of algorithms will be able to see microscopy images with an unbiased eye.

Acknowledgments Ida Sundvor Opstad's contribution was supported by UiT The Arctic University of Norway "Tematiske satsinger" program (VirtualStain; project number 2061348).

References

Abergel C, Legendre M, Claverie JM (2015) The rapidly expanding universe of giant viruses: Mimivirus, Pandoravirus, Pithovirus and Mollivirus. FEMS Microbiol Rev 39(6):779–796

Almeida A, Kaliki S, Shields CL (2013) Autofluorescence of intraocular tumours. Curr Opin Ophthalmol 24(3): 333–332

Alvarado DAA, Picón MAQ, Taborda-Murillo A, Ortiz-Arango N, Ospina SO, Arias LF (2021) Microscopía electrónica en biopsias renales: una evaluación de su utilidad en el siglo XXI (The relevance of electron microscopy in kidney biopsies to 21st century pathology). Rev Esp Patol 54(4):234–241

Anim JT, John B, Abdulsathar SS, Prasad A, Saji T, Akhtar N, Ali V, Al-Saleh M (2005) Relationship between the expression of various markers and prognostic factors in breast cancer. Acta Histochem 107(2): 87–93

Arganda-Carreras I, Kaynig V, Rueden C, Eliceiri KW, Schindelin J, Cardona A, Seung SH (2017) Trainable Weka segmentation: a machine learning tool for microscopy pixel classification. Bioinformatics 33(15):2424–2426

ASGE Technology Committee (2014) Confocal laser endomicroscopy. Gastrointest Endosc 80(6):928–938

Balcetis E, Dunning D (2006) See what you want to see: motivational influences on visual perception. J Pers Soc Psychol 91(4):612–625

Beck AH, Sangoi AR, Leung S, Marinelli RJ, Nielsen TO, van de Vijver MJ, West RB, van de Rijn M, Koller D (2011) Systematic analysis of breast cancer morphology uncovers stromal features associated with survival. Sci Transl Med 3(108):108ra113

Brandes N, Linial M (2019) Giant viruses-big surprises. Viruses 11(5):404

Casetta E (2020) Preformation vs. epigenesis: inspiration and haunting within and outside contemporary philosophy of biology. Riv Estet 74(74):119–138

Chapman JA, Lee LMJ, Swailes NT (2020) From scope to screen: the evolution of histology education. In: Rea PM (ed) Biomedical visualisation, advances in experimental medicine and biology, vol 1320. Springer, Cham, pp 75–107

Chase WG, Simon HA (1973) Perception in chess. Cogn Psychol 4(1):55–81

Ciocca DR, Elledge R (2000) Molecular markers for predicting response to tamoxifen in breast cancer patients. Endocrine 13(1):1–10

Croft WJ (2006) Under the microscope: a brief history of microscopy (chapter 2), vol 5. World Scientific

Demarchi MS, Karenovics W, Bédat B, Vito CD, Triponez F (2021) Autofluorescence pattern of parathyroid adenomas. BJS Open 5(1):zraa047

Deo RC (2015) Machine learning in medicine. Circulation 132(20):1920–1930

Dlamini Z, Francies FZ, Hull R, Marima R (2020) Artificial intelligence (AI) and big data in cancer and precision oncology. Comput Struct Biotechnol J 18:2300–2311

Dror IE (2011) The paradox of human expertise: why experts get it wrong. In: Kapur N (ed) The paradoxical brain. Cambridge University Press, Cambridge, pp 177–188

Dunning D, Balcetis E (2013) Wishful seeing: how preferences shape visual perception. Curr Dir Psychol Sci 22(1):33–37

Dunsby C (2008) Optically sectioned imaging by oblique plane microscopy. Opt Express 16(25):20306–20316

van Etten JL, Lane LC, Dunigan DD (2010) DNA viruses: the really big ones (giruses). Annu Rev Microbiol 64: 83–99

Evans AJ, Bauer TW, Bui MM, Cornish TC, Duncan H, Glassy EF, Hipp J, McGee RS, Murphy D, Myers C, O'Neill DG, Parwani AV, Rampy BA, Salama ME, Pantanowitz L (2018) US Food and Drug Administration approval of whole slide imaging for primary diagnosis: a key milestone is reached and new questions are raised. Arch Pathol Lab Med 142(11):1383–1387

Falk GW (2009) Autofluorescence endoscopy. Gastrointest Endosc Clin N Am 19(2):209–220

Goecks J, Jalili V, Heiser LM, Gray JW (2020) How machine learning will transform biomedicine. Cell 181(1):92–101

Higgins RA, Blankenship JE, Kinney MC (2008) Application of immunohistochemistry in the diagnosis of non-Hodgkin and Hodgkin lymphoma. Arch Pathol Lab Med 132(3):441–461

Hohwy J (2017) Priors in perception: top-down modulation, Bayesian perceptual learning rate, and prediction error minimization. Conscious Cogn 47:75–85

Horne N, Siemers P (2023) Re: viewing observation. The philosophy of medical imaging. In: Shapiro L, Rea PM (eds) Biomedical visualisation. Advances in experimental medicine and biology, vol 1392. Springer, Cham, pp 3–16

Ibrahim A, Gamble P, Jaroensri R, Abdelsamea MM, Mermel CH, Chen PHC, Rakha EA (2020) Artificial intelligence in digital breast pathology: techniques and applications. Breast 49:267–273

Jambor H, Antonietti A, Alicea B, Audisio TL, Auer S, Bhardwaj V, Burgess SJ, Ferling I, Gazda MA, Hoeppner LH, Ilangovan V, Lo H, Olson M, Mohamed SY, Sarabipour S, Varma A, Walavalkar K, Wissink EM, Weissgerber TL (2021) Creating clear and informative image-based figures for scientific publications. PLoS Biol 19(3):e3001161

Kubitscheck U (ed) (2017) Fluorescence microscopy: from principles to biological applications. Wiley-Blackwell, Hoboken

Laissue PP, Alghamdi RA, Tomancak P, Reynaud EG, Shroff H (2017) Assessing phototoxicity in live fluorescence imaging. Nat Methods 14(7):657661

Leong AS, Wright J (1987) The contribution of immunohistochemical staining in tumour diagnosis. Histopathology 11(12):1295–1305

Leong ASY, Cooper K, Leong FJWM (2003) Manual of diagnostic antibodies for immunohistology. Greenwich Medical Media Ltd, London

Levin JR, Anglin GJ, Carney RN (1987) On empirically validating functions of pictures in prose. In: Willows DM, Houghton HA (eds) The psychology of illustration, vol 1. Springer, New York, pp 51–86

Liu Y, Kohlberger T, Norouzi M, Dahl GE, Smith JL, Mohtashamian A, Olson N, Peng LH, Hipp JD, Stumpe MC (2019) Artificial intelligence-based breast cancer nodal metastasis detection: insights into the black box for pathologists. Arch Pathol Lab Med 143(7):859–868

Lüllmann-Rauch R, Asan E (2019) Taschenlehrbuch Histologie, 6th edn. Thieme, Stuttgart

Mansfield JR (2013) Multispectral imaging: a review of its technical aspects and applications in anatomic pathology. Vet Pathol 51(1):185–210

Mansy SS, AbouSamra MM (2022) Electron microscopy overview of SARS-COV2 and its clinical impact. Ultrastruct Pathol 46(1):1–17

Martin M (2012) C-path: updating the art of pathology. J Natl Cancer Inst 104(16):1202–1204

Mayer RE (2002) Multimedia learning. Psychol. Learn Motiv 41:85–139

Mayer RE (ed) (2014) The Cambridge handbook of multimedia learning, 2nd edn. Cambridge University Press, New York

Möckl L, Lamb DC, Bräuchle C (2014) Super-resolved fluorescence microscopy: Nobel prize in chemistry 2014 for Eric Betzig, Stefan hell, and William E. Moerner Angew Chem Int Ed 53(51):13972–13977

Morgan ML, Kaushik DK, Stys PK, Caprariello AV (2020) Autofluorescence spectroscopy as a proxy for chronic white matter pathology. Mult Scler 27(7): 1046–1056

Mukhopadhyay S, Feldman MD, Abels E, Ashfaq R, Beltaifa S, Cacciabeve NG, Cathro HP, Cheng L, Cooper K, Dickey GE, Gill RM, Heaton RPJ, Kerstens R, Lindberg GM, Malhotra RK, Mandell JW, Manlucu ED, Mills AM, Mills SE, Moskaluk CA, Nelis M, Patil DT, Przybycin CG, Reynolds JP, Rubin BP, Saboorian MH, Salicru M, Samols MA, Sturgis CD, Turner KO, Wick MR, Yoon JY, Zhao P, Taylor CR (2018) Whole slide imaging versus microscopy for primary diagnosis in surgical pathology: a multicenter blinded randomized noninferiority study of 1992 cases. Am J Surg Pathol 42(1):39–52

Nandakumar N, Buzney S, Weiter JJ (2012) Lipofuscin and the principles of fundus autofluorescence: a review. Semin Ophthalmol 27(5–6):197–201

Niazi MKK, Tavolara TE, Arole V, Lee C, Parwani A, Gurcan MN (2018) (MP58–06) Automated staging of T1 bladder cancer using digital pathologic H&E images: A deep learning approach. Poster presented at the American Urological Association’s 2018 Annual Meeting, Moscone Center, San Francisco, 18–21 May 2018

Opstad IS (2021). Bringing optical nanoscopy to life-Super-resolution microscopy of living cells. Dissertation, The Arctic University of Norway

Opstad IS, Godtliebsen G, Ahluwalia BS, Myrmel T, Agarwal K, Birgisdottir ÅB (2022a) Mitochondrial dynamics and quantification of mitochondria-derived vesicles in cardiomyoblasts using structured illumination microscopy. J Biophotonics 15(2):e202100305

Opstad IS, Godtliebsen G, Ströhl F, Myrmel T, Ahluwalia BS, Agarwal K, Birgisdottir B (2022b) Three-dimensional structured illumination microscopy data of mitochondria and lysosomes in cardiomyoblasts under normal and galactose-adapted conditions. Sci Data 9:98

Opstad IS, Wolfson DL, Øie CI, Ahluwalia BS (2018) Multi-color imaging of sub-mitochondrial structures in living cells using structured illumination microscopy. Nano 7(5):935–947

Renkl A, Scheiter K (2017) Studying visual displays: how to instructionally support learning. Educ Psychol Rev 29(3):599–621

Ricciardi CA, Gnudi L (2021) Kidney disease in diabetes: from mechanisms to clinical presentation and treatment strategies. Metabolism 124:154890

Robinson AL (1986) Electron microscope inventors share Nobel physics prize: Ernst Ruska built the first electron microscope in 1931; Gerd Binnig and Heinrich Rohrer developed the scanning tunneling microscope 50 years later. Science 234(4778):821–822

Saffarian S (2021) Application of advanced light microscopy to the study of HIV and its interactions with the host. Viruses 13(2):223

Sapoznik E, Chang BJ, Huh J, Ju RJ, Azarova EV, Pohlkamp T, Welf ES, Broadbent D, Carisey AF, Stehbens SJ, Lee K-M, Marín A, Hanker AB, Schmidt JC, Arteaga CL, Yang B, Kobayashi Y, Tata PR, Kruithoff R, Doubrovinski K, Shepherd DP, Millett-Sikking A, York AG, Dean KM, Fiolka RP (2020) A versatile oblique plane microscope for large-scale and high-resolution imaging of subcellular dynamics. elife 9:e57681

Schermelleh L, Ferrand A, Huser T, Eggeling C, Sauer M, Biehlmaier O, Drummen GPC (2019) Super-resolution microscopy demystified. Nat Cell Biol 21(1):72–84

Schindelin J, Arganda-Carreras I, Frise E, Kaynig V, Longair M, Pietzsch T, Preibisch S, Rueden C, Saalfeld S, Schmid B, Tinevez J-Y, White DJ, Hartenstein V, Eliceiri K, Tomancak P, Cardona A (2012) Fiji: an open-source platform for biological-image analysis. Nat Methods 9(7):676–682

Schönborn KJ, Anderson TR (2010) Bridging the educational research-teaching practice gap: foundations for assessing and developing biochemistry students' visual literacy. Biochem Mol Biol Educ 38(5):347–354

Scola BL, Audic S, Robert C, Jungang L, de Lamballerie X, Drancourt M, Birtles R, Claverie J-M, Raoult D (2003) A giant virus in amoebae. Science 299(5615):2033

Ströhl F, Hansen DH, Grifo MN, Birgisdottir B (2022) Multifocus microscopy with optical sectioning and high axial resolution. Optica 9(11):1210–1218

Wiederschain GY (2011) The molecular probes handbook. A guide to fluorescent probes and labeling technologies, 11th edn. Life Technologies, Carlsbad

World Health Organization (2005) Fluorescence microscopy for disease diagnosis and environmental monitoring. WHO Regional Publications, Cairo

von Wright JV (1992) Reflections on reflection. Learn Instr 2(1):59–68

Wunderlich L, Ströhl F, Ströhl S, Vanderpoorten O, Mascheroni L, Kaminski CF (2021) Superresolving the kidney: a practical comparison of fluorescence nanoscopy of the glomerular filtration barrier. Anal Bioanal Chem 413(4):1203–1214

Xiong Y-Q, Ma S-J, Hu H-Y, Ge J, Zhou L-Z, Huo S-T, Qiu M, Chen Q (2017) Comparison of narrow-band imaging and confocal laser endomicroscopy for the detection of neoplasia in Barrett's esophagus: a meta-analysis. Clin Res Hepatol Gastroenterol 42(1):31–39

Zhang L, Lu Q, Chang C (2020) Epigenetics in health and disease. In: Chang C, Lu Q (eds) Epigenetics in allergy and autoimmunity, vol 1253. Springer, Singapore, pp 3–55

2

Morphometric Image Analysis and its Applications in Biomedicine Using Different Microscopy Modes

Vesselina Merhar and Thajasvarie Naicker

Abstract

In biomedicine, morphometric image analysis is defined as the merging of geometry and histology. Morphometry refers to a quantitative analysis of the size and shape of geometric features of cells, cell organelles, and/or biomarkers. Modern morphometry utilizes advanced computer-assisted image analysis software to interface an image with geometric software that objectively measures specific histological characteristics. It may be accomplished on the whole image, or on a particular area of interest after image selection (segmentation).

Morphometric image analysis is widely used in biomedical studies and pathology. Its applications include differentiating between benign and malignant tissues based on the nuclear morphology of the cells, as well as quantitation of immunohistochemical or immunofluorescent assays for the expression of specific biomarkers in normal and/or pathological conditions. Accurate calibration of the microscope using standards and controls is crucial for precise and reproducible quantitation. Morphometric image analysis may be performed on plastic or paraffin-embedded and specifically stained tissue sections by use of conventional light, e.g., fluorescence microscopy or on thick specimens by means of confocal laser scanning microscopy, as well as at a subcellular level using transmission electron microscopy.

This review chapter defines, illustrates, and encapsulates the importance of morphometric image analysis in biomedical research using different microscopy modes. It also covers the methodology and problems related to quantitation using immunohistochemical, immunofluorescent, and immunoelectron images.

Keywords

Morphometry · Image analysis · Microscopy · Immunohistochemistry · Immunofluorescence

2.1 Background

Morphometry in biomedicine refers to the quantitative analysis of form, which is a perception that includes both the size (i.e., area or length and breadth) and the shape of an organism, organ, or cell organelle. Specific measurements may be

V. Merhar (✉)
Department of Biology, Medical Genetics and Microbiology, Faculty of Medicine, University Prof. Dr. Assen Zlatarov, Burgas, Bulgaria
e-mail: vmerhar@uniburgas.bg

T. Naicker
Optics and Imaging Centre, Doris Duke Medical Research Institute, College of Health Sciences, University of KwaZulu-Natal, Durban, South Africa
e-mail: naickera@ukzn.ac.za

© The Author(s), under exclusive license to Springer Nature Switzerland AG 2023

L. Shapiro (ed.), *Microscopy Techniques for Biomedical Education and Healthcare Practice*, Biomedical Visualization 2, https://doi.org/10.1007/978-3-031-36850-9_2

carried out on living organisms, cadavers, fossils, etc.

Morphometric analyses are primarily related to an approach called “traditional morphometrics,” which is characterized by measurement of the length and width of structures and distances between specific landmarks, as well as the changes in shape as a function of size (i.e., allometry) (Rohlf and Marcus 1993). Morphometric analysis is useful when either absolute or relative sizes are of particular interest, such as in studies of growth. Traditional morphometry is also useful when measurements of the size of the objects are of theoretical importance such as body mass and limb length in studies of functional morphology. However, these measurements have one important limitation: they contain little information about the spatial distribution of shape changes across the organism. This is because it is difficult to recover the shape of the original from the data of distance measurements.

In the last decade, a new approach in morphometric analyses, so-called “geometric morphometry,” or “landmark-based geometric morphometry” was explored (Dujardin 2011). This shift from traditional morphometrics to more complex geometric functions was facilitated by the development of image capturing and processing tools. The geometry of the structure being studied is captured in the form of two-dimensional (2D) or three-dimensional (3D) coordinates of morphological landmark points. The distances between the landmarks are then calculated from these coordinates. Geometric morphometry has become very effective in quantifying biological shape and shape variations among different species. It is now widely used by biologists, paleontologists, and anthropologists conducting studies of comparative morphology (Webster and Sheets 2010). It is also utilized in developmental biology studies since it enables the quantitative comparison of developmental routes across individuals, populations, and/or environments (Hallgrimsson et al. 2015; Mitteröcker 2021). A very important consideration is the record of homologous landmarks since this allows for a better comparison and more comprehensive biological interpretation of the results. If one is interested in the overall outline or surface of a structure (or only parts of a structure between landmarks in 2D or a surface in 3D), then “outline methods” (Rohlf and Marcus 1993) and other techniques exploring textures and surface patterning (Lestrel 2000) can be included.

There are now several alternative approaches that can analyze shape variation in a sample of organisms or compare shape differences among two or more samples. Among them, the superimposition methods (also called Procrustes methods) are very popular (Rohlf and Marcus 1993; Mitteroecker and Gunz 2009; Hallgrimsson et al. 2015). They are based on overlaying the images of two or more specimens, so that their homologous landmarks match as closely as possible. This preserves the geometry of the specimens and facilitates the geometric morphometric methods. Capturing the shape variation by measuring the Procrustes distances is considered to be the most reliable method to describe variations and relations among species and populations of insects (Dujardin 2011; Sendaydiego et al. 2013; Araña 2015). It is also utilized in the developmental studies, e.g., craniofacial development (Hallgrimsson et al. 2015).

2.2 Microscopic Imaging, Morphometry, and Quantification of the Results

The recent advance in computer-assisted image analysis systems has revolutionized morphometric evaluation. The microscopic image is recorded by a video camera and displayed on a computer screen, which makes it possible to trace the outlines of different features on the screen and then compute their areas and shapes using dedicated software. For morphometric assessment, the size (area, length, volume, layer thickness) and shape (roundness, aspect ratio) of the image features are measured. The quantitative data are obtained numerically in the form of tables, graphically or as histograms, which are then read by experts in the field (e.g., pathologists, anatomists, paleontologists, and anthropologists), who link them to the corresponding study, or in case of clinical observations, help with the diagnosis. Accurate calibration of the instrument and the use of standards and controls is essential for precise and reproducible quantitation.

Morphometric image analysis may be performed on plastic or paraffin-embedded and specifically stained tissue sections by use of conventional light, e.g., fluorescence microscopy, epoxy resin embedded ultrathin sections using transmission electron microscopy as well as on thick specimens by means of confocal laser scanning microscopy (Franchi et al. 2004; Chvátal et al. 2007; Abdalla et al. 2009; Curry et al. 2013; Varaden et al. 2019; Edgar et al. 2020; Merhar et al. 2022). In pathology, smears obtained by fine needle aspiration cytology (FNAC) techniques and subsequent Hematoxylin and Eosin (H&E) or Papanicolaou staining is routinely used in the nuclear morphometry and diagnosis of breast lumps (Kashyap et al. 2018; Pandian et al. 2021). The FNAC method is an accurate diagnostic test used in the initial evaluation of nodular thyroid disease (Jasim et al. 2015), prostate cancer (Buhmeida 2006), liver cancer (Wen et al. 2009), etc.

Despite the variety of software platforms, the steps to follow up are always the same: image acquisition; image capturing; image processing, and image analysis (Fig. 2.1).

Morphometric measurements can be performed on the whole image, or a specific region of interest (ROIs) after image segmentation. The objective of image segmentation is to partition an image into non-overlapping, constituent regions that are homogeneous with respect to intensity and texture (Gonzalez and Woods 2002). When applied to a stack of images, typical in medical imaging, the resulting contours post-segmentation enable 3D reconstructions of different organs, e.g., bone and brain cartilage (Balafar et al. 2010; Ambellan et al. 2019). Determining ROIs in the brain and applying morphometric analysis to them, helped to confirm that schizophrenia is an anatomical disorder of the brain, involving many discrete yet widely spread regions within the cortical gray matter (Levitt et al. 2010).

Image segmentation plays an essential role in the field of Magnetic Resonance Imaging (MRI) and Computed Tomography (CT) scans (Balafar et al. 2010). While MRI utilizes radio waves and magnets to form images, CT scan uses X-rays and together with computer-aided visualization creates 3D reconstructions of individual anatomical structures. Both techniques are essential in the diagnosis and choice selection of treatment modalities. In a recent work, Saood and Hatem (2021) proposed two computer-based segmentation techniques (SegNet and U-NET) for identifying and quantifying the infected lung regions on CT scan images from COVID-19 patients. The same segmentation techniques have been used by Daimary et al. (2020) to segment brain tumors from MRI images. These and other segmentation techniques are beneficial in medical imaging, because they not only assist in disease diagnosis but also help to estimate the severity of the illness.

The simplest and most widely used method for image segmentation is thresholding. It is useful in separating the “object” or foreground pixels from the background pixels to aid in image processing. By selecting an adequate threshold value, the grayscale or full-color image can be converted to a binary (black and white) image that contains all of the essential information about the position and shape of the objects of interest (foreground). The advantage of obtaining a binary image is that it reduces the complexity of the data and simplifies the process of recognition and classification of the object of interest (Al-amri et al. 2010).

Nonetheless, the imaging technique used for morphometric analysis requires the optimal contrast and detail of the image. Many such techniques exist for generating data for morphometric analysis in biology and medicine, including a variety of MRI morphometry techniques (Chang and Shukla 2018). A full review of these is beyond the scope of the present chapter. Instead, we will briefly describe two microscopic imaging techniques that are most widely used in biomedical research and highlight their

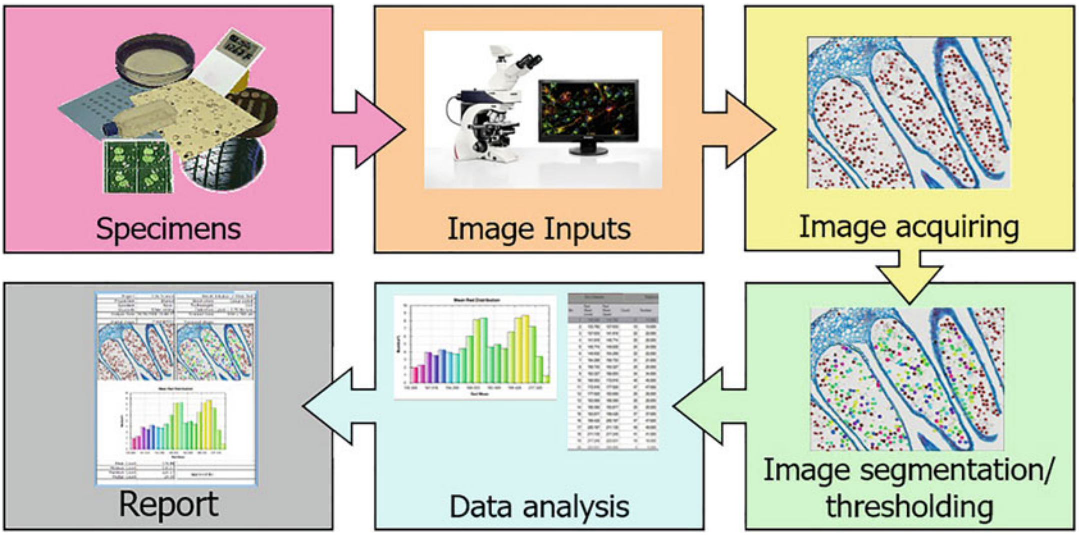

Fig. 2.1 Schematic view of the microscopic imaging and data analyzing process

advantages and limitations for morphometric analysis of tissues, cells, cell organelles, or biomarkers.

2.2.1 3D Confocal Cell Morphometry

Three-dimensional confocal cell morphometry combines the high image resolution offered by the confocal laser scanning microscopy (CLSM) with analysis of the time course of morphological changes of tissues and cells in situ and in vivo (Chvátal et al. 2007; Lauwers et al. 2008; Jonuscheit et al. 2011). Confocal laser scanning microscopy is a technique for obtaining high-resolution optical images with different depths. The key feature of CLSM is its ability to acquire in-focus images from selected depths, a process known as optical sectioning. Images are acquired point-by-point and reconstructed with a computer, allowing 3D reconstructions of topologically complex objects. This allows imaging of the interior structures of the specimen with a greatly enhanced quality over that of the conventional light microscope because image information from multiple depths in the specimen is not superimposed.

Aside from the advantage of recording and analyzing fine cell morphology, there are some limitations of confocal morphometry. Photobleaching is one of the main sources of artifacts when performing measurements, especially those of volumes and is considered the main limitation for morphometric analysis. It is due to damage of fluorochromes by high-power lasers used in CLSM, which results in a decrease in fluorescence. Photobleaching can be reduced to a minimum by choosing the lowest possible excitation light intensity, while still maintaining a reasonable signal-to-noise ratio in the acquired images. Another option is to minimize the signal loss by reducing the number of images in a stack and increasing the interlayer distance (Chvátal et al. 2007). The use of longer-lasting commercial fluorochromes is also an alternative.

Morphometry in vivo by real-time confocal microscopy is a very useful approach for quantifying changes in cell morphology over a certain period of time. Time-lapse microscopy is a powerful and constantly developing tool for real-time imaging of living cells. Versatility of this technique, its applications in modern biology and medicine, and its technical approaches are discussed in a recent review article by Collins et al. (2019). Disadvantages of time-lapse microscopy for morphometric analysis are its relatively low resolution, the complex data collection, and the possible phototoxic effect of the fluorescent dyes on the living cells. The long exposures to the lasers can lead to photobleaching of fluorescent probes, cell stress, and cell death. These effects can have a large impact on the data and lead to misinterpretation of the results. Furthermore, the calculations of the morphometric parameters are based on intracellular fluorescence, which sometimes overwhelms the image and fine cell changes cannot be visualized and quantified. Long term three-dimentional time-lapse imaging should be performed cautiously due to integrated light exposure. Fast Z-series acquisition is important in order to minimize motion artifacts due to cell movement and dynamics that occur during the acquisition period (Burke and Orth 2016).

Nevertheless, there are some exciting studies on the morphometric analysis by means of time-lapse microscopy. Araújo and Llimargas (2023) have demonstrated their results from tracheal development of *Drosophila*. Using time-lapse imaging (among others), the authors visualize larval tracheal terminal cell branching and lumen formation and perform a morphometric analysis on the tracheal cells. There are also increasing numbers of investigations using time-lapse microscopy which ask fundamental questions in cell biology ranging from cell motility and division, organelle dynamics, membrane trafficking, responses of cells to anticancer drugs or natural products, etc. (Burke and Orth 2016).

In vivo confocal microscopy is often used in clinical observations for the observation of living tissues. In ophthalmology, in vivo confocal microscopy (IVCM) is a noninvasive method of examining the living human cornea. It allows the obtaining of high-quality and magnification corneal images and presents new opportunities in anterior eye research (Bhattacharya et al. 2022).

Reflectance confocal microscopy (RCM) is another noninvasive in vivo imaging tool with a particular application in dermatology. It utilizes an 830-nm laser that penetrates the skin epidermis and gives a horizontal view of its structure until the superficial dermis. Microscopic tissue elements (especially melanin and keratin) reflect the light with different refractive indices resulting in white structures on a black background (Filoni and Alaibac 2019). Due to its accuracy in differentiating between benign and malignant skin neoplasms, RCM is used to diagnose and monitor several types of skin tumors. Nonetheless, care must be taken to avoid possible artifacts that may obscure the image and affect the interpretation of the results (Gill et al. 2019).

2.2.2 Electron Microscopy Morphometry

Electron microscopy (EM) reveals the fine-ultrastructure examination of cells and tissues. Unfortunately, using cell morphometry in these preparations may produce deviations from the real native shape and cell dimensions, because the tissue and its individual cellular elements are subjected to shrinkage caused by fixation and embedding in the course of the specimen preparation procedure. Nevertheless, there are some exciting studies on Transmission Electron Microscopy (TEM) and morphometry on brain and heart muscle sections, briefly described below.

With the aid of TEM images, Grosche et al. (2002) were able to reconstruct the 3D structure of Bergmann glial cell processes of the cerebellum. Furthermore, using morphometric analysis of glial cell processes, they detected basic construction principles involving the complex glial–neuronal relationships within the cerebellum; information that had been hidden in a previous 2D image view. Nonetheless, this is a labor-intensive process intertwined with complex measurements.

Transmission electron microscopy of white matter of the central nervous system has provided vital information on the ultrastructural features of axons, their myelin sheaths (Fig. 2.2), and the major cells of white matter; namely, oligodendrocytes, astrocytes, and microglia.

Fixation can have adverse effects on the morphometric parameters of the brain cells. Hence, the most detailed morphometric analyses of the white matter can be performed on well-preserved samples from animal models, perfusion fixed at the time of death. In a recent work, Edgar et al. (2020) describe methods for routine

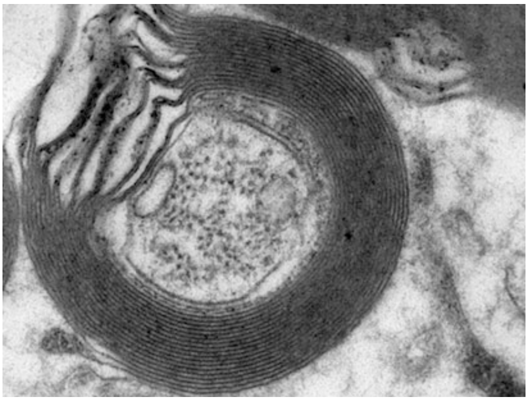

Fig. 2.2 Transmission electron micrograph showing myelin pathology—it facilitates easy measurement of myelin pathology (With permission from Naicker, 2023)

ultrastructural examination and morphometry of white matter samples using TEM of perfusion fixed tissue, with particular emphasis on axon and myelin pathology.

In earlier studies, Curry et al. (2013) investigated the morphological, morphometric, and ultrastructural characteristics of cardiomyocytes with a particular focus on mitochondria and in relation to aging. The experiments were performed on old (18 months of age) rats, which were euthanized using an overdose of anesthesia with transcardial perfusion. Samples were collected for light microscopy, transmission electron microscopy, and high-resolution scanning electron microscopy. Various morphometric measurements were performed, amongst them on an average sarcomere length of cardiomyocytes, wall thickness, mitochondrial shape, volume density, average area, average length, and an average mitochondrial cristae thickness. These data are important for researchers who focus on the changes in cardiac tissue, especially in relation to aging.

Transmission Electron Microscopy Morphometry is particularly valuable in the study of bacilli and viral ultrastructure. Applying a high magnification TEM, Joubert (2010) performed detailed calculations of the cell membrane and cell wall thickness of a bacilli-*Clamydia* (Fig. 2.3).

More recently a revolutionary approach was introduced, called ACSON (AutomatiC 3D Segmentation and morphometry Of axoNs) that enables full 3D analysis of the white matter ultrastructure (Abdollahzadeh et al. 2019). It utilized the advanced EM technique called serial block-face scanning electron microscopy (SBEM) (Denk and Horstmann 2004). SBEM combines scanning electron microscopy (SEM) with back-scattered electron detection and low beam energies. Images are acquired from the block-face of a sample each time an ultra-microtome inside the vacuum chamber removes the top section from a block-face to expose a new surface for imaging. The result is a stack of high-resolution and high-contrast 3D images of tissue. Applying the ACSON pipeline to the 3D images acquired by SBEM enabled Abdollahzadeh and co-workers to segment the white matter into myelin, intra-axonal space of myelinated and unmyelinated axons, cell bodies and their processes, and subcellular compartments, such as mitochondria and vacuoles. Their results showed that cross-sections of myelinated axons were elliptic rather than circular, and their diameter varies substantially along their longitudinal axis.

Another approach for ultrastructural quantification is immunoelectron microscopy. It is a simple reliable means of subcellular localization of antigens on thin sections (50 nm) of aldehyde fixed, plastic embedded biological material. It provides highly specific and sensitive labeling with negligible background since the gold-conjugated complex has little non-specific interaction with embedding matrices and cellular components. Additionally, the gold particles are easily detectable on thin sections because of their high electron density, and because their small size (10 nm) allowed for clear identification of the underlying cellular structure.

Immunoelectron microscopy provides important information on the in situ localization of the intracellular/extracellular antigens. The technique is vital for identifying antigens at a subcellular ultrastructural level by labeling them with specific immunogold antibodies either by pre- or post-embedding techniques (Fig. 2.4) (Naicker 2002).

Immunogold labeling enables the simultaneous detection and visualization of more than one antigen, by using antibodies conjugated to

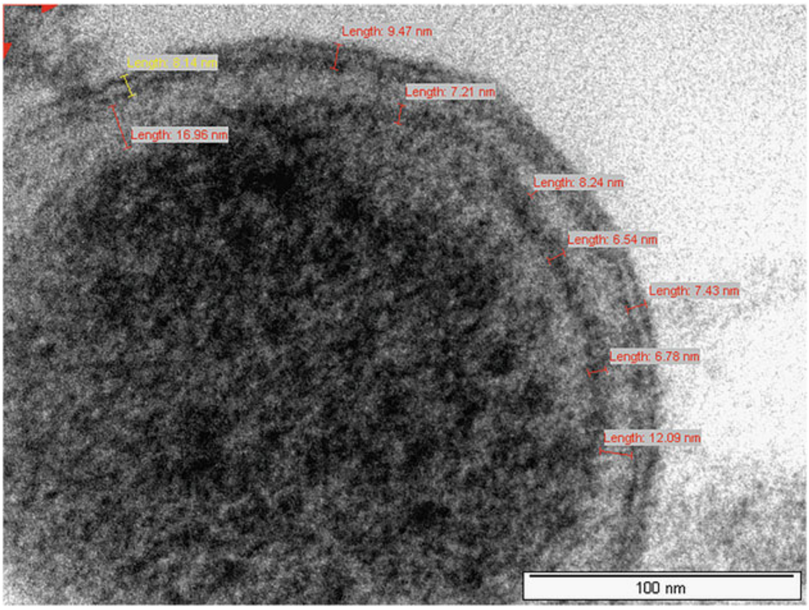

Fig. 2.3 Transmission electron micrograph at high magnification indicating calculation of membrane and wall thickness of a bacilli-*Clamydia* (with permission from Joubert 2010)

immunogold particles with different sizes, which are then quantified morphometrically (Naicker et al. 2013). It is also valuable in the study of viruses to show structural localization and organization of antigens within the virion (Gulati et al. 2019).

Application of immunoelectron microscopy requires several crucial conditions, including preservation of protein antigenicity, ability of antibodies to penetrate throughout the cell, and specificity of antigen–primary antibody recognition. Additionally, correct biological sample preparation is necessary, which includes fixation, selecting the right embedding resin, and having quick access to antibodies specific to the molecules whose ultrastructural position has to be established (De Paul et al. 2012). The combination of glutaraldehyde (1%) and paraformaldehyde (4%) may be used to ensure stability of cellular structures in order to obtain adequate immunoelectron localization of the antigen, preventing artifactual diffusion and replacement of antigenic material or its extraction, and effectively preserving cellular fine structure. Also, pre- or post-embedding labeling is a crucial decision and is dependent on the location of the cell antigens that need to be immunostained. Due to the issue of antigen accessibility on resin sections, several researchers strongly support cryo-ultramicrotomy, unless the antigen is plentiful or accessible on the section's surface (Griffiths and Sloth 1992).

2.3 Applications of Morphometrical Analysis in Biomedicine

Morphometric image analysis is widely used in biomedical studies and pathology. Some of its applications are locating tumors and other pathologies (Papaxoinis et al. 2009; Mudaliar and Hutchens 2013; Bostwick and Cheng 2020). Notably, its other value lies in measuring tissue volume (Levitt et al. 2010; Maduray et al. 2016), help with diagnosis, study of anatomical structure (Hallgrimsson et al. 2015; Edgar et al. (2020), surgery planning, virtual surgery simulation, intra-surgery navigation, etc. It is widely used in oncology for diagnosis of malignant tumors (Laishram 2017; Pandian et al. 2021). Its applications include differentiating between benign and malignant tissues, as well as quantitation of immunohistochemical or immunofluorescent assays for the expression of specific biomarkers in pathological conditions and to

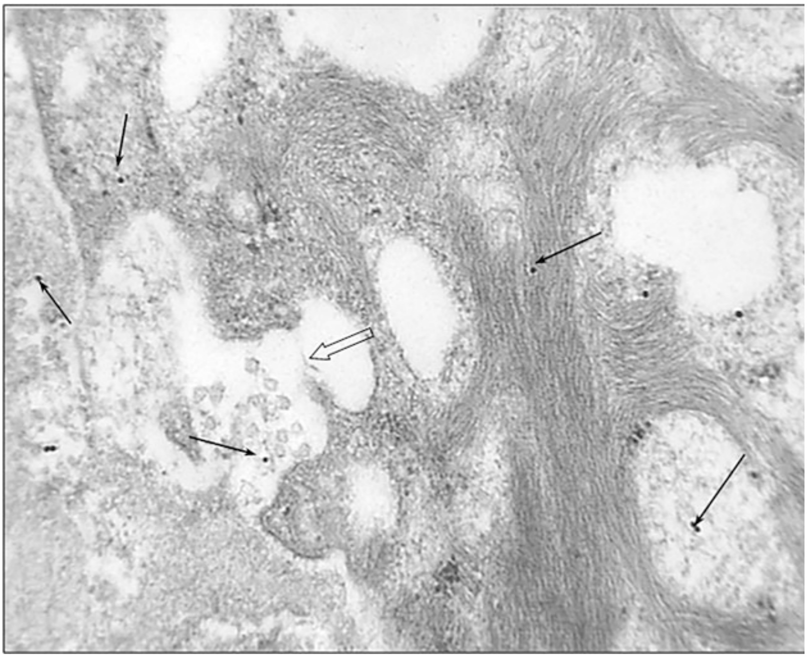

Fig. 2.4 Immunoreactive TGF-®$_1$ gold particles (arrow) occurring on the filamentous as well as fibrillar material of the cisternal pool of ER. Note the extrusion of proteinaceous material into the fibrinoid wall of the artery (open arrow). Mag X 48000 (With permission from Naicker, 2023)

compare them with the norm (Onyangunga et al. 2016; Merhar et al. 2022). Also, using dual immunohistochemical staining protocols interfaced with morphometric image analysis, Naicker et al. (2013) were able to demonstrate apoptosis of trophoblast cells in the uterine wall of pre-eclamptic women.

In 2016, Maduray et al. evaluated the functional efficiency of the placentae from pre-eclamptic deliveries using volume, diameter, and thickness measurements. Volume, length, thickness, and surface area of placental images were measured and were found to be lower in pre-eclampsia compared to normotensive pregnancies. These findings were then fed into a mathematical model and these researchers were able to show a reduction in placental functional efficiency in the hypertensive disorder of pre-eclampsia.

The application of morphometric analysis in biology and medicine is vast. In this chapter, we focus on the involvement of morphometry in tumor and brain studies, as well as in immunohistochemistry.

2.3.1 Morphometric Image Analysis in Tumor Researches and Diagnostics

Morphometric image analysis in pathology includes item classification and grading, point counting and intersection counting methods, and the use of various semi-automatic or automatic instruments (Young et al. 2011). It can be used as a statistical and diagnostic approach. In statistical morphometry, morphometrical parameters are collected from several disease cases and serve as a basis for disease classification and prognosis. Diagnostic morphometry, on the other hand, studies the sample of one individual and gives relevant data for diagnostic decisions. A huge advantage of morphometry is that it can detect structural and morphological aberrations in samples prepared by other methods and bring an element of accuracy to support the diagnostic decision.

Perhaps the most important application of morphometric image analysis in pathology is differentiating between benign and malignant tissues based on the nuclear morphology of the cells. Heiberg and Kemp in 1929 were the first to report an increase in the size of the nuclei of a tumor compared to normal cells (Buhmeida 2006). In the following decades, an increased interest in cancer research gave a strong impetus to morphological analysis in biomedicine and the application of morphometric analysis became increasingly popular and widely applied.

Now, nuclear morphometry is an efficient and successful tool in distinguishing benign and malignant lesions. The most popular morphometric markers representing the histopathological features are: nuclear size, nuclear shape, nuclear roundness, nuclear texture and density, size and number of nucleoli, and number of apoptotic bodies. The pleomorphism (variability in the size, shape, and staining of cells and/or their nuclei) appears to be the most reliable histopathological feature to distinguish benign tumors from malignant ones because it is resistant to methodological variation and can be easily compared to other image analysis studies (Mudaliar and Hutchens 2013). Cellular and nuclear pleomorphism is one of the earliest hallmarks of cancer progression and a feature characteristic of malignant neoplasms (Kashyap et al. 2018).

Studies have shown that abnormalities of nuclear morphology correlate with the increasing grade of a tumor as well as worsening of prognosis in various carcinomas such as breast cancer, renal cell carcinoma, prostate carcinoma, thyroid follicular neoplasms, and squamous neoplasms among others (Tosi et al. 1986; Gil et al. 2002; Wang et al. 2005; Mudaliar and Hutchens 2013; Bostwick and Cheng 2020). Hence, morphometric analysis can assist in the prognosis and treatment planning for various types of cancer.

Grading of tumors before surgery ideally should provide independent prognostic information and thus assist in the determination of tumor behavior in individual cases. It is also important in selecting the most appropriate therapy for patients. However, it is not perfect and has an element of subjectivity. Since the abnormalities in the nuclear morphology correlate with tumor progression and grade of breast cancer, they can be measured by the nuclear morphometry as nuclear size, nuclear shape, nuclear texture, and nuclear density. The role of nuclear morphometry in differentiating benign and malignant lesions has been well documented (Yang et al. 2001; Gil et al. 2002; Abdalla et al. 2009; Kashyap et al. 2018; Pandian et al. 2021). The strong correlation between the morphometric parameters and the size of the breast tumor, lymph node involvement, and mitotic activity implies that nuclear morphometry can augment the cytology grading of breast cancer and help in classifying patients into low and high-risk groups. When the diagnosis of aspirates of breast masses are questionable, nuclear morphometry can help in the further classification of such lesions, thereby allowing more appropriate albeit invasive surgical biopsy (Laishram 2017).

Aside from nuclear morphometry, the ultrastructural morphometric features of the nucleolus and the nucleolar area are also taken into consideration when grading some types of carcinomas. The nucleolar area appears to be the most useful in the reproducible and accurate grading of clear cell renal cell carcinoma (Lloreta-Trull et al. 2001; Delahunt et al. 2011).

It has been proved that morphometry is able to detect minor differences, which may escape the skilled and accurate pathologist. Hence, essential diagnostic and prognostic information can be obtained with this technique. An interesting report by Papaxoinis et al. (2009) revealed the high predictive value of nuclear morphometry for the diagnosis of malignant bile duct strictures. The authors performed nuclear morphometry on smears from 51 patients with bile duct strictures. Prior to this, the patients underwent endoscopic retrograde cholangiopancreatography (ERCP), but in 33 of them the diagnoses were inconsistent when conventional cytology methods were applied. After staining of smears for DNA visualization and assessing the nuclear morphometry on images acquired by a confocal laser scanning microscope, a distinctive nuclear morphometric pattern was observed in the 33 undiagnosed cases and attributed to malignant nuclei. After a follow-up period of 8 months, 19 of these cases were indeed diagnosed with malignant strictures and 14 with benign strictures. The study highlights the importance of nuclear morphometry for the diagnosis of malignant bile duct strictures when conventional cytology fails to do so.

2.3.2 Morphometric Analysis in Brain Research

Morphometric analysis is often applied to MRI images to study brain injuries. Voxel-based morphometry is an automated quantitative approach to compare the volume or density of the brain tissue between patient and control groups. It is a typical method of gray matter volumetry that also includes cortex measurement. Surface-based morphometry gives an estimation of the cortical morphology, such as volume, thickness, area, and gyrification. Together, these techniques help researchers and clinicians to obtain a better understanding of normal neurobiological processes of the brain. Furthermore, the use of both methods may improve the accuracy of the detection of morphological changes when comparing the data of patients and controls (Goto et al. 2022).

Structural MRI morphometry is a very useful approach in measuring brain atrophy. This has included parameters such as volume, surface area, and thickness in the cortical regions, with only volume and shape in the subcortical zone. Neuroimaging studies utilizing MRI morphometry have shown widespread brain atrophy in patients infected with human immunodeficiency virus (HIV). Among the features are volume losses in subcortical gray matter, white matter, and cerebellum, as well as cortical thinning of frontal, temporal, parietal, and cingulate cortices (Chang and Shukla 2018).

Morphometric analysis with CLSM is a useful approach in studies on cortical microcirculation because it allows for the attainment of space-related profiles and the performing of volumetric measurements. Using CLSM and a novel 3D computer-assisted morphometric analysis, Lawrence et al. (2008) extracted and analyzed hundreds of thousands of vascular segments within a large cortical area of thick sections of Indian ink-injected human brains. From this database they performed a morphometric analysis of the global densities, the statistical distributions of diameters and lengths, variations in volume density along the cortical depth and vectors parallel to the cortical surface. They also separated the tree- and net-like parts of the microcirculation and proposed a comprehensive model of the human cerebral cortex microcirculation.

Brain imaging studies have long reinforced that Schizophrenia is a disorder of the brain, involving many discrete and widely spread regions within the brain. In a review article, Levitt et al. (2010) summarized studies on volumetric and morphometric imaging of the cortical gray matter of patients with Schizophrenia. They screened only for those studies utilizing manual or manually edited image segmentation for determining ROIs and concluded that in almost all ROIs, cortical gray matter volume was reduced in patients diagnosed with Schizophrenia. These results clearly support that Schizophrenia involves an anatomical disorder of the brain, specifically a reduction of cortical gray matter in regions involved in higher cognition and emotional processing.

2.3.3 Morphometric Analysis in Immunohistochemical Investigations

Immunohistochemistry (IHC) has become a common tool in clinical and research laboratories as a more specific alternative to routine histochemical staining. It is widely used in research for immunodetection of specific biomarkers between treatment groups and also for visualizing the protein localization, trafficking pathways, and protein–protein interactions. The latter deal with cell imaging and for clarity are classified as immunocytochemistry (ICC). In the clinical field, IHC is a way to quickly visualize the presence of biomarkers in the context of tissue morphology. It is widely applicable as a routine diagnostic aid for many diseases, including breast cancer (Rexhepaj et al. 2008), lung cancer (Hirsch et al. 2017), prostate cancer (Bostwick and Cheng 2020), adrenal cortical carcinoma (Papathomas et al. 2016), melanoma (Phillips et al. 2018), and head and neck squamous cell carcinoma

(Franchi et al. 2004). A comprehensive review article by Matos et al. (2010) describes the principle of immunohistochemistry, its history, applications, importance, limitations, difficulties, problems, and some aspects related to interpretation and quantification of the results.

A variation of IHC is immunofluorescence (IF), where the specimens are stained with fluorescent antibody and then visualized by means of a fluorescent microscope, either conventional or CLSM. Both IHC and IF may be performed in vitro on cell culture samples. Coupled with morphometric analyses, they produce excellent quantitative results. A significant effort has been made toward developing in vivo IHC and IF morphometric assays coupled with high-resolution imaging. As discussed previously, the live imaging is a powerful technique, but at the same time, the staining can influence the viability and behavior of cells. Furthermore, the nature of live imaging and time-lapse microscopy is such that it is sometimes very difficult to capture and quantify the fine immunofluorescent labels of cells in motion.

Nevertheless, there are in vivo studies on morphometric analysis of immunolabeling with the main focus being molecular regulation of lymphatic development. In order to study lymphangiogenesis, Ny et al. (2013) created transgenic Tg (Flk1, eGFP) *Xenopus laevis* reporter lines expressing green fluorescent protein (GFP) in blood and lymph vessels and established novel in vivo models of spontaneous and induced lymphatic/vascular sprouting. The authors counted the number of blood and lymphatic sprouts and measured the cumulative length of the sprouts by means of computer-assisted morphometry.

Morphometric analysis of lymphatic vessels has gained a lot of interest due to the important role of lymphatics in various physiological and pathological conditions (Onyangunga et al. 2016; Varaden et al. 2019). Recent progress in computer-assisted lymphatic morphometry was facilitated by the discovery of molecular markers specifically expressed in lymphatic vessels. Antibodies raised against lymphatic markers such as podoplanin and the lymphatic vessel endothelial hyaluronan receptor-1 (LYVE-1) have been widely used to identify the role of the lymphatic vessels in the pathogenesis of numerous diseases (Onyangunga et al. 2016, 2018).

Evidence suggests that the formation of tumor-associated lymphatic vessels plays an active role in the metastatic spread of several human malignancies. In order to study the role of tumor-associated lymphangiogenesis in head and neck squamous cell carcinoma (HNSCC), Franchi et al. (2004) performed computer-assisted morphometric analysis on HNSCC paraffin sections, immunostained for the lymphatic marker D2–40. The authors found a correlation between lymphatic vessel density and size within the peritumoral area compared with the tumor area. Furthermore, the relative area of intratumoral and peritumoral lymphatics was significantly higher in HNSCC cases with lymph node metastasis. The study suggests that intratumoral lymphatics are essential for the metastatic spread and prognosis of HNSCC.

In our studies on the immunoexpression of the lymphatic markers (LYVE-1) and Podoplanin, we applied computer-assisted morphometric image analysis to quantify the IHC distribution of these markers in the placenta of HIV-infected normotensive versus pre-eclamptic women (Onyangunga et al. 2016; Merhar et al. 2022). Morphometric analysis of the IHC staining within the villi was challenging due to their unique and complicated morphologies. Primary stem villi give rise to intermediate villi from which arise the terminal (exchange) villous units. Performing morphometric analysis on stem villi was relatively easy, due to their large areas, which occupy almost the whole field of view (Fig. 2.5a, b). Hence, we performed manual segmentation (framing) at the edges of each stem villi and the amount of immunostaining (green) was expressed as a percentage per frame area (Fig. 2.5c). Within the terminal villi (red) the amount of label (green) was determined by a two-phase threshold and expressed as a total percentage of LYVE-1. Podoplanin is depicted within the frame area (Fig. 2.5d).

It is also possible to check accuracy of the segmentation by an overlay onto the actual

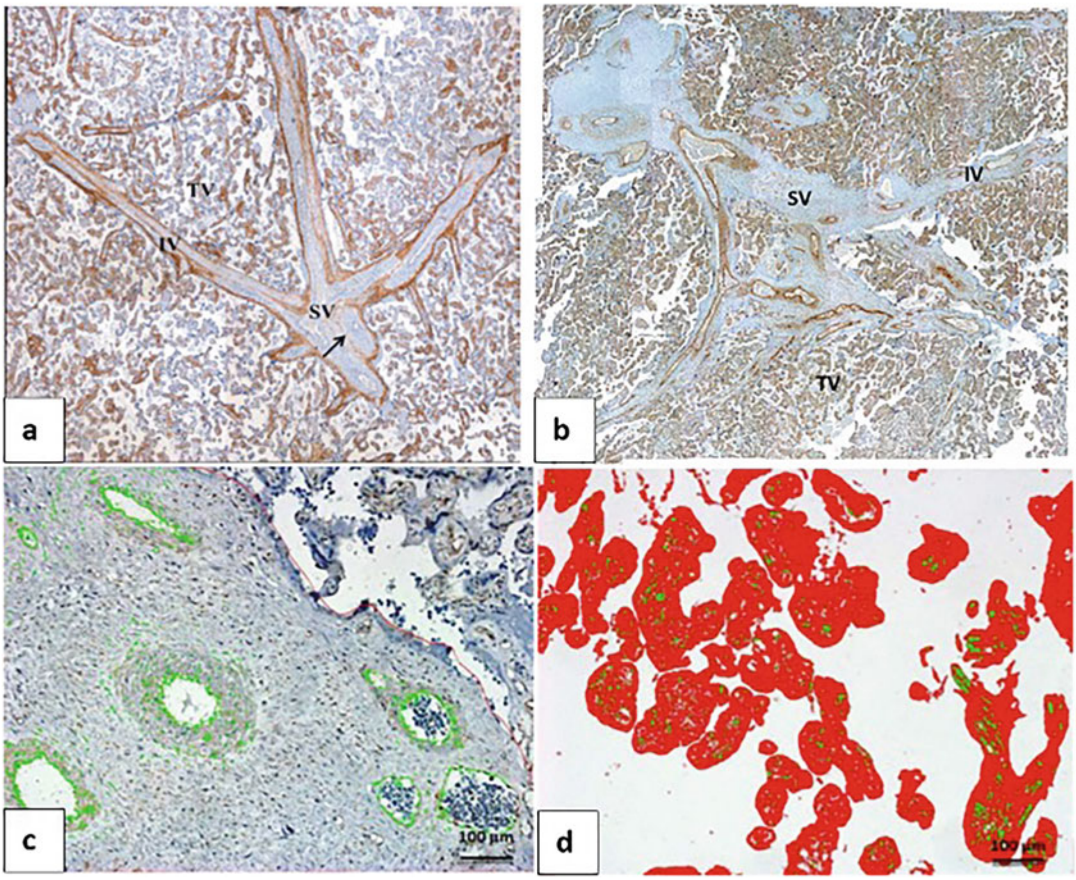

Fig. 2.5 Composite images of podoplanin (**a**) and LYVE-1 (**b**) immunostained placental villi and image segmentation of stem (**c**) and terminal (**d**) villi. (SV)—stem villi, (IV)—intermediate villi, and (TV)—terminal villi. Artery (black arrow). Initial magnification 5×

immunostained image. This is demonstrated in Fig. 2.6 where areas segmented are overlayed onto the original immunostained image of myometrial trophoblast cells immunostained with MNF 116 (a cytokeratin marker).

2.4 Essential Requirements for Precise and Reproducible Morphometric Analysis of Microscopic Images

Morphometric analysis is dependent on the quality of initial images. Note that the quality of images relies on a few adjustments of the microscope and hence facilitates accurate quantification.

Samples to be compared should be imaged with the same settings such as white balance and exposure. If exposure changes are required, they should be minimized so as not to affect the color balance. An important concept for this type of application (when comparing color renditions between samples for testing or diagnostic purposes) is that the white balance should only be performed for the light source and should not be corrected for each sample. When quantifying the staining intensity, it is important to have a uniform background throughout the whole image.

To compare numerous samples, staining, and image acquisition should be performed in parallel

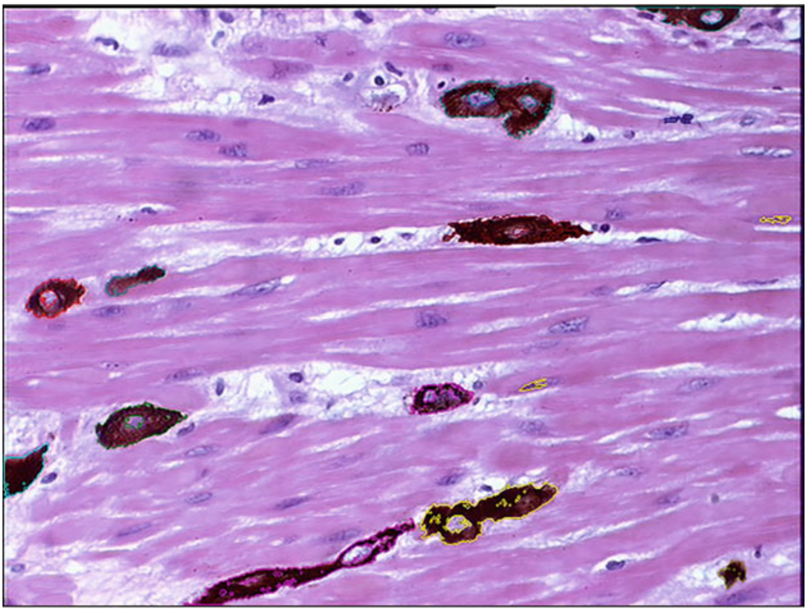

Fig. 2.6 Computed light micrograph to show areas measured. A mask image overlay surrounds the trophoblast cell within the myometrium. The mask image serves as the region validation check. Each color of the overlay depicts different intensity values of immunostaining (Naicker 2002)

for the whole set. Settings of the threshold must be the same in all images to be compared. It is recommended to measure particular ROIs as opposed to the entire image. With the imaging software, it is possible to choose particular areas for examination or deselect areas with undesirable features.

Accurate calibration of the instrument and the use of standards and controls are imperative for precise and reproducible quantification. Calibration can be done manually using a stage micrometer, or automatically. Automatic calibration is possible for motorized or encoded microscopes. The microscope takes into consideration the following components (set by the user): magnification of the objective, or the zoom factor in the case of a stereomicroscope, magnification factor of the camera adapter(s) used, the physical size of the pixels on the camera's CCD sensor and the binning mode used on the digital microscope camera.

For reproducible morphometric analysis, it is very important to keep the microscope capturing and measuring settings the same for all samples. Settings of microscopic light intensity, iris diaphragm, and condenser position as well as the workflow should be the same for both the samples within one batch and those from different batches. Hence, it is advisable to customize the interface to make repetitive tasks that will lead to reproducible results, an option that is offered by all modern microscopes.

Regarding the morphometric analysis in IHC, it is often unclear how to extract information from the IHC images, so that the morphometric analysis is reliable and reproducible. As with all types of imaging, if the images are of bad quality or if the experimental design was not well prepared, the analysis will inevitably be flawed. While image processing is a useful tool to enhance the images or to extract some useful information from them, it is not a good choice in IHC morphometric image analysis. This is because too much digitizing may mask the real IHC staining and cause certain deviations from its quantification. Similar to routine histological staining, IHC staining can be subject to many factors during the experiments which are inherent to the procedure or operator. These problems are now significantly reduced with automated specimen preparation. Nevertheless, the only way to properly answer the question as to whether or not a specific biomarker is present in the analyzed samples, is to compare the results with control samples that have gone through the same process. Negative and positive controls are essential for validating the specificity of the staining. More meaningful information can be extracted by quantifying the biomarker between individual cells of the image. In this case, segmentation of the edges of cells is essential in order to consider them on an individual basis. Tissue fixation and antigen retrieval are all critical factors for successful IHC quantification. Without doubt, the development of quantification methods for the immunohistochemistry technique, mainly those which are computer assisted, have increased not only the accuracy in the detection of markers, but also the reliability of their results.

2.5 Future Perspectives

In the era of global 4D imaging, microscopes and their associated morphometric applications will continue to undergo considerable advances to mitigate easier and exact representation of antigen immunolocalization and quantitation. Moreover, the interfacing of different types of microscopes with various mathematical logarithms that are specific to user needs will advance precise morphometric information with regard to quantitative cellular localization of antigens in biomedicine.

Notably, diagnostic criteria in medicine would be enhanced and more precise by morphometric image analysis of tissue pathology.

References

Abdalla F, Boder J, Markus R, Hashmi H, Buhmeida A, Collan Y (2009) Correlation of nuclear morphometry of breast cancer in histological sections with clinicopathological features and prognosis. Anticancer Res 29:1771–1776

Abdollahzadeh A, Belevich I, Jokitalo E, Tohka J, Sierra A (2019) Automated 3D axonal morphometry of white matter. Sci Rep 9(1):6084

Al-amri SS, Kalyankar NV, Khamitkar SD (2010) Image segmentation by using threshold techniques. J Comput 2(5):83–86

Ambellan F, Tack A, Ehlkeba M, Zachow S (2019) Automated segmentation of knee bone and cartilage combining statistical shape knowledge and convolutional neural networks: data from the Osteoarthritis initiative. Med Image Anal 52:109–118

Araña RVE (2015) Geometric morphometric analysis of individual variation in bumblebee wings. IAMURE Int J Ecol Conserv 11:1–15

Araújo SJ, Llimargas M (2023) Time-lapse imaging and morphometric analysis of tracheal development in drosophila. In: Margadant C (ed) Cell migration in three dimensions. Methods in molecular biology, vol 2608. Humana, New York, NY. https://doi.org/10.1007/978-1-0716-2887-4_11

Balafar MA, Ramli AR, Saripan MI, Mashohor S (2010) Review of brain MRI image segmentation methods. Artif Intell Rev 33:261–274

Bhattacharya P, Edwards K, Schmid KL (2022) Segmentation methods and morphometry of confocal microscopy imaged corneal epithelial cells. Cont Lens Anterior Eye 45(6):101720

Bostwick DG, Cheng L (2020) Neoplasms of the Prostate. In: Cheng L, Maclennan GT & Bostwick DG (eds) Urologic Surgical Pathology (Fourth Edition), chapter 9, pp. 415–525, Elsevier. ISBN 978-0323549417, https://doi.org/10.1016/B978-0-323-54941-7.00009-8

Buhmeida A (2006) Quantitative pathology: historical background, clinical research and application of nuclear morphometry and DNA image cytometry. Libyan J Med 1:126–139

Burke RT, Orth JD (2016) Through the looking glass: time-lapse microscopy and longitudinal tracking of single cells to study anti-cancer therapeutics. J Vis Exp 111:e53994

Chang L, Shukla DK (2018) Imaging studies of the HIV-infected brain. In: Handbook of Clinical Neurology, Vol. 152 (3rd series), Brew BJ, Ed. The Neurology of HIV Infection, Chapter 18, pp 229–264, Elsevier. https://doi.org/10.1016/B978-0-444-63849-6.00018-9

Chvátal A, Anderová M, Kirchhoff F (2007) Three-dimensional confocal morphometry—a new approach for studying dynamic changes in cell morphology in brain slices. J Anat 210:671–683

Collins JL, van Knippenberg B, Ding K, Kofman AV (2019) Time-lapse microscopy. Cell Culture. https://doi.org/10.5772/intechopen.81199

Curry DP, Dias FJ, Sosthenes MC, Dos Santos Haemmerle CA, Ogawa K, Da Silva MC, Mardegan Issa JP, Iyomasa MM, Watanabe IS (2013) Morphometric, quantitative, and three-dimensional analysis of the heart muscle fibers of old rats: transmission electron microscopy and high-resolution scanning electron microscopy methods. Microsc Res Tech 76(2):184–195

Daimary D, Bora MB, Amitab K, Kandar D (2020) Brain tumor segmentation from MRI images using hybrid convolutional neural networks. Procedia Comput Sci 167:2419–2428

De Paul AL, Mukdsi JH, Petiti JP, Gutiérrez S, Quintar AA, Cristina A. Maldonado CA, Torres AI (2012). Immunoelectron microscopy: a reliable tool for the analysis of cellular processes, applications of immunocytochemistry, Dr. Hesam Dehghani (Ed.). InTech

Delahunt B, Sika-Paotonu D, Bethwaite PB, William Jordan T, Magi-Galluzzi C, Zhou M, Samaratunga H, Srigley JR (2011) Grading of clear cell renal cell carcinoma should be based on nucleolar prominence. Am J Surg Pathol 35(8):1134–1139

Denk W, Horstmann H (2004) Serial block-face scanning electron microscopy to reconstruct three-dimensional tissue nanostructure. PLoS Biol 2(11):e329

Dujardin J-P (2011) Modern Morphometrics of Medically Important Insects. In: Tibayrenc M (ed) Genetics and Evolution of Infectious Diseases. chapter 16, pp. 473–501. Elsevier. ISBN 9780123848901. https://doi.org/10.1016/B978-0-12-384890-1.00016-9

Edgar JM, Smith RS, Duncan ID (2020) Transmission electron microscopy and morphometry of the CNS white matter. In: Babetto E (ed) Axon degeneration. Methods in molecular biology, vol 2143. Humana, New York, NY

Filoni A, Alaibac M (2019) Reflectance confocal microscopy in evaluating skin cancer: a Clinicians's perspective. Front Oncol 9:1457

Franchi A, Gallo O, Massi D, Baroni G, Santucci M (2004) Tumor lymphangiogenesis in head and neck squamous cell carcinoma: a morphometric study with clinical correlations. Cancer 101(5):973–978

Gil J, Wu H, Wang BY (2002) Image analysis and morphometry in the diagnosis of breast cancer. Microsc Res Tech 59(2):109–118

Gill M, Alessi-Fox C, Kose K (2019) Artifacts and landmarks: pearls and pitfalls for in vivo reflectance confocal microscopy of the skin using the tissue-coupled device. Dermatol Online J 25(8):1–13

Gonzalez R, Woods R (2002) Digital image processing, 2nd edn. Prentice-Hall, Upper Saddle River, NJ, USA

Goto M, Abe O, Hagiwara A, Fujita S, Kamagata K, Hori M, Aoki S, Osada T, Konishi S, Masutani Y, Sakamoto H, Sakano Y, Kyogoku S, Daida H (2022) Advantages of using both voxel- and surface-based morphometry in cortical morphology analysis: a review of various applications. Magn Reson Med Sci 21(1):41–57

Griffiths G, Sloth J (1992). Cryoultramicrotomy and immunolabelling workshop course notes. Electron Microscopy Unit, University of Natal, South Africa

Grosche J, Kettenmann H, Reichenbach A (2002) Bergmann glial cells form distinct morphological structures to interact with cerebellar neurons. J Neurosci Res 68:138–149

Gulati NM, Torian U, Gallagher JR, Harris AK (2019) Immunoelectron microscopy of viral antigens. Curr Protoc Microbiol 53(1):e86

Hallgrimsson B, Percival CJ, Green R, Young NM, Mio W, Marcucio R (2015) Morphometrics, 3D imaging, and craniofacial development. Curr Top Dev Biol 115:561–597

Hirsch FR, McElhinny A, Stanforth D et al (2017) PD-L1 immunohistochemistry assays for lung cancer: results from phase 1 of the blueprint PD-L1 IHC assay comparison project. J Thorac Oncol 12:208–222

Jasim S, Dean DS, Gharib H (2015) Fine-needle aspiration biopsy of the thyroid gland. In: Feingold KR et al (eds) Endotext [internet]. MDText.com, Inc., South Dartmouth (MA), p 2000

Jonuscheit IS, Doughty MJ, Ramaesh K (2011) *In vivo* confocal microscopy of the corneal endothelium: comparison of three morphometry methods after corneal transplantation. Eye (Lond) 25(9):1130–1137

Joubert, B C. (2010). The interaction of lymphogranuloma venereum and oculogenital chlamydia trachomatis with human keratinocytes and cervical epithelium. PhD thesis, UKZN, South Africa

Kashyap A, Jain M, Shukla S, Andley M (2018) Role of nuclear morphometry in breast cancer and its correlation with cytomorphological grading of breast cancer: a study of 64 cases. J Cytol 35(1):41–45

Laishram S (2017) Nuclear morphometric application in the quantitative description of breast lesions. J Med Res 3(5):255–257

Lauwers F, Cassot F, Lauwers-Cances V, Puwanarajah P, Duvernoy H (2008) Morphometry of the human cerebral cortex microcirculation: general characteristics and space-related profiles. NeuroImage 39(3):936–948

Lawrence D, Alvis R, Olson D (2008) Specimen preparation for cross-section atom probe analysis. Microsc Microanal 14(S2):1004–1005

Lestrel PE (2000) Morphometrics for the life sciences. World Scientific Publishing Company

Levitt JJ, Bobrow L, Lucia D, Srinivasan P (2010) A selective review of volumetric and morphometric imaging in schizophrenia. Curr Top Behav Neurosci 4:243–281

Lloreta-Trull J, Bielsa-Galí O, Domínguez-Solà D, Arumí-Uría M, Pavesi M, Gelabert A, Serrano-Figueras S (2001) Ultrastructural morphometry of nucleoli: potential usefulness for objective grading of clear cell renal cell carcinoma. Ultrastruct Pathol 25(2):105–110

Maduray K, Moodley J, Naicker T (2016) Morphometrical analysis of placental functional efficiency in normotensive versus pre-eclamptic south African black women. Hypertens Pregnancy 35(3):361–370

Matos LL, Trufelli DC, de Matos MG, da Silva Pinhal MA (2010) Immunohistochemistry as an important tool in biomarkers detection and clinical practice. Biomark Insights 5:9–20

Merhar V, Onyangunga O, Moodley J, Naicker T (2022) Comparative morphometric image analysis of LYVE-1 and Podoplanin in HIV infected preeclamptic women. In: Sotirov SS, Pencheva T, Kacprzyk J, Atanassov KT, Sotirova E, Staneva G (eds) Contemporary methods in bioinformatics and biomedicine and their applications. Springer publishing, pp 400–408

Mitteröcker P (2021) Morphometrics in evolutionary developmental biology. In: Nuño de la Rosa L, Müller GB (eds) Evolutionary developmental biology. Springer, Cham

Mitteroecker P, Gunz P (2009) Advances in geometric morphometrics. Evol Biol 36:235–247

Mudaliar K, Hutchens K (2013) Morphometric image analysis as a tool in the diagnosis of transected squamous neoplasms. J Clin Anat Pathol 1:1–5

Naicker T (2002). Immunolocalisation of transforming growth factor beta and its latent peptide in the placental bed of normal and hypertensive pregnancy. PhD thesis UKZN, South Africa

Naicker T, Dorsamy E, Ramsuran D, Burton GJ, Moodley J (2013) The role of apoptosis versus proliferation on trophoblast cell invasion in the placental bed of normotensive and hypertensive pregnancies. Hypertens Pregnancy 32(3):245–256

Naicker T (2023) Personal communication. University of KwaZulu-Natal, Optics & Imaging Centre

Ny A, Vandevelde W, Hohensinner P, Beerens M, Geudens I, Diez-Juan A, Brepoels K, Plaisance S, Krieg PA, Langenberg T, Vinckier S, Luttun A, Carmeliet P, Dewerchin M (2013) A transgenic Xenopus laevis reporter model to study lymphangiogenesis. Biol Open 2(9):882–890

Onyangunga O, Moodley J, Odun-Ayo F, Naicker T (2018) Immunohistochemical localiza-tion of podoplanin in the placentas of HIV-positive preeclamptic women. Turk J Med Sci 48:916–924

Onyangunga OA, Moodley J, Merhar V, Ofusori A, Naicker T (2016) Lymphatic vascular endothelial hyaluronan receptor-1 immunoexpression in placenta of HIV infected pre-eclamptic women. J Reprod Immunol 117:81–88

Pandian DJN, Ramdas A, Ambroise MM (2021) Image analysis-assisted nuclear morphometric study of benign and malignant breast aspirates. J Microsc Ultrastruct 9(3):114–118

Papathomas TG, Pucci E, Giordano TJ et al (2016) An international Ki67 reproducibility study in adrenal cortical carcinoma. Am J Surg Pathol 40:569–576

Papaxoinis K, Patsouris E, Athanassiadou P, Nicolopoulou-Stamati P (2009) Contribution of nuclear morphometry by confocal laser scanning microscopy to the diagnosis of malignant bile duct strictures. Acta Cytol 53(2):137–143

Phillips T, Millett MM, Zhang X et al (2018) Development of a diagnostic programmed cell death 1-ligand 1 immunohistochemistry assay for nivolumab therapy in melanoma. Appl Immunohistochem Mol Morphol 26:6–12

Rexhepaj E, Brennan DJ, Holloway P et al (2008) Novel image analysis approach for quantifying expression of nuclear proteins assessed by immunohistochemistry: application to measurement of oestrogen and progesterone receptor levels in breast cancer. Breast Cancer Res 10:1–10

Rohlf FJ, Marcus LF (1993) A revolution in morphometrics. Trends Ecol Evol 8(4):129–132

Saood A, Hatem I (2021) COVID-19 lung CT image segmentation using deep learning methods: U-Net versus SegNet. BMC Med Imaging 21(1):1–10

Sendaydiego JP, Torres MAJ, Demayo CG (2013) Describing wing geometry of Aedes aegypti using landmark-based geometric morphometrics. Int J Biosci Biochem Bioinforma 3(4):379–381

Tosi P, Luzi P, Baak JP, Miracco C, Santopietro R et al (1986) Nuclear morphometry as an important prognostic factor in stage I renal cell carcinoma. Cancer 58: 2512–2518

Varaden D, Moodley J, Onyangunga OA, Thajasvarie Naicker T (2019) Morphometric image analysis of placental C-type lectin domain family2, member D (CLEC2D) immuno-expression in HIV associatedpre-eclampsia. Eur J Obstet Gynecol Reprod Biol: X 3: 100039

Wang SL, Wu MT, Yang SF, Chan HM, Chai CY (2005) Computerized nuclear morphometry in thyroid follicular neoplasms. Pathol Int 55:703–706

Webster M, Sheets H (2010) A practical introduction to landmark-based geometric morphometrics. Paleontological Society Papers 16:163–188. https://doi.org/10.1017/S1089332600001868

Wen C, Huang M, Wang S, Su Y, Yang S, Chai C (2009) Diagnostic value of computerized nuclear morphometry for the prediction of malignancy in liver fine needle aspiration cytology. Acta Cytol 53:77–82

Yang Q, Mori I, Sakurai T, Yoshimura G, Suzuma T, Nakamura Y, Nakamura M, Taniguchi E, Tamaki T, Umemura T, Kakudo K (2001) Correlation between nuclear grade and biological prognostic variables in invasive breast cancer. Breast Cancer 8(2):105–110

Young JW, Locke JC, Altinok A, Rosenfeld N, Bacarian T, Swain PS et al (2011) Measuring single-cell gene expression dynamics in bacteria using fluorescence time-lapse microscopy. Nat Protoc 7(1): 80–88

3 The Shift in Power from Conventional to Digital and Virtual Microscopy

Shoohana Singh and Thajasvarie Naicker

Abstract

Since the eleventh century, manipulating lenses to magnify an object for enhanced viewing, launched the evolution of optical microscopes in, but not limited to the fields of clinical and medical sciences. The strides in technological advancements have transformed the use and application of traditional microscopy in the teaching and learning environment of medical sciences. The aim of this chapter is to discuss our experience in the transition from traditional microscopy to digital and virtual learning techniques in the study of histology within the clinical and medical sciences disciplines at a tertiary level.

Limitations of traditional microscopy include high cost, maintenance, colour fading and the need for a dedicated laboratory. Moreover, economic constraints in low- and middle-income countries make it impossible to provide microscopes to all learners within a class. In a class restricted by the number of optical microscopes available to teach a histology practical, digital and virtual microscopy has opened up the classroom beyond its physical location. Microscopes interfaced with large monitors and software have enabled images to be streamed to the entire class whilst simultaneously reducing the cost of buying each student a microscope. Pathologists worldwide can now simultaneously consult on a patient's outcome with the convenience of a virtual hub of histopathology tissue sections. The diagnostic accuracy of histological assessment of digitized virtual slides is similar to traditional glass slides. Additionally, studies have shown that grasping the concept of histology and improved understanding and recall of cellular structure and function are attributed to digital and virtual microscopy. Furthermore, when challenged with the COVID-19 pandemic where access to laboratories and lecture venues had been severely restricted, histology teaching and learning continued to thrive.

This chapter will highlight the benefits of virtual visualization from digitized histological slides over traditional microscopy such as the multimodal communication of images. Virtual microscopy is a visual stimulus that is an undeniable tool for improved teaching and learning of histology at the tertiary level of biomedicine. The positive pedagogic outcome of this type of visualization and learning is the outcome of the students' assessment.

Keywords

Virtual microscopy · Digital histology imaging · Histology practical · Optical microscope · Conventional microscopy

---

S. Singh (✉) · T. Naicker
Optics and Imaging Centre, Doris Duke Medical Research Institute, College of Health Sciences, University of KwaZulu-Natal, Durban, South Africa
e-mail: Singhs5@ukzn.ac.za; naickera@ukzn.ac.za

© The Author(s), under exclusive license to Springer Nature Switzerland AG 2023

L. Shapiro (ed.), *Microscopy Techniques for Biomedical Education and Healthcare Practice*, Biomedical Visualization 2, https://doi.org/10.1007/978-3-031-36850-9_3

3.1 Conventional Optical Microscopy and its Shortfalls

As early as the fifteenth century, the idea of the first microscope was put forward, which utilized ground glass lenses by the father and son duo Hans and Zacharias Janssen (Dutch spectacle makers) (Ball 1966). This addition of lenses improved magnification and resolution. The subsequent study of biological specimens by Robert Hooke in 1665, was with the first version of what would now be regarded as a compound microscope. In the same period, Antonie van Leeuwenhoek developed a single lens microscope that could magnify up to 200X, similar to the present-day stereomicroscope used in the dissection of insects and the study of bacteria. Carl Zeiss, Ernst Abbe and Otto Schott manufactured a high-performance stand-type microscope in 1857, which improved spatial resolution of the microscope to 0.2 μm (Araki 2017).

The manipulation of lenses unlocked studies in the field of biological specimens and enabled massive strides in progress in the medical realm. Microsurgery became a reality with the manufacture of the first binocular device in 1876. A microscope with coaxial illumination was created by Carl Zeiss Inc. to be used as an otoscope and a colposcope. It was rapidly modified for use in ocular surgery after it was made commercially accessible in 1953 (Barraquer 1980). Apart from biologists, medical scientists and surgeons, biochemists and material scientists also benefited from the advancements in optical microscopy development. By using expansion microscopy, biochemists attempted to evenly separate the biomolecules creating more space for the labels to bind (Mertz 2023). Whilst material scientists developed microsphere-assisted microscopy (MAM) as an effective method to improve microscopy resolution. In MAM, a microsphere is positioned close to the object to function as a magnifying glass and enhance resolution (Darafsheh and Abbasian 2023).

Despite light and lenses being used in the development of the modern-day microscope, their properties also create limitations in the use of the microscope. The development of the light microscope was hindered by the wavelength of light. The resolving power of a light microscope is affected by both wavelength and numerical aperture of the lens. Under the microscope, anything smaller than half the illumination source's wavelength is not visible. Furthermore, diffraction limits the resolution to approximately 0.2 μm. The cell's internal structures are transparent and colourless. The typical approach is to use specific dyes on various structures to enhance contrast, although this frequently necessitates killing and chemically fixing the specimen. An optical microscope can often magnify objects up to a maximum of 1500 times, typically between 50x and 1500x.

3.2 The Use of Microscopes in Teaching and Learning

Microscopes expose students to the multitude of invisible worlds that exist all around them. For many students, learning through practical sessions is significantly more effective than learning through hearing, writing or didactic teaching. Giving impressionable young students the opportunity to do practical tasks utilizing microscopes, demonstrates to them that biomedical science is not only to be found in textbooks. This also communicates to the student that the search for information and understanding is a proactive one.

Undergraduate students, especially those in low- and middle-income countries, may not have had the opportunity to explore much beyond the boundaries of their own communities. Notably, the use of microscopes in histology enables the examination of human tissue contributing to its integration into physiology and pathology. This promotes inquiry and study, which are crucial for making scientific discoveries. The true value and appreciation of workmanship that goes into creating a specimen slide for viewing can only be achieved if the student experiences it. Physical, practical sessions in histotechniques, histology, microscopy and pathology make this experience possible.

3.3 Limitations of Microscopes in Teaching and Learning

Despite the immense benefits of microscopes for teaching and learning, the cost of even a simple basic microscope is high. This high cost poses a serious challenge for low- and middle-income countries. In a science teaching environment, every student (or at least 2 students) should have access to a single microscope. Unfortunately, this is impossible in low- and middle-income countries. In the teaching and learning environment, tertiary institutions are also unable to furnish their laboratories with sufficient microscopes for practical sessions, particularly in the study of histology due to exorbitant costs. Furthermore, maintenance, servicing and replacement of these microscopes can run into significant sums of money, making a 2-yearly service agreement difficult.

Another problem encountered in histology teaching that hinders productive practical sessions, is that every student requires the same set of specimen slides. Glass slides are easily broken and stains fade over time. This makes maintaining and setting up for every practical session daunting, especially if student numbers per course or module are large.

3.4 Challenges in Teaching and Learning of Microscopy and Histology

The primary educational challenge in biomedical science is that students are finding it difficult to conceptualize dimensional orientation and the integration of histology, physiology and anatomy resulting in a lack of interest and poor performance in the subject.

Taking into account the limitations of the conventional light microscopy which involve the cost of microscopes, service costs and replacement of specimen slides within the large student practical laboratories, it would seem that a better approach would be to teach histology using a digital approach. The generation of learners, termed Millennials, Generation-Z and Generation Alpha are technology driven and better understand the use of computers and digital media (Oblinger 2003). Moreover, many of them see light microscopy hardware as archaic tools (Krippendorf and Lough 2005; Lakhtakia 2021). Consequently, the student loses enthusiasm for studying the subject matter. In addition, many undergraduate students in the fields of Sport Science, Physiotherapy, Occupational therapy and Medicine may never need to use a microscope in their career, but need to understand microanatomy in the form of histology and histopathology. It is therefore incumbent on educators to deliver the course content in such a manner as to be compatible with the students' future field of specialization, in order that they understand how the subject matter could improve proficiency in their career.

In low- and middle-income countries, inadequate laboratory infrastructure with limited space makes the delivery of histology teaching and meaningful learning problematic. For instance, at our tertiary institution, there are currently only 42 functional microscopes in the histology laboratory, accommodating 24 modules (Table 3.1) taught as either majors or electives in the Bachelor of Medical Science degree (Anatomy and Physiology) and Honours, Bachelor of Medicine and Surgery, Bachelor of Nursing, Bachelor of Pharmacy, Bachelor of Physiotherapy, Bachelor of Optometry, Bachelor of Occupational Therapy, Bachelor of Audiology, Bachelor of Speech-Language Therapy and Bachelor of Sport Science.

3.5 Reflection on Teaching Histology

This infrastructure limitation, including the sharing of a microscope between a number of students in a practical session, results in an unsatisfactory learning experience. Students subsequently struggle to master microscopy techniques as well as adequately interact with the teaching material. Most of the time, students were found to be viewing an incorrect area of the tissue under the individual light microscope and consequently are not

Table 3.1 Biomedical student numbers per semester at our tertiary institution

	Courses requiring microscopes	Student numbers
1	HPHS111 – Basic Human Physiology	163
2	HPHS112 – Physiological Changes in Exercise & Training72	72
3	HPHS221 – Homeostasis	256
4	HPHS222 – Integration and Communication	269
5	HPHS1NU – Physiology 1	76
6	HPHS2NU – Physiology 2	79
7	HPHS1H2 – Human Body: Form and Function	159
8	HPHS231 – Foundations of Physiology	125
9	HPHS232 – Cardiorespiratory and Renal Physiology	102
10	HPHS331 – Neuroendocrine Physiology	52
11	HPHS322 – Human Genetics Applied Physiology	61
12	HAEM301 – Haematology	83
13	MedM3M2 – Medical Microbiology	82
14	HMBC7MR – Research Methodology for Medical Sciences	41
15	HPHS7AL – Advanced Laboratory Techniques in Physiology	25
16	HPHS711 – Integrative Physiology	25
17	HPHS721 – Applied physiology	25
18	HPHS731 – Pathophysiology	25
19	HPHS7RP – Research Project	26
20	CMED1BF – Basic and Foundation Science for Medicine	250
21	CMED2CR – Homeostasis	250
22	CMED2NG – Co-ordination, protection and control	250
23	CMED3MN – Mental Health and Neuro-musculoskeletal problems	250
24	CMED3RH – Reproductive Health, Blood and AI, Infectious Diseases and Aids	250

able to correlate the practical aspect to the theoretical material. The conventional way in which histology was taught at our institution involved a pre-laboratory lecture that explained structure, function and location with the aid of PowerPoint presentations. Thereafter the student was supplied with glass slides, microscopes and a report worksheet to complete and submit a week later to be evaluated. The practical report would consist of labelled diagrams and short notes. Students often drew incorrect diagrams and became frustrated due to poor performance resulting from inadequate microscopy skills. At present, laboratory space is a major restricting factor when considering student enrolment into our school, and although we have been successful at meeting our student quota, sadly we have had to turn away potentially good students who have met the entry criteria. Furthermore, the workload, contact time and repetitive practicals were extremely taxing on the academic staff.

3.6 Virtual and Digital Microscopy

Virtual microscopy was developed over 25 years ago and has progressively become a popular substitute for traditional light microscopy (Dee 2009). It is now gradually dispensing with the conventional laboratory-based approach to teaching histology and pathology. Virtual microscopy image data files are easy to recreate, but high-end slide scanners and software to read the digital slides are required. Moreover, server storage and superior quality histologically stained slide are recommended. Notably, this is a one off cost hence cheaper and less cumbersome than microscopy hardware. Furthermore, the electronic image files, usually gigabytes large, are stored on a central server and can be obtained over the Internet or a local network. The technology mimics that of Google Earth (Google Inc., Mountain View, CA).

Students can examine these image data files on their computer screen by using one of the many digital viewer programmes or an Internet browser. Students may easily scroll over the image and zoom in or out to receive an overview of the entire slide or scrutinize details at higher magnification. Additionally, the ability to view images of the entire specimen on a monitor enables many students to examine the tissue sections without the use of a microscope. This encourages teamwork and strengthens productive debates for the benefit of technology users. Students usually respond positively to the introduction of virtual microscopy and several publications have reported a corresponding improvement in learning outcomes for students enrolled in histology or pathology courses (Francis et al. 2022; Sakthi-Velavan and Zahl 2023; Qing et al. 2022; Joaquim et al. 2022).

3.7 Teaching and Learning Using a Virtual Online Platform—Experience at our Laboratory Setting

After recognizing the difficulties encountered by students in the laboratory, our histology division embarked on transforming our conventional microscopy and histology teaching methods to a virtual and digital microscopy set-up.

3.8 Creation of Digitized Database

The initial step involved acquiring a digital slide scanner to perform whole slide imaging (WSI). Thereafter, a selection of our irreplaceable human tissue slides accrued over the years were scanned using sophisticated software (Leica SCN 400; Leica Microsystems, Germany). A secure digitized database was created on the university server accessible to specific biomedical course coordinators and to academics teaching on those courses. Fortunately, software for digital viewing (SlidePath Gateway Client 2.0; Leica Microsystems, Germany) was installed on the desktop computers of land area network (LAN) servicing the biomedical students. Only registered students were able to access the database by logging in using their username and password.

3.9 Remodelling of Laboratory and Lecture Venues to Accommodate Virtual Platform

Remodelling the conventional histology laboratory space to encompass our new virtual platform was a mammoth task. Desktop Personal Computers (PCs) were cost-effective at the period of set-up with the intention to change over to laptops in the future. Moreover, desktop PCs were cheaper than existing microscopes, hence we purchased one per student. Similar to the LAN, network points were connected to each PC, in addition to a wireless network hub to connect to the central server. Furthermore, several high-definition monitors (Samsung 46″ LED display panel) were strategically placed throughout the laboratory. These monitors were connected to a projection system interchangeable with a camera-linked microscope at the lecturer's front table. This enabled the lecturer to live broadcast a histology slide of interest with the ability of focusing on and drawing attention to features that may be missed if a student was to locate these features under individual microscopes.

Students were equipped with Smart wireless devices that would connect directly to the camera-linked microscope for easier viewing and recording the session. The lecturer could easily switch between output modes and interchange from the live slide to the theoretical information from their PowerPoint presentation to convey the objective of the practical session. In addition, a document viewer was also installed and connected to the interchangeable output system (Fig. 3.1a–c). This enabled easy viewing of documents, textbooks and biological samples. Due to the document viewer's zooming capability, a demonstration of tissue dissecting techniques could be projected to the students without them having to cluster around a dissecting table.

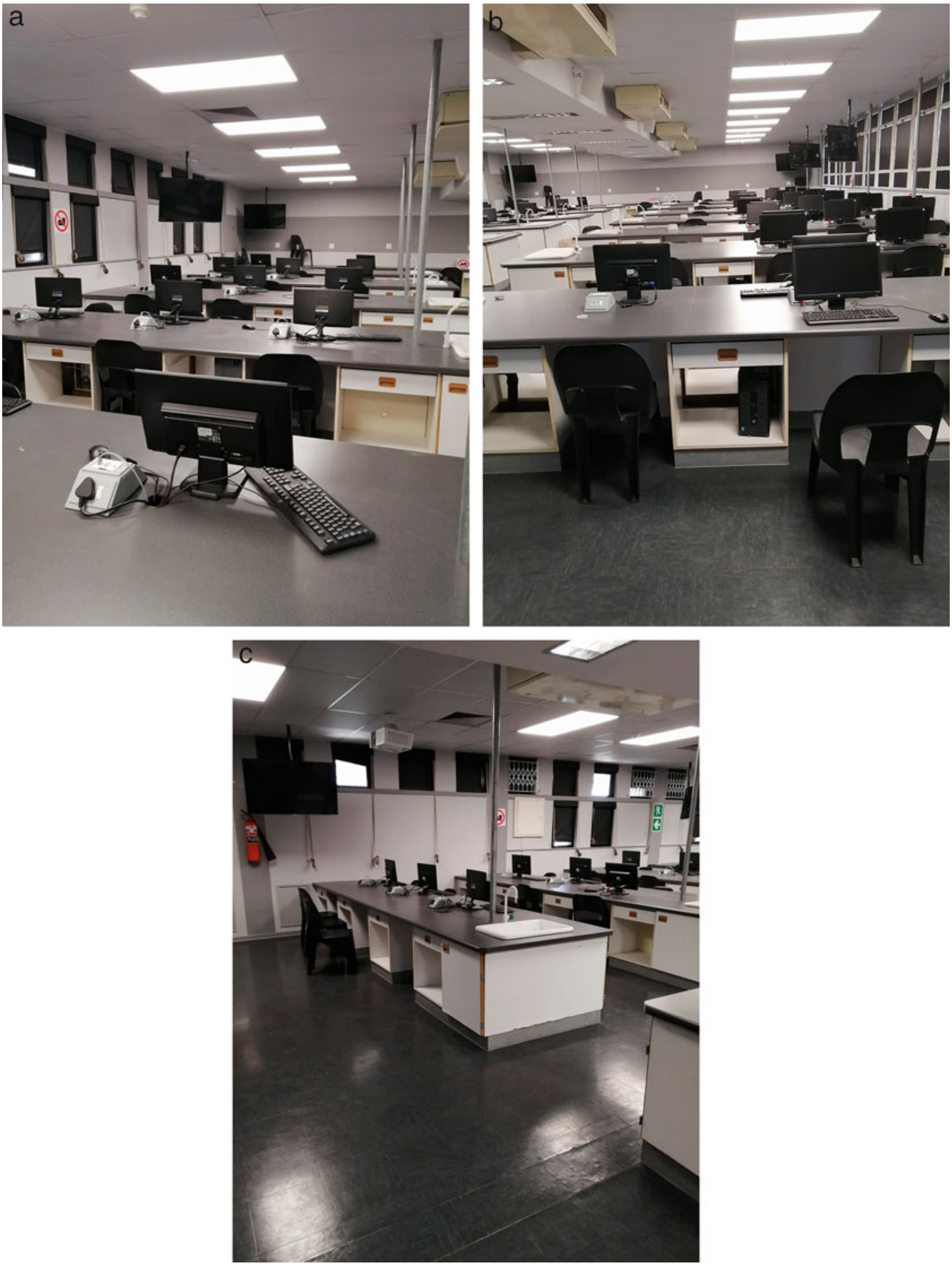

Fig. 3.1 (**a**) Desktop PCs with LAN. (**b**) Back-to-back seating can be accommodated by installing swivel display monitors. (**c**) A high-definition projector improves viewing quality

3.10 Delivering Histology Practical Sessions

The installation of the new virtual system required the colossal task of creating a virtual database of slides as well as equipping the laboratory for digital practical sessions. As such, traditional hardcopy histology practical session manuals had to be upgraded and converted to an electronic format with the addition of workflow instructions for software navigation.

The academics had the option to upload their pre-laboratory lecture material via the web-based communication system, University Learn Online Portal (ULOP), prior to the practical session for students to prepare towards the objectives and learning outcomes. Notably, all practical assessments were completed online and so reduced the cost of printing and paper consumption. This is a positive spin-off in reducing our carbon footprint and is considered as a Green initiative from our College.

Furthermore, to ensure conceptual understanding of specific areas within histology, the academic could select a few complicated tissue slides to project and navigate through with the camera-linked microscope for discussion within these virtual classrooms. Thereafter, students proceeded with logging into their desktop-based systems and accessed the database, in particular, the practical-specific folder along with the electronic practical manual (Figs. 3.2, 3.3, 3.4 and 3.5).

3.11 Assessments, Tutorials and Correspondence

Assessments and tutorials have moved away from paper-based methods and are now performed using our institute's online system with feedback made available timeously. Digital images captured from the virtual slides make identification-type assessments effortless for academics to set-up. Short and long question-type tutorials with reference to the virtual database allow for thorough interpretation and study. The online chatroom-based facility of the University Learn Online Portal (ULOP) allows for real-time interaction between students and academics, whereas the announcement facility serves to notify a particular course of students about practical schedules and any new postings or uploads. Announcements are geared to generate emails that are posted to individual students which also makes available another forum of one-on-one communication between the academic and student.

3.12 Impact of COVID-19 on Histology Practical Teaching

Many governments and institutions were unprepared for the impact that COVID-19 pandemic had on education and the disruption it caused (Tarkar 2020; Pokhrel and Chhetri 2021; Reimers 2022). Higher education institutions were compelled to use online instruction in order to rescue the academic year. Although we had created the database of virtual slides, we were never compelled to conduct an off-campus histology practical with the current technology. We had to encourage students to transition to attending online lectures and online learning. Fortunately, our institution had already begun the roll-out of laptops to all first-year Health Science students, making the transition for those students with laptops slightly easier. It was in March 2020 when South Africa had to adhere to strict national lockdown regulations that teaching and learning challenges began. Urgent deliveries of laptops to all our first-year Health Science students via already inundated courier services had to be completed. Negotiations with mobile service providers allowed our institute to allocate data bundles to every registered under- and postgraduate student, giving them Internet access. Pre-lab PowerPoint lectures had to be changed by adding audio recordings and full lecture recordings were possible with help from the Visual Learning Project (VLP) teams. Academics and students had to familiarize themselves with Zoom Video Communication, Inc. (San Hose,

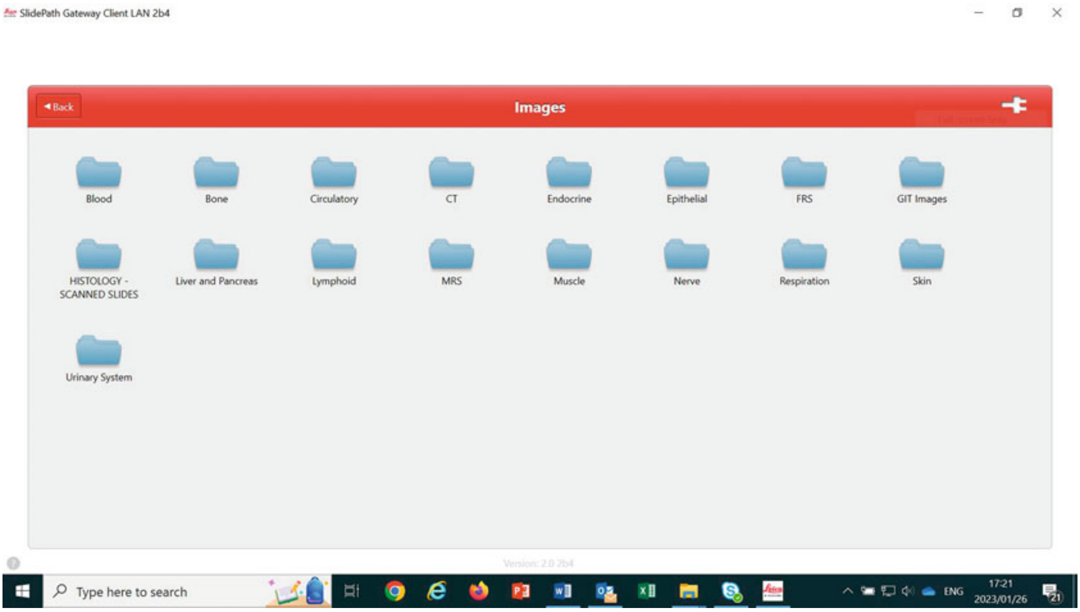
SlidePath Gateway Client LAN 2b4
Back
Images
Blood
Bone
Circulatory
CT
Endocrine
Epithelial
FRS
GIT Images
HISTOLOGY - SCANNED SLIDES
Liver and Pancreas
Lymphoid
MRS
Muscle
Nerve
Respiration
Skin
Urinary System
Version: 2.0 2b4
Type here to search
ENG
17:21
2023/01/26

Fig. 3.2 The Leica Microsystems Software displaying the database of virtual slides

California) and Microsoft Teams (USA) in order to engage with interactive sessions around lecture material.

Virtual Histology practical sessions became a reality with the use of Zoom meetings incorporated with our institute's virtual database. We used Microsoft Teams and SharePoint for software package sharing and installation in order for all our academics and students to download onto their laptops. In order to access the network drive, a pathway was mapped allowing academics and students to access the server along

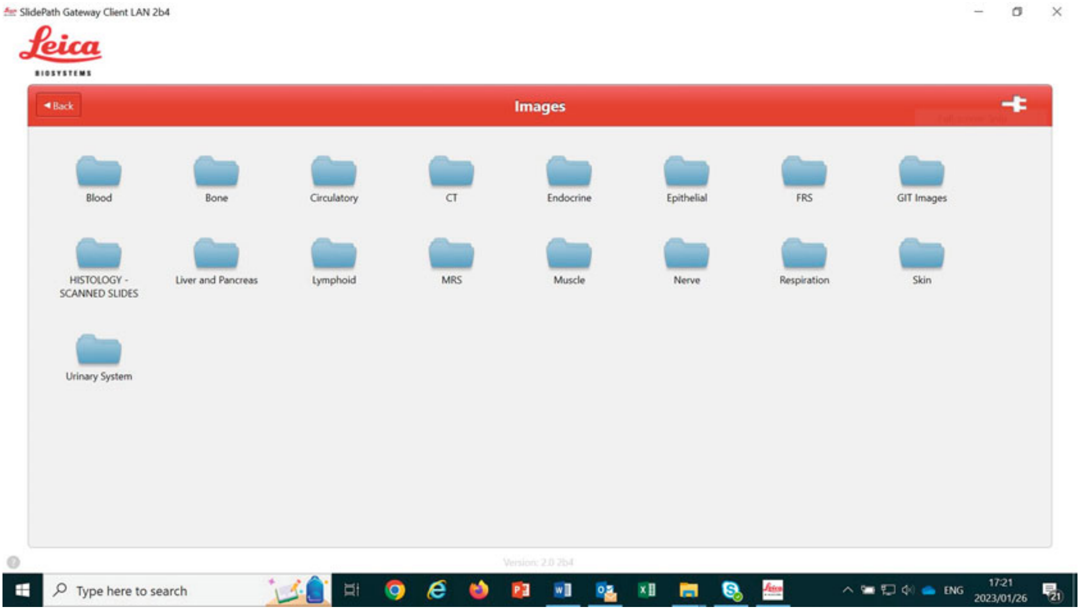
SlidePath Gateway Client LAN 2b4
Leica
BIOSYSTEMS
Back
Images
Blood
Bone
Circulatory
CT
Endocrine
Epithelial
FRS
GIT Images
HISTOLOGY - SCANNED SLIDES
Liver and Pancreas
Lymphoid
MRS
Muscle
Nerve
Respiration
Skin
Urinary System
Version: 2.0 2b4
Type here to search
ENG
17:21
2023/01/26

Fig. 3.3 Virtual slide population per practical folder with section numbers that correspond to the practical manual

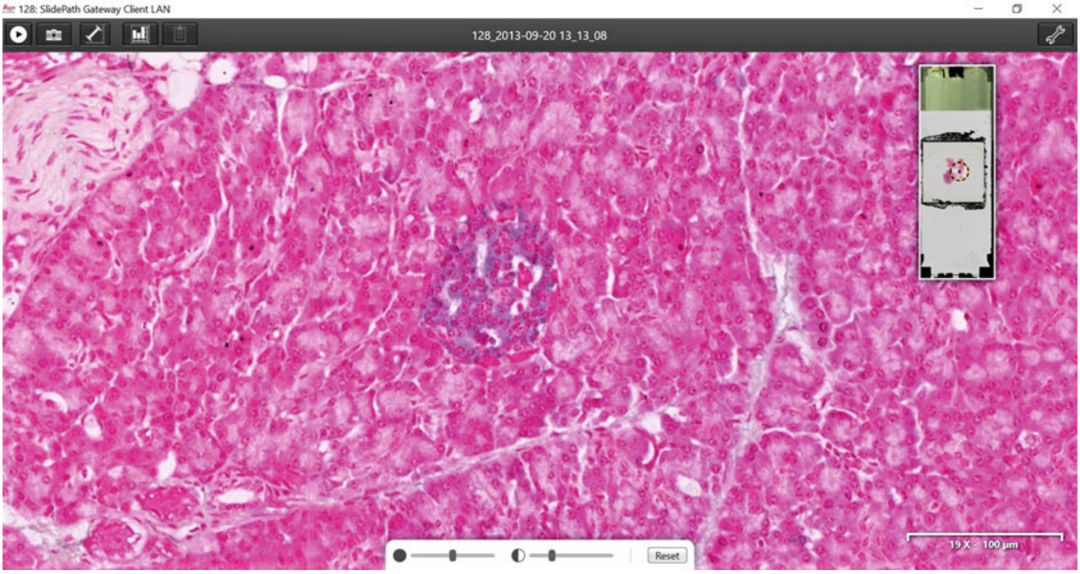

Fig. 3.4 Zoomed-in visual of database Section 128—Pancreas. The SlidePath Gateway Client 2.0 (Leica Microsystems, Germany) software offers a 'snapshot' tool allowing students to capture the image of interest for future reference. A mini 'navigation' slide pinpoints the viewing location

with the virtual database to visualize the tissue sections for each practical. It goes without saying that there were numerous teething problems and troubleshooting these made us adapt rapidly to the 'new normal'.

Zoom meeting sessions with the use of the virtual database enabled academic and students' interaction, interpretation and discussions to continue with regards to Histology practical sessions. The text chat feature of Zoom allowed students to put forward questions without disrupting the navigation of tissue sections. Whilst the recording feature made it possible to record the practical session which was later uploaded to the ULOP system where students could access and review the session at their leisure for revision (Fig. 3.6).

The following are examples of universities that have introduced and are currently using this technology: University of Minnesota; University of Turku, Finland (Helle et al. 2013); University of Virginia School of Medicine (Bloodgood 2012); Queen's University Belfast, UK (Hamilton et al. 2012); Maurice and Gabriela Golfschleger School of Dental Medicine (Ianculovici et al. 2012); University of Manchester (Choudhury and Gouldsborough 2012); Institute of Pathology, Germany (Kayser et al. 2004); New York City Department of Health and Mental Hygiene (Hemans-Henry et al. 2012) and University of Medical Science, Przybyszewski, Poland (Szymas and Lundin 2011). These aforementioned institutions noted that digital histology has been well received by their students and is seen as a significant advance in education and a more desirable method of learning. These systems, in the abovementioned universities, have helped to address workforce shortages whilst others have used this platform as refresher courses and assessment centres.

Universities which have fully digitized their slide libraries have emphasized the value of immortalizing their scarce slide resources which are pivotal in pathology teaching. The web-based environments they have created allow them to correspond with distance learning student populations (Makki et al. 2023). Advances in clinical pathology have been based on pilot systems like these to help diagnose and treat patients between medical professionals seated in different rooms. This technology facilitates the

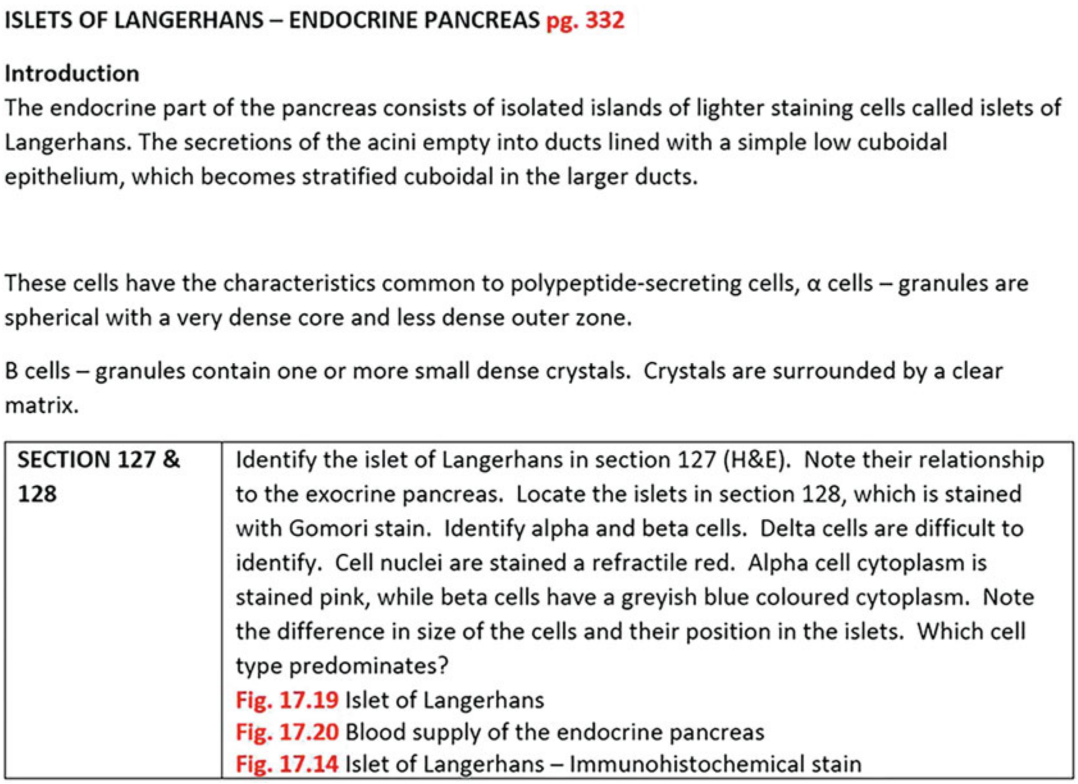

ISLETS OF LANGERHANS – ENDOCRINE PANCREAS pg. 332

Introduction

The endocrine part of the pancreas consists of isolated islands of lighter staining cells called islets of Langerhans. The secretions of the acini empty into ducts lined with a simple low cuboidal epithelium, which becomes stratified cuboidal in the larger ducts.

These cells have the characteristics common to polypeptide-secreting cells, α cells – granules are spherical with a very dense core and less dense outer zone.

B cells – granules contain one or more small dense crystals. Crystals are surrounded by a clear matrix.

SECTION 127 & 128	Identify the islet of Langerhans in section 127 (H&E). Note their relationship to the exocrine pancreas. Locate the islets in section 128, which is stained with Gomori stain. Identify alpha and beta cells. Delta cells are difficult to identify. Cell nuclei are stained a refractile red. Alpha cell cytoplasm is stained pink, while beta cells have a greyish blue coloured cytoplasm. Note the difference in size of the cells and their position in the islets. Which cell type predominates? Fig. 17.19 Islet of Langerhans Fig. 17.20 Blood supply of the endocrine pancreas Fig. 17.14 Islet of Langerhans – Immunohistochemical stain

Fig. 3.5 Example of the practical manual referring to the visuals in Fig. 3.4. Included in the practical manual are points of reference to the prescribed textbook, highlighted in red text

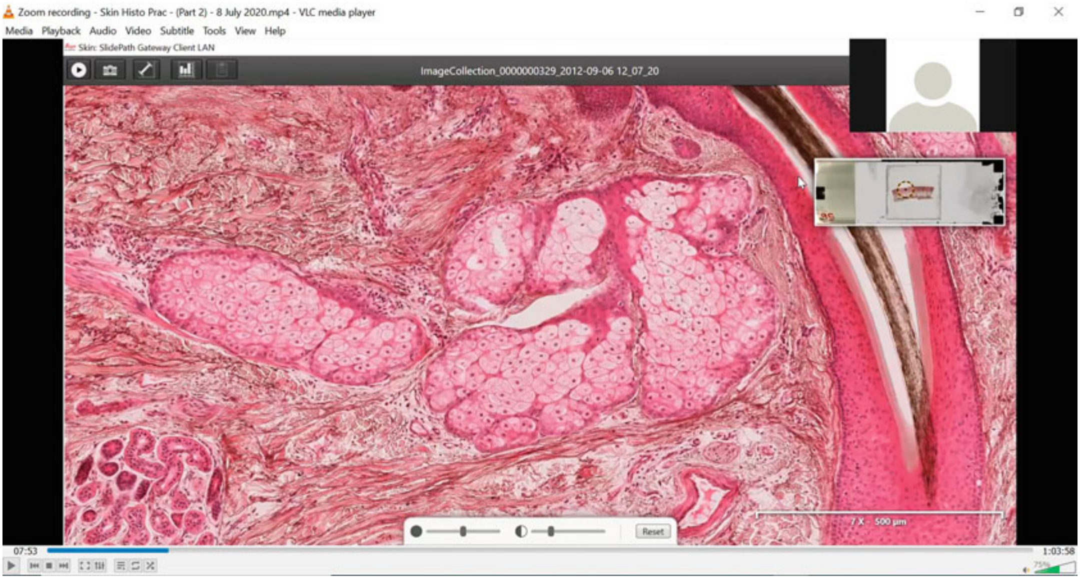
Zoom recording - Skin Histo Prac - (Part 2) - 8 July 2020.mp4 - VLC media player
Media Playback Audio Video Subtitle Tools View Help
Skin: SlidePath Gateway Client LAN
ImageCollection_0000000329_2012-09-06 12_07_20
7 X 500 µm
Reset
07:53
1:03:58
75%

Fig. 3.6 Screenshot of a Zoom Histology session

use of unusual and unique specimens for teaching and training, such as small tissue biopsies and other relevant patient materials that cannot be duplicated or reproduced due to limited samples. Examination and feedback are in real time, thus enhancing transferable skills. Notably, online learning may effectively integrate public health-orientated training into clinical residency courses (Kim and Bonk 2006; Wittich et al. 2017; Hemans-Henry et al. 2012).

Post-COVID-19, many institutes have opted for hybrid and blended methods of teaching and learning. In the comprehensive approach of hybrid learning, some students will attend the lecture or laboratory session in person whilst others will do so virtually. The academic instructs both their in-person and online students simultaneously, so virtual learners are not watching recordings but are actively participating. Whilst blended learning is more widely understood than hybrid learning, it combines traditional in-person instruction with online learning to extend the amount of time students spend in a physical lecture or laboratory venue. This blend of traditional in-person instruction with technology-enhanced online learning significantly increases student engagement across the multimodal learning spectrum. Recent studies indicate that students prefer and perform better in the hybrid and blended learning environment compared with the didactic method. This further demonstrates that the hybrid and blended teaching mode is superior to the traditional didactic teaching mode and may raise the calibre of histology instruction, encourage teacher–student interaction, and enhance both teaching and learning (Al-Alami et al. 2022; Huijie et al. 2022; Zhong et al. 2022a; Ruan et al. 2022; Zhong et al. 2022b). The future augurs well for institutes that have transitioned from traditional to virtual microscopy.

3.13 Digital and Virtual Microscopy as a Research Tool

A similar mind-set can be adopted for post-graduate histology-based research projects where access between supervisor and student is limited. Research units will no longer require bulky multi-head microscopes to focus on experimental slide work. Students will not need to spend many hours viewing and capturing images for their publications and thesis. The acquisition of the Leica SCN400 slide scanner enables us to offer whole slide imaging (WSI) services to other departments within our institute as well as to universities, schools and colleges external to our institute, resulting in numerous publications.

3.14 Conclusion

The forced move from didactic delivery of histology practical sessions to virtual microscopy practical sessions during the COVID pandemic, has contributed greatly to the successful study of histology. The true value of teaching using virtual microscopy will be seen as this highly adaptable medium continues to be applied to specific teaching and learning needs. We look forward to improved technologies, artificial intelligence, and machine learning building on and contributing positively to teaching and learning. We plan to develop online distance learning in an outreach programme aimed at benefiting students in remote locations who would otherwise have no access to the physical location of our institute. This will facilitate an exponential growth of student enrolment with reduced stress on infrastructure. Furthermore, virtual teaching mediates liaison with national and international experts in various fields of medical science by creating online information sharing and troubleshooting sessions.

3.15 Limitations of Digital and Virtual Microscopy

Higher education institutions in low- and middle-income countries may not be able to afford the initial cost of the hardware required to digitize microscopic glass slides. Another significant expense is the conversion of traditional histology facilities to accommodate the digital set-up. When conducting on-site or off-campus histology sessions, the inconsistent electrical power supply experienced in many of these countries presents a challenge. Virtual microscopy also demands well-maintained servers and high-bandwidth Internet.

References

Al-Alami ZM, Adwan SW, Alsous M (2022) Remote learning during Covid-19 lockdown: a study on anatomy and histology education for pharmacy students in Jordan. Anat Sci Educ 15(2):249

Araki T (2017) The history of the optical microscope. Mech Eng Rev 4(1):16-00242-16

Ball CS (1966) The early history of the compound microscope. Bios:51–60

Barraquer JI (1980) The history of the microscope in ocular surgery. Microsurgery 1(4):288–299

Bloodgood R (2012) Active learning: a small group histology laboratory exercise in a whole class setting utilizing virtual slides and peer education. Anat Sci Educ 5(6):367–373

Choudhury B, Gouldsborough I (2012) The use of electronic media to develop transferable skills in science students studying anatomy. Anat Sci Educ 5(3): 125–131

Darafsheh A, Abbasian V (2023) Dielectric microspheres enhance microscopy resolution mainly due to increasing the effective numerical aperture. Light Sci Appl 12(1):22

Dee FR (2009) Virtual microscopy in pathology education. Hum Pathol 40(8):1112–1121

Francis DV, Charles AS, Jacob TM, Ruban A, Premkumar PS, Rabi S (2022) Virtual microscopy as a teaching–learning tool for histology in a competency-based medical curriculum. Med J Armed Forces India. https://doi.org/10.1016/j.mjafi.2022.02.002

Hamilton PW, Wang Y, McCullough SJ (2012) Virtual microscopy and digital pathology in training and education. APMIS 120(4):305–315

Helle L, Nivala M, Kronqvist P (2013) More technology, better learning resources, better learning? Lessons from adopting virtual microscopy in undergraduate medical education. Anat Sci Educ 6(2):73–80

Hemans-Henry C, Greene CM, Koppaka R (2012) Integrating public health-oriented e-learning into graduate medical education. Am J Prev Med 42(6 Suppl 2): S103–S106. https://doi.org/10.1016/j.amepre.2012.03.019

Huijie Y, Lina Q, Yonghong Z, Ying D, Wei Z, Chaohong L et al (2022) The application of student-centered online and offline blended teaching model in histology and embryology. Med Res 4:3

Ianculovici C, Dvoyris V, Shenkman A (2012) Distance E-learning model for IDF dentists. Refu'at Ha-peh Veha-shinayim (1993) 29(1):48–53. 66

Joaquim DC, Hortsch M, Silva ASR, David PB, Leite ACRM, Girão-Carmona VCC (2022) Digital information and communication technologies on histology learning: what to expect?—an integrative review. Anat Histol Embryol 51(2):180–188

Kayser K, Kayser G, Radziszowski D, Oehmann A (2004) New developments in digital pathology: from telepathology to virtual pathology laboratory. Stud Health Technol Inform 105:61–69

Kim K-J, Bonk CJ (2006) The future of online teaching and learning in higher education. Educ Q 29(4):22–30

Krippendorf BB, Lough J (2005) Complete and rapid switch from light microscopy to virtual microscopy for teaching medical histology. Anat Rec B New Anat 285(1):19–25

Lakhtakia R (2021) Virtual microscopy in undergraduate pathology education: an early transformative experience in clinical reasoning. Sultan Qaboos Univ Med J 21(3):428

Makki Z, Malcolm J, Miguel JC (2023) COVID-19 adaptations with virtual microscopy. Biomedical visualisation. Springer, pp 173–197

Mertz L (2023) Advances in microscopy tech offer better views. IEEE Pulse 14(1):2–7

Oblinger D (2003) Boomers gen-xers millennials. Educ Rev 500(4):37–47

Pokhrel S, Chhetri R (2021) A literature review on impact of COVID-19 pandemic on teaching and learning. Higher Education for the Future 8(1):133–141

Qing J, Cheng G, Ni X-Q, Yang Y, Zhang W, Li Z (2022) Implementation of an interactive virtual microscope laboratory system in teaching oral histopathology. Sci Rep 12(1):1–11

Reimers FM. Learning from a pandemic. The impact of COVID-19 on education around the world. Primary and secondary education during Covid-19: Disruptions to educational opportunity during a pandemic. 2022:1–37

Ruan Y, Zhang J, Cai Q, Wang J, Liu G, Liu Y et al (2022) Evaluation of a prerequisite course of histology implementation for Chinese students of eight-year medical programme: a mixed quantitative survey. BMC Med Educ 22(1):514

Sakthi-Velavan S, Zahl S (2023) Integration of virtual microscopy podcasts in the histology discipline in osteopathic medical school: learning outcomes. Anat Sci Educ 16(1):157–170

Szymas J, Lundin M (2011) Five years of experience teaching pathology to dental students using the WebMicroscope. Diagnostic Pathology: BioMed Central. 1–6

Tarkar P (2020) Impact of COVID-19 pandemic on education system. Int J Adv Sci Technol 29(9):3812–3814

Wittich CM, Agrawal A, Cook DA, Halvorsen AJ, Mandrekar JN, Chaudhry S et al (2017) E-learning in graduate medical education: survey of residency program directors. BMC Med Educ 17:1–7

Zhong J, Li Z, Hu X, Wang L, Chen Y (2022a) Effectiveness comparison between blended learning of histology practical in flipped physical classrooms and flipped virtual classrooms for MBBS students. BMC Med Educ 22(1):1–8

Zhong TC, Saad MIM, Ahmad CNC (2022b) Integrating technology-mediated learning in biology education (histology): a systematic literature review. J ICT Educ 9(1):86–99

4

How Visualizations Have Revolutionized Taxonomy: From Macroscopic, to Microscopic, to Genetic

Andrew J. Lunn, Isabelle C. Winder, and Vivien Shaw

Abstract

We, as humans, are natural taxonomists, with a preference for classifying things as a means of understanding them. Taxonomy (the classification of all organisms) is central to our understanding of biodiversity and evolution, and, therefore, to our ability to conserve organisms and ecosystems. However, the way scientists classify organisms has changed over time as a series of new technological innovations have arisen, mainly focused on new ways of visualizing comparisons. These innovations, and the impact they have had on how we "see," are the focus of this chapter. First, we explore how Aristotle and Carl Linnaeus helped found taxonomy by developing schemes to classify organisms based on similarities and differences in their gross (macroscopic) anatomy. While many of these classifications are still accepted to this day, others have been refined as new lines of evidence arose. The invention of microscopy and the several types of visualizations associated with it, e.g., photomicrographs, allowed later scientists to start classifying smaller organisms and develop their understanding of the fundamental biology of large ones. Finally, the late twentieth-century emphasis on visualizing genes and not anatomy, has also driven significant reclassifications. Broadly speaking, anatomical-based definitions of taxonomy are better at showing ecological patterns, while genetic definitions help us to recognize underlying similarities between species that may look very different, or conversely to see that similar-looking animals are in fact completely distinct species that happen to have arrived at a similar body plan. Fundamentally, the way we do taxonomy, i.e., looking for similarities or differences, has remained the same, but integrating new visualizations into classifications has both clarified how organisms are related in terms of evolution, and progressed biological science as a whole.

Keywords

Taxonomy · Visualization · Classification · Macroscopic · Microscopic · Genetics

4.1 Introduction

Taxonomy is, in its simplest form, the science of describing, naming, and classifying organisms such as animals and plants based on characteristics including their genetic traits, biochemical processes, and behavioral and morphological characteristics (Convention on Biological

A. J. Lunn (✉) · I. C. Winder
School of Natural Sciences, Bangor University, Bangor, UK

V. Shaw
Academic Visitor at Hull York Medical School, Faculty of Health Sciences, University of Hull, Hull, UK

© The Author(s), under exclusive license to Springer Nature Switzerland AG 2023

L. Shapiro (ed.), *Microscopy Techniques for Biomedical Education and Healthcare Practice*, Biomedical Visualization 2, https://doi.org/10.1007/978-3-031-36850-9_4

Diversity 2010). The ability to explain and organize your surroundings using specific, distinct categories has been fundamental to human survival and is likely to have been practiced by our early ancestors. For example, the ability to distinguish effectively between edible and poisonous plants is a crucial one (Manktelow 2010). Even now, in our everyday lives, we place ordinary objects that surround us into distinct categories. For example, you probably would not choose to put a book in your kitchen cupboards with your pots and pans, or the fruit bowl in the bathroom. We, as humans, have a tendency to seek out patterns and have done so for thousands of years.

One of the first known collections of texts dedicated to medical botany, also known as a pharmacopeia, is the "*Shennong Ben Cao Jing*" ("Classic of the Materia Medica"/"Shennong's Herbal Classics") which originates from the Eastern Han dynasty of China and was compiled by multiple authors between 25 and 220 AD (Wachtel-Galor et al. 2011). This collection of texts is attributed to the mythological Chinese emperor "Shennong" also known as the "Divine Husbandman" or "Divine Farmer" (Fig. 4.1). Shennong was born in the twenty-eighth century BCE, and this work catalogs 365 species of medicinal plants across three volumes and describes their pharmacological uses (Britannica 2019a). One of the medicinal herbs discussed in the second volume (titled "Herbs: Middle Class") is *Gan Jiang*, or Ginger (*Zingiber officinale*), which is said to be used to combat vomiting, abdominal pain, headaches, nasal congestion, worm and insect bite toxins, and to promote sweating (Shou-zhong 1998). Another example of a herb described in ancient Chinese medicine is *Artemisia annua*, which was said to treat pain in joints (Shou-zhong 1998). In modern medicine, artemisinin and its derivatives are used in the treatment of malaria and the work underlying the development of this medicine won a share of the 2015 Nobel Prize in Physiology or Medicine (Klayman 1985; Krungkrai and Krungkrai 2016; Wang et al. 2019; Youyou 2017). Shennong's book represents one of the earliest texts that includes some taxonomy of plants, alongside information about their medicinal uses.

In Ancient Egypt (c. 1500 BCE), 13 centuries after Shennong's pharmacopeia, a compilation of medical texts called the Ebers Papyrus was produced detailing a range of remedies to cure a multitude of afflictions (Fig. 4.1) (Britannica 2019b). Some of the species included in this papyrus include opium, cannabis, myrrh, thyme, aloe, castor oil, and garlic (Aboelsoud 2010). Garlic, for example, was seen as an important substance that could be taken to treat sore throats and reduce the symptom severity of colds. While the efficacy of substances like garlic and ginger as cures is still debated (Anh et al. 2020; Arfeen et al. 1995; Josling 2001; Lissiman et al. 2014; Marx et al. 2017; Nantz et al. 2011), other discoveries such as artemisinin have proved to be very important. The fact that all are still recognizable plants/species under both the ancient Chinese/Egyptian and modern Western taxonomic schemes highlights just how ubiquitous the human urge to classify really is.

Taxonomy and classification are still important to medical science today. For example, establishing which antivenoms will work for a given snake bite (e.g., a rattlesnake) depends on where the venom stems from, as different snakes have different types of venom (Rogalski et al. 2017; Wüster 1996). The main uses of taxonomy in current scientific research, however, are in the protection and conservation of species and to help understand biodiversity and evolutionary histories (Mace 2004). The IUCN (International Union for Conservation of Nature) Red List is "the world's most comprehensive information source on the global extinction risk status of animal, fungi, and plant species," and requires formal taxonomic assessment to add a species to the list and collect and evaluate data on distributions, population trends, and conservation actions for as many species as possible (IUCN Red List 2022). The scale of this work is vast, and many citizen science projects exist to support the gathering of data via apps such as iNaturalist and Seek. These descriptions are made publically available via the IUCN, and the information enables us to better understand the ecological needs of these species and how best to approach protecting them (IUCN Red List 2023). Similarly, the biodiversity of a

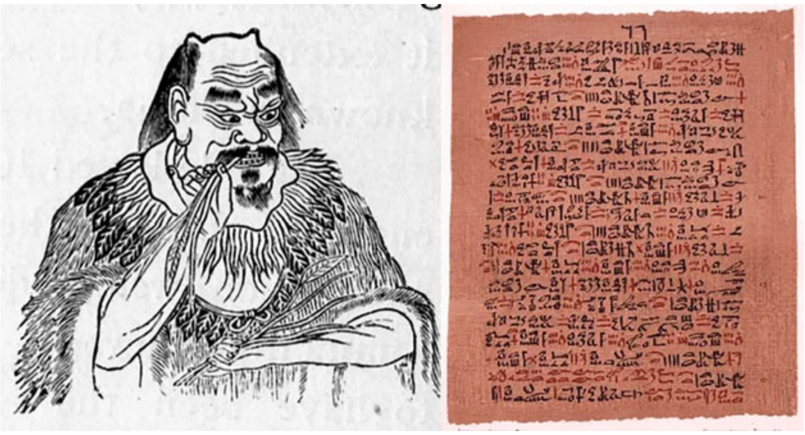

Fig. 4.1 (*Left*) Depiction of mythological Chinese ruler Shennong, also known as the "Divine Husbandman" or "Divine Farmer" as he consumes herbs to discover their qualities. Shennong is credited with originating some of the first collections of texts on medicinal botany and the pharmacological effects of plants. Image from the Outline of Chinese History by Li Ung Bing, Shanghai 1914 and licensed under creative commons, CC0 1.0 (PD-US-expired). (*Right*) Ancient Egyptian medical papyrus (titled "The Ebers Papyrus" c. 1550 BCE) detailing a range of medicinal uses for different plants and herbs. Image from the National Library of Medicine and licensed under creative commons, CC0 1.0 (PD-USGov)

particular area can be measured by looking at the variety of different organisms such as animals, plants, fungi, and microorganisms found at that site (Hancock and World Wildlife Foundation 2023). By definition, in order to measure them it is essential to be able to identify all the organisms within the area assessed. This is important to the sustainable maintenance of the varied ecosystems that we rely on so heavily (The Royal Society 2023). Finally, taxonomy using comparative anatomy (see Sects. 4.2–4.3) or genetics (discussed in Sect. 4.4), is also shedding light on the evolutionary histories of different lineages by exploring their relationships with one another. This, in turn, can help us demonstrate how different environmental pressures have shaped evolution and what this may mean for the current diversity of organisms on our planet.

Our primary aim in this chapter is to explore how the way in which we do taxonomy has evolved globally and through history. We will be looking at the technological developments that have created new ways in which we can "see" organisms, and how these new ways of seeing then accompany and support new forms of scientific understanding that were previously impossible. We move from macroscopic anatomical examination to the many new insights gained via microscopic examination, before finally looking at the genetic visualization of an organism, where the information we are looking at is completely abstracted away from the macroscopic or microscopic appearance of the animal or plant.

The macroscopic approach classifies organisms by examining their anatomy with the naked eye. As we have described, this kind of taxonomy was already important thousands of years ago in ancient China, Egypt, and Greece, and at least in some cases resulted in these societies having identified the same groups we would now call "species." We will explore this further (in Sect. 4.2) by looking at what seems to be the first systematic classification of animals, by the Greek philosopher Aristotle, before considering the work of the "father of modern taxonomy," Carl Linnaeus, who devised the system of binomial nomenclature (two-name naming system) (c. 1758) that is still used to this day (2023). Linnaeus used observations of macroscopic anatomical features such as bone and tooth morphology and behavioral observations to place animals into groups. However, in some cases, what we can see with the naked eye does not actually show us the whole picture. In Sect. 4.3, we summarize how the invention and effectiveness of the microscope, which allowed people to see what was previously invisible, caused the first revolution in taxonomic practice, allowing us to see beyond what is possible with the naked eye. Finally, in Sect. 4.4 we look at the most technologically advanced way of classifying organisms, genetic analysis. When we visualize an organism's genome, we can develop a taxonomic description of the code that underlies how it manifests in the world, giving us additional insights into not just how the organism is in the present day, but also where it fits into maps of the timeline of evolution of life on Earth.

By starting with gross anatomy and moving through ever more detailed, focused visualizations, scientists have effectively been shifting taxonomy onto an ever-increasing abstract basis. The fundamental approach to classification, i.e., looking for similarities and differences between organisms, has remained essentially the same, but it is these innovative visualization techniques that have caused fundamental shifts in the way that we understand evolutionary biology and the associated fields that draw on our ability to describe and classify organisms.

4.2 The Macroscopic: What Is Visible with the Naked Eye

4.2.1 The Aristotelian System

The Ancient Greek philosopher Aristotle (c. 384 BCE–322 BCE) wrote on a vast range of topics including biology, botany, philosophy of science, and zoology, but his work on classification dominated the field of taxonomy up until the eighteenth century (Amadio and Kenny 2023; Cain 2022). Aristotle was one of the first known scientists to classify animals and some of his broad groups, such as vertebrates and invertebrates, provided the basis of taxonomic keys where we can refine classifications according to different morphological elements (Manktelow 2010). His major taxonomic work, *De Partibus Animalium*, or "On the Parts of Animals," written c. 350 BCE, was dedicated to documenting animal anatomy and physiology (Table 4.1) (Aristotle and Ogle 1882a, b). Aristotle's taxonomy relied on organisms' physical characteristics, using an approach called phenetics. Phenetic research organizes animals into groups (taxa) on the basis of their overall morphological similarity without concern for evolutionary relationships (Choudhuri 2014). In the absence of microscopes, Aristotle's phenetic classifications focused solely on the macroscopic (visible) features of each animal.

Some of Aristotle's taxa are still recognized today (Table 4.1) and the macroscopic approach works remarkably well in many cases, even where classification is complex. For example, cetaceans (dolphins and whales), might at first be assumed to be closely related to fish, sharks, and other water living animals due to their superficial similarities, e.g., shape and shared environment. However, Aristotle correctly identified that cetaceans did not have gills as fish do, but rather had lungs like mammals. This meant that cetacea could not simply be classed as either "water-animals," or "land-animals," and so warranted their own unique classification which Aristotle nested within the Mammalia (Aristotle and Ogle 1882a, b, p.139, 205) (Table 4.1). Marine species, in particular, can be extremely difficult to classify as we are accustomed to the characteristics of animals that live on land, and marine animals—from sponges through to octopi via fish, jellyfish, and hydroids that look like plants and scallops—are in many cases considered to be fundamentally "other." As taxonomy advanced between c. 350 BCE and the middle of the eighteenth century, more and more groups were recognized and recorded using a system similar to Aristotle's, and much time was spent classifying and reclassifying borderline cases on the basis of their various macroscopic traits.

Table 4.1 A recreated and modified (by the author) table from Aristotle's "On the Parts of Animals" written c. 350 BCE, translated by William Ogle in 1882. Here Aristotle groups different animals depending on certain physical characteristics that he has observed. The first way in which Aristotle groups animals is according to whether they are Sanguineous (full of blood) or Bloodless. These words have now been replaced by Vertebrates and Invertebrates. Aristotle's second grouping characteristics (i.e., Vivipara or Ovipara) refer to whether the embryo develops inside the body as a fetus, or outside the body in an egg. While many of his further groupings are now defunct, having been renamed or changed to include different organisms, Aristotle's taxonomical groupings remain as accurate groupings based on the macroscopic characteristics of different types of animals

i.	Sanguineous Animals [*Vertebrata*].	
	A. Vivipara [*Mammalia*].	1. Man. [now a part of primates]
		2. Quadrupeds.
		3. Cetacea.
	B. Ovipara.	
	α. With perfect ovum.	4. Birds.
		5. Quadrupeds and Apoda [*reptiles and Amphibia*].
	β. With imperfect ovum.	6. Fishes.
ii.	Bloodless Animals [*Invertebrata*]	
	α. With imperfect ovum.	7. Malacia [*Cephalopods*, e.g., octopus and squid.].
		8. Malacostraca [*Crustacea*, e.g., crab and lobster].
	β. With scolex.	9. Insecta [*Remaining Arthropoda,* e.g., spiders *and some Vermes,* defunct taxon equivalent to worms].
	γ. With generative slime, buds, or spontaneous generation.	10. Ostracoderma or Testacea [*Mollusca,* snails, oysters, etc. *excepting Cephalopods*].
	δ. With spontaneous generation only.	11. [*Zoophytes*, e.g., coral or sea anemone].

4.2.2 The Linnaean System

4.2.2.1 Linnaeus and Binomial Nomenclature

Carl Linnaeus (Carolus Linnæus or Carl von Linné) was a Swedish zoologist, botanist, taxonomist, and physician living between 1707 and 1778. He is best known for creating a standardized system for naming a group of organisms (taxa) known as "binomial nomenclature" (Müller-Wille 2023). Binomial nomenclature gives each organism a unique name composed of two parts and is still in use, governed by organizations such as the *International Commission of Zoological Nomenclature* (ICZN 2023), the *International Association For Plant Taxonomy* (IAPT 2023), or the *International Commission on the Taxonomy of Fungi* (ICTF 2023). A binomial (bi = two, nomial = name) is made up of two parts; the first part referring to the broad group (or genus) that the organism belongs to, and the second to a specific species. In the scientific field of taxonomy, a species is defined as a group of individual organisms that "are more closely related to each other than they are to any other organisms," while the genus is a broader category that contains a group of species that are very closely related and share many physical similarities (Britannica 2023). For example, the binomial name for humans is *Homo sapiens*, meaning we are part of the same genus (*Homo*) as are some other human relatives such as the Neanderthals, but a separate distinct species (*Homo sapiens* as opposed to *Homo neanderthalensis*). Binomial names allow for global consistency when studying or conversing about organisms regardless of language. The common name for example for *Lynx pardinus* is "Iberian Lynx" in English, but in Spain the only place where they are still extant (Rodríguez and Calzada 2015) is "Lince ibérico." Using the binomial allows us to be sure we are talking about the same thing with greater precision.

The binomial system introduced by Linnaeus stems from his rank-based system of classification. We have already discussed the categories "Genus" and "Species" above, which are the two lowest ranks within Linnaeus' hierarchy. He also introduced, in ascending order, "Kingdom," "Class," and "Order," with the Kingdom level positioned above the Genus level. Biological Kingdoms are the broadest categories in this hierarchy, with "Animalia" housing all multicellular, eukaryotic organisms while "Plantae" contained predominantly photosynthetic eukaryotes. As one moves down Linnaeus' hierarchy, one gradually sees increasingly specific characteristics that organisms within that group share with one another, until you eventually arrive at the level of recognizing unique species (Fig. 4.2). It is important to note that since Linnaeus employed his hierarchal system, the biological classification levels "Domain" (Woese et al. 1990), "Phylum," and "Family" have all been added to it, as well as prefixes such as "sub," "infra," and "super" which allow scientists to further distinguish more taxonomic levels in between the standard ones.

This hierarchical system of formally naming species proved incredibly influential in the biological sciences, earning Linnaeus the title of the "father of modern taxonomy" (Calisher 2007; Manktelow 2010). Linnaeus' books not only proposed these new systems for taxonomy but also included detailed observational notes and put his new classification process into practice for hundreds of organisms. This provided more and more information for taxonomic keys, so we can identify known species according to different morphological elements, as well as recognize new ones.

4.2.2.2 How Linnean Classification Visualizes Organisms?

Linnaeus's method of classification was similar to Aristotle's (Sect. 4.2.1), in that he classified organisms based on overall macroscopic morphological similarities and differences, i.e., what he could physically see. While some species have since been reclassified, a lot of the names he assigned have remained in use. In the book *Systema Naturæ* (1735), Linnaeus classified organisms into three kingdoms—animals (Regnum Animale), plants (Regnum Vegetabile), and minerals (Regnum Lapideum) before dividing them further into different classes (Linnaeus and Salvius 1758). Although there are some similarities, this system builds on and goes far beyond Aristotle's earlier work on animals to create a classification system to describe the whole of the natural world. Volume two of this monumental work is concerned with classifying plants. As an example of his method, we can look at the Decandria (Fig. 4.3), or flowers with ten stamens (a stamen is the male reproductive part of a flower (Bhatia 2015)). One of the species of flower that Linnaeus then classified under his Decandria was *Kalmia latifolia*, (Mountain Laurel) an evergreen shrub with pale pink flowers in large clusters and ten stamens (Fig. 4.3) (Royal Horticultural Society 2023).

Here, Linnaeus took a visible feature (stamens) and used it to group certain plant species together on the basis of observations of varying stamen numbers. The category Decandria no longer exists but the binomial name assigned by Linnaeus to *Kalmia latifolia* is still in use and taxonomists still use observations of visible anatomy alongside newer approaches to classification.

Since Linnaeus, taxonomy has progressed significantly, with major changes even in his own lifetime between the first and tenth editions of the *Systema Naturæ* (1735 and 1758, respectively) as observations of organisms were repeated and standardized. For instance, the first edition contains a now-defunct taxon called Anthropomorpha which included humans (*Homo)*, monkeys and apes (*Simia*), and sloths (*Bradypus*) (Sherborn, et al. 1933). By the tenth edition Anthropomorpha had been replaced with Primates, sloths had been moved to a different order and two new genera (*Lemur*, a type of primate that lives in Madagascar, and *Vespertilio*, a group of bats) had been added (Fig. 4.4).

But why did Linnaeus classify bats as primates? The answer comes down to the fact that primates and bats shared morphological features that Linnaeus could physically see. He wrote that they can be grouped because they all

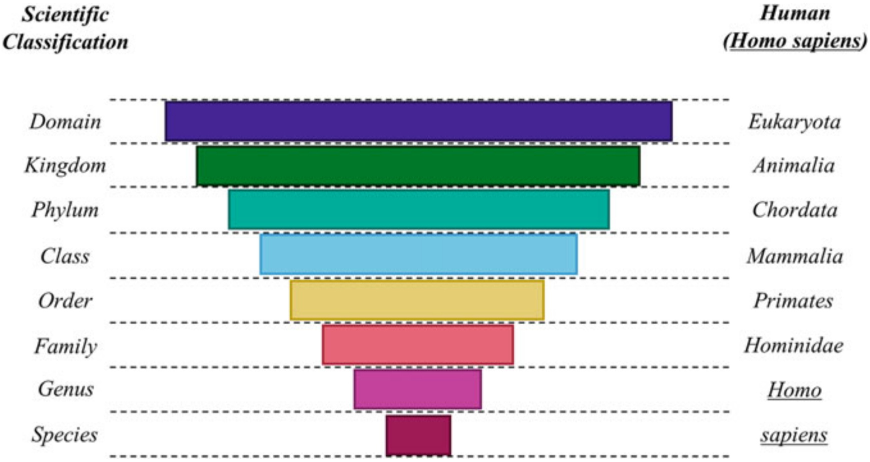

Fig. 4.2 The hierarchy used for modern classification which was first partially implemented by Carl Linnaeus in the tenth edition of *Systema Naturæ* (1758) and *Species Plantarum* (1753). Domain, Phylum, and Family have all been added since, to distinguish further levels. As you move down the hierarchy, the groups are more and more narrowly defined. This means that a Domain is the broadest category, containing a huge diversity of organisms, while species is the most specific and singles out a set of organisms that are more closely related to one another than any other organism. On the right of the figure is an example of human classification starting with the domain Eukaryota and kingdom Animalia before being given the specific binomial name *Homo sapiens*. Figure created by the chapter author using a color pallet by Tol (2021) for accessibility and clarity

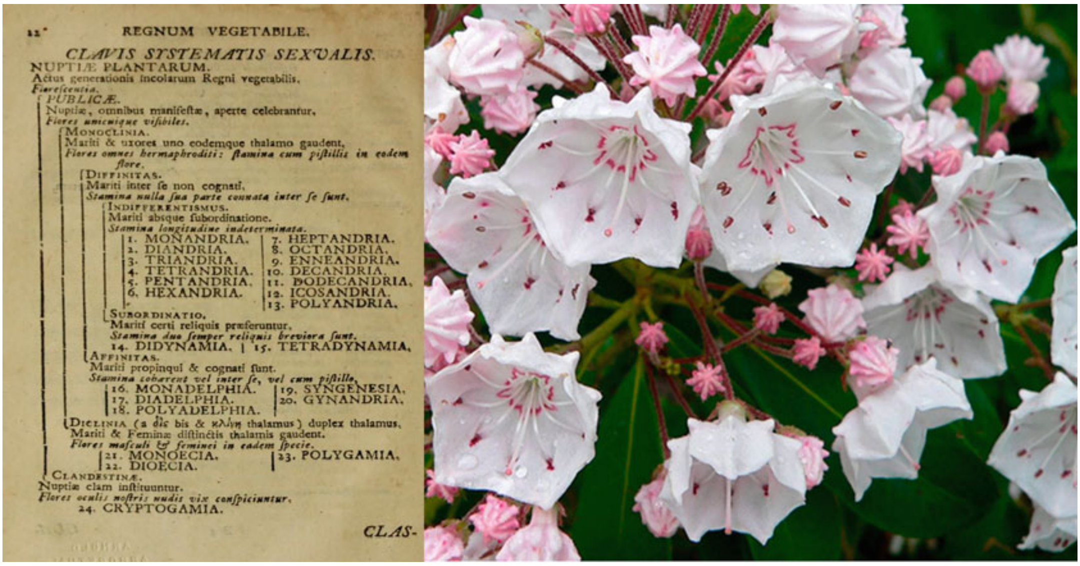
12* REGNUM VEGETABILE.

CLAVIS SYSTEMATIS SEXUALIS.

NUPTIÆ PLANTARUM.
Actus generationis incolarum Regni vegetabilis.
Floreſcentia.
PUBLICÆ.
Nuptiæ, omnibus manifeſtæ, aperte celebrantur.
Flores unicuique viſibiles.
MONOCLINIA.
Mariti & uxores uno eodemque thalamo gaudent.
Flores omnes hermaphroditi: ſtamina cum piſtillis in eodem flore.
DIFFINITAS.
Mariti inter ſe non cognati.
Stamina nulla ſua parte connata inter ſe ſunt.
INDIFFERENTISMUS.
Mariti abſque ſubordinatione.
Stamina longitudine indeterminata.
1. MONANDRIA.
2. DIANDRIA.
3. TRIANDRIA.
4. TETRANDRIA.
5. PENTANDRIA.
6. HEXANDRIA.
7. HEPTANDRIA.
8. OCTANDRIA.
9. ENNEANDRIA.
10. DECANDRIA.
11. DODECANDRIA.
12. ICOSANDRIA.
13. POLYANDRIA.
SUBORDINATIO.
Mariti certi reliquis præferuntur.
Stamina duo ſemper reliquis breviora ſunt.
14. DIDYNAMIA. | 15. TETRADYNAMIA.
AFFINITAS.
Mariti propinqui & cognati ſunt.
Stamina cohærent vel inter ſe, vel cum piſtillo.
16. MONADELPHIA.
17. DIADELPHIA.
18. POLYADELPHIA.
19. SYNGENESIA.
20. GYNANDRIA.
DICLINIA (a δὶς bis & κλίνη thalamus) duplex thalamus.
Mariti & Feminæ diſtinctis thalamis gaudent.
Flores maſculi & feminei in eadem ſpecie.
21. MONOECIA.
22. DIOECIA.
23. POLYGAMIA.
CLANDESTINÆ.
Nuptiæ clam inſtituuntur.
Flores oculis noſtris nudis vix conſpiciuntur.
24. CRYPTOGAMIA.

CLAS-

Fig. 4.3 (*Left*) A page from Linnaeus's *Systema Naturæ* tenth edition, volume two, discussing Regnum Vegetabile (the biological kingdom encompassing plants), and certain classes devised by Linnaeus based on morphological features, such as stamen count. Image sourced from the Biodiversity Heritage Library and licensed under creative commons, CC0 1.0 (PD-US-expired) (Linnaeus, 1767). (*Right*) *Kalmia latifolia*, named by Linnaeus, with ten stamens and therefore originally placed in Decandria class. Image titled *Kalmia latifolia in North Carolina* sourced from Arx Fortis and licensed under CC BY-SA 3.0

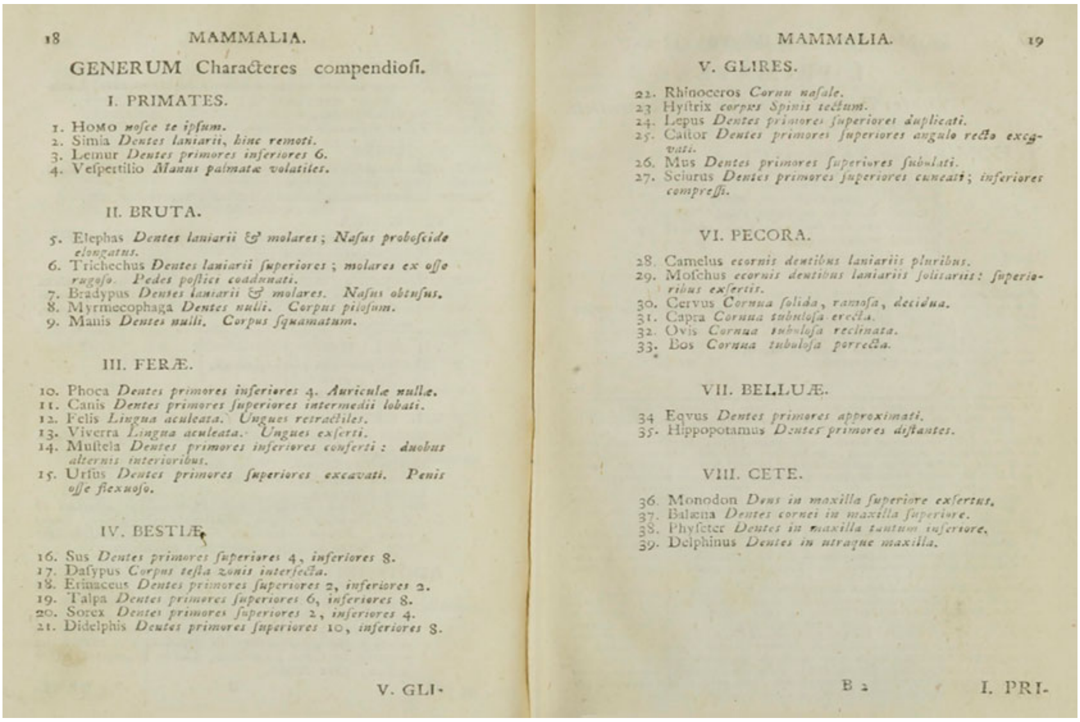

18 MAMMALIA.

GENERUM Characteres compendioſi.

I. PRIMATES.

1. Homo *noſce te ipſum.*
2. Simia *Dentes laniarii, hinc remoti.*
3. Lemur *Dentes primores inferiores 6.*
4. Veſpertilio *Manus palmatæ volatiles.*

II. BRUTA.

5. Elephas *Dentes laniarii & molares; Naſus proboſcide elongatus.*
6. Trichechus *Dentes laniarii ſuperiores; molares ex oſſe rugoſo. Pedes poſtici coadunati.*
7. Bradypus *Dentes laniarii & molares. Naſus obtuſus.*
8. Myrmecophaga *Dentes nulli. Corpus piloſum.*
9. Manis *Dentes nulli. Corpus ſquamatum.*

III. FERÆ.

10. Phoca *Dentes primores inferiores 4. Auriculæ nullæ.*
11. Canis *Dentes primores ſuperiores intermedii lobati.*
12. Felis *Lingua aculeata. Ungues retractiles.*
13. Viverra *Lingua aculeata. Ungues exſerti.*
14. Muſtela *Dentes primores inferiores conferti: duobus alternis interioribus.*
15. Urſus *Dentes primores ſuperiores excavati. Penis oſſe flexuoſo.*

IV. BESTIÆ.

16. Sus *Dentes primores ſuperiores 4, inferiores 8.*
17. Daſypus *Corpus teſta zonis interſecta.*
18. Erinaceus *Dentes primores ſuperiores 2, inferiores 2.*
19. Talpa *Dentes primores ſuperiores 6, inferiores 8.*
20. Sorex *Dentes primores ſuperiores 2, inferiores 4.*
21. Didelphis *Dentes primores ſuperiores 10, inferiores 8.*

V. GLI-

MAMMALIA. 19

V. GLIRES.

22. Rhinoceros *Cornu naſale.*
23 Hyſtrix *corpus Spinis tectum.*
24. Lepus *Dentes primores ſuperiores duplicati.*
25. Caſtor *Dentes primores ſuperiores angulo recto excavati.*
26. Mus *Dentes primores ſuperiores ſubulati.*
27. Sciurus *Dentes primores ſuperiores cuneati; inferiores compreſſi.*

VI. PECORA.

28. Camelus *ecornis dentibus laniariis pluribus.*
29. Moſchus *ecornis dentibus laniariis ſolitariis: ſuperioribus exſertis.*
30. Cervus *Cornua ſolida, ramoſa, decidua.*
31. Capra *Cornua tubuloſa erecta.*
32. Ovis *Cornua tubuloſa reclinata.*
33. Bos *Cornua tubuloſa porrecta.*

VII. BELLUÆ.

34 Eqvus *Dentes primores approximati.*
35. Hippopotamus *Dentes primores diſtantes.*

VIII. CETE.

36. Monodon *Dens in maxilla ſuperiore exſertus.*
37. Balæna *Dentes cornei in maxilla ſuperiore.*
38. Phyſeter *Dentes in maxilla tantum inferiore.*
39. Delphinus *Dentes in utraque maxilla.*

B 2 I. PRI-

Fig. 4.4 Pages 18 and 19 from Linnaeus & Salvius, (1758) detailing general characteristics for 39 genera within 8 taxonomic orders. Linnaeus grouped these genera by looking at their visible physical characteristics. For example, *Vespertilio* (bats) are grouped within the primates due to their palmed hands, while other genera are grouped together due to tooth morphology. Image sourced from the Biodiversity Heritage Library and licensed under creative commons, CC0 1.0 (PD-US-expired)

have four upper front teeth and palmed hands (Fig. 4.4). Today, with the addition of microscopic and genetic evidence on top of the macroscopic traits described, we know that bats are actually more related to carnivores, cetaceans, and odd-toed ungulates such as zebras, rhinos, or horses (perissodactyls) than to primates (Lin and Penny 2001; Madesn et al. 2001; Nikaido et al. 2000).

There are many other examples of taxa grouped by Linnaeus on the grounds of their shared visible features. The order Feræ, for example, was described by Linnaeus as having "Primary superior teeth of fex, sharp" (i.e., sharp superior teeth or canines) (Linnaeus and Salvius 1758. pp. 37) and there are several examples of animals in this order below (Fig. 4.5). Linnaeus primarily grouped these species together because of their sharp superior teeth or, as they are more commonly referred to, "canine teeth." These single-cusped, single-rooted teeth are located next to the incisors and are adapted for holding and gripping food which, in the case of carnivores, is vital to survival and explains why carnivore canines are so pronounced in comparison to those of other animals (Encyclopaedia Britannica 2014). Figure 4.5 explicitly shows this feature, and it is easy to see why Linnaeus assumed that the species showing this visually distinctive canine morphology must be more closely related to one another than any other species.

While many of Linnaeus's groupings remain in use, there are a few groups where his morphological groupings were not so long lived. One of the features Linnaeus associated with his "Beastiæ" group was a "nose protruding beyond the mouth" (Linnaeus and Salvius 1758. pp. 49),

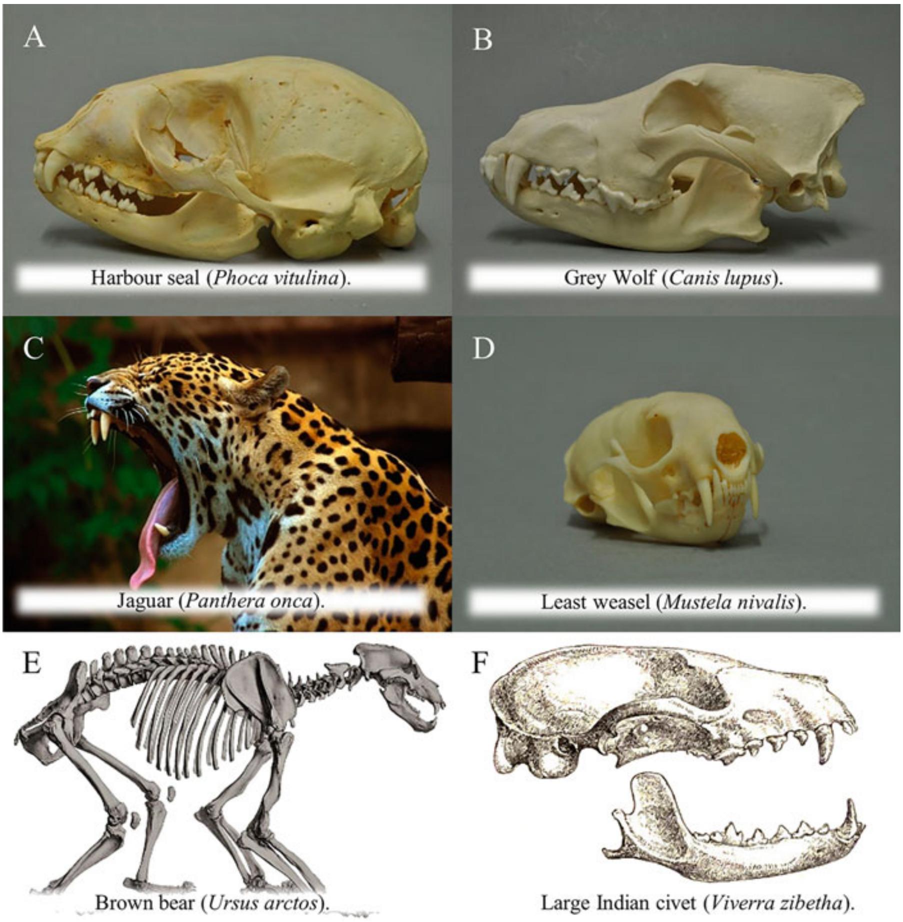
A
Harbour seal (*Phoca vitulina*).
B
Grey Wolf (*Canis lupus*).
C
Jaguar (*Panthera onca*).
D
Least weasel (*Mustela nivalis*).
E
Brown bear (*Ursus arctos*).
F
Large Indian civet (*Viverra zibetha*).

Fig. 4.5 Example of the animals within one of Linnaeus's groups, titled *Feræ (*Linnaeus and Salvius 1758*)*, whose classification matches closely with what is accepted today as the Order Carnivora. Linnaeus described Feræ as having "*Primary superior teeth of fex, sharp"* and these images show this anatomical feature. (**a**) Harbor seal (*Phoca vitulina*) skull and (**b**) Gray wolf (*Canis lupus*) skull Images by Klaus Rassinger and Gerhard Cammerer, Museum Wiesbaden and licensed under CC BY-SA 3.0. (**c**) Jaguar (*Panthera onca*) with canines on display Image taken at Toronto Zoo by MarcusObal and licensed under CC BY-SA 3.0. (**d**) Least weasel (*Mustela nivalis*) skull. Image by Klaus Rassinger and Gerhard Cammerer, Museum Wiesbaden, and licensed under CC BY-SA 3.0. (**e**) Brown bear (*Ursus arctos*) full skeleton, note the particularly visible teeth. Image by Blainville and Henri-Marie Ducrotay and licensed under creative commons, CC0 1.0 (PD-US-expired). (**f**) Large Indian civet (*Viverra zibetha*) skull. Image by W T Blanford from the Fauna of British India, Mammals and licensed under creative commons, CC0 1.0 (PD-US-expired)

like a pig's snout, or the pointy nose of a hedgehog or mole. He, therefore, grouped pigs (*Sus*), armadillos (*Dasypus*), hedgehogs (*Erinaceus*), moles (*Talpa*), shrews (*Sorex*), and opossums (*Didelphis*) together based on this feature (Fig. 4.6). Today however, we do not consider nose shape to be particularly informative about taxonomic relationships. Scientists still group hedgehogs, moles, and shrews together (Nikaido et al. 2003), but opossums, armadillos, and pigs have been placed in separate orders (Scornavacca et al. 2019; Spaulding et al. 2009; Tarver et al. 2016).

Macroscopic anatomy is still a starting point for modern taxonomists interested in organisms visible to the naked eye, but the appearance of the

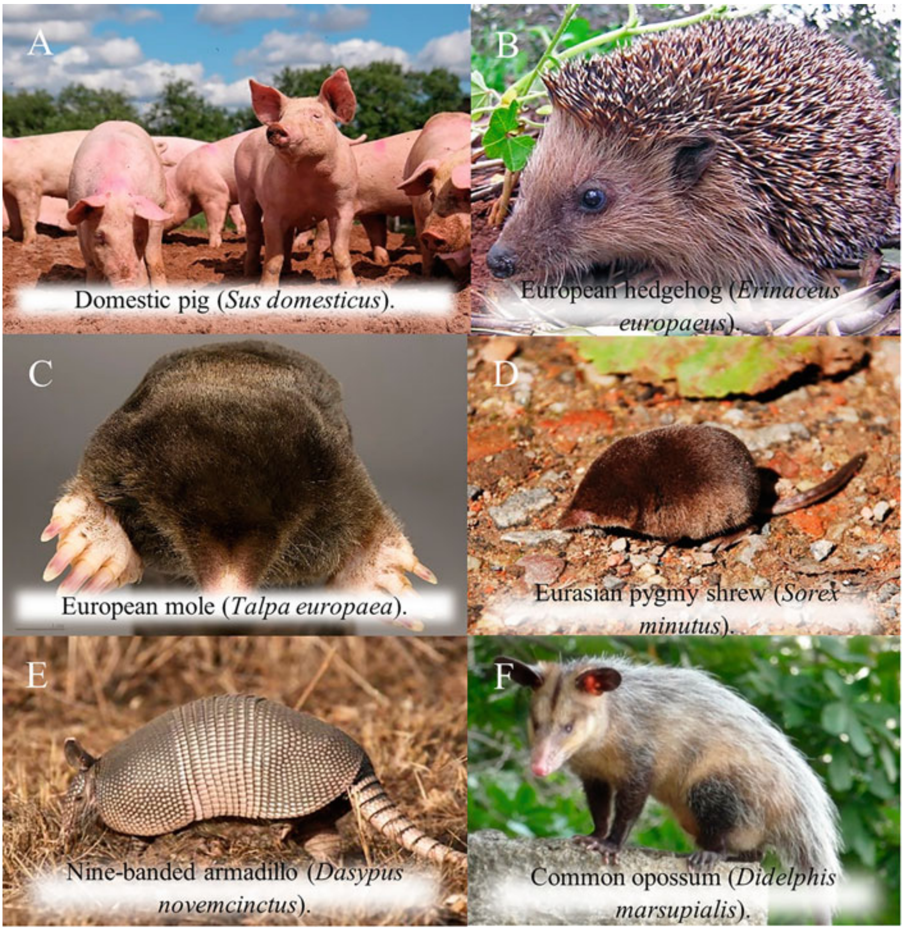
A
Domestic pig (*Sus domesticus*).
B
European hedgehog (*Erinaceus europaeus*).
C
European mole (*Talpa europaea*).
D
Eurasian pygmy shrew (*Sorex minutus*).
E
Nine-banded armadillo (*Dasypus novemcinctus*).
F
Common opossum (*Didelphis marsupialis*).

Fig. 4.6 Example of the animals within one of Linnaeus's groups, Bestiæ (Linnaeus and Salvius 1758), which is not accepted today. Linnaeus described Bestiæ as having "*a nose that extends beyond the mouth"* and these images show this anatomical feature. (**a**) Domestic Pig (*Sus domesticus*). Image of a pig farm in Vampula, Finland by Kallerna and licensed under CC BY-SA 4.0. (**b**) European Hedgehog (*Erinaceus europaeus*). Image by Gibe and licensed under CC BY-SA 3.0. (**c**) European Mole (*Talpa europaea*). Image taken by Didier Descouens as part of the Muséum de Toulouse and licensed under CC BY-SA 3.0. (**d**) Eurasian pygmy shrew (*Sorex minutus*). Image by Importé sur Commons par Salix. Sur Flikr par Polandeze and licensed under CC BY 2.0. (**e**) Nine-banded armadillo (*Dasypus novemcinctus*). Image taken at Quivira National Wildlife Refuge by Jerry Segraves and free of any copyright, CC0 1.0. (**f**) Common opossum (*Didelphis marsupialis*). Image by Juan Tello, modified by WolfmanSF and licensed under CC BY 2.0

microscope—which allowed scientists to see smaller organisms and smaller parts of organisms than they can view unaided—added a new layer of complexity to taxonomy. Its use led to reclassifications and additions to Linnean taxonomy, and in the next section, we explore the effects of these first tools that made the invisible visible.

4.3 The Microscopic

4.3.1 How Many Species Are There?

The number of new species described each year shows no sign of abating, with the Natural History Museum in London alone describing 351 new species in 2022 (Davis 2022). We may never truly know how many unique life-forms are present on our planet, but estimates range from ~5 ± 3 million to ~8.7 ± 1.3 million without us even contemplating bacterial and viral organisms (Costello et al. 2013 and Mora et al. 2011, respectively). Of this huge number, the IUCN Red List estimates that as of 2022, only ~2.16 million species have been formally described (The IUCN Red List 2022). Roughly 3.4% of these are vertebrates (mammals, birds, reptiles, amphibians, fishes) with the rest being invertebrates (70.4%), plants (19.6%), and fungi/protists (6.5%) (see The IUCN Red List 2022, Table 4.1a for further details). As discussed in Sect. 4.2, the macroscopic morphology-based classifications which dominated the field of taxonomy since Aristotle in 350 BCE could only work with organisms that one could see with one's own eyes, and with a particular focus on terrestrial organisms as there were inherent difficulties with observing marine species. As these estimates suggest, the species we can physically see—while iconic and very prevalent in our culture—make up a very small amount of the total number of organisms on this planet. The invention of the microscope allowed scientists their first glimpse of organisms and features beyond what they could see themselves and this drove the first visual revolution in taxonomy.

4.3.2 The Invention of the Microscope

The exact date of the creation of the microscope remains uncertain, but Dutch inventor and spectacle maker Zacharias Janssen is famous in part because he is thought to have created some of the earliest microscope models around the year 1600 (The Science Museum Group 2019). A simple microscope works by manipulating the way in which light enters your eye using a convex lens (where the lens is curved outward on both sides). Light reflects off the object under inspection and passes through the convex lens. As it does so, the light is bent toward the eye which makes the object look bigger than it actually is (National Geographic Society 2022). The use of the microscope thus revolutionized the way in which we do taxonomy by allowing us to visualize features too small to be visible to the naked eye.

4.3.3 The Uses of Microscopy

4.3.3.1 Early Microscopy and Taxonomy

Arguably the first significant and influential piece of work relating to microscopy was a book written by English scientist Robert Hooke in 1665 entitled *Micrographia*, which contained detailed illustrations of insects, plants, and fungi that Hooke had observed under a microscope (The British Library 2023; Encyclopaedia Britannica 2023; Hooke 1665) (Fig. 4.7). Hooke's imagery of a flea under a microscope is perhaps the most iconic image from his book (Fig. 4.7c). This skillfully produced illustration is an engraving that folds out to become almost four times larger than the book itself and is a highly detailed and faithful representation of the flea. It is especially significant because the microscopic components of the natural world had not been visualized until this point. Hooke has also been credited as one of the first to visualize plant cells and coin the term "cell" when referring to them (Fig. 4.7b). Hooke presented detailed written observations on organisms that had previously been unobservable by way of magnification. One example is his description of blue mold (Observ. XX in Hooke 1665, p. 125). Hooke described and visualized the microscopic structure of a mold spot (Fig. 4.7a), and then used his microscope to try and understand how this species (now classified in genus *Mucor*; Gest, 2004) reproduces.

While Hooke noted that once he could see the microscopic world, all that was needed to understand it was a sincere hand, and a faithful eye, he also realized that he could not yet capture nature exactly as he saw it. He stated when describing the eye of a fly that:

> In the Sunshine they look like a Surface covere'd with golden Nails; in another posture, like a Surface cover'd with Pyramids; in another with Cones.
>
> (Hooke 1665 pp. Preface).

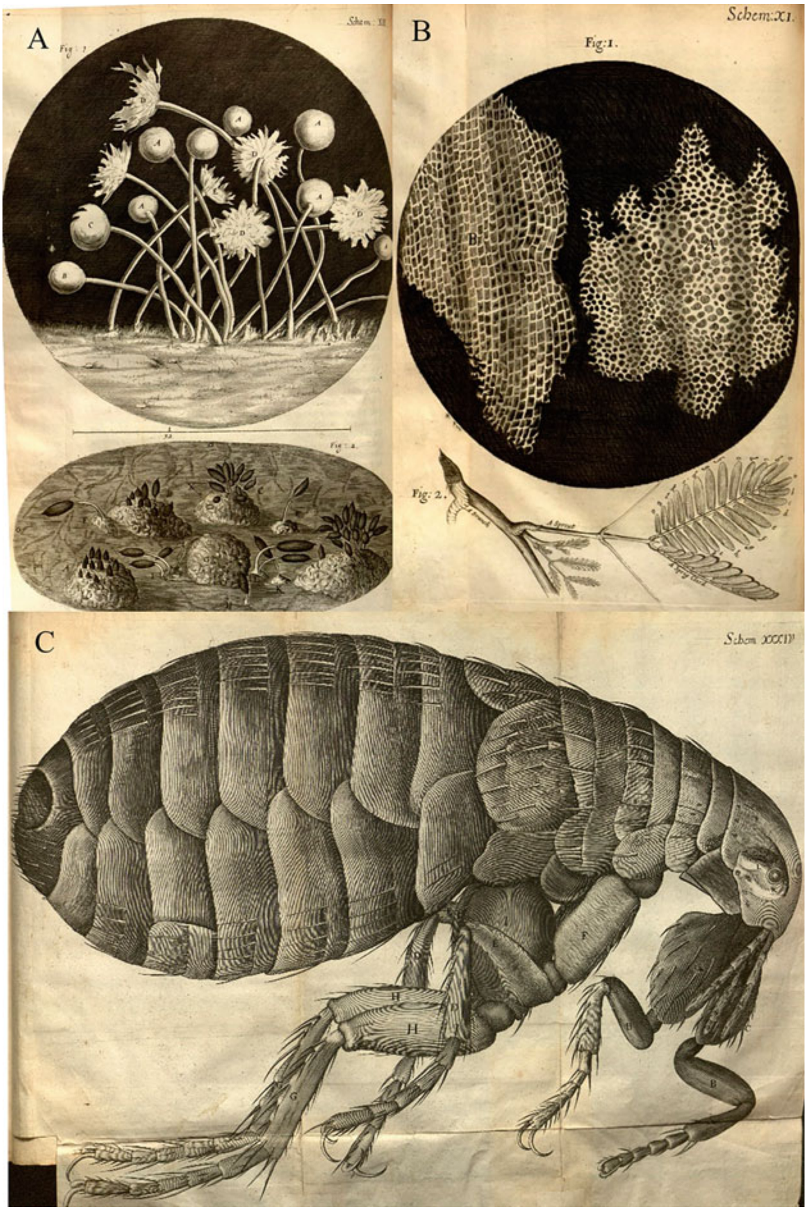

Fig. 4.7 Three iconic visualizations from Robert Hooke's historically significant book *Micrographia* which is commonly referred to as the first piece of influential work in the world of microscopy (Hooke 1665). (**a**) A blue mold spot (later classified in the genus *Mucor (Gest, 2004)*) was viewed under a microscope. (**b**) The cells of a plant are seen under a microscope. (**c**) Perhaps the most iconic engraving from Micrographia of a highly detailed flea viewed under a microscope. All images are sourced from the Biodiversity Heritage Library and licensed under CC0 1.0 (PD-US-expired)

As this statement suggests, Hooke carefully explored how different lighting conditions and angles affected the way light reflected off the fly. While some people note that microscopic images were ambiguous and relied on personal expertise or interpretation to convey the right answers (Fara 2009), it is advancements in microscopy and photomicrography that have helped provide an accurate depiction of the microscopic world.

4.3.3.2 The Development of Microscopy

As science, in general, progressed from making hand-crafted visualizations to digital ones of increased clarity (Lunn et al. 2022), so did microscopy. Photography in the laboratory progressed from placing scientists in front of the camera describing their specimens and results to photographing the specimens themselves, which reduced the rate of human error and ensured accurate depictions of what was being observed under a microscope (Fara 2009).

While this did have multiple subsequent benefits for taxonomy (as we will discuss in Sect. 4.3.3.3), one of the key innovations that sprang from this advancement in visualization was the visualization of model organisms. Some examples of model organisms include the fruit fly (*Drosophila melanogaster*), the mouse (*Mus musculus*), and the bacterium (*Escherichia coli*). These are all extensively studied due to their experimental advantages (for example, easy care, low maintenance costs, and rapid reproduction), and the results can be subsequently applied to other species that are harder to study, such as humans (Fields and Johnston 2005). One of the most famous works on model organisms is Sydney Brenner's, which established the free-living roundworm *Caenorhabditis elegans* (or *C. elegans*), as a model organism for developmental biology, and subsequently led to him being awarded a share in the 2002 Nobel Prize in Physiology or Medicine (Brenner 1974; Friedberg 2019). While Brenner's *C. elegans* work was primarily focused on genetics and developmental biology rather than taxonomy, he still needed to visualize it, and his work neatly illustrates the great power that arises from the combination of microscopy and photography (Fig. 4.8) (Brenner 1974). Using a dissecting microscope illuminated from below Brenner created a selection of photomicrographs (a graphic representation, in the form of a digital picture, of an object shown under a microscope) showing natural *C. elegans* and a selection of mutants (Fig. 4.8). The ease with which those seeing his pictures could see the difference between the characteristic features (e.g., length and width) of the mutant worms depicted, amply illustrates the huge potential photomicrography offered for taxonomies based on microscopic traits. Having a microscope in itself was a great advantage but having the ability to capture and share the things one saw through it allowed scientists to share their findings widely through writing scientific papers, allowing their colleagues around the world to see the work for themselves.

4.3.3.3 Modern Microscopy and Taxonomy

It is only in recent history that scientific visualization has broken free from the constraints of printing, with the move to online publication becoming the norm. This has resulted in a tendency for researchers to provide more and more visual evidence based on digital images as part of their work. In taxonomy, a good example is a paper by Laudurner, et al., (2005) which describes a new species of free-living flatworm (*Macrostomum lignano*), and proposes its use as a model organism. Here, the authors use a microscope to observe the species as well as a digital microscope video camera to accurately produce "extensive digital micrographical documentation" that they offer to distribute to other researchers (Fig. 4.9).

Figure 4.9 (showing Fig. 4.3 from Laudurner et al. 2005 with labels) begins with a very similar photomicrograph (Fig. 4.9a) overview of a free-living flatworm to Brenner's 1974 image (Fig. 4.8), but is much more detailed. These images can be difficult to interpret when you are not already familiar with what you are looking at as they then proceed to show smaller physical details, such as the brain, eyes, and pharynx in 9B, and the mouth in 9C. It can take a while to "get your eye in" and be able to understand what you are looking at, but when you do the power of this technique is phenomenal. The rest of the figure really plays to the strengths of digital capture technology and advanced microscopy techniques, as we can visualize some of the smallest parts of the organism, such as glands and parts of the brain that are typically smaller than 20 μm (or 0.002 cm). Previously, photomicrographs were much harder to produce due to problems associated with early photography techniques, such as long exposures increasing the difficulty of capturing moving organisms or lens imperfections (Fara 2009). Modern photography has vastly improved this and now the possibilities for describing species using microscopy have increased dramatically, just as in the case described above.

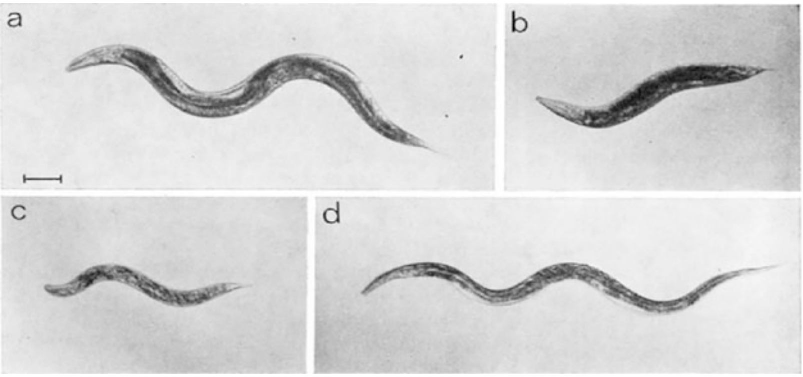

Fig. 4.8 Fig. 4.1 from Brenner, (1974) depicting photomicrographs of *C. elegans* and a selection of its mutants. This work described *C. elegans* as a model organism for developmental biology and the photomicrographs are produced using a dissecting microscope illuminated from below. Reprinted by permission from Oxford University Press: Oxford University Press, Genetics, *Brenner, S.* 1974. *The genetics of Caenorhabditis elegans. 77 (1) pp. 71–94.* https://doi.org/10.1093/genetics/77.1.71

While microscopy-based taxonomy using a compound or light microscope is still common (see Schultz 2002; and Ullah et al. 2021 for examples), it is still limited by the optical limitations of light. These limitations mean that scientists struggle to see anything with a magnification ratio (how much larger the image of an object appears compared to its actual size) greater than ×1500 or a resolution (the minimum distance between two distinct points where you can distinguish details) beyond 200 nanometers (nm) (or 0.00002 centimeters!) (Holgate and Webb 2003). Just as many organisms were not visible to the naked eye before the invention of the microscope, there are still many organisms that are smaller than 200 (nm) which therefore remain unobservable even with a traditional microscope.

To bypass the problems associated with light, a beam of electrons can be used instead; this is called an electron microscope. Electrons have a much shorter wavelength than photons in visible light, and so the magnification of electron microscopes can reach ×1,000,000 with resolutions of 1–2 nm (Marion 1981; National Renewable Energy Laboratory 2023). By using them, we can start to look more closely at organelles within cells and classify organisms that were previously inaccessible, such as viruses and bacteria (Ackermann and Prangishvili 2012; Akkari et al. 2013; Goldsmith and Miller 2009). Electron microscopy can additionally be used to reveal new details about the taxonomy and ecology of species we can physically see. For example, Dillon et al. (2017) researched whether it was possible to identify shark taxons and therefore, shark communities, by the tough tooth-like scales (dermal denticles) that they shed (Fig. 4.10).

These authors discuss the five different shapes that dermal denticles can take when they are optimized for different functions, and show how denticle shape tends to be influenced by shark family, but also show links to function as well (Fig. 4.10). For example, the ten denticles present in part 1 of the figure are all specialized for drag reduction and belong to either the requiem sharks, such as the tiger or lemon sharks (Family: Carcharhinidae and denticles A, B, D, E, F, and H), or the hammerhead sharks (Family: Sphyrnidae and denticles C and G). In this case, the final denticle specialized for drag reduction (denticle I) belongs to a thresher shark (not pictured in Fig. 4.10), and there are no denticles specialized for drag reduction from the carpet sharks (e.g., nurse sharks from the family Ginglymostomatidae) likely as a product of their life mode. The first denticle identified in this

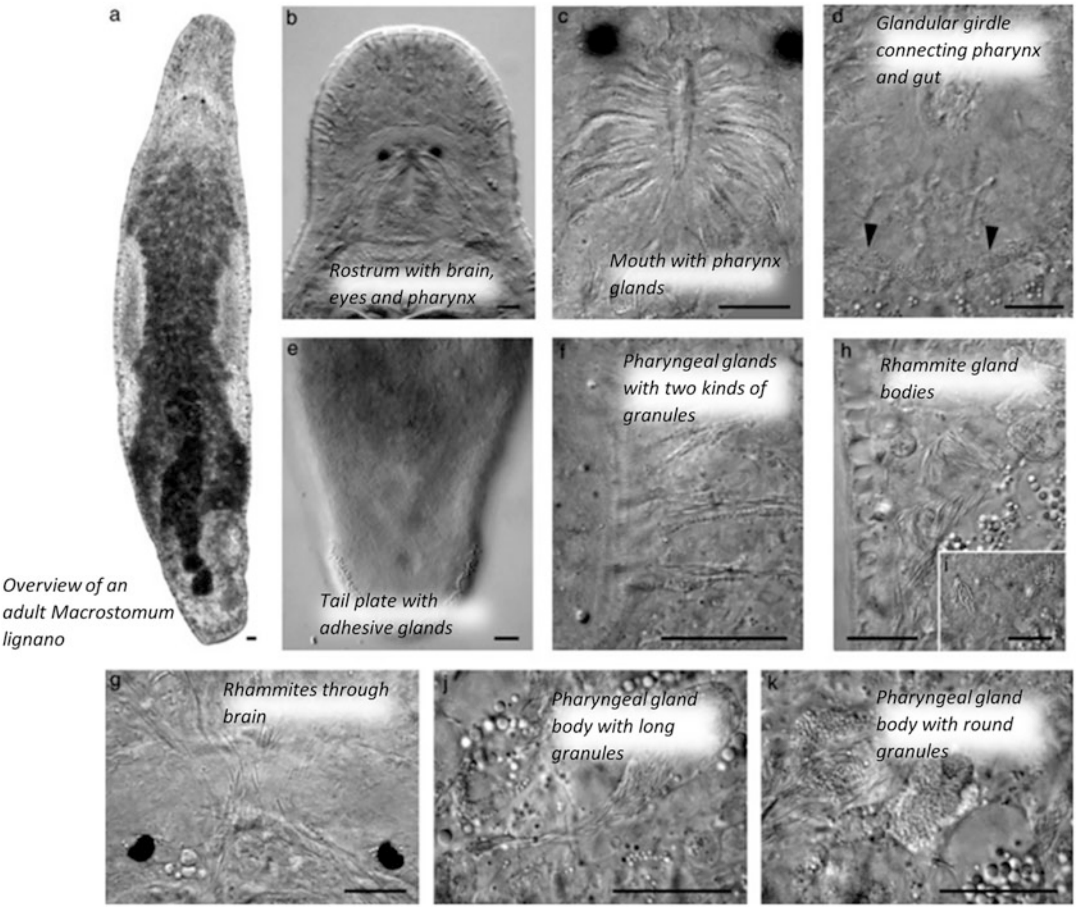
a
Overview of an adult Macrostomum lignano
b
Rostrum with brain, eyes and pharynx
c
Mouth with pharynx glands
d
Glandular girdle connecting pharynx and gut
e
Tail plate with adhesive glands
f
Pharyngeal glands with two kinds of granules
h
Rhammite gland bodies
i
g
Rhammites through brain
j
Pharyngeal gland body with long granules
k
Pharyngeal gland body with round granules

Fig. 4.9 Fig. 4.3 from Laudurner, et al. (2005) with additional labels depicting photomicrographs of *Macrostomum lignano*. It is from the extensive photomicrographs produced here that the authors classify this as a new species and propose it as a model organism. Photomicrographs are produced using a compound microscope and a digital microscope video camera. Scale bar equates to 20 μm. Reprinted by permission from John Wiley and Sons: John Wiley and Sons, *Journal of Zoological Systematics and Evolutionary Research*, Laudurner et al. 2005. *A new model organism among the lower Bilateria and the use of digital microscopy in taxonomy of meiobenthic Platyhelminthes: Macrostomum lignano, n.* sp. *(Rhabditophora, Macrostomorpha). 43 (2) pp. 114–126.* https://doi.org/10.1111/j.1439-0469.2005.00299

family is specialized for "abrasion strength" (denticles K and N).

This study showed how, by using a scanning electron microscope, it is possible to identify shed dermal denticles to at least the family level and therefore reconstruct the community that would have lived at a specific site. In this way, one would know, for example, if an area was frequented by tiger sharks or hammerheads. Further research using scanning electron microscopes on dermal denticles has shown that adult and juvenile denticles differ, suggesting that age patterns in these communities could be reconstructed (Soares et al. 2016). As such, by using microscopes to study denticles, we gain valuable information about community structure which is relevant to conservation. Microscopes can improve our understanding of how these (microscopic) features can be shaped by their different functions, e.g., drag resistance or abrasion strength, as well as how they are inherited, allowing us to add these identifying

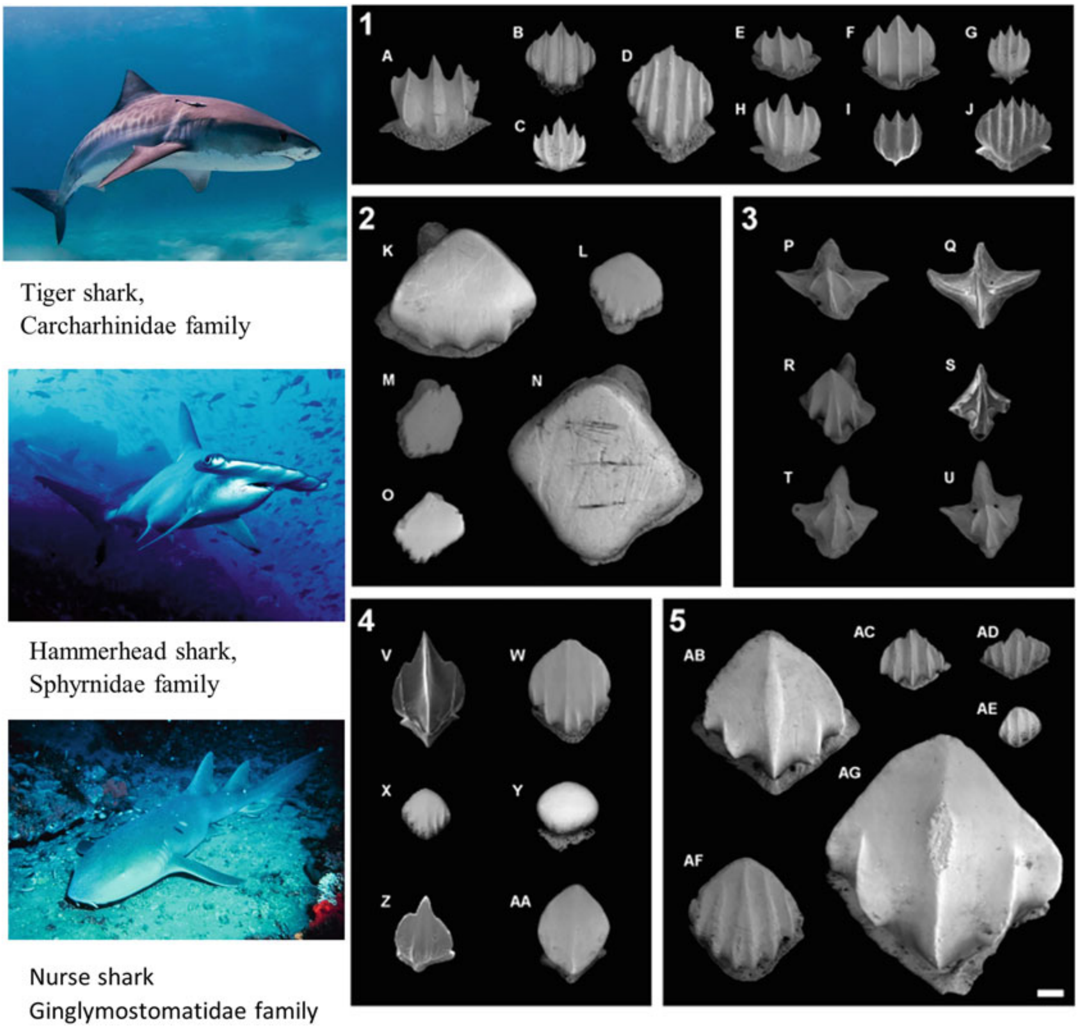
Tiger shark,
Carcharhinidae family

Hammerhead shark,
Sphyrnidae family

Nurse shark
Ginglymostomatidae family

Fig. 4.10 Composite figure created for this text. The right-hand side images show scanning electron microscope images of dermal denticles demonstrating morphological variation across shark families and for different functions (Dillon et al. 2017; their Fig. 4.2a). Each photograph shows denticles with a different core function in "(1) drag reduction, (2) abrasion strength, (3) defense, (4) generalized functions, and (5) ridged abrasion strength. The letters by each dermal denticle represent the specific shark species as Identified in Dillon et al. (2017)'s manuscript. Scale bar = 100 µm. Reprinted by permission from Inter-Research Science Publisher: Inter-Research Science Publisher, Marine Ecology Progress Series, Dillon et al. 2017. Dermal denticles as a tool to reconstruct shark communities. 566 pp. 117–134. https://doi.org/10.3354/meps12018. The left of the figure shows the three main taxonomic families that these sharks fall under (Carcharhinidae, Sphyrnidae, and Ginglymostomatidae). These images are sourced from Albert Kok, Barry Peters, and Dr. Mathew Gilligan and are licensed under CC BY-SA 2.5, CC BY 2.0, and CC0 1.0 (PD-USGov), respectively

characteristics into the arsenal of features that we then use to underpin our taxonomy.

Both the development of the microscope and the associated advances in visualization and image-capture techniques are fundamental to the way we do taxonomy. Taxonomists are now able to see and classify microscopic organisms and use the microscopic features of larger animals to tell them apart from one another. Microscopy has also helped in aiding several vital scientific breakthroughs by facilitating the visualization of model organisms and encouraging functional morphology, which bridges taxonomy and ecology. However, taxonomy undertaken through the microscope still relies on the "comparative morphological" approach—i.e., looking for similarities and differences that one can physically see. A microscope can improve one's vision of the microscopic, but even a photomicrograph can only record what it can detect through the lens, and this remained a constraint on taxonomy until the last decades of the twentieth century.

4.4 Genetics

4.4.1 A Brief Introduction to Genetics

The capacity for genetic analysis has arguably created one of the biggest paradigm shifts in the biological sciences. In 1866, Austrian scientist Gregor Mendel laid the foundations for genetics by exploring the principles of heredity using his famous garden pea experiments (Mendel 1866). Mendel grew different varieties of pea, some with purple flowers and some with white flowers. When they started to produce pollen ready for fertilization, he removed the stamens and carefully collected the pollen from each plant. He was then able to control how the plants were fertilized by using a fine brush with which to individually cross-pollinate them. He kept meticulous records of which plants he was cross-breeding and continued his experiments over multiple generations of pea plants to see how their color and shape traits changed. The observable characteristic produced by a certain set of genes, in this case, the color of the flower, is known as its phenotype. Mendel observed how the traits that he was interested in were passed down through the plant generations as distinct phenotypes and calculated the underlying rules that determined what color the flowers would become for any particular set of plant "parents" (see Fig. 4.11). While it is now evident that the traits that Mendel used to develop his theory are much simpler than most phenotypes, Mendelian inheritance became the backbone for what we now call genetic analysis (Cobb 2006; National Human Genome Research Institute 2013; Schacherer 2016; Winchester 2023).

The observable characteristics (phenotypes) of an organism arise from the interaction between its genes and the surrounding environment. Genes are small sections of deoxyribonucleic acid (DNA) that contain the information needed to determine how an organism will grow. In reality, growth is complex, and multiple genes interact in order to develop an organism (Campbell et al. 2018a). The ability to analyze genes and the different characteristics they influence has facilitated great strides in the field of medicine, which uses model animals, such as "knockout mice" which have had one or more genes removed (knocked out), as a way of understanding the exact role that different genes play in development (Centers for Disease Control and Prevention 2021; Frank 2004; Genetic Alliance 2006; Holtzman and Marteau 2000; Nussbaum et al. 2016).

Ecology, evolution, and taxonomy have also been hugely impacted by our capacity to map genome sequences. The nature versus nurture debate has been an ongoing one. However, where genetics is concerned, it can be shown that although genes often underpin how a structure develops, the environment that the structure develops in can have an equally powerful effect, particularly where evolution is concerned, and this interaction is something that we discuss in more detail in Sect. 4.4.3. Genetic analysis has become increasingly useful as it can be used to distinguish between pairs of species that look similar through adapting in similar ways to a shared environment, and pairs that actually share recent common ancestors. Conversely, genetic analysis can also identify when organisms that look very different in fact share an evolutionary history.

4.4.2 Evolutionary Biology and Taxonomy

To better understand how genetics has revolutionized taxonomy we will briefly summarize the role of evolutionary theory. Prior to the

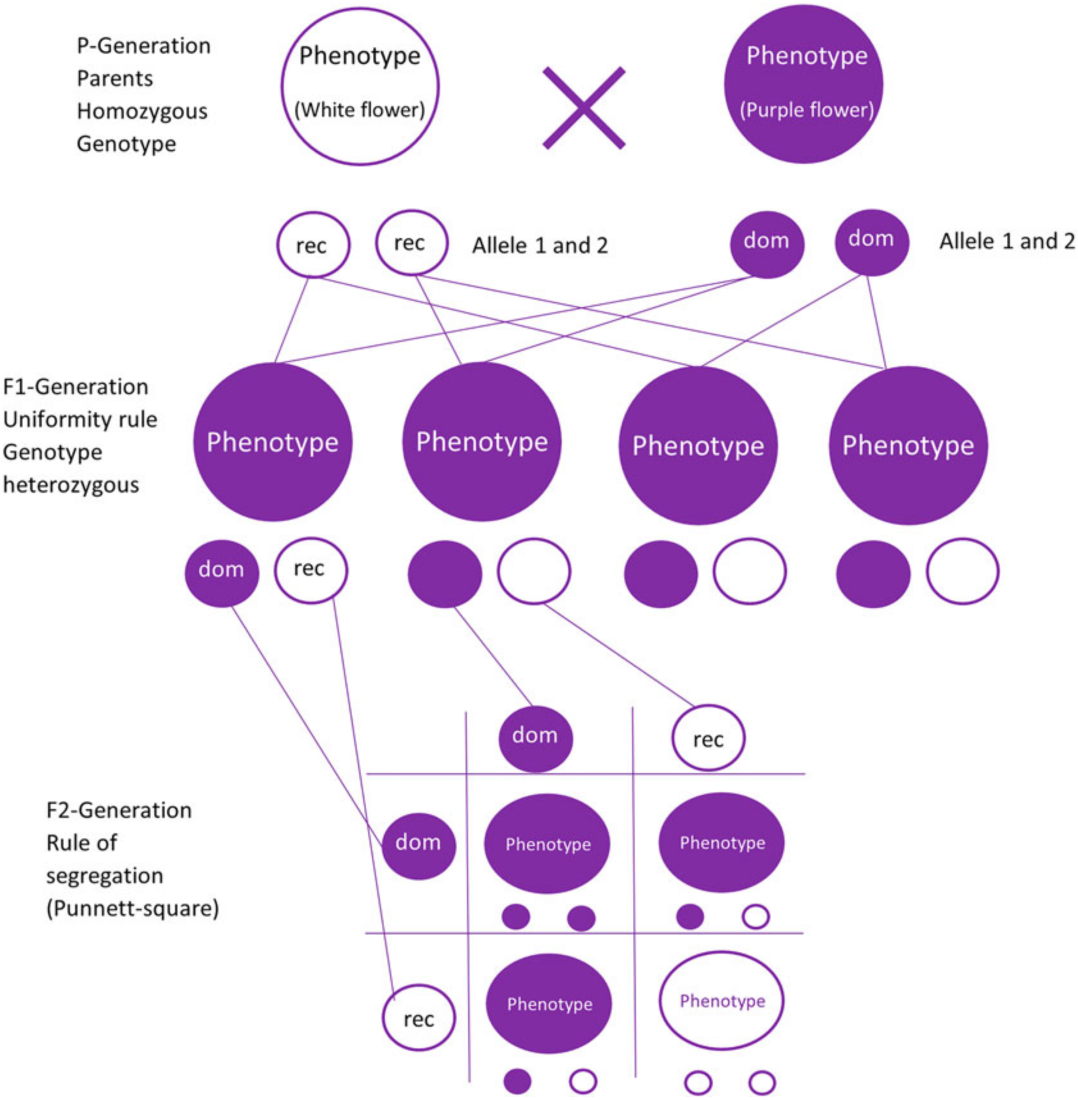
P-Generation
Parents
Homozygous
Genotype
Phenotype
(White flower)
Phenotype
(Purple flower)
rec
rec
Allele 1 and 2
dom
dom
Allele 1 and 2
F1-Generation
Uniformity rule
Genotype
heterozygous
Phenotype
Phenotype
Phenotype
Phenotype
dom
rec
dom
rec
F2-Generation
Rule of
segregation
(Punnett-square)
dom
Phenotype
Phenotype
rec
Phenotype
Phenotype

Fig. 4.11 This is a copy of Gregor Mendel's iconic model of heredity (Mendel 1866). In this specific diagram, Mendel describes cross-breeding true-breeding purple and white flowered plants. The parent generation's phenotypes (observable characteristics) were produced by two identical genes, either two purple alleles or two white ones. The first hybrid generation produced by these parents, the F1 hybrids, were all purple in phenotype but all had two different alleles—one purple and one white. In this case, the purple allele is called dominant and the white allele is recessive, because when you have both present, it is the purple color that is expressed and the white allele has no visible effect. When these F1 hybrids were themselves crossed, however, the next generation (F2) plants were mixed, with purple or white flowers in a ratio of 3:1 respectively (Campbell et al. 2018a). This is demonstrated best by the punnett square on the figure, which puts the genes they could get from one parent along the top and those from the other down the sides and then creates crosses in the middle boxes. Image was recreated based on one from Sciencia58 that is in the public domain (CC0 1.0)

mid-nineteenth century, there were many competing theories for how species and other taxa came to emerge, but the theory of evolution by natural selection (Fig. 4.12), originally independently conceived by Charles Darwin and Alfred Russel Wallace (Darwin and Wallace 1858; Darwin

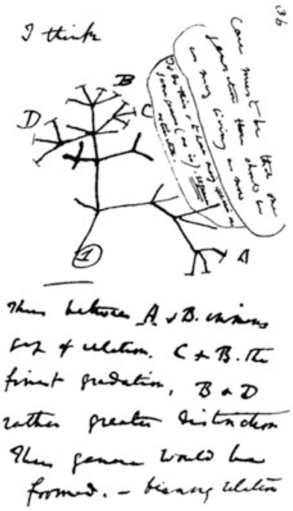
I think
A
B
C
D
1
Then between A & B. immense gap of relation. C & B. the finest gradation, B & D rather greater distinction. Thus genera would be formed. – bearing relation

1) Individuals in a population have different morphologies, physiologies, and behaviours (phenotypic variation)

1) Different phenotypes have different rates of survival and reproduction in different environments (differential fitness)

1) Phenotypes that prove successful in survival and reproduction are passed down to offspring (fitness is heritable). Less successful phenotypes fail to reproduce and eventually die out

1) This process continues over generations and distinct species are formed as successful phenotypes become established

Fig. 4.12 (*Left*) The famous first sketch of an evolutionary tree drawn by Charles Darwin in his first notebook on the Transmutation of Species (1837). In this sketch, labeled branches (A, B, C, and D) indicate living species while unlabelled ones indicate extinct ones. The general idea proposed here is that there can be such a difference in morphology between closely related specimens because organisms that would fill the "morphological gap" are now extinct due to events beyond their control (i.e., geographical/climatic change or predator changes for example) or because they were less fit in the face of natural selection. Darwin also demonstrated in this image how species share common related ancestors—even those who look very morphologically distinct. Image sourced from Charles Darwin and in the public domain, CC0 1.0 (PD-US-expired). (*Right*) The process of natural selection as described by Darwin (1859) and Lewontin (1970)

1859), now dominates work in taxonomy as it does in the broader field of biology. There are four key parts to this theory:

Darwin's first sketch of what we now call an "evolutionary tree" (Fig. 4.12) is now considered an important cultural milestone in evolutionary biology. This was how he visualized his "Big Idea" that different organisms were related to one another through shared ancestors; there is a shared ancestor at every point on the tree where two or more branches diverge. Darwin also used it to visualize why some closely related species can look so different, i.e., be morphologically distinct. On his sketch, labeled branches indicated species that exist now, while unlabeled ones indicated extinct ones. The general idea was that species that fill the "morphological gap" between two related species are likely to have become extinct, leaving a gap in what might originally have been a continuum. For example, the three species of elephant are most closely related to the manatees and hyraxes pictured below, despite looking very different from them (Fig. 4.13).

It is reported that there are at least seven lineages related to elephants that have become extinct over the past 32 million years (Campbell et al. 2018b), indicating that Darwin's idea seems to hold true in many instances. As such, adjacent branches on a tree may contain species that are very similar to one another or ones that are more distant neighbors whose common ancestors lived much longer ago. While each cluster shares a common ancestor, the amount of change, both in terms of their genetic material and their phenotype, can vary as can the amount of time since species separated.

Evolutionary trees tell us about relationships and overall similarities, including which ones share recent common ancestors. We also know that there are multiple ways new species can appear, called allopatric (literally: allo-different, patric-homeland), peripatric (around the

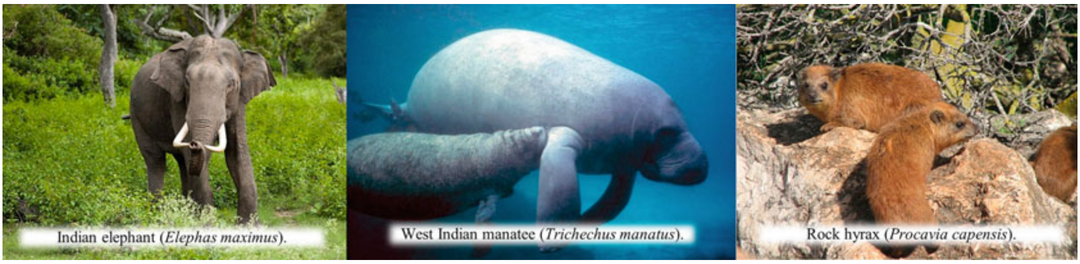
Indian elephant (*Elephas maximus*).
West Indian manatee (*Trichechus manatus*).
Rock hyrax (*Procavia capensis*).

Fig. 4.13 Composite image of the Indian elephant (*Elephas maximus*), West Indian manatee (*Trichechus manatus*), and the rock hyrax (*Procavia capensis*) to show how the three living species of elephant (*Elephas maximus*, *Loxodonta Africana*, and *Loxodonta cyclotis*) are most closely related to manatees and hyraxes despite the physical appearance being very different from one another. Images sourced from (left to right), Yathin S Krishnappa, Galen Rathbun as part of the USFWS Digital Library, and Arikk, and licensed under CC BY-SA 3.0, CC0 1.0 (PD-USGov), and CC BY-SA 3.0, respectively

homeland), parapatric (next to the homeland), and sympatric (same homeland) speciation (Fig. 4.14).

These forms of speciation are distinguished because they have different geographical patterns. Allopatric speciation is perhaps the most common of the four types. Here, an original population splits because of the appearance of a geographical barrier such as a large river that separates one population into two, preventing them from reaching each other with the result that they can no longer interbreed. Over time, each new population is exposed to different selective pressures (i.e., different predators, climates, and food sources), and begins to adapt to them. This results in them gradually diverging from their cousins on the other side of the river to form a new and distinct species (Rutledge et al. 2022). Peripatric and parapatric speciations are similar but occur as a result of a small subpopulation either moving into a completely new habitat, such as a different forest that is not attached to the current one (peripatric), or following population expansion into adjacent areas of a large range by staying in the same big forest but moving to a different section of it (parapatric). Sympatric speciation, where two species arise while coexisting, is theoretically possible but seems to be rare; it may happen when some individuals experience genetic change and stop breeding with their fellows.

While speciation is all about divergence and development away from a given genetic starting point, some species also undergo convergent evolution. Convergent evolution occurs when different lineages evolve similar traits because they are adapting to similar selective pressures and environments, despite not being closely related (there are examples in Sect. 4.4.3) (Gabora 2013). This is where genetic analysis may become the most useful tool in a taxonomist's arsenal. If you were to classify organisms based solely on similarities in their macroscopic features (like Aristotle and Linnaeus), you would likely consider these broad similarities indicative of a close relationship, though it is now known that they might instead result from convergence. By creating an abstraction of the organism, through analysis of its genes, we can move beyond merely seeing physical similarities and differences and begin to understand their history as well as their ecological function.

4.4.3 What Genetics Reveals about Taxonomy: Divergence and Convergence

One of the best examples of convergent evolution comes from the aquatic adaptations many species of mammals have independently acquired (Chikina et al. 2016). Whales are not closely related to seals or dugongs despite all three

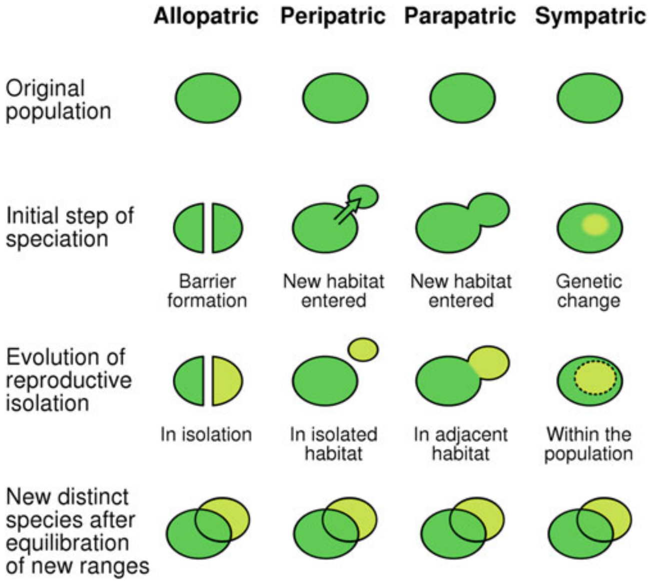
Allopatric
Peripatric
Parapatric
Sympatric
Original population
Initial step of speciation
Barrier formation
New habitat entered
New habitat entered
Genetic change
Evolution of reproductive isolation
In isolation
In isolated habitat
In adjacent habitat
Within the population
New distinct species after equilibration of new ranges

Fig. 4.14 The four geographic processes of speciation (formation of new distinct species) (Rutledge et al. 2022). Once the original population has been separated into two or more sub-groups by barriers, range expansion, or mutation, different selective pressures (environmental or ecological for example) force each population to evolve differently. In doing this, the populations begin to diverge from one another and sometimes the original population until you get one or more new distinct species. Image created by Ilmari Karonen, courtesy of Wikimedia and is within the public domain (CC0 1.0)

animals looking very similar (Fig. 4.15). They share macroscopic traits such as streamlined bodies, reduced limbs (Fish and Hui 1991; Fish et al. 2008), and in some cases adapted respiratory systems to cope with deep diving or hypoxia (Andersen 1966; Kooyman 2006).

Genetic analysis reveals that the last common ancestors of whales and dugongs, and whales and seals, lived 99 and 76 million years ago, respectively (Kumar et al. 2017). However, both have more recent common ancestors with other species that live on land. For instance, dugongs and sea cows share a common ancestor with elephants that lived 60 million years ago, while whales diverged from semi-aquatic hippopotami 53 million years ago (Kumar et al. 2017). The shared adaptations of whales and dugongs that allow both species to live in the aquatic environments thus arose convergently, with both animals originating from land-based ancestors in the Paleogene period when there was a rapid diversification of mammals after a mass extinction (Meredith et al. 2011).

Similarly, Figs. 4.16 and 4.17 demonstrate how two species that look physically similar do not actually have to be closely related from an evolutionary perspective.

In Fig. 4.16a and b, we have a lesser hedgehog tenrec (*Echinops telfairi*) and a European hedgehog (*Erinaceus europaeus*). These insectivorous animals have always been challenging to classify, with Linnaeus in 1758 noting “a nose that extends beyond the mouth” and as we mentioned earlier, placing them in his Bestiæ category along with opossums, armadillos, and even pigs (Linnaeus and Salvius 1758) (Fig. 4.6). In 1821, the order Insectivora was established and included a wide range of species, including shrews, hedgehogs, moles, and their relatives. However, the only specific, defining characteristic that all members of Insectivora shared was that they were small, placental mammals that fed on insects. This meant that the order was effectively a place

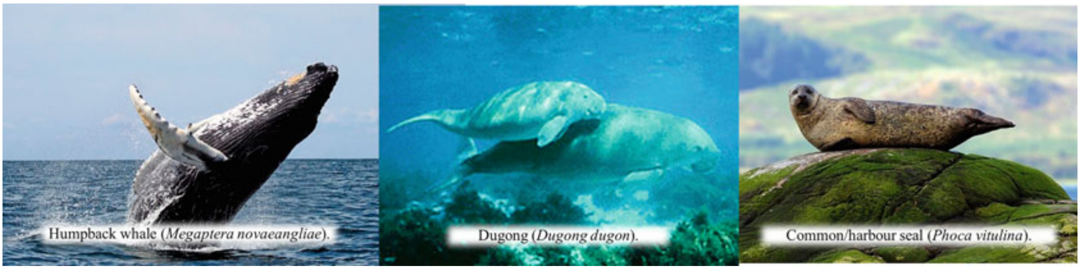
Humpback whale (*Megaptera novaeangliae*).
Dugong (*Dugong dugon*).
Common/harbour seal (*Phoca vitulina*).

Fig. 4.15 Composite image of the humpback whale (*Megaptera novaeangliae*), dugong (*Dugong dugon*), and the common/harbor seal (*Phoca vitulina*) to show how these three species share some macroscopic traits despite not being closely related. They have likely evolved these similarities due to convergence and similar selective pressures. Images sourced from (left to right), Whit Welles, the marine mammal commission, and Charles J. Sharp, and licensed under CC BY 3.0, CC0 1.0 (PD-USGov), and CC BY-SA 4.0, respectively

where animals were grouped if they did not fit anywhere else, called a "wastebasket taxon" (Musser 2018). After more than a century of research, Insectivora is now thought to be polyphyletic, meaning that their members are not all descended from a common ancestor. Groups that are polyphyletic often share their key traits because of convergence, not shared history (Symonds 2007; Stanhope et al. 1998). Another example of a polyphyletic group would be if one were to group birds and bats together because of their ability to fly, despite knowing that their flight is convergent and that they are not actually closely related, having diverged as much as 319 million years ago (Kumar et al. 2017).

So, while hedgehogs and tenrecs may look similar with their small, stout bodies, they are likely to have evolved these features independently and are not closely related. Genetic analysis of the six taxonomic families that once made

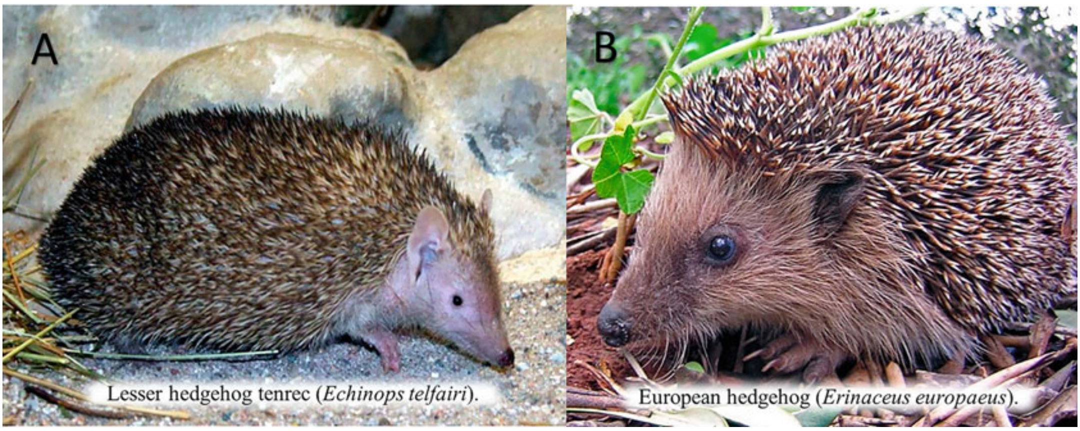
A
Lesser hedgehog tenrec (*Echinops telfairi*).
B
European hedgehog (*Erinaceus europaeus*).

Fig. 4.16 Composite figure showing the lesser hedgehog tenrec (*Echinops telfairi*) (**a**) and the European hedgehog (*Erinaceus europaeus*) (**b**). While these species share a lot of physical characteristics, and were in fact classified together for many years, genetic analysis has revealed they are actually only distantly related. The tenrec is now classified in the order Afrosoricida within the superorder Afrotheria which includes elephants, dugongs and manatees, and the aardvark. The hedgehog is in the order Eulipotyphla and superorder Laurasiatheria which also includes bats, carnivores, and ungulates (Mouchaty et al. 2008; Stanhope et al. 1998). The tenrec is thus more closely related to an elephant than it is to the physically similar hedgehog! Images by Wilfried Berns and Gibe and licensed under CC BY-SA 2.0 DE and CC BY-SA 3.0, respectively

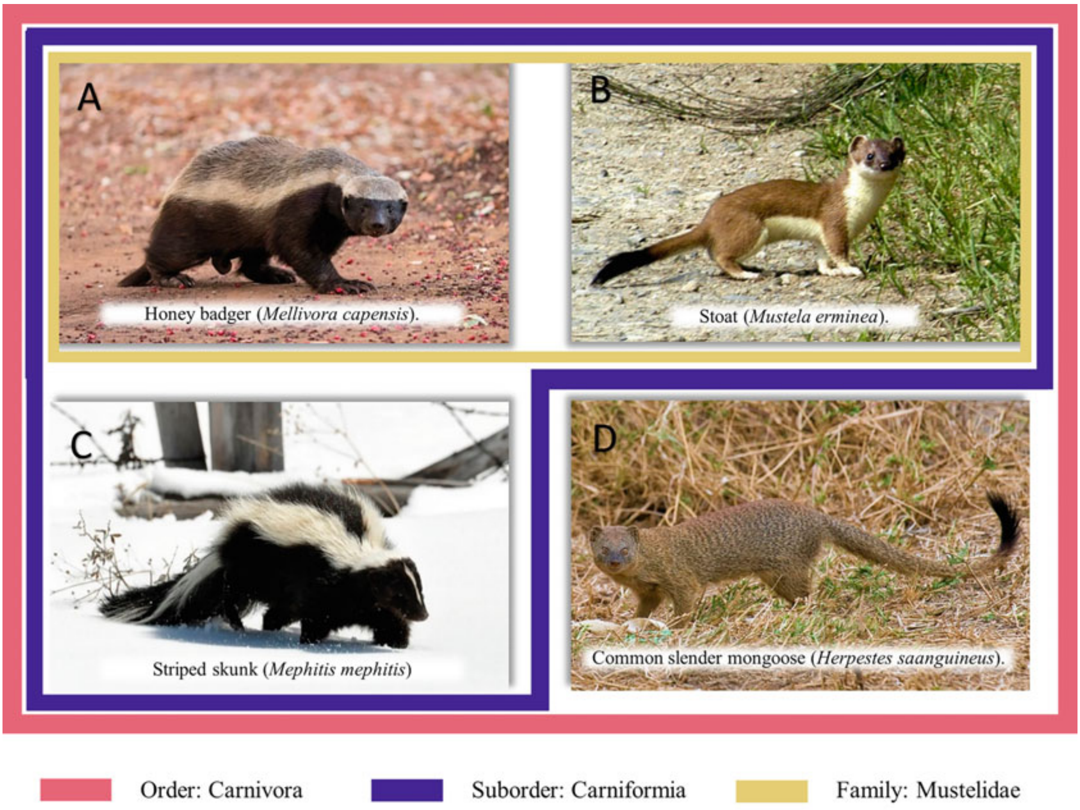
A
Honey badger (*Mellivora capensis*).
B
Stoat (*Mustela erminea*).
C
Striped skunk (*Mephitis mephitis*)
D
Common slender mongoose (*Herpestes saanguineus*).
Order: Carnivora
Suborder: Carniformia
Family: Mustelidae

Fig. 4.17 Composite figure showing four species—the honey badger (*Mellivora capensis*) (**a**), the stoat (*Mustela erminea*) (**b**), the striped skunk (*Mephitis mephitis*) (**c**), and the common slender mongoose (*Herpestes sanguineus*) (**d**). All four species are classified in the order Carnivora (as illustrated by the pale red box). Only **A**, **B**, and **C** are in the suborder Carniformia (the blue box) while **D** is in Feliformia. The point of showing **D** is to demonstrate how it looks very physically similar to **B** specifically, even down to the black tip on the end of their tails, despite being in different suborders whose most recent common ancestor lived 55 million years ago (Kumar et al. 2017). The honey badger (**a**) perhaps looks most similar to the skunk (**c**), but they are in different families. The badger is actually in the same family as the stoat (Family: Mustelidae; the yellow box). Genetic evidence has been used to better visualize these species' relationships and understand how convergence and shared ancestry have shaped their phenotypes. Images by Sumeet Moghe, James Lindsey at Ecology of Commanster, Dan & Lin Dzurisin using Flickr, and Yathin S Krishnappa, and licensed under CC BY-SA 4.0, CC BY-SA 2.5, CC BY 2.0, and CC BY-SA 3.0, respectively

up Insectivora confirms this, showing that tenrecs and golden moles are most closely related to elephants, manatees, dugongs, and aardvarks (Stanhope et al. 1998; Mouchaty et al. 2008). The remaining families have now been grouped into an order that contains hedgehogs, moles and true-shrews, and Insectivora is no longer recognized. The tenrec is thus more closely related to an elephant than it is to the physically similar hedgehog!

Our next example in Fig. 4.17 shows four species that also have a more complex classification than would be expected.

The honey badger, stoat, striped skunk, and common slender mongoose are all members of the order Carnivora. However, the first major classification difference is that honey badgers, stoats, and striped skunks are in a different suborder to the mongoose which is in the suborder Feliformia, which contains cats, lions, and hyenas among other animals (Duszynski et al. 2018; Flynn and Nedbal 1998; Veron et al. 2004; Zhou et al. 2017). However, when you look at the stoat and the mongoose (Fig. 4.17b and d), with their small, slender bodies and darkened tail tip, it is hard to recognize the substantial taxonomic gap between them.

The honey badger and striped skunk (Fig. 4.17a and c), are within the same suborder but different families (Dragoo and Honeycutt 1997). However, they look far more similar to one another than the honey badger (Fig. 4.17a) and the stoat (Fig. 4.17b) despite the fact that the badger and the stoat are more closely related to each other than the badger and the skunk. All of these examples show once again how genetic analysis can reveal whether two species that look physically similar inherited their shared traits from a common ancestor or gained them through convergence.

Conversely, genetic analysis can also help us see when organisms that look very different are actually more closely related than one might initially suspect. The four species in Fig. 4.18, the blue whale (*Balaenoptera musculus*), hippopotamus (*Hippopotamus amphibius*), Bactrian camel (*Camelus bactrianus*), and domesticated Suffolk sheep (*Ovis aries*) look very different from one another, yet are closely related.

Linnaeus realized that cetaceans (whales and dolphins) shared features in common with all mammals, and it has now been widely accepted, thanks to genetic analysis, that they do indeed share their evolutionary history with sheep, hippopotami and Bactrian camels (Graur and Higgins 1994; Montgelard et al. 1997), having separated from a common ancestor around 76 million years ago (Kumar et al. 2017). While this sounds like a relatively long time ago, the last common ancestor of the tenrec and hedgehog discussed above, was around 99 million years ago, which in evolutionary terms is relatively much more recent despite the huge changes in their physical appearance.

The natural next step in classification, if we were looking purely at physical features, would be to assume that whales were the first group to diverge because they look so different from the other three species in Fig. 4.18. However, it was the camels that branched off first (~64 million years ago), before the two suborders consisting of whales/hippopotami, and hoofed herbivorous mammals (e.g., sheep) last shared a common ancestor around 58 million years ago (Beck et al. 2006; doe Reis et al. 2012; Kumar et al. 2017; Song et al. 2012) (Fig. 4.19). These four animals which show such different physical appearances actually share a closer evolutionary history, with their morphological differences likely to be the result of adaptation to different selective pressures.

This section has shown how adding knowledge of genetics improves our ability to classify organisms, especially where macroscopic anatomy is not a good indicator of the relationships between species. But how do taxonomists *visualize* genetics in order to incorporate them into their classification schemes? Gene sequences are much too long and complex to use in isolation, so new visualization techniques have been crucial to this taxonomic revolution.

4.4.4 How we Visualize Genetics?

Genetic-based taxonomy is fundamentally similar to early taxonomy. In the case of both macro and microscopic taxonomies, taxonomists were looking for similarities and differences. Genetic taxonomy involves something very similar, but rather than describing, drawing, or taking a photograph of an organism, geneticists create a visual abstraction of it, by visualizing its DNA or a sequence of numbers derived from that DNA.

Just as the letters in our alphabet spell different words when arranged in different orders, a genetic sequence is made up of different arrangements of nucleotides, the building blocks of DNA. Nucleotide names are abbreviated to A (adenine), T (thymine), C (cytosine), and G (guanine), and these nucleotides occur in a sequence that gives a unique string of code. Variations in the sequence of these letters create different genes, which in turn produce different observable characteristics and phenotypes, just as was described earlier in the case of Mendel's purple

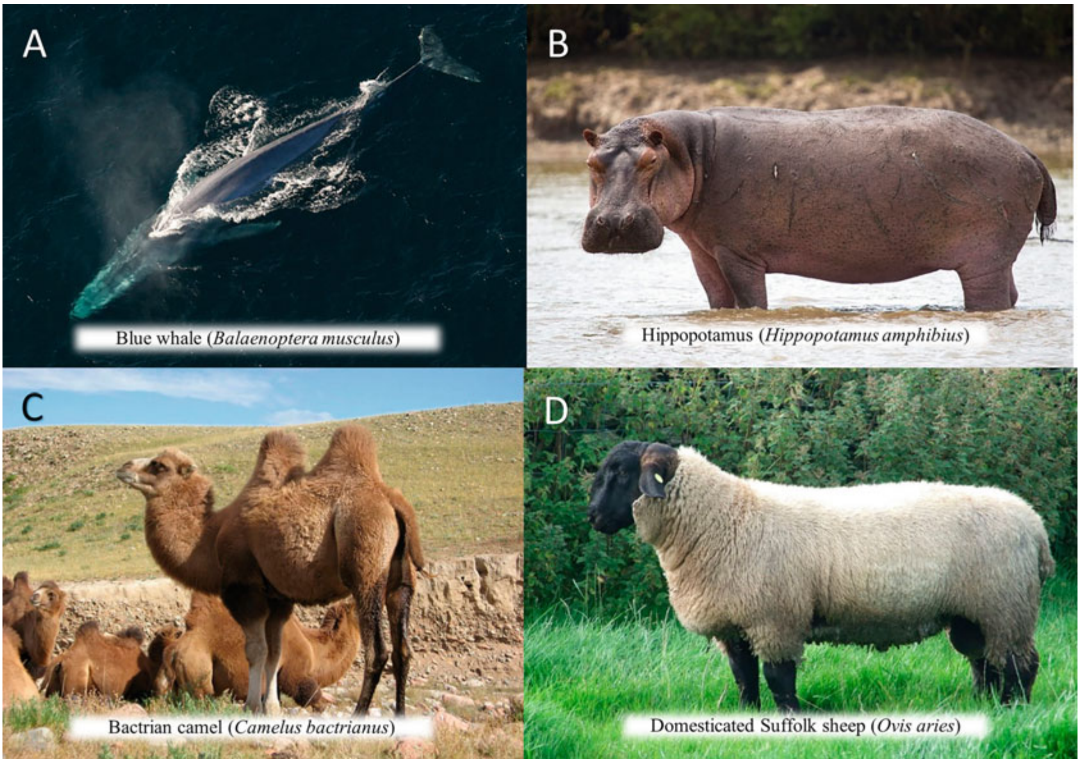
A
Blue whale (*Balaenoptera musculus*)
B
Hippopotamus (*Hippopotamus amphibius*)
C
Bactrian camel (*Camelus bactrianus*)
D
Domesticated Suffolk sheep (*Ovis aries*)

Fig. 4.18 Composite figure showing four species, the blue whale (*Balaenoptera musculus*) (**a**), hippopotamus (*Hippopotamus amphibius*) (**b**), Bactrian camel (*Camelus bactrianus*) (**c**), and domesticated Suffolk sheep (*Ovis aries*) (**d**). While these four species look very different, they are all classified within the order Artiodactyla meaning they shared a common ancestor 76 million years ago, less distantly than the hedgehog and tenrec whose last common ancestor lived around 99 million years ago (Kumar et al. 2017). Images from NOAA Photo Library, Muhammad Mahdi Karim, Yaan, and J Gareth p at the English Wikipedia and licensed under CC0 1.0 (PD-USGov), CC BY-SA 4.0, CC BY-SA 3.0, and CC BY-SA 3.0, respectively

or white flowers. Genetic analysis is about extracting the specific sequence of letters that makes up an organism's DNA and visualizing not only differences in the overall use of each letter, but also the differences in sequence. The raw output of this looks very similar to computer code and usually requires a background in genetics to make sense of it (Fig. 4.20).

Figure 4.20 shows short sections of the DNA sequences of a total of ten specimens of African elephant (*Loxodonta*), Asian elephant (*Elephas*), and mammoth (*Mammuthus*) (Thomas et al. 2000). In this case, Fig. 4.20 literally displays the nucleotide sequence (the letters A, T, C, and G in the order they appear), with dots indicating the same nucleotide as the reference animal at the top (labeled Lox-ref). A letter thus indicates that the animal has a different nucleotide than the reference individual. The sequences in our example Fig. 4.20 are very short, but they make it easy to see why whole genome analysis cannot rely on visualizations of full sequences. The entire genome for the African elephant is 3196.74 Mb (megabases) long, meaning that if one letter represents one nucleotide base, then the entire African elephant genome would have 3,196,740,000 letters in it (National Center for Biotechnology Information 2023). To compare the sequences systematically, we need programs capable of handling vast quantities of genetic data—and visualization techniques that can summarize and synthesize the results.

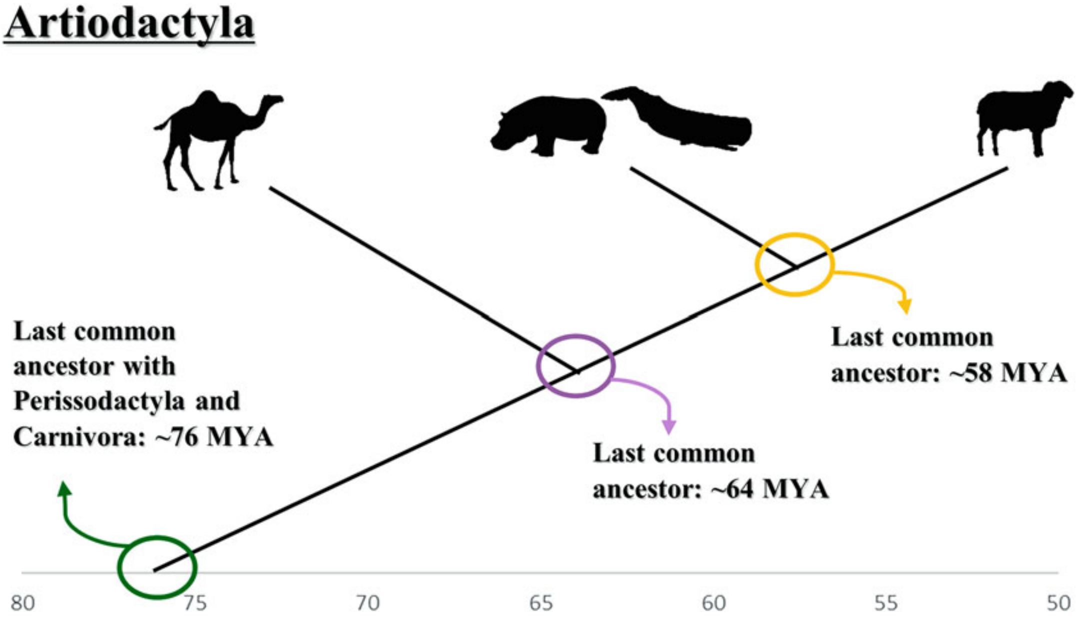
Artiodactyla
Last common ancestor with Perissodactyla and Carnivora: ~76 MYA
Last common ancestor: ~64 MYA
Last common ancestor: ~58 MYA
80
75
70
65
60
55
50

Fig. 4.19 A simplified cladogram showing the last common ancestors in millions of years (MYA) for four species, the dromedary camel (*Camelus dromedarius*), the hippopotamus (*Hippopotamus amphibius*), the sperm whale (*Physeter macrocephalus*), and the domestic sheep (*Ovis aries*). Despite all four looking vastly different, they are all part of the same order (Artiodactyla) which last had a common ancestor with the orders Perissodactyla and Carnivora around 76 MYA. Camels were the first group to diverge around 64 MYA before whales/hippopotami diverged from some hoofed mammals such as sheep around 58 MYA. Figure created by using data from Kumar, et al., (2017) and iconography from PhyloPic, and specifically uploaded by Katy Lawler, Margot Michaud, and Jody Taylor. All images are available and in the public domain (CC0 1.0)

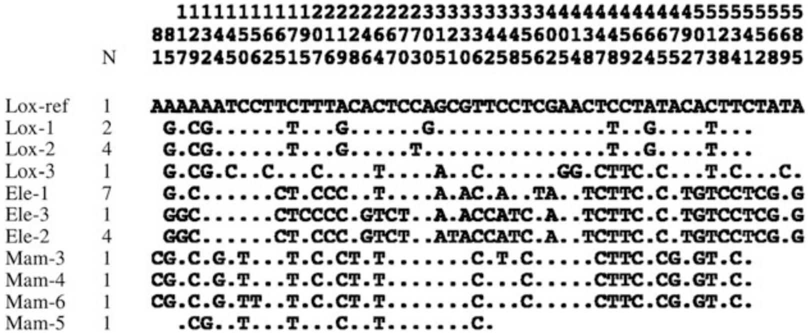

```
                  11111111111222222222333333333344444444444455555555 5
                 88123445566790112466770123344456001344566679012345668
           N     15792450625157698647030510625856254878924552738412895

Lox-ref    1     AAAAAATCCTTCTTTACACTCCAGCGTTCCTCGAACTCCTATACACTTCTATA
Lox-1      2      G.CG......T...G......G...............T..G....T...
Lox-2      4      G.CG......T...G.....T................T..G....T...
Lox-3      1      G.CG.C..C...C....T....A..C......GG.CTTC.C...T.C...C.
Ele-1      7      G.C......CT.CCC..T....A.AC.A..TA..TCTTC.C.TGTCCTCG.G
Ele-3      1      GGC......CTCCCC.GTCT..A.ACCATC.A..TCTTC.C.TGTCCTCG.G
Ele-2      4      GGC......CT.CCC.GTCT..ATACCATC.A..TCTTC.C.TGTCCTCG.G
Mam-3      1     CG.C.G.T...T.C.CT.T.......C.T.C.....CTTC.CG.GT.C.
Mam-4      1     CG.C.G.T...T.C.CT.T.......C...C.....CTTC.CG.GT.C.
Mam-6      1     CG.C.G.TT..T.C.CT.T.......C...C.....CTTC.CG.GT.C.
Mam-5      1       .CG..T...T...C..T.......C.
```

Fig. 4.20 Genetic sequences from Thomas et al. (2000)'s analysis of ten individuals from three genera, *Loxodonta* (African elephant), *Elephas* (Asian elephant), and *Mammuthus* (mammoth). A dot means the nucleotide base at that locality is the same as in the reference species (Lox-ref, at the top), while a letter represents a base that is different from the one that is in the reference species. Reprinted by permission from the Royal Society: Royal Society, Proceedings of the Royal Society of London. Series B: Biological Sciences. Thomas et al. 2000. *Molecular and morphological evidence on the phylogeny of the Elephantidae. 267 (1461) pp. 2493–2500.* https://doi.org/10.1098/rspb.2000.1310

One of the most common ways of visualizing the results of genetic analysis is through a phylogenetic tree or cladogram. Both trees and cladograms show the relationship between organisms, but the length of the branches in a phylogenetic tree is proportional to a measure of evolutionary (usually genetic) distances between taxa, while a tree (like Darwin's in Fig. 4.12) is usually not proportional. The two examples seen below in Fig. 4.21, are genetic cladograms for living primates (Fig. 4.21a, from Perelman et al. 2011) and carnivores (Fig. 4.21b, from Flynn et al. 2005). These cladograms visually represent the overall similarities in the sequences of the organisms by calculating measures of overall similarity between them and drawing out the branching sequence of their ancestors as reflected in those similarities.

Beginning on the left-hand side in each case, one sees the last common ancestor of the whole group of species splitting into two taxa that split again and again until reaching the present-day species on the right. For example, using Fig. 4.21a we can follow a lineage from the base of the tree on the left through branching points B, C, G, and H, and see that humans (*Homo*) are most closely related to chimpanzees and bonobos who make up the genus *Pan*. In Fig. 4.21b, we can start with Caniformia, go to Arctoidea, then Pinnipedia to see that seals (Otariida) are most closely related to walruses (Odobenidae) and very distantly related to cats (Felidae) despite all three animals being carnivores. There are, of course, many different pathways that can be traced in each tree, which is what gives these cladograms their huge explanatory power: they show the relationships and histories of all the depicted lineages, as they were captured in the specific bit of DNA analyzed. Many cladograms, like these two, add a great amount of contextual information in the form of color, images of taxa, labels, and lettering with a key, which allows them to effectively convey a lot more than the raw data can (Lunn et al. 2022). There are many ways to visualize genetic trees, and a good genetic tree can convey a lot of information in a small image.

Modern taxonomic visualizations can also combine genetic evidence with data from other sources such as the biogeographical information found in Fig. 4.22. This image accompanies a paper presenting a new orangutan species, *Pongo tapanuliensis*, to the academic community and includes three different visuals: a map showing the geographical distribution of this species and its close relatives, as well as two visualizations of genetic data.

Instead of presenting a genetic tree, Nater et al. (2017) have shown us a plot that visualizes the outputs of a statistical analysis of gene sequences (Fig. 4.22b). On this plot, the dots that are spread out in the box with a group in the top left- and right-hand corner, as well as a group in the bottom left of the plot, represent individual orangutans. The dot colors show their species, and the distance between dots indicates how similar their sequences are. This image visualizes the fact that the two established orangutan species *Pongo abelii* and *Pongo pygmaeus* are genetically distinct from each other and cluster in opposite corners of the PCA plot, therefore demonstrating different characteristics from one another. The visual and genetic distance between them is roughly the same as it is between each of them and the new proposed *Pongo tapanuliensis* species. Therefore, these authors suggest that this indicates that this species is substantially different from previously known species and so worthy of recognition in its own right. The second visualization shows where each of the genes for each individual orangutan studied seems to have originated from, with each vertical bar representing an individual and the colors identifying populations. The colors on all three images coincide so that the populations and sub-populations that are geographically close also cluster together in terms of genetic distances and tend to have exchanged genes only with each other. The red and orange groups seem to make up one species, the yellow group a separate (new) species, and the blue, green, and purple groups a third species. However, the small number of yellow points and individuals with yellow ancestry in the genetic visualizations also point to an inherent weakness of this analysis: it was forced to rely

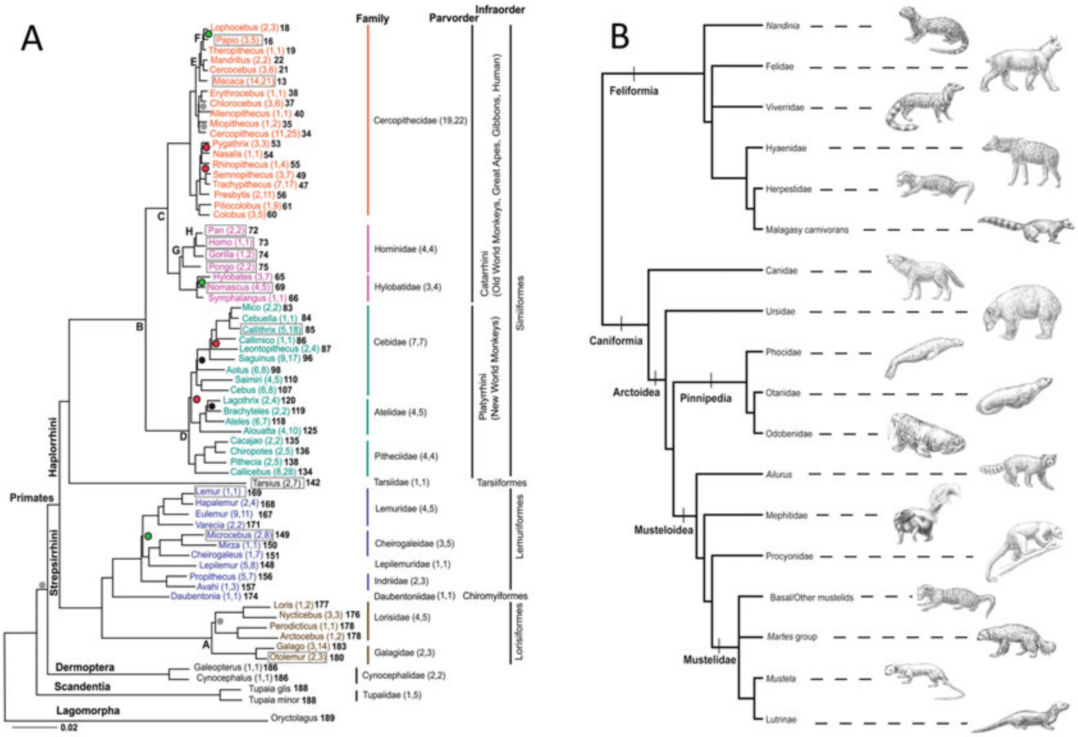
A
Family
Parvorder
Infraorder
Lophocebus (2,3) 18
F
Papio (3,5) 16
Theropithecus (1,1) 19
E
Mandrillus (2,2) 22
Cercocebus (3,6) 21
Macaca (14,21) 13
Erythrocebus (1,1) 38
Chlorocebus (3,6) 37
Allenopithecus (1,1) 40
Miopithecus (1,2) 35
Cercopithecus (11,25) 34
Pygathrix (3,3) 53
Nasalis (1,1) 54
Rhinopithecus (1,4) 55
Semnopithecus (3,7) 49
Trachypithecus (7,17) 47
Presbytis (2,11) 56
Piliocolobus (1,9) 61
Colobus (3,5) 60
C
H
Pan (2,2) 72
Homo (1,1) 73
G
Gorilla (1,2) 74
Pongo (2,2) 75
Hylobates (3,7) 65
Nomascus (4,5) 69
Symphalangus (1,1) 66
Mico (2,2) 83
Cebuella (1,1) 84
Callithrix (5,18) 85
B
Callimico (1,1) 86
Leontopithecus (2,4) 87
Saguinus (9,17) 96
Aotus (6,8) 98
Saimiri (4,5) 110
Cebus (6,8) 107
Lagothrix (2,4) 120
Brachyteles (2,2) 119
Ateles (6,7) 118
Alouatta (4,10) 125
D
Cacajao (2,2) 135
Chiropotes (2,5) 136
Pithecia (2,5) 138
Callicebus (8,28) 134
Tarsius (2,7) 142
Haplorrhini
Primates
Lemur (1,1) 169
Hapalemur (2,4) 168
Eulemur (9,11) 167
Varecia (2,2) 171
Microcebus (2,8) 149
Mirza (1,1) 150
Cheirogaleus (1,7) 151
Lepilemur (5,8) 148
Propithecus (5,7) 156
Avahi (1,3) 157
Daubentonia (1,1) 174
Strepsirrhini
Loris (1,2) 177
Nycticebus (3,3) 176
Perodicticus (1,1) 178
Arctocebus (1,2) 178
A
Galago (3,14) 183
Otolemur (2,3) 180
Dermoptera
Galeopterus (1,1) 186
Cynocephalus (1,1) 186
Scandentia
Tupaia glis 188
Tupaia minor 188
Lagomorpha
Oryctolagus 189
0.02
Cercopithecidae (19,22)
Hominidae (4,4)
Hylobatidae (3,4)
Cebidae (7,7)
Atelidae (4,5)
Pitheciidae (4,4)
Tarsiidae (1,1)
Lemuridae (4,5)
Cheirogaleidae (3,5)
Lepilemuridae (1,1)
Indriidae (2,3)
Daubentoniidae (1,1)
Lorisidae (4,5)
Galagidae (2,3)
Cynocephalidae (2,2)
Tupaiidae (1,5)
Catarrhini (Old World Monkeys, Great Apes, Gibbons, Human)
Platyrrhini (New World Monkeys)
Simiiformes
Tarsiiformes
Lemuriformes
Chiromyiformes
Lorisiformes
B
Feliformia
Nandinia
Felidae
Viverridae
Hyaenidae
Herpestidae
Malagasy carnivorans
Caniformia
Canidae
Ursidae
Arctoidea
Pinnipedia
Phocidae
Otariidae
Odobenidae
Ailurus
Musteloidea
Mephitidae
Procyonidae
Basal/Other mustelids
Martes group
Mustelidae
Mustela
Lutrinae

Fig. 4.21 Two figures that visualize complex genetic data in an accessible way, in the form of a phylogenetic tree or cladogram. (**a**) shows "the molecular phylogeny of 61 Primate genera, two Dermoptera [colugos] genera, and one Scandentia [treeshrew] genus and rooted by Lagomorpha [hares, rabbits, and pikas]" (Fig. 4.1 from Perelman et al. 2011). (**b**) shows "a schematic cladogram representing the major evolutionary relationships recovered in this analysis of Carnivora." Illustrations of representative taxa for major lineages are available in the original manuscript (Fig. 4.5 from Flynn et al. 2005). Figure 4.21a reprinted from *Perelman P, Johnson WE, Roos C, Seuánez HN, Horvath JE, Moreira MAM,* et al. (2011) *A Molecular Phylogeny of Living Primates. PLoS Genetics 7(3): e1001342*. https://doi.org/10.1371/journal.pgen.1001342 and made available under the Creative Commons CC0 public domain direction. Figure 4.21b reprinted by permission from Oxford University Press: Oxford University Press, Systematic Biology, *Flynn, J.J., Finarelli, J.A., Zehr, S., Hsu, J. and Nedbal, M.A.* 2005. *Molecular Phylogeny of the Carnivora (Mammalia): Assessing the Impact of Increased Sampling on Resolving Enigmatic Relationships. 54 (2) pp. 317–337.* https://doi.org/10.1080/10635150590923326

on genetic samples from just two individuals of the proposed new species. Combining this data with behavioral and macroscopic anatomical evidence was therefore key to the argument that *Pongo tapanuliensis* was a separate species.

Genetic analysis has undoubtedly been one of the biggest changes to the field of taxonomy since Carl Linnaeus implemented his binomial nomenclature naming system. By moving to the smallest parts of an organism (its DNA), it is now possible to visualize evolutionary history as recorded in a different, but complementary medium—the genotype as opposed to the phenotype. Being able to effectively visualize genetic sequences and distances has been very important for our ability to classify organisms, as macroscopic and microscopic anatomy can be used alongside genetics to understand evolution in new ways. A combination of all the evidence is stronger than any single piece of evidence in isolation.

4.5 Conclusions

In this chapter, we have shown how several notable changes in visualization techniques have each

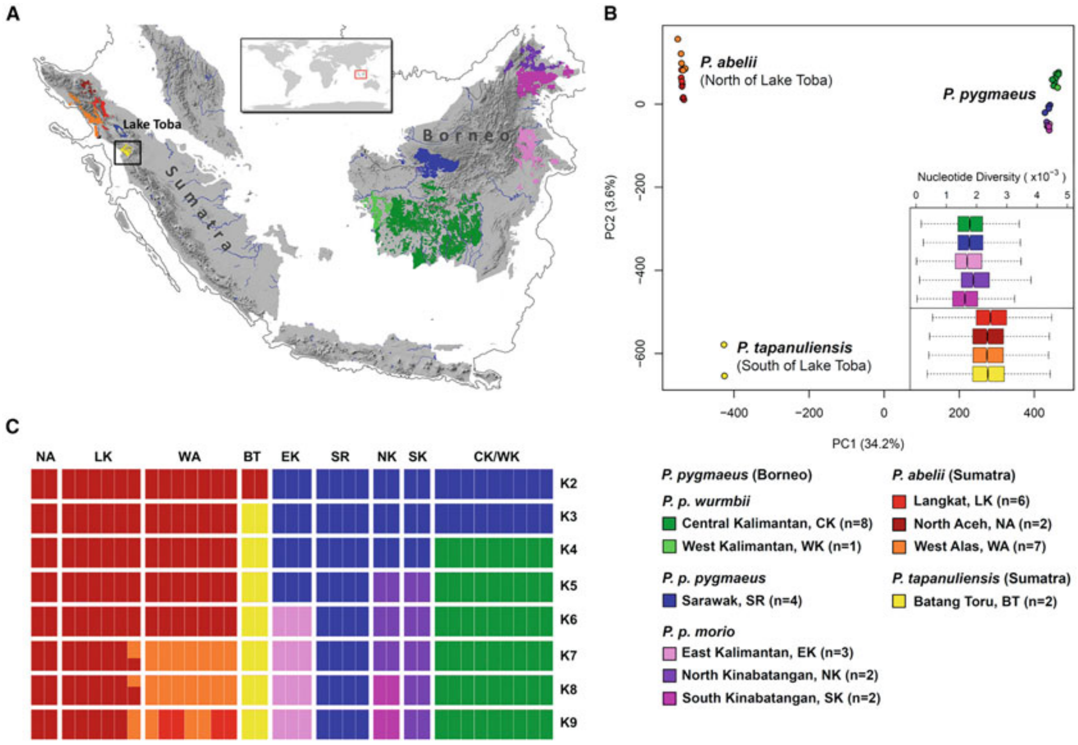

Fig. 4.22 "Distribution, Genomic Diversity, and Population Structure of the Genus *Pongo*" (Nater et al. 2017, Fig. 4.2). (**a**) "Sampling areas across the current distribution of orangutans. The contour indicates the extent of the exposed Sunda Shelf during the Last Glacial Maximum." (**b**) "PCA of genomic diversity in Pongo. Axis labels show the percentages of the total variance explained by the first two principal components." A PCA plot reduces the data set to a single component value that explains the variance in the data. Plotting the first two principal components (the ones which explain most of the variance) allows for easier comparisons in big data sets. (**c**) "Bayesian clustering analysis of population structure using the program ADMIXTURE. Each vertical bar depicts an individual, with colors representing the inferred ancestry proportions with different assumed numbers of genetic clusters (K, horizontal sections)." Reprinted by permission from Elsevier: Elsevier, Current Biology, Nater et al. 2017. *Morphometric, Behavioural, and Genomic Evidence for a New Orangutan Species. 27 (22) pp. 3487–3498.* https://doi.org/10.1016/j.cub.2017.09.047

revolutionized the way we do taxonomy. The fundamental approach to classification, i.e., looking for similarities and differences between organisms, has remained essentially the same regardless of changes in method or technology. However, it is the developments in the way that we visualize an organism that has allowed us to describe progressively more and more species and classify them more and more precisely. For hundreds of years, taxonomy was done on a macroscopic scale using physical features that could be seen with the naked eye. The invention of the microscope allowed for the same morphology-based taxonomy but using features too small to be resolved with the human eye. Advancements in microscopy and the visualizations that accompanied this, allowed for the reclassification and understanding of large organisms on the basis of their microscopic anatomical details (e.g., the shapes and functions of shark denticles) and facilitated early classifications of microscopic organisms like Hooke's mold spot, as well as supporting multiple and vital scientific breakthroughs by helping us to visualize and identify model organisms. More recently, the advent of genetics has added a new strand of evidence to taxonomists' arsenals, allowing them to classify not only on visible macroscopic and microscopic grounds but also by visualizing a more abstract characterization of the organism through sequencing its genome.

Some have argued that genetically based taxonomies should gradually replace anatomical ones, but here we have instead suggested that it is by having all of these lines of evidence together that allows for the greatest insight. Cases where only one line of evidence is available, as for fossil species, are always more challenging. The half-life of DNA is only 521 years, meaning that on average, half of a specimen's DNA will have disappeared 500 years after its death (Kaplan 2012). While this may allow us to extract genetic information from near prehistory, with some human relatives for example (Green et al. 2006; Ovchinnikov et al. 2000), this is virtually impossible for earlier animals like dinosaurs. Microscopic structures can also be fundamentally changed during fossilization, resulting in paleontological finds typically still being classified using macroscopic anatomy. The natural history museum in London described at least three new significant species last year alone (Agnolín et al. 2022; Davis 2022; Hui et al. 2022; Yao et al. 2022), so methods of identifying species using macroscopic and microscopic approaches to examine fossilized remains will never go out of fashion!

Macroscopic, microscopic, and genetic taxonomies each have their own strengths and weaknesses. In order to gain a thorough understanding of ancient life-forms and how taxa have evolved, being able to visualize both the anatomical and the genetic levels is invaluable. Through examining different species at differing scales and resolutions, we can gain the insight and detail needed to develop robust, systematic classifications for the organisms we share the planet with and live alongside.

References

Aboelsoud NH (2010) Herbal medicine in ancient Egypt. J Med Plant Res 4(2):82–86

Ackermann H-W, Prangishvili D (2012) Prokaryote viruses studied by electron microscopy. Arch Virol 157:1843–1849. https://doi.org/10.1007/s00705-012-1383-y

Agnolín FL et al (2022) First definitive abelisaurid theropod from the late cretaceous of northwestern Argentina. J Vertebr Paleontol 41(4):e2002348. https://doi.org/10.1080/02724634.2021.2002348

Akkari N, Cheung DK-B, Enghoff H, Stoev P (2013) Revolving SEM images visualising 3D taxonomic characters: application to six species of the millipede genus *Ommatoiulus* Latzel, 1884, with description of seven new species and an interactive key to the Tunisian members of the genus (Diplopoda, Julida, Julidae). Zookeys 328:5–45. https://doi.org/10.3897/zookeys.328.5763

Amadio AH, Kenny AJ (2023) Aristotle. Encylopedia Britannica [Online] Available at: https://www.britannica.com/biography/Aristotle. Accessed 22 Feb 2023

Andersen HT (1966) Physiological adaptations in diving vertebrates. Physiol Rev 46(2):212–243. https://doi.org/10.1152/physrev.1966.46.2.212

Anh NH et al (2020) Ginger on human health: a comprehensive systematic review of 109 randomized controlled trials. Nutrients 12(1):157. https://doi.org/10.3390/nu12010157

Arfeen Z et al (1995) A double-blind randomized controlled trial of ginger for the prevention of postoperative nausea and vomiting. Anaesth Intensive Care 23(4):449–452. https://doi.org/10.1177/0310057X9502300406

Aristotle, Ogle W (1882a) On the parts of animals. K. Paul, French & Company. https://doi.org/10.5962/bhl.title.30294

Aristotle, Ogle W (1882b) The main groups of animals. In: On the parts of animals. K. Paul, French and Company, p 33. https://doi.org/10.5962/bhl.title.30294

Beck RM et al (2006) A higher-level MRP supertree of placental mammals. BMC Evol Biol 6:1–14. https://doi.org/10.1186/1471-2148-6-93

Bhatia S (2015) Chapter 2–plant tissue culture. In: Modern applications of plant biotechnology in pharmaceutical sciences. Academic Press, Elsevier, Oxford, pp 31–107. https://doi.org/10.1016/B978-0-12-802221-4.00002-9

Brenner S (1974) The Genetics of Caenorhabditis Elegans. Genetics 77(1):71–94. https://doi.org/10.1093/genetics/77.1.71

Britannica EE (2023) Biological classification. Enyclopedia Britannica Kids Available at: https://kids.britannica.com/students/article/biological-classification/611149#. Accessed 27 Feb 2023

Britannica EE (2019a). Shennong. Encyclopedia Britannica. [Online] Available at: https://www.britannica.com/topic/Shennong. Accessed 21 Feb 2023

Britannica EE (2019b) Ebers papyrus. Encyclopedia Britannica. [Online] Available at: https://www.

britannica.com/topic/Ebers-papyrus. Accessed 21 Feb 2023

Cain AJ (2022) Taxonomy. Encyclopedia Britannica. [Online] Available at: https://www.britannica.com/science/taxonomy. Accessed 22 Feb 2023

Calisher CH (2007) Taxonomy: What's in a name? Doesn't a rose by any other name smell as sweet? Croatian Medical Journel 48(2):268–270

Campbell NA et al (2018a) Unit 3–the genetic basis of life. In: Biology–a global approach, 11th edn. Pearson, New York, pp 303–498

Campbell NA et al (2018b) Unit 4–Evolution. In: Biology–a global approach. Pearson, New York, pp 499–606

Centers for Disease Control and Prevention (2021) Genetics 101. [Online] Available at: https://www.cdc.gov/genomics/about/basics.htm. Accessed 11 Mar 2023

Chikina M, Robinson JD, Clark NL (2016) Hundreds of genes experienced convergent shifts in selective pressure in marine mammals. Mol Biol Evol 33(9):2182–2192. https://doi.org/10.1093/molbev/msw112

Choudhuri S (2014) Chapter 2–fundamentals of molecular evolution. In: Bioinformatics for beginners: genes, genomes, molecular evolution, databases and analytical tools. Academic Press, Elsevier, s.l., pp 27–53. https://doi.org/10.1016/B978-0-12-410471-6.00002-5

Cobb M (2006) Heredity before genetics: a history. Nat Rev Genet 7(12):953–958. https://doi.org/10.1038/nrg1948

Convention on Biological Diversity (2010) Global taxonomy initiative. [Online] Available at: https://www.cbd.int/gti/taxonomy.shtml#:~:text=Taxonomy%20is%20the%20science%20of,and%20microorganisms%20of%20the%20world. Accessed 14 Feb 2023

Costello MJ, May RM, Stork NE (2013) Can we name Earth's species before they go extinct? Science 339(6118):413–416. https://doi.org/10.1126/science.1230318

Darwin C, Wallace A (1858) On the tendency of species to form varieties; and on the perpetuation of varieties and species by natural means of selection. J Proc Linn Soc London Zool 3(9):45–62. https://doi.org/10.1111/j.1096-3642.1858.tb02500.x

Darwin C (1859) On the origin of species. John Murray, London. https://doi.org/10.5962/bhl.title.28875

Davis J (2022) Museum scientists described 351 new species in 2022. [online] Available at: https://www.nhm.ac.uk/discover/news/2022/december/natural-history-museum-scientists-describe-351-new-species-in-2022.html. Accessed 6 Mar 2023

Dillon EM, Norris RD, O'Dea A (2017) Dermal denticles as a tool to reconstruct shark communities. Mar Ecol Prog Ser 566:117–134. https://doi.org/10.3354/meps12018

doe Reis M et al (2012) Phylogenomic datasets provide both precision and accuracy in estimating the timescale of placental mammal phylogeny. Proc R Soc B Biol Sci 279(1742):3491–3500. https://doi.org/10.1098/rspb.2012.0683

Dragoo JW, Honeycutt RL (1997) Systematics of mustelid-like carnivores. J Mammal 78(2):426–443. https://doi.org/10.2307/1382896

Duszynski DW, Kvičerová J, Seville RS (2018) Chapter 1–introduction. In: The biology and identification of the Coccidia (Apicomplexa) of carnivores of the world. Academic Press, London, pp 1–6. https://doi.org/10.1016/B978-0-12-811349-3.00001-3

Encyclopaedia Britannica, T. E. o (2014) Canine tooth. Enylocpedia Britannica. [Online] Available at: https://www.britannica.com/science/canine-tooth. Accessed 3 Mar 2023

Encyclopaedia Britannica, T. E. o (2023) Robert Hooke. Encyclopedia Britannica. [Online] Available at: https://www.britannica.com/biography/Robert-Hooke. Accessed 6 Mar 2023

Fara P (2009) A microscopic reality tale. Nature 459(7247):642–644. https://doi.org/10.1038/459642a

Fields S, Johnston M (2005) Whither model organism research? Science 307(5717):1885–1886. https://doi.org/10.1126/science.1108872

Fish FE, Howle LE, Murray MM (2008) Hydrodynamic flow control in marine mammals. Integr Comp Biol 48(6):788–800. https://doi.org/10.1093/icb/icn029

Fish FE, Hui CA (1991) Dolphin swimming–a review. Mammal Rev 21(4):181–195. https://doi.org/10.1111/j.1365-2907.1991.tb00292.x

Flynn JJ et al (2005) Molecular phylogeny of the Carnivora (Mammalia): assessing the impact of increased sampling on resolving enigmatic relationships. Syst Biol 54(2):317–337. https://doi.org/10.1080/10635150590923326

Flynn JJ, Nedbal MA (1998) Phylogeny of the Carnivora (Mammalia): congruence vs incompatibility among multiple data sets. Mol Phylogenet Evol 9(3):414–426. https://doi.org/10.1006/mpev.1998.0504

Frank SA (2004) Genetic predisposition to cancer—insights from population genetics. Nat Rev Genet 5(10):764–772. https://doi.org/10.1038/nrg1450

Friedberg E (2019) Sydney Brenner (1927-2019). Nature 568(7753):459. https://doi.org/10.1038/d41586-019-01192-9

Gabora L (2013) Convergent evolution. In: Maloy S, Hughes K (eds) Brenner's encyclopedia of genetics. Acadmic Press, pp 178–180. https://doi.org/10.1016/B978-0-12-374984-0.00336-3

Alliance G (2006) A guide to genetics and health. Genetic Alliance, Washington (DC)

Goldsmith CS, Miller SE (2009) Modern uses of electron microscopy for detection of viruses. Clin Microbiol Rev 22(4):552–563. https://doi.org/10.1128/CMR.00027-09

Graur D, Higgins DG (1994) Molecular evidence for the inclusion of cetaceans within the order Artiodactyla. Mol Biol Evol 11(3):357–364. https://doi.org/10.1093/oxfordjournals.molbev.a040118

Green RE et al (2006) Analysis of one million base pairs of Neanderthal DNA. Nature 444(7117):330–336. https://doi.org/10.1038/nature05336

Hancock L, World Wildlife Foundation (2023) What is biodiversity? WWF [Online] Available at: https://www.worldwildlife.org/pages/what-is-biodiversity. Accessed 22 Feb 2023

Holgate JH, Webb J (2003) MICROSCOPY | light microscopy and histochemical methods. In: Caballero B (ed) Encyclopedia of food sciences and nutrition, 2nd edn. Academic Press, pp 3917–3922. https://doi.org/10.1016/B0-12-227055-X/00778-1

Holtzman NA, Marteau TM (2000) Will genetics revolutionize medicine? N Engl J Med 343(2):141–144. https://doi.org/10.1056/NEJM200007133430213

Hooke R (1665) Micrographia, or, some physiological descriptions of minute bodies made by magnifying glasses: with observations and inquiries thereupon, 1st edn. Royal Society, London. https://doi.org/10.5962/bhl.title.904

Hui D et al (2022) New stegosaurs from the middle Jurassic lower member of the Shaximiao formation of Chongqing, China. J Vertebrate Paleontol 41(5): e1995737. https://doi.org/10.1080/02724634.2021.1995737

IAPT (2023) International association for plant taxonomy. [online] Available at: https://www.iaptglobal.org/. Accessed 27 Feb 2023

ICTF (2023) International commission on the taxonomy of fungi. [online] Available at: https://www.fungaltaxonomy.org/. Accessed 27 Feb 2023

ICZN (2023) International commission on zoological nomenclature. [online] Available at: https://www.iczn.org/. Accessed 27 Feb 2023

IUCN Red List (2022) Background & history–the IUCN red list. [Online] Available at: https://www.iucnredlist.org/about/background-history. Accessed 1 April 2023

IUCN Red List (2023) Taxonomic Sources. IUCN Red List. [Online] Available at: https://www.iucnredlist.org/resources/tax-sources. Accessed 22 Feb 2023

Josling P (2001) Preventing the common cold with a garlic supplement: a double-blind, placebo-controlled survey. Adv Ther 18:189–193. https://doi.org/10.1007/BF02850113

Kaplan M (2012) DNA has a 521-year half-life. [online] Available at: https://www.nature.com/articles/nature.2012.11555. Accessed 14 Mar 2023

Klayman DL (1985) Qinghaosu (artemisinin): an antimalarial drug from China. Science 228(4703):1049–1055. https://doi.org/10.1126/science.3887571

Kooyman GL (2006) Mysteries of adaptation to hypoxia and pressure in marine mammals–the Kenneth S. Norris lifetime achievement award lecture. Mar Mamm Sci 22(3):507–526. https://doi.org/10.1111/j.1748-7692.2006.00069.x

Krungkrai J, Krungkrai SR (2016) Antimalarial qinghaosu/artemisinin: the therapy worthy of a Nobel prize. Asian Pac J Trop Biomed 6(5):371–375. https://doi.org/10.1016/j.apjtb.2016.03.010

Kumar S, Stecher G, Suleski M, Hedges SB (2017) TimeTree: a resource for timelines, Timetrees, and divergence times. Mol Biol Evol 34(7):1812–1819. https://doi.org/10.1093/molbev/msx116

Ladurner P, Schärer L, Salvenmoser W, Rieger RM (2005) A new model organism among the lower Bilateria and the use of digital microscopy in taxonomy of meiobenthic Platyhelminthes: *Macrostomum lignano*, n. sp. (Rhabditophora, Macrostomorpha). J Zool Syst Evol Res 43(2):114–126. https://doi.org/10.1111/j.1439-0469.2005.00299.x

Lewontin RC (1970) The units of selection. Annu Rev Ecol Syst 1(1):1–18. https://doi.org/10.1146/annurev.es.01.110170.000245

Linnaeus C, Salvius L (1758) Caroli Linnaei. . .Systema naturae per regna tria naturae: secundum classes, ordines, genera, species, cum characteribus, differentiis, synonymis, locis, 10th edn. Impensis Direct. Laurentii Salvii, Holmiae. https://doi.org/10.5962/bhl.title.542

Lin Y-H, Penny D (2001) Implications for bat evolution from two new complete mitochondrial genomes. Mol Biol Evol 18(4):684–688. https://doi.org/10.1093/oxfordjournals.molbev.a003850

Lissiman E, Bhasale AL, Cohen M (2014) Garlic for the common cold. Cochrane Database Syst Rev 11: CD006206. https://doi.org/10.1002/14651858.CD006206.pub4

Lunn AJ, Shaw V, Winder IC (2022) The evolution of scientific visualizations: a case study approach to big data for varied audiences. In: Shapiro L, Rea PM (eds) Biomedical visualization volume 12–the importance of context in image-making. Advances in experimental medicine and biology, vol 1388. Springer, Cham, pp 51–84. https://doi.org/10.1007/978-3-031-10889-1_3

Mace GM (2004) The role of taxonomy in species conservation. Philos Trans R Soc Lond B Biol Sci 359(1444): 711–719. https://doi.org/10.1098/rstb.2003.1454

Madesn O et al (2001) Parallel adaptive radiations in two major clades of placental mammals. Nature 409:610–614. https://doi.org/10.1038/35054544

Manktelow M (2010) History of taxonomy. lecture from Dept. of systematic biology, Uppsala University. [online] Available at: http://www.atbi.eu/summerschool/files/summerschool/Manktelow_Syllabus.pdf. Accessed 14 Feb 2023

Marion JB (1981) 17–electrons and photons. In: Marion JB (ed) Physics in the modern world, 2nd edn. Academic Press, New York, pp 469–491. https://doi.org/10.1016/B978-0-12-472280-4.50020-4

Marx W et al (2017) The effect of a standardized ginger extract on chemotherapy-induced nausea-related quality of life in patients undergoing moderately or highly Emetogenic chemotherapy: a double blind, randomized, Placebo Controlled Trial. Nutrients 9(8): 867. https://doi.org/10.3390/nu9080867

Mendel G (1866) Versuche über Pflanzen-Hybriden. Im Verlage des Vereines, Brünn. https://doi.org/10.5962/bhl.title.61004

Meredith RW et al (2011) Impacts of the cretaceous terrestrial revolution and KPg extinction on mammal diversification. Science 334(6055):521–524. https://doi.org/10.1126/science.1211028

Montgelard C, Catzeflis FM, Douzery E (1997) Phylogenetic relationships of artiodactyls and cetaceans as deduced from the comparison of cytochrome b and 12S rRNA mitochondrial sequences. Mol Biol Evol 14(5):550–559. https://doi.org/10.1093/oxfordjournals.molbev.a025792

Mora C et al (2011) How many species are there on earth and in the ocean? PLoS Biol 9(8):e1001127. https://doi.org/10.1371/journal.pbio.1001127

Mouchaty SK, Gullberg A, Janke A, Arnason U (2008) Phylogenetic position of the tenrecs (Mammalia: Tenrecidae) of Madagascar based on analysis of the complete mitochondrial genome sequence of *Echinops telfairi*. Zool Scr 29(4):307–317. https://doi.org/10.1046/j.1463-6409.2000.00045.x

Müller-Wille S (2023) Carolus linnaeus. Encyclopedia britannica. [Online] Available at: https://www.britannica.com/biography/Carolus-Linnaeus. Accessed 27 Feb 2023

Musser G (2018) Insectivore. Encyclopedia britannica. [Online] Available at: https://www.britannica.com/animal/insectivore. Accessed 12 Mar 2023

Nantz MP et al (2011) Supplementation with aged garlic extract improves both NK and γδ-T cell function and reduces the severity of cold and flu symptoms: a randomized, double-blind, placebo-controlled nutrition intervention. Clin Nutr 31(3):337–344. https://doi.org/10.1016/j.clnu.2011.11.019

Nater A et al (2017) Morphometric, behavioral, and genomic evidence for a new orangutan species. Curr Biol 27(22):3487–3498. https://doi.org/10.1016/j.cub.2017.09.047

National Center for Biotechnology Information, N. L. o. M (2023) Loxodonta africana (African savanna elephant). [Online] Available at: https://www.ncbi.nlm.nih.gov/genome/224. Accessed 13 Mar 2023

National Geographic Society (2022) Microscopes. [Online] Available at: https://education.nationalgeographic.org/resource/microscopes/. Accessed 6 Mar 2023

National Human Genome Reserach Institute (2013) 1865: Mendel's Peas. [Online] Available at: https://www.genome.gov/25520230/online-education-kit-1865-mendels-peas. Accessed 11 Mar 2023

National Renewable Energy Laboratory (2023) Scanning electron microscopy. [Online] Available at: https://www.nrel.gov/materials-science/scanning-electron.html. Accessed 10 Mar 2023

Nikaido M et al (2003) Mitochondrial phylogeny of hedgehogs and monophyly of Eulipotyphla. Mol Phylogenet Evol 28(2):276–284. https://doi.org/10.1016/S1055-7903(03)00120-9

Nikaido M et al (2000) Monophyletic origin of the order Chiroptera and its phylogenetic position among Mammalia, as inferred from the complete sequence of the mitochondrial DNA of a Japanese Megabat, the Ryukyu flying fox (*Pteropus dasymallus*). J Mol Evol 51:318–328. https://doi.org/10.1007/s002390010094

Nussbaum RL, McInnes RR, Willard HF (2016) Thompson & Thompson Genetics in medicine, 8th edn. Elsevier, Philadelphia

Ovchinnikov IV et al (2000) Molecular analysis of Neanderthal DNA from the northern Caucasus. Nature 404(6777):490–493. https://doi.org/10.1038/35006625

Perelman P et al (2011) A molecular phylogeny of living primates. PLoS Genet 7(3):e1001342. https://doi.org/10.1371/journal.pgen.1001342

Rodríguez A, Calzada J (2015) Lynx pardinus (errata version published in 2020). The IUCN red list of threatened species. [online] Available at: https://www.iucnredlist.org/species/12520/174111773. Accessed 2023 Feb 2023

Rogalski A et al (2017) Differential procoagulant effects of saw-scaled viper (Serpentes: Viperidae: *Echis*) snake venoms on human plasma and the narrow taxonomic ranges of antivenom efficacies. Toxicol Lett 280:159–170. https://doi.org/10.1016/j.toxlet.2017.08.020

Royal Horticultural Society (2023) Kalmia latifolia. [Online] Available at: https://www.rhs.org.uk/plants/9708/kalmia-latifolia/details. Accessed 27 Feb 2023

Rutledge K et al. (2022) Speciation. [online] Available at: https://education.nationalgeographic.org/resource/speciation/. Accessed 11 Mar 2023

Schacherer J (2016) Beyond the simplicity of Mendelian inheritance. C R Biol 339(7–8):284–288. https://doi.org/10.1016/j.crvi.2016.04.006

Schultz M (2002) Microscopic investigation in fossil hominoidea: a clue to taxonomy, functional anatomy, and the history of disease. Anat Rec 257(6):225–232. https://doi.org/10.1002/(SICI)1097-0185(19991215)257:6<225::AID-AR8>3.0.CO;2-S

Scornavacca C et al (2019) OrthoMaM v10: scaling-up orthologous coding sequence and exon alignments with more than one hundred mammalian genomes. Mol Biol Evol 36(4):861–862. https://doi.org/10.1093/molbev/msz015

Sherborn CD, Soulsby BH, Brittish Museum (Natural History) Library (1933) A catalogue of the works of Linnæus (and publications more immediately relating thereto). In: Preserved in the libraries of the British Museum (Bloomsbury) and the British Museum (natural history), 2nd edn. South Kensington, London. https://doi.org/10.5962/bhl.title.99948

Shou-zhong Y (1998) Herbs: middle class. In: The divine Farmer’s Materia Medica: a translation of the Shen nong ben Cao Jing. Blue Poppy Press, INC., Boulder, CO, p 50

Soares KD, Gomes UL, De Carvalho MR (2016) Taxonomic review of catsharks of the *Scyliorhinus haeckelii* group, with the description of a new species (Chondrichthyes: Carcharhiniformes: Scyliorhinidae). Zootaxa 4066(5):501–534. https://doi.org/10.11646/zootaxa.4066.5.1

Song S, Liu L, Edwards SV, Wu S (2012) Resolving conflict in eutherian mammal phylogeny using phylogenomics and the multispecies coalescent model. PNAS 109(37):14942–14947. https://doi.org/10.1073/pnas.1211733109

Spaulding M, O'Leary MA, Gatesy J (2009) Relationships of Cetacea (Artiodactyla) among mammals: increased taxon sampling alters interpretations of key fossils and character evolution. PLoS One 4(9):e7062. https://doi.org/10.1371/journal.pone.0007062

Stanhope MJ et al (1998) Molecular evidence for multiple origins of Insectivora and for a new order of endemic African insectivore mammals. PNAS 95(17): 9967–9972. https://doi.org/10.1073/pnas.95.17.9967

Symonds MR (2007) Phylogeny and life histories of the 'Insectivora': controversies and consequences. Biol Rev 80(1):93–128. https://doi.org/10.1017/S1464793104006566

Tarver JE et al (2016) The interrelationships of placental mammals and the limits of phylogenetic inference. Genome Biol Evol 8(2):330–344. https://doi.org/10.1093/gbe/evv261

The British Library (2023) Micrographia by Robert Hooke, 1665. [Online] Available at: https://www.bl.uk/collection-items/micrographia-by-robert-hooke-1665. Accessed 6 Mar 2023

The IUCN Red List (2022) Summary statistics. [online] Available at: https://www.iucnredlist.org/resources/summary-statistics#Summary%20Tables. Accessed 6 Mar 2023

The Royal Society (2023) Why is biodiversity important? The Royal Society [Online] Available at: https://royalsociety.org/topics-policy/projects/biodiversity/why-is-biodiversity-important/?gclid=CjwKCAiAl9efBhAkEiwA4TorisksJwMK9Ny7VJ1eGVR9gYzk7BCD6FWWLHIZtrUtHnFpgfGlF4vLpRoC4uUQAvD_BwE. Accessed 22 Feb 2023

The Science Museum Group (2019) The microscope. [online] Available at: https://www.sciencemuseum.org.uk/objects-and-stories/medicine/microscope. Accessed 6 Mar 2023

Thomas MG et al (2000) Molecular and morphological evidence on the phylogeny of the Elephantidae. Proc R Soc Lond Ser B Biol Sci 267(1461):2493–2500. https://doi.org/10.1098/rspb.2000.1310

Ullah F et al (2021) Pollen morphology and its taxonomic potential in some selected taxa of Caesalpiniaceae observed under light microscopy and scanning electron microscopy. Microscopy Reserach and Technique 85(4):1410–1420. https://doi.org/10.1002/jemt.24004

Veron G et al (2004) Molecular systematics and origin of sociality in mongooses (Herpestidae, Carnivora). Mol Phylogenet Evol 30(3):582–598. https://doi.org/10.1016/S1055-7903(03)00229-X

Wachtel-Galor S, Yuen J, Buswell JA, Benzie IF (2011) *Ganoderma lucidum* (Lingzhi or Reishi): a medicinal mushroom. In: Benzie IF, Wachtel-Galor S (eds) Herbal medicine biomolecular and clinical aspects. Taylor & Francis Group, New York, pp 175–200

Wang J et al (2019) Artemisinin, the magic drug discovered from traditional Chinese medicine. Engineering 5(1):32–39. https://doi.org/10.1016/j.eng.2018.11.011

Winchester AM (2023) Genetics. Encyclopedia britannica. [Online] Available at: https://www.britannica.com/science/genetics/DNA-and-the-genetic-code. Accessed 11 Mar 2023

Woese CR, Kandler O, Wheelis ML (1990) Towards a natural system of organisms: proposal for the domains archaea, bacteria, and Eucarya. PNAS 87(12): 4576–4579. https://doi.org/10.1073/pnas.87.12.457

Wüster W (1996) Taxonomic changes and toxinology: systematic revisions of the asiatic cobras (*Naja naja* species complex). Toxicon 34(4):399–406. https://doi.org/10.1016/0041-0101(95)00139-5

Yao X et al (2022) A new early branching armored dinosaur from the lower Jurassic of southwestern China. eLife 11:e76248. https://doi.org/10.7554/eLife.75248

Youyou T (2017) Chapter 6–studies on pharmacological actions of Artemisia annua. In: From Artemisia Annua L. to Artemisinins: the discovery and development of Artemisinins and antimalarial agents. Academic Press, pp 109–138. https://doi.org/10.1016/B978-0-12-811655-5.00006-4

Zhou Y, Wang S-R, Ma J-Z (2017) Comprehensive species set revealing the phylogeny and biogeography of Feliformia (Mammalia, Carnivora) based on mitochondrial DNA. PLoS One 12(3):e0174902. https://doi.org/10.1371/journal.pone.0174902

5 Bright New World: Principles of Fluorescence and Applications in Spectroscopy and Microscopy

John G. Woodland

The title of this chapter is adapted from the title of Aldous Huxley's novel Brave New World (1932), which itself is a quotation from William Shakespeare's play *The Tempest. In the same way that Miranda is dazzled by the "many goodly creatures" on her island (Thompson et al. 2001), so too have biologists discovered whole new worlds of structural and functional detail under the fluorescence microscope. This chapter is based on material from my doctoral thesis (Woodland 2016) and is dedicated to the memory of Professor Timothy Egan (1962–2022), my PhD supervisor at the University of Cape Town, who passed away prematurely and who encouraged my first explorations in fluorescence. He is greatly missed by the South African and global scientific communities.*

Abstract

The study of fluorescence has revolutionized biomedical research. Since it was first described almost two centuries ago, fluorescence has transformed the scientific enterprise by facilitating unprecedented insights into the intricacies of biological systems on small and large scales. This chapter presents an overview of this curious photophysical phenomenon and the ways in which fluorescence can be harnessed to enrich our understanding of chemical and biological systems through spectroscopy and microscopy.

J. G. Woodland (✉)
Department of Chemistry and Holistic Drug Discovery and Development (H3D) Centre, University of Cape Town, Cape Town, South Africa

South African Medical Research Council Drug Discovery and Development Research Unit, Institute of Infectious Disease and Molecular Medicine, University of Cape Town, Cape Town, South Africa
e-mail: john.woodland@uct.ac.za

Keywords

Fluorescence · Microscopy · Spectroscopy · Image analysis

5.1 Introduction

Fluorescence-based techniques have recently enjoyed remarkable growth across many disciplines, culminating in the award of the 2014 Nobel Prize in Chemistry to William E. Moerner, Stefan Hell, and Eric Betzig for the development of super-resolution fluorescence microscopy. This recognition represents the pinnacle of a century-and-a-half of investigation that now permits the imaging of single proteins inside living cells with exquisite precision (Fig. 5.1). Technologies exploiting fluorescence are characterized by rapid speeds of response, high spatial resolution, and ultra-high sensitivity, meaning that fluorescence has become the technique of choice for probing the structure and dynamics of biological systems. Although modern fluorescence instruments enjoy single parts-per-trillion sensitivity over large

© The Author(s), under exclusive license to Springer Nature Switzerland AG 2023
L. Shapiro (ed.), *Microscopy Techniques for Biomedical Education and Healthcare Practice*, Biomedical Visualization 2, https://doi.org/10.1007/978-3-031-36850-9_5

concentration ranges, yielding superior contrast and specificity compared to visible light microscopy, the susceptibility of electronically-excited states to deactivation means that experiments must be planned carefully to avoid the pervasive effects of interference.

5.2 Historical Context

The origin of the term “fluorescence” is not immediately clear. Readers might assume that the prefix “fluor” may refer to the element fluorine, which is not itself fluorescent! Instead, “fluorescence” was coined by Sir George Stokes (1819–1903), a nineteenth-century physicist and mathematician who carefully observed solutions of the naturally occurring alkaloid quinine (Stokes 1852; Stokes 1853). Incidentally, the history of fluorescence is intimately linked to quinine because its reputation as a famous antimalarial at the time meant that it was a molecule of intense interest among scientists (Woodland and Chibale 2022).

Stokes’s studies of the alkaloid followed those of Sir John Herschel (1792–1871), a famous polymath,[1] who was the first to observe the unusual blue phenomenon at the surface of an acidic solution of quinine in sunlight. About the solution, Herschel wrote:

> Though perfectly transparent and colourless when held between the eye and the light . . . it yet exhibits . . . under certain incidences of light an extremely vivid and beautiful celestial blue colour. (Herschel 1845)

Later, it was Stokes who demonstrated that the phenomenon was a photophysical process that occurred after the absorption of light. In an elegant experiment, Stokes formed the solar spectrum by means of a prism (Valeur and Brochon 2001). When he moved the quinine solution through the visible part of the spectrum, the solution simply remained transparent. But beyond the violet portion of the spectrum (that is, in the region corresponding to ultraviolet radiation), the solution glowed with a blue light (Valeur 2001). Stokes wrote: “It was certainly a curious sight to see the tube instantaneously light up when plunged into the invisible rays; it was literally *darkness visible*” (Stokes 1852).

Stokes initially called this phenomenon “dispersive reflexion” but in a footnote wrote: “I do not like this term. I am almost inclined to coin a word, and call the appearance *fluorescence*, from *fluorspar*, as the analogous term opalescence is derived from the name of a mineral” (Stokes 1853). It is now known that, while calcium fluoride (the major constituent of fluorspar) is not fluorescent, fluorspar *appears* fluorescent due to the presence of small amounts of fluorescent lanthanide atoms (Valeur 2001).

Together, these observations by Herschel and Stokes laid the foundation for a century-and-a-half of intense development in the field of fluorescence. Edmond Becquerel (1820–1891), a French physicist and the father of Henri Becquerel who discovered radioactivity, described the apparent “fluorescence” of calcium sulfide and was the first to articulate that the emitted light is of longer wavelength than the incident light (Valeur 2001). Calcium sulfide is, in fact, *phosphorescent* and the first theoretical distinction between these two processes was provided by Francis Perrin (1901–1992) who also worked on a quantitative model of fluorescence quenching and polarized fluorescence (Valeur 2001). In 1948, Theodor Förster (1910–1974) published his quantum mechanical theory of dipole-dipole energy transfer (Sect. 5.3.4). Spectroscopy and microscopy, and our understanding of complex biological systems, would never be the same again.

---

[1] Sir John Frederick William Herschel was a British astronomer, mathematician, chemist, and photographer. It is an interesting reflection for this author that, in 1833, Herschel embarked on a journey to South Africa with his wife to catalog the stars, nebulae, and other objects of the southern skies. During their stay in the Cape, the Herschels also produced over 100 illustrations of Cape flora.

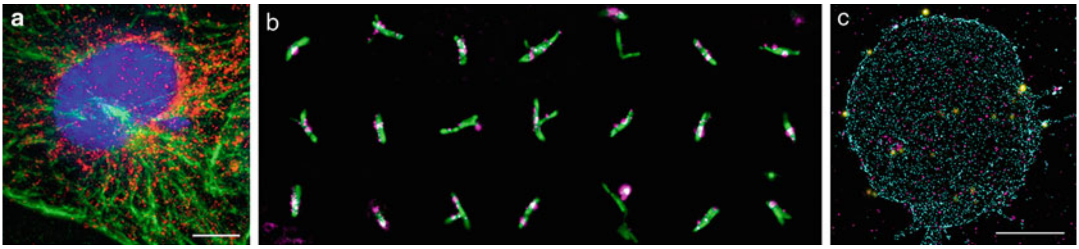

Fig. 5.1 Three images showcasing the breadth of meaningful biological information that can be acquired through fluorescence microscopy. (**a**) A Chinese hamster ovary cell illuminated with green fluorescent protein (GFP)-linked microtubulin (green) and GAPDH mRNA (red). The nucleus is stained blue and the scale bar represents 10 μm. (**b**) GFP-labeled mycobacteria (cytosolic expression) tagged at the surface with a human-derived monoclonal antibody (purple). (**c**) A single-molecule localization microscopy image of a human T-cell with super-resolved cell surface CD4 receptor (turquoise), HIV glycoprotein gp120 (magenta), and diffraction-limited HIV Gag protein (yellow) (scale bar represents 5 μm). Dr. Caron Jacobs (University of Cape Town) is gratefully acknowledged for these images

5.3 Characteristics of Fluorescence Excitation and Emission

5.3.1 Photophysical Processes

Fluorescence is a photophysical process in which light of a particular wavelength is absorbed by a molecule, exciting an electron to a higher energy level. This is followed by the release of light of lower energy as the electron returns to the ground state.

More accurately, fluorescence is the emission of light from a *singlet excited state*. In the singlet state, the electron in the excited orbital is paired by opposite spin to the electron in the ground state orbital (Fig. 5.2). Return to the ground state is spin-allowed and typically occurs within nanoseconds. Emission of light from a *triplet excited state*, in which the excited electron is no longer paired with the ground state electron, is spin-forbidden but still observed as a result of spin-orbit coupling. As a result, transitions to the ground state from the triplet excited state (called phosphorescence) are much slower and typically occur within milliseconds or seconds.

The Perrin-Jabłoński diagram is a partial energy-level diagram for photoluminescent systems and is a useful illustration of the photophysical processes relevant to fluorescence excitation and emission. The Polish physicist Alexander Jabłoński (1898–1950) is regarded as the “father” of fluorescence spectroscopy and the diagram is named after him along with Francis Perrin and his father, the physicist Jean Perrin (1872–1942) (Valeur 2001).

The singlet ground state and first and second excited states are depicted by S_0, S_1, and S_2, respectively (Fig. 5.3). At each of these electronic energy levels the molecules can exist in a number of vibrational states (depicted by 0, 1, 2, etc.) and further rotational energy levels (not illustrated). Transitions between states are indicated by vertical lines to indicate the almost-instantaneous nature of light absorption or emission. Dotted lines are used to indicate transitions between states resulting from internal conversion or non-radiative relaxation processes.

At room temperature, thermal energy is not sufficient to populate excited vibrational states. At this temperature, an even larger energy difference between ground and excited singlet states does not allow for thermal population of S_1. Consequently, as absorption and emission typically occur from molecules in their lowest vibrational energy states, light is used to induce fluorescence and not heat (Lakowicz 2010).

Fluorescence is typically governed by three important events, all of which occur on timescales separated by several orders of magnitude. When a photon is rapidly absorbed by a susceptible molecule (a femtosecond event), the molecule is

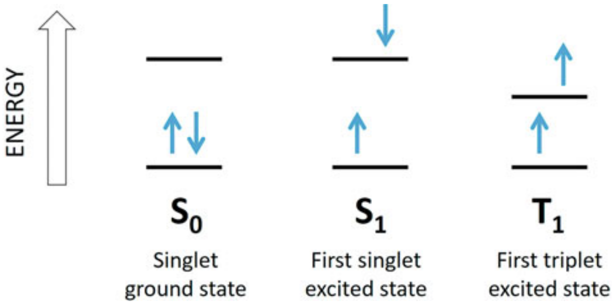
ENERGY
S_0
Singlet ground state
S_1
First singlet excited state
T_1
First triplet excited state

Fig. 5.2 An illustration of singlet and triplet electronic states. Note that the triplet excited state is less energetic than the corresponding singlet excited state

excited to a higher vibrational level of either of the electronically excited singlet states, S_1 or S_2. These higher states then rapidly relax to the lowest vibrational level of S_1 by the slower processes of *vibrational relaxation* or *internal conversion* which are together measured on the picosecond scale. The excess energy is dissipated to solvent molecules as heat.

The final process, emission of a photon and return to the ground state which typically manifests as fluorescence, is longer still on the order of nanoseconds. Fluorescence almost inevitably occurs from a thermally equilibrated excited state, i.e., the lowest vibrational state of S_1. Return to the ground state typically occurs to a higher vibrational level of S_0 which then rapidly (10^{-12} s) reaches thermal equilibrium to the lowest vibrational level in the ground state. Consequently, the fluorescence emission spectrum is often a mirror image of the absorbance spectrum of the $S_0 \rightarrow S_1$ transition which reflects the manifold of closely-spaced vibrational modes of the ground state to which the fluorophore may return.

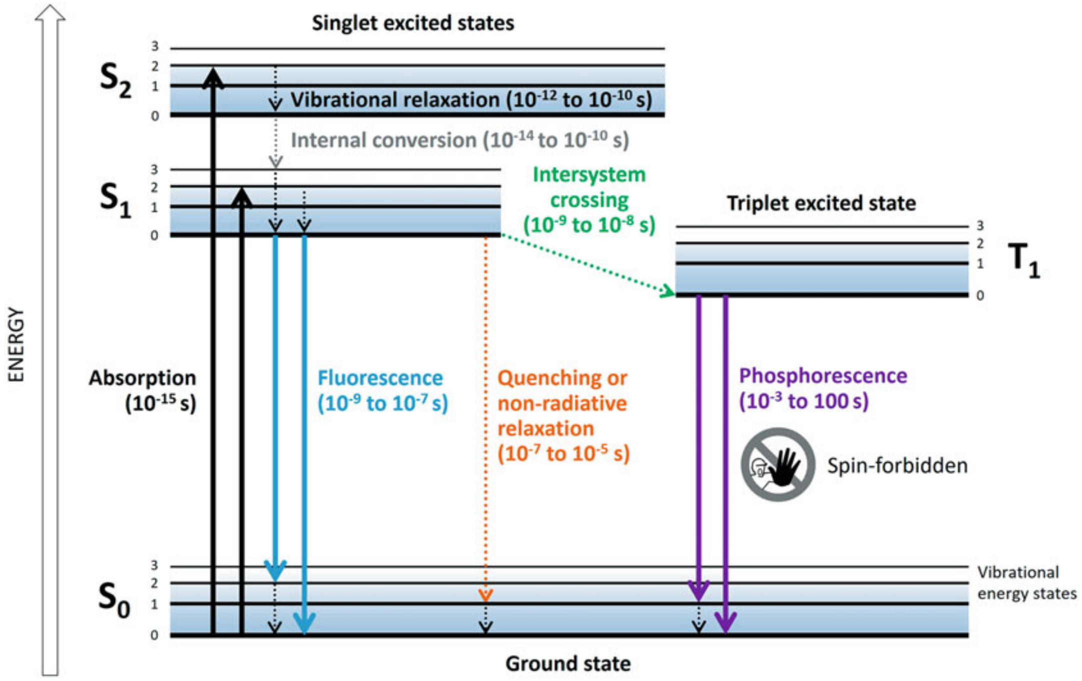
Singlet excited states
S_2
3
2
1
0
Vibrational relaxation (10^{-12} to 10^{-10} s)
Internal conversion (10^{-14} to 10^{-10} s)
S_1
Intersystem crossing (10^{-9} to 10^{-8} s)
Triplet excited state
T_1
ENERGY
Absorption (10^{-15} s)
Fluorescence (10^{-9} to 10^{-7} s)
Quenching or non-radiative relaxation (10^{-7} to 10^{-5} s)
Phosphorescence (10^{-3} to 100 s)
Spin-forbidden
Vibrational energy states
S_0
Ground state

Fig. 5.3 A Perrin-Jabłoński diagram indicating energy levels and states leading to fluorescence, phosphorescence, and non-radiative relaxation processes. Typical timescales for these events are indicated

Although the entire fluorescence lifetime, from excitation to emission, is measured in billionths of a second, the phenomenon is a stunning manifestation of the interaction between light and matter which forms the foundation for the expansive fields of fluorescence spectroscopy and microscopy. Most fluorophores repeat this excitation and emission cycle many hundreds of thousands of times before the highly reactive excited state molecule is photobleached, resulting in destruction of the fluorophore.

Several other excitation pathways with varying degrees of probability compete with the fluorescence emission process. The excited state can be dissipated non-radiatively as heat, either through a quenching mechanism or via energy transfer to a second molecule in another non-radiative process. These intermolecular deactivation processes are broadly termed *external conversion*.

Alternatively, molecules in S_1 can also undergo spin conversion to the first triplet state (T_1) via *intersystem crossing*. As mentioned previously, emission from the triplet state is termed phosphorescence and generally occurs at longer wavelengths than fluorescence. As the transition to the triplet state is a forbidden process which violates the spin selection rule, these processes exhibit rate constants much lower than those for fluorescence and may occur on a timescale from milliseconds to dozens of seconds. Consequently, phosphorescence is seldom observed in solution as it is outcompeted by non-radiative quenching processes.

5.3.2 Characterizing Fluorophores

Three fundamental parameters are commonly used to describe and compare fluorophores: the *molar absorption coefficient*, the *fluorescence quantum yield*, and the *fluorescence lifetime*.

The molar absorption coefficient (ε) is a direct measure of the molecule's ability to absorb light. Fluorophores with a large molar absorption coefficient typically have a high probability of fluorescence emission. The fluorescence quantum yield (Φ) or quantum efficiency is defined as the ratio of the number of photons emitted as fluorescence to the number of photons absorbed. The brightest fluorophores have fluorescence quantum yields approaching unity. As the fluorescence quantum yield of a compound is determined by the relative rate constants of processes by which the lowest excited singlet state is deactivated, the fluorescence quantum yield is susceptible to a variety of other factors such as pH, solvent polarity, and concentration. The reciprocal of the fluorescence decay rate constant is called the intrinsic lifetime of a fluorophore (τ_0), which is defined as the lifetime of the excited state in the absence of all processes that compete for excited state deactivation.

Useful information about fluorophores can be summarized in their absorption and fluorescence emission spectra. These spectra for quinine are presented as an example (Fig. 5.4). Primary and secondary absorption peaks are observed at λ_{max} 345 nm and 320 nm, respectively. The lower-energy band corresponds to a transition to the first excited singlet state ($S_0 \rightarrow S_1$) while the higher-energy band corresponds to the $S_0 \rightarrow S_2$ transition which rapidly relaxes to S_1. Hence fluorescence is observed only from S_1 and not from the second singlet excited state. Consequently, the emission spectrum is a mirror image of only the $S_0 \rightarrow S_1$ absorption spectrum.

Because the energy associated with the fluorescence emission transition ($S_1 \rightarrow S_0$) is almost invariably less than that of the absorption process, the emitted photons have less energy and hence longer wavelengths. This gives rise to the *Stokes shift* which is the difference between the positions of the two band maxima of the absorption and emission spectra of the same electronic transition.

It has been mentioned before that local environmental factors such as temperature, pH, and solvent polarity have profound effects on the emission spectra of fluorophores. The effects of these parameters vary widely from one fluorophore to another. *Solvatochromism* is the shift in fluorescence maxima resulting from changes in solvent polarity. An increase in the Stokes shift may also be observed due to solvent effects, with more polar solvents resulting in larger Stokes shifts than less polar solvents due

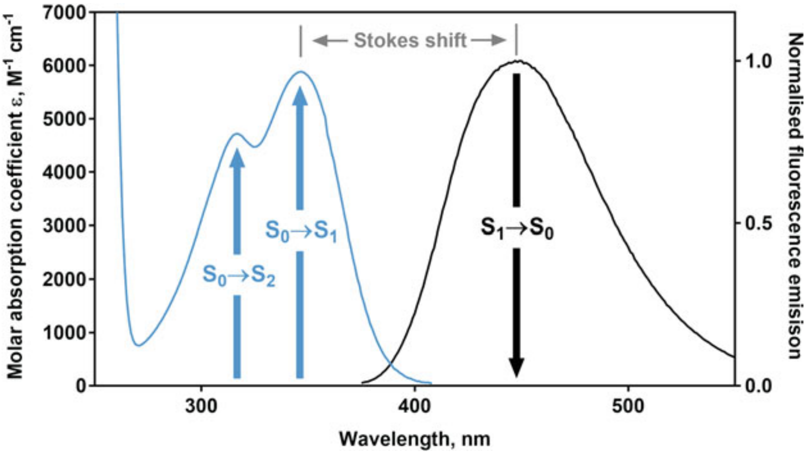

Fig. 5.4 The absorption spectrum of quinine in 0.5 M sulfuric acid and its corresponding fluorescence emission spectrum following excitation at 333 nm. Vertical arrows indicate electronic transitions and the horizontal arrows indicate a large Stokes shift between the absorption and emission maxima

to solvent-specific relaxation effects during the excited state.

5.3.3 Fluorescence Quenching

The intensity of fluorescence emission is also susceptible to changes in pH, temperature, and solvent polarity. Perhaps the most important measurements of changes in the intensity of fluorescence emission are those caused by quenching. These are decreases in fluorescence intensity arising from competing intermolecular processes that induce non-radiative relaxation of excited state electrons to the ground state.

While processes such as fluorescence and phosphorescence are examples of *intra*molecular deactivation processes, *inter*molecular deactivation processes usually fall into two groups. *Static quenching* (also referred to as contact quenching) arises from the formation of a non-fluorescent complex between the fluorophore and the quencher that serves to limit absorption by reducing the population of active, excitable molecules (Lakowicz 2010). Static quenching occurs when the molecules form a complex in the ground state before excitation occurs. The complex has its own unique properties such as being non-fluorescent and having its own absorption spectrum. The fluorescence emission is therefore reduced without altering the average lifetime of the excited state.

On the other hand, *collisional* (or *dynamic*) *quenching* occurs when the excited state is deactivated upon interaction with another non-fluorescent molecule in solution. Neither of the molecules is chemically altered in the collisional quenching process. Mechanisms for collisional quenching include electron transfer, spin-orbit coupling (usually in the presence of the heavier halogens), and intersystem crossing to the excited triplet state. Typically, higher temperatures and lower viscosities accelerate the quenching process as they lead to increased collisions between molecules and hence diminished fluorescence.

5.3.4 Fluorescence Resonance Energy Transfer

A fluorophore in the first singlet excited state can variously lose its excitation energy by conversion into light (fluorescence), via thermal equilibration (vibrational relaxation), or by the formation of a non-fluorescent ground state complex with another molecule (static quenching).

Yet another mechanism, first described by Theodor Förster in 1948, is a non-radiative energy transfer process that is regarded as a dynamic quenching mechanism because energy transfer occurs while the donor is in the excited state (Förster 1948). *Fluorescence resonance energy transfer* (FRET) is a long-range electrodynamic phenomenon that has found countless applications, particularly in biological systems in which its distance-dependence means that it can be used as a "spectroscopic ruler."

The premise of Förster's theory is that the "donor" fluorophore can be treated as an oscillating dipole at a particular resonant frequency in a manner analogous to the behavior of coupled oscillators. FRET occurs between a donor in its excited state and an "acceptor" in its ground state. Energy transfer occurs without the appearance of a photon and is the result of long-range dipole–dipole interactions between the donor and acceptor. The transfer of energy is manifested both by quenching of the donor fluorescence emission in the presence of the acceptor and increased fluorescence emission from the acceptor (Lakowicz 2010).

5.3.5 The "Dark Side" of Fluorescence

In the excited triplet state, the fluorophore interacts with molecules around it (usually molecular oxygen) causing a reaction. *Photobleaching* is the permanent loss of electrons from the productive cycle of fluorescence emission due to photochemical change, in which a fluorophore loses its fluorescence due to damage induced by light. Practical advice for avoiding photobleaching includes staining samples in dim conditions, keeping samples in dark containers or wrapped in foil, short excitation or exposure times while imaging, and reducing excitation or laser power as much as possible.

5.4 Spectrofluorimetry

The direct relationship between fluorescence intensity and the concentration of the fluorophore allows relatively simple electronics and optics to be used in a spectrofluorimeter (Fig. 5.5). The light source is generally a xenon lamp that illuminates equally in all directions. Two monochromators are usually employed, the first of which selects the excitation wavelength. Radiation from the excitation monochromator is split with part of the radiation passing to a reference photomultiplier tube and part to the sample. After fluorescence emission occurs from the sample in all directions, the second monochromator determines the emission wavelengths to be transmitted to the detector. Following dispersion by the emission monochromator, the light is detected using a second sensitive photocell (Valeur 2001).

Fluorescence intensity is a linear function of the concentration of the fluorophore with zero intercepts under "ideal" conditions. However, these conditions are met only when the attenuation of light at both excitation and emission wavelengths is negligible over the pathlengths of interest. Absorption of excitation and/or emission radiation by a sample reduces the fluorescence intensity and results in a nonlinear relationship between the observed fluorescence intensity and the concentration of the fluorophore. This is called the *inner-filter effect* and care should be taken to minimize it. When new fluorophores are prepared, they will typically be characterized in a spectrofluorimeter. Their absorption and emission spectra will be measured as well as several other parameters that are important before such a molecule can be used in a biological microscopy experiment.

5.5 Fluorescence Microscopy

> *The purpose of microscopy is insight not images.*
> —R. W. Hamming (Electron Microscope Unit, University of Cape Town 2023)

Fluorescence is arguably at its most powerful when it is used in biological imaging. Modern fluorescence microscopy offers the possibility to probe the dynamics of living cells at high spatial resolution and in a minimally invasive manner. With the vast number of fluorescent stains that are readily available, fluorescence microscopy also allows for the rapid identification of subcellular components with a high degree of specificity.

An important technical consideration is the ability of the microscope to form an image in the focal plane with simultaneous suppression of out-of-plane emission. This is the advantage of

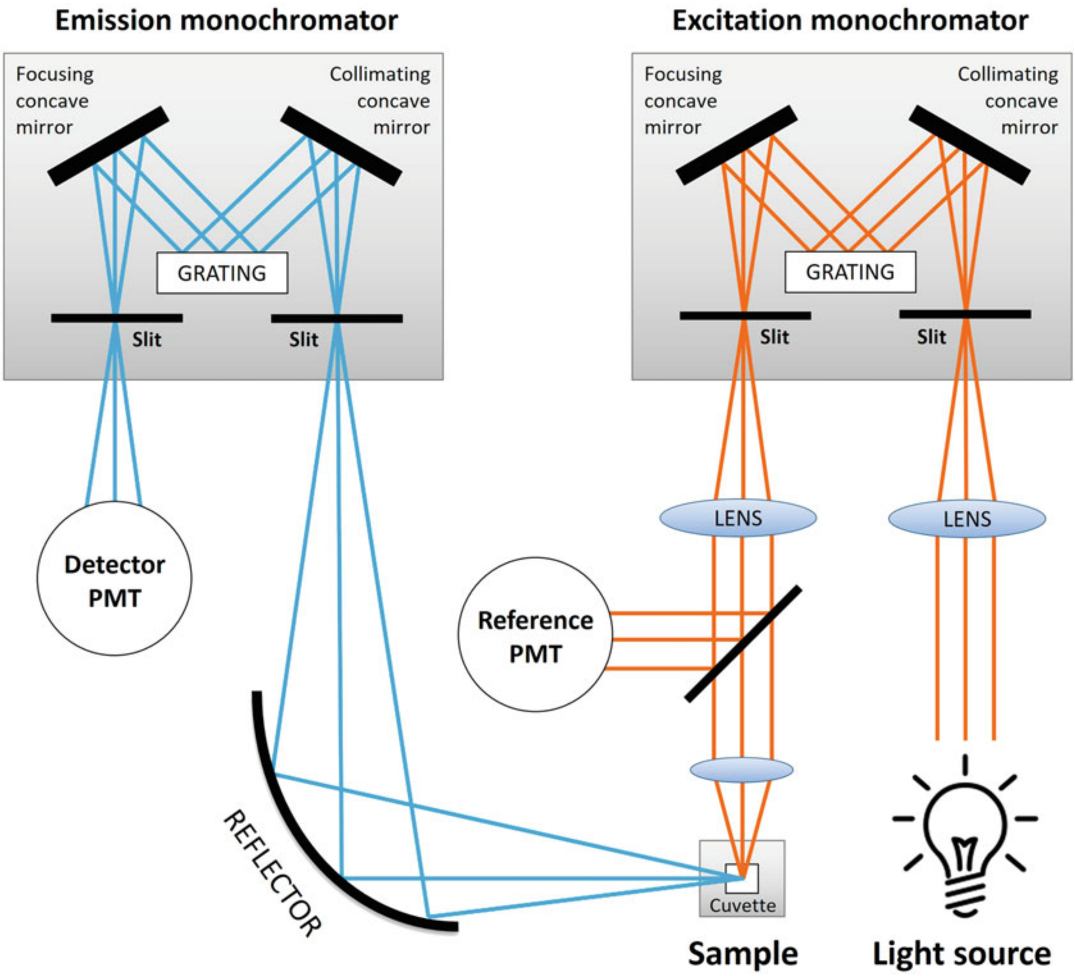
Emission monochromator
Focusing concave mirror
Collimating concave mirror
GRATING
Slit
Slit
Excitation monochromator
Focusing concave mirror
Collimating concave mirror
GRATING
Slit
Slit
Detector PMT
LENS
LENS
Reference PMT
REFLECTOR
Cuvette
Sample
Light source

Fig. 5.5 Schematic of a typical spectrofluorimeter. Orange rays indicate incident radiation while blue rays indicate fluorescence leaving the sample following excitation

confocal microscopy over traditional widefield methods, as detailed below. Meanwhile, the limit of spatial resolution in fluorescence microscopy is dictated by the wavelength of light that is used and is known as the “diffraction limit.” The German physicist Ernst Abbe (1840–1905) defined this limit as the ability of a lens-based optical microscope to discern only those details that are longer than half the wavelength of the incident light. However, this limit has been surpassed by a suite of super-resolution techniques that have given rise to the field of nanoscopy.

5.5.1 Widefield Microscopy

Widefield microscopy is the most popular fluorescence microscopy technique. In this configuration, excitation and observation occur from *above* the specimen and hence it is also known as “epifluorescence” microscopy. This is in contrast to common optical microscopes that collect light that is transmitted through the sample (Demchenko 2010).

The light source passes bright white light through a filter to produce the excitation beam (Fig. 5.6). This is reflected by a dichroic mirror that passes the beam through the objective to

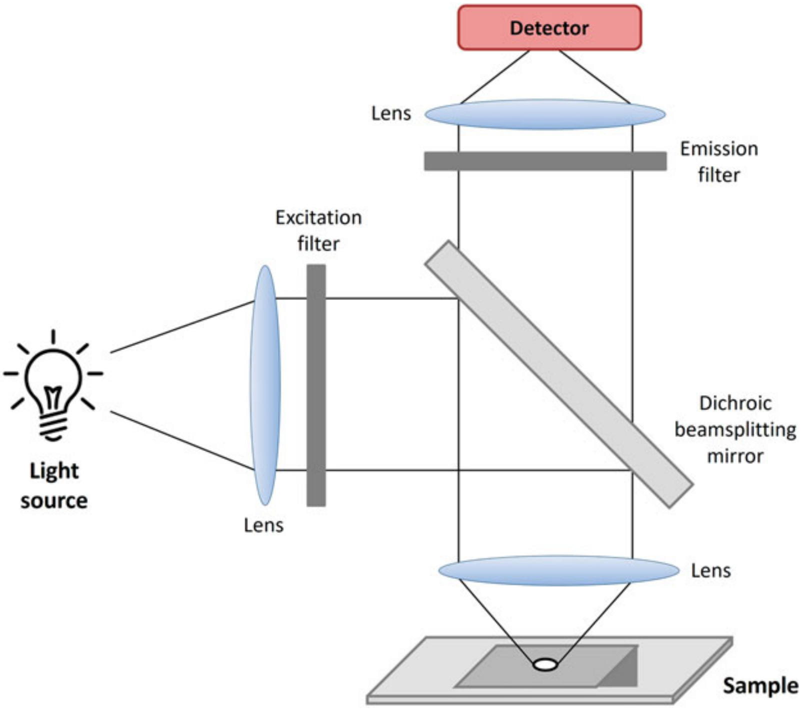

Fig. 5.6 Schematic of a simple widefield microscope. Excitation light, after passing through the first optical filter, is focused on the specimen from above. Fluorescence is directed to the detector after passing through the emission filter that rejects reflected and scattered excitation light

interact with the sample. Fluorescence emission from the sample is passed back through the objective and the dichroic mirror transmits only the (weaker) fluorescence light. Finally, the fluorescence is passed through the emission filter and is captured with a detector.

5.5.2 Confocal Microscopy

Confocal microscopy offers a different principle for forming sharp images. While the excitation of out-of-focus fluorophores by the incident beam is not avoided, an optical configuration of the instrument allows the rejection of their emission by means of a confocal pinhole that provides geometric restriction to the transmission of this out-of-focus emission. The application of this principle allows the rendering of sharp images due to a dramatically improved signal-to-noise ratio.

A schematic of a typical confocal microscope is shown in Fig. 5.7. Because a higher intensity of photons is required for excitation in comparison to widefield microscopes, lasers are typically employed. The beam enters the microscope and passes through the excitation filter and a dichroic mirror. Next, two scanning mirrors (not indicated in Fig. 5.7) move the beam in a raster across the sample. Fluorescence emission then passes back through the objective and is de-scanned by reflecting off both of the scanning mirrors. The light is then reflected off the dichroic mirror. Importantly, only in-focus light is allowed to proceed through the pinhole and emission filter to the detector. Out-of-focus light is rejected by the pinhole and does not reach the detector.

The great advantage of confocal microscopy is the ability to adjust the focal plane. This enables one to scan the object at different *z*-levels so that cross-sections at various depths can be obtained. These two-dimensional sections can then be reconstructed to form a three-dimensional image of the object. The disadvantage of the confocal microscope is the need to use high-intensity lasers for excitation and to illuminate the sample with a large volume of light, not only within the focal plane. As a result, this increases the possibility of photobleaching and phototoxicity, especially when imaging live cells (Demchenko 2010).

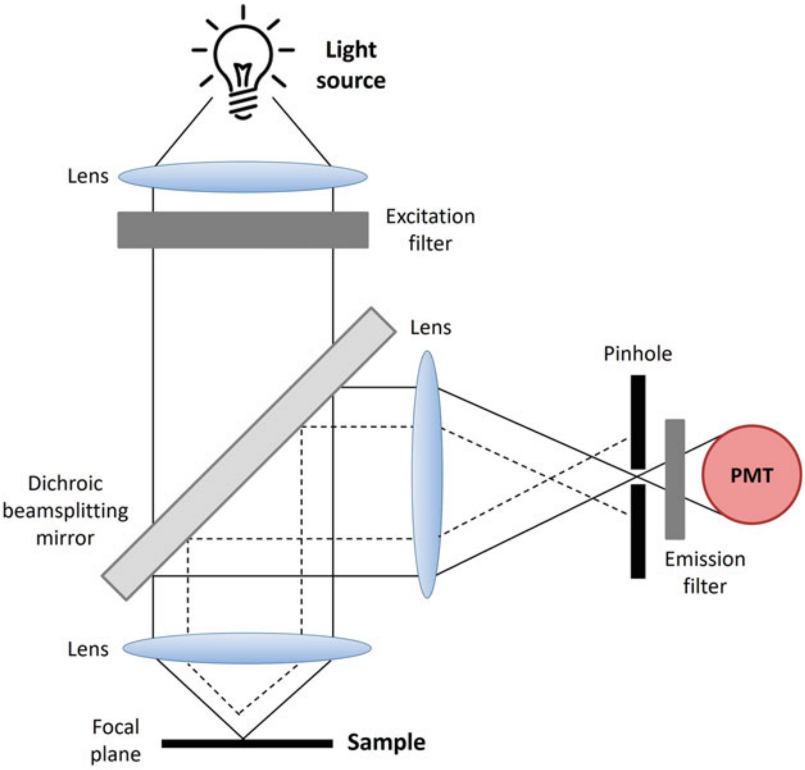

Fig. 5.7 Schematic of a typical confocal microscope showing the beam geometry that allows rejection of photons emitted from outside the focal plane. The solid lines indicate in-focus photons that pass through the pinhole while the dashed lines indicate out-of-focus photons that are rejected by the pinhole

5.5.3 The Diffraction Limit and the Advent of Super-Resolution Microscopy

Toward the end of the nineteenth century, Ernst Abbe (Abbe 1873) and Lord Rayleigh (Rayleigh 1896) found that light of wavelength λ, traveling in a medium with refractive index n and converging with angle θ, will form a focal "spot" with radius d as described by Eq. 5.1:

$$d = \frac{\lambda}{2n\ sin\theta} \tag{5.1}$$

Consequently, widefield and confocal microscopes are constrained by this *diffraction limit*. When light is focused by the objective of a microscope, the notion of light rays converging to an infinitely sharp focal point does not occur. Instead, the light forms a blurry focal spot with a finite size due to diffraction.

A single-point emitter such as a fluorescent molecule, therefore, appears as a blurry "smudge" with a finite size when imaged through a microscope. The intensity profile of this smudge defines the *point spread function* of the microscope and has approximately the same width as the focal spot defined above. Consequently, two identical emitters separated by a distance less than the width of the point spread function will appear as a single object and are thus unresolvable from one another (Huang et al. 2010).

Practically, this means that for green light of wavelength 500 nm passing through a microscope objective with a high numerical aperture (1.2–1.5), the Abbe limit is about 200 nm perpendicular to the direction of light propagation (laterally) and about 500 nm parallel to the direction of the light propagation (axially, or in the z-direction). These dimensions may be small compared to most cells (1–100 μm) but not viruses (100 nm) or proteins (10 nm). Structures as small as these are unresolvable by light microscopy.

Typically, electron microscopes have been used to overcome these resolution problems but electron microscopy cannot be used for imaging live cells. Furthermore, electron microscopy typically requires extensive sample preparation and suffers from a lack of contrast in biological samples, making the identification of subcellular components very challenging.

For almost a century-and-a-half it was believed that this limit of resolution could not be surpassed. However, a number of different techniques have subsequently been developed that overcome this limit. These technologies, with a resolving power exceeding the diffraction limit, are collectively known as *super-resolution microscopy*.

Stimulated emission depletion (STED) microscopy was developed and demonstrated by Stefan Hell in the 1990s. This method creates super-resolution images by the selective deactivation of fluorophores, minimizing the area of illumination of the focal point and thus increasing the resolution. Two laser sources are used; one excites the fluorophores while the other quenches all the fluorophores except those surrounding the nanometer-sized region of interest. Quenching occurs by forcing these outer fluorophores into higher vibrational levels of the ground state without emission of fluorescence (stimulated depletion). The energy of the second laser is therefore lower than the excitation energy and is generally in the far-red region. However, the high intensities required for STED microscopy mean that photobleaching is problematic when working with live cells. Special fluorophores are typically required.

Eric Betzig and William E. Moerner, who were awarded the 2014 Nobel Prize in Chemistry jointly with Hell, separately laid the foundations for a second way of performing super-resolution microscopy. Their method relies on photoswitchable fluorophores that alternate between “on” (fluorescent) and “off” (dark) states. Typically, only a few of these molecules are “on” during a single image acquisition. The center of each spot can be found by fitting the observed emission profile to a known geometrical function. Superimposing these partial fluorescent representations yields a dense, super-resolved image; essentially, this is a pointillist representation of the coordinates of all the localized molecules. The two most popular variations on this theme are photoactivated localization microscopy (PALM) and stochastic optical reconstruction microscopy (STORM).

A third kind of super-resolution technology, structured-illumination microscopy (SIM), is based upon the idea of patterning the excitation light. By allowing the patterned light (usually a fine grid) to interfere with the structures in the sample, a characteristic pattern is produced. By rotating the grid between the acquisition of each image set and transforming the images into frequency space, additional spatial information may be retrieved. The reverse Fourier transform returns the reconstructed super-resolution image.

5.6 Fluorescent Reporters

As described above, fluorescence is an essential tool for examining biological systems and processes, whether single cells or complete organisms. Originally, fluorescence was observed from small organic dyes attached to antibodies which displayed high specificity for the protein of interest. However, antibody targeting of intracellular proteins normally requires cell fixation and permeabilization which perturbs the biological system and may introduce artifacts.

Later, fluorophores were developed to recognize organelles directly and even nucleic acids and ions in living cells. Over the past few decades, fluorescent proteins have enabled non-invasive imaging of reporter gene expression, protein trafficking, and dynamic biochemical signals. The jellyfish *Aequorea victoria* is the source of the bioluminescent photoprotein aequorin and its partner, the green fluorescent protein (GFP). Roger Y. Tsien, Osamu Shimomura, and Martin Chalfie were awarded the 2008 Nobel Prize in Chemistry for their discovery and development of GFP.

Semiconductor nanocrystals (quantum dots) have been developed with superior brightness and photostability compared to previous fluorophores, but their use in cells and tissues remains challenging (Giepmans et al. 2006).

These crystals are typically the size of a small fluorescent protein and must be coated with a biocompatible material such as lipid or polyethylene glycol.

Fluorescence in situ hybridization is a molecular cytogenetic technique that allows the localization of a specific DNA sequence or an entire chromosome in a cell. These days, biomolecules can even be labeled *within living cells* using the toolkits of bioorthogonal and click chemistry that were together recognized with the 2022 Nobel Prize in Chemistry, awarded to Carolyn Bertozzi, Morten Meldal, and K. Barry Sharpless.

Organic dyes have remained the most common fluorescence reporters. The benefits of these dyes are that they are usually inexpensive, readily available, and are often small compared to their substrates. Many possess superior photostability and brightness, but most important is their versatility. There is immense variation in their chemical, photophysical, and spectroscopic properties meaning that their use can be adapted to almost any system. Unsurprisingly, a one-size-fits-all or "ideal" fluorescent dye does not exist and so compromises have to be made depending on the role of the fluorescent reporter and the system in question.

Microscopy, and especially live-cell imaging, is usually more challenging than spectroscopic studies in a cuvette. Nevertheless, some of the desired properties of a fluorophore for bioimaging include a high molar absorbance (large extinction coefficient, ε), high fluorescence quantum yield (Φ), optimal excitation and emission wavelengths (λ), a large Stokes shift ($\Delta\nu$), high photostability, optimal fluorescence lifetime (τ) and optimal solubility, penetration, and reactivity.

5.7 Image Analysis

> Beware of determining and declaring your opinion suddenly on any subject; for imagination often gets the start of judgement, and makes people believe they see things which better observations will convince them could not be seen: therefore, assert nothing till after repeated experiments and examinations in all lights and in all positions. When you employ a microscope shake off all prejudice, nor harbor any favorite opinions.
>
> —Advice of an eighteenth century microscopist (Baker 1742)

One of the most common applications of fluorescence microscopy is to compare the subcellular distributions of two fluorescent molecules. Often the goal is to probe the localization of a fluorescently-tagged substrate and thus the second fluorophore is usually a commercially available tracker dye that is specific for a subcellular region or organelle.

"Colocalization" is a term that has received much criticism but appears ubiquitously in the literature. The term refers to the general spatial overlap between two (or more) different fluorescence signals; however, even super-resolution images cannot identify the physical apposition of two molecules merely by comparing their fluorescence signals. Hence, the term "codistribution" may be preferred in which it is asked whether the molecules tend to associate with the same structures (Dunn et al. 2011). This, in turn, may be thought of as a combination of *co-occurrence* (the spatial overlap of probes in a fluorescence image) and *correlation* (distribution in proportion to one another within and between structures).

Qualitative methods of image analysis rely on a comparison of separate fluorescence channels. Typically, images are displayed in different channels using pseudo-coloring (usually green and red) and regions of overlap are identified in a dual-channel image (in this case, regions of overlap would appear yellow). Quantitative methods, on the other hand, involve global statistical analysis of the pixel intensity distribution and are called *intensity correlation coefficient-based analyses*. This involves statistical analysis of the correlation of the intensity values of the pixels in the dual-channel image and is usually done using correlation coefficients that measure the strength of the linear relationship between two values.

A simple way of measuring the dependency of pixels in dual-colored images is to plot the pixel intensity values of the two images against one another and to display the result in a pixel distribution diagram, also called a scatterplot or *cytofluorogram*. If the intensities of both pixel distributions are proportional to one another and if detection has been carried out in the linear range, the resulting scatterplot should form a dot cloud in the shape of a line, the slope of which reflects the relative (unique) stoichiometry of both fluorophores. The spread of this distribution with respect to a fitted line, calculated by linear regression, may be estimated by calculating the *Pearson correlation coefficient* which is a standard procedure in pattern recognition for matching one image with another and is used to describe the degree of overlap between two patterns, providing a useful first estimate of colocalization (Bolte and Cordelières 2006). Various other metrics can be used to quantify aspects of fluorescence microscopy images, generating further insights into the structure and function of biological systems.

5.8 Conclusion

Instruments that detect and measure fluorescence are now ubiquitous in the modern scientific laboratory, demonstrating their value as an indispensable approach for interrogating and visualizing biological events. Today, new developments in the arena of fluorescence permit ever richer data acquisition that can more readily elucidate biological processes through space and time and help to accelerate, for instance, the discovery of new medicines.

For example, the synthesis of brighter dyes in the near-infrared range has prompted tremendous advances in corresponding technologies such as LED-light engines and automated microscopy systems optimized to take advantage of these dyes. Other benefits of near-infrared dyes include enhanced photostability, decreased autofluorescence, and deep-tissue imaging with less light scattering. Meanwhile, advances in live-cell imaging have been facilitated by the development of protein tags such as HaloTags and SNAP-Tags in which a modified enzyme covalently binds to synthetic ligands which themselves may be bioorthogonally attached to a variety of useful substrates such as fluorescent dyes, affinity handles, or solid surfaces.

Techniques in fluorescence-guided surgery are also emerging that selectively illuminate cancer cells, enhancing the distinction between tumors and surrounding tissues with the potential for single-cell sensitivity. In the environmental sciences, new fluorescent sensors for the detection of pollutants in the atmosphere and water are being developed. More recently, high-content imaging systems have been coupled with artificial intelligence and machine learning algorithms to detect patterns that are not readily apparent to the human eye.

It is exhilarating to witness how the applications of fluorescence continue to expand and evolve, facilitating ever-greater insights into chemical and biological systems—and illuminating the way to a brighter future for all.

References

Abbe E (1873) Beiträge zur Theorie des Mikroskops und der mikroskopischen Wahrnehmung. Arch Mikrosk Anat 9:413–468

Baker (1742) The microscope made easy, London

Bolte S, Cordelières FP (2006) A guided tour into subcellular colocalization analysis in light microscopy. J Microsc 224:213–232

Demchenko P (2010) Introduction to fluorescence sensing. Springer, New York

Dunn KW, Kamocka MM, McDonald JH (2011) A practical guide to evaluating colocalization in biological microscopy. Am J Physiol Cell Physiol 300:C723–C742

Electron Microscope Unit, University of Cape Town. Lecture 1: Intro to EM for Biologists. http://www.emu.uct.ac.za/intro-em-biologists-lecture-1. Accessed 17 April 2023

Förster T (1948) Zwischenmolekulare Energiewanderung und Fluoreszenz. Ann Phys (Berlin) 437:55–75

Giepmans BNG, Adams SR, Ellisman MH, Tsien RY (2006) The fluorescent toolbox for assessing protein location and function. Science 312:217–224

Herschel JFW (1845) On a case of superficial colour presented by a homogeneous liquid internally colourless. Phil Trans 135:143–145

Huang B, Babcock H, Zhuang X (2010) Breaking the diffraction barrier: super-resolution imaging of cells. Cell 143:1047–1058

Lakowicz JR (2010) Principles of fluorescence spectroscopy. Springer, New York

Rayleigh L (1896) On the theory of optical images, with special reference to the microscope. Philos Mag 42: 167–195

Thompson A, Kastan DS, Proudfoot R (eds) (2001) The Arden Shakespeare complete works. Arden Shakespeare, London

Stokes GG (1852) On the change of Refrangibility of light. Phil Trans 142:463–562

Stokes GG (1853) On the change of Refrangibility of light. No. II. Phil Trans 143:385–396

Valeur B (2001) Molecular fluorescence: principles and applications. Wiley-VCH Verlag GmbH, Federal Republic of Germany

Valeur B, Brochon J (eds) (2001) New trends in fluorescence spectroscopy. Springer-Verlag GmbH, Heidelberg

Woodland JG (2016) Insights into the mechanism of action of quinoline antimalarials against plasmodium falciparum revealed by novel fluorescent analogues and chemical proteomics. University of Cape Town, Thesis

Woodland JG, Chibale K (2022) Quinine fever. Nat Chem 14:112

6

An Introduction to Particle Tracking Techniques with Applications in Biomedical Research

Sourav Bhattacharjee

Abstract

Due to their inherent complexity and diverse range of functions, biological systems—both at the cellular and tissue levels—continue to challenge the prowess of modern science. Despite significant advances toward understanding the core mechanisms driving such systems, unknown domains continue to hold back scientific progress. The advent of microscopy tools, especially epifluorescence and confocal microscopy for live cell imaging, has strengthened biology research. Emerging modalities of super-resolution microscopy are now providing crisp resolution, and the availability of tailor-made dyes for labeling biological samples, have also inspired the current generation of microscopists to investigate biological structures down to the *nanoscale*. Particle tracking techniques, especially single particle tracking that emerged as a component of a fast-evolving fluorescence microscopy landscape, are now pushing the current limits of technological excellence even further. With high-resolution imagery data acquisition, often conducted in a time-lapse mode, particle tracking tools are providing crucial insights into how the cells function with emphasis on metabolism, cytoskeletal dynamics, cell division, and phagocytosis. The further kinematic analysis delves deeper into the hitherto unknown realms of (nano)particulate transport, with or without receptor mediation, across biological membranes, followed by cellular internalization and intracellular fate, including subcellular compartmentalization. Such novel insights are not only widening the current knowledge base on complex biological systems but also guiding researchers toward developing effective theranostic agents for advanced drug delivery and biomedical imaging, including preparation of nanomedicinal formulations. This chapter revisits the current state-of-the-art particle tracking platforms while drawing inspiration from its wide range of biomedical applications, including therapeutics. In this journey, the chapter will present a balanced critique of the available tracking software packages along with their strengths and weaknesses. Finally, it will present some future perspectives from a vantage of current paradigms, caution the research community on the challenges that lie ahead, and highlight some approaches that need to be integrated into current concepts while progressing ahead.

Keywords

Single particle tracking · Track analysis · Confocal microscopy · Biomembranes · Intracellular transport · Nanomedicine

---

S. Bhattacharjee (✉)
School of Veterinary Medicine, University College
Dublin, Belfield, Dublin 4, Ireland
e-mail: sourav.bhattacharjee@ucd.ie

© The Author(s), under exclusive license to Springer Nature Switzerland AG 2023

L. Shapiro (ed.), *Microscopy Techniques for Biomedical Education and Healthcare Practice*, Biomedical Visualization 2, https://doi.org/10.1007/978-3-031-36850-9_6

6.1 Introduction

Biological systems are remarkably dynamic and often behave in a time-dependent manner, especially when considering cells and interactions with their surroundings (Assmus et al. 2006). The structure and physiology of a cell, including its collection of a wide variety of organelles—floating in viscous cytoplasm and allocated with a precise set of tasks—hold the keys to the mystery of life (Saminathan et al. 2022) and have intrigued researchers to delve deeper. As biological entities, cells are metabolically active, bear shape-shifting attributes, such as the cytoskeleton (Ross et al. 2019), and resort to various ways of dealing with alterations or oscillations, including biochemical parameters, in their milieu (Cretel et al. 2008).

Naturally, scientific investigations in the field have tried to probe the dynamics of both intracellular and extracellular events, such as cytoskeletal motility during cell division (Fletcher and Mullins 2010) and migration (Tang and Gerlach 2017), membrane characteristics, including transport (Guan 2022) of a gamut of external agents often delivered as vesicles (Cui et al. 2022), genetic transcription and intracellular transport (Fig. 6.1) to name a few. A surge in such investigations is further endorsed by the arrival of advanced and sophisticated microscopy platforms that can reveal information on complex cellular events based on time-lapse microscopy (Muzzey and van Oudenaarden 2009).

The emergence of time-lapse microscopy, with or without data acquisition as multiple slices of uniform thickness and often predetermined thickness enabling digital three-dimensional (3D) reconstruction of the sample, has already provided a wealth of information while leaving a fertile ground for further exploration. Integration of advanced light microscopy platforms, with an improvement of the already existing ones, such as confocal laser scanning microscopy (Fig. 6.2), may revolutionize the way cellular behavior and interactions have traditionally been investigated. The arrival of super-resolution microscopic techniques, for example, stimulated emission depletion microscopy (Vicidomini et al. 2018), stochastic optical reconstruction microscopy (Lelek et al. 2021), and photo-activated localization microscopy (Khater et al. 2020) have further expanded the scope of such platforms.

While cells interact with a wide range of alterations in their biochemical ambiance, including fluctuating pH (Taylor 1962), temperature (Lepock 2005), and ionic strength (Spitzer and Poolman 2009), one crucial external agent often responsible for paving the way for such changes is the *particles*. In a biological context, an interpretation of the term “particle” can be vast and often with conceptually opaque boundaries. It is prudent to accept that the scope of the expression “particle” can be quite generic in biology (and at times confusing), whereas realistically and from a working point of view, it can be taken as an isolated entity often present in clusters consisting of high numbers, with or without agglomeration. As isolated entities, particles are confined in 3D space and, unless otherwise specified, are envisioned as a spherical or geometrically comparable (e.g., elliptical or oblong) species in biology.

Cellular interactions, including receptor-mediated binding (Schlessinger 1997; Jackson et al. 2022), internalization (Rennick et al. 2021), and intracellular compartmentalization (Barton and Kagan 2009), are a fast-evolving field of research. It is particularly important from the perspective of understanding the functional machinery of a cell (given that a significant fraction of molecular traffic traveling in or out of the cells is realized with the aid of particulate agents), such as vesicles (Ortega et al. 2022), that act as carriers to transport cargo of physiologically relevant molecules, and at times, theranostic agents (Xing et al. 2020). Hence, acquiring a robust understanding of how these particulate matters negotiate with the cells, from reaching its periphery to cellular uptake and accessing the intracellular target sites, can provide crucial insights into the principles of cellular functioning, the way cells interact with their environment or an exposure scenario, including metabolism, energy audit, and cytotoxicity (DeBerardinis and Thompson 2012).

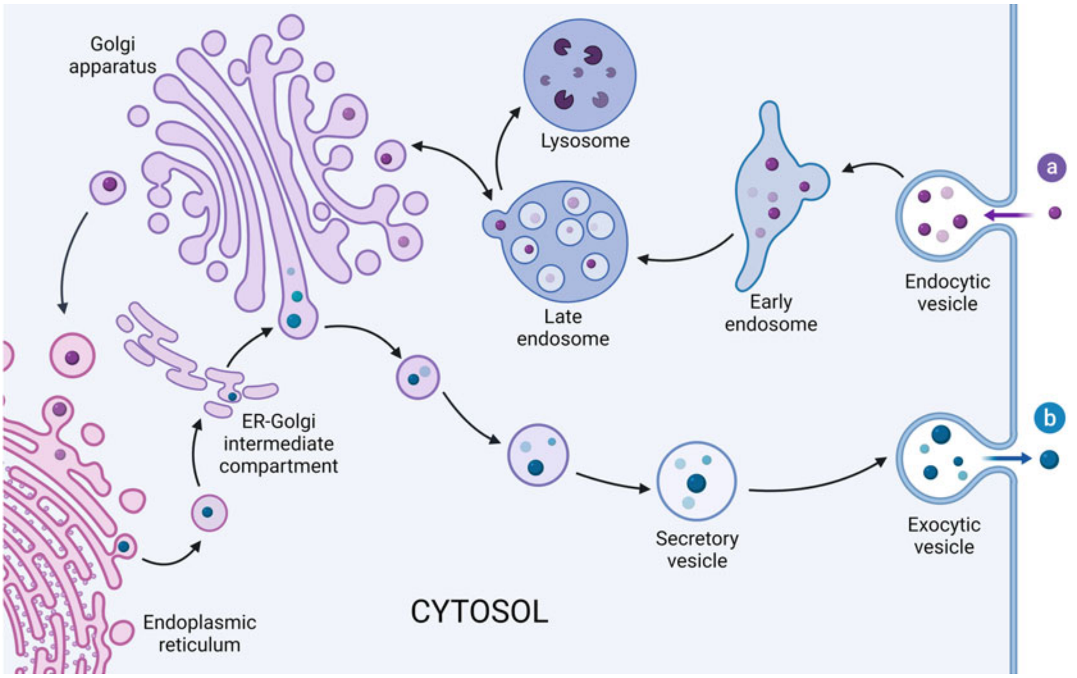

Fig. 6.1 Scheme showing the pathway of intracellular transport of vesicles. The ports for entry into and exit from the cell are marked as “a” and “b,” respectively. Figure created using Biorender.com

Moreover, such knowledge strengthens our current understanding and, in certain instances, improves the extant ways of intervening or modulating how cells interact with particles with theranostic attributes, for example, the nanoparticles (NPs). Due to their minuscule sizes, often <100 nm, the NPs are highly reactive species, can engage diverse biomolecules and simultaneously reach those sites of a human body that are otherwise inaccessible to larger microparticles, due to a sheer size advantage (Bhattacharjee et al. 2013; Garcés et al. 2021).

Thus, over the last few decades, a great deal of research has been streamlined toward developing NPs as drug delivery systems where the deliverable therapeutic agents are either grafted to the nanoparticulate surfaces or encapsulated inside the NP, typically in a core-shell construct. Inherent surface reactivity of NPs allied to advances achieved in synthetic techniques has enabled researchers in the field of nanomedicine to prepare a range of nanoparticulate vectors for the delivery of widely used and life-saving drugs, including anticancer agents, antimicrobials, and endocrinal biomacromolecules (Bhattacharjee and Brayden 2021).

To attain facilitated drug delivery, surface decoration of the NPs with grafted ligands targeting overexpressed receptors on cellular surfaces in affected tissues (Rosenblum et al. 2018; Mitchell et al. 2021), such as folate receptors in breast cancer (Fasehee et al. 2016), has demonstrated improved therapeutic efficacy in vitro and in vivo. Furthermore, improved synthetic protocols have now enabled preparing multimodal nanomedicinal platforms that, other than therapeutic molecules, are also able to deliver imaging agents such as fluorophores (May et al. 2020), contrast agents for magnetic resonance imaging (Reeβing and Szymanski 2019) and positron emission tomography (Goel et al. 2017), in a controlled and site-specific manner. This chapter will only explore the craft of particle tracking from data obtained by light microscopy and refrain from discussing the same in magnetic resonance imaging, computed tomography, and

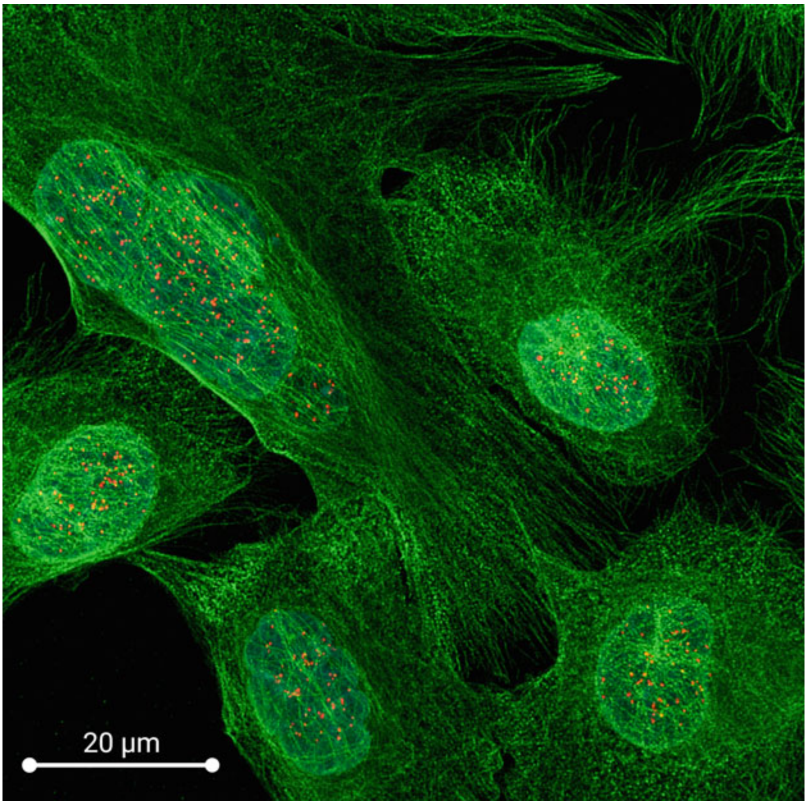

Fig. 6.2 Confocal microscopy on fluorophore-labeled HeLa cells, with the nuclei stained with DAPI ($\lambda_{ex} = 405$ nm, $\lambda_{em} = 425–495$ nm), cytoplasmic tubulin with Alexa Fluor 488 ($\lambda_{ex} = 496$ nm, $\lambda_{em} = 505–575$ nm), and centrioles with Cy5 ($\lambda_{ex} = 649$ nm, $\lambda_{em} = 655–725$ nm) dyes. A scaler bar of 20 µm is embedded within the figure. Reproduced with permission from Dr. Sara Barozzi, IFOM–FIRC Institute of Molecular Oncology, Milan, Italy

positron emission tomographic datasets; however, relevant literature is cited for further consultation (Shapiro et al. 2004; Pore et al. 2015; Dallet et al. 2021; Schultze et al. 2021; Tumpa et al. 2022).

6.2 Conceptualizing a *Particle* in Biological and Virtual Realms

An essential requisite to progress further with the discussion is to understand what a particle entails in biology and microscopy, or as advanced microscopy data now displayed on digital screens, in virtual platforms. As stated earlier, in real terms, a particle within biological auspices typically denotes an isolated or clustered entity, often isotropic, confined within a 3D space, and frequently spherical in shape, or at least with some symmetry in the case of aspherical particles. Additionally, physiologically relevant particles are typically within a few µm with the size of NPs, often <100 nm (e.g., viruses—although therapeutic NPs, including vesicular constructs like liposomes and exosomes—may easily reach 200–300 nm), a size range popularly known as nanoscale (Torchilin 2005; Doll et al. 2013; Herrmann et al. 2021; Tenchov et al. 2022).

On the contrary, a particle in a digital environment means a pixelated space confined in 2D or 3D with defined boundaries demarcating it from its surrounding/background pixels/voxels. Unlike biological particles, virtual particles are not constrained by a size threshold. Thus, larger entities, such as cells of 20–30 µm size, can be considered particles. A lack of size threshold while defining a particle in virtual domains thus allows tracking of larger cells (single-cell tracking) apart from smaller particulates in the form of single particle tracking (SPT).

Another important difference between them, especially from a tracking point of view, is that virtual particles, as their name suggests, are virtual and created by the digital interpretation of a microscopy-derived light signal—often aided with algorithms with editable features customized as per user needs—both in a 2D or 3D coordinate system (Shen et al. 2017; Cui et al. 2018).

Such differences render particle tracking from microscopy datasets conducted exclusively by digital means somewhat semi-quantitative and warrants caution while considering the reliability of such analyses at face value. It needs to be emphasized for future researchers that the data obtained by such tracking on microscopy datasets, despite providing an informative visual package of real-life incidents taking place in biological spheres, unfortunately, bear certain caveats in addition to the inadequacy of results that are vulnerable to alterations made in user settings. Thus, depending on their variation, different user settings may yield varied outputs from the same dataset, which need to be factored in.

6.3 Principles of Particle Tracking

Particle tracking in microscopy is fundamentally a kinematic analysis, and most measured parameters (e.g., speed, velocity, and acceleration) are time dependent. Thus, time-lapse microscopy has emerged as a core competency in particle tracking. Unfortunately, a detailed discussion on time-lapse microscopy falls beyond this chapter's scope, although relevant literature is quoted here for further comprehension (Tvaruskó et al. 1999; Dzyubachyk et al. 2010; Neumann et al. 2010; Comes et al. 2019).

Time-lapse microscopy captures images of the same visual field at various, usually evenly spaced, predetermined time points (Cheng et al. 2022). Upon completion of the acquisition process, these images are stitched together and played as a movie file to identify the structures within the microscopy dataset that have changed their position, or their x- and y-coordinates, to be more precise. As the total span of acquisition is known, various kinematic parameters such as mean and total displacement, speed, velocity, and acceleration, can be computed. Furthermore, modern software interfaces also provide path analysis data, for example, total and average path length and path straightness, that can help better understand the particle movement in granular detail (Schindelin et al. 2012; Gautier and Ginsberg 2021).

In 3D data acquisition, multiple images are recorded at various heights, also called z-stacks, inside the sample. Later, these images are stacked in a virtual environment and projected in a 3D hyperspace (Fig. 6.3). Advanced microscopy platforms now provide possibilities to run both z-stacking and time-lapse acquisition simultaneously. When integrated into a virtual environment, the obtained data provides the ability to check the movements of particles in 3D inside the sample with an assessment of the same kinematic parameters as 2D. However, combining multiple modalities in a single acquisition session requires advanced microscopic systems and more computational ability, as discussed later in this chapter.

Finally, a preliminary requirement is that the particles under investigation emit enough light signals to gather quality data. It is usually achieved by labeling the particles with fluorophores that, upon illumination with light of a certain wavelength (excitation wavelength), emit in a particular spectral region (emission wavelength). For particles made up of materials with large scattering cross sections, such as the gold-NPs (Wan et al. 2014) and quantum dots (Zahid et al. 2018), simple scattering of the incident laser without any fluorophore tag often provides an adequate signal for tracking.

6.4 Methodological Considerations

It needs to be noted that particle tracking and the quality of extracted data output are related to the quality of input. Therefore, the acquired microscopy imagery dataset must be above a pre-set quality threshold. The focus should be placed on microscopic data acquisition, while the coding and in silico analysis can be tackled later. It can be tricky as biological samples, such as tissue blocs, are often incompatible with light microscopy due to their inherent opacity and granularity,

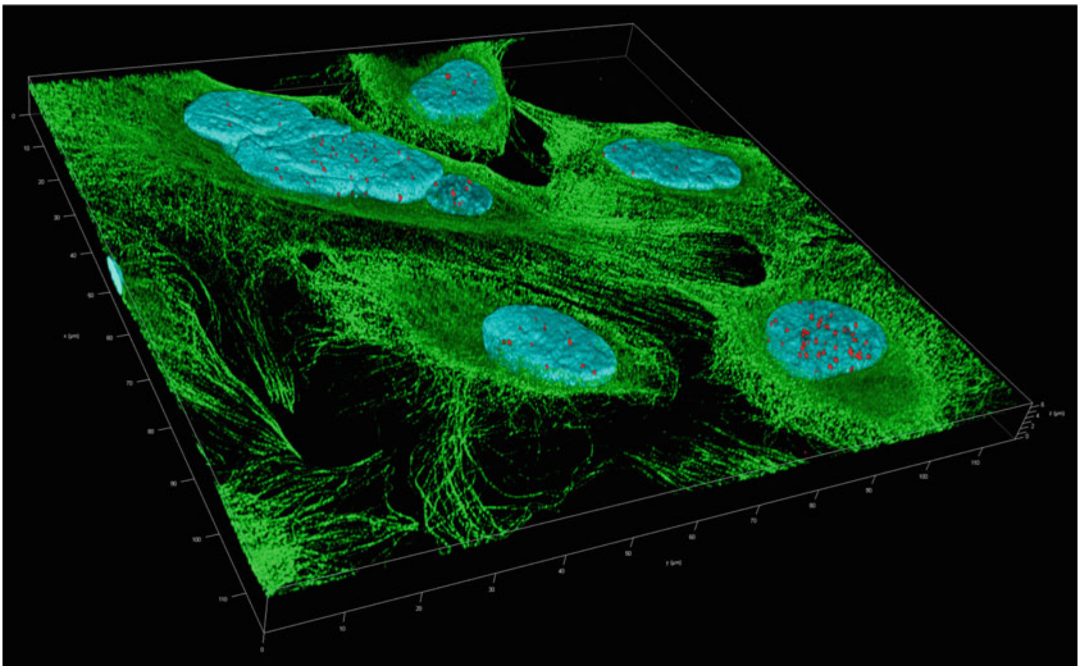

Fig. 6.3 A digital 3D reconstruction of HeLa cells from acquired *z*-stacks. The nuclei were stained with DAPI ($\lambda_{ex} = 405$ nm, $\lambda_{em} = 425$–495 nm), cytoplasmic tubulin with Alexa Fluor 488 ($\lambda_{ex} = 496$ nm, $\lambda_{em} = 505$–575 nm), and centrioles with Cy5 ($\lambda_{ex} = 649$ nm, $\lambda_{em} = 655$–725 nm) dyes. The dimensions of the 3D grid box are also shown. Reproduced with permission from Dr. Sara Barozzi, IFOM – FIRC Institute of Molecular Oncology, Milan, Italy

causing light scattering (Popp et al. 2003; Steelman et al. 2019; Chorfi et al. 2020) and loss of resolution. The compatibility of samples with advanced light microscopy must be affirmed first, and it is only fair to expect that sometimes there will be difficulties in optimizing the experimental platforms.

In a compatible sample, the study design should move on to the next phase, where further granular investigative details must be planned. Perhaps, such a discussion begins with understanding the available microscope (Fig. 6.4), its working principles, the constraints under which it is to be used, and the expected outputs. Usually, these are complex discussions that require plenty of system optimization and modulation of experimental protocols in the absence of set guidelines. Multiple factors related to the microscope should also be included, such as the light source, detector, camera, the range of available control settings, need for temperature control (37 °C), and supply of moist carbon dioxide during live cell imaging, stability of the stage in time-lapse acquisition, available objectives (with or without oil immersion), and the software package installed for data visualization or analysis.

Factors related to the sample, including its preparation and mounting, any autofluorescence that may intensify background noise, transparency, and ability to withstand exposure to laser illumination for a prolonged period, affect data acquisition. During tissue fixation, the fixing medium's desiccative effect on the sample should be factored in. Making the right choice about the mounting medium is also crucial (Szczurek et al. 2018).

A wide range of dyes is now available for sample labeling, each providing precise spectral properties to help custom design the experimental plan. However, each of them has its strengths and weaknesses. For example, some dyes are more prone to bleaching or are photochemically

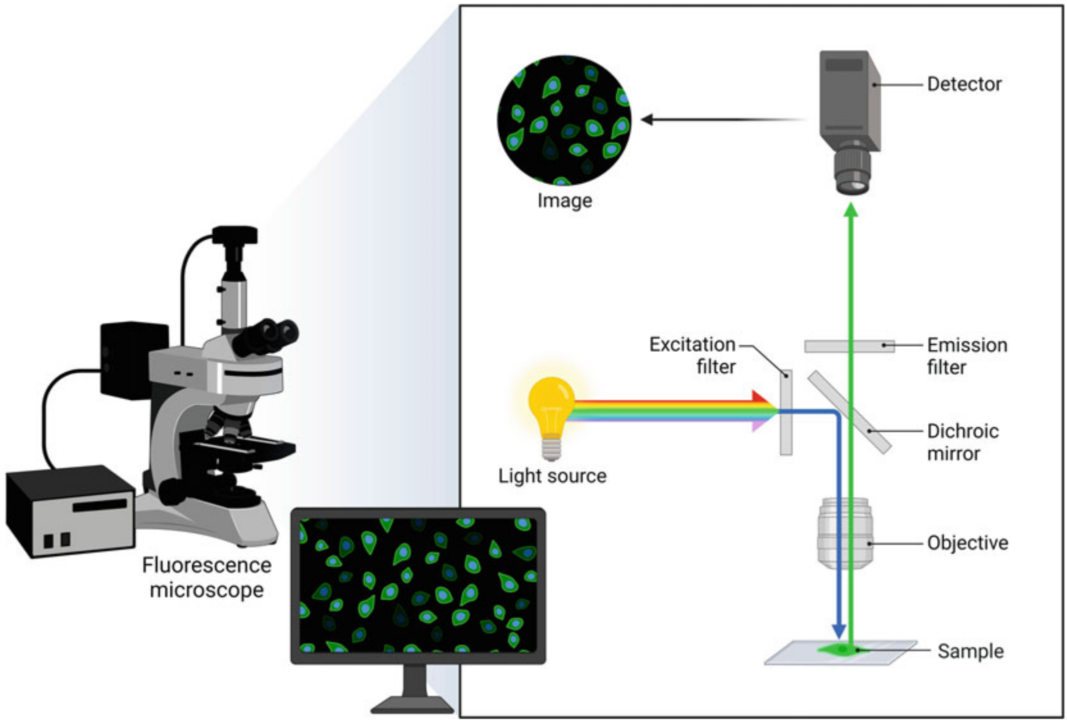

Fig. 6.4 Scheme showing the working principle of a fluorescence microscope, including the light source, dichroic mirror, sample, objective, and detector. Figure created using Biorender.com

unstable when exposed to intense light for some time. Similarly, some do not demonstrate the desired emission properties, including adequate quantum yield, while others need complex multistep bioconjugation processes under harsh reaction conditions that risk causing damage to the tissue fabric. Still, the inventory of available dyes (including Alexa and Cyanine group of dyes (Fig. 6.5) in addition to organelle-specific ones, such as MitoTracker and LysoTracker to track the cellular mitochondria and lysosomes, respectively), tailor-made for specific experiments has expanded recently. Thus, it often becomes difficult, if not confusing, to decide which one to select. Some prior experience or guidance while designing experiments can be useful. Particle tracking is now also done with super-resolution microscopy (Blom and Widengren 2017), and a separate catalog of dyes is available for such applications.

During microscopy, the total exposure period should be chosen in a way that does not bleach the fluorophores. For time-lapse acquisition, particularly where the number of repetitions is high, care must be taken that the stage remains stable and the sample in focus until the entire acquisition is over. Such stage instability may occur, especially when time-lapse *z*-stacking is underway, and should be avoided. It is also important that the proper exposure parameters are chosen in the acquisition settings, as every microscope has a refractory period after each acquisition and before it can start with the next run. Realistically, the actual acquisition runs slightly longer than the theoretical span or of what is included in the acquisition settings. Such lag is also catered for by shutter and camera speeds. Therefore, care must be taken to leave enough time gap between successive acquisitions and avoid overlapping.

Advanced microscopy platforms also provide opportunities for multipoint acquisition where

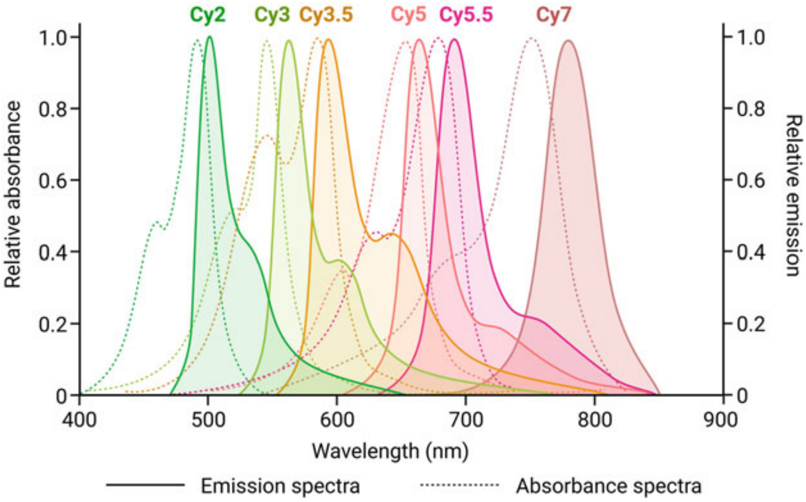

Fig. 6.5 The spectral profile, including the absorbance and emission, of the Cyanine dyes. Figure created using Biorender.com

predetermined focal points in the sample can be included in the time-lapse acquisition. The stage keeps moving the sample systematically and brings the chosen points under focus. The process is usually fully automated and controlled by the operating software, which records the *x*-, *y*-, and *z*-coordinates of the pre-set points and moves the stage periodically in accordance with the image acquisition. Although a time-saving process, such maneuvers risk losing focus on certain points after a few rounds of periodic stage movement. Fortunately, such glitches are less encountered in advanced microscopes due to their robust assembly, improved stability of the moving stages and superior software control.

Once the dataset is generated upon completion of the acquisition, it should be stored and visualized before progressing with further tracking analysis. Such time-lapse acquisition of high-resolution imagery datasets are inevitably bulky files and, depending on how long the acquisition ran, can consume large amounts of storage space on computers or servers. The operating software in the microscopes usually provides adequate rendering of the data both in 2D and 3D environments that helps with a quick preview of the acquired images and video files generated from time-lapse acquisition. A decision is usually made at this stage if any pre-processing or filtering of the data is needed, although such tunability is also available while the particle tracking is ongoing. Additionally, the software interface often provides scope for embedding scale bars into the images and time stamps into the video files to help better interpret the results.

6.5 Software Packages

There are a number of software packages, both commercial and open-source, that are now available for particle tracking analysis. It is difficult, and maybe even unfair, to compare the commercial (e.g., Imaris, Oxford Instruments, Abingdon, United Kingdom; Amira, Thermo Fisher Scientific, Waltham, MA, USA) and freely available software packages (ImageJ, National Institutes of Health, Bethesda, MD, USA; Icy, Institute Pasteur and France-BioImaging, Paris, France) as they have their strengths and weaknesses. Additionally, each researcher has a personal inclination toward certain tools based on prior experience, skill set, comfort level, the job at hand as well as the practical constraints of funding. In general, commercial software packages are more user-friendly and, in the author's opinion, easy to train as the entire interfacial planning often emerges out of years of meticulous planning and a customer-centric approach. It is envisaged that at some point in the future, there is a logic ingrained within the syntax of these tools, which facilitates comprehension of its design and workflow. It is also often easier to perform complex analyses with them.

However, as a downside, these platforms are often exorbitantly priced, both for purchase and technical support, and inadvertently need institutional licensing and backup, including installation and maintenance of dedicated facilities with huge data storage servers. It is also difficult to use them for profit-making purposes due to complex legal paperwork, a need for profit sharing with the software developing organization, and copyright issues. Thus, these software packages often prove difficult to be accessed by small and medium-sized enterprises, including tech startups, unless there is significant capital backing them.

On the contrary, open-source software is free of most of these licensing barriers and copyright issues with less paper trail. They also often do not need a lot of computer power and can be run on personal computers or laptops. To put matters into context, on a brisk initial assessment, open-source software might not deliver complex analysis or data visualization but often excel at achieving the desired results in the long run, especially when the needs are simpler.

They might also appear chaotic especially at the training stage, as they did not emerge as a result of catering to a set of client needs, but as a result of a natural outgrowth from the participation of an online community. Obtaining advice in case of encountered problems, such as “bugs,” can also be frustrating and delayed as the feedback or action needed to solve an issue is often offered pro bono. The quality of advice received from the online support community is often mixed, and unsupervised. Hence, users need to be cautious about the information that they accept from online forums. The welcome news is that over the last few years, from the perspective of developing a strongly knit, collaborative, and supportive online community that advocates the use of freewares for biomedical research, improvements are visible with good reasons to be hopeful about its future.

In biomedical research, single-cell tracking and SPT are often converged into a common interface, and in this chapter, unless otherwise stated, only SPT will be discussed. Perhaps this is also fair given that much of such tracking analyses are conducted on live cells and tissue blocs where a combination of these possibilities is required to gather maximum information. It also needs to be emphasized that almost all of these software packages come with opportunities for installing plug-ins, such as TrackMate in Fiji is just ImageJ (FIJI) (Tinevez et al. 2017), are custom designed to deal with certain types of datasets, and deliver the precise information or data that the investigators seek. These tailor-made programs are algorithms, sometimes written by lab researchers or biomedical engineers while handling a particular dataset. Many research labs have developed their own algorithms and fortunately, have shared them with the wider research community gratis.

In the author’s opinion, the relationship between a choice of software package and the quality of extracted data is often not linear, and when used skillfully, open-source software programs provide data not inferior to commercial software packages. Thus, from the viewpoint of particle tracking analysis, user skill, and experience may often act as a leveling factor between them.

6.6 Overview of the Data Derived from Particle Tracking

As stated earlier in this chapter, particle tracking is fundamentally a kinematic exercise where the movement of a particle, solitary or part of a larger cluster, is measured. The edges of a rectangular field of view typically become the metric field’s abscissa and ordinate. In the case of 3D reconstruction from *z*-stacks, the vertical depth scanned inside the sample acts as the third (*z*-axis) dimension. Each particle, moving in isolation or as part of a cohort, is assigned its coordinates at the initial frame based on the pixel in 2D or voxel in 3D tracking. In time-lapse acquisition, the selected particle(s), or the pixel(s)/voxel(s) are tracked frame-by-frame based on their coordinates. It is, therefore, crucial to understand that in particle tracking, rather than the particle, a light signal emerging out of that particle is being tracked in a virtual 2D or 3D space.

Such tracking of a particle, or the light signal it emits that is later digitally projected as a spot deconvoluted based on point-spread function (Shechtman et al. 2015; Yu et al. 2016), does bear certain caveats that will be discussed later in this chapter. Of interest from an application point of view is that by coordinate geometry calculations, the displacement vector of the particle, from the initial to final frame of acquisition, can be determined. From a mathematical perspective, if the position vector of a particle under tracking is denoted by r, and the total acquisition time is t, then the velocity vector v can be derived as:

$$v = \frac{dr}{dt} = i.\frac{\partial x}{\partial t} + j.\frac{\partial y}{\partial t} + k.\frac{\partial z}{\partial t} \tag{6.1}$$

Here i, j, and k are unit vectors in x-, y, and z-axes, respectively. Similarly, the acceleration vector a can be ascertained as:

$$a = \frac{d^2r}{dt^2} \tag{6.2}$$

A temporal pixel/voxel-wise estimation of a particle's position also enables the software to display the particle track(s) with a series of mathematical derivations, such as (average) length and duration of the tracks as well as its straightness shown in an arbitrary scale of $0 - 1$, where a value of 0 means null straightness, while a unitary value demonstrates perfect linearity. The software produces color-coded infographics on the various particulate tracks it analyzed, with a classification of them marked in a color scale.

Some of the available software packages also provide an interactive digital environment for the users to estimate the tracks, edit the set parameters or thresholds, and filter the tracks relevant to the experiment. The numerical data from the analyzed tracks could also be exported as spreadsheets for further statistical analysis, including determining the mean value and standard deviation, followed by data plotting and fitting. Additionally, excellent visual projection with a virtual rendering of the particulate movements across the tracks provides an experience for the users that, despite being virtual, appears real and easy to interpret.

The mathematical deductions shown so far were meant for particles moving or flowing with the same or similar directionalities within a visual field. However, particle tracking can also be done without a fixed directionality where, for example, the NPs are exhibiting random movements under Brownian motion. An important parameter that can be extracted from such instances is the mean square displacement (MSD), and it will gradually transpire in the later sections of this chapter how informative this parameter can be, especially while designing mucopermeative NPs for drug delivery.

A knowledge of MSD indicates the mode of displacement exhibited by the particle and the diffusion coefficient to mark if any binding is taking place between the particles and the surrounding matrix over time. The measurement of MSD can be achieved by determining the Cartesian coordinates of the centroid of a particulate system exhibiting random movement by the following equation (Wang et al. 2021a):

$$\left\langle \Delta r^2(\tau) \right\rangle = \left\langle (r(t+\tau) - r(t))^2 \right\rangle \tag{6.3}$$

Here, $r(t + \tau)$ and $r(t)$ denote the position vectors of the particle at two instances separated by a time interval of τ and $\langle \ldots \rangle$ denotes if it is time-averaged (TA) or ensemble-averaged (EA). Let us assume that in a particulate system of a total N number of particles eliciting random movement, the total acquisition time is T while the time lag of measurement is $t^{'}$.

Thus, the time-averaged MSD is:

$$\left\langle \Delta r^2(t') \right\rangle_{TA} = \frac{1}{T-t'} \int_0^{T-t\prime} [r(t+t') - r(t)]^2.dt \tag{6.4}$$

Similarly, the ensemble-averaged MSD would be:

$$\left\langle \Delta r^2(t') \right\rangle_{EA} = \frac{1}{N} \sum\nolimits_{i=1}^{N} [r_i(\tau) - r_i(0)]^2 \tag{6.5}$$

The slope (α) of the MSD plotted against time provides information on the diffusion pattern of the particles (Fig. 6.6): $\alpha < 1$ for sub-diffusion due to particle binding with its matrix, such as NPs binding with mucin (Li et al. 2013); $\alpha = 1$ for Brownian motion; and $\alpha > 1$ for super-diffusion—an anomalous diffusion triggered by active transport—and is reported in cells (Reverey et al. 2015; Kalwarczyk et al. 2017; Song et al. 2021).

The diffusion coefficient (D) of the particles in a system of d dimensions ($d = 2$ in 2D and $d = 3$ in 3D) can be deduced from the following equation:

$$\left\langle \Delta r^2(\tau) \right\rangle = 2dD\tau \tag{6.6}$$

The viscoelastic modulus of a complex fluid, such as intracellular cytoplasm, indicative of its resistance against deformation and flow under applied stress, can also be further determined from the diffusion coefficient (D) by mathematical deductions.

6.7 Some Interesting Applications of Particle Tracking in Biomedical Systems

6.7.1 Designing Mucopermeative NPs for Drug Delivery

The mucus layer that bathes the epithelial surfaces of the respiratory, gastrointestinal, and female reproductive tracts acts as a formidable physiological barrier against NP-mediated drug delivery (Bhattacharjee et al. 2017). When administered, the NPs often adhere to the mucus layer and, rather than reaching their target sites, are recycled with the mucus layer inside human body every 3–4 h (Lai et al. 2009a). Thus, a considerable and unpredictable fraction, often as high as 90% of the administered dose, is dissipated (Lai et al. 2009b). In addition, it increases the production cost with wastage of excipients and other valuable resources.

The mechanism of mucus-NP binding is still not adequately explained. However, an observation that anionic NPs demonstrate higher mucopermeation than their cationic counterparts has indicated that such binding is surface charge driven. By weight composition, mucus is >90% water, while the solid part is mostly composed of mucin, a biopolymer that, due to its high content of glycoproteins, can hold water molecules (Siddhanta et al. 2019). Hence, mucin swells and contributes to mucus hydrogel in an aqueous environment. At physiological pH of 7.2–7.4, mucin is overall anionic, and due to electrostatic repulsion, anionic NPs experience lower binding with the mucin mesh that in turn facilitates mucopermeation. On the contrary, cationic NPs bind more with the mucin, discouraging their capacity to permeate through mucus (Wang et al. 2011). Interestingly, human mucus is exposed to various degrees of pH variation throughout the human body. For example, it is slightly alkaline in the respiratory tract while acidic in the stomach and proximal duodenum (Lieleg et al. 2010).

Particle tracking was used to investigate the dynamics of rhodamine-labeled liposomes (120–130 nm) of various surface charges (cationic and anionic) inside porcine jejunal mucus. The harvested mucus was filled inside microchannels fabricated on an optically translucent microslide, and time-lapse acquisition under an inverted 40× objective was achieved. The data divulged intricate details of how the surface chemistry of NPs plays an important role in determining their passage through a column of mucus, with lessons important for designing nanomedicines. It was also shown with the help of fluorescence lifetime imaging microscopy that not only did the cationic liposomes bind to the mucin mesh but also triggered its irreversible agglomeration (Bhattacharjee et al. 2018). Such agglomeration of mucus by cationic NPs, despite enhancing mucopermeation, may simultaneously compromise the safeguarding role of mucus against external pathogens and toxins (Fahy and Dickey 2010).

Finally, SPT on fluorescent NPs, while permeating mucus in real-time, maybe an interesting tool for microrheological investigations. This is especially important given that the viscoelasticity of mucus is relevant in maintaining homeostasis. Optimal viscoelasticity ensures that

Fig. 6.6 The MSD vs. time plot shows the typical patterns in diffusion, sub-diffusion, and super-diffusion

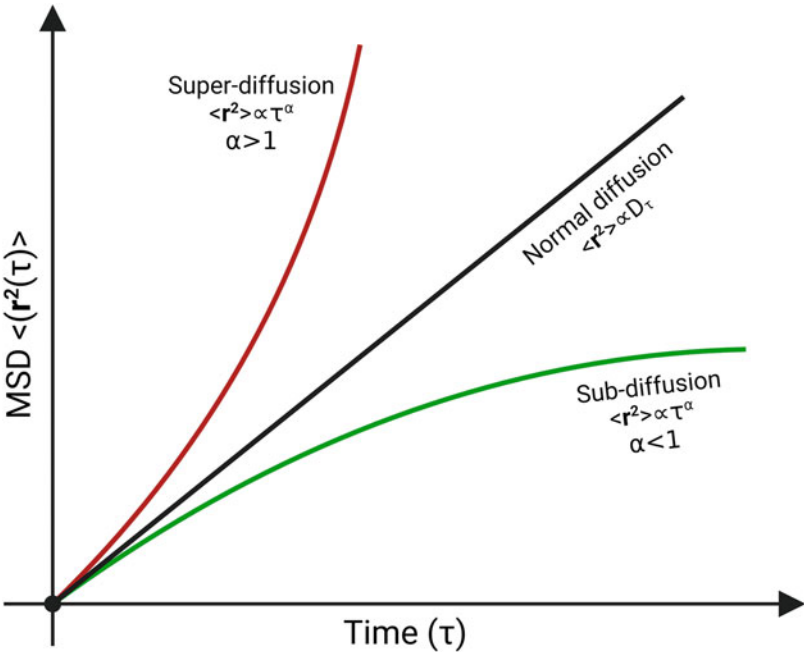

the mucus hydrogel acts as a barrier against harmful external agents and concurrently allow access to the beneficial biomolecules, including nutrients and administered therapeutics (Yuan et al. 2015). Such permeability threshold will inevitably be low for a thinner mucus layer with lessened viscosity that, in addition to the beneficial molecules, would also grant undesirable passage to some harmful agents. On the contrary, a thicker mucus, such as the respiratory tract mucus in cystic fibrosis patients (Comegna et al. 2021), will be dysfunctional in many ways. For example, in cystic fibrosis, other than inviting infections by opportunistic pathogens, such as *Pseudomonas aeruginosa* (Waters and Goldberg 2019), a viscous mucus layer makes the respiratory tract congested and breathing difficult (Morrison et al. 2019).

6.7.2 Cellular Microrheology and Biomechanics

Particle track analysis has provided fresh impetus in microrheology by delivering information on the physical (viscosity) and rheological attributes (elastic and viscous moduli) of a cell (Ladoux and Mège 2017; Rigato et al. 2017; Fläschner et al. 2021). This information is important for understanding how cells react to environmental changes, including exposure to physicochemical stress and toxicants. It can also provide information on the intracellular variance in viscosity within various compartments, such as the cytoplasm and nucleus.

The viscoelasticity and its alterations during cell division of human cervical cancer-derived HeLa cells were examined using particle tracking techniques. Fluorescent ($\lambda_{ex/em} = 585/605$ nm) polystyrene beads (100 nm) were injected into the cells using a biolistic particle delivery system at a range of 5–26 particles/cell (average 11 particles/cell). The Brownian motion of the particles inside the cells was imaged in an inverted Nikon Eclipse Ti (Tokyo, Japan) microscope with oil-immersion objective (100×) connected to a charge-coupled device camera. Further settings included a frame rate of 100 frames-per-second, 512 × 512 pixels-per-frame, and an image resolution of 0.169 μm/pixel. The video files were analyzed to extract multiple numerical readouts, including the elastic, viscous, and complex moduli, plus MSD. The results showed that the intracellular viscosity increased from metaphase to anaphase while remaining static from anaphase onward until telophase. Such a rise in intracellular viscosity was attributed to an accumulation of microtubules as part of spindle formation that required redistribution of the molecular motors (Yin-Quan et al. 2013).

Similarly, tracking of the chromatin granules exhibiting Brownian motion inside the nuclei of acute lymphocytic leukemia-derived cell lines, viz., Jurkat, CCRF-CEM, and Reh, revealed that the isolated nuclei of high-risk leukemia cells elicited higher viscosity than normal ones. Interestingly, the isolated nuclei of cells derived from relapsed leukemia patients were even more viscous than the high-risk category. These isolated nuclei were immunostained with Hoechst 33342 dye and imaged in an SPE confocal microscope with a 40× oil-immersion objective. The image analysis and quantification were done with FIJI, while multiple particle tracking was conducted by Speeded Up Robust Features algorithm (Herráez-Aguilar et al. 2020).

In a different study, carboxylate-terminated anionic and amine-terminated cationic polystyrene NPs of 100 and 200 nm sizes were microinjected into Swiss 3T3 fibroblast cells cultured on 35 mm glass bottom dishes. The acquisition was performed under physiological conditions (37 °C) in an inverted epifluorescence microscope fitted with a 100 Plan Fluor oil-immersion objective. The investigations demonstrated that both the endocytosed carboxylate- and amine-terminated NPs (endocytosed or injected) showed non-specific interactions with cellular proteins while their directional motions were detected in the cytoplasm (Tseng et al. 2002).

An understanding of the mechanical properties of cancer cells, including their increased deformability, has been linked to their metastatic potential. To investigate, human breast cancer (MDA-MB-23) and human breast epithelial (MCF-10A) cells labeled with an enhanced green fluorescent protein, were microinjected with carboxylate-terminated anionic polystyrene NPs (200 nm) aided by a ballistic particle injector. Both the cell types were less deformable in vivo compared to a 2D cell culture in vitro. Over time, the deformability of normal epithelial cells remained static, although it increased in cancer cells. Particle tracking revealed that the mechanical properties of a 3D spheroid constructed out of these cells on collagen matrices simulated the in vivo condition (Wu et al. 2020).

Particle microrheology could be a useful way of investigating how chemotherapy alters the elasticity of cancer cells. To demonstrate, carboxylate-modified anionic and fluorescent polystyrene NPs of 190 nm sizes were microinjected into breast cancer-derived MCF-7 cells, with or without being exposed to a mitotic inhibitor anticancer agent, paclitaxol. Both the elastic and viscous moduli of the cells increased up to 12 h after the paclitaxol exposure and continued with an upward trend even after 24 h (El Kaffas et al. 2013).

6.7.3 Understanding the Dynamics of Biomembranes

Particle tracking has been used to probe the dynamics of various membrane components and estimate the lateral diffusion on the membrane. A single molecule tracking exercise on the HeLa cells demonstrated that the chemokine CXCR4 receptor on the cell membrane undergoes a complex formation when activated by a ligand. Furthermore, these complexes demonstrated a 2.5× higher cellular internalization than the monomers utilizing a clathrin-dependent pathway. The single molecule fluorescence imaging was done in a Nikon total internal reflection fluorescence microscope with a 100× oil-immersion objective. The exposure time for each frame was 50 ms, and a deep-learning algorithm was used to differentiate the monomeric CXCR4 receptors from their complex forms (Wang et al. 2021b).

SPT of immobilized quantum dots on the Madin-Darby canine kidney or MDCK II cells expressing cystic fibrosis transmembrane conductance regulator-3 hemagglutinin (CFTR-3HA) receptors enabled modeling of confined diffusion of CFTR chloride channels in the cell membrane.

The diffusion coefficient was determined to be ~0.004 μm^2/s, while the particle tracking data fitting resembled an attractive potential depicted by a spring, that is, $V(r) = k.\ r^2$ where the value of spring constant k was 2.6 ± 0.8 pN/μm. The spring constant was relatively unaffected when the cells were exposed to jasplakinolide, an actin-stabilizing agent, at a concentration of 2.5 mM for 5–10 min. On the contrary, it declined with a 5–10 min exposure to 250 nM latrunculin, an inhibitor of actin polymerization. The collective data demonstrated the role of actin filaments in elastic behavior of the CFTR. The imaging was done in an inverted epifluorescence microscope with an oil-immersion objective. The SPT was accomplished using 15 ms acquisitions for 20 s (Jin et al. 2007).

Tracking of single fluorescent lipid molecules in an artificial phospholipid membrane was able to deduce the lateral diffusion coefficient as 1.42 (±0.13) × 10^{-8} cm^2/s. The acquisition was done in a Zeiss Axiovert microscope ($\lambda_{ex} = 514$ nm) under a 100× oil-immersion objective (Schmidt et al. 1996). Similarly, SPT on a gold-NP labeled solid supported lipid bilayer with an increasing concentration of GM_1 gangliosides enabled the determination of percolation threshold (22% GM_1). The anionic gold-NPs adhered to the cationic ethyl phosphatidylcholine lipid in the bilayer. In bilayers devoid of GM_1, 92% of the gold-NPs elicited random diffusion with a mean diffusion coefficient of 4.3 (±4.5) × 10^{-9} cm^2/s. In bilayers with 14% GM_1 content, 62% of the gold-NPs were confined within a microdomain created by the GM_1 clusters. At 22% GM_1 content (percolation threshold), almost all the gold-NPs were restricted within the GM_1 clusters. The microscopic acquisition was done in an inverted microscope with a 100× oil-immersion objective (Sagle et al. 2012).

6.7.4 Mechanistic Investigations on Intracellular and Intercellular Transport

Particle tracking has successfully probed cellular internalization and intracellular transport of vesicles that play a major role in cellular dynamics, including phagocytosis and apoptosis. For example, tracking synaptic vesicles in neurons of hippocampal cell cultures from Wistar rats showed that the mobility of synaptic vesicles was low in absence of electrical stimulation (resting condition) or even during synaptic activity. The recycling pool of the synapses and synaptic vesicles were stained with fluorescence dyes FM5–95 and FM1–43, respectively. The acquisition was done in a Leica SP2 confocal microscope equipped with a 63× objective (Lemke and Klingauf 2005).

Similar particle tracking studies on Rhodamine-B-labeled fluorescent silica NPs (70 nm) and submicron silica particles (300 and 1000 nm) in human lung cancer-derived A549 cells showed that the size of silica particles did not affect the motility of early or late-endosomes and lysosomes. However, the vesicles containing 70 nm silica NPs moved faster inside the cells when compared with the 300 nm and 1000 nm ones. Thus, particle size affected the membrane traffic of the endosomes. The acquisition was done in a custom-designed inverted total internal reflection fluorescence microscope with a 100× oil-immersion objective (Aoyama et al. 2017).

In a separate study, dengue viruses labeled with DiD dye were tracked inside *Aedes albopictus* C6/36 cells. The results confirmed cellular internalization of the viral particles via clathrin-mediated endocytosis. The viruses first diffused on the cell membrane surfaces before being trapped by the clathrin-coated pits. Once internalized by the cells, the viral particles were transported in Rab5+ endosomes, although with maturation, the endosomes lost Rab5 and gained Rab7. The fusion between the viral membrane with the endosomes was mostly noticed in the late endosomes (van der Schaar et al. 2008).

Similarly, tracking membrane vesicles labeled with FM1–43 dye showed their movement in live *Escherichia coli* bacterium. When exposed to antimicrobials, such as ciprofloxacin and chloramphenicol, the production and traffic of vesicles increased, perhaps due to reduced bacterial surface appendages caused by the antimicrobials. The microscopy was done in a Zeiss ApoTome inverted wide-field microscope fitted with a Plan Apo 63× objective (Bos et al. 2021).

6.7.5 Mechanistic Investigations on Cellular Uptake

Particle tracking can provide crucial insights into cellular uptake mechanisms. In such a study, tetrahedral DNA nanostructures labeled with Cy3 were tracked while internalized by the HeLa cells. It was noted that the cells took up DNA nanostructures via caveolin-mediated pathways, and the nanostructures were confined within lysosomes. The researchers functionalized the DNA nanostructures with nuclear localization signals as a next step. For particle tracking on these functionalized DNA nanostructures, the nuclear localization signals were labeled with TAMRA dye, while the nanostructures were tagged with Alexa 488. The nuclei of the HeLa cells were labeled with Hoechst 33342. SPT of these labeled DNA nanostructures functionalized with nuclear localization signals demonstrated that the nanostructures could escape the lysosomes and enter the cellular nuclei. The live cell imaging was done in a Leica TCS SP5 confocal microscope under a 63× oil-immersion objective and 37 °C temperature (Liang et al. 2014).

In another study, colloidal carboxylated particles of various sizes were tracked in transfected 3T3 fibroblasts to understand the mechanism of cellular uptake. The imaging was conducted using a combination of label-free total internal reflection and reflectance fluorescence microscopy. The obtained data confirmed that the particles were taken up by clathrin-mediated endocytosis, although there was an upper size threshold for such internalization. For example, colloidal latex particles of up to 500 nm size engaged with clathrin receptors while larger particles, such as 1 μm, did not (Byrne et al. 2015).

The mechanism of cellular internalization and intracellular fate of filamentous M13 bacteriophages in *Escherichia coli* bacteria (ER2738 and XL1-Blue strains) was investigated by SPT. The surfaces of the bacteriophages were functionalized with cell-penetrating peptides, viz., light chain variable domain 3D8 VL transbody (3D8 VL-M13) and TAT peptide (TAT-M13), to facilitate bacterial uptake. The 3D8 VL-M13 variant showed higher uptake than the TAT-M13. Additionally, the 3D8 VL-M13 was internalized primarily by a caveolin-mediated pathway upon interacting with the heparan sulfate proteoglycan receptors on bacterial surfaces, whereas the TAT-M13 triggered both clathrin and caveolin pathways (Fig. 6.7) via the chondroitin sulfate proteoglycan receptors. Furthermore, internalized 3D8 VL-M13 remained stable and distributed in the cytosol for 18 h from uptake inside the bacterial cells without any visible compartmentalization. On the contrary, the TAT-M13 rapidly clustered into various subcellular compartments and was degraded in lysosomes within 2 h (Kim et al. 2012).

Using SPT, another study reported an induced autophagy of octa-arginine peptide R8-conjugated poly(styrene-*co*-maleic anhydride) polymeric Pdots (85 nm) in HeLa cells with accelerated internalization. Image acquisition was done in a Leica TCS SP8 confocal microscope equipped with a 63× oil-immersion objective, while the track analysis was done in FIJI software. The R8-modified polymeric NPs were taken up mostly by caveolin-dependent pathways without being entrapped in lysosomes clustered in the perinuclear regions of the HeLa cells (Luo et al. 2019).

3D SPT of endosomes with endocytosed carboxylated fluorescent polystyrene NPs of 100 nm size in human lung carcinoma-derived A549 cells showed that the particle motion inside the cells gradually transforms from a 3D-constrained pattern to quasi-2D motion. The action of microtubules on the vesicular transport introduces anisotropy and heterogeneity in intracellular endosomal dynamics, for example, in lateral movements. On the contrary, the axial movement was noticed to be more homogeneous. Furthermore, it was shown by tracking that the endocytosed cargo remained near the internal

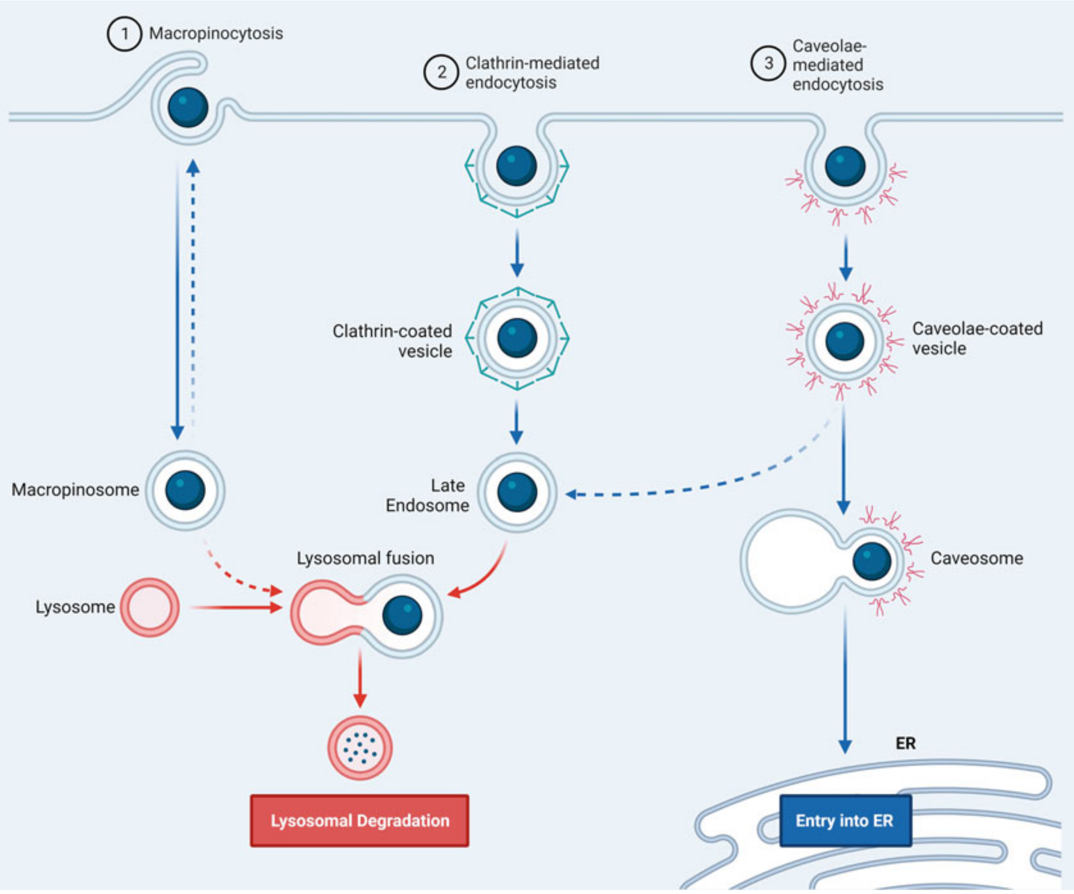
1 Macropinocytosis
2 Clathrin-mediated endocytosis
3 Caveolae-mediated endocytosis
Clathrin-coated vesicle
Caveolae-coated vesicle
Macropinosome
Late Endosome
Caveosome
Lysosomal fusion
Lysosome
ER
Lysosomal Degradation
Entry into ER

Fig. 6.7 Scheme showing the different non-phagocytic endocytosis pathways, including the clathrin- and caveolae-mediated ones. Figure created using Biorender.com

membrane surfaces of the endosomes while eliciting lateral diffusion (Jiang et al. 2022).

6.8 Future Perspectives

As an analytic tool, SPT has come a long way since its inception, with a great deal of technical advances during this journey. Improved microscopy and better computational capability have empowered current microscopists to create their niche and provide a fertile ground for collaboration with biologists. Admittedly, particle tracking has provided a wealth of information on how biological systems work and the repercussions felt when exposed to fluctuations in their physicochemical environments. Additionally, SPT has revealed intriguing details on the core principles of cellular functioning, at times in molecular detail, that, when embroidered together, present a much clear understanding of the cellular machinery than what we possessed even a decade back. Emerging SPT modalities, such as single particle orientation and rotational tracking (Gu et al. 2013), are providing fresh hopes of pushing the current limits further with unpacking of more mysteries in cellular physiology.

However, there is a long way ahead for such emerging systems to bridge many of the gaps that still exist in our understanding of cells, tissues, and a wide spectrum of other biomaterials that are present in human body, for example, the mucus hydrogel that formed a crucial component in the discussion thus far. The algorithms need to be better equipped to manage biological datasets that, unlike many physical systems in research labs, can be incompatible and tedious. The microscopy platforms need similar advancements to continue a descent along the size scale. In a way, SPT is already possible on even single molecules, but as a technique, it still has plenty of ground to cover while dealing with diverse biological samples.

The emergence and gradual evolution of super-resolution microscopy are a welcome development from that perspective. Some of these platforms can achieve resolution down to <50 nm/pixel, which is truly a technological marvel. However, the fact that these platforms can offer unprecedented resolution makes them more complex and challenging. They are expensive and personnel need intensive training before sustained data output can be expected. Pressing logistic demands also makes them less feasible in resource-poor countries. Moreover, the biomedical research community is still adapting to such high-end microscopy. In summary, super-resolution microscopy, despite having promising potential, at least in the current scenario, is predominantly confined within some expert groups, although awareness is growing and the future seems promising.

The range of dyes now available to microscopists for particle tracking has widened significantly over the last few years. The photochemistry of some of these dyes is unique and well-tuned to the requirements of many complex acquisitions. Unfortunately, the conjugation of these dyes is not trivial and, once more, leads to complex processes that ultimately make the entire process strenuous, expensive, time-consuming, and labor-intensive, which might discourage some researchers from engaging. In this regard, collaboration and regular exchange of ideas between microscopists, chemists, and biologists is indispensable, and it is only through these dialogs that such an interdisciplinary research field can be explored. Perhaps it is also time to prioritize unconventional fluorophores, such as quantum dots (Gardini et al. 2015), gold-NPs (Dosumu et al. 2021), and fluorescent organic NPs (Genin et al. 2014), in such microscopic ventures as they often provide neat results and simultaneously address many of the issues related to the popular dyes, including insufficient quantum yield, poor photostability, and photobleaching.

There is currently a heightened focus toward improving the algorithms. Integration of advanced data analysis tools, such as deep neural network-based platforms as part of both the hope and hype associated with artificial intelligence-driven research, are expected to enhance the depth of analysis further. It will be interesting to monitor the progress on that front. Despite a commendable initiative, it is the author’s position that perhaps a major focus should be on the pre-acquisition and acquisition stage, as that is where major obstacles remain. A recent study (Chenouard et al. 2014) has confirmed that different algorithms used on similar datasets, did not make much difference to the outcomes, while the manuscript categorically stated, “Our results indicate that, at present, there exists no universally best method for particle tracking. Users should be aware that a method reported to work for certain experiments may not be the right choice for their application.” A robust microscopy dataset should not deliver much difference in calculations as long as an adequate algorithm is applied, while in biological samples, there are obvious variations in results. However, this statement needs to be viewed in its proper context and should not be taken as a discouragement toward developing better algorithms, but rather as a word of caution that needs to be considered with gravity.

Acknowledgments The author remains grateful to Professor Dimitri Scholz from the Bioimaging Core Facility at the University College Dublin Conway Institute of Biomolecular and Biomedical Research and Dr. Massimiliano Garrè from the Super-Resolution Imaging Consortium at the Royal College of Surgeons in Ireland, for being excellent teachers and mentors in advanced microscopic techniques, including single particle tracking. Many of the pearls of wisdom conveyed in the manuscript were passed on to the author by these two amazing colleagues and scientists over stimulating discussions and enjoyable training sessions.

Funding The author would like to thank UCD Research Output Based Research Support Scheme (OBRSS) for funding.

Conflict of Interest None declared.

Ethics Approval Not required.

Data Availability Statement No novel data was reported in the manuscript. Further information on the reported data may be obtained from the author upon reasonable request.

References

Aoyama M, Yoshioka Y, Arai Y et al (2017) Intracellular trafficking of particles inside endosomal vesicles is regulated by particle size. J Control Release 260:183–193

Assmus HE, Herwig R, Cho K-H, Wolkenhauer O (2006) Dynamics of biological systems: role of systems biology in medical research. Exp Rev Mol Diagn 6:891–902

Barton GM, Kagan JC (2009) A cell biological view of toll-like receptor function: regulation through compartmentalization. Nat Rev Immunol 9:535–542

Bhattacharjee S, Brayden DJ (2021) Addressing the challenges to increase the efficiency of translating nanomedicine formulations to patients. Expert Opin Drug Discov 16:235–254

Bhattacharjee S, Gaspar MM, Scholz D, Almeida AJ, Brayden DJ (2018) Track analysis of the passage of rhodamine-labeled liposomes across porcine jejunal mucus in a microchannel device. Ther Deliv 9:419–433

Bhattacharjee S, Mahon E, Harrison SM et al (2017) Nanoparticle passage through porcine jejunal mucus: microfluidics and rheology. Nanomedicine NBM 13: 863–873

Bhattacharjee S, Rietjens IMCM, Singh MP et al (2013) Cytotoxicity of surface-functionalized silicon and germanium nanoparticles: the dominant role of surface charges. Nanoscale 5:4870–4883

Blom H, Widengren J (2017) Stimulated emission depletion microscopy. Chem Rev 117:7377–7427

Bos J, Cisneros LH, Mazel D (2021) Real-time tracking of bacterial membrane vesicles reveals enhanced membrane traffic upon antibiotic exposure. Sci Adv 7: eabd1033

Byrne GD, Vllasaliu D, Falcone FH, Somekh MG, Stolnik S (2015) Live imaging of cellular internalization of single colloidal particle by combined label-free and fluorescence total internal reflection microscopy. Mol Pharm 12:3862–3870

Cheng H-J, Hsu C-H, Hung C-L, Lin C-Y (2022) A review for cell and particle tracking on microscopy images using algorithms and deep learning technologies. Biom J 45:465–471

Chenouard N, Smal I, De Chaumont F et al (2014) Objective comparison of particle tracking methods. Nat Methods 11:281–289

Chorfi H, Ayadi K, Bouamama L, Boufendi L (2020) Contribution to the study of cancer tissues by light scattering. Optik 221:165094

Comegna M, Conte G, Falanga AP et al (2021) Assisting PNA transport through cystic fibrosis human airway epithelia with biodegradable hybrid lipid-polymer nanoparticles. Sci Rep 11:6393

Comes MC, Casti P, Mencattini A et al (2019) The influence of spatial and temporal resolutions on the analysis of cell-cell interaction: a systematic study for time-lapse microscopy applications. Sci Rep 9:6789

Cretel E, Pierres A, Benoliel A-M, Bongrand P (2008) How cells feel their environment: a focus on early dynamic events. Cell Mol Bioeng 1:5–14

Cui L, Li H, Xi Y et al (2022) Vesicle trafficking and vesicle fusion: mechanisms, biological functions, and their implications for potential disease therapy. Mol Biomed 3:29

Cui Y, Yu M, Yao X, Xing J, Lin J, Li X (2018) Single-particle tracking for the quantification of membrane protein dynamics in living plant cells. Mol Plant 11: 1315–1327

Dallet L, Stanicki D, Voisin P, Miraux S, Ribot EJ (2021) Micron-sized iron oxide particles for both MRI cell tracking and magnetic fluid hyperthermia treatment. Sci Rep 11:3286

DeBerardinis RJ, Thompson CB (2012) Cellular metabolism and disease: what do metabolic outliers teach us? Cell 148:1132–1144

Doll TAPF, Raman S, Dey R, Burkhard P (2013) Nanoscale assemblies and their biomedical applications. J R Soc Interface 10:20120740

Dosumu AN, Claire S, Watson LS et al (2021) Quantification by luminescence tracking of red emissive gold nanoparticles in cells. JACS Au 1:174–186

Dzyubachyk O, Essers J, Cappellen WAV et al (2010) Automated analysis of time-lapse fluorescence microscopy images: from live cell images to intracellular foci. Bioinformatics 26:2424–2430

El Kaffas A, Bekah D, Rui M, Carl Kumaradas J, Kolios MC (2013) Investigating longitudinal changes in the mechanical properties of MCF-7 cells exposed to paclitaxol using particle tracking microrheology. Phys Med Biol 58:923

Fahy JV, Dickey BF (2010) Airway mucus function and dysfunction. N Engl J Med 363:2233–2247

Fasehee H, Dinarvand R, Ghavamzadeh A et al (2016) Delivery of disulfiram into breast cancer cells using folate-receptor-targeted PLGA-PEG nanoparticles: in vitro and in vivo investigations. J Nanobiotechnol 14:32

Fläschner G, Roman CI, Strohmeyer N, Martinez-Martin-D, Müller DJ (2021) Rheology of rounded mammalian cells over continuous high-frequencies. Nat Commun 12:2922

Fletcher DA, Mullins RD (2010) Cell mechanics and the cytoskeleton. Nature 463:485–492

Garcés M, Cáceres L, Chiappetta D, Magnani N, Evelson P (2021) Current understanding of nanoparticle toxicity mechanisms and interactions with biological systems. New J Chem 45:14328–14344

Gardini L, Capitanio M, Pavone FS (2015) 3D tracking of single nanoparticles and quantum dots in living cells by out-of-focus imaging with diffraction pattern recognition. Sci Rep 5:16088

Gautier MK, Ginsberg SD (2021) A method for quantification of vesicular compartments within cells using 3D reconstructed confocal *z*-stacks: comparison of ImageJ and Imaris to count early endosomes within basal forebrain cholinergic neurons. J Neurosci Methods 350:109038

Genin E, Gao Z, Varela JA et al (2014) "Hyper-bright" near-infrared emitting fluorescent organic nanoparticles for single particle tracking. Adv Mater 26:2258–2261

Goel S, England CG, Chen F, Cai W (2017) Positron emission tomography and nanotechnology: a dynamic duo for cancer theranostics. Adv Drug Deliv Rev 113: 157–176

Gu Y, Ha JW, Augspurger AE, Chen K, Zhu S, Fang N (2013) Single particle orientation and rotational tracking (SPORT) in biophysical studies. Nanoscale 5: 10753–10764

Guan L (2022) Structure and mechanism of membrane transporters. Sci Rep 12:13248

Herráez-Aguilar D, Madrazo E, López-Menéndez H, Ramírez M, Monroy F, Redondo-Muñoz J (2020) Multiple particle tracking analysis in isolated nuclei reveals the mechanical phenotype of leukemia cells. Sci Rep 10:6707

Herrmann IK, Wood MJA, Fuhrmann G (2021) Extracellular vesicles as a next-generation drug delivery platform. Nat Nanotechnol 16:748–759

Jackson CB, Farzan M, Chen B, Choe H (2022) Mechanisms of SARS-CoV-2 entry into cells. Nat Rev Mol Cell Biol 23:3–20

Jiang C, Yang M, Li W, Dou S-X, Wang P-Y, Li H (2022) Spatiotemporal three-dimensional transport dynamics of endocytic cargos and their physical regulations in cells. iScience 25:104210

Jin S, Haggie PM, Verkman AS (2007) Single-particle tracking of membrane protein diffusion in a potential: simulation, detection, and application to confined diffusion of CFTR cl^{-} channels. Biophys J 93:1079–1088

Kalwarczyk T, Kwapiszewska K, Szczepanski K et al (2017) Apparent anomalous diffusion in the cytoplasm of human cells: the effect of probes' polydispersity. J Phys Chem B 121:9831–9837

Khater IM, Nabi IR, Hamarneh G (2020) A review of super-resolution single-molecule localization microscopy cluster analysis and quantification methods. Patterns 1:100038

Kim A, Shin T-H, Shin S-M et al (2012) Cellular internalization mechanism and intracellular trafficking of filamentous M13 phages displaying a cell-penetrating transbody and TAT peptide. PLoS One 7:e51813

Ladoux B, Mège R-M (2017) Mechanobiology of collective cell behaviours. Nat Rev Mol Cell Biol 18:743–757

Lai SK, Wang Y-Y, Hanes J (2009b) Mucus-penetrating nanoparticles for drug and gene delivery to mucosal tissues. Adv Drug Deliv Rev 61:158–171

Lai SK, Wang Y-Y, Wirtz D, Hanes J (2009a) Micro- and macrorheology of mucus. Adv Drug Deliv Rev 61:86–100

Lelek M, Gyparaki MT, Beliu G et al (2021) Single-molecule localization microscopy. Nat Rev Methods Primers 1:39

Lemke EA, Klingauf J (2005) Single synaptic vesicle tracking in individual hippocampal boutons at rest and during synaptic activity. J Neurosci 25:11034

Lepock JR (2005) How do cells respond to their thermal environment? Int J Hyperth 21:681–687

Li LD, Crouzier T, Sarkar A, Dunphy L, Han J, Ribbeck K (2013) Spatial configuration and composition of charge modulates transport into a mucin hydrogel barrier. Biophys J 105:1357–1365

Liang L, Li J, Li Q et al (2014) Single-particle tracking and modulation of cell entry pathways of a tetrahedral DNA nanostructure in live cells. Angew Chem Int Ed 53:7745–7750

Lieleg O, Vladescu I, Ribbeck K (2010) Characterization of particle translocation through mucin hydrogels. Biophys J 98:1782–1789

Luo Y, Han Y, Hu X et al (2019) Live-cell imaging of octaarginine-modified polymer dots via single particle tracking. Cell Prolif 52:e12556

May JN, Golombek SK, Baues M et al (2020) Multimodal and multiscale optical imaging of nanomedicine delivery across the blood-brain barrier upon sonopermeation. Theranostics 10:1948–1959

Mitchell MJ, Billingsley MM, Haley RM, Wechsler ME, Peppas NA, Langer R (2021) Engineering precision nanoparticles for drug delivery. Nat Rev Drug Discov 20:101–124

Morrison CB, Markovetz MR, Ehre C (2019) Mucus, mucins, and cystic fibrosis. Pediatr Pulmonol 54:S84–S96

Muzzey D, van Oudenaarden A (2009) Quantitative time-lapse fluorescence microscopy in single cells. Annu Rev Cell Dev Biol 25:301–327

Neumann B, Walter T, Hériché J-K et al (2010) Phenotypic profiling of the human genome by time-lapse microscopy reveals cell division genes. Nature 464: 721–727

Ortega MA, Fraile-Martinez O, Garcia-Montero C et al (2022) An updated view of the importance of vesicular trafficking and transport and their role in immune-mediated diseases: potential therapeutic interventions. Membranes 12:552

Popp AK, Valentine MT, Kaplan PD, Weitz DA (2003) Microscopic origin of light scattering in tissue. Appl Opt 42:2871–2880

Pore M, Ong GH, Boyce CM et al (2015) A comparison of magnetic resonance, X-ray and positron emission particle tracking measurements of a single jet of gas entering a bed of particles. Chem Eng Sci 122:210–218

Reeβing F, Szymanski W (2019) Following nanomedicine activation with magnetic resonance imaging: why, how, and what's next? Curr Opin Biotechnol 58:9–18

Rennick JJ, Johnston APR, Parton RG (2021) Key principles and methods for studying the endocytosis of biological and nanoparticle therapeutics. Nat Nanotechnol 16:266–276

Reverey JF, Jeon J-H, Bao H, Leippe M, Metzler R, Selhuber-Unkel C (2015) Super-diffusion dominates intracellular particle motion in the supercrowded cytoplasm of pathogenic *Acanthamoeba castellanii*. Sci Rep 5:11690

Rigato A, Miyagi A, Scheuring S, Rico F (2017) High-frequency microrheology reveals cytoskeleton dynamics in living cells. Nat Phys 13:771–775

Rosenblum D, Joshi N, Tao W, Karp JM, Peer D (2018) Progress and challenges towards targeted delivery of cancer therapeutics. Nat Commun 9:1410

Ross TD, Lee HJ, Qu Z, Banks RA, Phillips R, Thomson M (2019) Controlling organization and forces in active matter through optically defined boundaries. Nature 572:224–229

Sagle LB, Ruvuna LK, Bingham JM, Liu C, Cremer PS, Van Duyne RP (2012) Single plasmonic nanoparticle tracking studies of solid supported bilayers with ganglioside lipids. J Am Chem Soc 134:15832–15839

Saminathan A, Zajac M, Anees P, Krishnan Y (2022) Organelle-level precision with next-generation targeting technologies. Nat Rev Mater 7:355–371

van der Schaar HM, Rust MJ, Chen C et al (2008) Dissecting the cell entry pathway of dengue virus by single-particle tracking in living cells. PLoS Pathog 4: e1000244

Schindelin J, Arganda-Carreras I, Frise E et al (2012) Fiji: an open-source platform for biological-image analysis. Nat Methods 9:676–682

Schlessinger J (1997) Direct binding and activation of receptor tyrosine kinases by collagen. Cell 91:869–872

Schmidt T, Schütz GJ, Baumgartner W, Gruber HJ, Schindler H (1996) Imaging of single molecule diffusion. Proc Natl Acad Sci U S A 93:2926–2929

Schultze B, Karbasi P, Sarosiek C et al (2021) Particle-tracking proton computed tomography—data acquisition, pre-processing, and preconditioning. IEEE Access 9:25946–25958

Shapiro EM, Skrtic S, Sharer K, Hill JM, Dunbar CE, Koretsky AP (2004) MRI detection of single particles for cellular imaging. Proc Natl Acad Sci U S A 101: 10901–10906

Shechtman Y, Weiss LE, Backer AS, Sahl SJ, Moerner WE (2015) Precise three-dimensional scan-free multiple-particle tracking over large axial ranges with tetrapod point spread functions. Nano Lett 15:4194–4199

Shen H, Tauzin LJ, Baiyasi R et al (2017) Single particle tracking: from theory to biophysical applications. Chem Rev 117:7331–7376

Siddhanta S, Bhattacharjee S, Harrison SM, Scholz D, Barman I (2019) Shedding light on the trehalose-enabled mucopermeation of nanoparticles with label-free Raman spectroscopy. Small 15:1901679

Song Y, Geng Y, Shen L (2021) Visualizing super-diffusion, oligomerization, and fibrillation of amyloid-β peptide chains along tubular membranes. ACS Macro Lett 10:1295–1299

Spitzer J, Poolman B (2009) The role of biomacromolecular crowding, ionic strength, and physicochemical gradients in the complexities of life's emergence. Microbiol Mol Biol Rev 73:371–388

Steelman ZA, Ho DS, Chu KK, Wax A (2019) Light-scattering methods for tissue diagnosis. Optica 6:479–489

Szczurek A, Contu F, Hoang A, Dobrucki J, Mai S (2018) Aqueous mounting media increasing tissue translucence improve image quality in structured illumination microscopy of thick biological specimen. Sci Rep 8: 13971

Tang DD, Gerlach BD (2017) The roles and regulation of the actin cytoskeleton, intermediate filaments and microtubules in smooth muscle cell migration. Respir Res 18:54

Taylor AC (1962) Responses of cells to pH changes in the medium. J Cell Biol 15:201–209

Tenchov R, Sasso JM, Wang X, Liaw W-S, Chen CA, Zhou QA (2022) Exosomes─Nature's lipid nanoparticles, a rising star in drug delivery and diagnostics. ACS Nano 16:17802–17846

Tinevez J-Y, Perry N, Schindelin J et al (2017) TrackMate: an open and extensible platform for single-particle tracking. Methods 115:80–90

Torchilin VP (2005) Recent advances with liposomes as pharmaceutical carriers. Nat Rev Drug Discov 4:145–160

Tseng Y, Kole TP, Wirtz D (2002) Micromechanical mapping of live cells by multiple-particle-tracking microrheology. Biophys J 83:3162–3176

Tumpa TR, Acuff SN, Gregor J, Bradley Y, Fu Y, Osborne DR (2022) Data-driven head motion correction for PET using time-of-flight and positron emission particle tracking techniques. PLoS One 17:e0272768

Tvaruskó W, Bentele M, Misteli T et al (1999) Time-resolved analysis and visualization of dynamic processes in living cells. Proc Natl Acad Sci U S A 96: 7950–7955

Vicidomini G, Bianchini P, Diaspro A (2018) STED super-resolved microscopy. Nat Methods 15:173–182

Wan X-Y, Zheng L-L, Gao P-F et al (2014) Real-time light scattering tracking of gold nanoparticles-bioconjugated respiratory syncytial virus infecting HEp-2 cells. Sci Rep 4:4529

Wang Q, He H, Zhang Q et al (2021b) Deep-learning-assisted single-molecule tracking on a live cell membrane. Anal Chem 93:8810–8816

Wang Y-Y, Lai SK, So C, Schneider C, Cone R, Hanes J (2011) Mucoadhesive nanoparticles may disrupt the protective human mucus barrier by altering its microstructure. PLoS One 6:e21547

Wang Z, Wang X, Zhang Y, Xu W, Han X (2021a) Principles and applications of single particle tracking in cell research. Small 17:2005133

Waters CM, Goldberg JB (2019) *Pseudomonas aeruginosa* in cystic fibrosis: a chronic cheater. Proc Natl Acad Sci U S A 116:6525–6527

Wu P-H, Gambhir SS, Hale CM, Chen WC, Wirtz D, Smith BR (2020) Particle tracking microrheology of cancer cells in living subjects. Mater Today 39:98–109

Xing Y, Cheng Z, Wang R, Lv C, James TD, Yu F (2020) Analysis of extracellular vesicles as emerging theranostic nanoplatforms. Coord Chem Rev 424:213506

Yin-Quan C, Chia-Yu K, Ming-Tzo W et al (2013) Intracellular viscoelasticity of HeLa cells during cell division studied by video particle-tracking microrheology. J Biomed Opt 19:011008

Yu B, Yu J, Li W et al (2016) Nanoscale three-dimensional single particle tracking by light-sheet-based double-helix point spread function microscopy. Appl Opt 55:449–453

Yuan S, Hollinger M, Lachowicz-Scroggins ME et al (2015) Oxidation increases mucin polymer cross-links to stiffen airway mucus gels. Sci Transl Med 7:276ra27

Zahid MU, Ma L, Lim SJ, Smith AM (2018) Single quantum dot tracking reveals the impact of nanoparticle surface on intracellular state. Nat Commun 9:1830

7

An Exploration of the Practice of CT Modalities to Evaluate Anterior Cranial Deformities in Craniosynostosis

Anil Madaree, Vensuya Bisetty, Nivana Mohan, Courtney Barnes, and Lelika Lazarus

Abstract

Craniosynostosis is a condition of the premature fusion of one or more cranial sutures, which results in characteristic skull-shape deformities and facial asymmetry accompanied by varying functional consequences. In most forms of craniosynostosis, the anterior cranial fossa (ACF) is affected. The most common forms include scaphocephaly, trigonocephaly, anterior plagiocephaly (AP), and brachycephaly. Diagnostic imaging is necessary to assess and analyze accompanying skull deformities, intracranial pathology, and other complications in craniosynostoses. The analysis of the morphometric changes in the ACF is best elicited by computed tomography (CT) scans due to its superior bone depiction. To quantify and describe the extent to which the ACF is affected, one can measure the dimensions of the ACF and compare it to suitable normal/unaffected controls. In unilateral cases, the ACF dimensions can be compared to the non-synostotic side of the same patient. In order to get the most accurate and consistent assessment of the ACF, one needs to find fixed anatomical landmarks which are used as the basis of the morphometric analyses. Literature regarding the morphometry of the ACF in craniosynostoses is limited. Therefore, this study aimed to evaluate the anterior cranial deformities in three types of craniosynostosis, viz. scaphocephaly, trigonocephaly, and AP, by analyzing the morphometry (length and width) of the ACF on 3D-CT scans. The findings of this study provide insight into the changes that occur within the ACF in patients with scaphocephaly, trigonocephaly, and AP. The measurements obtained can be used in the planning of surgical correction and in the postoperative analysis of surgical outcomes. All of the topics in this chapter represent novel approaches to the anatomical basis of ACF deformities in these rare craniosynostoses within the South African context.

Keywords

Anterior cranial fossa · Computed tomography · Craniosynostosis · Deformities

---

A. Madaree
Department of Plastic and Reconstructive Surgery, Inkosi Albert Luthuli Central Hospital, Durban, South Africa
e-mail: madaree@ukzn.ac.za

V. Bisetty · N. Mohan · C. Barnes · L. Lazarus (✉)
Discipline of Clinical Anatomy, School of Laboratory Medicine and Medical Sciences, College of Health Sciences, University of KwaZulu-Natal, Durban, South Africa
e-mail: Ramsaroopl@ukzn.ac.za

© The Author(s), under exclusive license to Springer Nature Switzerland AG 2023

L. Shapiro (ed.), *Microscopy Techniques for Biomedical Education and Healthcare Practice*, Biomedical Visualization 2, https://doi.org/10.1007/978-3-031-36850-9_7

7.1 Introduction

Craniosynostosis is a birth defect which results from the premature fusion of one or more sutures of the skull (Ciurea et al. 2011). Early sutural closure may result in a multitude of morphological and functional changes regarding craniofacial and neurological development (Van Veelen-Vincent et al. 2010; Ciurea et al. 2011). Various types of craniosynostoses exist, viz. scaphocephaly, trigonocephaly, anterior plagiocephaly (AP), posterior plagiocephaly, and brachycephaly (Kajdic et al. 2017). The range of complications and the effect on a child's neurodevelopmental outcome is based on the number of sutures involved. Three-Dimensional (3D) Computed Tomography (CT) scanning is the preferred diagnostic imaging technique used in craniosynostoses as it is rapid and provides extensive information on the changes in cranial morphology. The use of these scans is highly beneficial in surgical planning as well as postoperative evaluation (Ciurea et al. 2011). This chapter focuses on the use of 3D-CT scans to evaluate the anterior cranial deformities in three types of non-syndromic craniosynostosis, viz. scaphocephaly, trigonocephaly, and AP. These types were selected as (1) they are the most prevalent of the craniosynostoses and (2) all three present with a certain degree of deformation to the anterior aspect of the skull.

Scaphocephaly, also known as sagittal synostosis, results from the premature fusion of the sagittal suture. The resultant skull shape is elongated in the anteroposterior direction and narrowed in the transverse direction (Ghizoni et al. 2016). Scaphocephaly is the most common form of simple non-syndromic craniosynostosis, with an incidence of 1 in 2000–7000 births and is more prevalent in males than females (Ciurea et al. 2011; Calandrelli et al. 2020).

Trigonocephaly, also known as metopic synostosis, occurs as a result of the premature fusion of the metopic suture. It is characterized by a ridge over the midline of the forehead, resulting in a triangular-shaped head, and restricted lateral growth of the frontal bones (Wang et al. 2016). Trigonocephaly is the second most common type of craniosynostosis and is responsible for 25% of all non-syndromic craniosynostosis cases (Wang et al. 2016). Trigonocephaly has an incidence of 1 in 2100–2500 births and occurs more predominantly in males compared to females (Ghizoni et al. 2016).

AP, also known as unilateral coronal synostosis (UCS), is the premature fusion of one of the coronal sutures, resulting in either left- or right-sided UCS (LUCS or RUCS) (Kronig et al. 2020). It is the third most common type of isolated single-suture craniosynostosis, following scaphocephaly and trigonocephaly, accounting for 13%–16% of all craniosynostoses (Calandrelli et al. 2018). AP causes a twisting deformity that asymmetrically affects the majority of the craniofacial skeleton (Dvoracek et al. 2021). AP occurs more frequently in females than in males and has an incidence of 1 per 10,000 live births (Spazzapan et al. 2017).

Few studies that investigate the morphometry of the ACF in the craniosynostoses using CT modalities are available (Captier et al. 2003; Calandrelli et al. 2016, 2018, 2020; Chandler et al. 2021). Furthermore, the parameters of interest in this study have not been adequately evaluated in the existing literature. Therefore, this chapter aimed to evaluate the anterior cranial deformities in scaphocephaly, trigonocephaly, and AP by analyzing the morphometry (length and width) of the anterior cranial fossa (ACF) in 3D-CT scans. All of the topics in this chapter represent novel approaches to the anatomical basis of ACF deformities in these rare craniosynostoses within the South African context.

7.2 Anatomy of the Infant Skull

7.2.1 Gross Anatomy

The human skull is a complex structure composed of the neurocranium, which is responsible for enclosing and protecting the brain, and the viscerocranium, which is responsible for forming the facial skeleton (Jin et al. 2016). The neurocranium can be further categorized into a cartilaginous portion, which is responsible for forming the base of the skull, and a membranous portion, which is responsible for forming the calvarium (Jin et al. 2016). The calvarium is composed of the paired frontal and parietal bones, the squamous portions of the temporal bones, and the interparietal portion of the occipital bone (Jin et al. 2016). These bones are united by fibrous joints called cranial sutures (Johnson and Wilkie 2011). The calvarium is comprised of four major sutures—metopic, sagittal, coronal, and lambdoid—and three minor sutures, viz. frontonasal, temporal squamosal, and frontosphenoidal. The frontal bones are separated by the metopic suture, and the parietal bones via the sagittal suture. The coronal suture separates the frontal from the parietal bones, and the lambdoid suture separates the occipital from the parietal bones (Johnson and Wilkie 2011; Ghizoni et al. 2016). The bones of the newborn skull meet at the intersection of the sutures, forming spaces called fontanelles. The cranial sutures and fontanelles permit movement of the cranial bones to facilitate the passage of the newborn's skull through the birth canal during parturition (Johnson and Wilkie 2011; Nagaraja et al. 2013; Ghizoni et al. 2016; Kajdic et al. 2017). The posterior fontanelle closes 3 months after birth, the sphenoidal in the third month, and the anterior fontanelle usually closes within 18 months of birth, while the posterolateral fontanelle remains open until the second year (Gray and Standring 2016). Postnatally, the cranial vault sutures allow enlargement of the calvaria to accommodate the growing brain (Johnson and Wilkie 2011; Ghizoni et al. 2016; Kajdic et al. 2017). These sutures fuse over time and are rendered immovable. The closure intervals of each suture vary; the metopic suture typically fuses between 3 and 9 months of age, closure of the sagittal suture usually commences at 22 years of age, followed by the coronal suture at 24 years of age and the lambdoid suture at 26 years of age. In most cases, these sutures may become fully closed only at 35, 41, and 47 years of age, respectively (Som and Curtin 2011; Anderson et al. 2019).

7.2.2 Embryogenesis

During the embryonic phase of development, the calvarium develops from mesenchymal cells (Kajdic et al. 2017). Initially, it is positioned as a capsular membrane that surrounds the developing brain (Kajdic et al. 2017). With continuous growth and development, the outer mesenchymal tissue layer is formed via intramembranous ossification (Kajdic et al. 2017). During development, the brain is enclosed by dural fibers, which are strongly adhered to the sutural system (Kajdic et al. 2017). The sutures of the calvarium are formed during the embryonic phase of development at the same approximate positions as the membranous bones and will later on signify the main areas of bone expansion within the skull (Kajdic et al. 2017). This development involves a combination of (1) the accumulation of osteoid at the boundaries of the sutures, (2) surface placement and reconstruction of the bone, and (3) outward displacement due to brain expansion (Kajdic et al. 2017). The dura mater is responsible for controlling the fusion of sutures, and also communicates with the tissues overlying the calvarium (Kajdic et al. 2017). The premature fusion of the sutures (as in the case of craniosynostosis) by the joining of bones at the suture areas inhibits any further bone formation in this area (Jin et al. 2016). Therefore, the absence of sutural growth areas produces an inability to assist fast and expansive growth of the neurocranium and, as a result, leads to abnormal compensatory growth throughout the skull and usually causes craniofacial dysmorphology (Jin et al. 2016).

7.3 What Is Craniosynostosis?

Craniosynostosis is a rare congenital deformity characterized by an abnormal head shape resulting from premature fusion of one or more cranial sutures (Van Veelen-Vincent et al. 2010; Ciurea et al. 2011). It is one of the most common causes of craniofacial abnormalities in children, with an incidence of 1 in 2100–2500 live births (Johnson and Wilkie 2011; Kajdic et al. 2017). In craniosynostosis, the skull compensates for its inability to expand perpendicular to the affected suture by growing more in the direction parallel to the unaffected sutures, resulting in facial and/or head shape abnormalities (Van Veelen-Vincent et al. 2010). Craniosynostosis follows an additional three rules involving compensatory growth, viz. (1) compensatory growth is greatest at adjacent sutures, (2) compensatory growth is symmetrical if the adjacent suture is roughly parallel to the fused suture, and (3) if the adjacent suture is parallel to the fused suture, compensatory growth occurs from the bone distal to the fused suture (Jane et al. 2000; Massimi et al. 2012). If left untreated, craniosynostosis can lead to a variety of issues, including developmental delays, sensory, respiratory, and neurological dysfunction, abnormalities affecting the eye, as well as psychological disturbances. Therefore, early diagnosis, expert surgical techniques, postoperative care, and adequate follow-up are of paramount importance in the treatment of craniosynostosis (Johnson and Wilkie 2011; Kajdic et al. 2017).

The exact cause of craniosynostosis is unknown; however, it may be caused by environmental factors such as in utero head constraint, abnormal position, oligohydramnios, prenatal exposure to teratogens, maternal smoking, and antiepileptic drugs such as valproic acid and phenytoin or genetic factors including single-gene mutations, chromosome abnormalities, and polygenic background (Johnson and Wilkie 2011; Kajdic et al. 2017). Genetic causes contribute to approximately 20% of all craniosynostoses and are usually associated with complex craniosynostosis and extracranial complications. Most genetically linked craniosynostoses are characterized by autosomal dominant inheritance or, in some cases, new mutations (Johnson and Wilkie 2011; Kajdic et al. 2017).

The classifications of craniosynostosis vary depending on the underlying mechanism, the number of fused sutures, or the presence of other disorders. Primary craniosynostosis is the result of a primary defect in the ossification process, while secondary craniosynostosis occurs due to known systemic diseases, with hematologic or metabolic dysfunction. Secondary craniosynostosis may also develop in newborns with microcephaly due to lack of brain growth or after shunt placement in children with hydrocephalus. The term “simple craniosynostosis” is used to describe the premature closure of a single suture; conversely, “complex craniosynostosis” refers to early fusion involving several sutures of the skull. Craniosynostosis is further classified into syndromic, where it occurs with other dysmorphisms including Apert, Crouzon, or Pfeiffer syndrome, and non-syndromic, where it develops as an isolated disease (Van Veelen-Vincent et al. 2010; Ghizoni et al. 2016; Kajdic et al. 2017) (Fig. 7.1). Non-syndromic craniosynostosis is more commonly encountered and typically involves a single suture, whereas multiple sutures are affected in syndromic craniosynostosis (Van Veelen-Vincent et al. 2010).

Various types of craniosynostoses exist, viz. scaphocephaly (sagittal synostosis), trigonocephaly (metopic synostosis), anterior plagiocephaly (unilateral coronal synostosis), posterior plagiocephaly (unilateral lambdoid synostosis), and brachycephaly (bicoronal and/or bilambdoid synostosis) (Kajdic et al. 2017). The frequency in which each of the cranial sutures fuses varies among the craniosynostoses, with the most common non-syndromic craniosynostosis being sagittal synostosis (scaphocephaly), followed by metopic synostosis (trigonocephaly), uni- and bilateral-coronal synostoses (anterior plagiocephaly and brachycephaly), lambdoid synostosis (posterior plagiocephaly or brachycephaly), and other types of multiple suture synostosis (Van Veelen-Vincent et al. 2010; Johnson and Wilkie 2011). This chapter only focuses on the three most common types of non-syndromic craniosynostosis.

7.3.1 Scaphocephaly

The term scaphocephaly is derived from the Greek words “*skaphe*” meaning boat, and “*kephale*” meaning head. Scaphocephaly (sagittal synostosis) is the morphological consequence of premature fusion of the sagittal suture, the suture joining the paired parietal bones in the median

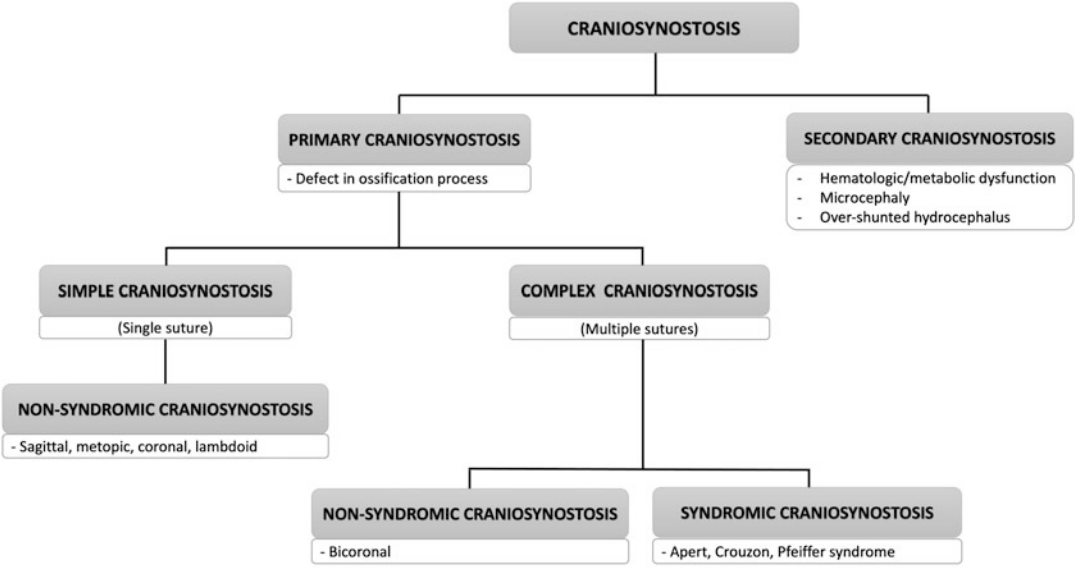
CRANIOSYNOSTOSIS
PRIMARY CRANIOSYNOSTOSIS
- Defect in ossification process
SECONDARY CRANIOSYNOSTOSIS
- Hematologic/metabolic dysfunction
- Microcephaly
- Over-shunted hydrocephalus
SIMPLE CRANIOSYNOSTOSIS
(Single suture)
COMPLEX CRANIOSYNOSTOSIS
(Multiple sutures)
NON-SYNDROMIC CRANIOSYNOSTOSIS
- Sagittal, metopic, coronal, lambdoid
NON-SYNDROMIC CRANIOSYNOSTOSIS
- Bicoronal
SYNDROMIC CRANIOSYNOSTOSIS
- Apert, Crouzon, Pfeiffer syndrome

Fig. 7.1 Classification of craniosynostosis

plane (Seeberger et al. 2016). The appearance of the skull is an elongated one with an increase in the anteroposterior diameter and a decrease in the biparietal diameter (Ghizoni et al. 2016) (Fig. 7.2). Progression of sagittal synostosis along the sagittal arch may involve the metopic suture and/or the minor sutures of the cranial base (ethmoido-frontal sutures) as well as the anterior fontanelle (Calandrelli et al. 2020). Scaphocephaly may be accompanied by additional morphological changes including frontal bossing, biparietal narrowing, temporal protrusion, sagittal ridging, coronal constriction, anteroposterior elongation, changes in the cervico-occipital angle, and occipital protuberance (David et al. 2009; Van Veelen-Vincent et al. 2010; Ghizoni et al. 2016; Calandrelli et al. 2019). The cranial dysmorphism in scaphocephaly varies considerably among affected individuals, depending on the age of onset, anatomical location, presence of prominent anatomical features, degree of premature suture closure and compensatory growth, as well as the severity of the deformity (Jane et al. 2000; Ruiz-Correa et al. 2006; David et al. 2009; Massimi et al. 2012; Tatum et al. 2012; Calandrelli et al. 2019). Scaphocephaly is the most frequently encountered form of simple non-syndromic craniosynostosis, accounting for more than 50% of all reported cases (Ciurea et al. 2011). The condition has a general incidence ranging from 1 in 2000 to 1 in 7000 births, with a male-to-female predominance of 2–4:1 (Calandrelli et al. 2020).

7.3.2 Trigonocephaly

The term trigonocephaly originates from the Greek words “*trigonon*” which means triangle, and “*kephale*” which means head (Van der Meulen 2012). Trigonocephaly, also known as metopic synostosis, is the second most common type of craniosynostosis, and accounts for approximately 25% of all non-syndromic craniosynostosis cases. The metopic suture is the first to fuse physiologically, starting at approximately 3 months of age. However, the occurrence of the premature fusion of the metopic suture results in a clear ridge located over the midline of the forehead and also the restricted lateral growth of the frontal bones (Wang et al. 2016) (Fig. 7.2). Trigonocephaly can additionally be characterized by the shortening of the anterior cranial fossa, supraorbital retrusion, hypotelorism, bitemporal narrowing, and occipitoparietal widening (Van

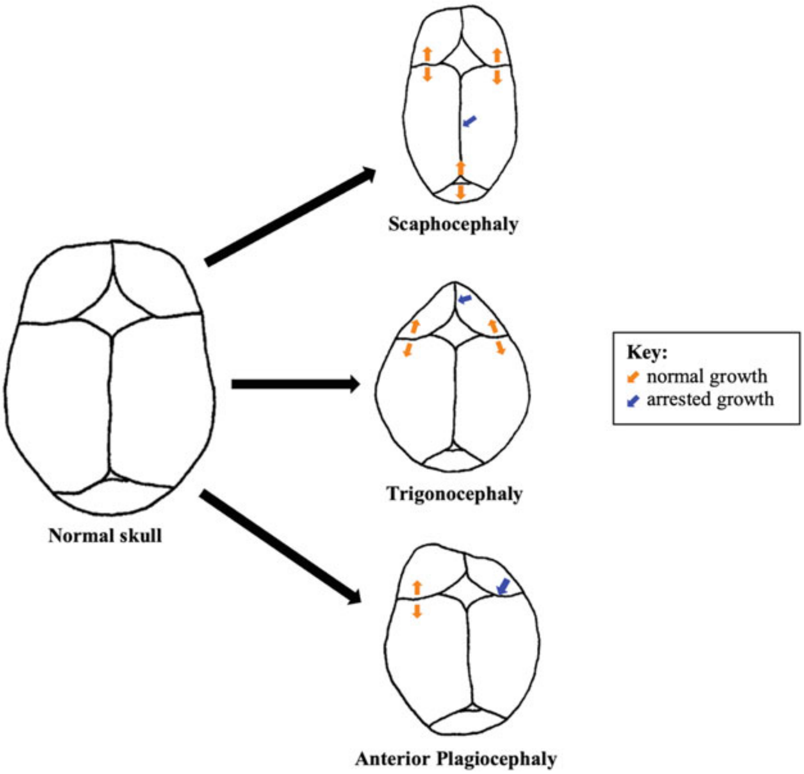

Fig. 7.2 Schematic representation of normal skull growth versus restricted skull growth as a result of different anterior deformities in the craniosynostoses being investigated

der Meulen 2012; Wang et al. 2016). In 50% of cases, the anterior fontanelle also fuses prematurely (Baş and Baş 2021). The insufficient lateral orbital rims in trigonocephalic patients promote supraorbital retrusion and bitemporal indentations (Van der Meulen 2012). At the medial orbital walls, hypotelorism is evident and in some cases combined with ethmoidal hypoplasia. The orbits are typically described as a teardrop shape and are angled in the direction of the midline of the forehead (Van der Meulen 2012). As a result of the hypotelorism appearance, a decrease in the interorbital distance is highly prevalent (Van der Meulen 2012). Trigonocephaly has an incidence of 1 in 2100–2500 births and occurs more predominantly in males compared to females with a prevalence ratio of 3:1 (Ghizoni et al. 2016).

7.3.3 Anterior Plagiocephaly

The term "*plagiocephaly*," derived from the Greek term "*plagio kephale*" which means slanted or oblique head, has been used to define either acquired or congenital developmental cranial deformities that result in severe asymmetry and scoliosis of the craniofacial skeleton (Di Rocco et al. 2012). Plagiocephaly affects every part of the skull bone, particularly the calvaria, which accounts for seven-eighths of the cranial volume in infants (Captier et al. 2003). Anterior (frontal) plagiocephaly (AP) also known as unilateral coronal synostosis (UCS), is a rare pathological cranial malformation caused by premature fusion of the coronal suture on one side (Calandrelli et al. 2018; Kronig et al. 2020). This can result in either left- or right-sided UCS (LUCS or RUCS), naturally depending on which side the suture is fused (Kronig et al. 2020). AP causes pronounced side-to-side craniofacial asymmetry, with a spectrum of features ranging from mild to severe asymmetry (Moderie et al. 2019). It involves vertical, transverse, and sagittal facial asymmetry, as well as lower facial asymmetry, resulting in a "C-shaped" malformation that is always visible on the face (Dvoracek et al. 2021; Kronig et al. 2021). This asymmetrical appearance results in constricted growth on one side of the skull and compensatory growth on the other (Moderie et al. 2019) (Fig. 7.2). The side of the head with the synostosis is termed "ipsilateral," and the opposite side is termed "contralateral" (Di Rocco et al. 2012). Most of the facial structures in AP deviate to the side of the synostosis (Marsh et al. 1986). This deformity is distinguished by some of the following characteristics: underdevelopment of the ipsilateral frontal bone, supraorbital ridge, and anterior cranial fossa (ACF), resulting in a flattened appearance; the ipsilateral orbit is elongated and narrow (harlequin orbit); anterior shift of ear, petrous bone, and zygoma; and ipsilateral deviation of the nasal root (Captier et al. 2003; Raposo-do-Amaral et al. 2011; Di Rocco et al. 2012; Spazzapan et al. 2017). On the contralateral side, there is frontal and temporal bossing, deviation of the nasal tip and chin, as well as rotation of the middle and lower face toward the non-fused side (Oh et al. 2008). AP is the third most prevalent type of simple craniosynostosis, following scaphocephaly and trigonocephaly, representing 13%–16% of all craniosynostoses (Calandrelli et al. 2018). The incidence of AP is 1 per 10,000 live births, with a 1.6 to 3.6:1 female preponderance (Dias et al. 2020). Furthermore, it has been reported that right-sided AP (RUCS) is reported to occur twice as frequently as left-sided AP (LUCS) (Heuzé et al. 2012; Kajdic et al. 2017).

7.4 Imaging Modalities Used in the Evaluation of Craniosynostosis

Imaging plays a crucial role in the precise diagnosis, surgical planning, posttreatment assessment, and detection of concomitant defects and complications related to craniosynostosis (Kim et al. 2016). Various imaging modalities have been and are currently being used in the evaluation of craniosynostosis; some of these are discussed below.

7.4.1 Plain Skull Radiography and Bone Scintigraphy

Plain skull radiography and bone scintigraphy were one of the first imaging modalities used to radiologically diagnose patients with craniosynostosis (Podda et al. 2022). Skull radiography is the radiographic examination of the skull vault and related bony structures (Murphy et al. 2022). Since multiple views are required to completely evaluate the skull for suture synostosis, plain skull radiography is considered less accurate in diagnosing craniosynostosis (Podda et al. 2022). In the absence of a CT, plain radiography of the skull is usually the last option in trauma imaging in modern medicine (Kajdic et al. 2017; Podda et al. 2022). A bone scan, also known as skeletal scintigraphy, is a unique kind of nuclear medicine treatment that employs minuscule amounts of radioactive material to identify and evaluate the severity of a number of bone diseases and conditions, such as fractures, infections, and cancer (Kajdic et al. 2017; Podda et al. 2022). However, scintigraphy is not as reliable as a plain film for the evaluation of craniosynostosis (Podda et al. 2022).

7.4.2 Computed Tomography

A Computed Tomography (CT) scan combines a number of X-ray images taken from various angles all over the body and uses computer processing to produce cross-sectional images (slices) of the bones, blood vessels, and soft tissues within the body. The advent of CT transformed the diagnosis of craniosynostosis. CT scanning is regarded as the most reliable and accurate imaging technique to diagnose craniosynostoses as it allows for all sutures to be rapidly assessed for patency. Closed sutures appear sclerosed or obliterated on CT bone windows; defects in parenchyma and ventricle spaces can be evaluated on soft tissue windows (Podda et al. 2022). Compared to traditional X-rays, CT scan images have a significant advantage as they provide more detailed information of the specified area in cross-section, eliminating the superimposition of images (Patel and De Jesus 2022). Three-dimensional rendering of CT data provides a model of the cranial vault including a depiction of the patient's sutures and fontanelles, and can also allow for evaluation of the brain for possible structural abnormalities (Podda et al. 2022).

CT scans assist in enhancing the clinician's judgement, therefore increasing the accuracy and reliability of a diagnosis (Kajdic et al. 2017). Additionally, CT scans consist of numerous slices, of varying sizes, which enable a completed image of the skull to be visualized. This further increases the accuracy of diagnosis and aids in surgical planning, as the greater the number of slices that a CT scan is composed of, the increased visualization of the deformity and any additional morphological abnormalities that may be paired with different types of craniosynostosis (Kajdic et al. 2017). Furthermore, the accuracy and efficiency of CT scanning are improving with newer generations of CT software (Podda et al. 2022).

7.4.3 Magnetic Resonance Imaging and Sonography

Magnetic Rresonance Iimaging (MRI) is an imaging technique that uses a magnetic field and computer-generated radio waves to produce detailed images of the organs and tissues in the body. The invention of MRI for use in medical research has significantly advanced diagnosis, especially with the avoidance of exposure to potentially hazardous ionizing radiation. Due to reduced costs and improved accessibility, the use of MRI in clinical practice is expanding (Grover et al. 2015). Diagnostic ultrasound, also known as sonography or diagnostic medical sonography, is a type of imaging technique that uses sound waves to create images of the internal organs and other structures in the body. The images can provide important information for diagnosing and determining the best treatment option for a variety of diseases and illnesses (Proisya et al. 2019).

More recently, MRI and sonography have been used to assess cranial sutures. MRI is a favored modality for the assessment of cerebral structures; however, it is less accurate in visualizing the cranial sutures compared to CT. MRI is generally reserved for patients in which CT reveals cerebral anomalies. Sonography allows for the patency of cranial sutures to be evaluated in utero without the use of ionizing radiation. Since prenatal intervention for a nonfatal condition is not advisable, the use of ultrasonography for early diagnosis of congenital anomalies is considered controversial (Kajdic et al. 2017; Podda et al. 2022).

MRI is a critical imaging modality when used in conjunction with ultrasound testing, especially in infants with suspected intracranial abnormalities and related craniosynostosis complications. However, CT continues to be the gold standard for diagnosing craniosynostosis until methods that permit safe prenatal diagnosis and treatment are developed (Kajdic et al. 2017; Podda et al. 2022).

7.5 A Novel Approach to Analyze ACF Morphometry in Craniosynostosis

7.5.1 Patients

This retrospective study was conducted using preoperative CT scans that were obtained from the databases of the Departments of Plastic and Reconstructive Surgery and Neurosurgery at the Inkosi Albert Luthuli Central Hospital (IALCH), Durban, South Africa. The sample population consisted of pediatric patients with a CT-confirmed diagnosis of scaphocephaly, trigonocephaly, and AP who presented to the craniofacial clinic at IALCH. In AP, finding an equivalent control to compare the morphometry is a challenge. It is acknowledged that there may be compensatory changes on the non-synostotic (contralateral) side of patients with AP (UCS) and some authors may question the normality of this control. However, if normal CT scans are used, the variability of age, sex, individual variations, and other factors would lead to many variables that may render the outcomes of a study less scientific. While the authors of this study do concede that there are compensatory changes on the non-synostotic side of AP patients, the authors are of the opinion that comparison with the non-synostotic side is the most effective way to minimize the variables. On the other hand, since the entire anterior region of the skull is affected in scaphocephaly and trigonocephaly, controls were required to fully evaluate the extent of the deformities. The controls consisted of non-affected/normal pediatric patients, who underwent clinically indicated CT scanning of the head for non-head-shape indications and had comparable CT scan information available. Only those that had met the inclusion criteria were selected for analysis.

7.5.2 Inclusion and Exclusion Criteria

7.5.2.1 Inclusion Criteria

Patients

- Pediatric patients with a CT-confirmed diagnosis of scaphocephaly who had presented to the craniofacial clinic at IALCH between 2014 and 2020.
- Pediatric patients with a CT-confirmed diagnosis of trigonocephaly who had presented to the craniofacial clinic at IALCH between 2014 and 2019.
- Pediatric patients with a CT-confirmed diagnosis of AP who had presented to the craniofacial clinic at IALCH between 2004 and 2020.

Controls

- Non-affected/normal pediatric patients who underwent clinically indicated CT scanning of the head for non-head-shape indications, and with comparable CT scan information available.
- Fine-cut CT scans with a slice thickness of 0.6 mm.

7.5.2.2 Exclusion Criteria

Patients

- Pediatric patients with multiple suture involvement.
- Pediatric patients diagnosed with syndromic craniosynostoses.
- Pediatric patients who had undergone surgical correction and postoperative CT scans.
- Pediatric patients with insufficient CT scan information and CT scans of poor quality where distinct anatomy could not be clearly defined.

Controls

- Pediatric patients with an abnormal skull shape.
- Pediatric patients with insufficient CT scan information and CT scans of poor quality where distinct anatomy could not be clearly defined.
- CT scans with a slice thickness $<$ or $>$ 0.6 mm.

7.5.3 Sample Size

Patients

Preoperative CT scans of all consecutive patients with a CT-confirmed diagnosis of:

- Scaphocephaly, presenting to the craniofacial clinic at IALCH from 2014 to 2020 and which met the inclusion criteria. A total of 37 patients with scaphocephaly were identified; however, only 24 were included in this study. The mean age at the time of the CT scan was 2.47 ± 2.36 years (range: 0.17–7.67 years).
- Trigonocephaly, presenting to the craniofacial clinic at IALCH from 2014 to 2019 and which met the inclusion criteria. A total of 12 cases were identified; however, only 8 of them were included in this study. The mean age at the time of the CT scan was 0.92 ± 0.66 years (range: 0.06–2.00 years).

– AP, presenting to the craniofacial clinic at IALCH from 2004 to 2020 and which met the inclusion criteria. A total of 29 cases were acquired; however, only 18 of them were included in this study. The mean age at the time of the CT scan was 1.23 ± 1.40 years (range: 0.50–5.75 years).

Controls
Preoperative CT scans of non-affected/normal pediatric patients, undergoing clinically indicated CT scanning of the head for non-head-shape indications, with comparable CT scan information available, and which met the inclusion criteria.

- Scaphocephaly: Of the 39 non-affected/normal patients that were identified, 14 had met the inclusion criteria (mean age: 3.35 ± 2.81 years, range: 0.08–8.42 years).
- Trigonocephaly: Of the 14 non-affected/normal patients who were identified, 6 had met the inclusion criteria (mean age: 1.32 ± 0.73 years, range: 0.08–2.00 years).

7.5.4 Ethical Considerations

Ethical clearance was obtained from the Biomedical Research Ethics Committee of the University of KwaZulu-Natal (UKZN) (BREC/00002084/2020; BREC/00002129/2020; BREC/00004342/2022). Since this study involved the use of retrospective CT scans, patient-informed consent was not required. Patient identification information was anonymized to maintain confidentiality. All data is saved on password protected electronic devices which are only accessible by the investigators. Data will be stored for a period of 5 years and thereafter, destroyed.

7.5.5 Image Acquisition

CT scans of selected patients were retrieved from IALCH's Picture Archiving and Communication System (PACS) and saved onto a hard drive in DICOM (Digital Imaging and Communication in Medicine) format. CT images were acquired in the clinical routine with either a 128-slice SOMATOM Definition AS scanner or SOMATOM Definition Flash CT Scanner (Siemens Healthineers, Forcheim, Germany). The scans of the patient groups had a slice thickness ranging from 1 to 5 mm. All CT scans of the control groups were fine-cut and had a slice thickness of 0.6 mm.

7.5.6 Image Analysis

The scans were viewed and analyzed using the Horos software version 3.3.6 (Horos Project, Annapolis, MD, USA), on an offline MacBook workstation (Apple, Cupertino, CA, USA). The CT scan images were automatically calibrated by the DICOM viewer and verified manually. CT scans were aligned in the orbitomeatal plane, which is defined by a line passing through the outer canthus of the eye and the midpoint of the external acoustic meatus (Otake et al. 2018). All measurements were performed on CT images on the bone window setting using the built-in length tool. To ensure accuracy and reliability, all measurements were performed in triplicate.

7.5.7 Current Approach to Analyzing ACF Morphometry in the Craniosynostoses

7.5.7.1 Scaphocephaly

There is a dichotomy of opinion with regard to the description of the ACF in the literature consulted. Calandrelli et al. (2020) used endocranial anatomical landmarks to measure the length of the ACF. This measurement, however, did not reflect the true length of the ACF because it was captured diagonally as opposed to being captured in an anteroposterior direction. Furthermore, no previous literature reported on the width of the ACF in patients with scaphocephaly.

7.5.7.2 Trigonocephaly

Chandler et al. (2021) utilized the midpoint of the sella turcica as a reference landmark to measure the anterior-posterior distance (length) of the ACF. However, due to the high variability in the morphology and size of the sella turcica, especially between different sexes, using the midpoint of the sella turcica may decrease the accuracy and reproducibility of the anterior-posterior distance of the ACF. Additionally, to ensure that the maximum transverse distance (width) of the ACF is measured with maximum accuracy and reproducibility, the width of the ACF should be measured in the same plane as the length of the ACF.

7.5.7.3 Anterior Plagiocephaly

Different authors used different methods and anatomical landmarks to define the ACF length parameter. Previous studies used anatomical landmarks that captured the length of the ACF diagonally, rather than using landmarks that provided a straight anteroposterior diameter to determine the true length of the ACF (Captier et al. 2003; Calandrelli et al. 2016, 2018). There is also no prior literature referencing the ACF width parameter.

The literature revealed that there is a need to revise the anatomical landmarks in order to accurately evaluate the ACF dimensions in the craniosynostoses.

7.5.8 Use of Novel Anatomical Landmarks to Analyze ACF Morphometry in the Craniosynostoses

The authors believe that the midline anteroposterior and transverse diameter measurements between fixed anatomical points better represent lengths and widths, respectively. Therefore, anatomical landmarks characteristic of the ACF were chosen accordingly, between which midline anteroposterior and transverse diameters were measured to obtain the true length and width of the ACF, respectively.

All CT scans were analyzed in the axial plane and a set of fixed anatomical landmarks characteristic of the ACF were selected to obtain the maximum anteroposterior and transverse diameters for length and width measurements, respectively. Landmarks were chosen by a plastic surgeon, neurosurgeon, and an anatomist on the basis of being easily identifiable, being able to characterize the morphology of the fossae for optimal measurements to be taken, as well as being reproducible.

The landmarks chosen to measure the length of the ACF in the craniosynostoses provide a more accurate representation of the posterior boundary of the ACF, and as a result, provided more accuracy and reproducibility when the anterior-posterior distance (length) of the ACF was measured. Similarly, to ensure that the maximum transverse distance (width) of the ACF was measured with maximum accuracy and reproducibility, the width of the ACF in this study was measured in the same plane as the length of the ACF.

7.5.8.1 ACF Length and Width in Scaphocephaly

To obtain the length of the ACF, the midpoint of the limbus sphenoidale was identified as a reference landmark and transcended to the level at which the ACF was observed to be at its maximal length. The anteroposterior diameter in the midpoint of the ACF was measured perpendicularly from the transcended point (LS*) to the inner table of the frontal bone (ITF) (Fig. 7.3a and b). The maximum transverse diameter (width) of the ACF was measured as the lateral distance between the points on the inner tables of the frontal bones that were most remote from each other in the ACF (ITF to ITF); at the same level at which the maximum length was obtained (Fig. 7.3a and b) (Bisetty et al. 2022).

7.5.8.2 ACF Length and Width in Trigonocephaly

The midpoint of the limbus sphenoidale was selected as a reference landmark. At the level at which the ACF was observed to be at its maximal length, the maximum anterior-posterior distance

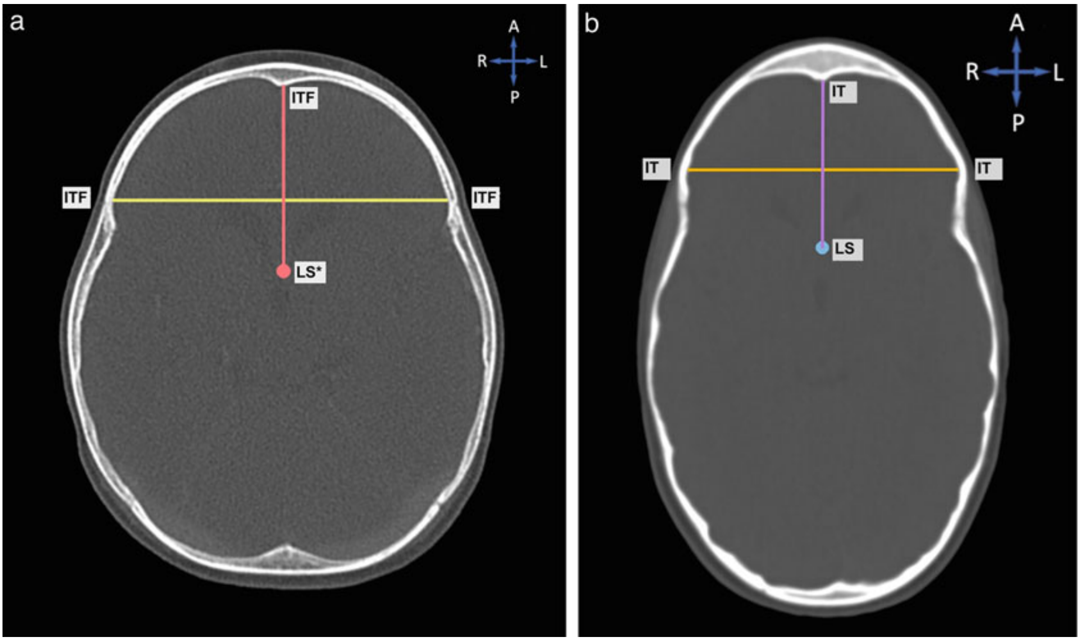

Fig. 7.3 Anterior cranial fossa (ACF) parameters [length = LS* to ITF, width = ITF to ITF] on axial CT scan of (**a**) a non-affected/normal patient (**b**) a patient with scaphocephaly. *Key: LS** Transcended point of midpoint of limbus sphenoidale, *ITF* Inner table of frontal bone

(length) was measured from the referenced landmark (LS*) and perpendicularly extrapolated to the inner table of the frontal bone (ITF) (Fig. 7.4a and b). To obtain the ACF width, the maximum transverse distance was measured between the inner tables of the frontal bones that were observed to display the widest transverse distance, in the same plane that the maximum anterior-posterior distance was measured (Fig. 7.4a and b).

7.5.8.3 ACF Length and Width in AP

Measurements were taken in the axial plane at the level where the inferior extent of the fused coronal suture was first observed to be the most prominent. The posterior margin of the crista galli was used as a reference landmark. This landmark was transcended to the level at which the inferior extent of the fused coronal suture was first observed to be the most prominent. At that level, the width was determined on the contralateral side by constructing a line from the coronal suture to the transcended landmark, whereas on the ipsilateral side, a line was constructed from the inferior extent of the fused coronal suture to the transcended landmark (Fig. 7.5). The midpoints of those two lines created by the width were calculated and the length of the ACF on either side was measured by constructing a perpendicular line from the midpoint to the inner table of the ACF (Fig. 7.5).

It is important to note that for all parameters measured in AP, the difference in the measurements between the ipsilateral and contralateral sides was calculated. This difference was expressed as a percentage of the contralateral side:

$$\begin{aligned}&\%\text{Difference}\\&\quad=[(\text{Ipsilateral}-\text{Contralateral})/(\text{Contralateral})]\times 100\end{aligned}$$

When comparing the ipsilateral to the contralateral side, the increase or decrease in a specific parameter of the ACF on the ipsilateral side are

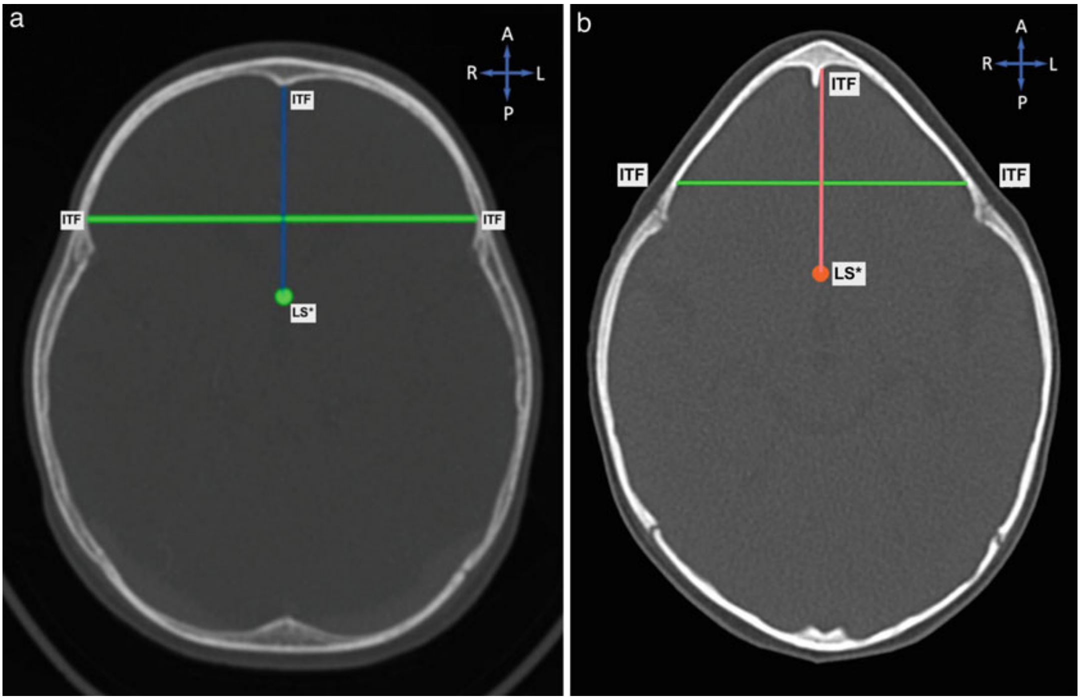

Fig. 7.4 Anterior cranial fossa (ACF) parameters [length = LS* to ITF, width = ITF to ITF] on axial CT scan of (**a**) a non-affected/normal patient (**b**) a patient with trigonocephaly. *Key: LS** Transcended point of midpoint of limbus sphenoidale, *ITF* Inner table of frontal bone

denoted with negative (−) and positive (+) signs, respectively. However, for reporting purposes the (+) sign has not been shown, e.g., +1.5 was reported as 1.5. In some instances, the absolute (i.e., the magnitude of the value irrespective of sign) measurements were considered (Mohan et al. 2022).

7.5.9 Statistical Data Analysis

Statistical data analysis was performed using R Statistical Computing Software of the R Core Team (R Studio, Boston, MA, USA). The results were presented in the form of descriptive statistics. Data were assessed for normality and the

Fig. 7.5 Anterior cranial fossa (ACF) parameters [length = M—ITA, width = CS—*c*] on axial CT scan of a patient with AP—LUCS. *Key: CS* Coronal suture, *FS* Fused coronal suture, *ITA* Inner table of ACF, *M* Midpoint, *c* Transcended point of posterior margin of crista galli

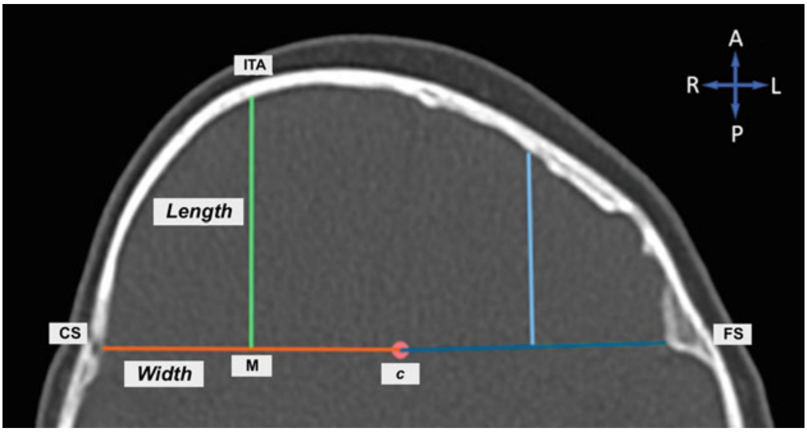

Table 7.1 Maximal anterior cranial fossa (ACF) dimensions in patients with scaphocephaly vs. Control group

Dimensions (mm)	Scaphocephaly($n = 24$) (mean ± SD)	Control ($n = 14$) (mean ± SD)	p-value[a]	% Change[#]
ACF length	60.7 ± 5.17	56.9 ± 5.71	**0.041**	**6.8**
ACF width	94.2 ± 5.76	95.6 ± 8.72	0.568	−1.5

Note: *ACF* Anterior cranial fossa. *SD* Standard deviation

[a] *t*-test

[#] % Change = (mean value of dimension in scaphocephalic patients—mean value of dimension in control group) ÷ (mean value of dimension in control group) × 100

Statistically significant results ($p < 0.05$)

relevant statistical test was performed (t-test or Wilcoxon). A p-value of less than 0.05 was considered statistically significant.

7.6 A New and Improved Approach to ACF Morphometry

7.6.1 ACF Morphometry in Scaphocephaly

The maximal dimensions of the ACF were compared between scaphocephalic and control patients. The mean length of the ACF was significantly larger ($p = 0.041$) in patients with scaphocephaly (60.7 ± 5.17 mm) compared to the control group (56.9 ± 5.71 mm) by 3.8 mm (6.8%). The width of the ACF was generally smaller in scaphocephalic patients; however, this did not reach statistical significance ($p = 0.568$) (Table 7.1). The findings reveal that most of the change occurs along the AP plane, and very little change occurs in the transverse plane. The larger length of the ACF may be attributed to (1) the compensatory anteroposterior expansion of the skull as a result of premature fusion of the sagittal suture and/or (2) the varying degrees of the compensatory anterior deformities associated with scaphocephaly, i.e., bossing of the frontal bone (Bisetty et al. 2022).

7.6.2 ACF Morphometry in Trigonocephaly

The mean length of the ACF was significantly larger ($p = 0.014$) in patients with trigonocephaly (51.86 ± 4.48 mm) compared to control patients (51.76 ± 5.53 mm). The mean width of the ACF was significantly smaller ($p = 0.027$) in patients with trigonocephaly (83.86 ± 7.96 mm) compared to control patients (86.62 ± 10.69) (Table 7.2). This coincides with similar findings observed by Chandler et al. (2021), who reported that the mean length of the ACF was significantly larger ($p = 0.003$) in trigonocephaly patients compared to control patients, and the mean width of the ACF was significantly smaller ($p = <0.001$) in trigonocephaly patients compared to control patients.

The common triangular ridge located over the midline of the forehead, due to the premature fusion of the metopic suture, accounts for the significant increase in the length of the ACF in trigonocephaly patients. Additionally, due to bitemporal narrowing of the skull, the width of the ACF is observed to be significantly smaller in

Table 7.2 Craniometric dimensions of the anterior cranial fossa (ACF) in patients with trigonocephaly vs control group

Dimensions (mm)	Trigonocephaly ($n = 8$) (mean ± SD)	Control ($n = 6$) (mean ± SD)	p-Value[a]
ACF length	51.86 ± 4.48	51.76 ± 5.53	**0.014**
ACF width	83.86 ± 7.96	86.62 ± 10.69	**0.027**

Note: *ACF* Anterior cranial fossa, *SD* Standard deviation

[a] *t*-test

Statistically significant results ($p < 0.05$)

Table 7.3 Means for anterior cranial fossa (ACF) parameters of ipsilateral vs. contralateral sides in patients with AP ($n = 18$)

Dimensions (mm)	Ipsilateral (mean ± SD)	Contralateral (mean ± SD)	p-Value[a]
ACF length	26.6 ± 6.71	33.1 ± 5.36	<0.001
ACF width	42.8 ± 4.87	50.7 ± 5.84	<0.001

Note: *ACF* Anterior cranial fossa, *AP* Anterior plagiocephaly, *SD* Standard Deviation, mm = millimeter
[a] *t*-test (The comparisons were based on the paired test, although the group means were displayed)
Statistically significant results ($p < 0.05$)

trigonocephaly patients. Furthermore, the degree of severity, as well as age, are some of the factors that can influence the dimensions of the ACF, as a result of differences in the occurrence of the prematurely fused metopic suture and the overall growth of the skull, respectively.

7.6.3 ACF Morphometry in AP

The mean ACF width values for the ipsilateral and contralateral sides were 42.8 ± 4.87 mm and 50.7 ± 5.84 mm, respectively; this was statistically significant ($p < 0.001$) (Table 7.3). Although the group means are stated, the comparisons were based on the paired test. The average percentage of the width based on the paired differences was −15.3% ± 7.53% (range: −34.4% to −5.37%) between both sides (Table 7.4). The mean ACF length values for the ipsilateral and contralateral sides were 26.6 ± 6.71 mm and 33.1 ± 5.36 mm, respectively; this was statistically significant ($p < 0.001$) (Table 7.3). The average percentage difference in the length was −20.2% ± 9.91% (range: −39.6% to −1.59%) between the ipsilateral and contralateral sides (Table 7.4). Overall, the ipsilateral side had significantly reduced mean values when compared to the contralateral side for both ACF parameters. The length on the ipsilateral side decreased the most by −20.2 ± 9.91% %, while the width decreased the least by −15.3% ± 7.53% (Table 7.4).

Previous studies reported that the length was significantly reduced on the ipsilateral side when compared to the contralateral side (Captier et al. 2003; Calandrelli et al. 2016, 2018). This study observed a similar pattern and revealed a statistically significant difference, with an average difference of −20.2% between the ipsilateral and contralateral sides (Table 7.4). The width of the ACF was found to be significantly narrower on the ipsilateral side when compared to the contralateral side, with an average difference of −15.3% (Table 7.4). The findings revealed that the ACF was asymmetric, with reduced growth on the ipsilateral side. Furthermore, the findings indicated that the length of the ACF was the most asymmetrical because it decreased the most, while the width of the ACF was the least asymmetrical because it decreased the least (Table 7.4). Since growth perpendicular to the suture is inhibited, these results could be attributed to the ipsilateral flattening of the frontal bone, including the supraorbital rim. As a result of these anatomical differences, the ACF length

Table 7.4 Overall mean percentage differences for anterior cranial fossa (ACF) parameters in patients with AP ($n = 18$)

Dimensions (mm)	% diff. = ipsilateral-contralateral (mean ± SD)	(%) Range	p-Value[a]
ACF length	−20.2 ± 9.91	−39.6 to −1.59	**<0.001**
ACF width	−15.3 ± 7.53	−34.4 to −5.37	**<0.001**

Note: *ACF* Anterior cranial fossa, *AP* Anterior plagiocephaly, *SD* Standard Deviation
% diff. = Percentage difference
[a] *t*-test
Statistically significant results ($p < 0.05$)

and width are affected, resulting in a much shorter and narrower ACF on the ipsilateral side (Mohan et al. 2022).

7.7 Limitations

A limitation of this study includes the relatively small sample size in all of the patient groups as well as the control group. Another limitation is the lack of age-, sex-, and population-matched control group. These limitations hampered possible detailed statistical analyses. The limited sample size of the patient groups are mainly due to the rarity of these conditions and the fact that the data was collected from a single craniofacial center. The restricted sample size of the control group is attributed to the fact that CT scans are not routinely performed in pediatric patients due to the radiation involved; therefore, obtaining CT material in this regard was a challenge.

7.8 Recommendations

Further studies with a larger sample size are recommended by (1) broadening the time frame for retrospective analysis, (2) including CT scans of patients with craniosynostosis from other craniofacial centers in the country (this will also provide a more inclusive representation of a South African craniosynostotic population as the present study provides data based only on a single unit), and (3) including normal-patient reference CT material from other institutions to expand the control database. Additionally, this study can be used as a reference for future research by comparing preoperative and postoperative data to monitor surgical outcomes and assess the improvement of the deformity. Long-term follow-up of these patients and a larger sample size would provide more information on craniofacial changes with age and growth, as well as the need for any surgical revision in adulthood.

7.9 Conclusion

This chapter presents novel morphometrical data based on a South African population. It employs the use of 3D-CT modalities to provide insight into the changes that occur within the ACF in patients with scaphocephaly, trigonocephaly, and AP. To date, CT imaging is considered the gold standard for the diagnosis of craniosynostosis and is known to have yielded the most reliable and reproducible measurements of complex craniofacial anomalies. 3D reconstructed CT scans provided the clearest identification of all the hallmark characteristics allowing the anterior cranial deformities in the craniosynostoses to be adequately investigated. The morphometric dimensions obtained from this study may be beneficial to craniofacial surgeons during corrective surgery by indicating the degree of the severity of the deformity, making it easier to plan the techniques as well as determine the extent of surgical correction required.

Overall, this chapter endeavored to bridge a gap in the literature by providing an anatomical basis of the anterior cranial deformities in these rare congenital conditions using 3D-CT scans. This chapter adds to the existing body of knowledge on craniosynostosis by providing previously unrecorded morphometrical data within a select South African population.

References

Anderson BW, Kortz MW, Black AC, Kharazi KAA (2019) Anatomy, head and Neck. Skull, StatPearls. Available at: https://www.ncbi.nlm.nih.gov/books/NBK499834/. Accessed: January 19, 2023

Baş NS, Baş S (2021) Craniometric measurements and surgical outcomes in Trigonocephaly patients who underwent surgical treatment. Cureus J Med Sci 13(3):e13676. https://doi.org/10.7759/cureus.13676

Bisetty V, Lazarus L, Harrichandparsad R, Madaree A (2022) Morphometric analysis of the cranial fossae in scaphocephalic patients: an anatomical basis. J Craniofac Surg 33(5):1375–1380. https://doi.org/10.1097/scs.0000000000008552

Calandrelli R, D'Apolito G, Massimi L, Gaudino S, Visconti E, Pelo S, Di Rocco C, Colosimo C (2016) Quantitative analysis of craniofacial dysmorphology in infants with anterior synostotic plagiocephaly. Childs Nerv Syst 32(12):2339–2349. https://doi.org/10.1007/s00381-016-3218-8

Calandrelli R, Pilato F, Massimi L, Panfili M, Colosimo C (2020) A systematic quantitative morpho-volumetric analysis in infants with sagittal craniosynostosis and relationship with the severity of scaphocephalic deformity. Radiol Med 125(6):585–594. https://doi.org/10.1007/s11547-020-01150-w

Calandrelli R, Pilato F, Massimi L, Panfili M, Di Rocco C, Colosimo C (2018) Quantitative analysis of cranial-orbital changes in infants with anterior synostotic plagiocephaly. Childs Nerv Syst 34(9):1725–1733. https://doi.org/10.1007/s00381-018-3824-8

Calandrelli R, Pilato F, Massimi L, Panfili M, Di Rocco C, Colosimo C (2019) The unseen third dimension: a novel approach for assessing head shape severity in infants with isolated sagittal synostosis. Childs Nerv Syst 35(8):1351–1356. https://doi.org/10.1007/s00381-019-04246-5

Captier G, Leboucq N, Bigorre M, Canovas F, Bonnel F, Bonnafé A, Montoya P (2003) Plagiocephaly: morphometry of skull base asymmetry. Surg Radiol Anat 25(3–4):226–233. https://doi.org/10.1007/s00276-003-0118-x

Chandler L, Park KE, Allam O, Mozaffari MA, Khetpal S, Smetona J, Pourtaheri N, Lu X, Persing JA, Alperovich M (2021) Distinguishing craniomorphometric characteristics and severity in metopic synostosis patients. Int J Oral Maxillofac Surg 50:1040–1046. https://doi.org/10.1016/j.ijom.2020.11.022

Ciurea A, Toader C, Mihalache C (2011) Actual concepts in scaphocephaly (an experience of 98 cases). J Med Life 4(4):224–431

David L, Glazier S, Pyle J, Thompson J, Argenta L (2009) Classification system for sagittal Craniosynostosis. J Craniofac Surg 20(2):279–282. https://doi.org/10.1097/SCS.0b013e3181945ab0

Di Rocco C, Paternoster G, Caldarelli M, Massimi L, Tamburrini G (2012) Anterior plagiocephaly: epidemiology, clinical findings, diagnosis, and classification. A review. Child's Nerv Sys 28(9):1413–1422. https://doi.org/10.1007/s00381-012-1845-2

Dias M, Samson T, Rizk E, Governale L, Richtsmeier J (2020) Identifying the misshapen head: Craniosynostosis and related disorders. Pediatrics 146(3). https://doi.org/10.1542/peds.2020-015511

Dvoracek L, Bykowski M, Foglio A, Ayyash A, Pfaff M, Losee J, Goldstein J (2021) Objective analysis of Fronto-orbital Dysmorphology in unilateral coronal Craniosynostosis. J Craniofac Surg 32(7):2266–2272. https://doi.org/10.1097/SCS.0000000000007748

Ghizoni E, Denadai R, Raposo-Amaral C, Joaquim A, Tedeschi H, Raposo-Amaral C (2016) Diagnosis of infant synostotic and nonsynostotic cranial deformities: a review for pediatricians. Revista Paulista de Pediatria (English Edition) 34(4):495–502. https://doi.org/10.1016/j.rpped.2016.01.004

Gray H, Standring S (2016) Gray's anatomy: The anatomical basis of clinical practice, 41st edn. Elsevier, Amsterdam

Grover VP, Tognarelli JM, Crossey MM, Cox IJ, Taylor-Robinson SD, McPhail MJ (2015) Magnetic resonance imaging: principles and techniques: lessons for clinicians. J Clin Exp Hepatol 5(3):246–255. https://doi.org/10.1016/j.jceh.2015.08.001

Heuzé Y, Martínez-Abadías N, Stella J, Senders C, Boyadjiev S, Lo L, Richtsmeier J (2012) Unilateral and bilateral expression of a quantitative trait: asymmetry and symmetry in coronal craniosynostosis. J Exp Zool B Mol Dev Evol 318(2):109–122. https://doi.org/10.1002/jezb.21449

Jane J, Lin K, Jane J (2000) Sagittal synostosis. Neurosurg Focus 9(3):1–6. https://doi.org/10.3171/foc.2000.9.3.4

Jin SW, Sim KB, Kim SD (2016) Development and growth of the normal cranial vault: an embryologic review. J Korean Neurosurg Soc 59(3):192–196. https://doi.org/10.3340/jkns.2016.59.3.192

Johnson D, Wilkie A (2011) Craniosynostosis. Eur J Hum Genet 19(4):369–376. https://doi.org/10.1038/ejhg.2010.235

Kajdic N, Spazzapan P, Velnar T (2017) Craniosynostosis–recognition, clinical characteristics, and treatment. Bosn J Basic Med Sci 18(2):110–116. https://doi.org/10.17305/bjbms.2017.2083

Kim HJ, Roh HG, Lee IW (2016) Craniosynostosis: Updates in Radiologic Diagnosis. J Korean Neurosurg Soc 59(3):219–226. https://doi.org/10.3340/jkns.2016.59.3.219

Kronig S, Kronig O, Vrooman H, Veenland J, Van Adrichem L (2020) Quantification of severity of unilateral coronal synostosis. Cleft Palate Craniofac J 58(7):832–837. https://doi.org/10.1177/1055665620965099

Kronig S, Kronig O, Zurek M, Van Adrichem L (2021) Orbital volume, ophthalmic sequelae and severity in unilateral coronal synostosis. Childs Nerv Syst 37(5):1687–1694. https://doi.org/10.1007/s00381-021-05065-3

Marsh J, Gado M, Vannier M, Stevens W (1986) Osseous anatomy of unilateral coronal synostosis. Cleft Palate J 23:87–100. https://doi.org/10.1007/978-3-642-82875-1_21

Massimi L, Caldarelli M, Tamburrini G, Paternoster G, Di Rocco C (2012) Isolated sagittal craniosynostosis: definition, classification, and surgical indications. Childs Nerv Syst 28(9):1311–1317. https://doi.org/10.1007/s00381-012-1834-5

Moderie C, Govshievich A, Papay F, Fearon J, Gosain A, Doumit G (2019) Current trends in Management of non-syndromic Unilateral Coronal Craniosynostosis: a cross-sectional survey. Plast Reconstr Surg Glob Open 7(5):e2229. https://doi.org/10.1097/GOX.0000000000002229

Mohan N, Lazarus L, Harrichandparsad R, Madaree A (2022) Anterior Synostotic Plagiocephaly: a quantitative analysis of craniofacial features using computed tomography. J Craniofac Surg 33(8):2339–2349. https://doi.org/10.1097/SCS.0000000000008746

Murphy A, Er A, Bell D, Sharma R (2022) Skull radiography: radiology reference article, Radiopaedia Blog RSS. Radiopaedia.org. Available at: https://radiopaedia.org/articles/skull-radiography. Accessed January 19, 2023

Nagaraja S, Anslow P, Winter B (2013) Craniosynostosis. Clin Radiol 68(3):284–292. https://doi.org/10.1016/j.crad.2012.07.005

Oh A, Wong J, Ohta E, Rogers G, Deutsch C, Mulliken J (2008) Facial asymmetry in unilateral coronal synostosis: long-term results after Fronto-orbital advancement. Plast Reconstr Surg 121(2):545–562. https://doi.org/10.1097/01.prs.0000297639.48289.9e

Otake S, Taoka T, Maeda M, Yuh WTC (2018) A guide to identification and selection of axial planes in magnetic resonance imaging of the brain. Neuroradiol J 31(4):336–344. https://doi.org/10.1177/1971400918769911

Patel PR, De Jesus O (2022) CT scan. StatPearls. Available at: https://www.ncbi.nlm.nih.gov/books/NBK567796/. Accessed January 19, 2023

Podda S, Ciminello FS, Wolfe SA (2022) Congenital synostoses, overview, embryology and development, pathogenesis. Medscape Available at: https://emedicine.medscape.com/article/1280365-overview#a5. Accessed December 29, 2022

Proisya M, Bruneau B, Riffaud L (2019) How ultrasonography can contribute to diagnosis of craniosynostosis. Neurochirurgie 65(5):228–231. https://doi.org/10.1016/j.neuchi.2019.09.019

Raposo-do-Amaral C, Silva M, Menon D, Somensi R, Raposo-do-Amaral C, Buzzo C (2011) Anthropometric study of craniofacial asymmetry in unilateral coronal Craniosynostosis. Brazilian J Plast Surg 26(1):27–31. https://doi.org/10.1590/S1983-51752011000100007

Ruiz-Correa S, Sze R, Starr J, Lin H, Speltz M, Cunningham M, Hing A (2006) New Scaphocephaly severity indices of sagittal Craniosynostosis: a comparative study with cranial index quantifications. Cleft Palate Craniofac J 43(2):211–221. https://doi.org/10.1597/04-208.1

Seeberger R, Hoffmann J, Freudlsperger C, Berger M, Bodem J, Horn D, Engel M (2016) Intracranial volume (ICV) in isolated sagittal craniosynostosis measured by 3D photocephalometry: a new perspective on a controversial issue. J Cranio-Maxillofac Surg 44(5):626–631. https://doi.org/10.1016/j.jcms.2016.01.023

Som PM, Curtin HD (2011) Head and Neck Imaging, 5th edn. Elsevier, Canada

Spazzapan P, Bošnjak R, Velnar T, Cassisi A (2017) Anterior Plagiocephaly–a report of a case and operative technique. Slovenian Med J 86:1–2. https://doi.org/10.6016/ZdravVestn.1768

Tatum S, Jones L, Cho M, Sandu R (2012) Differential management of scaphocephaly. Laryngoscope 122(2):246–253. https://doi.org/10.1002/lary.22463

Van der Meulen J (2012) Metopic synostosis. Child's Nervous System 28(9):1359–1367. https://doi.org/10.1007/s00381-012-1803-z

Van Veelen-Vincent M, Mathijssen I, Arnaud E, Renier D, Di Rocco F (2010) Craniosynostosis. Neurosurgery:501–528. https://doi.org/10.1007/978-3-540-79565-0_29

Wang JY, Dorafshar AH, Liu A, Groves ML, Ahu ES (2016) The metopic index: an anthropometric index for the quantitative assessment of trigonocephaly from metopic. Journal of Neurosurgery Pediatrics 18(3):275–280. https://doi.org/10.3171/2016.2.PEDS15524

Part II

Anatomical and Cell Biology Education

The Use of Biomedical Imaging in Visuospatial Teaching of Anatomy

8

Sashrika Pillay-Addinall, Nhlanhla L. Japhta,
and Sabashnee Govender-Davies

Abstract

Anatomy is the cornerstone of medicine, and a clear understanding of human anatomy relies in part on the visuospatial understanding of different parts of the body and the way they relate to each other. The ability to visualise structures in multiple planes and to further translate 2D information into 3D domains is vital for student learning and clinical practice. Dissection continues to be an important tool for the visualisation of anatomical structures within the body. However, the availability of cadavers in many countries is increasingly challenged by restrictive laws which limit their acquisition. Biomedical imaging modalities are fast becoming an alternative to traditional cadaver-based learning and as a student-centred teaching aid. Imaging modalities such as the Anatomage virtual dissector, 3D printing, MacroView imaging and ultrasound all have the ability to bridge the visuospatial gap in teaching and learning, and have a positive impact on student performance.

The incorporation of three-dimensional-printed models in the standard anatomy PowerPoint lecture and cadaver-side teaching dramatically shortens the amount of time students take to spatially orientate and keep up with the teaching session. Anatomage provides an interactive visuospatial alternative to standard dissection with no cadaver preservation fumes and cadaver availability challenges. Anatomage three-dimensional capabilities allow for integrated curricular development in a vertical alignment (first year—final year).. Ultrasound provides students with real-time visualisation of structures and spatial orientation within the volume of the anatomy. Live ultrasound scanning takes learning from a static pedagogical medium in a dynamic direction, aligning with vertical integration and preparing students for future clinical scenarios. MacroView imaging is effective in multi-angle imaging achieved through real-time specimen repositioning on the image capturing platform. It enables focus on specific areas of interest with real-time annotations and the availability of high-quality images for student's self-study and revision sessions.

Biomedical imaging modalities enhance visuospatial understanding of human anatomy, improving student knowledge and performance in assessments. A pilot study on a select group of students revealed student enthusiasm towards a multi-imaging modalities approach rather than the conventional anatomy teaching method, and demonstrated improved

---

S. Pillay-Addinall · N. L. Japhta ·
S. Govender-Davies (✉)
Department of Anatomy and Histology, School of Medicine, Sefako Makgatho Health Sciences University, Ga-Rankuwa, South Africa
e-mail: Sabashnee.govender@smu.ac.za

© The Author(s), under exclusive license to Springer Nature Switzerland AG 2023

L. Shapiro (ed.), *Microscopy Techniques for Biomedical Education and Healthcare Practice*, Biomedical Visualization 2, https://doi.org/10.1007/978-3-031-36850-9_8

performance in assessments compared with a conventional teaching control group.

Keywords

Imaging modalities · Visuospatial · Biomedical imaging · Anatomy · Teaching

8.1 Introduction

Anatomy has been the foundation of medical disciplines for centuries. A thorough knowledge of human anatomy relies on the visuospatial understanding of body structures. The ability to visualise structures in multiple planes as well as to translate two dimension (2D) information into three dimension (3D) domains is vital. Hence, the primary modality employed for centuries has been the dissection of the human body. As early as the third century BC, anatomists carried out dissections on the human body to further their knowledge. It was only in the late thirteenth and fourteenth centuries that anatomy was starting to gain acceptance as science and cadavers were introduced as teaching material (Malomo et al. 2006). This revolutionised the course of medical and scientific practice, as well as forming the framework that we rely on at present. With further advancements in technology, microscopic anatomy became a new imaging modality of specialisation. As expected, anatomy is inherently visual. Conventional, in-class lecturing aims to translate theoretical anatomical information into a 3D picture in the mind of a student. Unfortunately, it remains a challenge for many students, especially first-year candidates.

Dissection continues to be an important tool for the visualisation of anatomical structures within the body and body donations are the primary source of cadaveric material. Many countries have strict laws surrounding the acquisition of ‘corpses’ for use as cadavers (Santana et al. 2022) and this has led to a dwindling supply of cadavers. There are religious beliefs and cultural practices, as well as bioethical debates, that surround the use of deceased individuals for research and teaching purposes (Santana et al. 2022) has further limited the supply of cadavers for dissection. Throughout history, dissection was met had many negative connotations attached to it. During the seventeenth and eighteenth centuries, there was a general perception that undergoing a dissection was a matter of great dishonour for the individual, as the cadaver would be rendered distorted and denied a proper burial. Executed criminals were then legislated to be a legal course of cadaver acquisition. The increase in demand for cadavers and the slow supply, lead to the mandate for use of unclaimed bodies. This spurred unethical practices such as grave robbing, body snatching, and even murder (Ghosh 2015). These practises have been curtailed over the years, however, many still consider it unethical, owing to the belief that the body is disrespected or mutilated during the act of dissecting. In many regions, especially those in Asia and Africa, there are a series of religious rights that are required for the deceased’s soul to reach the afterlife peacefully. After one has passed there is usually a time frame in which these rights are to be carried out. In many religions, it is therefore deemed unacceptable to have one’s body dissected. In South Africa, a study conducted by Gama and Satyapal assessed the attitudes of undergraduate students towards body donation. They found that out of the total number of students surveyed, 68.7% were unwilling to donate their bodies. Twenty-eight percent of these students stated religious beliefs to be the deciding factor. These barriers make acquiring cadavers difficult and therefore making physical dissections more challenging.

Biomedical imaging modalities have the ability to bridge the visuospatial gap in teaching and learning, as well as mitigate the lack of cadavers. This can be achieved by using the potential of technology to explore tailored anatomical teaching. Conventional lecturing aims to translate theoretical anatomical information into a 3D image, in the mind of a student. Unfortunately, this remains a challenge for many students, especially first-year candidates.

Studies focusing on anatomy in biomedical education revealed anatomy ‘experts’ have higher spatial visualisation skills than their colleagues within their field (Ivanusic et al. 2010). Additionally, students exposed to visual-spatial activities during teaching and learning tend to have a better understanding of the anatomical region (Carter et al. 2016). Hence, it is vital that new avenues be explored to enhance the teaching and learning experience. This can be achieved by using the potential of technology to explore tailored anatomical teaching. Historically, visual representations have aided in the teaching of anatomy for decades. Previous research findings from educational neuroscience and cognitive psychology studies support the idea that the process of drawing is valuable for learning and the enhancement of student engagement through interactivity and innovation (Friedlander et al. 2011; Tyler and Likova 2012). Additionally, by incorporating the visual arts into anatomy teaching and learning, deep neural integrative pathways can be activated, further suggesting that artistic engagement could increase cognitive functions linked to the development of motor skills (Tyler and Likova 2012).

As such, this pilot study aims to explore the use of multimodal biomedical visualising technology in traditional anatomical teaching. The general trend in traditional anatomical teaching is your basic lecture. In the current age, these are usually administered via a PowerPoint presentation. By introducing multimodal biomedical imaging systems such as 3D printed structures, ultrasound imaging and digital dissection tables, within the lecture, students gain a better understanding of the structures before entering a dissection hall furthermore, we would like to assess students' perceptions, attitudes and knowledge retention when incorporating biomedical equipment into teaching and learning. As this would be a different style of lecturing from what they are usually accustomed to, assessing whether they find the imaging modalities useful and whether it aids in understanding and translation of the content is a secondary aim.

Visuospatial awareness is the key to mastering the study of anatomy. Spatial ability has been defined as the ability to create, retain, rotate and organise structured visual shapes to sustain our daily lives (Aydın et al. 2020). Spatial ability plays a role in the comprehension of complex anatomical structures and their distribution in space. This further helps clinicians and physicians to correlate findings from physical examinations with anatomical knowledge in order to determine if the underlying structures are within normal limits (Gonzales 2019). Various studies conducted emphasise the positive correlation that exists between visuospatial abilities and the understanding of educational anatomy (Lufler et al. 2012; Luursema et al. 2017; Gonzales 2019; Aydın et al. 2020; Roach et al. 2021). Study results revealed improvement in both practical and theoretical components (Lufler et al. 2012). Furthermore, students with higher spatial abilities were reported to be more successful in their clinical practice, making fewer mistakes during allocated tasks (Gonzales 2019; Aydın et al. 2020).

In a study conducted by Aydin and colleagues, the authors concluded their study by stating that the use of multisensory tools such as visual and haptic observations lead to an enhanced holistic understanding of the 3D spatial anatomy (Aydın et al. 2020). This is an ultimate goal when incorporating biomedical imaging in the teaching of anatomy.

8.2 History of Traditional Anatomical Teaching Techniques

Anatomy, in its most fundamental form, is a science that constitutes the study of the development, composition and structure of the human body and other species (Queiroz 2005; Malomo et al. 2006; Santana et al. 2022). The study of anatomy dates back to the early third century BC. Ancient Greece was amongst the first to pioneer advancements in medical practice through dissections of pigs and monkeys with Claudius Galen at the forefront. Although the translation between animal dissections to human structures and the subsequent theories he formed were not entirely accurate, the knowledge that he generated still dominated and continued to influence much of the third century through to the Renaissance.

With the rise of the Renaissance, the advancement of human learning was achieved. Ideas and technological advancements reached new heights, with the free availability of teaching materials such as books (Calkins et al. 1999). Public dissections by Mondino de Liuzzi, were performed and the first dissection manual was established (Santana et al. 2022). Leonardo da Vinci broke further barriers with his pictorial works that contributed scientific progression in our understanding of the inner workings of the human body. His most notable artwork is the Vitruvian Man, which depicts groups of nerves, muscles, bone and vessels in, what later was termed the 'anatomical position' (Santana et al. 2022).

The pursuit of anatomical knowledge continued and from early 1500 modern anatomy was born, with the introduction of further and more precise illustrations of the human body and together with the dynamic teaching methods developed and refined by Andreas Vesalius, the figure of the cadaver lost much of its superstitious and religious affiliations. Teaching and learning continued to pave the way and inform the more advanced medical professionals.

Conventionally, the most universally employed teaching method was and often still is that of the 'chalk and board' which is used to convey information to future physicians. Whilst the lecture is being performed, pertinent sentences and key terms are noted down on the chalkboard together with illustrations of the body structures for a more holistic view of the topic being taught (Benly 2014). We have since moved on to PowerPoint presentations that can easily portray three-dimensional, animated images. However, illustrations on a chalkboard are still important tools for displaying the structural components of different parts. Thereafter students would be seated around anatomical tables in a dissection hall with direct exposure to the anatomical structures. The lecturer would demonstrate the cadaveric structures and introduce the class to the dissection method (Sugand et al. 2010). Dissection reinforced 3D visualisation of structures and helped students to orientate these structures within the body volume. Hence, dissection formed a key and important aspect of anatomical teaching (Iwanaga et al. 2021).

Dissection remains the single most traditional anatomical teaching method and to date is still employed in most tertiary institutions (Sugand et al. 2010; Zhang et al. 2019). From a surgical perspective, dissection is an invaluable method in the education of future clinicians. Medical students are able to hone their tissue manipulation skills, as well as improve their manual dexterity, teamwork and professional communication. They are exposed to the emotional implications of death and are able to develop ways to handle the impact thereof. During dissections, students are also exposed to different anatomical variations that are generally absent in other teaching modalities (Reindenberg and laitman 2002). A further benefit of this modality is the presence of connective tissues. Most prosected or pre-dissected specimens have the connective tissue removed or partially absent (Iwanaga et al. 2021). This is not a true representation of the structures and how they are found in vivo, especially in a theatre setting (Arráez-Aybar et al. 2008). Therefore, during dissections, students can observe the blended, non-discreet connective tissue layers as they follow the dissection process. With all the benefits dissection brings, it is still an inadequate modality *when considered as a singular teaching modality*. Demonstrations of functional neuroanatomy and neurovascular elements are largely deficient in cadaveric samples. Additionally, the acquisition of cadaveric material remains a challenge in many countries, making dissection a potentially difficult mode of teaching. To date, this remains a barrier in many countries (Simão et al. 2016).

Many countries rely on body donations in order to obtain cadavers, but there are still many bioethical and religious, as mentioned previously, issues involved when dealing with a deceased individual. This hinders the collection of corpses significantly (Simão et al. 2016). Owing to this obstacle and the increasing number of medical students, cadavers have become limited to specific medical groups and larger groups of students are allocated to a single cadaver. This is not the optimal teaching environment and many students fall behind or lose interest in this vital exercise and experience.

In order to alleviate and bring some resolution to this situation, models and plastinated specimens became a useful complement to didactic lectures and dissection. These tools allow for the visualisation of structures that are otherwise difficult to access in cadavers. Furthermore, synthetic models can be enlarged to better portray the structures at hand, making it easier to observe these structures that may sometimes be invisible to the naked eye (Benly 2014). Plastinated specimens involve replacing the organic tissue such as blood, fluid and fat in a fresh prosected specimen, thus, preserving the region and structures therein perfectly, and allowing for better observation. The amalgamation of these teaching tools into the curriculum provides institutions with a viable supplement to conventional dissections and lectures.

8.3 Modernisation of Anatomical Teaching

Technology has revolutionised many industries and anatomical education is no exception. As mentioned previously, dissection forms the fundamental baseline for the effective teaching of anatomy. Although instrumental, the ever-increasing cost of embalming and bioethical considerations form some of the most pertinent issues. Technology has provided many different avenues for development and students are no longer limited to sometimes outdated textbooks and crowded dissection halls. A wide range of online resources as well as 3D visualisation tools now exists to diversify and broaden the pool of visual and textual information and make it available to everyone.

The introduction of multimodal teaching methods has caused some controversy in the medical community, as it often comes at the expense of traditionalist teaching methods such as dissection. Some educators strongly disagree with the advancements whilst others welcome them (Older 2004; Slotnick and Hilton 2006). The replacement of traditional cadaveric dissection with modern teaching technologies, such as 3D software was not embraced wholly by all educators. There is a belief that teaching and learning anatomy is inseparable from cadaveric dissection. The cadaver hall provides students with more than just a tactile and spatial appreciation and understanding of the layers and composition of the human body. It also plays an intricate role in moulding the students' emotional response to death. Furthermore, Cadaveric dissections were implemented out of programme for courses that could not accommodate it, in order to improve the deficiencies in physical examination skills, surgical procedures and general anatomical knowledge. Therefore, many educators deem it vital for a tougher grasp of anatomical concepts. Nevertheless, multimodal teaching methods such as problem-based learning, computer-based learning and 3D software are fast gaining traction. Problem or clinical-based learning presents an out-of-the-box way of delivering anatomical information. It ties together theoretical and practical knowledge and allows students to apply it to real-time situations. Student-centred problem-solving techniques are employed which stimulate teamwork, communication and conceptualisation over the rote memorisation of facts (Sugand et al. 2010).

Computer-based learning has revolutionised the concept of basic anatomical teaching. Computerised learning packages help students to prepare section topics beforehand, giving them a precis of what to expect (Collins 2008). This is particularly useful in non-surgical disciplines, where dissection time is limited or not implemented within the curriculum. The incorporation of 3D interactive software, such as 3D atlases, transforms a conventional lecture into an interactive session. The importance of computer-based learning cannot be understated, as evidenced during the SARS-CoV-2 pandemic. With little to no access to dissection halls and lecture theatres, the world turned to electronic-based communication. Many studies have shown that students show an increased interest in technologies such as virtual and augmented reality, thus making the teaching experience more enjoyable and memorable (Estai and Bunt 2016). Anatomy as a whole is an inherently visual subject and therefore can be better understood with effective visual aids.

Students who had access to online visual aids scored significantly higher in examinations than those who did not (Sugand et al. 2010). This reinforces the importance of diversifying and embracing the adoption of a multimodal teaching and learning environment. Conversely, students exposed primarily to online activities showed no significant increase in performance when compared to their previous year's counterparts (Attardi et al. 2018; Iwanaga et al. 2021).

Emerging technologies such as imaging software and computer-based learning are slowly phasing out cadaveric activities (Estai and Bunt 2016). With all the controversial and conflicting viewpoints when considering anatomical education, the most effective approach seems now to be blended learning. Merging both traditional and technological methods yields a more holistic approach (Dahle et al. 2002). This hybrid model allows educators to select methods based on their purpose rather than the method's inherent abilities, therefore tailoring the teaching approach to fit the discipline in question and better equipping students with multifaceted skills rather than a single-modal technique.

Didactic lectures and models are also considered to be the traditional way of delivering anatomical teachings. Although these modalities have evolved and progressed over the years, they are still considered outdated (Hu et al. 2017).

8.4 The Benefits of Incorporating Biomedical Technology in Teaching Anatomy

Among the various imaging modalities available, modalities used in a clinical setting can be incorporated into the teaching of anatomy. By introducing imaging technologies into the teaching and learning procedure educators can utilise a vast quantity of visual aids to improve the learning process by making it more interactive and engaging, while activating long-term memory retention (Dev 1999). Imaging modalities have the ability to further provide surplus information which includes measuring physical parameters related to the anatomical structures in the body and analysing metabolic processes, or functional performance of the tissue systems. Additionally, by incorporating these methods as a supplement to traditional teaching methods students are able to (i) translate 2D information into 3D structures, (ii) understand in vivo relationships and (iii) obtain an understanding and visuospatial awareness of structures and interrelationships (Schramek et al. 2013). 3D imaging technologies with haptic stimuli enhance the learning process by allowing the navigation of applications via a touchscreen interface which is intuitive and mimics the usability of smart devices. In this way, it allows the user to focus on the anatomy rather than the functionality of the device (Allen et al. 2019). Moreover, it further transforms complex static anatomical relationships into comprehensible dynamic affiliations (Alfalah et al. 2019). Additionally, with the advancements in technology, there is a call to create a stronger link between basic science education and its eventual role in the clinical setting. By doing this, the transition from a pre-clinical environment to a future clinical setting will be easier amongst students (Jurjus et al. 2014), further reinforcing the vertical curriculum alignment.

8.5 Three-Dimensional Printing

Tertiary institutions use the full potential of the three-dimensional printing (3Dp) technology to help bridge the spatial challenge and improve the understanding of human anatomy. For many years and continuing today, students suffered the drawback of a lack of depth perception and spatial orientation in the 2D images in the textbooks and atlases whilst studying outside of the dissection hall (Sakas 2002; Patankar and Padasalagi 2017). Despite 3Dp models lacking the feel and look of cadaveric tissue (Yuen 2020), they provide adequate alternative solutions when there is limited or no availability of models and prosected specimens to demonstrate the structures and anatomical concepts which are challenging to comprehend using 2D images in textbooks and atlases, magnetic resonance imaging (MRI) and computer tomography (CT) prints. To date, the incorporation of 3Dp in conventional teaching has been shown to significantly improve anatomy knowledge and student performance in assessment. Students struggling with visual thinking considerably improve test scores after exposure to 3D models (Salewski et al. 2022). In applied clinical anatomy, 3D models would help the student understand how the integrity of the bone is affected by chronic diabetes by comparing the normal and diabetic 3D trabecular architecture.

8.5.1 Three-Dimensional Modelling Software

Timeous preparation is essential when incorporating 3Dp models in routine lectures and practical sessions. Depending on the size and complexity of the part of the human body or organ, printing may take well over 24 h to complete. Duplicating one model for a bigger group session would require even more time for the 3Dp to be ready for the planned session. It would be ideal for an institution to invest in a 3D scanner to enable the capture and creation of a museum of rare anomalies and abnormalities in the human body, and as a library for the incorporation of 3Dp models in routine lectures and practical sessions. As a cost-effective alternative, 3D images of various parts of the human body and related clinical conditions are readily available on the Internet, and in formats compatible with different types of 3Dp printers. In this regard, the *MakerBot Replicator Z18* (MakerBot Industries, Brooklyn, NY, USA) (Fig. 8.1) is compatible with the standard triangle language and geometry definition file formats which are developed from computer-aided design software. Several other 3D image file formats such as STEP, 3MF and SCAD are compatible with 3D printers and are available from various 3D platforms, as well as complex file formats that require advanced graphic designer skills. *MakerBot Desktop* software, freely available and downloadable from makerbot websites, is user friendly even to non-3Dp professionals.

The *MakerBot Desktop* software enables the manipulation of the image into the desired size before 3Dp, with 3Dp support structures such as pillars and bridges (Fig. 8.2). Guided by available budgets, several printing materials such as nylon, polylite, tough, polymax PC and ABS-R durabio may be used as alternatives to the polylactic acid filament. Different colour polylactic acid filaments may be used to highlight specific structures or areas of the 3Dp.

8.5.1.1 Incorporation of 3Dp in a Lecture Series

The inclusion of 3Dp models in the standard anatomy PowerPoint lecture and cadaver-side teaching variably shortens the amount of time students take to spatially orientate and keep up with the session. In the preparation of the lecture, a pre-selected organ may be a 3D scanned or 3D image sourced from the Internet. For example, a 3Dp kidney may be printed two or three times its normal size for ease of demonstration. Each structural component may be printed individually, such as the renal pelvis, renal artery and vein and cortex (Fig. 8.3). This enables the students, in the session and during revision time, to assemble the printed parts anatomically corrected for the normal kidney and in the process enhance their understanding of the topography and functional relation of the structures passing through the renal hilum. A kidney with an anomaly or abnormality of interest may be 3Dp to bridge the spatial orientation gap from the 2D images. When the lecture or practical facility is fitted with multiple monitors, MacroView may provide the real-time view of the prosected specimen or cadaver with kidney of interest, in situ on one of the monitors. MacroView is a windows based system with streaming capabilities for the benefit of groups of students in multiple venues and on or off-campus (online) students. This coupling of modalities provides students with tactile input from a 3Dp model (Yuen 2020), enabling them

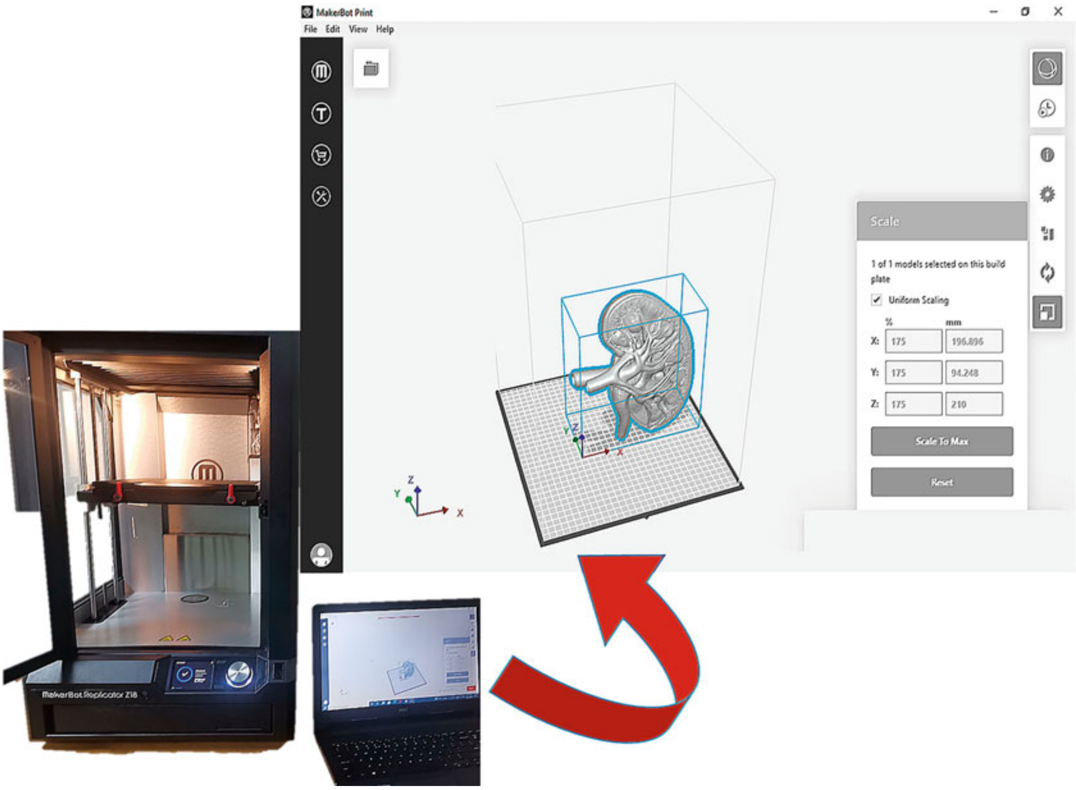

Scale

1 of 1 models selected on this build plate

☑ Uniform Scaling

	%	mm
X:	175	196.896
Y:	175	94.248
Z:	175	210

Fig. 8.1 MakerBot Replicator Z18 3D printer and MakerBot Desktop printing software with a user-friendly interactive platform to configure STL/OBG image formats to desired models

to make sense of the structural topography and providing them with the platform to question and clarify aspects of the lecture or practical, whilst multiple learning aids are focused on the structure of interest.

3D modelling is increasingly used in teaching bone morphology and related changes from various bone-affecting diseases (Müller-Stich et al. 2013; Wu et al. 2018). The addition of 3Dp trabeculae in the osteology lecture helps students to understand the micro-architecture of the bone (Fig. 8.4). This enables the student, at the undergraduate level, to understand and differentiate how diseases of the bone affect the integrity of the bone-supporting architecture, the trabeculae. 3Dp osteology models allow tactile input in the learning process through haptic stimulus. Moreover, it allows students to view the trabeculae, both normal and diseased from multiple angles. The benefit of 3D osteology models is highlighted in improved student assessment scores when compared with those exposed to conventional teaching and learning material (Wu et al. 2018).

Specific parts of the heart may be printed either to enhance the understanding or to put emphasis on the topography, structural or functional relations. The three-dimensional-printed structural relation of the cardiac valves, atrioventricular and semilunar valves may allow a visual perspective that is 10 folds better than a poorly sectioned heart (Fig. 8.5). The printed model of the atrio-venrticular cusps, chorda tendineae and papillary muscle or the Purkinje fibres with or without ventricular walls enables the student to better understand how the structures within the heart function in relation to each other.

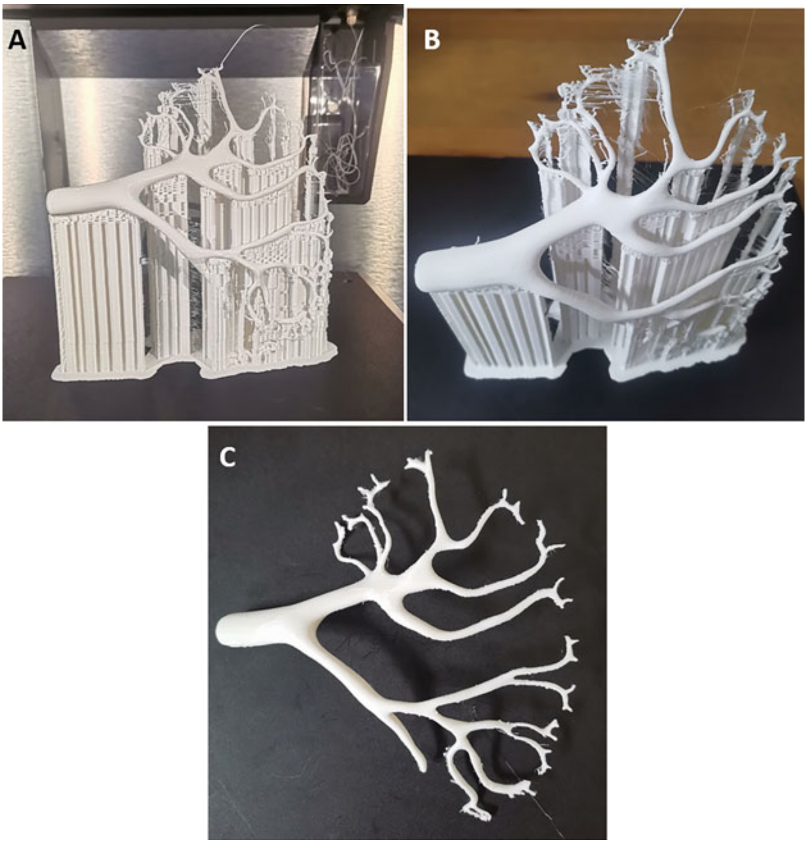

Fig. 8.2 A-C Renal vessel 3Dp at different stages of printing and processing

8.6 MacroView

MacroView DM 5 is a mobile digital imaging system commonly used in forensic post-mortem investigations. The design and functionality of the MacroView make it an efficient tool of choice in a multimodality cadaver-based anatomy teaching and learning environment (Fig. 8.6). It provides a simple platform for capturing images of the full body, a region or organ of interest, and the capability to record videos and upload images. This helps make teaching challenging aspects of anatomy to students at different levels of study much easier when compared to the traditional single modality, PowerPoint presentation. Its design allows ease of operation in between cadavers in the dissection hall, around wet or dry specimen stations, and in a seminar room or lecture hall with or without multiple projection monitors.

The MacroView's height adjustable arm enables positioning of the built-in high-resolution camera to capture specimens, especially, from angles that are not possible with ceiling mounted high-zoom cameras. The digital imaging module with a control panel allows the facilitator to zoom and focus the image on a particular structure or area of the body, record the discussion and save the picture for annotation without moving away from the specimen (Fig. 8.7). The running software is calibrated and provides a reliable measurement tool for structural dimensions and spatial relations of the structure or organ of interest.

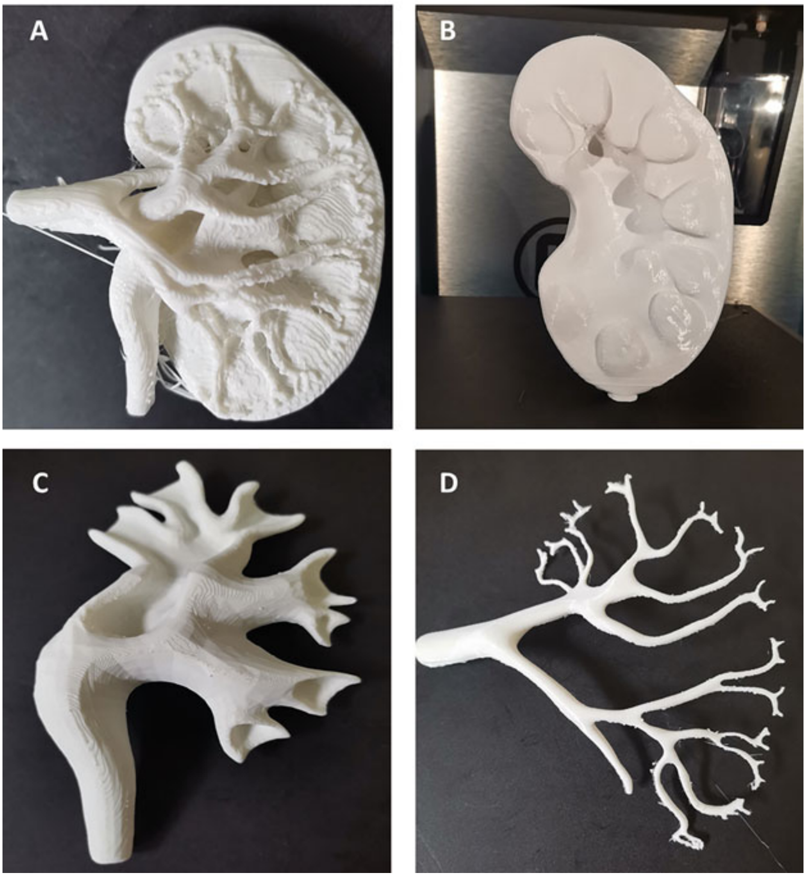

Fig. 8.3 3Dp remodel (**a**) and individual components (**b**-**d**) for the ease of explaining structural relationships and students' appreciation of spatial orientation in the renal hilum

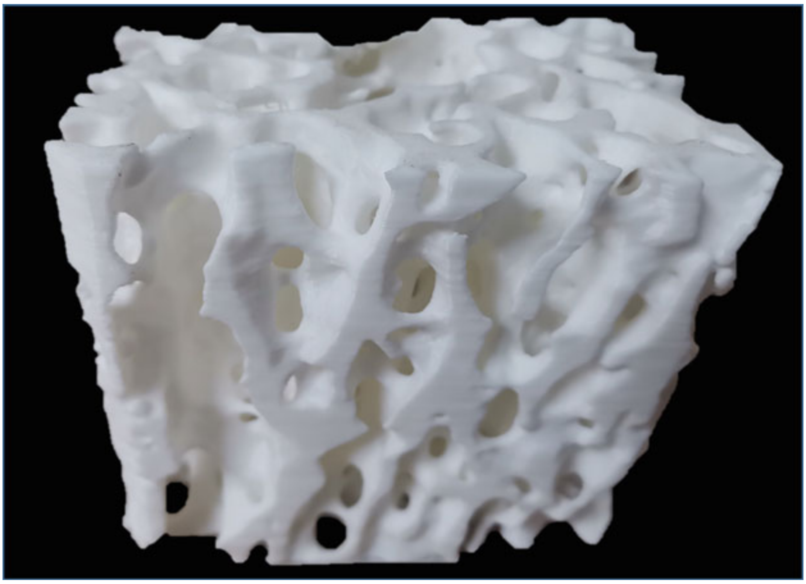

Fig. 8.4 3Dp micro-architecture of the bone which can be used in anatomy teaching as well as in clinical training, to illustrate disease progression on the bone

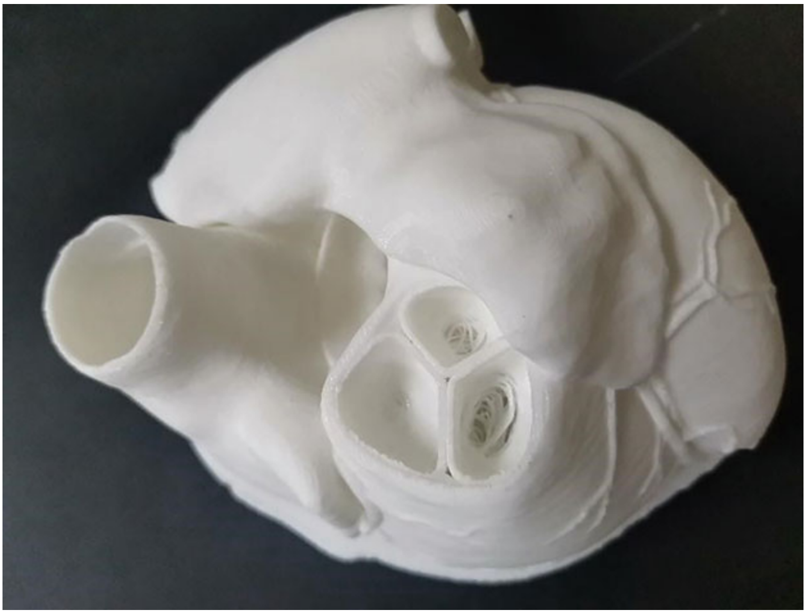

Fig. 8.5 Specific orientation of the heart to show the topography of semilunar valves

8.6.1 Role of MacroView in Lecture Series

The MacroView may be added to PowerPoint-based lectures as an additional teaching aid or as a stand-alone tool, especially during dissection hall sessions. Equally, it may be used in small group discussions and tutorials. During a lecture or practical session the MacroView may be used to demonstrate a structure or organ of interest, giving the class a 3D perspective with the option to zoom in on particular structures whilst emphasising their importance (Fig. 8.8). The ability to reposition the specimen for the students to view different angles and to have a better spatial appreciation is an added advantage.

The inclusion of MacroView in teaching and learning allows for effective real-time responses to questions students may have on the area or organ of interest. The MacroView's built-in HD camera may be used to take a still picture of the specimen, which is annotated during teaching and learning, addressing questions students may have raised (Fig. 8.9). Spatial understanding may be enhanced by repositioning the specimen, taking a picture and highlighting the structure of interest from a different viewpoint or angle. Even more beneficial to students, annotation and explanation of the structure(s) of interest may be recorded with the aid of a built-in microphone in the digital imaging unit. Annotated pictures and video recordings may be uploaded to a learning management system which students have access to, during self-study and revision sessions. In addition, the MacroView provides quality HD images (Fig. 8.9) that may be used to create databases downloadable to external storage for later use in tutorials, lectures and supplementary material for student revision. The quality of images from in-house cadaver material may substitute the images adapted from atlases in computer-based assessments. In this case, students are exposed to and assessed on the material they are familiar with from practical and dissection sessions.

8.7 Ultrasound

Ultrasound guidance is a non-invasive method in which sound waves are employed to visualise various tissue structures within the body (Royer 2016). It is a safe, non-radiating tool used to view internal structures in real time (Royer 2016). These waves occur at a frequency greater than 20,000 Hertz, which is inaudible to the human ear. Most clinical applications require frequencies

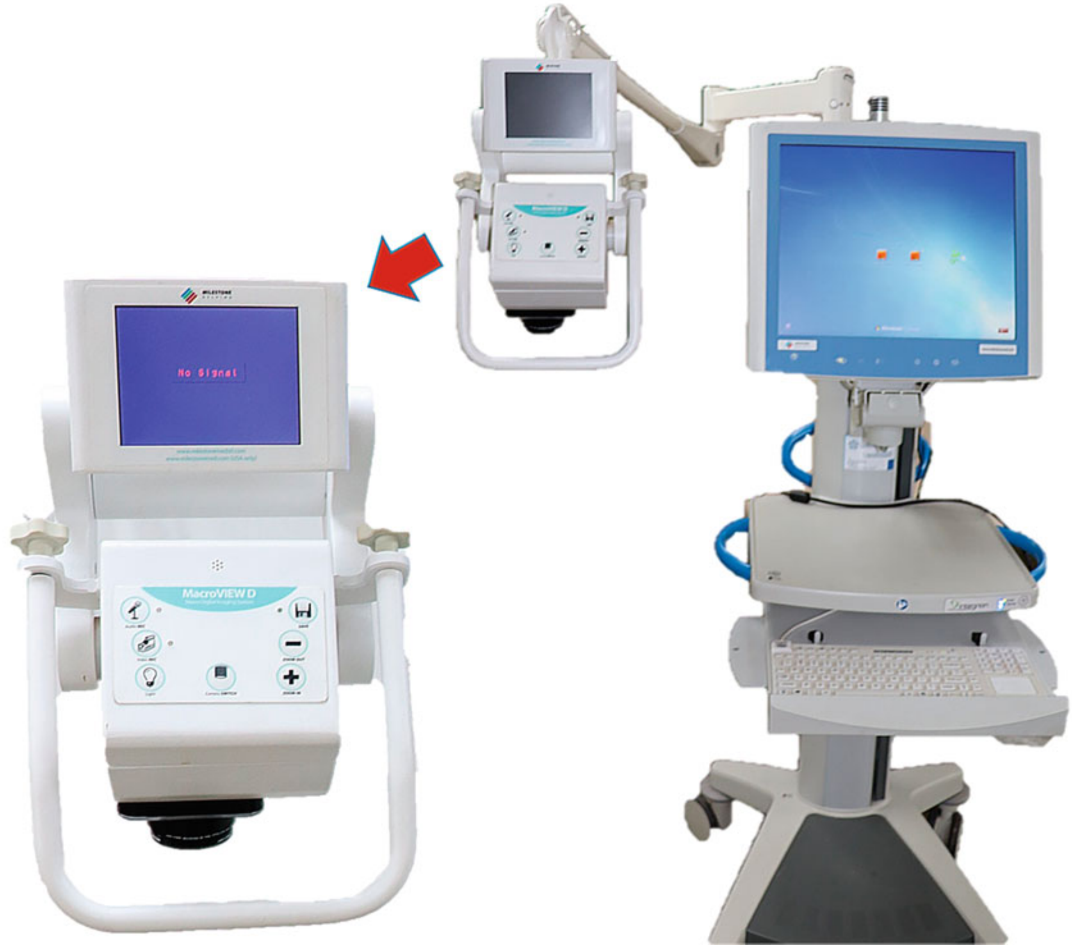

Fig. 8.6 Mobile MacroView DM 5 imaging unit with high definition (HD) camera fitted on spring, height adjustable arm with the control panel on the digital imaging module

ranging between 1 and 15 MegaHertz (MHz) (Venables 2011; Gerrard and Roberts 2012). Piezoelectric material is found within the transducer contract and expands as a voltage is applied across them, acting as the source of the sound waves. Sound waves, in the form of electrical energy, are directed into the body, travelling until it encounters an acoustic interface. Upon the encounter, a portion of the sound wave, in the form of an echo is reflected towards the transducer. Each echo carries mechanical energy, which is then converted back into electrical energy by the piezoelectric crystals in the transducer. These voltage values are then used to determine the brightness of the image produced (Venables 2011). Additionally, sound waves cannot be propagated through air, therefore, ultrasound gel is utilised as a conduction medium. The ultrasound gel acts as a coupling agent and reduces interference that might occur (Govender n.d.). Higher frequency transducers with a higher resolution are recommended for superficial structures, as the penetration depth is less. Whilst lower frequency transducers are recommended for deeper structures with a greater penetration depth but at a detriment to the resolution.

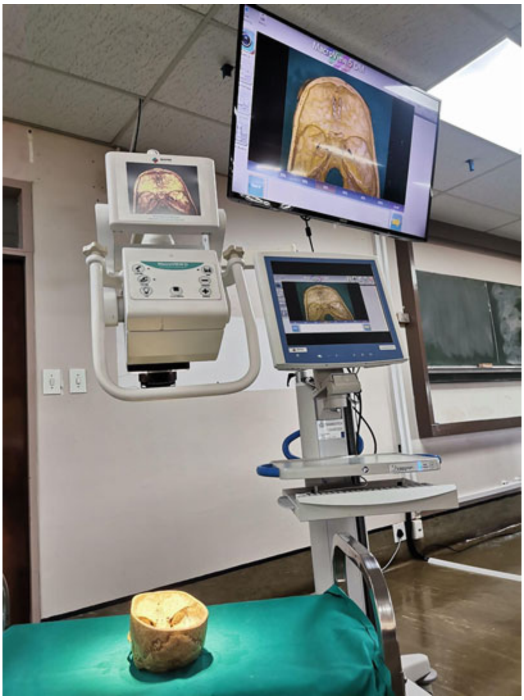

Fig. 8.7 Multiple screen projection of specimen captured with MacroView digital imaging module

8.7.1 Echogenicity

Echogenicity refers to the ability of the tissue to reflect sound waves in the context of its surrounding tissue (Ihnatsenka and Boezaart 2010). Based on this, structures can be characterised as hyper-, hypo- or an-echoic. Anechoic structures such as bone, do not allow sound waves to pass through them, therefore appearing black on the ultrasound screen with a hyperechoic or white rim (Fig. 8.10). Since sound waves cannot penetrate bone, they will create an acoustic shadow beyond the bone itself. Tissues and structures rich in water, such as blood, cartilage and lymph nodes, allow sound waves to partially penetrate, reflecting fewer sound waves and therefore, appearing grey or darker on the ultrasound screen. These are called hypoechoic structures. Hyperechoic structures such as tendons, ligaments and fat do not allow sound waves to pass through them and will, therefore, reflect more of the sound waves towards the transducer. These appear white on the ultrasound screen (Fig. 8.10) (Govender n.d.). In any

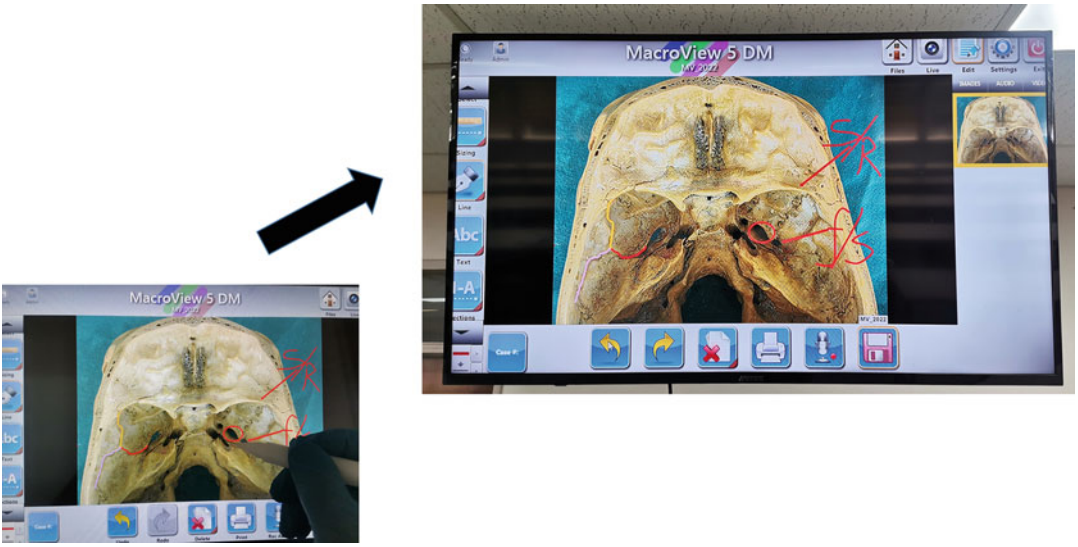

Fig. 8.8 Annotation of pictures with freehand or standard keyboard function projected to monitors in the lecture room

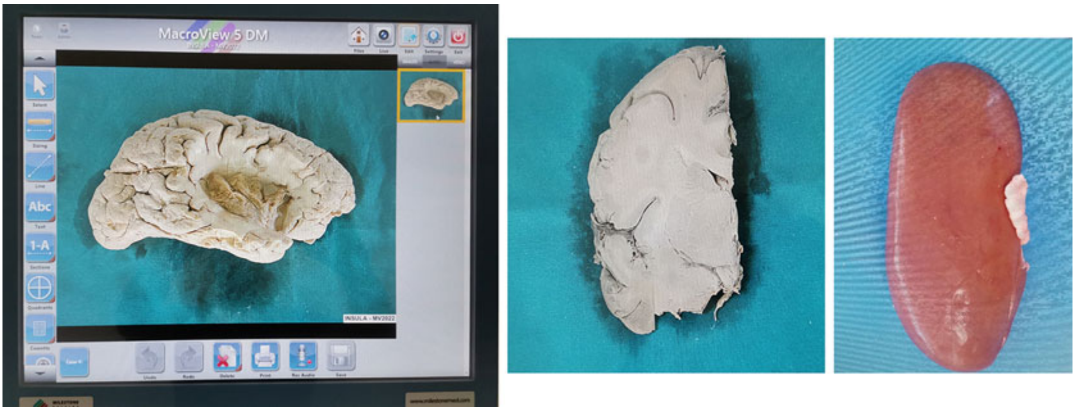

Fig. 8.9 MacroView images downloadable to be used in a lecture session or computer-based assessment

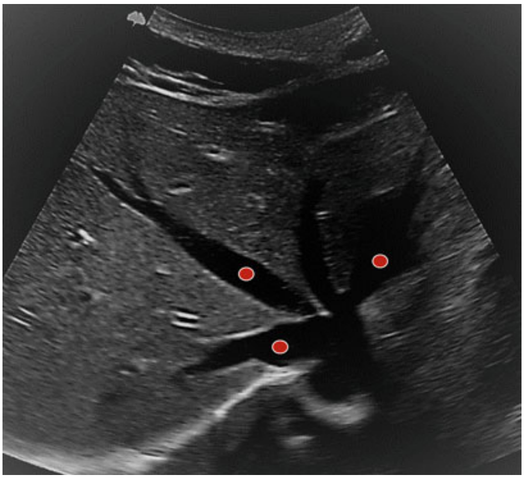

Fig. 8.10 Ultrasound scan displaying the hypoechoic (red dots) blood vessels of the liver, compared to the surrounding hyperechoic structures

diagnostic applications of ultrasound, it is imperative to identify what is 'real' and what is an 'artefact' on the ultrasound image (Venables 2011). An artefact is a structure or feature that is not usually present, but visible on the ultrasound screen. The ability to recognise and remedy potentially correctable ultrasound artefacts is important for image quality improvement and optimal patient care (Feldman et al. 2009).

8.7.2 Transducers

To capture the best image, 'the right tool' is needed. Based on the area of interest, choosing the right type of ultrasound transducer is important. The type of transducer is directly related to the frequency and application.

8.7.2.1 Curvilinear Transducer

This transducer has a relatively large and rounded footprint. Therefore, the beam produced fans outwards, allowing for better resolution. As such, this transducer is ideal for viewing structures larger than the beam. The frequency of the transducer usually ranges from 2 to 6 MHz and its applications include general abdomen, pelvic and vascular scanning. Scans produced appear as a wider arch-shaped image.

8.7.2.2 Linear Transducer

The linear transducer has a smaller, narrower footprint as compared to the curvilinear transducer. The beam produced runs parallel, therefore when introduced to a medium it tends to transect structures perpendicularly. Scans produced have a rectangular-shaped image. The frequency of the transducer ranges from 5 to 15 MHz, providing higher resolution. Its general application is to visualise structures of the musculoskeletal system, structures of the thoracic region, superficial soft tissue in the neck and the genitals.

8.7.2.3 Phased Array Transducer

The phased array transducer has a minimal (smaller and flatter) footprint, with a high penetration depth. It is also known as an echo transducer and is mainly used in echocardiography. The beam produced tends to fan outwards, displaying a similar image to the curvilinear transducer. The frequency produced from this transducer ranges from 1 to 5 MHz.

Each of these transducers contains an orientation marker or indicator. This corresponds to the orientation marker on the ultrasound image, allowing the user to orient themselves during scanning. *A tip, the indicator should always be orientated towards the patient's cranial or right side.* Whilst scanning there are various transducer movements and manipulation that can be applied to obtain the optimal image. These include sliding, tilting, rotating, rocking and compression.

Sliding involves moving the entire transducer along the long or short axis to obtain the appropriate image window. Tilting or fanning involves moving the transducer from side to side along the short axis. This movement produces multiple cross-sectional images of the structure of interest. Rotation involves turning the transducer in either a clockwise or counter-clockwise direction along a central axis. This is mainly used when switching between long- and short-axis views. Rocking entails 'rocking' the transducer towards the user and then away from the user (in line with the transducer indicator). This movement produces an image along the long axis of the structure of interest. Compression is mainly involved with assessing veins versus arteries. It requires the user to apply downward pressure on the transducer to evaluate the compressibility of the underlying structure(s).

8.7.3 Frequency and Resolution

Setting the frequency is directly related to the structure(s) of interest. Higher frequencies produce shorter wavelengths, whereas lower frequencies produce longer wavelengths. The shorter the wavelength the more easily the wavelengths are absorbed. Therefore, higher frequencies have poor penetration but higher resolution. Whilst lower frequencies have deeper penetration but poor resolution.

8.7.4 Knobology

For each ultrasound machine, the general functions and basic settings are similar. Below is a general rule guide to follow when setting up the device for scanning. Please note the following steps are specific to the Vinno A5, portable Doppler ultrasound machine.

Step 1: Power button

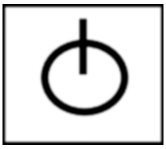

→

The power symbol appears on the top left-hand side of the control panel.

Step 2: Selecting the correct transducer

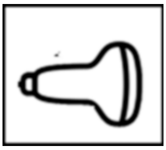

→

The transducer icon allows you to select your transducer of choice. Most ultrasound machines allow for multiple transducers to be plugged in simultaneously. This enables the user to switch between transducers.

Step 3: Body pattern

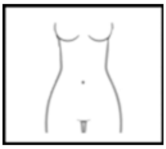

→

This allows you to select the body region you will be scanning. Use the trackball to navigate to the body region of interest, once the cursor is hovering over the region, press enter to confirm the body region.

Step 4: Application preset

→ Once the above settings have been selected, the next step is to select the correct application preset for the transducer. Application presets are specific to the transducer based on its frequency and footprint. The application preset will automatically set the ultrasound settings (frequency, depth, gain etc.) specific to that scan. Application presets include abdomen(Abdo), cardiac, renal, gynaecology (gynea), obstetrics (obs), musculoskeletal (msk) and vascular.

Step 5: Depth

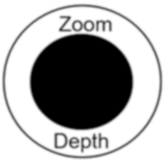

→

Although the application presets will apply factory settings, further adjusting during scanning may be needed to optimise the image. Ultrasound depth is an indication of how deep the beam should travel to scan the structure(s). A tip is to apply the depth needed for that specific structure whilst avoiding unnecessary ‘blank’ space. The scale on the right side of the screen correlates to the depth of the structure from the footprint of the transducer in centimetres. As you increase the depth (turning the dial), the numbers on the side scale will increase accordingly.

Step 6: Gain

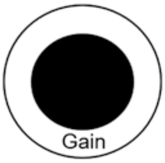

→

Gain is an indication of how bright or dark the structure(s) on the scan appears. The colours of the structure are a representation of the sound waves returning to the transducer. Under-gain makes the image appear too dark, whilst over-gain makes the image appear too bright. The optimal gain (which is ideal for the optimal image) is an equal balance between the bright and dark shades. An additional function known as time gain compensation can also be used to adjust the overall gain. This feature allows the user to adjust the gain at specific depths of the greyscale ultrasound image. The sliding bars correlate to different areas in the scan which can be adjusted individually.

Step 7: Focus

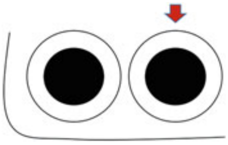

→

This function is ideal for further optimising your image as it adjusts the focus over a specific structure(s). By adjusting the focus, the sound waves are concentrated at a specific depth on the image to maximise the resolution. To adjust the focus, turn the second dial on the left side of the control pad. Each turn of the dial correlates to a cursor position on the right-hand side of the screen.

The next couple of steps are important for freezing images, taking various measurements or capturing ultrasound images or videos.

Step 8: Freeze

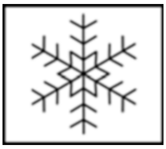

→

This function takes a screenshot of the current view and ‘freezes’ the image frame. This allows you the opportunity to view structures in more detail over time. Additionally, by moving the trackball, you can scroll between frames taken 10–30 seconds before freezing the image

Step 9: Measure

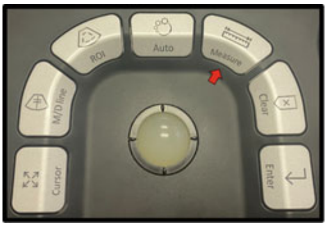

→

The calliper tool allows you to take various measurements on images. These include distance, area, volume and pluses.

Step 10: Saving images or videos etc.

P1 →

Images or videos taken during scanning can be saved by pressing the P1 button. Files captured will be saved under the patient's file.

8.7.4.1 Basic Ultrasound Modes

Two-dimensional

2D →

Also known as B-Mode or bright mode. This setting created a 2D grayscale image. For advanced scanning, this mode needs to be mastered as it forms the basis for scanning in other modes or reconstruction. *Tip*, if you are in the present and would like to navigate back to the factory setting, simply select 2D.

M Mode

M →

Also known as motion mode. This mode does scanning whilst taking into account motion and time. The motion is represented by the *Y* axis (left side of the screen), whilst time is represented by the *X* axis (bottom of the screen). To achieve M-mode, begin scanning using B-mode to obtain the structure of interest (in the centre of the screen), and press M-mode for a cursor line to appear. Place the cursor line over/along the structure of interest, then press M-mode again. In summary, M-mode takes a slice of the B-mode image over a period of time. By placing the cursor over the area that section will be subjected to M-mode. The image can then be frozen to take measurements.

Colour Doppler

CF →

This function is used to characterise the flow within the medium. Flow can be classified as a moving or stationary source. Depending on the direction of flow either towards or away from the transducer, structures will appear red or blue. Flow towards the transducer tends to have a higher frequency and is displayed as red. Whilst flowing away from the transducer, it tends to have a lower frequency and is displayed as blue. Important to note, the transducer should be held parallel to the flow (rather than 90 degrees) in order to detect movement. To activate this function, select the CF button. The frequency and gain options can be further adjusted whilst the colour Doppler function is active to further optimise images.

Pulse Wave

PW →

This function allows the user to measure the velocity of blood flow at a single point. To activate this function press the PW button. A selection box with a sample gate (parallel lines) will appear. Place the sample box over the area of interest whilst positioning the sample gate over the vessel using the cursor. Press the PW button again to activate Pulse Wave Doppler mode. The image can then be frozen to take measurements.

8.7.4.2 Incorporation of Ultrasound in Lecture Series

Ultrasound has been incorporated into teaching and learning as it has a direct clinical context. The addition of real-time visualising has taken teaching and learning from a static to a dynamic direction. By doing this, students are able to spatially orientate themselves when learning various body systems or regions. Additionally, it aligns with vertical teaching, preparing students for future clinical sessions. Ultrasound specifically is mobile and portable, making it an ideal modality for teaching and learning (Smith et al. 2018a, 2018b).

8.8 Anatomage Table 8

The Anatomage table is a multimodal interface, used for 3D virtual dissection of a life-size simulated cadaver (Allen et al. 2019; Baratz et al. 2019; et al., 2022). In addition, it can be used for pre- and perioperative planning, as it allows for the practice of surgical approaches. By repeating dissection scenarios and replicating operative fields, this tool can be used to support training whilst reducing the need for expensive teaching and learning models (Kazoka and Pilmane 2019). This interactive tool includes systemic, segmental and regional anatomy in real time. Various presets or tools can be used to manipulate the anatomy on multiple levels or planes to further enhance teaching and learning.

The main toolbar provides the following options contained in folders (Fig. 8.11): OpenFile, Import PACs, Gross Anatomy, High Res Regional Anatomy, Physiology, Case Library, Histology, Curriculum and prosections.

These options are designed to provide quick access to the various features. Files saved in the Digital Imaging and Communication (DICOM) format on an external device can be accessed using the OpenFile function. These files can be uncompressed CT or MRI scans, similar to those found in the case library. However, these files do not have full visualisation and dissection capabilities as the simulated models. The import PACs options allow users to import files from the Picture Archiving and Communication Systems (PACs). The Gross Anatomy option allows access to the simulated models including the full-body CT section scans. Further navigation in this section will be discussed later. The High Res Regional Anatomy option includes regional scans taken at 0,2 millilitres resolutions. These model scans are more detailed than the scans found under the Gross Anatomy folder. The Physiology option allows the user to explore physiology simulations and pathways. The Case Library folder contains a collection of CT or MRI scans, both normal and diseased. These scans are divided into regions, including embryology and four-dimensional as well as other categories that allow you to explore specific sections. The Histology option provides access to a library collection of microscopic histological slices found in each system. The search function in both these libraries allows for quicker access to heading titles and descriptions. The Curriculum option provides a menu for segmented and DICOM Anatomy options specific to region-based anatomy. The prosection option provides the user with real-life cadaveric prosections of anatomical regions or tissue organs. Since these are real-life images, dissection or exploratory functions cannot be performed on the images. However, annotations cannot be done via the pen and pin functions (Allen et al. 2019).

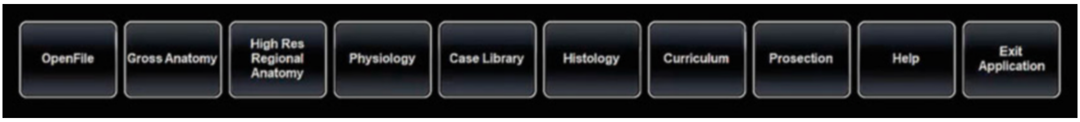

Fig. 8.11 Screen shot of the main tool bar of the Anatomy table 8

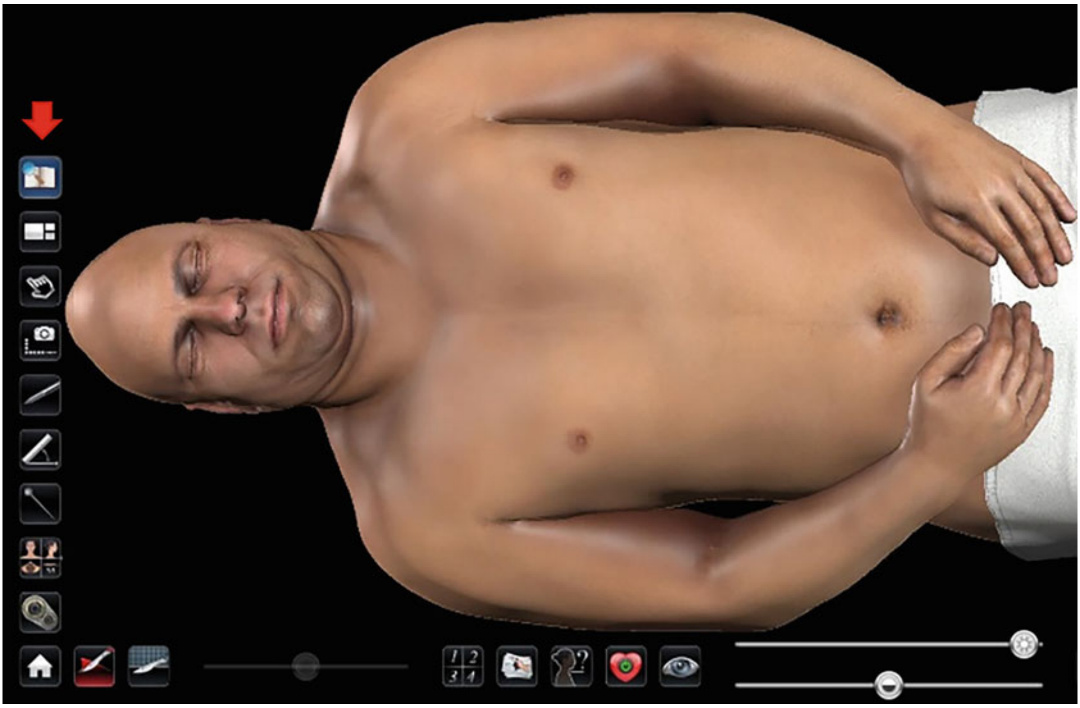

Fig. 8.12 Image displaying the navigation pane (left side indicated by the red arrow) when using the gross anatomy feature on the Anatomage table

8.8.1 Gross Anatomy Folder

The navigation pane is set up to provide simple access to commonly used tools, features or icons (Allen et al. 2019), whilst the touchscreen function makes the application of the tools easier to control. These tools/features include the overall view and positioning of the models, dissection and saving options (Fig. 8.12).

The volume orientation feature allows the user to rotate or move the model into various viewing orientations (Baratz et al. 2019). Three hundred and sixty-degree rotations can be done using one figure to revolve the model accordingly. Whilst positioning can be done using two fingers to reposition, drag and drop the model on the screen. Both these features can be done by swiping anywhere on the table-top. Any selected view can be further zoomed in or out by using the pinching motion with your fingers. To zoom in on the model, spread your fingers apart. To zoom out on the model, move your fingers closer together. Both these features require the use of two fingers either on the same hand or different hands. To return the model back to its anatomical position (anterior) without having to manipulate it, the icon with the model facing anteriorly can be selected. The double tap function of this icon further allows for the model to be turned into a posterior position. The icon of the model lying in a supine position (lateral view), allows for a lateral view (both sides) of the model. The icon with the eye allows for the model to be positioned either cranially or caudally (double tap function). The icon that displays a 1:1 symbol is helpful to obtain the life-size perspective of the model on the table, this feature can be manipulated to change the size appearance of the model. These icons can be found on the side navigation bar.

The blue scalpel icon allows for quick cuts. This tool can be used to perform virtual incisions, controlling the length, direction and deep (Kazoka and Pilmane 2019). By selecting the scalpel icon, lines representing the incision can

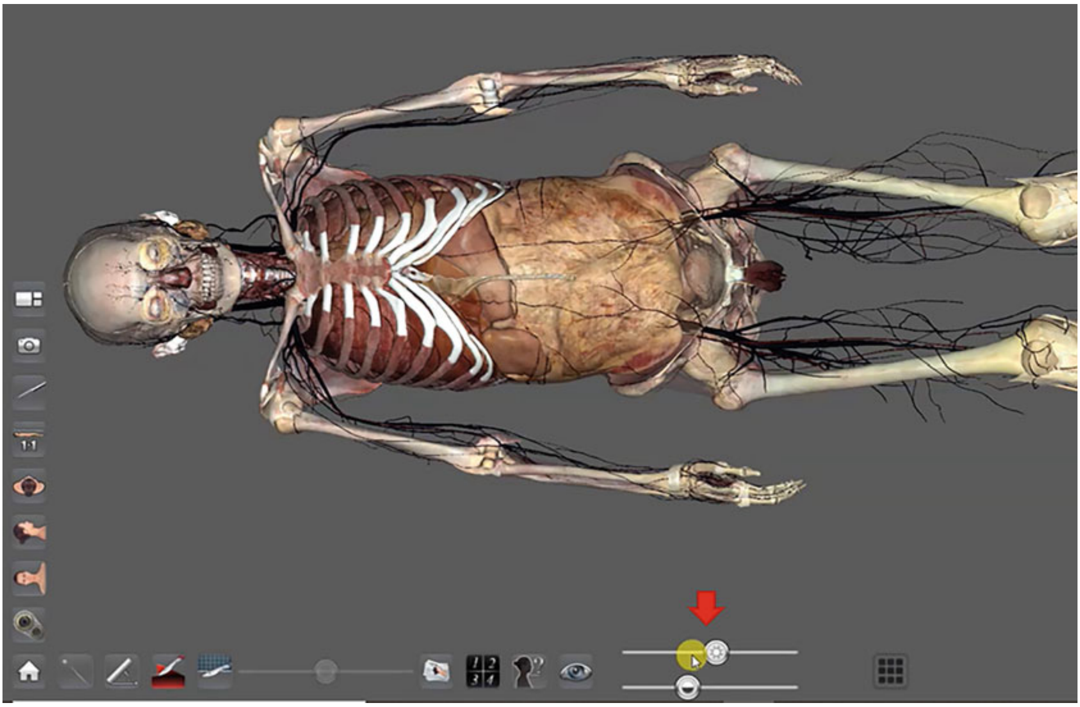

Fig. 8.13 Image displaying the scroll bars responsible for adding or removing layers (red arrow) on the Anatomage table

be made using freehand motions. Alternatively, quick tool preset features can also be used to perform dissections. The icon with a sagittal slice through the model will produce a sagittal cut through the entire model. The same applies to the icon with a transverse or coronal slice through the model. Cuts can be further adjusted using the scroll bar next to the scalpel icon. More customised cuts can be done using the red scalpel icon. This feature allows for organic, curved or straight cuts. Likewise, these cuts can be further adjusted using the scroll bar next to the scalpel icon.

Towards the bottom right of the navigation pane, there are two scroll bars (Fig. 8.13). The top scroll bar represents the brightness, but also functions to remove structures from superficial to deep. The bottom scroll bar represents the various body systems, allowing you to add or remove system by system. The reset option provides the possibility to undo previous steps, allowing for repetition during training or the production of body segments during teaching and learning.

Structures such as arteries, veins or lymphatics can be customised according to colour. The setting wheel/gear icon can be used for this feature. By navigating to the properties tab, you can adjust the colours of the various structures. This gear icon also allows them to feature lock the table to prohibit model manipulation. An alternative route to navigate to system/structures is by using the visibility menu, on the bottom navigation bar. This menu displays all the systems visible on the model. Each system is further subdivided into categories which further list the individual structures (both left and right if available) in the system. Structures that have a tick in the check box will be displayed, alternatively these checkboxes can be deselected to remove structures. Additionally, annotations can be added or removed by further selecting the annotation box. Structures can be colour customised by selecting the colour icon. This colour icon can further highlight the origin and insertion of muscles as well as bony landmarks (Fig. 8.14). Additionally, when using the volume feature in

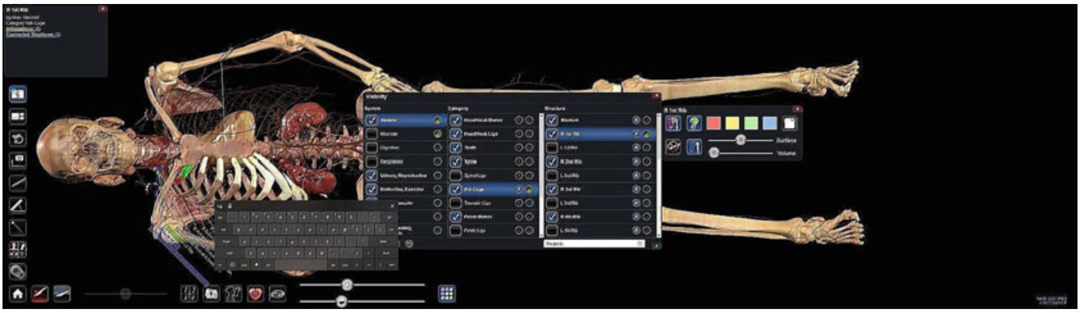

Fig. 8.14 Image displaying the visibility function on the Anatomage table

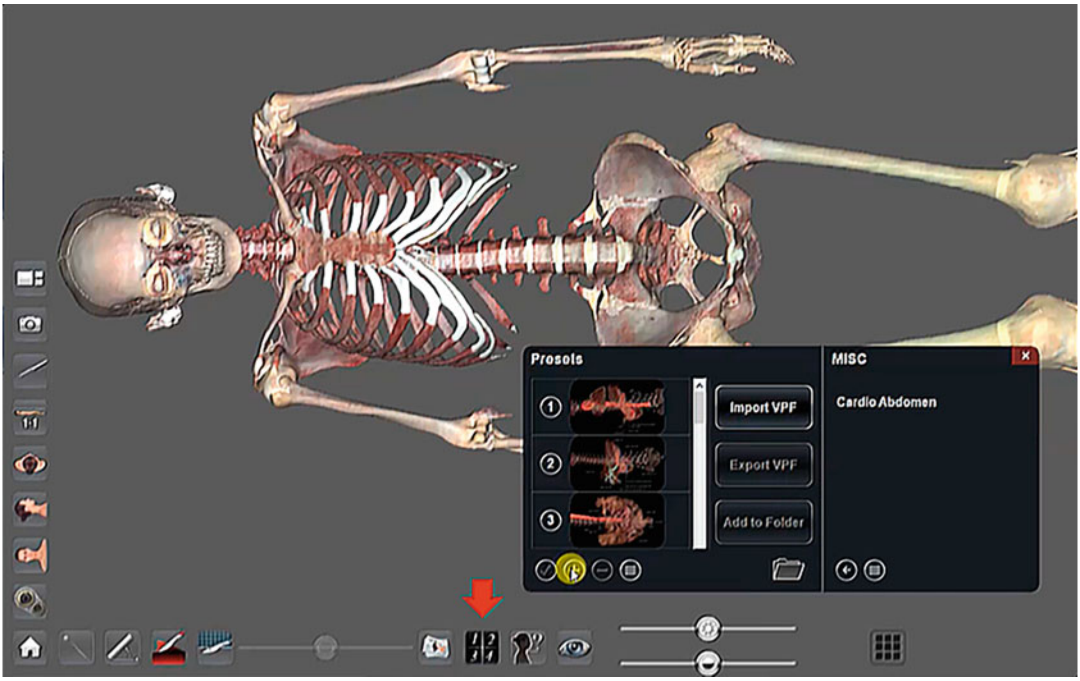

Fig. 8.15 Image displaying the presets function (red arrow) on the Anatomage table

combination with the surface feature, structures can be made transparent to view internal structures.

By double tapping on structures, an action menu will appear. This menu is a shortcut menu to the above-mentioned functions: check box, transparency, colour, annotation, origins and insertion, cuts, reset the preset function, which appears as the 123 icon can be programmed to customise settings prior to navigation. Presets can be added or removed using the plus and minus buttons (Fig. 8.15). This function allows for quick navigation to preview the system or structure during teaching and learning. These presets can be saved and exported to an external device.

Additional features include the pen icon, apart from annotations it can be used for measuring structures, either straight or curved, accurate to real-life structures. Whilst the pin tool (pin icon), allows the user to click and drop up to 10 pins anywhere on the model (Fig. 8.16).

The pen tool (pen icon), further has colour options, freehand text, text box, and arrow placements (Fig. 8.17). The camera icon, which

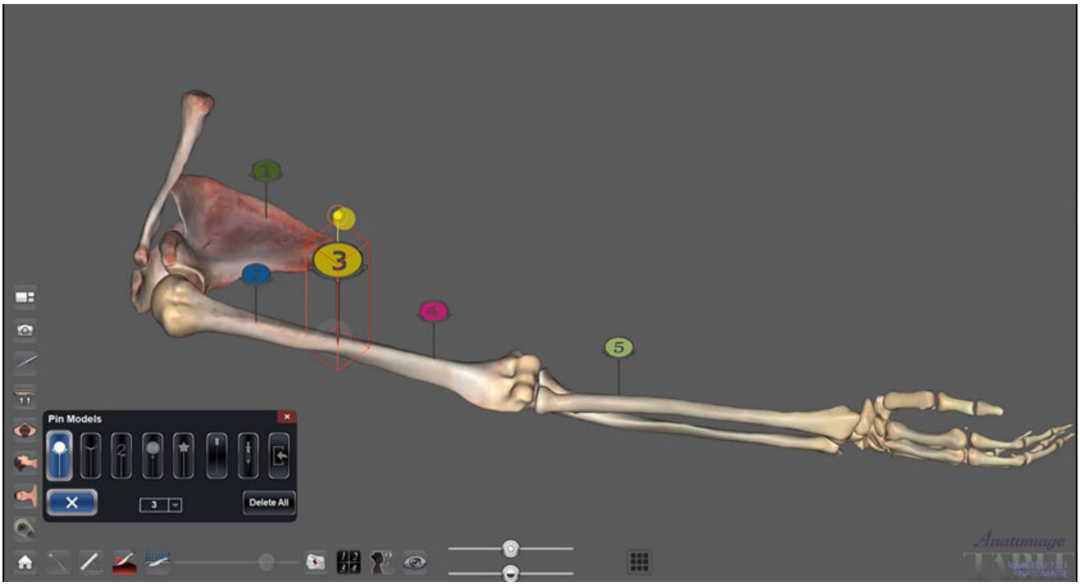

Fig. 8.16 Image displaying the pin function on the Anatomage table

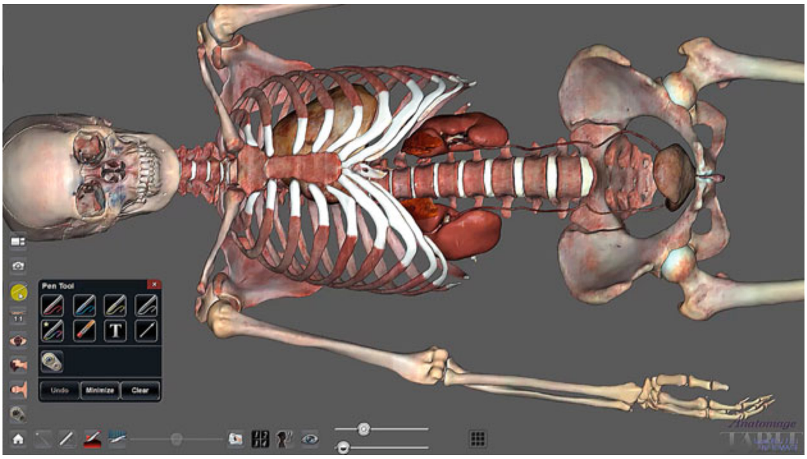

Fig. 8.17 Image displaying the pen function on the Anatomage table

is the screenshot function, can section images that can be saved as JPEG and PNG files. Lastly, the layout tool can customise the model to correlate with a section scan or image (CT or MRI scans).

8.8.2 Assessments

Assessment tools for the Anatomage table include feature lock and quiz mode. These can be employed for self-study or instructional assessments. To utilise feature lock, a preset must be created that can include pins, bony landmarks or origin and insertion points. To access the feature lock, as previously mentioned, navigate to the setting wheel/gear icon. Select feature lock options to further manipulate the image control, presets, pin placements, draw tool, cutting, screenshot, measurement and slider bars. By selecting enable, you will be prompted to select a password. This generated password will allow the facilitator to enable/disable the feature

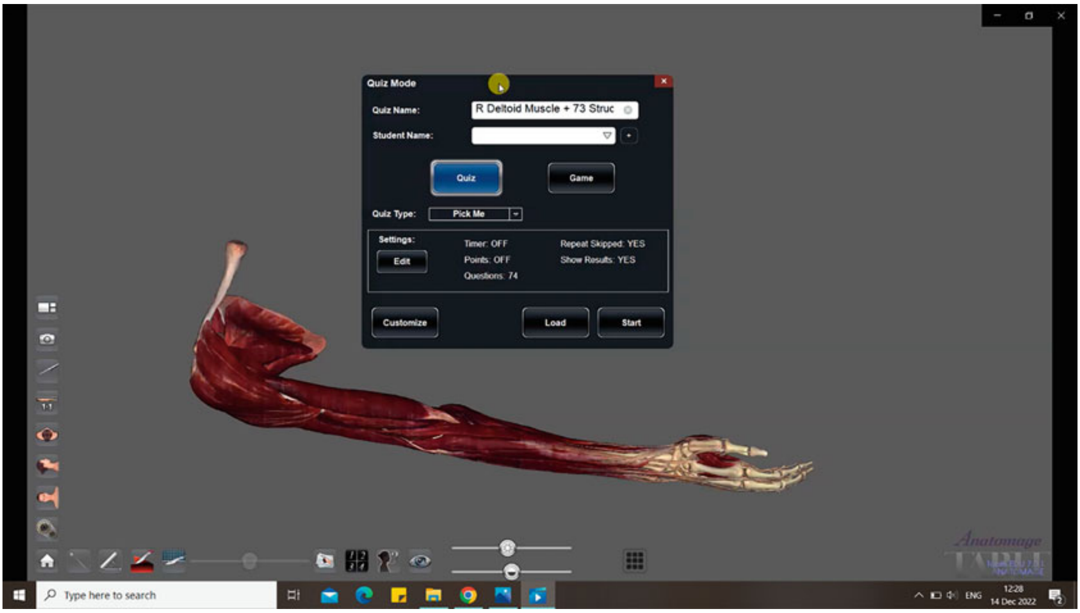

Quiz Name: R Deltoid Muscle + 73 Struc
Student Name:
Quiz Type: Pick Me
Settings:
Timer: OFF
Points: OFF
Questions: 74
Repeat Skipped: YES
Show Results: YES

Fig. 8.18 Image displaying the assessment function of the Anatomage table

lock or to further modify the setting options. Alternatively, assessments can be done using quiz mode (Fig. 8.18).

Each quiz type can be customised according to four options: (i) pick me quiz mode, (ii) flash card, (iii) multiple choice and (iv) highlight. The first option requires the user to identify the structure prompted on the screen by tapping on the structure, without providing feedback. A summary of the quiz is provided upon completion (Allen et al. 2019). Additionally, several views are available per question. The second option is similar to the first option, however, feedback is provided after each question. The third option, provides the user with a highlighted structure, along with a list of options from which you select the correct option. No feedback is provided, however, a summary is displayed upon completion. Whilst the last option highlights structures for users to identify. As these structures are not annotated this method requires the users to know the structure without prompting and is mainly used for oral assessments or review purposes (Allen et al. 2019). This option allows for one view per question of which students have control of the cutting function only. Each option can be edited to allow some access to the students, randomise the question, select the highlight colours, control time and alter the mark allocation. Additionally, you can customise the quiz by creating section views.

8.8.2.1 Incorporation of Anatomage in Lecture Series

The Anatomage table has been introduced into teaching and learning since its inception. Furthermore, this virtual dissection tool is fast becoming a replacement for cadaveric material due to multiple rising issues. The interactive interface serves as an alternative method to learning 3D anatomy. Overall, the Anatomage table has several advantages over the use of cadaveric material such as less expenditure, and less time consumption incurred during the embalming and disposal procedures. Moreover, students develop visuospatial skills as they learn anatomy across multiple planes, sections and regions. This tool encourages students to explore on their own, further enhancing the teaching and learning processes by creating a sense of intrigue. The additional assessment function also serves as a self-testing tool at the end of learning sections or regions. Overall, the Anatomage table provides virtual dissections, which further reinforces the visuospatial relationships between anatomical structures (Allen et al. 2019; Bork et al. 2019).

8.9 Pilot Study

This study consisted of a pilot component in which the above-mentioned biomedical imaging modalities (3D printed models, Macroview, ultrasound, Anatomage) were introduced as a supplement to the traditional teaching and learning methods of anatomy. Ethical approval was obtained prior from the relevant committees. The aim of the study was to engage with students using questionnaires to obtain an understanding of their perceptions and experience of incorporating technology (imaging modalities) in the teaching and learning process.

8.9.1 Material and Methods

This study included first-year occupational therapy and second-year physiotherapy students from Sefako Makgatho Health Sciences University. The classes consisted of 35 and 74 students, respectively. These two cohorts attend lectures and practical's together, as well as write the same practical assessments. Since all students from both cohorts were included in the study (there were no exclusion criteria.

The physiotherapy group served as a control group which employed traditional teaching methods, in the form of a straightforward lecture presented in a lecture hall. Whilst the occupational therapy group was the intervention group exposed to imaging modalities; ultrasound scanning, an interactive Anatomage table, a MacroView, an overhead high-zoom HD camera and 3D printed models, as a supplement to the teaching methods.

The focus area for this study was the abdominal region, specific to the urinary system. Following theory lectures, students from both cohorts were asked to complete a questionnaire to obtain an understanding of the students' comprehension of the topic. The lecture encompassed the posterior abdominal wall as well as the organs (kidney, ureter and bladder) of the urinary system. Prior to the start of the lecture, both cohorts were given a traditional questionnaire to assess their basic knowledge of the components of the urinary system being taught. As this was a face-to-face lecture, students were dispersed throughout the venue to ensure each student had a clear view of the educator and PowerPoint material. For the intervention group three prosected abdominal specimens, each displaying various urinary organs in situ against the posterior abdominal wall were placed under the overhead high-zoom HD camera. Whilst the lecture was being presented, teaching modes cycled between the conventional lecture and the overhead High-zoom HD camera with the prosected specimens. Information regarding the anatomical structures was disseminated to students with the use of the PowerPoint lecture and further reiterated using the prosected specimens.

Subsequently, the imaging modalities were set up at different stations in the same venue. At the conclusion of the lecture, the intervention cohort was split into four groups which cycled through each modality station. The stations were as follows:

Station 1—Anatomage: Images of the posterior abdominal wall and the urinary system, in real time, were displayed. Students had the advantage of viewing different cross-sectional images at various levels of the urinary system with animated blood flow.

Station 2—3D printed specimens: Students were given the opportunity to view the internal structures of the kidney and piece together the different components, such as the renal pelvis and vessels. This allowed students to orientate the organ as well as visualise the internal components.

Station 3—Ultrasound machine: From each group, a student volunteer was scanned to visualise the individual components of the urinary system in real time. They further gained clarity on the spatial orientation and relationships of the surrounding structures.

Students were also exposed to transverse and longitudinal orientation planes of each organ.

Station 4—MacroView with prosected specimens: Although students were already exposed to the specimens during the course of the lecture, they now had the opportunity to review the structures on their own. With the use of this modality, smaller structures on prosected specimens could be zoomed into and visualised.

The control cohort was exposed to the conventional lecture, without the use of any imaging modalities. The lecture was held in an online setting, concurrent with the intervention cohort. At the conclusion of the lecture session, both cohorts were presented with a follow-up questionnaire. These aimed to evaluate the level of information retained by each cohort and to further assess whether the introduction of imaging modalities made a significant improvement in their conceptual visualisation of the structures at hand. The traditional and follow-up questionnaires consisted of a five-point Likert scale (strongly agree to strongly disagree) assigned to statements/questions. All questionnaires were kept confidential and anonymous. Subsequently, an average score was determined for the answers to each question provided by the students.

8.10 Results and Outcomes

Below is a short report and comparison of the students' reactions to the different teaching and learning methods used in the pilot study.

Occupational therapy first-year students showed a large degree of uncertainty with regards to the anatomy of the urinary system and the relationships of the kidney. Fifty-six percent (56%) of students indicated that they do not understand the visuospatial orientation of the kidney and its relationship with the urinary system as a whole. When looking at the gross anatomy and layers of the kidney a large number of students (52% and 43%, respectively) could not positively identify structures.

Physiotherapy students, like occupational therapy students, could not visualise the orientation and relationships of the kidney within the urinary system. However, physiotherapy students seemed more unsure of their knowledge than occupational therapy, with 36% neutral responses to the visuospatial orientation, 40% and 42% neutral responses to the gross anatomy and layering of the kidney, respectively.

A comparison of the post-lecture surveys (Figs. 8.21 and 8.22) shows a significant increase in the level of understanding, of the visuospatial orientation of structures in the urinary system and gross anatomy of the kidney. For the occupational therapy students, 43% of students indicated their understanding of the visuospatial orientation, this is a significant increase from 7% (Fig. 8.19). Physiotherapy students reflected a greater level of uncertainty again, with 45% of students remaining neutral. Only 35% of the class indicated that they have a basic understanding. Fifty-eight percent of the physiotherapy class agreed that the introduction of imaging modalities would have helped them better understand the urinary system and the structures related, whilst the occupational therapy students displayed a high level of satisfaction with the introduction of imaging modalities. Students found the Anatomage to be the most effective in aiding visualisation of the different planes and gross anatomy of the urinary system, with 50% of students strongly agreeing to its efficiency.

8.11 Discussion

The primary goal of a medical educator is to teach students how to perform complex clinical procedures, with minimal risks of complication and maximum patient benefits (Nguyen et al. 2014). Moreover, advances within the medical field have led to the incorporation of innovative teaching and learning resources such as 3D computer models, body painting, clay modelling, hand-held manipulation, plastinated specimens and haptic simulators (Preece et al. 2013). Therefore, it should be a priority for educators to incorporate additional teaching and learning methods

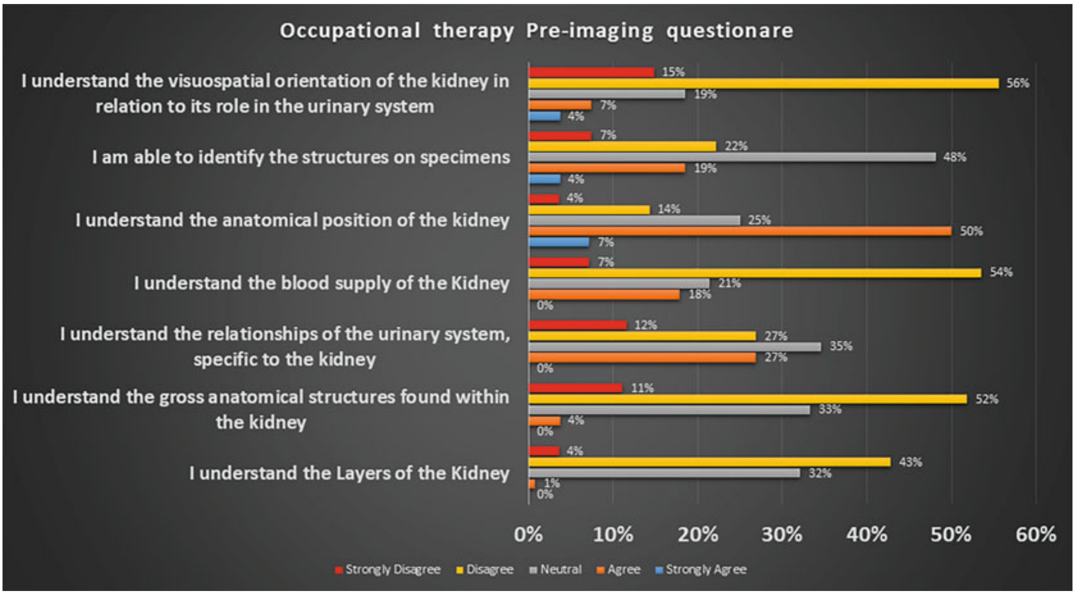

Question	Strongly Agree	Agree	Neutral	Disagree	Strongly Disagree
I understand the Layers of the Kidney	0%	1%	32%	43%	4%
I understand the gross anatomical structures found within the kidney	0%	4%	33%	52%	11%
I understand the relationships of the urinary system, specific to the kidney	0%	27%	35%	27%	12%
I understand the blood supply of the Kidney	0%	18%	21%	54%	7%
I understand the anatomical position of the kidney	7%	50%	25%	14%	4%
I am able to identify the structures on specimens	4%	19%	48%	22%	7%
I understand the visuospatial orientation of the kidney in relation to its role in the urinary system	4%	7%	19%	56%	15%

Fig. 8.19 Table showing percentages per question for occupational therapy (intervention group) pre-imaging lecture survey

that simulate similar clinical scenarios at an early stage. Results from this study revealed that enhancing students' visuospatial ability leads to greater retention of anatomical knowledge (learning). Which in turn results in strengthened anatomy performance outcomes (Roach et al. 2021).

The intervention cohort displayed a high level of interest in the imaging modalities employed, the Anatomage and 3D-printed specimens being the most effective in helping them with visualising the internal and external structures of the kidney as well as its relation to other urinary structures. Fifty percent (50%) of the class found that the theory portion of the lecture was well supplemented with the subsequent dissection planes observed on the Anatomage (Fig. 8.19). Prior to the lecture, the majority of the class could not visualise the gross anatomy (52%) of the kidney or the orientation/visuospatial planes that it occupies in the body (56%). At the conclusion of the session, students were far more confident in their abilities to comprehend and identify the different aspects of the urinary system, with 53% of the class stating that they are able to identify the various structures on cadaveric specimens.

The control cohort showed a less significant increase in their understanding of the different components of the urinary system. When assessing pre-lecture statistics, students were mainly undecided on their level of comprehension of the topic, with 36% of the students unable to visualise the different orientation planes and 36% neutral on the subject. With regards to the gross anatomy and layering of the kidney, students fared worse with 40% undecided or neutral and 30% completely unable to identify the structures of the kidney (Fig. 8.20). Unlike their Occupational therapy counterparts, the physiotherapy students remained neutral on their stance concerning the visuospatial orientation of the kidney with 45% of the cohort still neutral or undecided. There was an increase in their understanding of the basic structures found in the kidney when compared with the pre-lecture survey, however, 48% of the cohort was neutral on their abilities to identify these structures on cadaveric specimens. Students expressed a great interest in incorporating imaging technologies in their lectures, with 58% of learners believing they would have fared better if imaging modalities were supplemented with traditional lectures (Figs. 8.19, 8.20, 8.21 and 8.22).

By incorporating biomedical technologies such as the Anatomage table, students are able to learn in a safe environment which allows them to explore, reverse errors and replicate procedures (Dev 1999). Further incorporation of the Anatomage table in teaching and learning has demonstrated increased learning performance. Amongst its benefits the terms 'engaging', 'interactive' and 'self-directed learning', all of which increase the spatial understanding of anatomy, have been used by multiple authors (Baratz et al. 2019; Bork et al. 2019). Additionally, as the Anatomage table is considered a haptic tool, it is linked to longer memory retention as it mimics everyday smart device activities (Allen et al. 2019). However, even though this tool evokes more excitement and intrigue in the teaching and learning of anatomy, as a modality it measures equivalent to cadaveric dissections for learning specific anatomical regions (Allen et al. 2019; Baratz et al. 2019).

Schramek and colleagues conducted a study incorporating imaging modalities such as ultrasound, radiography, CT and MRI imaging as an adjuvant to embalmed cadavers as a teaching tool for anatomy. The study outcomes revealed an increase in the overall understanding of medical imaging, further improving the students' long-term ability to identify anatomical structures in vivo and on medical imaging files. Whilst ultrasound was the imaging tool of choice for dynamic teaching and learning of anatomy, CT scans were the most suitable to teach students to identify the pathological changes in the skeletal system (Schramek et al. 2013).

In another study, the authors compared the effectiveness of anatomists versus clinicians in teaching anatomy with the aid of ultrasound. Results revealed that anatomists were just as effective educators when compared to clinicians (Jurjus et al. 2014). This speaks to the disadvantage some authors propose when incorporating ultrasound in teaching, stating that there is a lack of experienced clinicians available to teach

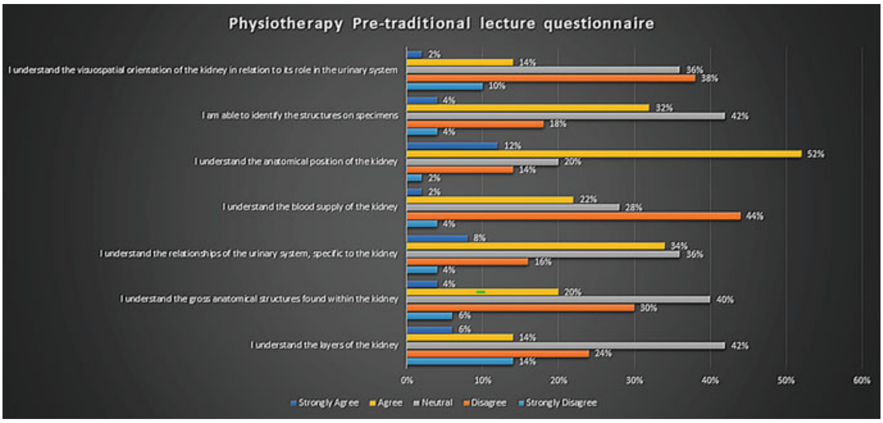

Question	Strongly Disagree	Disagree	Neutral	Agree	Strongly Agree
I understand the layers of the kidney	14%	24%	42%	14%	6%
I understand the gross anatomical structures found within the kidney	6%	30%	40%	20%	4%
I understand the relationships of the urinary system, specific to the kidney	4%	16%	36%	34%	8%
I understand the blood supply of the kidney	4%	44%	28%	22%	2%
I understand the anatomical position of the kidney	2%	14%	20%	52%	12%
I am able to identify the structures on specimens	4%	18%	42%	32%	4%
I understand the visuospatial orientation of the kidney in relation to its role in the urinary system	10%	38%	36%	14%	2%

Fig. 8.20 Table showing percentages per question for the physiotherapy students (control group) before the traditional lecture was conducted

(Kapur et al. 2016). Overall, most authors favour the integration of ultrasound, as it allows for better 3D teaching and learning, including the surface anatomy correlation. Furthermore, apart from gaining the skills to perform and interpret ultrasound, students will also be able to analyse and apply this knowledge to physiological, surgical and diagnostic imaging concepts ('Teaching musculoskeletal ultrasound in the undergraduate medical curriculum–Tshibwabwa–2007–Medical Education–Wiley Online Library,' n.d.; Smith et al. 2018a, b).

Previous studies have revealed positive outcomes when incorporating the use of additional imaging modalities in teaching and learning. Preece and colleagues reported

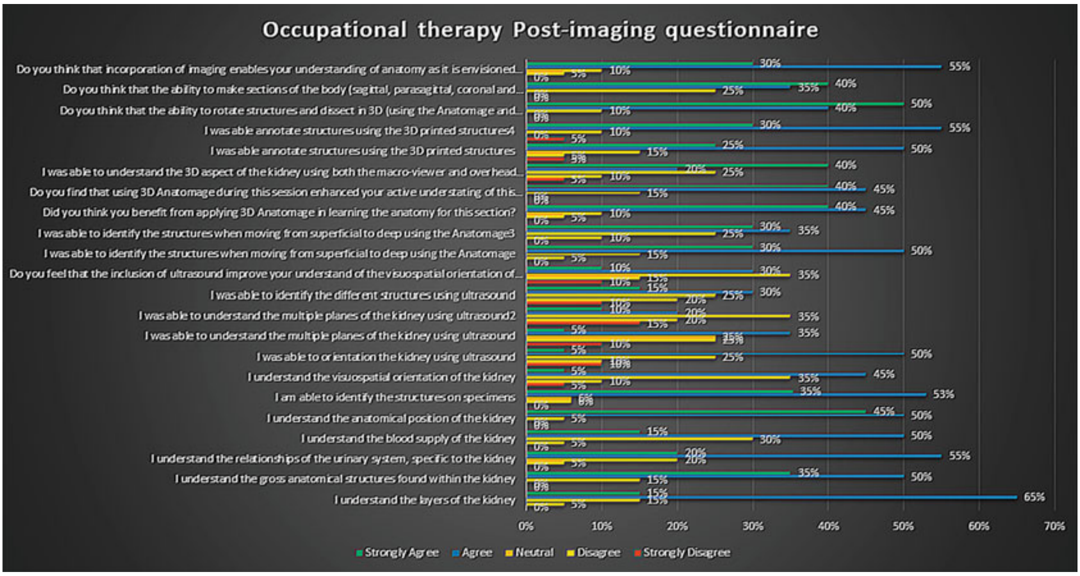

Fig. 8.21 Table showing percentages per question for the occupational therapy (intervention group) students after the imaging lecture

significantly higher performance scores when using 3D computer-printed models when compared to the standard textbook instruction. The authors concluded their study by stating there are significant advantages associated when using physical printed models in enhancing students' visuospatial appreciation and understanding of complex anatomical architecture (Preece et al. 2013). However, reports from more recent studies revealed that using 3D graphs and models to teach anatomy is the current trend, however, there are no additions to the advantages of this method when compared to traditional 2D material (Gonzales 2019).

In another comparative study conducted on a group of radiology students, the authors assessed two approaches of integration in a basic imaging module. The first was the integration of imaging modalities under a subject area, whilst the second was the integration of a subject area under one imaging modality. Results reveal a favourable response from students towards the second approach. This approach allowed students to identify and augment images whilst doing multiple comparisons (AlQahtani 2018).

Various authors have advocated for the growth potential of biomedical technology in medical education as an adjuvant or replacement for traditional teaching and learning methods (Alfalah et al. 2019). As this speaks to the demand to modernise conventional teaching methods on par with emerging technology. Additionally, by incorporating imaging modalities into teaching and learning, there is a direct relevance and link to clinical situations, as well as the application for future clinical work (Nyhsen et al. 2013). Results from this pilot study further emphasise the positive outcomes when combining biomedical technology with teaching and learning.

Question	Strongly Disagree	Disagree	Neutral	Agree	Strongly Agree
I understand the layers of the kidney	0%	5%	15%	65%	15%
I understand the gross anatomical structures found within the kidney	0%	0%	15%	50%	35%
I understand the relationships of the urinary system, specific to the kidney	0%	5%	20%	55%	20%
I understand the blood supply of the kidney	0%	5%	30%	50%	15%
I understand the anatomical position of the kidney	0%	0%	5%	50%	45%
I am able to identify the structures on specimens	0%	6%	6%	53%	35%
I understand the visuospatial orientation of the kidney	5%	10%	35%	45%	5%
I was able to orientation the kidney using ultrasound	10%	10%	25%	50%	5%
I was able to understand the multiple planes of the kidney using ultrasound	10%	25%	25%	35%	5%
I was able to understand the multiple planes of the kidney using ultrasound2	15%	20%	35%	20%	10%
I was able to identify the different structures using ultrasound	10%	20%	25%	30%	15%
Do you feel that the inclusion of ultrasound improve your understand of the visuospatial orientation of the kidney?	10%	15%	35%	30%	10%
I was able to identify the structures when moving from superficial to deep using the Anatomage	0%	5%	15%	50%	30%
I was able to identify the structures when moving from superficial to deep using the Anatomage3	0%	10%	25%	35%	30%
Did you think you benefit from applying 3D Anatomage in learning the anatomy for this section?	0%	5%	10%	45%	40%
Do you find that using 3D Anatomage during this session enhanced your active understanding of this topic?	0%	0%	15%	45%	40%
I was able to understand the 3D aspect of the kidney using both the macro-viewer and overhead projector	5%	10%	25%	20%	40%
I was able annotate structures using the 3D printed structures	5%	5%	15%	50%	25%
I was able annotate structures using the 3D printed structures4	5%	0%	10%	55%	30%
Do you think that the ability to rotate structures and dissect in 3D (using the Anatomage and ultrasound) helps in visualizing the body system	0%	0%	10%	40%	50%
Do you think that the ability to make sections of the body (sagittal, parasagittal, coronal and transverse) using imaging modalities enhanced your understanding of the location and relationships of the internal structures for this topic?	0%	0%	25%	35%	40%
Do you think that incorporation of imaging enables your understanding of anatomy as it is envisioned through medical imaging?	0%	5%	10%	55%	30%

Fig. 8.21 (continued)

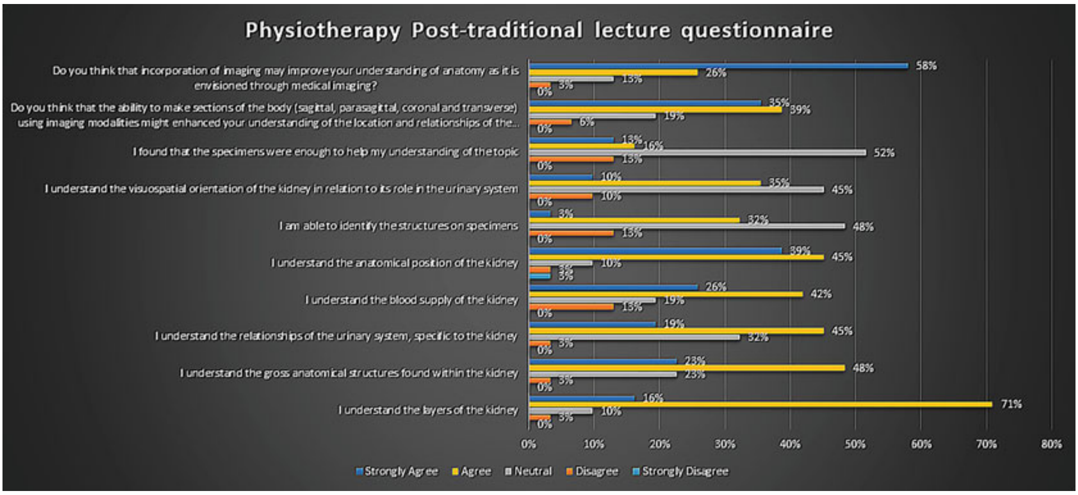

Question	Strongly Disagree	Disagree	Neutral	Agree	Strongly Agree
I understand the layers of the kidney	0%	3%	10%	71%	16%
I understand the gross anatomical structures found within the kidney	0%	3%	23%	48%	23%
I understand the relationships of the urinary system, specific to the kidney	0%	3%	32%	45%	19%
I understand the blood supply of the kidney	0%	13%	19%	42%	26%
I understand the anatomical position of the kidney	3%	3%	10%	45%	39%
I am able to identify the structures on specimens	0%	13%	48%	32%	3%
I understand the visuospatial orientation of the kidney in relation to its role in the urinary system	0%	10%	45%	35%	10%
I found that the specimens were enough to help my understanding of the topic	0%	13%	52%	16%	13%
Do you think that the ability to make sections of the body (sagittal, parasagittal, coronal and transverse) using imaging modalities might enhanced your understanding of the location and relationships of the internal structures for this topic?	0%	6%	19%	39%	35%
Do you think that incorporation of imaging may improve your understanding of anatomy as it is envisioned through medical imaging?	0%	3%	13%	26%	58%

Fig. 8.22 Table showing percentages per question for the physiotherapy students (control group) after the traditional lecture

8.12 Conclusion

Anatomy is a discipline that has gone through multiple transitions that are linked to the expansion of medical knowledge, the implementation of integrated clinical-based teaching and learning, a decrease in the availability of cadaveric material and the exponential advancements in technology. New pedagogical techniques can be developed whilst integrating biomedical imaging modalities within the objective-driven anatomy curricula. This can lead to improved visuospatial abilities, resulting in greater retention of anatomical knowledge and enhanced clinical skills. Overall this study revealed that students at a first and second-year level lack a basic understanding of visuospatial and 3D spatial plane orientation. However, if exposed at an early stage to imaging modalities through teaching and learning these gaps can be bridged, setting the foundation for developing clinical skills and providing the visuospatial awareness of anatomical structures. We believed that this can be achieved through technology as long as there is a balance between memorisation, understanding, spatial orientation and visualisation in order to meet the necessitating intellectual effort of learning anatomy.

Acknowledgements The authors would like to thank the students for their enthusiasm to participate in the study. As well as the families, that consistently provide support.

References

Alfalah SFM, Falah JFM, Alfalah T, Elfalah M, Muhaidat N, Falah O (2019) A comparative study between a virtual reality heart anatomy system and traditional medical teaching modalities. Virtual Reality 23:229–234. https://doi.org/10.1007/s10055-018-0359-y

Allen MA, Kirkpatrick N, Agosto ER (2019) Anatomage table 6. J Electron Res Med Libr 16:59–66. https://doi.org/10.1080/15424065.2019.1638866

AlQahtani F (2018) Radiology learning or teaching subject areas vs modalities: students&#39; perspective and experience at Albaha University. AMEP 9:791–799. https://doi.org/10.2147/AMEP.S171977

Arráez-Aybar LA, Castaño-Collado G, Casado-Morales MI (2008) Dissection as a modulator of emotional attitudes and reactions of future health professionals. Med Educ 42(6):563–571

Attardi SM, Barbeau ML, Rogers KA (2018) Improving online interactions: lessons from an online anatomy course with a laboratory for undergraduate students. Anat Sci Educ 11:592–604. https://doi.org/10.1002/ase1776

Aydın M, Yılmaz MT, Şeker M (2020) Evaluation of the relationship between spatial abilities and anatomy learning. Anatomy 14:139–144. https://doi.org/10.2399/ana.20.769500

Azer SA, Eizenberg N (2007) Do we need dissection in an integrated problem-based learning medical course? Perceptions of first- and second-year students. Surg Radiol Anat 29:173–180

Baratz G, Wilson-Delfosse AL, Singelyn BM, Allan KC, Rieth GE, Ratnaparkhi R, Jenks BP, Carlton C, Freeman BK, Wish-Baratz S (2019) Evaluating the Anatomage table compared to cadaveric dissection as a learning modality for gross anatomy. Med Sci Educ 29:499–506. https://doi.org/10.1007/s40670-019-00719-z

Benly P (2014) Teaching methodologies on anatomy- a review. J Pharm Sci Res 6:242–243

Bork F, Stratmann L, Enssle S, Eck U, Navab N, Waschke J, Kugelmann D (2019) The benefits of an augmented reality magic mirror system for integrated radiology teaching in gross anatomy: anatomical sciences education. Anat Sci Educ 12:585–598. https://doi.org/10.1002/ase.1864

Calkins CM, Franciosi JP, Kolesari GL (1999) Human anatomical science and illustration: the origin of two inseparable disciplines. Clin Anat 12:120–129

Carter JL, Hocum G, Pellicer R, Patel A, Benninger B (2016) Integration of 3D/4D ultrasound in teaching medical anatomy. Med Sci Educ 26:343–348. https://doi.org/10.1007/s40670-016-0271-6

Castro FS, Landeira-Fernandez J (2011) Soul, body and the ancient greek civilization: the first observations of brain functioning and mental activities. Psicol Reflex Crit 24:798–809

Collins JP (2008) Modern approaches to teaching and learning anatomy. BMJ 337:a1310

Dahle LO, Brynhildsen J, Behrbohm Fallsberg M, Rundquist I, Hammar M (2002) Pros and cons of vertical integration between clinical medicine and basic science within a problem-based undergraduate medical curriculum: examples and experiences from Linköping, Sweden. Med Teach 24:280–285

Dev P (1999) Imaging and visualization in medical education. IEEE Comput Grap Appl 19:21–31. https://doi.org/10.1109/38.761545

Estai M, Bunt S (2016) Best teaching practices in anatomy education: a critical review. Ann Anat 208:151–157

Feldman MK, Katyal S, Blackwood MS (2009) US Artifacts. Radio Graphics 29:1179–1189. https://doi.org/10.1148/rg.294085199

Friedlander MJ, Andrews L, Armstrong EG, Aschenbrenner C, Kass JS, Ogden P, Schwartzstein R, Viggiano TR (2011) What can medical education learn from the neurobiology of learning? Acad Med 86:415–420. https://doi.org/10.1097/ACM.0b013e31820dc197

Gerrard C, Roberts S (2012) Ultrasound-guided regional Anaesthesia in the Paediatric population. ISRN Anesthesiol 2012:1–7. https://doi.org/10.5402/2012/169043

Ghosh SK (2015) Human cadaveric dissection: a historical account from ancient Greece to the modern era. Anat Cell Biol 48(3):153–169. https://doi.org/10.5115/acb.2015.48.3.153. Epub 2015 Sep 22. PMID: 26417475; PMCID: PMC4582158

Govender S (n.d.) Critical analysis of the macro- and sonographic anatomy of the brachial plexus

Hu YY, Mazer LM, Yule SJ, Arriaga AF, Greenberg CC, Lipsitz SR, Gawande AA, Smink DS (2017) Complementing operating room teaching with video-based coaching. JAMA Surg 152(4):318–325

Gonzales DRA (2019) The impact of spatial awareness training on spatial ability, anatomy learning, manual dexterity and surgical skills 215

Gutierrez JC (2019) Spatial and visual reasoning in biomedical education: the possible contributions of anatomical learning. AJBSR 1:214–216. https://doi.org/10.34297/AJBSR.2019.01.000545

Ihnatsenka B, Boezaart AP (2010) Ultrasound: basic understanding and learning the language. Int J Shoulder Surg 4:55–62. https://doi.org/10.4103/0973-6042.76960

Ivanusic J, Cowie B, Barrington M (2010) Undergraduate student perceptions of the use of ultrasonography in the study of "Living Anatomy.". Anat Sci Educ 3:318–322. https://doi.org/10.1002/ase.180

Iwanaga J, Loukas M, Dumont AS, Tubbs RS (2021) A review of anatomy education during and after the COVID-19 pandemic: revisiting traditional and modern methods to achieve future innovation. Clin Anat 34:108–114

Jurjus RA, Dimorier K, Brown K, Slaby F, Shokoohi H, Boniface K, Liu YT (2014) Can anatomists teach living anatomy using ultrasound as a teaching tool? Ultrasound for teaching anatomy. Am Assoc Anat 7:340–349. https://doi.org/10.1002/ase.1417

Kapur J, Han T, Quek ST, Kanagasuntheram R, Ng YK, Lim A, Chong YS, Yeoh KG, Lee SS, Samarasekera D (2016) The role of ultrasound in teaching clinical anatomy to first year medical students. Med EdPublish 5:29. https://doi.org/10.15694/mep.2016.000029

Kazoka D, Pilmane M (2019) 3D dissection tools in Anatomage supported interactive human anatomy teaching and learning. SHS Web Conf 68:02015. https://doi.org/10.1051/shsconf/20196802015

Lufler RS, Zumwalt AC, Romney CA, Hoagland TM (2012) Effect of visual-spatial ability on medical students' performance in a gross anatomy course. Anat Sci Ed 5:3–9. https://doi.org/10.1002/ase.264

Luursema J-M, Vorstenbosch M, Kooloos J (2017) Stereopsis, visuospatial ability, and virtual reality in anatomy learning. Anat Res Int 2017:1–7. https://doi.org/10.1155/2017/1493135

Malomo AO, Idowu OE, Osuagwu FC (2006) Lessons from history: human anatomy, from the origin to the renaissance. Int J Morphol 24:24

Müller-Stich BP, Löb N, Wald D, Bruckner T, Meinzer H-P, Kadmon M, Büchler MW, Fischer L (2013) Regular three-dimensional presentations improve in the identification of surgical liver anatomy–a randomized study. Randomized Controlled Trial 13:131

Nguyen N, Mulla A, Nelson AJ, Wilson TD (2014) Visuospatial anatomy comprehension: the role of spatial visualization ability and problem-solving strategies: spatial anatomy task performance. Am Assoc Anat 7:280–288. https://doi.org/10.1002/ase.1415

Nyhsen CM, Steinberg LJ, O'Connell JE (2013) Undergraduate radiology teaching from the student's perspective. Insights Imaging 4:103–109. https://doi.org/10.1007/s13244-012-0206-8

Older J (2004) Anatomy: a must for teaching the next generation. Surgeon 2:79–90

Patankar SB, Padasalagi GR (2017) Three-dimensional versus two-dimensional laparoscopy in urology: a randomized study. Indian J Urol 33:226–229

Preece D, Williams SB, Lam R, Weller R (2013) "Let's get physical": advantages of a physical model over 3D computer models and textbooks in learning imaging anatomy: let's get physical. Am Assoc Anat 6:216–224. https://doi.org/10.1002/ase.1345

Queiroz CAF (2005) The user human corpses as a tool to build up knowledge from a bioethical view. In: Dissertation. Goiânia (GO): postgraduate program in environmental sciences and health. Catholic University of Goiás

Raja B, Chandra A, Azam M, Das S, Agarwal A (2022) Anatomage–the virtual dissection tool and its uses: a narrative review. J Postgrad Med 68:156. https://doi.org/10.4103/jpgm.jpgm_1210_21

Reidenberg JS, Laitman JT (2002) The new face of gross anatomy. Anat Rec 269(2):81–88

Roach VA, Mi M, Mussell J, Van Nuland SE, Lufler RS, DeVeau KM, Dunham SM, Husmann P, Herriott HL, Edwards DN, Doubleday AF, Wilson BM, Wilson AB (2021) Correlating spatial ability with anatomy assessment performance: a meta-analysis. Anat Sci Educ 14:317–329. https://doi.org/10.1002/ase.2029

Royer DF (2016) The role of ultrasound in graduate anatomy education: current state of integration in the United States and faculty perceptions: ultrasound in graduate anatomy education. Am Assoc Anat 9:453–467. https://doi.org/10.1002/ase.1598

Sakas G (2002) Trends in medical imaging: from 2D to 3D. Comput Graph 26:577–587

Salewski C, Nemeth A, Sandoval Boburg R, Berger R, Hamdoun H, Frenz H, Spintzyk S, Hahn JK, Schlensak C, Krüger T (2022) The impact of 3D printed models on spatial orientation in echocardiography teaching. BMC Med Educ 22:180

Santana LI, Buchaim DV, Hamzé AL, Reis CHB, de Souza Bueno CR et al (2022) The history of anatomy, its importance and new trends in the teaching/learning process. Arch Anat Physiol 7:001–004

Schramek GGR, Stoevesandt D, Reising A, Kielstein JT, Hiss M, Kielstein H (2013) Imaging in anatomy: a comparison of imaging techniques in embalmed human cadavers. BMC Med Educ 13:7

Smith CF, Tollemache N, Covill D, Johnston M (2018a) Take away body parts! An investigation into the use of 3D-printed anatomical models in undergraduate anatomy education. Anat Sci Educ 11:44–53. https://doi.org/10.1002/ase.1718

Simão TRP, Miglino MA, da Silva JB, Mcmanus C, Liberti EA (2016) Implementation of a program of voluntary body donation for anatomical study in the University of São Paulo, Brazil. Int J Morphol 34: 1494–1501

Slotnick HB, Hilton SR (2006) Proto-professionalism and the dissecting laboratory. Clin Anat 19:429–436

Smith JP, Kendall JL, Royer DF (2018b) Improved medical student perception of ultrasound using a paired anatomy teaching assistant and clinician teaching model: anatomy TA-clinician teaching model for ultrasound. Am Assoc Anat 11:175–184. https://doi.org/10.1002/ase.1722

Sugand K, Abrahams P, Khurana A (2010) The anatomy of anatomy: a review for its modernization. Anat Sci Educ 3:83–93

Teaching musculoskeletal ultrasound in the undergraduate medical curriculum–Tshibwabwa–2007–Medical Education–Wiley Online Library [WWW Document] (n.d.). URL https://onlinelibrary-wiley-com.uplib.idm.oclc.org/doi/full/10.1111/j.1365-2929.2007.02745.x. Accessed 13 Dec 22

Tyler C, Likova L (2012) The role of the visual arts in enhancing the learning process. Front Hum Neurosci 6

Venables H (2011) How does ultrasound work? Ultrasound 19:44–49. https://doi.org/10.1258/ult.2010.010051

Wu A-M, Wang K, Wang J-S, Chen C-H, Yang X-D, Ni W-F, Hu Y-Z (2018) The addition of 3D printed models to enhance the teaching and learning of bone spatial anatomy and fractures for undergraduate students: a randomized controlled study. Ann Transl Med 6:403

Yuen J (2020) What is the role of 3D printing in undergraduate anatomy education? A scoping review of current literature and recommendations. Med Sci Educ 30:1321–1329

Zargaran A, Turki MA, Bhaskar J, Spiers HVM, Zargaran D (2020) The role of technology in anatomy teaching: striking the right balance. Adv Med Educ Pract 11: 259–266. https://doi.org/10.2147/AMEP.S240150

Zhang X, Yang J, Chen N, Zhang S, Xu Y, Tan L (2019) Modelling and simulation of an anatomy teaching system. Vis Comput Ind Biomed Art 2(1):1–8

Ultrasound Imaging for Musculoskeletal Research

9

Nkhensani Mogale

Abstract

Ultrasound (US) imaging has seen major advancements over the last few decades, with this imaging modality becoming routinely used during the initial clinical assessment. The use of US as a medical imaging device can be traced back to 1942 and has been in use since. The cost, ease of access, and pain-free applications associated with US imaging, makes this imaging modality preferred by patients. US skills coupled with anatomical knowledge make clinical diagnosis using US more accurate in patient care.

US is used in both inflammatory and non-inflammatory diseases. Rheumatologists have advanced the treatment of various forms of arthritis and have employed US as a means of assessing the type of arthritis present and determining the appropriate treatment plan. Medical examinations using US are advantageous to patient education and provide the rationale for the treatment choice. The advancement of US imaging has improved extensively and is in some settings documented as being as effective as MRI and CT imaging. US imaging in the treatment of musculoskeletal diseases has seen many improvements, with some applications noted in the assessment of pressure ulcers in patients presenting with a spinal cord injury. US is used to evaluate the tissue found superficial to the ischial tuberosity and is used to document tissue properties that make patients susceptible to the development of pressure ulcers.

This chapter outlines the history of US imaging and its role in the treatment of various musculoskeletal diseases such as arthritis. Probe selection plays an important role in diagnosis as it allows for the optimization of an image and as such disease monitoring. The role of US in the investigation of tissue composition below the ischial tuberosity and its role in the evaluation of pressure ulcers will be covered in this chapter, as well as the future direction of US imaging. Fusion imaging, 3D imaging and contrast-enhanced US are some of the recent advances made in rheumatology, which seek to combine and overcome the limitations associated with MRI and CT imaging. The high learning curve associated with US imaging when weighed against its benefits, makes point of care ultrasound (POCUS) ideal for the clinical setting.

Keywords

Ultrasound imaging · Pressure ulcers · Ischial tuberosity · Musculoskeletal ultrasound

---

N. Mogale (✉)
Department of Anatomy, School of Medicine, Faculty of Health Sciences, University of Pretoria, Pretoria, South Africa
e-mail: nkhensani.mogale@up.ac.za

© The Author(s), under exclusive license to Springer Nature Switzerland AG 2023

L. Shapiro (ed.), *Microscopy Techniques for Biomedical Education and Healthcare Practice*, Biomedical Visualization 2, https://doi.org/10.1007/978-3-031-36850-9_9

9.1 Introduction

Ultrasound (US) is a term used to refer to non-audible, high-frequency sound waves of over 20 kHz (kilohertz). This form of imaging is desirable due to the cost-effective nature and safety associated with US sonography. US as an imaging modality has been used as a medical diagnostic tool since 1942 (Dussik 1942). The use of US by radiologists was first documented in 1972 (McDonald and Leopold 1972). Due to ease of access and portability of this technology, more clinicians are using US sonography for routine clinical examinations. Rheumatologists have started using US for earlier detection and treatment plan for patients presenting with inflammatory arthritis. Early and aggressive therapy for inflammatory arthritis has been shown to alter prognosis significantly. The use of US as a screening tool plays an important role in accurate disease diagnosis, the assessment of tissue damage, disease monitoring, and assessment of the effectiveness of the treatment plan. The quick scan time without radiation and noninvasive nature of US provides the benefit of imaging multiple joints in one session. Radiologists are also able to perform contralateral examinations within a reasonable time (Dasgupta and Patil 2012). The ability of US to, in real-time, allow the visualization of something like a needle during guided procedures without the threat of metal artifacts, such as the case of magnetic resonance imaging (MRI), makes it an ideal imaging modality. Metal implants that are used in various surgical reconstructive procedures produce metal artifacts which result in distorted images when using MRI. Patients who have had reconstructive surgery may require additional imaging in preparation for revision procedures, as failure rates following procedures such as spinal fusion can be as high as 30–40% (Javid and Hadar 1998; Ryken et al. 2003; Mekhail et al. 2011). Patients may also have other metallic articles such as fixation screws or surgical pins, surgical clips, dental fillings, and some intrauterine devices (IUDs) which may not be compatible with the MRI imaging environment. MRI devices are magnetic which may cause ferromagnetic objects to react to the static magnetic field. Some implants may heat up due to their interaction with the radiofrequency fields produced by the MRI (Kanal et al. 1990; Wildermuth et al. 1998; Nitz et al. 2001).

US use is displayed by various animals such as dolphins and dogs, who communicate using ultrasonic sounds. Species such as bats use US to navigate their surroundings in flight as well as to locate food. The experiment carried out by Lazzaro Spallanzani (1729–1799) on bats is often associated with discussions around US imaging (Eisenberg 1992). Following Spallanzani's findings, further investigations by Donald R. Griffin and Robert Galambos (1949) were conducted with a sonic detector to record the ultrasonic waves emitted by bats (Griffin and Galambos 1941). US has been used as a highly effective way of detecting objects and measuring distances by submarines and battleships. The term "echolocation" is used to describe directional sound reflection, and was initially developed for nautical purposes following the sinking of the *Titanic*. In 1912, Reginal A. Fessenden patented devices using echolocation leading to the building of the first sonar in 1914 which could detect an iceberg from a distance of 3.22 km (2 miles). This technology was superseded by Paul Langevin and Constantin Chilowsky who constructed an underwater sound generator using quartz crystals and two steel plates. This became the prototype for modern US devices (Hill 1973). The development of medical diagnostic US therefore owes its development to military and industrial applications.

In 1942, US became a medical diagnostic tool and was used by Karl Dussik in his attempt to locate brain tumors and cerebral ventricles (Dussik 1942). These findings were expanded upon by John Julian Wild, a Cambridge medical graduate, who went on to lay the foundation for ultrasonic tissue diagnosis. Wild published the A-mode (amplitude mode) of the intestinal and breast malignancies and in 1955 developed a linear handheld B-mode (brightness mode) device, the earliest known description of an endoscopic A-mode scanning transducer, used for transrectal and transvaginal scanning (Shampo and Kyle 1997).

A critical figure in the development of medical US in the clinical setting is Professor Ian Donald whose interest in medical US was sparked by meeting John Wild. Donald's initial encounter with US was during World War II when he served in the Royal Air Force. Following becoming the Regius Professor in Midwifery at the University of Glasgow, Donald and colleagues started numerous studies which led to the establishment of the role of medical ultrasound. Donald used a "flaw detector" to differentiate between solid and cystic abdominal masses. In 1958, this technology led Donald and colleagues to publish their findings following the diagnosis of a simple ovarian cyst initially thought to be a terminal carcinoma. This was a significant milestone in medical diagnosis (Donald et al. 1958). In 1960, Donald and colleagues developed an automatic scanner following the development of a two-dimensional scanner, and made the first antepartum diagnosis of placenta previa using US. In 1962, further advancements were made with the development of a method for measuring the biparietal diameter of the fetal head. In 1963, Donald contributed to another medical first, by utilizing the full bladder to detect pregnancy of about 6–7 weeks gestation (Kurjak 2000).

9.1.1 History of Musculoskeletal US

In 1958, Dussik published the first report on musculoskeletal ultrasonography. In his report, he measured acoustic attenuation of articular and periarticular tissues including skin, adipose tissue, muscle, tendon, articular capsule, articular cartilage, and bone (Dussik et al. 1958). The work published by Dussik lay a foundation for musculoskeletal US through the investigation of the effects of different pathological processes in articular tissues on US attenuation (Kane et al. 2004). The first B-scan image which included the differentiation of Baker's cysts from thrombophlebitis was described by Daniel McDonald and George Leopold in 1972 (McDonald and Leopold 1972). This knowledge has built the foundation for improvements in ultrasonography with these including power Doppler, linear array technology, and improved computer processing. Marnix van Holsbeeck (1991) and Bruno Fornage (1995) improved on this foundation which has now contributed to the description of the musculoskeletal system in health and disease (Van Holsbeeck and Introcaso 1991; Fornage 1995). The practical application of US musculoskeletal disease diagnosis relating to congenital dislocation of the hip was led by an orthopedic surgeon, Reinhard Graf in 1980. The ideas as set out by Graf (1980) led to the way in which musculoskeletal US imaging was performed, with this knowledge extending to clinical obstetrics (Kane et al. 2004).

US imaging among rheumatologists was responsible for advances in the diagnosis of rheumatoid diseases. Synovitis in rheumatoid arthritis was first demonstrated by Peter L. Cooperberg, who in 1978 correlated his grayscaled imagery of joint infusion and related synovial thickening with treatment using yttrium-90 injection in the clinical setting (Cooperberg et al. 1978). The first detailed features of synovitis and tenosynovitis were in a rheumatoid hand and the published description of rheumatoid erosion detection using US was captured in 1988 by De Flaviis (De Flaviis 1988). In 1994 Newman reported on the first application using power Doppler in soft tissue hyperemia in a case of musculoskeletal disease (Newman et al. 1994). A report on using US-guided techniques for joint aspirations took place in 1981 and was described by Brian M. Gompels (Gompels and Darlington 1981). The sensitivity of US has improved over the years, with documented cases of rheumatoid erosion imaging (Wakefield et al. 2000), scleroderma (Cosnes et al. 2003), joint studies (Wakefield et al. 2003), US-guided joint aspiration (Balint et al. 2002), and US-guided joint injection (Naredo et al. 2004).

9.1.2 The Role of US in Musculoskeletal Applications

Musculoskeletal US is used for a variety of soft tissue ailments which present as both inflammatory and noninflammatory diseases. Ultrasound is able to detect features that are unique to each ailment, which results in more precise diagnosis, resulting in better treatment plans. Evaluation of muscle volume and thickness was carried out by English et al. (2012) who in their study evaluated the upper and lower limb muscles in individuals with neuromusculoskeletal disorders as well as healthy individuals (English et al. 2012). Previous studies by van Drongelen et al. (2007) and Fournier et al. (2017) evaluated the supraspinatus and biceps tendon thickness by looking at the echogenicity of these muscles in wheelchair users (van Drongelen et al. 2007; Fournier et al. 2017). Other applications of US in musculoskeletal applications include the assessment of skin thickness in individuals with spinal cord injuries (Yalcin et al. 2013), the thickness of adipose tissue in young adult participants (Leahy et al. 2012) as well as the course of the median nerve in healthy participants compared with individuals with carpal tunnel syndrome (Paquette et al. 2015). Ultrasonography has been used in the skin assessments of vascular surgery patients in the heels and coccygeal areas (Porter-Armstrong et al. 2013).

Features that are unique to various forms of arthritis can be detected using US imaging. In inflammatory arthritis, US is able to detect tenosynovitis, synovitis with hypervascularity, joint effusions, and erosions. The detection of a tendon rupture and swelling of the median nerve are features that can also be detected by US. Osteoarthritis is also a common US feature and is seen as presenting with effusion, osteophytes, and joint space narrowing. During clinical examination of osteoarthritis, US may also detect a notch sign, synovitis, tenosynovitis, ganglions, and nerve sheath deposits. Crystal arthritis is usually present in US as synovitis, joint effusions, gouty erosions, tophi, and chondrocalcinosis. Possible findings of crystal arthritis may also appear as a double contour sign “snowstorm” appearance detected by the US (Dasgupta and Patil 2012).

Clinical rheumatologists use US imaging to detect inflammatory arthritis and enthesitis and monitor ongoing disease activity and changes in patients who have already been diagnosed with arthritis. The joints commonly imaged are the shoulder, elbow, wrist, hand, knee, ankle, and foot where nerve entrapments and periarticular pain may be present. This imaging modality is also used for needle-guided techniques such as aspirations, biopsies of synovial tissue, and injections (Hassan 2018) particularly of deep joints such as the hip joint in obese patients in whom such procedures may be challenging.

Rheumatoid Arthritis

Rheumatoid arthritis, an autoimmune disease where the body’s own immune system attacks a patient’s own body’s tissue, affects many joints including the joints of the hands and feet. This chronic inflammatory disorder affects the inner lining of joints, resulting in painful swelling that can result in deformity of the joints and bone erosion. In the treatment action plan for rheumatoid arthritis, it appears that early diagnosis has an impact on the patient outcome. Noninflammatory diseases such as fibromyalgia can mimic inflammatory arthritis, making it difficult to diagnose during an initial examination. A study by Damjanov et al. (2012) showed a more accurate diagnosis of rheumatoid arthritis when US was used, which assists clinicians in predicting joint damage by assessing the disease activity (Damjanov et al. 2012). As such, the use of US during clinical assessment helps to remove challenges which would otherwise make such diagnoses difficult (Dasgupta and Patil 2012).

Synovitis

Synovial joints are lined with a synovial membrane which at times becomes inflamed, resulting in a medical condition known as synovitis. The use of US for the diagnosis of synovitis is more accurate and sensitive than clinical examination (Grassi 2003; Kane et al. 2003). MRI imaging techniques are not feasible for imaging rheumatoid arthritis due to the associated cost, availability, and patient tolerance for this imaging modality, it therefore remains a second- or third-line imaging tool after X-ray and US (Di Matteo et al. 2020). CT is unable to image soft tissue and uses ionizing radiation. Damjanov et al. (2012) documented a reliable Disease Activity Score (DAS) when US was used in 90 patients with active rheumatoid arthritis. In their study, Damjanov et al. (2012) noted the reliability of US in assessing disease activity and found US to be better at anticipating future joint damage. Ultrasound is able to detect synovial and tenosynovial effusion, soft tissue edema, bone erosions, and loss of cartilage and tendon tears (Filippucci et al. 2014; Bruyn et al. 2019). US can also be used to assess treatment responses by using power Doppler (Teh et al. 2003). Advances in US using Doppler imaging have shown the accuracy of synovitis diagnosis to be comparable with dynamic contrast-enhanced MRI (Szkudlarek et al. 2001; Terslev et al. 2003).

Erosions

A key feature of rheumatoid disease is bone erosion, which are defined as the discontinuity of the echogenic bone cortex larger than 2 mm in diameter (Wakefield et al. 2005; Bajaj et al. 2007). Rheumatoid arthritis not only damages the joint but can progressively lead to erosion of the bone as well. The presence and detection of erosion in the early stages of the disease normally require an aggressive treatment approach (Van Der Heijde et al. 1992). US sonography is documented as the best way to assess this damage in patients with rheumatoid arthritis, which is important in determining the prognosis for recovery (Bajaj et al. 2007). In the initial stages of the disease, this form of imaging is even more sensitive than the results of X-ray (Wakefield et al. 2000).

Tenosynovitis

Inflammation of the fluid-filled synovium found within the tendon sheath is a clinical term used to describe tenosynovitis. This presents clinically as swelling, pain, and contractures in the tendons of mostly the hand, wrist, and foot is a common feature of rheumatoid arthritis (Hmamouchi et al. 2011). The presence of tenosynovitis is not easy to detect as it may be diagnosed as a side effect of rheumatoid arthritis. Ultrasound has therefore become the gold standard in the detection and diagnosis of tenosynovitis (Grassi et al. 2000).

Psoriatic Arthritis

US is used in the detection of intra- and extra-articular psoriatic arthritis which causes affected joints to become swollen, stiff, and painful. This form of arthritis presents in some individuals as the skin condition known as psoriasis and can progressively worsen with time, leading to functional impairment in 50% of the patients (Gladman et al. 1987). De Simone et al. (2011) in their publication mentioned that routine screening of patients with psoriasis for musculoskeletal involvement assisted with the early detection of psoriatic arthritis (De Simone et al. 2011).

Osteoarthritis

US as an imaging modality is indicated as ideal for patients presenting with osteoarthritis (Koutroumpas et al. 2010). Osteoarthritis, which is sometimes referred to as a degenerative joint disease, is the most common form of arthritis. Osteoarthritis causes a breakdown of the cartilage lining the joint while also changing the underlying bone. These changes are commonly noted in the hips, knees, and hands and are commonly noted by loss of flexibility in the affected joint, pain, grating sensation to the joint, and joint stiffness. US imaging is used to detect various presentations associated with osteoarthritis.

Crystal Arthritis

This form of arthritis develops in individuals with deposits of calcium pyrophosphate crystals in their joints. The crystal deposits found in the joints reflect the US waves more strongly than the surrounding tissue within the joint. This makes US imaging ideal in the diagnosis of this type of clinical condition (Dasgupta and Patil 2012). Crystal arthritis usually presents with impaired use of the joint and with swelling, warmth, and joint pain being accompanying symptoms.

Medial and Lateral Epicondylitis

Epicondylitis is a clinical condition that results in pain on either side of the elbow. Medial epicondylitis, also called “golfer’s elbow” can result in weakness of the hands and stiffness of the elbow. Lateral epicondylitis, also referred to as “tennis elbow” usually results following overuse of the common extensor tendons, mainly the extensor carpi radialis brevis (Levin et al. 2005). Ultrasound is a useful tool for determining the presence of these two conditions and the extent of tendon damage in the affected patients. A lesion of the medial collateral ligament can be distinguished from medial epicondylitis using US imaging (Dasgupta and Patil 2012).

Enthesitis and Bursitis in Seronegative Spondyloarthropathy

Enthesitis refers to inflammation at the site where the tendons or ligaments insert onto the bone, while bursitis is inflammation of the bursae, which act as a cushion at the joints. Seronegative spondyloarthropathy is a term used to describe a family of joint disorders that are inclusive of reactive arthritis (previously known as Reiter syndrome), inflammatory bowel disease-associated arthritis, psoriatic arthritis, ankylosing spondylitis, and undifferentiated spondyloarthropathy. US is currently used in the clinical examination of peripheral enthesitis and spondyloarthropathy in adults and children (Gutierrez et al. 2011; Jousse-Joulin et al. 2011).

Carpal Tunnel Syndrome

Carpal tunnel syndrome, which is caused by compression on the median nerve within the carpal tunnel, presents as tingling or weakness in the arm and hand. US is used to detect the changes to the nerve and thereby affect the surgical approach and action plan. US is used to measure the cross-sectional area of the nerve, which if greater than 9 mm at the level of the pisiform, is a clear sign of median nerve compression (Duncan et al. 1999).

Polymyalgia Rheumatica

This inflammatory disorder is commonly associated with pain and stiffness around the hip joint and shoulder joint. Advancements in US technology have made it easier to diagnose polymyalgia rheumatica with typical findings noting bilateral subacromial bursitis, trochanteric bursitis, and biceps long-head tenosynovitis (Falsetti et al. 2011). Ultrasound, therefore, plays an important role in the assessment and diagnosis of various musculoskeletal diseases.

Vasculitis

The medical condition that results in the inflammation of blood vessels remains a mystery. The causes of vasculitis are mostly unknown, however, it is suspected to be caused by an infection or medication. Various authors have reported on the application of US in the diagnosis of vasculitis in large vessels (Schmidt et al. 2002, 2006; Schmidt and Blockmans 2005).

Giant cell arteritis diagnosis has increased due to the use of US, thereby preventing irreversible visual loss associated with the medical condition. This form of diagnosis is less invasive than the commonly used temporal artery biopsy which has a complication rate of 0.5%. The use of US as a diagnostic alternative allows the visualization of characteristic findings in the temporal artery (Arida et al. 2010).

Pediatric Rheumatology

The use of US imaging in place for other imaging modalities, which may produce radiation in young patients, makes this imaging modality ideal for this patient population in the treatment of musculoskeletal diseases. The use of US in young patients can be challenging, as cooperation from the patient is necessary in order to get the best image quality. US is also used to detect some pediatric-related arthritis and to evaluate the number of joints that may be affected. US can also detect changes to the affected joint when compared with what is deemed to be normal anatomy. A study by Wakefield et al. (2004) documented subclinical synovitis in two-thirds of the patients scanned while a study by Spârchez et al. (2010) found power Doppler use in children to be a superior form of imaging (Spârchez et al. 2010; Wakefield et al. 2004).

9.1.3 Advantages and Limitations of Using US for Diagnostic Purposes in Musculoskeletal Injuries

The noninvasive and cost-effective nature of US imaging makes it a well-accepted imaging modality for the patient population. Clinicians alike prefer using US as it allows for contralateral imaging without the threat of metal artifacts, which are a concern when using MRI. Needle-guided techniques using US make this form of imaging preferred due to real-time feedback (Del Cura 2008).

US imaging is beneficial for a variety of musculoskeletal applications including visualization of tendon instability as documented by Bianchi et al. (2001) and impingement of the shoulder as published by Bureau et al. (2006).

Limitations

Although US imaging has a variety of benefits, there are some limitations that are associated with this imaging modality. US is said to be user dependent and takes extensive training to be fully competent. Interpretation of US imagery also takes time, as artifacts may be detected which may be mistaken for some form of pathology. US imaging has the ability to limit the user's view in comparison to what is seen with MRI, and has the inability to penetrate structures such as bone (Hassan 2018). Pressure exerted over the tissue also plays a role in how the image is projected as well as transducer rotation which affects the geometric and grayscale measurements of the projected image (Whittaker et al. 2009; Ishida and Watanabe 2012; Ishida et al. 2017a, b).

9.2 Types of Transducers for Musculoskeletal Imaging

Advances in technology have led to the development of high-resolution transducers that can image superficial structures such as joints, tendons, and nerves in great detail and with a lateral and axial resolution of 0.1 mm.

Probe selection is important during US imaging, low-frequency curvilinear probes (3–5 MHz) (Fig. 9.1) target deeper structures and are better suited for imaging joints such as the hip and knee joints. These types of probes allow the US to penetrate to deeper structures. However, the resolution of the image may be poorer as a result (Louis 2008).

Linear probes (Fig. 9.2) with higher frequencies (7–15 MHz) lack the ability to penetrate to deeper structures during imaging and are therefore best used for needle-guided procedures to superficial structures (McNally and Rees 2007; Nazarian 2008).

Phased array transducers (Fig. 9.3) are named according to the arrangement of the piezoelectric crystals. These low-frequency transducers (2–7.5 MHz) have a small footprint to fit between ribs and are mostly used in cardiac imaging. The phased array transducer is also used for abdominal, brain, and transesophageal examinations (De Luca et al. 2018). In imaging the heart, the phased array transducer can be operated at different frequencies depending on the patient population: 4–12 MHz for neonates, 2–12 MHz for a

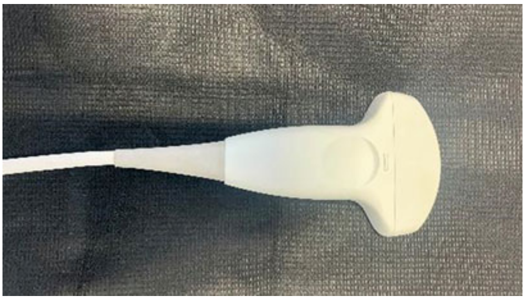

Fig. 9.1 Curvilinear probe (3–5 MHz) for imaging deeper structures including joints of the hip and knee

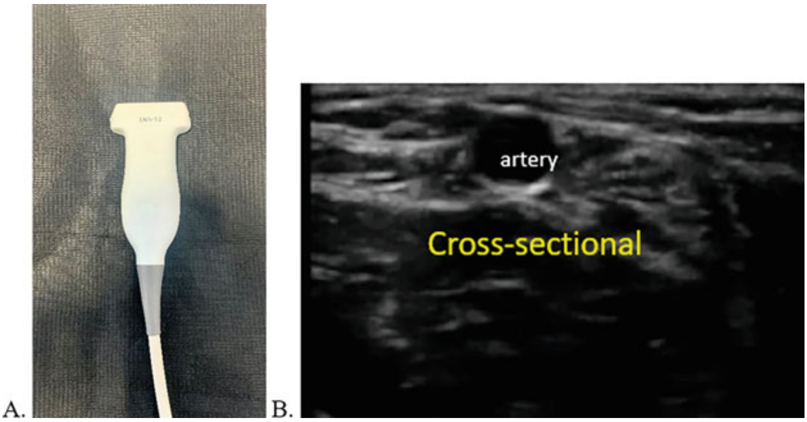

Fig. 9.2 (**a**) Linear probe (7–15 MHz) used for needle-guided procedures to superficial structures. (**b**) Cross-section through the forearm showing the radial artery imaged with a linear probe

pediatric sample, and 1–5 MHz for adults (Wildes and Smith 2012).

High-frequency probes such as the hockey stick transducers allow for better contact between small irregular surfaces and have a smaller footprint. These transducers are best used for guiding injections around the foot and hand (Fessell et al. 2000).

9.3 US Imaging for Seated Anatomy

9.3.1 The Role of US in the Early Detection of Pressure Ulcers

Background

The role of US imaging in the assessment of musculoskeletal diseases cannot be discounted, where in some instances it is comparable with more expensive imaging modalities such as MRI. US imaging is used in the assessment of pressure ulcers, which if not treated could lead to morbidity and mortality. This type of deep tissue injury could lead to osteomyelitis, sepsis, myocardial infarction, renal failure, or multiple organ failure (Agam and Gefen 2007).

Pressure ulcers resulting from long-term wheelchair use are commonly noted in individuals with spinal cord injuries. Pressure injuries, a resultant combination of shear forces and pressure, occur over bony prominences in the body, and can develop as early as 2 h following immobility (Bansal et al. 2005; NPUAP 2018). Various authors have alluded to the link between the development of pressure ulcers and tissue deformity (Oomens et al. 2003; Stekelenburg et al. 2006; Loerakker et al. 2011; Sprigle and

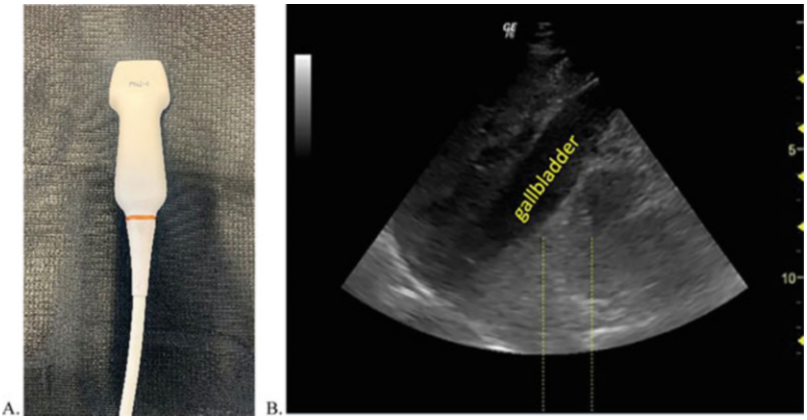

Fig. 9.3 (**a**) Phased array ultrasound probe, suited for cardiac imaging. (**b**) Ultrasound imaging of the gallbladder using a phased array probe. (**c**) Ultrasound imaging of the heart using a phased array probe

Sonenblum 2011; Oomens et al. 2015), with 50% of the spinal cord injured population developing pressure ulcers during their lifetime (Krause and Broderick 2004; Saunders et al. 2012). The spinal cord injured population includes individuals who suffer from a variety of ailments including multiple sclerosis, cerebral palsy, spina bifida, and other medical conditions which impact mobility and cause limited tissue sensation (LCD 2013). These individuals are mostly wheelchair dependent which puts them at risk of the development of pressure ulcers, which in seated individuals develop predominantly where body weight is distributed including areas such as the ischial tuberosity and related soft tissue (Stekelenburg et al. 2006). In their meta-analysis output, Gefen (2014) alludes to the changes caused by prolonged sitting following spinal cord injury. Challenges such as fluctuating weight, muscle atrophy, flattening of the ischial tuberosity and increased fat deposits in skeletal muscles, prolonged sitting due to the use of the wheelchair, are highlighted as contributing factors to the development of tissue injury (Gelis et al. 2009; Gefen 2014).

Pressure ulcers, a second most common complication, are estimated to be prevalent in 30–47% of the spinal cord injured population, with 15% of the pressure ulcers developing within the first-year post-injury (Donovan et al. 1984; McKinley et al. 1999; Wann-Hansson et al. 2008; Cowan et al. 2019). Two studies that reported on individuals living with spinal cord injuries for 20 and 25 years, noted the prevalence of pressure ulcers in 39% and 56%, respectively, in the population studied (Liem et al. 2004; Werhagen et al. 2012). A common pressure ulcer associated with prolonged wheelchair use is a sitting-acquired deep tissue injury that mostly develops in the gluteus muscle and the related soft tissue located under the ischial tuberosity (Gefen 2014). Deep tissue ulcers develop as a result of sustained loading, especially in the area found adjacent to bony prominences and present as blood-filled blisters or purple and blue colored areas over the skin (NPUAP 2018). These types of pressure ulcers are often diagnosed at a late stage as they start in the underlying tissue and are often only detected at an advanced stage. The cause of pressure ulcers is mostly unknown with speculations ranging from muscle atrophy, wheelchair design, and the type of cushion used in the wheelchair (Gefen 2014). Various speculating theories have implicated ischemia perfusion injury (Ytrehus et al. 1995; Blaisdell 2002; Tsuji et al. 2005), lymphatic drainage, and impaired interstitial fluid flow (Krouskop et al. 1978; Miller and Seale 1981; Reddy and Cochram 1981; Braden and Bergstrom 1987), and deformation of cells (Landsman et al. 1995; Bouten et al. 2003; Wang et al. 2005). Certain risk factors such as humidity, heat, and shearing make one more susceptible to developing pressure ulcers. This creates the need to better understand the anatomy of the buttocks and thighs and the tissues susceptible to pressure ulcers (Sonenblum et al. 2020). Call et al. (2017), Brienza et al. (2018), and Sonenblum et al. (2018, 2020) are some of the authors who have investigated the tissue under the ischium in an attempt to better understand seating anatomy. In their studies, various methods and imaging modalities were used, with US being the most accessible for such studies.

The advantages associated with US imaging include being portable, noninvasive, with few contraindications and rapid result interpretation (Yabunaka et al. 2009; Quintavalle et al. 2006; Lucas et al. 2014; Molinari et al. 2015). These advantages, therefore, make the use of US an attractive option for studying tissue changes and related treatment options.

When pressure is experienced in the body, this pressure stemming from an external source causes tissue deformity by relaying the pressure to the muscle, adipose tissue, and connective tissue, resulting in reduced blood flow, mechanical cell damage, and damage to the lymphatic system (Bouten et al. 2003; Oomens et al. 2015). Diagnostic US can therefore be used to identify individuals who are at risk of developing deep tissue injuries prior to presenting with the pressure ulcer.

In the detection of pressure ulcers using US, previous studies have detected the susceptibility to the development of this deep tissue injury as the appearance of less dense tissue with lower signal intensity when visualized with US. Additional detection of unclear layered structures or hypoechoic lesions is noted as common deep tissue injury presentations (Gnaidecka and Quistorff 1996; Johnson et al. 1998; Quintavalle et al. 2006). In the study by Swaine et al. (2018), US was used to detect abnormal tissue signs in 42% of their study sample. These signs were detected through the appearance of solid, cystic regions or a combination of solid and cystic regions over the lowest points of the ischial tuberosity. This is the point that experiences the most pressure when the sitting position is assumed (Swaine et al. 2018).

The movement toward studying seated anatomy has been limited, with some of the early work dating back to Dhami et al. (1985). In their study, Dhami et al. (1985) studied the contours of the ischial region by seating the participants in soft clay which created impressions and then comparing the findings between the participants. Deeper and sharper contours were documented in paraplegic participants with a history of pressure ulcers when compared with able-bodied participants (Dhami et al. 1985). The study by Wu and Bogie (2013) compared the muscle quality and quantity of the gluteus maximus muscle in able-bodied individuals and those with spinal cord injuries. Wu and Bogie (2013) reported on fatty infiltrations in the gluteus maximus muscle. However, findings from this study could not be properly compared as participants were scanned in a supine position, making it impossible to translate the findings to a seated position (Wu and Bogie 2013).

A paucity in the literature still exists relating to investigation of the tissue found beneath the ischial tuberosity in the seated position (Fig. 9.4). Studies present with different methodologies and different ideal imaging positions when the ischial tuberosity is imaged. The influence of the assumed position (prone, upright seated or lateral decubitus position) seems to play a role in the type of tissue present below the ischial tuberosity and the presence of the gluteus maximus muscle. Seat cushions and their role in deforming tissue anatomy were highlighted by Sonenblum et al. (2018), who in their study looked at the role of seat cushion design and its impact on tissue deformation. In their study, Sonenblum et al. (2018) used three cushion types; an orthotic offloading cushion (Java, Ride Designs), a pressure redistribution cushion made with contoured foam (Matrix Vi,

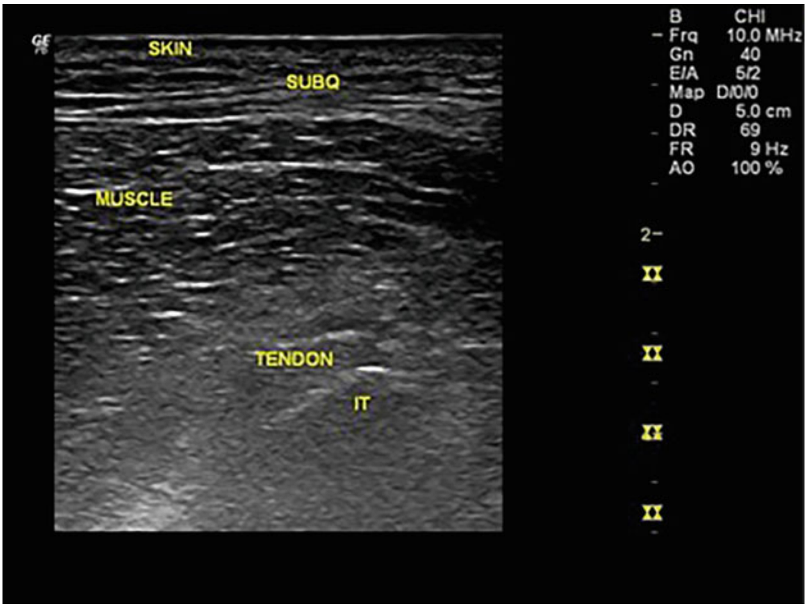

Fig. 9.4 US image of the unloaded tissue below the ischial tuberosity (IT). The image shows the skin, subcutaneous tissue (SUBQ), the muscle, tendon of the hamstrings, and the ischial tuberosity (IT)

Invacare), and a pressure redistribution cushion that uses air flotation (Roho HP, Permobil). Although the study made sure to offload the ischium in all the imaging procedures and align participants to have a neutral pelvis, the findings showed that tissue deformation was variable depending on the type of seat cushion used. The tissue type present below the ischial tuberosity was also influenced by the seat cushion type, indicating that seat cushion design plays a role in tissue deformity, which may also play a role in the development of pressure ulcers in individuals with spinal cord injuries who use wheelchairs for mobility (Sonenblum et al. 2018).

9.3.1.1 US Imaging of the Ischial Tuberosity

Diagnostic US is seen as an efficient tool for determining changes to soft tissue components such as the epidermis, dermis, subcutaneous tissue, muscle, tendons, and joints of the body.

Echogenicity is used to measure tissue integrity by evaluating the mean echogenicity values and contrasting the values with the muscle density and the presence of intramuscular adipose tissue (Reimers et al. 1993; Sipilä and Suominen 1993). Diagnostic US is able to detect changes in the muscle tissue, as muscle tissue which has disease present loses its striated pattern, appearing more brightly spotted and hyperechoic when using US (Heckmatt et al. 1982). Echogenicity, therefore, allows for the distinction and detection of muscle tissue changes (Whittaker et al. 2007; Pillen and van Alfen 2011) and allows the clinician to determine tissue integrity in the scanned muscle (Moghimi et al. 2010). Evaluation of individuals at risk of developing pressure ulcers is achieved using US. Clinical presentations such as dermal edema have been diagnosed by evaluating the changes in the echogenicity of the imaged tissue (Quintavalle et al. 2006; Lucas et al. 2014). Various other changes can be detected using US, which is useful for clinical diagnosis. US can be used to evaluate the progression of healing by studying the changes in tissue homogeneity (Rippon et al. 1998).

In the evaluation of the tissue overlying the ischial tuberosity, US imaging can be used in healthy participants to establish baseline measures for tissue composition. In a study by Akins et al. (2016), comparisons were made between two imaging modalities, MRI and B-mode US for evaluating tissue thickness overlying the ischial tuberosity. Akins et al. (2016) found comparable measurements between findings made using US with MRI measurements (Akins et al. 2016). Swaine et al. (2017) evaluated the operator reliability when imaging the soft tissue thickness below the ischial tuberosity under loaded and unloaded tissue conditions using US. Findings made by Swaine et al. (2017) showed good reliability between operators when able-bodied individuals and individuals with a spinal cord injury were imaged using US (Swaine et al. 2017). However, Akins et al. (2016) and Swaine et al. (2017) did not focus on echogenicity in their studies.

Soft tissue found below the ischial tuberosity (skin, subcutaneous tissue, hamstring tendons, and muscle) has varying viscoelastic properties, making it challenging to come up with one-size-fits-all solution for the prevention of pressure ulcers (van Loocke et al. 2008). A study by Courtney H. Lyder and Elizabeth A. Ayello (2008) recommended below 32 mmHg external pressure maintenance for tissue overlying the ischial tuberosity. Tissue stiffness is variable, muscle tissue for instance is more susceptible to applied loads compared to adipose tissue, while skin is more tolerant to compressive forces than muscle and adipose tissue. This suggests that muscle tissue may be more sensitive to applied loads when compared with adipose tissue and skin (van Loocke et al. 2008; Thorfinn et al. 2009). The difficulty to unload the ischial tuberosity for 2 min of every 15 min of sitting (due to immobility caused by the spinal cord injury) contributes to the development of pressure ulcers (Stockton and Parker 2002; Coggrave and Rose 2003; Houghton et al. 2013). However, it is worth noting that skin, subcutaneous tissue, and muscle undergo changes following a spinal cord injury as a result of disuse (Agrawal and Chauhan 2012;

Gefen 2014). Skin, although the tissue is less susceptible to pressure injuries, is found to lose 25% of its thickness over the ischial tuberosity in the spinal cord injured population (Makhsous et al. 2008; Yalcin et al. 2013). Dietary changes resulting in malnutrition, microvascular changes to the skin, reduced fibroelastic activity, and dehydration contribute to changes in the anatomy of the skin and result in less collagen being formed. A reduction in collagen production and the reduction in the thickness of the skin make individuals with spinal cord injuries more susceptible to the development of pressure ulcers during periods of increased loading to the ischial tuberosity (Stover et al. 1980; Claus-Walker and Halstead 1982; Vaziri et al. 1992; Dealey 2009; Yalcin et al. 2013; Gefen 2014). Muscles below the level of injury in individuals with spinal cord injury begin to atrophy as early as 4 weeks post-injury. Evidence of fat infiltration, reduced number of slow oxidative fibers, a greater presence of low-density muscles, macrovascular and microvascular changes are some of the changes to the anatomy that the spinal cord injured population experience (Giangregorio and McCartney 2006; Linder-Ganz et al. 2008; Carda et al. 2013; Wu and Bogie 2013; Gefen 2014).

9.4 Recent US Imaging Advances

Advances in US imaging are ongoing with a movement toward better image quality and coordination between various imaging modalities. Modern US devices are able to generate sound waves in the ranges of 2–15 MHz (Mega Hertz). US imaging works through a power source causing the vibration of piezoelectric crystals in the transducer to vibrate, which produce sound waves that course through the probe and into the body through a coupling medium which is the US gel. Upon encountering changes in the density between two adjacent tissues, some of the sound waves reflect back to the probe while the rest travel to deeper tissue in the body. The soundwaves that are reflected back into the probe are converted into electrical signals and will be seen as black and white images on the screen when the US is in B-mode (brightness mode). Structures that appear whiter when reflected back are said to be hyperechoic and this is caused by differences in the acoustic interfaces, such as what is noted between bone and cartilage, while bone produces a hyperechoic image. In instances where there is no density difference between two tissues, the sound waves travel straight through, giving the image a black appearance as seen when fluid is present in the body. As such, tissue echogenicity is classified as hyperechoic, hypoechoic (darker than surrounding structures), and anechoic (appearing black). Tissue echogenicity with normal characteristics displays tendon and ligament as hyperechoic structures, muscle and nerves with mixed echogenicity, and vessels as hypoechoic or at times anechoic (Smith and Finnoff 2009a, b; Hassan 2018).

Blood vessels can be further imaged and seen using the power Doppler (Fig. 9.5), which detects the movement of blood vessels and displays them in color. This is an essential tool used to detect pathology in areas normally properly vascularized, but now having limited blood flow or smaller blood vessels (Hassan 2018).

In brightness mode (B-mode), US allows for the imaging of tissue thickness, muscle sizes, and quality, progression of inflammation in the body and the orientation of blood vessels (Fig. 9.6) (English et al. 2012). In this mode, diagnostic US produces grayscale images which allow clinicians to assess soft tissue injury, wound healing, and changes to scar tissue as well as to clearly note muscle atrophy if present following the use of steroids (Rippon et al. 1998; Dyson et al. 2003). B-mode US has been validated and shown to be reliable for use in the evaluation of skeletal muscle size, and is comparable to both computerized tomography (CT) (Thomaes et al. 2012) and MRI, the current gold standards for imaging (Ahtiainen et al. 2009; Lucas et al. 2014). Musculoskeletal and neuromuscular diseases are also assessed with the grayscale

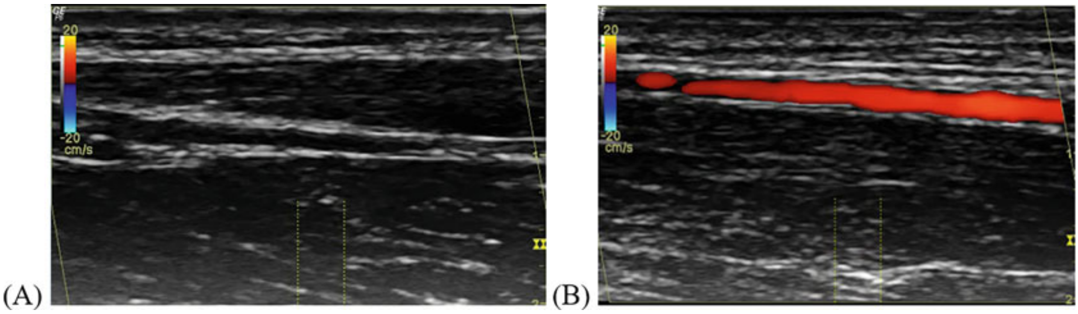

Fig. 9.5 (**a**) Ultrasound image of the longitudinal view of the radial artery through the brachium using a linear probe, (**b**) Doppler imaging is turned on to allow for viewing the artery

image, showing the importance and use of diagnostic US in the assessment of healthy tissue versus disease progression (Dudley-Javoroski et al. 2010; English et al. 2012; Thomaes et al. 2012).

Gray Level Co-occurrence Matrix (GLCM) is also used in ultrasonography by examining patterns of the pixel in pairs. This imaging is carried out by assigning each pixel a numeric value and comparing the pixel to those in close proximity to it by defining the pixel in a direction and space. The number of times the pixel pairs occur is then summarized and analysis is carried out by calculating the probability of occurrence of that pixel pair in an orthogonal direction (10). This analysis is used to yield information about tissue texture of the imaged tissue. In grayscale images analysis of US images, the pixel is assigned a numerical value in the range of 0–255, where 0 is equivalent to black and 255 to white (Gabison et al. 2018).

Contrast-Enhanced US

Doppler imaging, although effective, has some limitations in its ability to detect low-volume blood flow in very small vessels. Contrast agents compatible with US allow for increased sensitivity of color Doppler examination (Cimmono and Grassi 2008). The US contrast agents are becoming an important feature in the evaluation of disease progression. The use of contrast medium in imaging is more established for MRI imaging of

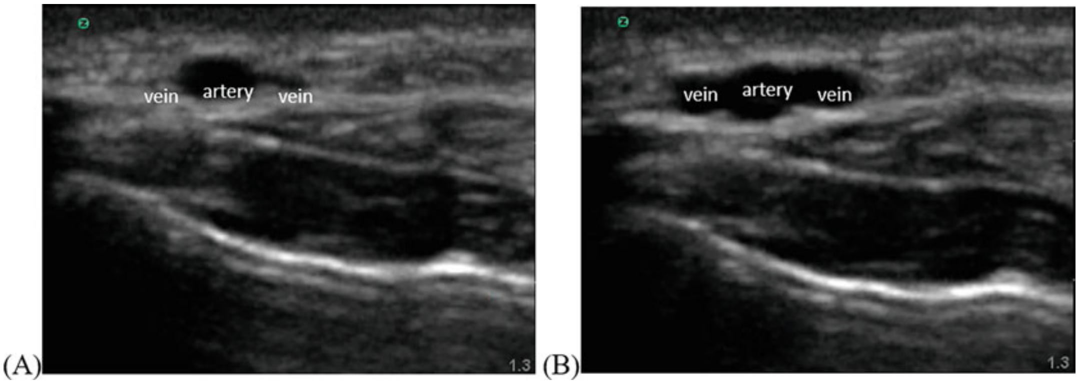

Fig. 9.6 (**a**) Cross section through the forearm showing the radial artery and accompanying venae comitantes compressed during imaging with the linear probe. (**b**) The radial artery can be better visualized with the venae comitantes no longer compressed

musculoskeletal anatomy and less so for US imaging (Dasgupta and Patil 2012).

Three-Dimensional (3D) US

Improvements and advances in imaging have allowed better visualization of the joint. This volumetric imaging technology has become widely used in obstetrics (fetal imaging), cardiology, and image-guided interventional procedures.

The early 1970s development of CT revolutionized imaging through the introduction of three-dimensional imaging, with the first commercial system only appearing in 1989. Future advancements which led to the introduction of MRI and positron emission tomography (PET) as well as multi-slice and cone beam CT imaging, have allowed for an improvement in applications in diagnostic and interventional medicine (Fenster et al. 2011).

US imaging, which has now introduced 3D imaging, has seen an improvement in this noninvasive imaging modality with more companies incorporating 3D imaging into US used in biopsy and therapy-related interventions (Chin et al. 1996, 1998; Smith et al. 2001; Wei et al. 2004; Carson and Fenster 2009).

A variety of benefits come with the use of 3D US imaging, including better visualization of the anatomy and pathology without the user needing to integrate various 2D images in order to arrive at a diagnosis. The viewing of planes parallel to the skin and accurate measurement of organs or lesions is also challenging with 2D US. These challenges can be overcome with the use of 3D US in which linear, tilt, and rotational scanners are used (Fenster et al. 2011).

Fusion Imaging

This is an imaging technique that fuses two different imaging modalities such as MRI, CT, or PET/CT data with US, allowing for more accurate diagnoses. In a study by Klauser et al. (2010), fusion imaging was used for improved accuracy in the injection of the sacroiliac joint, by combining real-time US imaging with previously obtained CT scans (Klauser et al. 2010).

9.5 Conclusion

US imaging has come a long way since its original inception and has become an important tool in musculoskeletal imaging. The quick access, portability, safe, and cost-effectiveness of US have made it an ideal imaging modality in the assessment of various musculoskeletal diagnoses, including arthritis. US use has also been noted to, in some instances, be as effective an imaging tool as MRI, without the ionizing radiation associated with MRI. US is able to, in real time, allow radiologists to image multiple joints in one session and come up with the best treatment options for diverse forms of arthritis. US imaging, despite its high learning curve, has been shown to be ideal in the early detection and treatment of musculoskeletal diseases. Recent advances in US imaging which include fusion imaging, 3D US, contrast-enhanced US are seeking to overcome some of the limitations associated with MRI and CT imaging while attempting to increase diagnostic accuracy.

References

Agam L, Gefen A (2007) Pressure ulcers and deep tissue injury: a bioengineering perspective. J Wound Care 16(8):336–342

Agrawal K, Chauhan N (2012) Pressure ulcers: back to the basics. Indian J Plast Surg 45:244–254

Ahtiainen JP, Hoffren M, Hulmi JJ, Pietikäinen M, Mero AA, Avela J, Häkkinen K (2009) Panoramic ultrasonography is a valid method to measure changes in skeletal muscle cross-sectional area. Eur J Appl Physiol 108(2):273–279

Akins JS, Vallely JJ, Karg PE, Kopplin K, Gefen A, Poojary-Mazzotta P, Brienza DM (2016) Feasibility of freehand ultrasound to measure anatomical features associated with deep tissue injury risk. Med Eng Phys 38(9):839–844

Arida A, Kyprianou M, Kanakis M, Sfikakis PP (2010) The diagnostic value of ultrasonography-derived edema of the temporal artery wall in giant cell arteritis: a second meta-analysis. BMC Musculoskelet Disord 11:44

Bajaj S, Lopez-Ben R, Oster R, Alarcon GS (2007) Ultrasound detects rapid progression of erosive disease in early rheumatoid arthritis: a prospective longitudinal study. Skelet Radiol 36(2):123–128

Balint PV, Kane D, Hunter J, McInnes IB, Field M, Sturrock RD (2002) Ultrasound guided versus conventional joint and soft tissue fluid aspiration in rheumatology practice: a pilot study. J Rheumatol 29:2209–2213

Bansal C, Scott R, Stewart D, Cockrell CJ (2005) Decubitus ulcers: a review of the literature. Dermatology 44:805–810

Bianchi S, Martinoli C, Sureda D, Rizzatto G (2001) Ultrasound of the hand. Eur J Ultrasound 14(1):29–34

Blaisdell FW (2002) The pathophysiology of skeletal muscle ischemia and the reperfusion syndrome: a review. Cardiovasc Surg 10:620–630

Bouten CV, Oomens CW, Baaijens FP, Bader DL (2003) The etiology of pressure ulcers: skin deep or muscle bound? Arch Phys Med Rehabil 84(4):616–619

Braden B, Bergstrom N (1987) A conceptual schema for the study of the etiology of pressure sores. Rehabil Nurs 12:8–12

Brienza D, Vallely J, Karg P, Akins J, Gefen A (2018) An MRI investigation of the effects of user anatomy and wheelchair cushion type on tissue deformation. J Tissue Viability 27(1):42–53

Bruyn GA, Iagnocco A, Naredo E, OMERACT Ultrasound Working Group et al (2019) OMERACT definitions for ultrasonographic pathologies and elementary lesions of rheumatic disorders 15 years on. J Rheumatol 46(10):1388–1393

Bureau NJ, Beauchamp M, Cardinal E, Brassard P (2006) Dynamic sonography evaluation of shoulder impingement syndrome. Am J Roentgenol 187:216–220

Call E, Hetzel T, McLean C, Burton JN, Oberg C (2017) Off loading wheelchair cushion provides best case reduction in tissue deformation as indicated by MRI. J Tissue Viability 26(3):172–179

Carda S, Cisari C, Invernizzi M (2013) Sacropenia or muscle modifications in neurologic diseases: a lexical or pathophysiological difference? Eur J Phys Rehabil Med 49:119–130

Carson PL, Fenster A (2009) Anniversary paper: evolution of ultrasound physics and the role of medical physicists and the AAPM and its journal in that evolution. Med Phys 36(2):411–428

Chin JL, Downey DB, Onik G, Fenster A (1996) Three-dimensional prostate ultrasound and its application to cryosurgery. Tech Urol 2(4):187–193

Chin JL, Downey DB, Mulligan M, Fenster A (1998) Three-dimensional transrectal ultrasound guided cryoablation for localized prostate cancer in nonsurgical candidates: a feasibility study and report of early results. J Urol 159(3):910–914

Cimmono MA, Grassi W (2008) What is new in ultrasound and magnetic resonance imaging for musculoskeletal disorders? Best Pract Res Clin Rheumatol 22:1141–1148

Claus-Walker J, Halstead LS (1982) Metabolic and endocrine changes in spinal cord injury: II (section 1). Consequences of partial decentralization of the autonomic nervous system. Arch Phys Med Rehabil 63:569–575

Coggrave MJ, Rose LS (2003) A specialist seating assessment clinic: changing pressure relief practice. Spinal Cord 41:692–695

Cooperberg PL, Tsang I, Truelove L, Knickerbocker WJ (1978) Gray scale ultrasound in the evaluation of rheumatoid arthritis of the knee. Radiology 126(3):759–763

Cosnes A, Anglade MC, Revuz J, Radier C (2003) Thirteen-megahertz ultrasound probe: its role in diagnosing localized scleroderma. Br J Dermatol 148(4):724–729

Cowan LJ, Ahn H, Flores M, Yarrow J, Barks LS, Garvan C et al (2019) Pressure ulcer prevalence by level of paralysis in patients with spinal cord injury in long-term care. Adv Skin Wound Care 32:122–130

Damjanov N, Radunovic G, Prodanovic S, Vukovic V, Milic V, Pasalic KS et al (2012) Construct validity and reliability of ultrasound disease activity score in assessing joint inflammation in RA: comparison with DAS-28. Rheumatology 51(1):120–128

Dasgupta B, Patil P (2012) Role of diagnostic ultrasound in the assessment of musculoskeletal diseases. Ther Adv Musculoskel Dis 4(5):341–355

De Flaviis L, Scaglione P, Nessi R, Ventura R, Calori G (1988) Ultrasonography of the hand in rheumatoid arthritis. Acta Radiol 29(4):457–460

De Luca R, Dattoma T, Forzoni L, Bamber J, Palchetti P, Gubbini A (2018) Diagnostic ultrasound probes: a typology and overview of technologies. Curr Dir Biomed Eng 4(1):49–53

De Simone C, Caldarola G, D'agostino M, Carbone A, Guerriero C, Bonomo L et al (2011) Usefulness of ultrasound imaging in detecting psoriatic arthritis of fingers and toes in patients with psoriasis. Clin Dev Immunol (in press)

Dealey C (2009) Skin care and pressure ulcers. Adv Skin Wound Care 22(9):421–428

Del Cura JL (2008) Ultrasound-guided therapeutic procedures in the musculoskeletal system. Curr Probl Diagn Radiol 37(5):203–218

Dhami LD, Gopalakrishna A, Thatte RL (1985) An objective study of the dimensions of the ischial pressure. Br J Plast Surg 38:243–251

Di Matteo A, Mankia K, Azukizawa M, Wakefield RJ (2020) The role of musculoskeletal ultrasound in the rheumatoid arthritis continuum. Curr Rheumatol Rep 22(8):41

Donald I, MacVicar J, Brown TG (1958) Investigation of abdominal masses by pulsed ultrasound. Lancet 1(7032):1188–1195

Donovan WH, Edward Carter R, Bedbrook GM, Young JS, Griffiths ER (1984) Incidence of medical complications in spinal cord injury: patients in specialised, compared with non-specialised centres. Paraplegia 22:282–290

Dudley-Javoroski S, McMullen T, Borgwardt MR, Peranich LM, Shields RK (2010) Reliability and responsiveness of musculoskeletal ultrasound in subjects with and without spinal cord injury. Ultrasound Med Biol 36(10):1594–1607

Duncan I, Sullivan P, Lomas F (1999) Sonography in the diagnosis of carpal tunnel syndrome. AJR Am J Roentgenol 173(3):681–684

Dussik KT (1942) On the possibility of using ultrasound waves as a diagnostic aid. Z Neurol Psychiatr 174:153–168

Dussik KT, Fritch DJ, Kyriazidou M, Sear RS (1958) Measurements of articular tissues with ultrasound. Am J Phys Med 37(3):160–165

Dyson M, Moodley S, Verjee L, Weinman J, Wilson P (2003) Wound healing assessment using 20 MHz ultrasound and photography. Skin Res Technol 9(2): 116–121

Eisenberg R (1992) Radiology: an illustrated history. Mosby, St. Louis

English C, Fisher L, Thoirs K (2012) Reliability of real-time ultrasound for measuring skeletal muscle size in human limbs in vivo: a systematic review. Clin Rehabil 26(10):934–944

Falsetti P, Acciai C, Volpe A, Lenzi L (2011) Ultrasonography in early assessment of elderly patients with polymyalgic symptoms: a role in predicting diagnostic outcome? Scand J Rheumatol 40(1):57–63

Fenster A, Parrage G, Bax J (2011) Three-dimensional ultrasound scanning. Interface. Focus 1(4):503–519

Fessell DP, Jacobson JA, Craig J, Habra G, Prasad A, Radcliff A et al (2000) Using sonography to reveal and aspirate joint effusions. AJR Am J Roentgenol 174(5):1353–1362

Filippucci E, Di Geso L, Grassi W (2014) Progress in imaging in rheumatology. Nat Rev Rheumatol 10(10):628–634

Fornage BD (1995) Musculoskeletal ultrasound. Churchill Livingstone, New York

Fournier BA, Gagnon DH, Routhier F, Roy JS (2017) Ultrasonographic measures of the acromiohumeral distance and supraspinatus tendon thickness in manual wheelchair users with spinal cord injury. Arch Phys Med Rehabil 98(3):517–524

Gabison S, Mathura S, Verriera MC, Nussbaum E, Popovic MR, Gagnon DH (2018) Quantitative ultrasound imaging over the ischial tuberosity: an exploratory study to inform tissue health. J Tissue Viability 27:173–180

Gefen A (2014) Tissue changes in patients following spinal cord injury and implications for wheelchair cushions and tissue loading: a literature review. Ostomy Wound Manage 60(2):34–45

Gelis A, Dupeyron A, Legros P, Benaïm C, Pelissier J, Fattal C (2009) Pressure ulcer risk factors in persons with SCI: part I: acute and rehabilitation stages. Spinal Cord 47(2):99–107

Giangregorio L, McCartney N (2006) bone loss and muscle atrophy in spinal cord injury: epidemiology, fracture prediction, and bone loss and muscle atrophy in spinal cord injury. J Spinal Cord Med 29:489–500

Gladman DD, Shuckett R, Russell ML, Thorne JC, Schachter RK (1987) Psoriatic arthritis (PSA) - an analysis of 220 patients. Q J Med 62(238):127–141

Gnaidecka M, Quistorff B (1996) Assessment of dermal water by high-frequency ultrasound: comparative studies with nuclear magnetic resonance. Br J Dermatol 135(2):218–224

Gompels BM, Darlington LG (1981) Septic arthritis in rheumatoid disease-causing bilateral shoulder dislocation: diagnosis and treatment assisted by grey scale ultrasonography. Ann Rheum Dis 40:609–611

Graf R (1980) The diagnosis of congenital hip-joint dislocation by the ultrasonic Combound treatment. Arch Orthop Trauma Surg 97(2):117–133

Grassi W (2003) Clinical evaluation versus ultrasonography: who is the winner? J Rheumatol 30(5):908–909

Grassi W, Filippucci E, Farina A, Cervini C (2000) Current comment sonographic imaging of tendons. Arthritis Rheum 43(5):969–976

Griffin DR, Galambos R (1941) The sensory basis of obstacle avoidance by flying bats. J Exp Zool 86(3): 481–506

Gutierrez M, Filippucci E, De Angelis R, Salaffi F, Filosa G, Ruta S et al (2011) Subclinical entheseal involvement in patients with psoriasis: an ultrasound study. Semin Arthritis Rheum 40(5):407–412

Hassan M (2018) Overview of musculoskeletal ultrasound for the clinical rheumatologist. Clin Exp Rheumatol 36(114):S3–S9

Heckmatt JZ, Leeman S, Dubowitz V (1982) Ultrasound imaging in the diagnosis of muscle disease. J Pediatr 101(5):656–660

Hill CR (1973) Medical ultrasonics: an historical review. Br J Radiol 46(550):899–905

Hmamouchi I, Bahiri R, Srifi N, Aktaou S, Abouqal R, Hajjaj-Hassouni N (2011) A comparison of ultrasound and clinical examination in the detection of flexor tenosynovitis in early arthritis. BMC Musculoskelet Disord 12:91

Houghton PE, Campbell KE (2013) Canadian best practice guidelines for the prevention and management of pressure ulcers in people with spinal cord injury. In: A resource handbook for clinicians. Katika Integrated Communications Inc., Mississauga, p 317

Ishida H, Watanabe S (2012) Influence of inward pressure of the transducer on lateral abdominal muscle thickness during ultrasound imaging. J Orthop Sports Phys Ther 42(9):815–818

Ishida H, Suehiro T, Suzuki K, Watanabe S (2017a) Muscle thickness and echo intensity measurements of the rectus femoris muscle of healthy subjects: intra and interrater reliability of transducer tilt during ultrasound. J Bodyw Mov Ther 22(3):657–660

Ishida H, Suehiro T, Suzuki K, Yoneda T, Watanabe S (2017b) Influence of the ultrasound transducer tilt on muscle thickness and echo intensity of the rectus femoris muscle of healthy subjects. J Phys Ther Sci 29(12):2190–2193

Javid M, Hadar E (1998) Long-term follow-up review of patients who underwent laminectomy for lumbar stenosis: a prospective study. J Neurosurg Pediatr 89(1): 1–7

Johnson R, Gerhart KA, McCray J, Menconi JC, Whiteneck GG (1998) Secondary conditions following spinal cord injury in a population-based sample. Spinal Cord 36(1):45–50

Jousse-Joulin S, Breton S, Cangemi C, Fenoll B, Bressolette L, De Parscau L et al (2011) Ultrasonography for detecting enthesitis in juvenile idiopathic arthritis. Arthritis Care Res 63:849–855

Kanal E, Shellock F, Talagala L (1990) Safety considerations in mr imaging. Radiology 176(3): 593–606

Kane D, Balint PV, Sturrock RD (2003) Ultrasonography is superior to clinical examination in the detection and localization of knee joint effusion in rheumatoid arthritis. J Rheumatol 30:966–971

Kane D, Grassi W, Sturrock R, Balint PV (2004) A brief history of musculoskeletal ultrasound: 'From bats and ships to babies and hips'. Rheumatology 43:931–933

Klauser AS, De Zordo T, Feuchtner GM, Djedovic G, Weiler RB, Faschingbauer R et al (2010) Fusion of real-time US with CT images to guide sacroiliac joint injection in vitro and in vivo. Radiology 256:547–553

Koutroumpas AC, Alexiou IS, Vlychou M, Sakkas LI (2010) Comparison between clinical and ultrasonographic assessment in patients with erosive osteoarthritis of the hands. Clin Rheumatol 29:511–516

Krause JS, Broderick L (2004) Patterns of recurrent pressure ulcers after spinal cord injury: identification of risk and protective factors 5 or more years after onset. Arch Phys Med Rehabil 85(8):1257–1264

Krouskop TA, Reddy NP, Spencer WA, Secor JW (1978) Mechanisms of decubitus ulcer formation—an hypothesis. Med Hypotheses 4:37–39

Kurjak A (2000) Ultrasound scanning—Prof. Ian Donald (1910–1987). Eur J Obstet Gynecol Reprod Biol 90: 187–189

Landsman AS, Meaney DF, Cargill RS, Macarak EJ, Thibault LE (1995) William J. Stickel Gold Award. High strain rate tissue deformation. A theory on the mechanical etiology of diabetic foot ulcerations. J Am Podiatr Med Assoc 85:519–527

Leahy S, Toomey C, Mccreesh K, O'Neill C, Jakeman P (2012) Ultrasound measurement of subcutaneous adipose tissue thickness accurately predicts total and segmental body fat of young adults. Ultrasound Med Biol 38(1):28–34

Levin D, Nazarian LN, Miller TT, O'Kane PL, Feld RI, Parker L et al (2005) Lateral epicondylitis of the elbow: US findings. Radiology 237:230–234

Liem NR, McColl MA, King W, Smith KM (2004) Aging with a spinal cord injury: factors associated with the need for more help with activities of daily living. Arch Phys Med Rehabil 85:1567–1577

Linder-Ganz E, Shabshin N, Itzchak Y, Yizhar Z, Siev-Ner I, Gefen A (2008) Strains and stresses in subdermal tissues of the buttocks are greater in paraplegics than in healthy during sitting. J Biomech 41:567–580

Loerakker S, Manders E, Strijkers GJ, Nicolay K, Baaijens FP, Bader DL et al (2011) The effects of deformation, ischemia, and reperfusion on the development of muscle damage during prolonged loading. J Appl Physiol 111(4):1168–1177

Louis LJ (2008) Musculoskeletal ultrasound intervention: principles and advances. Radiol Clin N Am 46(3): 515–533

Lucas VS, Burk RS, Creehan S, Grap MJ (2014) Utility of high-frequency ultrasound: moving beyond the surface to detect changes in skin integrity. Plast Surg Nurs 34(1):34–38

Lyder CH, Ayello EA (2008) Pressure ulcers: a patient safety issue

Makhsous M, Venkatasubramanian G, Chawla A, Pathak Y, Priebe M, Rymer WZ et al (2008) Investigation of soft-tissue stiffness alteration in denervated human tissue using an ultrasound indentation system. J Spinal Cord Med 31:88–96

McDonald DG, Leopold GR (1972) Ultrasound B-scanning in the differentiation of Baker's cyst and thrombophlebitis. Br J Radiol 45:729–732

McKinley WO, Jackson AB, Cardenas DD, DeVivo MJ (1999) Long-term medical complications after traumatic spinal cord injury: a regional model systems analysis. Arch Phys Med Rehabil 80:1402–1410

McNally EG, Rees JL (2007) Imaging in shoulder disorders. Skelet Radiol 36(11):1013–1016

Mekhail N, Wentzel D, Freeman R, Quadri H (2011) Counting the costs: case management implications of spinal cord stimulation treatment for failed back surgery syndrome. Prof Case Manag 16(1):27–36

Miller GE, Seale J (1981) Lymphatic clearance during compressive loading. Lymphology 14:161–166

Moghimi S, Baygi MHM, Torkaman G, Mahloojifar A (2010) Quantitative assessment of pressure sore generation and healing through numerical analysis of high-frequency ultrasound images. J Rehabil Res Dev 47(2): 99–108

Molinari F, Caresio C, Acharya UR, Mookiah MRK, Minetto MA (2015) Advances in quantitative muscle ultrasonography using texture analysis of ultrasound images. Ultrasound Med Biol 41(9):2520–2532

Naredo E, Cabero F, Beneyto P, Mondéjar B, Uson J, Palop MJ, Crespo M (2004) A randomized comparative study of short-term response to blind injection versus sonographic-guided injection of local corticosteroid in patients with painful shoulder. J Rheumatol 31(2):308–314

National Pressure Ulcer Advisory Panel (2018) NPUAP pressure injury stages. [cited 2018 June 28, 2018]; Available from: http://www.npuap.org/resources/

Nazarian LN (2008) The top 10 reasons musculoskeletal sonography is an important complementary or alternative technique to MRI. AJR Am J Roentgenol 190(6): 1621–1626

Newman JS, Adler RS, Bude RO, Rubin JM (1994) Detection of soft tissue hyperemia: value of power Doppler sonography. Am J Roentgenol 163:385–389

Nitz W, Oppelt A, Renz W, Manke C, Lenhart M, Link J (2001) On the heating of linear conductive structures as guide wires and catheters in interventional MRI. J Magn Reson Imaging 13(1):105–114

Oomens CW, Bressers OF, Bosboom EM, Bouten CV, Blader DL (2003) Can loaded interface characteristics influence strain distributions in muscle adjacent to bony prominences? Comput Methods Biomech Biomed Eng 6(3):171–180

Oomens CW, Bader DL, Loerakker S, Baaijens F (2015) Pressure induced deep tissue injury explained. Ann Biomed Eng 43(2):297–305

Paquette P, Lamontagne M, Higgins J, Gagnon DH (2015) Repeatability and minimal detectable change in longitudinal median nerve excursion measures during upper limb neurodynamic techniques in a mixed population: a pilot study using musculoskeletal ultrasound imaging. Ultrasound Med Biol 41(7):2082–2086

Pillen S, van Alfen N (2011) Skeletal muscle ultrasound. Neurol Res 33(10):1016–1024

Porter-Armstrong A, Adams C, Moorhead AS, Donnelly J, Nixon J, Bader D et al (2013) Do high frequency ultrasound images support clinical skin assessment? Nursing 8:1–5

Quintavalle PR, Lyder CH, Mertz PJ, Phillips-Jones C, Dyson M (2006) Use of high-resolution, high-frequency diagnostic ultrasound to investigate the pathogenesis of pressure ulcer development. Adv Skin Wound Care 19(9):498–505

Reddy NP, Cochran GV (1981) Interstitial fluid flow as a factor in decubitus ulcer formation. J Biomech 14:879–881

Reimers K, Reimers CD, Wagner S, Paetzke I, Pongratz DE (1993) Skeletal muscle sonography: a correlative study of echogenicity and morphology. J Ultrasound Med 12:73–77

Rippon MG, Springett K, Walmsley R, Patrick K, Millson S (1998) Ultrasound assessment of skin and wound tissue: comparison with histology. Skin Res Technol 4(3):147–154

Ryken T, Eichholz K, Gerszten P, Welch W, Gokaslan Z, Resnick D (2003) Evidence-based review of the surgical management of vertebral column metastatic disease. Neurosurg Focus 15(5):1–10

Saunders LL, Krause JS, Acuna J (2012) Association of race, socioeconomic status, and health care access with pressure ulcers after spinal cord injury. Arch Phys Med Rehabil 93(6):972–977

Schmidt WA, Blockmans D (2005) Use of ultrasonography and positron emission tomography in the diagnosis and assessment of large-vessel vasculitis. Curr Opin Rheumatol 17:9–15

Schmidt WA, Nerenheim A, Seipelt E, Poehls C, Gromnica-Ihle E (2002) Diagnosis of early Takayasu arteritis with sonography. Rheumatology 41:496–502

Schmidt WA, Wernicke D, Kiefer E, Gromnica-Ihle E (2006) Colour duplex sonography of finger arteries in vasculitis and in systemic sclerosis. Ann Rheum Dis 65:265–267

Shampo MA, Kyle RA (1997) John Julian Wild—pioneer in ultrasonography. Mayo Clin Proc 72:234

Sipilä S, Suominen H (1993) Muscle ultrasonography and computed tomography in elderly trained and untrained women. Muscle Nerve 16:294–300

Smith J, Finnoff JT (2009a) Diagnostic and interventional musculoskeletal ultrasound: part 2. Clinical applications. PMR 21(2):162–177

Smith JF, Finnoff JT (2009b) Diagnostic and interventional musculoskeletal ultrasound: part 1. Fundamentals. PMR 1:64

Smith WL, Surry K, Mills G, Downey D, Fenster A (2001) Three-dimensional ultrasound-guided core needle breast biopsy. Ultrasound Med Biol 27:1025–1034

Sonenblum SE, Ma J, Sprigle SH, Hetzel TR, McKay Cathcart J (2018) Measuring the impact of cushion design on buttocks tissue deformation: an MRI approach. J Tissue Viability 27(3):162–172

Sonenblum S, Seola D, Sprigleb SH, McKay Cathcart J (2020) Seated buttocks anatomy and its impact on biomechanical risk. J Tissue Viability 29:69–75

Spârchez M, Fodor D, Miu N (2010) The role of power Doppler ultrasonography in comparison with biological markers in the evaluation of disease activity in juvenile idiopathic arthritis. Med Ultrason 12:97–103

Sprigle S, Sonenblum S (2011) Assessing evidence supporting redistribution of pressure for pressure ulcer prevention: a review. J Rehabil Res Dev 48(3): 203–213

Stockton L, Parker D (2002) Pressure relief behaviour and the prevention of pressure ulcers in wheelchair users in the community. J Tissue Viability 12:84–99

Stover SL, Gay RE, Koopman W, Sahgal V, Gale LL (1980) Dermal fibrosis in spinal cord injury patients. Arthritis Rheumatol 23:1312–1317

Stekelenburg A, Oomens CW, Strijkers GJ, Nicolay K, Bader DL (2006) Compression-induced deep tissue injury examined with magnetic resonance imaging and histology. J Appl Physiol 100(6):1946–1954

Swaine JM, Moe A, Breidahl W, Bader DL, Oomens CWJ, Lester L et al (2017) Adaption of a MR imaging protocol into a real-time clinical biometric ultrasound protocol for persons with spinal cord injury at risk for deep tissue injury: a reliability study. J Tissue Viability:1–10

Swaine JM, Moe A, Breidahl W, Bader DL, Oomens CWJ, Lester L et al (2018) Adaptation of a MR imaging protocol into a real-time clinical biometric ultrasound protocol for persons with spinal cord injury at risk for deep tissue injury: a reliability study. J Tissue Viability 27(1):32–41

Szkudlarek M, Court-Payen M, Strandberg C, Klarlund M, Klausen T, Ostergaard M (2001) Power Doppler ultrasonography for assessment of synovitis in the metacarpophalangeal joints of patients with rheumatoid arthritis: a comparison with dynamic magnetic resonance imaging. Arthritis Rheum 44:2018–2023

Teh J, Stevens K, Williamson L, Leung J, McNally EG (2003) Power Doppler ultrasound of rheumatoid synovitis: quantification of therapeutic response. Br J Radiol 76:875–879

Terslev L, Torp-Pedersen S, Savnik A, Von Der Recke P, Qvistgaard E, Danneskiold-Samsoe B, Bliddal H (2003) Doppler ultrasound and magnetic resonance imaging of synovial inflammation of the hand in rheumatoid arthritis: a comparative study. Arthritis Rheum 48:2434–2441

Thomaes T, Thomis M, Onkelinx S, Coudyzer W, Cornelissen V, Vanhees L (2012) Reliability and validity of the ultrasound technique to measure the rectus femoris muscle diameter in older CAD-patients. BMC Med Imag 12(1):7–13

Thorfinn J, Sjoberg F, Lidman D (2009) Sitting can cause ischaemia in the subcutaneous tissue of the buttocks, which implicates multilayer tissue damage in the development of pressure ulcers. Scand J Plast Reconstr Surg Hand Surg 43:82–89

Tsuji S, Ichioka S, Sekiya N, Nakatsuka T (2005) Analysis of ischemia-reperfusion injury in a microcirculatory model of pressure ulcers. Wound Repair Regen 13:209–215

Van Der Heijde DM, Van Riel PL, Van Leeuwen MA, Van't Hof MA, Van Rijswijk MH, Van De Putte LB (1992) Prognostic factors for radiographic damage and physical disability in early rheumatoid arthritis. A prospective follow-up study of 147 patients. Br J Rheumatol 31:519–525

Van Drongelen S, Boninger ML, Impink BG, Khalaf T (2007) Ultrasound imaging of acute biceps tendon changes after wheelchair sports. Arch Phys Med Rehabil 88(3):381–385

Van Holsbeeck M, Introcaso JH (1991) Musculoskeletal ultrasound. Mosby, St. Louis

Van Loocke M, Lyons CG, Simms CK (2008) Viscoelastic properties of passive skeletal muscle in compression: stress-relaxation behaviour and constitutive modelling. J Biomech 41:1555–1566

Vaziri ND, Eltorai I, Gonzales E, Winer RL, Pham H, Bui TD et al (1992) Pressure ulcer, fibronectin, and related proteins in spinal cord injured patients. Arch Phys Med Rehabil 73:803–806

Wakefield RJ, Gibbon WW, Conaghan PG, O'Connor P, McGonagle D, Pease C, Green MJ, Veale DJ, Isaacs JD, Emery P (2000) The value of sonography in the detection of bone erosions in patients with rheumatoid arthritis: a comparison with conventional radiography. Arthritis Rheum 43:2762–2770

Wakefield RJ, Brown AK, O’Connor PJ, Emery P (2003) Power Doppler sonography: improving disease activity assessment in inflammatory musculoskeletal disease. Arthritis Rheum 48:285–288

Wakefield RJ, Green MJ, Marzo-Ortega H, Conaghan PG, Gibbon WW, McGonagle D, Proudman S, Emery P (2004) Should oligoarthritis be reclassified? Ultrasound reveals a high prevalence of subclinical disease. Ann Rheum Dis 63:382–385

Wakefield RJ, Balint PV, Szkudlarek M, Filippucci E, Backhaus M, D’agostino MA et al (2005) Musculoskeletal ultrasound including definitions for ultrasonographic pathology. J Rheumatol 32:2485–2487

Wang YN, Bouten CVC, Lee DA, Bader DL (2005) Compression-induced damage in a muscle cell model in vitro. Proc Inst Mech Eng 219:1–12

Wann-Hansson C, Hagell P, Willman A (2008) Risk factors and prevention among patients with hospitalacquired and pre-existing pressure ulcers in an acute care hospital. J Clin Nurs 17:1718–1727

Wei Z, Wan G, Gardi L, Mills G, Downey D, Fenster A (2004) Robot-assisted 3D-TRUS guided prostate brachytherapy: system integration and validation. Med Phys 31:539–548

Werhagen L, Aito S, Tucci L, Strayer J, Hultling C (2012) 25 years or more after spinal cord injury: clinical conditions of individuals in the Florence and Stockholm areas. Spinal Cord 50:243–246

Whittaker J, Teyhen D, Elliott J, Cook K, Langevin H, Dahl H, Stokes M (2007) Rehabilitative ultrasound imaging: understanding the technology and its applications. J Orthop Sports Phys Ther 37:434–449

Whittaker JL, Warner MB, Stokes MJ (2009) Induced transducer orientation during ultrasound imaging: effects on abdominal muscle thickness and bladder position. Ultrasound Med Biol 35(11):1803–1811

Wildermuth S, Dumoulin C, Pfammatter T, Maier S, Hofmann E, Debatin J (1998) Mr-guided percutaneous angioplasty: assessment of tracking safety, catheter handling and functionality. Cardiol Interv Radiol 21(5):404–410

Wildes DG, Smith LS (2012) Advanced ultrasound probes for medical imaging. In AIP Conference Proceedings

Wu GA, Bogie KM (2013) Not just quantity: gluteus maximus muscle characteristics in able-bodied and SCI individuals–implications for tissue viability. J Tissue Viability 22(3):74–82

Yabunaka K, Lizaka S, Nakagami G, Aoi N, Kadono T, Koyanagi H, Uno M, Ohue M, Sanada S, Sanada H (2009) Can ultrasonographic evaluation of subcutaneous fat predict pressure ulceration? J Wound Care 18(5):192–198

Yalcin E, Akyuz M, Onder B, Unalan H, Degirmenci I (2013) Skin thickness on bony prominences measured by ultrasonography in patients with spinal cord injury. J Spinal Cord Med 36(3):225–230

Ytrehus K, Reikeras O, Huseby N, Myklebust R (1995) Ultrastructure of reperfused skeletal muscle: the effect of oxygen radical scavenger enzymes. Int J Microcirc Clin Exp 15:155–162

Skill Acquisition in Histology Education

10

Rachael Door

Abstract

Histology has traditionally formed a key part of medical education. Increasing demands on the curriculum have resulted in a decline in time available for this complex topic. Previous research has identified that students struggle to apply their knowledge, instead favouring rote memorisation. This chapter explores how to shift the focus of histology education for medical students away from content memorisation and towards the development of problem-solving skills and the application of core knowledge. Several resources were investigated, at the core of which was a decision tree, a framework of yes–no questions in a flowchart arrangement that allows the learner to determine tissue type from an unknown specimen by linking structure to function.

The project was conducted in three phases, or cycles, to allow flexible and timely adjustments based on staff and student feedback on the changes made. Cycle 1 investigated the use of a pre-constructed histology decision tree in practical sessions to show students how to apply their knowledge. Cycle 2 investigated the usefulness of this resource when made available as an online resource (a website), supplemented by worked examples and quizzes with feedback. Cycle 3 expanded this website to include more detailed worked examples and images on the decision tree.

Qualitative and quantitative data was collected through anonymous online questionnaires, website data (quiz scores and worked example responses), and summative exam results. In addition, field notes provided subjective data on the use of the decision tree in practical sessions.

Ninety-seven percent of students found the decision tree helpful in their histology practical sessions. Students stated that the decision tree provided a structured framework for the consolidation of knowledge and showed them how to apply this knowledge. Students required a demonstration of how to use the decision tree with 94% of students finding the worked examples helpful. Eighty-three percent of students reported that they were able to identify more tissues in Quiz 2 following use of the decision tree and worked examples. Summative Objective Structured Skills Exam (OSSE) results also improved following use of the website when compared to the control group (the previous cohort). Importantly, testing and feedback opportunities were considered important amongst students and improved their confidence in the subject (free text comments).

Supplementary Information: The online version contains supplementary material available at https://doi.org/10.1007/978-3-031-36850-9_10.

R. Door (✉)
School of Medicine, Keele University, Staffordshire, UK
e-mail: r.e.door@Keele.ac.uk

© The Author(s), under exclusive license to Springer Nature Switzerland AG 2023

L. Shapiro (ed.), *Microscopy Techniques for Biomedical Education and Healthcare Practice*, Biomedical Visualization 2, https://doi.org/10.1007/978-3-031-36850-9_10

In summary, students require supported opportunities to develop the skills necessary to apply their knowledge, and a digital decision tree acts as an appropriate format. In addition, students learn best when provided with opportunities for formative assessment with timely and appropriate feedback.

Keywords

Histology · Anatomy · Medical education · Skill development · Active learning

10.1 Introduction

Histology is the study of the microstructure of tissues and is studied in years one and two of the medical curriculum at Keele University. These practical sessions involve students identifying various tissues at the microscopic level, linking structures to the function of the tissue. This is a content-heavy area and students typically struggle, becoming overwhelmed with the volume of new information. The literature examining approaches to histology teaching focuses primarily around the provision of *content*, either via digital images or via virtual microscopes, rather than the acquisition of *skills* (Heidger et al. 2002; Bloodgood and Ogilvie 2006; Sherman and Jue 2009). Students, therefore, attempt to memorise the content through rote learning rather than understanding the content and its significance. This led to a lack of enthusiasm and engagement in sessions which was reflected in exam results. As such, two key research questions were established:

1. How can students develop the skills necessary to apply their knowledge?
2. How can feedback in histology teaching be improved?

To answer these questions, an Action Research (AR) project was developed to investigate whether the use of a decision tree in histology education enables students to apply their knowledge by asking appropriate questions, and whether opportunities for formative assessment are perceived as helpful.

10.1.1 Traditional Histology Education

This project focused on histology practical sessions for first-year undergraduate medical students. In the medical curriculum at Keele University, histology is taught through a hands-on approach using microscopes and slides of human and animal tissue. The practical sessions run weekly, last for 2 h, and are delivered as a series of three repeats for students in sets A, B, and C with a total cohort of 130 students. The objective of the sessions is for the students to understand how the microstructure of tissues allows the physiological needs of the organ to be met; effectively to act as a bridge between the study of gross anatomy and physiology and a foundation for their future study of pathology.

Histology is traditionally taught through self-directed learning, with some institutions providing no academic support in practical sessions (Sherman and Jue 2009). At Keele, sessions are primarily led by anatomy lecturers, with some support from histopathology foundation year two (FY2) doctors in a demonstrator role. The content of the session is introduced by the academic lead and the students are then encouraged to study the tissues in pairs using their own microscopes. This incorporates several pedagogical methods identified by Sherman and Jue typically used in the teaching of histology; self-guided learning, co-operative learning, and motor-based learning, amongst others, and is an intentional approach to provide different learning environments (Steffe and Gale 1995; Prince 2004).

Observation of student behaviour during these sessions highlighted that students find the volume of content overwhelming. Academic staff leading the sessions identified that students typically displayed an inability to focus on one structure at a time and a lack of confidence as to where to start when discriminating features of a tissue. This was reinforced by comments directly from the students in which they vocalised their worries, and during summative Objective Structured Skills Exams (OSSEs). Students struggle to integrate the structure into the function of the tissue, and therefore do not understand why the knowledge is important for them as future clinicians. Students try to overcome these issues by attempting to memorise the content and inevitably obtain only a very basic understanding of the topic, and no concept of how it links to the physiology of the region. This is a significant area for concern as it has been found to impact an individual's ability to integrate core science and clinical concepts in diagnostic reasoning (Kulasegaram et al. 2013; Lisk et al. 2016). It is paramount that these medical students understand how the microstructure of the tissues allows the organ to fulfill its function, and ultimately how this will be altered in disease. As such, the rote memorisation of content is insufficient to meet the objectives of the histology practical sessions. It was therefore apparent that there was a need for a structured, logical approach to tissue identification, that not only removed confusion between different tissues, but also emphasised how structure linked to function. In addition, the literature surrounding higher education (HE) in general, and more specifically histology education, highlighted the growing need to provide students with feedback on their learning (Steffe and Gale 1995; Prince 2004; Draper and Brown 2004; Jisc 2005). There is, however, very little research on methods to improve feedback for students during histology teaching, aside from the author's own work on the use of clickers in histology practical sessions (Quinn 2017). This work introduced an electronic voting system and integrated quizzes in practical histology sessions to provide an opportunity for formative assessment and immediate feedback. Results highlighted that in-practical formative assessments allowed students to identify gaps in their knowledge (96%), and that students preferred to use such systems to anonymously answer questions (92%).

Prior to commencement of the project, Fanghanel's filters (2007) were used to identify the constraints present in this context. These 'filters' are seven factors that impact an academic's practice around teaching and learning, and are categorised into Micro, Meso, and Macro levels. Micro factors revolve around the individual and their pedagogical beliefs, Meso factors are at the department and discipline level, and Macro factors are at the institutional level. The use of these filters allowed a realistic approach as to what aspects of the educational context were open to modification. This in turn encouraged a reflexive approach and an awareness of how such changes may affect others (Door 2014). At the Micro level, the author's pedagogic beliefs have always focused on active learning environments and hands-on opportunities to self-discover knowledge. This is at odds with much histology teaching where the educational environment focuses on content delivery (Sherman and Jue 2009). At the Meso level, there are certain constraints on what is possible due to departmental restrictions. As an example, the heavy teaching load on staff and availability of contact time within the medical degree timetable restricts additional teaching opportunities. Similarly, technology with in-built cameras is not permitted within the laboratories and this limits opportunities for innovations using mobile phones, laptops, or tablets. At the wider discipline level, teaching on a medical curriculum comes with further restraints in that the content delivered must meet the guidelines set out by the General Medical Council. Looking more broadly at scholarship in general, many academics do not regularly share their practice outside of their sphere of influence and as such it is challenging to know what is working or perhaps more importantly, not working outside of one's own immediate context. At the Macro level, equity of access to the learning opportunity is essential and feedback has been identified as a key factor in ensuring that the learners are fully supported.

10.1.2 Action Research

Action research (AR) involves academics asking practical questions about core fundamentals of their own working environment (Bartlett and Burton 2006), and as such promotes reflective thinking that results in action (Ponte 2002). In addition, AR has the capacity to enhance the quality of teaching and learning (Kember 2000), improving the student experience and their knowledge of the subject. As a result, AR enables academics to better understand the process of teaching and learning (Freeman 1998) and contribute to the theory surrounding education (Wahlstrom and Ponte 2005). In the context of this project, an additional benefit of AR is that it is a collaborative process that treats all participants as equals (McNiff 2016).

AR can be defined as having seven key characteristics that must be fulfilled for a project to be considered truly AR: be social, aim at improvement, be cyclical, involve systematic enquiry, be reflective, be participative, and led by practitioners (Kember 2000 from Carr and Kemmis' 1986 work). Furthermore, it is generally agreed that AR should be collaborative, whereby researcher and participant are equally invested in the process (Norton 2009; Stringer 2013). This is important in AR as students may be better informed than the researcher (Munn-Giddings and Winter 2013), and the academics commitment to learning values may influence the way the context is perceived (Polanyi 2012). The nature of AR ensures that the researcher is embedded in the research environment, and this provides a subjective aspect to the research that is specific to AR. This means that the process must be rigorous, ensuring no bias, so that the results can be considered valid and generalisable.

10.1.3 Teaching in the Context of Medicine

Kember (1997) outlines two main conceptions of teaching: teaching as information transmission and teaching as supporting students' learning. In HE it is vital that students construct their own knowledge through a process of self-discovery, and that educators should facilitate them in this process by providing them with the tools necessary to construct that knowledge rather than didactically transferring content; teachers should be a 'guide on the side' and not the 'sage on the stage' (King 1993).

The specific context in which this project occurs must also be considered here. Students studying professional, high-demand courses such as Medicine are often mature or postgraduate, and highly motivated towards achieving their goals (Mcloughlin and Luca 2002). In general, HE emphasises the importance of 'learning' whilst professional education prioritises operational outcomes and skills. The personal transferable skills required of such professionals include the ability to integrate theoretical and practical knowledge, communication skills, and reflection on one's own knowledge (Oliver and McLoughlin 2000). Furthermore, HE typically places emphasis on propositional knowledge (knowledge that something is the case), whilst professional education requires not only propositional knowledge but also process and personal knowledge (Eraut 1994). The traditional style of teaching occurring throughout HE focuses on the transmission of content and produces inert knowledge that is insufficient for professional degrees such as Medicine. Medical students must question and apply knowledge, becoming self-directed in their approach to learning.

10.1.4 Ensuring Quality and Rigour in AR

It is important to consider what markers of quality and rigour should be used as a benchmark against which the project, and its outcomes, can be assessed. This is particularly important in AR as the rigour of this style of research is often brought into question amongst more traditional researchers (Seider and Lemma 2004). For this, the GROVER model was used; Generalisability, Reliability, Objectivity, Validity, Ethics, and Repeatability (Prof. Jackie Potter, personal communication during MA Learning and Teaching in HE). Outlining the expectations for each of these markers prior to the commencement of the project ensured that the goals of the project were clear, and established the standards to which the researcher would hold themselves. These standards in relation to the outcomes of the project are discussed further in Sect. 10.6.

10.2 Aims for the Research Project

Several aims were established:

1. Generation of new knowledge.
2. Achievement of action-oriented outcomes.
3. Education of researcher and participants.
4. Results that are relevant to the local setting.
5. Sound and appropriate research methodology.

These aims provided benchmarks against which the validity of the project outcomes could be assessed (Sect. 10.6).

10.3 Project Overview

This project investigated how students can develop the necessary skills to apply their knowledge, and how feedback can be improved in histology teaching. A framework of yes–no questions in a flowchart arrangement, hereon termed a ‘decision tree’, was created to examine whether this structure helped the students to apply their knowledge. The tree can be seen in Figs. 10.1a, b and 10.2a, b and a larger version can be accessed by scanning the associated quick response (QR) code. First, the use of the decision tree was investigated in the practical setting alone. Then, the decision tree was provided in an online format in a Google Site with quizzes and examples of how to work through the decision tree for specific tissues, hereon termed ‘worked examples’. This allowed the investigation of how formative assessment and feedback are perceived by students.

10.4 Methods

10.4.1 Ethics

Ethical approval was granted by the Keele Student Project Ethics Committee (SPEC) as this project was completed as part of the MA in Learning and Teaching in Higher Education. See Sect. 10.4.6 for more information on ethical considerations for this project.

10.4.2 Methods Overview

In the five stages of this project (Pre-cycle, Cycle 1, Cycle 2, Cycle 2.5, Post-cycle, see Fig. 10.3, Cycle Overview), online questionnaires, field notes, and exam results were used to examine the status quo, the immediate impact of the innovation, and the long-term effects on the cohort. In addition, in Cycles 2 and 2.5, the data from the Google Site also provided important feedback in the form of quiz scores and responses to the worked examples.

10.4.3 Creation of the Resources

The decision tree was created in Microsoft PowerPoint using the in-built SmartArt graphics option. The online resources were created using Google Sites, Google Forms, Google Slides, and YouTube. These digital tools were selected to allow the resources to be easily replicated by other educators.

10.4.4 Data Collection

10.4.4.1 Questionnaires

Online questionnaires were used to collect data for Cycle 1 (in situ decision tree), Cycle 2 (digital decision tree and worked examples), and Cycle 2.5 (modified digital decision tree and expanded worked examples, Fig. 10.3). SmartSurvey was selected to create the questionnaires because it is free and can be accessed by anyone who has the link to the questionnaire. The surveys generated were anonymous, as SmartSurvey creates a unique identification for each participant that cannot be traced back to the identity of the individual. This was important to help ensure that students were open and honest in their feedback. Google was not an appropriate tool because at the time of the project Keele used Google to host their email accounts and therefore the student’s name would be linked to any submission.

On accessing the questionnaire, participants were informed that completion of the

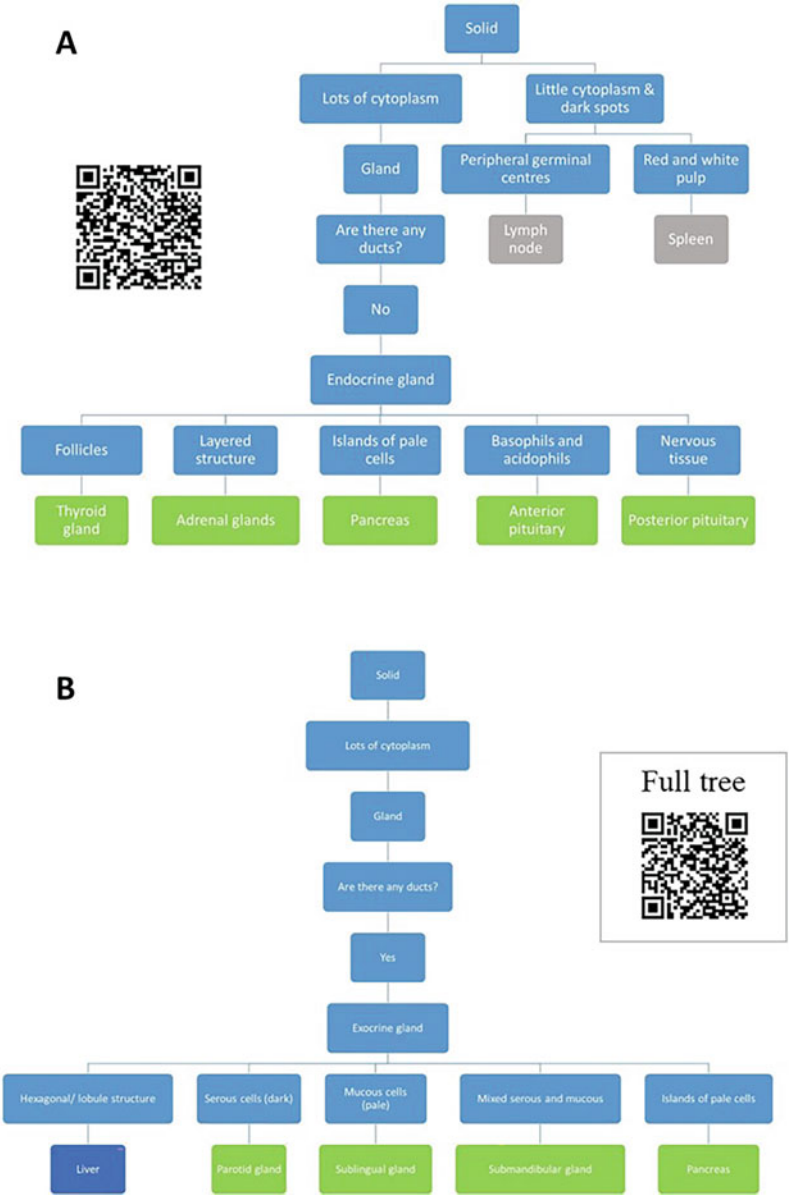
A
Solid
Lots of cytoplasm
Little cytoplasm & dark spots
Gland
Peripheral germinal centres
Red and white pulp
Are there any ducts?
Lymph node
Spleen
No
Endocrine gland
Follicles
Layered structure
Islands of pale cells
Basophils and acidophils
Nervous tissue
Thyroid gland
Adrenal glands
Pancreas
Anterior pituitary
Posterior pituitary
B
Solid
Lots of cytoplasm
Gland
Are there any ducts?
Yes
Exocrine gland
Hexagonal/ lobule structure
Serous cells (dark)
Mucous cells (pale)
Mixed serous and mucous
Islands of pale cells
Liver
Parotid gland
Sublingual gland
Submandibular gland
Pancreas
Full tree

Fig. 10.1 (**a** and **b**) The histology decision tree. This image depicts the decision tree divided into parts based on tissue shape. (**a**) shows the questions asked if the tissue is solid with either little cytoplasm or no ducts. (**b**) shows the pathway if the tissue is solid with ducts. A larger version of each sub-tree can be seen by scanning the associated QR code. The full tree can be seen by scanning the QR code in the inset

questionnaire would signify consent for their answers to be used in the project and they were encouraged to contact the project coordinator if they had any questions or concerns. An email address was supplied for this purpose. Potential participants were not able to progress without agreeing to this step. By embedding the consent process within the questionnaire, it was ensured that all participants were fully informed and willing to participate.

The questionnaires (1, 2, and 2.5) each consisted of eight questions, with a combination of open-ended questions, closed questions, and attitude scales in the form of Likert scales (Supplementary File 10.1) (Norton 2009). This combination of quantitative and qualitative approaches was intentionally selected to maximise the validity of the data obtained and the analysis performed (Jick 1979; Johnson 2008; McNiff 2016). All first-year Medicine students

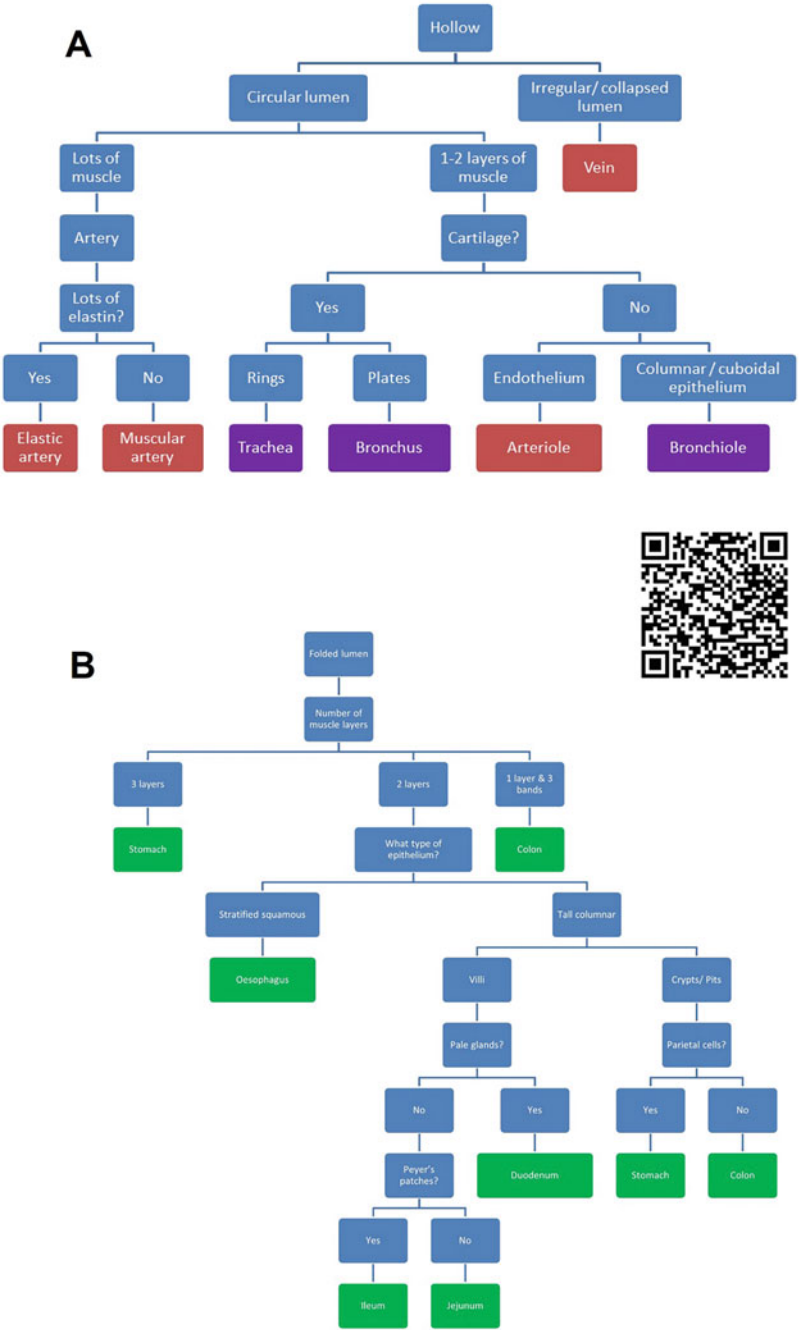
A
Hollow
Circular lumen
Irregular/ collapsed lumen
Lots of muscle
1-2 layers of muscle
Vein
Artery
Cartilage?
Lots of elastin?
Yes
No
Yes
No
Rings
Plates
Endothelium
Columnar / cuboidal epithelium
Elastic artery
Muscular artery
Trachea
Bronchus
Arteriole
Bronchiole
B
Folded lumen
Number of muscle layers
3 layers
2 layers
1 layer & 3 bands
Stomach
What type of epithelium?
Colon
Stratified squamous
Tall columnar
Oesophagus
Villi
Crypts/ Pits
Pale glands?
Parietal cells?
No
Yes
Yes
No
Peyer's patches?
Duodenum
Stomach
Colon
Yes
No
Ileum
Jejunum

Fig. 10.2 (**a** and **b**) The histology decision sub-trees. This image depicts the decision tree divided into parts based on tissue shape. (**a**) shows the questions asked if the tissue is hollow with a circular lumen. (**b**) shows the pathway if the tissue has a folded lumen. A larger version of each sub-tree can be seen by scanning the associated QR code

(130) were emailed a link to the questionnaires to maximise the response rate and thus the validity and generalisability of the data obtained.

Online questionnaires were selected, as opposed to either interviews or focus groups, for several reasons. Firstly, the students would be able to complete the questionnaires in their own time, within approximately 5 min (per questionnaire), and thus there was no pressure to prioritise this research over their study time and educational needs, as could be the case with a focus group. This also meant that feedback was obtained in

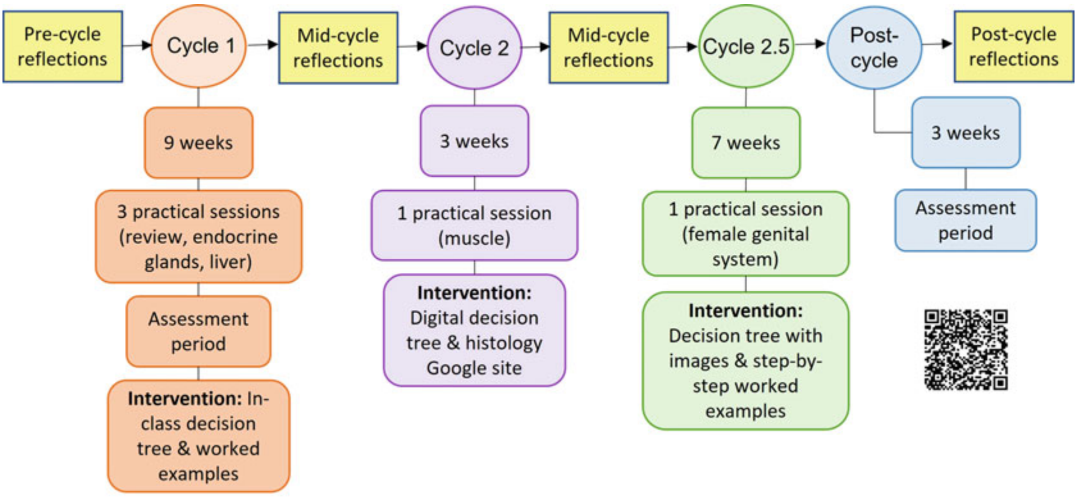
Pre-cycle reflections
Cycle 1
Mid-cycle reflections
Cycle 2
Mid-cycle reflections
Cycle 2.5
Post-cycle
Post-cycle reflections
9 weeks
3 practical sessions (review, endocrine glands, liver)
Assessment period
Intervention: In-class decision tree & worked examples
3 weeks
1 practical session (muscle)
Intervention: Digital decision tree & histology Google site
7 weeks
1 practical session (female genital system)
Intervention: Decision tree with images & step-by-step worked examples
3 weeks
Assessment period

Fig. 10.3 Cycle overview. This diagram outlines the stages involved in the project and the key information for each cycle. Pre- and mid-cycle reflections offered an important opportunity to plan and evaluate the innovations made and ensured the project was reflective in nature. For access to the current version of the Google Site referenced in Cycles 2 and 2.5 scan the QR code in the image

real-time and thus changes to the project in response to feedback could be made within a short period of time, as was the case with the introduction of Cycle 2.5 (Brown and Knight 2012). Secondly, the online feedback meant that students had time to provide considered answers that they could reflect on freely, rather than being requested to provide an in-session, time-restricted response. Thirdly, the questionnaires provided an opportunity for the students to provide completely anonymous feedback on the sessions that they may not feel comfortable providing in either an interview or focus group (Orne 2017). Fourthly, the questionnaires allowed many students to provide feedback on the innovation, thus maximising the generalisability of the data obtained.

The blend of open-ended questions, closed questions, and Likert scales provided a combination of quantitative and qualitative data that allowed categorisation of feedback through thematic analysis, in addition to statistical analysis. The addition of an ‘Other’ category to the Likert scales allowed the advantages of both open and closed questions, as students could provide an answer that had not been considered by the researcher, highlighting unknown unknowns. In the Likert scales, five categories were provided in addition to the ‘Other’ category; strongly agree, agree, neither agree nor disagree, disagree, and strongly disagree. A scale of five was selected as the traditional alternative of seven seemed surplus to requirement as respondents typically stay within the middle categories, preferring not to select either extreme (Jamieson 2004; Cohen et al. 2002). In addition, it was important to provide a neutral response (neither agree nor disagree), so that students could respond even if they did not hold any view on the matter, and they had the option of expanding on their answer in the free text box.

The free text options provided an important opportunity for Interpretive Phenomenological Inquiry (IPI) where lived experiences of those affected by the innovations are examined (Frechette et al. 2020). This form of qualitative analysis is an emerging methodology in medical education where assumptions are critically analysed, and subjective data is examined. The focus on understanding the experience of individuals differs from generic qualitative studies where the aim is action. This feedback, naturally, differs from person to person highlighting how individuals experience the same situation differently (Norton 2009). By incorporating a combination of approaches a more comprehensive insight is obtained.

When constructing the questionnaire, it was important to avoid questions that engendered socially desirable responses or patterns where respondents answered automatically rather than consciously (Norton 2009). To ensure this, open formats were chosen over leading questions, and Likert scales were interspersed with closed Yes/No options and free text boxes to prevent pattern clicking. Furthermore, the questions were designed to explicitly target one focused aspect of the project at a time, so that students did not feel committed to agreeing with the question as a whole when in reality they only agreed with part of it. The questionnaires were all tested before they were sent to students to ensure they were clear, concise, and took no longer than the stated 5 min to complete.

10.4.4.2 Field Notes

The academic leading the five histology practical sessions were able to observe the students using the decision tree. This took the form of informal direct observation, in that the students were aware of the research project prior to the session as part of the ethical approval process, questionnaires, and Google Site, but this was not explicitly stated in the session. Arguably this could therefore be considered a form of naturalistic observation over one with artificial experimental conditions (Bressers et al. 2020). Through the descriptions of people and their habits in their normal environment, these observations added an ethnographic component to the data as the academic was not perceived as an outsider there for purely research purposes.

10.4.4.3 Quiz and Assessment Results

The data from the Google Sites, in combination with the OSSE practical results, provided objective feedback as to the students' use of the decision tree and overall understanding of histology. This quantitative data allowed statistical analysis and thus comparison of the control groups with the research groups. This data was entirely anonymous and analysed using Microsoft Office Excel. The mean was selected as an appropriate measure of central tendency for the worked examples, quizzes, and exam data.

10.4.5 Control Groups

The previous cohort was used as a control group for the field notes and the summative exam scores. In addition, the current cohort prior to the project was also used as the control for the field notes. No control group was used to parallel the study group. This was due to the potential ethical implications of withholding a learning resource that was hypothesised to be helpful. This 'repeated measures' design does potentially open the study to the carry over effect where students improve with practice (Norton 2009) and was considered when the data was analysed, and conclusions drawn.

10.4.6 Ethical Considerations

Three key principles exist when considering the ethics surrounding research: informed consent, privacy and confidentiality, and protection from harm (Norton 2009; BERA 2011). Each of these was considered and addressed at each stage of the project.

- *Informed consent*—Students were provided with an information sheet attached to each email in Cycles 1, 2, and 2.5. The information sheet included information such as the aims of the project, the expectations of participants, and any benefits/risks associated with participation. The emails were sent to all 130 first-year students so that not all those receiving the email would be required to participate to provide sufficient data for appropriate analysis. This was important as in the context of AR the researcher is also the teacher and therefore has a unique position of power and this must not be abused. The first page of the questionnaires informed the participants that completion of the questionnaire would signify their consent for their answers to be used in the project.

- *Privacy and confidentiality*—The British Educational Research Association's ethical guidelines for educational research (BERA 2011), were used as a framework for the project. The questionnaires were stand-alone from the students' Google identity and thus could not be traced back to the individual student. The exam results were obtained from the assessments team in an anonymous format to ensure their analysis was objective. The field notes are unavoidably open to issues of confidentiality; however, no names or distinguishing quotes have been included here, maintaining both anonymity, and confidentiality. Covert breaches in confidentiality are, however, inevitable in AR as the researcher is investigating their own environment and therefore their name and role reveal their study group, be it peers or students. This should be considered when sharing the outcomes of an AR project and be controlled where possible.
- *Protection from harm*—In AR this aspect relates more to psychological harm than the physical harm seen in other studies, such as the impact on a student's confidence, or their study time. The questionnaires were kept intentionally brief to ensure they could be completed within approximately 5 min so as not to have a negative impact on the students' study time. In addition, the project focused on increasing students' confidence surrounding histology through the provision of quizzes, work examples, and detailed feedback.

10.5 Cycle Overview

The project consisted of three cycles of action. Figure 10.3 outlines the stages involved in the project. Each cycle was informed by reflections and triggered reflections on the outcomes. Cycles 1, 2, and 2.5 all involved practical sessions. Cycle 1 and the Post-cycle period both involved an assessment.

10.5.1 Pre-Cycle

As educator and researcher, there is a unique opportunity for prior teaching experience to inform the research project. The academic team (three lecturers, including the author, who all lead histology practical sessions) had previously noted that students typically disengaged with much of the active learning occurring in the session and appeared to do little or no self-study for histology, preferring instead to rote memorise the content contained within the PowerPoint slides. As they neared the assessment period the students appeared to resort to cramming in an attempt to 'learn' the vast amount of material that had been delivered over the year. Inevitably this resulted in surface learning at best, with less than half of the students correctly identifying the tissue in their OSSE practical exam in the pre-study control group.

10.5.2 Cycle 1: Use of a Decision Tree in the Practical Setting

The aim of Cycle 1 was to identify whether students found the use of the decision tree helpful during their practical histology sessions. This cycle covered a 9-week period in semester two, consisting of three practical sessions (Fig. 10.3). These sessions included a review of the semester one content, a session on endocrine glands, and a final session on the microanatomy of the liver. During this period there was also a written summative assessment for the whole cohort.

10.5.2.1 Cycle 1 Outline

Cycle 1 was designed to identify whether students found the introduction of a flowchart-based decision tree useful during histology sessions. This cycle was entirely lab-based as the students were only provided with the decision tree during the in situ practical sessions and were actively discouraged from copying the tree for use outside of this setting. The reason for this restriction on the use of the decision tree was primarily down to the hypothesis that students would gain more from the resource if they used it to scaffold their own decision analysis tree, instead of attempting to memorise the pre-constructed format. The generation of the decision tree was considered as important, if not more so, than the application of the tree to identify tissues. In addition, it was important to observe the students' use of the tree to inform the later cycles of the research project; by informally helping the students to apply the tree to the session content it was possible to identify what needed development or expansion as the project progressed.

10.5.2.2 Cycle 1 Logistics

Two A3 full colour printouts of the decision tree were provided. These printouts were located on the two front benches in the histology lab. The tree was also displayed in the PowerPoint presentation used in the session, and two tissues (submandibular gland and oesophagus, haematoxylin and eosin stain) were used as examples and ran through the tree to allow their identification. These two tissues were chosen as they follow very different paths within the tree and therefore show how to apply the tree to different contexts.

10.5.2.3 Cycle 1 Field Notes

Students were initially slow to approach the histology tree, and several appeared to struggle to follow the path to identify a tissue. The initial impulse of nearly all students appeared to be to try and copy the tree word for word, even after they were strongly discouraged from doing so. This was observed in all three repeats of the first histology session using the tree, to the extent where one student even tried to hide what they were doing and tried to deny copying it down despite the researcher (and session lead) directly observing them doing so.

10.5.2.4 Cycle 1 Questionnaire Data

Data from Cycle 1 was collected via an anonymous online questionnaire. SmartSurvey was used to create a questionnaire composed of Likert scales, closed questions, and free text boxes (questions available in Supplementary File 10.1). All first-year students who participated in the histology practical sessions were emailed (130 students). At this stage, the students had used the decision tree in three practical sessions and had sat a written exam assessing histology content. Fifty-nine questionnaires were completed (three students only viewed the questions, submitting no answers, and as such these were taken as non-submissions). Students from all three sets completed the questionnaire in proportionate amounts (31% set A, 42% set B, 27% set C), ensuring that feedback was received for all practical sessions and could be applied to the student population as a whole. The outcomes from the feedback are as follows:

- *Students find the decision tree helpful*—97% of students either agreed or strongly agreed that the decision tree was helpful (64% strongly agree). One student disagreed, and one selected ‘Other’. The student who selected ‘Other’ as their response commented that they had not had a chance to use it but that it sounded helpful. Similarly, the student who responded ‘Disagree’ commented that it was helpful knowing that a tree should be made and that it can help reach a decision. This resulted in some confusion as surely the more appropriate Likert response would have been ‘Agree’. Other comments provided by the students fit into two main themes; encouraged a logical thought process, and highlighted similarities and differences between tissues. Students highlighted how the tree allowed them to see a pattern, and how the summarised content in the tree was reassuring when students typically struggle with histology. Several students also commented on how they used the tree in the January summative exams, which provided positive feedback on its implementation in the practical sessions prior to this assessment. One student commented that they found it useful, however, that they could not remember most of it when they left the class. They continued to say that they feel they would have been able to learn the content more quickly and accurately if the tree was made available outside of the classroom. This insight re-enforced concerns about the students' desire to memorise the content rather than learn how the structure related to the function of the tissue.

- *The simplified content provided a logical thought process*—The students were asked what was helpful about the decision tree. This question was in the form of free text comments. The responses were categorised into four main themes: highlighted similarities and differences, simplified, provided a logical thought process, and removed the need to memorise the content. Students highlighted how the tree allowed them to distinguish tissues based on their key characteristics, and how they could eliminate tissues by answering just a few simple questions. They noted how the tree provided a starting point to distinguish differences, and encouraged comparison, rather than trying to learn them all separately. The simplified content made the task more manageable; students liked the ability to see all the (basic) content on a single page. The clear and concise nature of the diagram allowed the students to visualise the information more clearly. The students also commented on how it allowed them to see the 'big picture', and how the different tissues relate to each other. The step-by-step nature of the tree provided a guide on how to approach the identification process. The comments highlighted the importance of knowing how to *apply* the information, over purely knowing the content. The tree provided the framework in which to apply the content taught in the practical sessions. The students highlighted that the tree removed the need to memorise the content. One student commented '*the tree teaches us that it is important to understand and follow logical paths, rather than memorise. I reckon this is how doctors should think*'. This showed that there had been a shift in learning from rote memorisation towards the application of knowledge.
- *A widely available decision tree with images would provide a useful tool*—The students were asked what could be improved about the decision tree. This question was in the form of free text comments. The responses were categorised into three main themes: addition of images, more detailed descriptions, and wider availability. Students commented that the addition of images of each example tissue would facilitate identification and understanding of the various structures. Furthermore, some students suggested that a list of common structures found in each tissue would help their understanding. This is interesting when compared with the fact that many students liked the simplified and concise nature of the tree. One student commented that they did not feel like they went into sufficient detail when revising as they simply learned the tree—this is something that was hoped to be avoided by encouraging the students to construct their own tree. Students repeatedly requested that the tree be made available outside of the practical setting. Some noted that if the tree was made available at the start of the academic year, they would have a framework on which they could construct their knowledge throughout the practical sessions. Several students identified the small size of the font on the printed decision tree as an issue as it was slightly difficult to read.
- *The innovation encouraged students to construct their own decision tree*—54% of students responded that they had created their own decision tree, with 32% stating that they intended to. Some commented that the use of the tree in the practical setting had encouraged them to compare and contrast the tissues more, and one even said they were going to make a '*guess who histology game*'. Seventy-three percent of students reported that they either agreed or strongly agreed that creating their own decision tree was a helpful process. Students also noted that they believed the process would be helpful in preparation for their practical histology exams (OSSEs).

10.5.2.5 Cycle 1 Discussion

The results collected through the anonymous online questionnaire provided a detailed insight into how the students used the decision tree, and how they thought it could be improved.

Some students reported that only one decision tree was available at the front of the practical session, and this provided interesting 'food for thought' on how students interact with learning resources. There were, as mentioned previously, two copies of the decision tree available in the sessions. It is interesting to consider whether students disengage from potential learning opportunities if they cannot 'own' the resource, i.e. if they cannot copy it and memorise it. This highlights the growing need to encourage students to engage with all learning opportunities.

One student commented that they believed they would be able to 'learn' the content more quickly and accurately if the tree was available outside of the classroom. Such comments showed that students favour information recall over understanding—they may be able to memorise the structures in the tree, but they are not understanding *why* the structure is needed to fulfil the function of the tissue. It is important to remember that the students are not enrolled on a histology degree; they are studying histology to complement their study of gross anatomy and physiology, tie the two together and ultimately be able to predict how the structure would be affected in pathology. It is the responsibility of educators to break the cycle of rote memorisation to pass exams. It is not sufficient to memorise an image (for that is all the decision tree is in essence) and this does not prove that the student has learnt about the microstructure of the tissue.

One student commented that sufficient help was provided by the tutor prior to the observation of the tissue, so that the tree was surplus to requirement. This is interesting to consider in relation to HE teaching as a whole; should less help be provided in the form of content transfer, and more support in the form of showing students *how* to learn? It is *assumed* that students know how to learn appropriately by the time they reach HE, but very different outcomes are expected in terms of learning than is required at A-level. This reiterates the need to help the students to understand what is expected of them, and how they can best achieve that standard.

10.5.2.6 Cycle 1 Reflections for Implementation in Cycle 2 (Table 10.1)

10.5.3 Cycle 2: Use of the Decision Tree in a Digital Format

The aim of Cycle 2 was to investigate how to help students to apply the theory behind the histology decision tree. This cycle covered a 3-week period in semester two, consisting of one practical session on muscle (Fig. 10.3).

10.5.3.1 Cycle 2 Outline

It was hypothesised that an understanding of *why* the questions were being asked, and *how* they resulted in the answers they did, was more important than the students trying to rote learn the diagram. This cycle, therefore, incorporated the introduction of the Google Site containing a digital representation of the decision tree, in addition to two quizzes and three worked examples. Since this project, the Google Site has undergone numerous changes, however, if the reader is interested in viewing a similar version to that introduced in Cycle 2 it can be accessed *here* or by scanning the QR code shown in Fig. 10.3.

10.5.3.2 Cycle 2 Logistics

In response to student feedback, the two printouts of the decision tree were replaced by two digital versions of the tree. These were made available on two touchscreen computers at the front of the labs in histology practical sessions. In addition, a Histology Google Site was also created. This Site allowed the students to access the decision tree outside of the practical sessions. To minimise rote learning, the document was converted into a Google Slide embedded within the Site. To help the students to apply the decision tree to unknown tissues, the Site also consisted of three worked examples (trachea, submandibular gland, and ileum, all haematoxylin and eosin). These were presented in the format of Google Forms and embedded within the Google Site (Fig. 10.4).

Table 10.1 Reflections on Cycle 1

Reflection on Cycle 1	Change for Cycle 2
The time-limited availability of the decision tree appeared to impact how the students interacted with the resource.	In Cycle 2, the decision tree would be made more accessible within the practical setting and provided outside of these sessions.
The decision tree should be concise and not try to fulfil all the needs of the learning environment. Instead, students need to be shown how to use the resource effectively.	The students must be provided with worked examples to demonstrate the decision tree in action. In addition, the students should be encouraged to revisit the content from the session to develop their own aspects of the tree.
The decision tree can be difficult to interpret when all the tissues are included on one sheet.	The decision tree should be made available in digital format where the students can magnify the area of interest.

The worked examples demonstrated the key questions that the students should ask when identifying a tissue, all of which were taken directly from the decision tree. The final part of the website was the opportunity for the students to test their level of understanding. This component of the Site was split into two quizzes where students were asked to identify eight tissues. The students were encouraged to complete Quiz 1 prior to accessing the decision tree and using the worked examples, this was to test their base level of understanding. The second quiz was designed to be used after the worked examples and was meant to determine whether the students had increased their understanding of the structures of the tissues. On completion of Quiz 1, the students received feedback on which tissues had been incorrectly identified. In Quiz 2, this was developed further so that students, in addition to being supplied with their score, also received feedback on each of the tissues, independent of whether they identified them correctly or not.

10.5.3.3 Cycle 2 Field Notes

The students accessed the decision tree throughout the session, after the tissue was introduced.

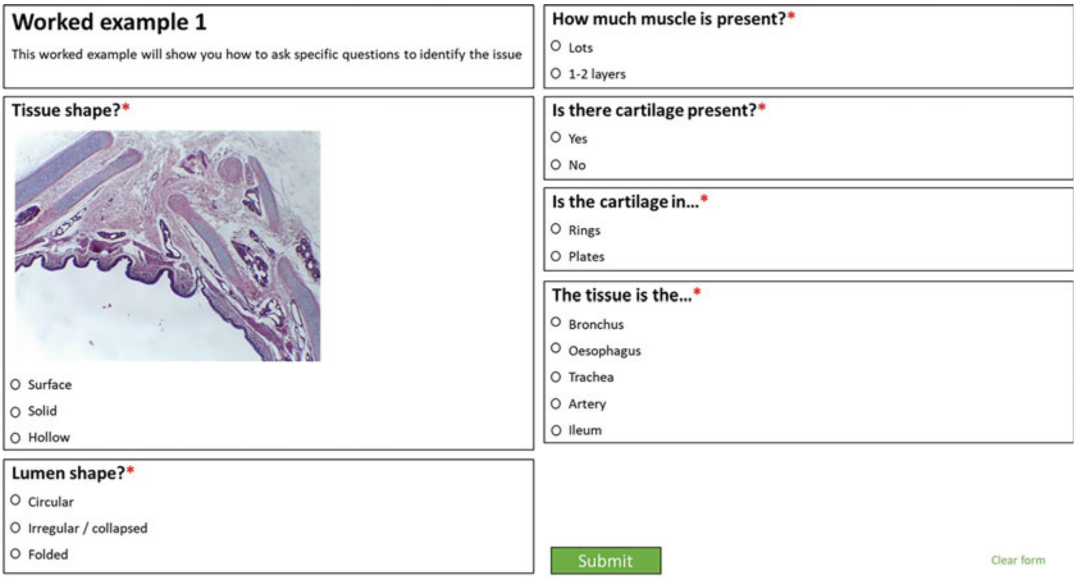

Worked example 1

This worked example will show you how to ask specific questions to identify the issue

Tissue shape?*

○ Surface
○ Solid
○ Hollow

Lumen shape?*

○ Circular
○ Irregular / collapsed
○ Folded

How much muscle is present?*

○ Lots
○ 1-2 layers

Is there cartilage present?*

○ Yes
○ No

Is the cartilage in...*

○ Rings
○ Plates

The tissue is the...*

○ Bronchus
○ Oesophagus
○ Trachea
○ Artery
○ Ileum

Fig. 10.4 Worked Example 1. This image shows the steps in Worked Example 1 on the Google Site. The questions shown are taken directly from the decision tree and are designed to allow the student to identify the tissue as the Trachea

When using the tree, they were no longer copying down the content, but were instead working through the questions (often in pairs) and discussing the results. There was clearly a shift from individual rote memorisation to group-based peer learning, where students were able to self-discover new content. Encouragingly, students also started to question *why* an answer was correct, and debate amongst themselves. This was a positive advancement and to have sparked discussion and debate amongst the students indicates, to some extent, interest, or at least investment, in the outcome. The students appeared able to navigate the Google Site with ease, with all content on a single page and no login process required.

10.5.3.4 Cycle 2 Questionnaire Data

Feedback on Cycle 2 was collected via an anonymous online questionnaire. As in Cycle 1, SmartSurvey was used to create a questionnaire composed of Likert scales, closed questions, and free text boxes. All first-year students who participated in the histology practical sessions (130 students) were emailed the survey. Cycle 2 included one practical session and ran for 3 weeks. Six questionnaires were completed (one student viewed the questionnaire but submitted no answers, and consequently this was taken as a non-submission). Students from all three sets (A, B, and C) completed the questionnaire in proportionate amounts (33.3% per set), ensuring that feedback was received for all practical sessions and could be applied to the student population. The outcomes from the feedback are as follows:

- *Students found the worked examples helpful for identifying tissues*—67% of respondents said they found the three worked examples provided on the website helpful when identifying unknown tissues. Free text comments on the worked examples focused on the lack of feedback on the answers provided by the students.
- *Students were able to correctly identify more tissues after using the worked examples*—83% of students responded that they identified more tissues correctly after reviewing the worked examples on the Google Site. This was based on their scores in Quiz 1 (completed before using the worked examples) compared to Quiz 2 (completed after reviewing the worked examples).
- *Quizzes and worked examples helped the students to identify tissues*—66% of students found both the quizzes and worked examples helpful, whilst 17% preferred the quizzes specifically, and 17% did not find the Site helpful. Feedback from respondents who did not find the Site helpful focused on the lack of feedback in the worked examples.

10.5.3.5 Quiz and Worked Example Results

In Cycle 2, 22 responses were recorded for Quiz 1, and 7 responses for Quiz 2. The average score for Quiz 1 was 53% and the average for Quiz 2 was 70%.

Twelve responses were recorded for Worked Example 1, six for Worked Example 2, and four for Worked Example 3. Thirty-three percent of students identified the correct tissue in Worked Example 1, 83% in Worked Example 2, and 50% in Worked Example 3. This resulted in an average score of 55% for correct tissue identification in the worked examples.

10.5.3.6 Cycle 2 Discussion

Feedback from Cycle 2 was based on six questionnaires. It was important to keep this in mind when reviewing the feedback as it was difficult to extrapolate this data and apply it to the cohort as a whole when so few responses were received. It was important, however, to implement changes that would benefit the students as soon as possible, and this led to the closure of Cycle 2 after 3 weeks and the implementation of Cycle 2.5 changes. The feedback also reflected the informal comments made by students during the practical sessions as well as staff reflections on the innovation.

In the questionnaire, students responded that they struggled to follow the worked examples which did not provide feedback as to whether the answer submitted was correct or incorrect.

The worked examples were designed to suggest to students the style of questions to ask when identifying a tissue. The activity was not necessarily about getting a ‘correct’ answer, but more about teaching the students how to ask specific questions about the structure and function of a tissue. This highlights the growing need to break the habit of teaching to an exam. This tendency is often acquired at secondary or further education level where the exam content is treated as core to the learner’s study. In this project, the ‘exam’ is instead part of the learning process, an example of assessment *for* learning rather than assessment *of* learning (Germany 2015). If a student has fully understood the process, they should know whether they have correctly identified the tissue or not. The worked examples should, ideally, be used in conjunction with the decision tree—if the students are sufficiently equipped to answer each of the series of questions, they should be left with no other option than the correct tissue. If they are selecting answers at random, rather than making informed decisions, and following a guided process, then they will have multiple tissues available to them. The use of the worked examples alongside the decision tree was not explicitly encouraged and was a point for reflection and development. In addition, the quizzes provided feedback on whether students had provided the correct answer. Both Quiz 1 and Quiz 2 informed students which answers were correct or incorrect, and Quiz 2 provided feedback on all answers, both correct and incorrect (Fig. 10.5).

Eighty-three percent of students responded that they had been able to correctly identify more tissues in Quiz 2 after reviewing the worked examples. Comparison with the data obtained from the two quizzes confirms this response, with the average score increasing from 50% in Quiz 1 to 75% in Quiz 2. However, the same eight tissues were examined in both quizzes, although in a different order, and three of these tissues were used in the worked examples. There is, therefore, some question as to whether the improved scores were due to revisiting the same tissues, or whether the worked examples themselves were the reason for the improvement.

10.5.3.7 Cycle 2 Reflections for Implementation in Cycle 2.5 (Table 10.2)

10.5.4 Cycle 2.5: Modification of the Digitally Available Resources

The aim of Cycle 2.5 was to improve the quality and usefulness of the resources made available on the Google Site. This cycle covered a 7-week period in semester two, consisting of one practical session on the female genital system (Fig. 10.3).

10.5.4.1 Cycle 2.5 Outline

Cycle 2.5 evolved as part of the mid-cycle reflections during Cycle 2 and in response to early feedback from students; both online questionnaire returns and data from the Google Site (quizzes and worked examples). Students appeared to struggle to apply the decision tree to the unidentified tissues in the quizzes and worked examples. The theory was that students would develop a deeper understanding of histology as a discipline, if they understood *why* the questions were being asked, and *how* they resulted in the answers that they did (essentially linking structure to function), than if they tried to memorise the diagram, however, it was evident that this was not something that the students had grasped.

10.5.4.2 Cycle 2.5 Logistics

In Cycle 2.5, the decision tree continued to be available in the practical setting in digital format. In addition, the Google Site was redeveloped to aid student understanding of how to apply the decision tree (Fig. 10.6). This online resource was increasingly important as several sessions were delivered by members of staff who did not use the decision tree in the session, and the assessment period was approaching so students were preparing by revising previous content outside of the practical setting. In response to feedback from Cycle 2, the decision tree was updated to include images of each tissue type. These images

Fig. 10.5 Quiz 2 feedback. This image shows the feedback provided to the students on completion of Quiz 2. All students were provided with feedback, whether they identified the tissue correctly or incorrectly

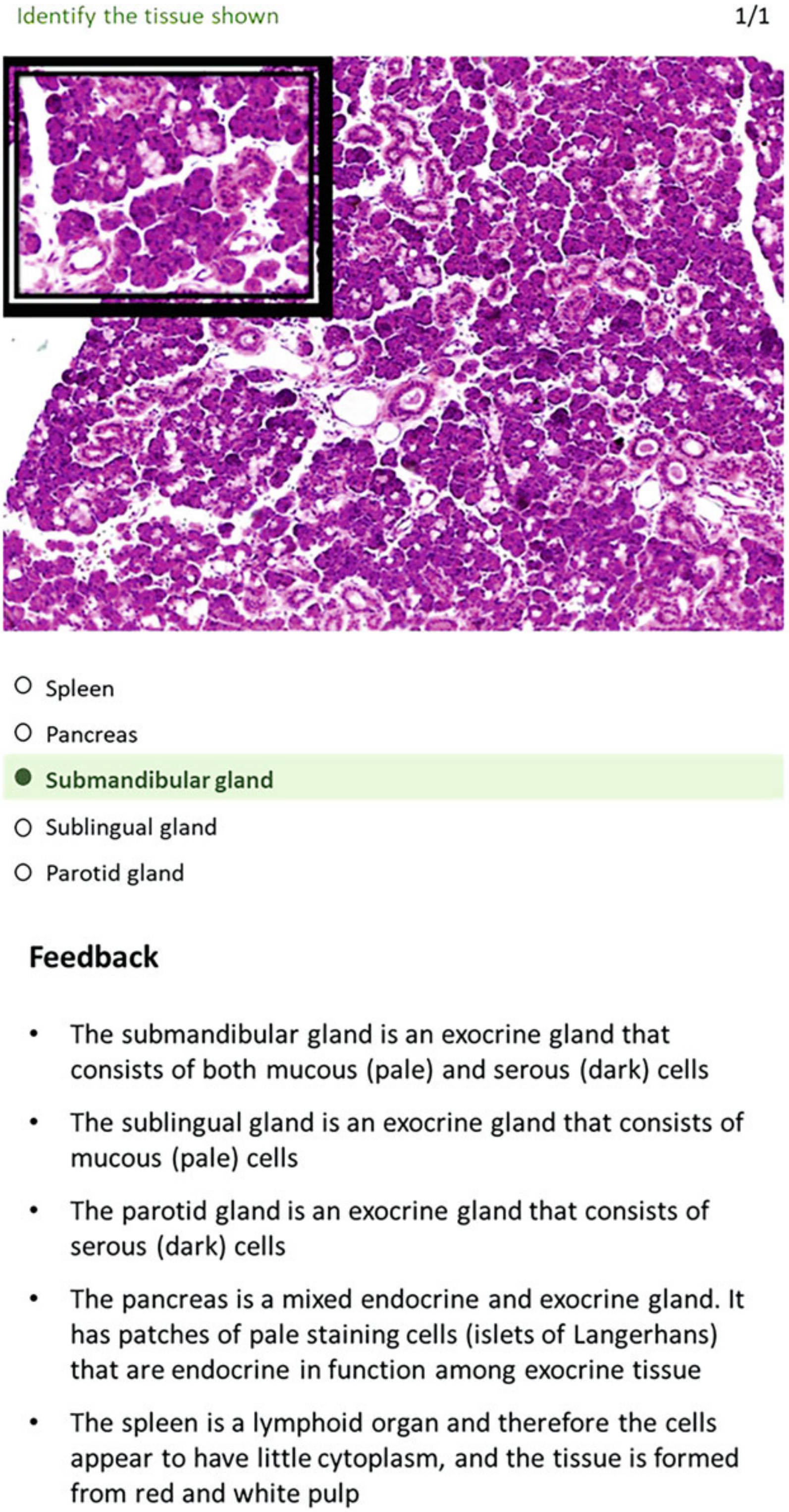

Identify the tissue shown 1/1

○ Spleen
○ Pancreas
● **Submandibular gland**
○ Sublingual gland
○ Parotid gland

Feedback

- The submandibular gland is an exocrine gland that consists of both mucous (pale) and serous (dark) cells
- The sublingual gland is an exocrine gland that consists of mucous (pale) cells
- The parotid gland is an exocrine gland that consists of serous (dark) cells
- The pancreas is a mixed endocrine and exocrine gland. It has patches of pale staining cells (islets of Langerhans) that are endocrine in function among exocrine tissue
- The spleen is a lymphoid organ and therefore the cells appear to have little cytoplasm, and the tissue is formed from red and white pulp

Table 10.2 Reflections on Cycle 2

Reflection on Cycle 2	Change for Cycle 2.5
Students reported that they found the worked examples hard to follow. These were not designed to inform the students of the correct answer, but to show them the *process* of using the tree to ask targeted questions in tissue identification. It appears that more help should be provided in showing the students *how* to apply the tree to unknown tissues.	Students should be provided with step-by-step instructions on how to apply the tree in specific examples.
Feedback again highlighted the need for greater detail on the decision tree. Inclusion of images of each tissue type next to their location on the tree may help the students to compare and contrast the different tissues and therefore more effectively consolidate their knowledge.	Images should be added to the decision tree.

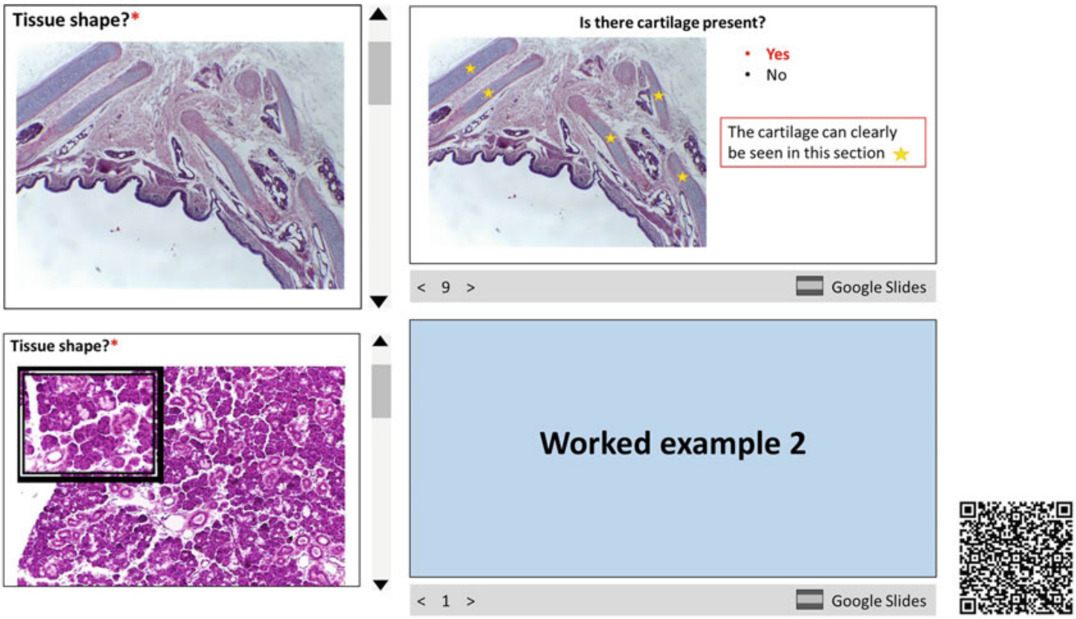

Tissue shape?*

Is there cartilage present?

- Yes
- No

The cartilage can clearly be seen in this section ★

Tissue shape?*

Worked example 2

Fig. 10.6 Histology Google Site, Version 2. This image shows some of the content of the Cycle 2.5 Google Site. Images of tissues were added to the decision tree, and step-by-step guides for the worked examples were provided. The current Google Site can be accessed by scanning the QR code

were produced by photographing the slides that the students used in their practical sessions. The website also included three Google Slide documents that worked through each of the worked examples in a step-by-step manner, highlighting structures that differentiated the tissue from alternative options (Fig. 10.6). This was in response to feedback from Cycle 2 where students relayed that they did not know if they had correctly identified the tissue in the worked example, and consequently could not evaluate whether they had used it appropriately.

10.5.4.3 Cycle 2.5 Field Notes

The students accessed the decision tree throughout the session and were clearly working through the process of tissue identification in a logical manner. Most students appeared to understand the importance of looking at the slide with the naked eye before even approaching the microscope—up to two-thirds of potential tissues could be ruled out if the sample was clearly a solid tissue for example. The practical session in Cycle 2.5 involved examination of different regions of the uterine tube. As part of this exercise, the students were asked to identify three different regions from the uterine tube on a single slide, and many students were able to do this with just the naked eye. This provided positive feedback for the students on the importance of asking simple questions, the answers to which can even be established without any magnification—e.g. what does the lumen look like? (a stage 2 question if tissue shape is used as a stage 1 question on the decision tree.)

The students appeared to be calmer and more rational when approaching tissue identification and several commented that they felt better equipped with the availability of the decision tree. The addition of the slides detailing the step-by-step process of tissue identification made the task of applying the tree significantly easier. Three worked examples appeared to be sufficient to show students how to ask structure-function questions, whilst also discouraging rote memorisation and a passive form of knowledge acquisition.

10.5.4.4 Cycle 2.5 Questionnaire Data

Feedback on Cycle 2.5 was collected via anonymous online questionnaire. As in Cycles 1 and 2, SmartSurvey was used to create a questionnaire composed of Likert scales, closed questions, and free text boxes. All first-year students who participated in the histology practical sessions were emailed (130 students). Cycle 2.5 included one practical session and ran for 7 weeks. Sixteen questionnaires were completed (four students viewed the questionnaire but submitted no answers, and consequently these were taken as non-submissions). Students from all three sets (A, B, and C) completed the questionnaire in proportionate amounts (37.5% set A, 25% set B, 37.5% set C), ensuring that feedback was received for all practical sessions and could be applied to the student population as a whole. The outcomes from the feedback are as follows:

- *Students benefited from greater help in following worked examples*—94% of respondents indicated that they found the three worked examples provided on the website helpful when identifying unknown tissues. In Cycle 2.5, additional help was provided with regards to how to proceed through the worked examples, with specific features highlighted in a Google Slide document (Fig. 10.6). Students commented on how helpful the step-by-step process (shown in the 'worked examples explained' section of the Site) was when identifying characteristic features in different tissues. One noted that it would be very helpful if there was a bank of such guides. The student who reported that the worked examples were not helpful stated that they wanted to be able to magnify the pictures to make out the cells and structures shown.
- *Students were able to correctly identify more tissues after using the worked examples*—88% of students responded that they identified more tissues correctly after reviewing the worked examples on the Google Site; an increase from 83% in Cycle 2.
- *Quizzes and worked examples helped the students to identify tissues*—75% of students found both the quizzes and worked examples helpful (an increase from 66% in Cycle 2), whilst 12.5% preferred specifically the quizzes, and 12.5% preferred the worked examples. No students responded that they found the Site unhelpful, compared to 1 student in Cycle 2. Students commented on how the worked examples showed them how to apply the decision tree, and the quizzes allowed them to test their understanding, boosting their confidence when they scored better than they expected. Several students even requested more quizzes, highlighting how timely and appropriate feedback can help students to see the benefit of assessment *for* learning.

10.5.4.5 Quiz and Worked Example Results

In Cycle 2.5, 71 responses were recorded for Quiz 1 and 18 responses for Quiz 2. The average score for Quiz 1 was 56% (cf. 53% in Cycle 2) and the average for Quiz 2 was 84% (cf. 70% in Cycle 2).

Twenty-eight responses were recorded for Worked Example 1, 17 for Worked Example 2, and 12 for Worked Example 3. Forty-three percent of students identified the correct tissue in Worked Example 1, 71% in Worked Example 2, and 66% in Worked Example 3. Overall, this gave an average score for correct tissue identification in the worked examples of 60% (cf. 55% in Cycle 2).

10.5.4.6 Cycle 2.5 Discussion

General feedback concerning the decision tree in Cycle 2.5 reflected the same feedback obtained during Cycle 2. Students found the decision tree helpful in their practical sessions; however, the small font size was still an issue. Overall, Cycle 2.5 saw a 21% increase in the number of students who responded that the decision tree was helpful in their practical sessions, when compared with Cycle 2 (67% compared to 88%). This highlighted how embedded use of a new learning resource is important for its adoption by students (Jisc 2005).

The worked examples, with the addition of the step-by-step guide with key characteristics highlighted, proved very popular with students. One student commented that they would have liked to have been able to magnify the images in the worked examples. The worked examples were not designed to replace the resources provided in the taught sessions but to complement these alongside their own self-study. As such, if the images were not sufficiently clear then the student could access the physical slides in their resource room and re-visit the content in the PowerPoint from the practical session. In Cycle 2.5 there was a 27% increase in the number of students responding that they found the worked examples helpful when compared to Cycle 2, highlighting the importance of showing the students how to use a novel learning resource appropriately.

Students scored higher on the quizzes in Cycle 2.5 than in Cycle 2, with an increase in Quiz 2 from 70% in Cycle 2 to 84% in Cycle 2.5. This may have been a result of the same students re-visiting the content, or an impact of the new worked examples and greater familiarity with the process.

Students appeared to relish the opportunity to test their level of understanding through both the quizzes and worked examples. This was stressed in the free text comments where students requested more quizzes and said how doing well boosted their confidence. This was a reminder of the importance of assessment and feedback *for* learning, not just as the end result (Germany 2015).

10.5.5 Post-cycle

The Post-cycle period involved the students' use of the resources without any additional innovations. Data was collected regarding the students' use of (and scores on) the quizzes and worked examples. In addition, there was a practical assessment of the students' histology skills in the form of an OSSE station (Fig. 10.3). This data is reported and discussed here.

10.5.5.1 Quiz and Worked Example Results

During the Post-cycle period, 93 responses were recorded for Quiz 1, and 35 for Quiz 2. The average score for Quiz 1 was 66% and the average for Quiz 2 was 91%. This data, combined with the data obtained during Cycles 2 and 2.5 is shown in Fig. 10.7.

Forty-one responses were recorded for Worked Example 1, 18 for Worked Example 2, and 14 for Worked Example 3. Seventy-eight percent of students identified the correct tissue in Worked Example 1, 72% in Worked Example 2, and 79% in Worked Example 3. This resulted in an average score of 76% for correct tissue identification in the worked examples. This data, combined with the data obtained during Cycles 2 and 2.5 for Worked Example 1 is shown in Fig. 10.8. Figure 10.9 shows the responses selected for the unidentified tissue in Worked Example 1 through Cycles 2, 2.5, and Post-cycle. A clear decline in the incorrect selection of 'Bronchus', and a rise in the correct selection of 'Trachea' can be seen throughout the cycles.

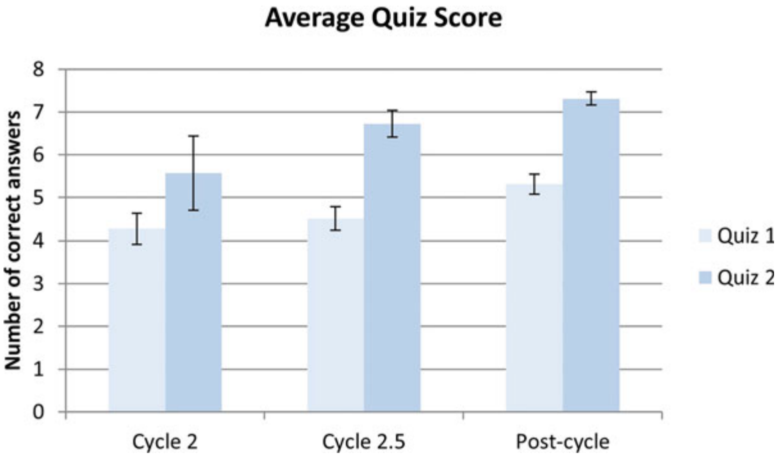

Fig. 10.7 Average quiz scores. This graph represents the average quiz scores, for Quiz 1 and 2, across Cycles 2, 2.5, and during the Post-cycle period. There was a clear improvement in Quiz 2 scores between Cycle 2 and the Post-cycle period

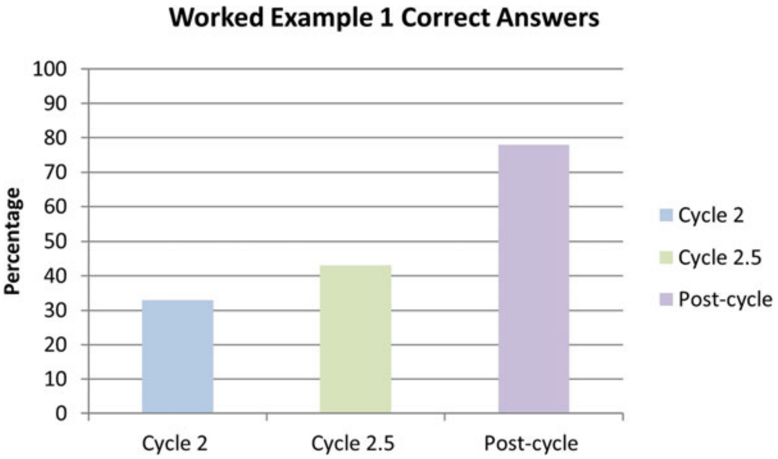

Fig. 10.8 Worked Example 1 correct answer results. The number of participants who correctly identified the tissue in Worked Example 1 increased from 33% in Cycle 2 to 78% during the Post-cycle period

10.5.5.2 Summative Practical Exam (OSSE) Results and Field Notes

Histology practical exams for year 1 Medicine students are held annually in June. Pre-innovation, 46% of students were able to correctly identify the tissue in the practical exam. Post-innovation, 81% of students were able to correctly identify the tissue. In addition, the number of students passing the histology station also increased from 86% pre-innovation to 94% post-innovation.

The OSSE practical exam provided a valuable opportunity to see the impact the decision tree and Google Site had on the students. As an examiner on the station, it was possible to observe how the students' entire approach to the tissue identification process had changed. Students had always been told to look at the slide with the naked eye. However, during previous exams, it had been clearly evident that the students were applying a very superficial approach at this stage of the process, purely to satisfy the examiner and in the hope of gaining some marks. After the innovation, however, students clearly took this step seriously and several students were able to make appropriate conclusions about the tissue even before looking at it with the microscope. In addition, students appeared calmer and appeared to be following a logical approach to the identification of the tissue, ruling out hollow structures and surfaces (the tissue was a solid section). This targeted approach allowed the students to rule

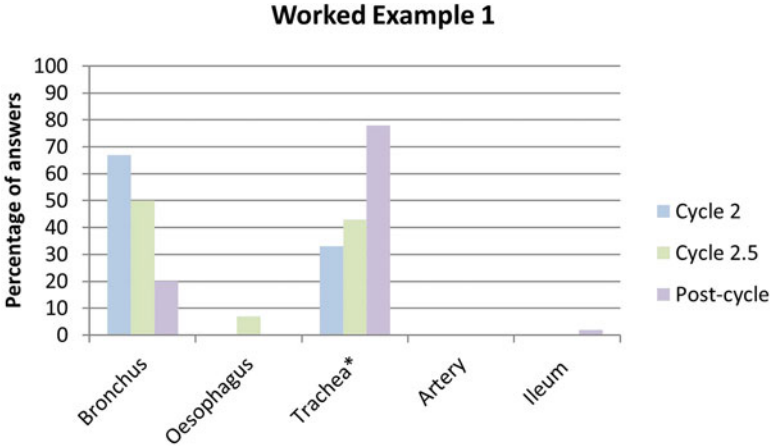

Fig. 10.9 Worked Example 1 submission. There was a gradual decline in the number of participants incorrectly identifying 'Bronchus' as the tissue across the cycles, and a subsequent rise in the number correctly identifying 'Trachea'. * Indicates correct tissue

out a large proportion of potential tissues, removing some of the panic that is often seen at a histology station. This highlighted that showing students *how* to apply their knowledge is as important as providing them with the tools to acquire that knowledge in the first place.

10.5.5.3 Post-cycle Discussion

Analysis and comparison of the data from the four key stages of the project (Cycle 1, Cycle 2, Cycle 2.5, and Post-cycle) has shown that the decision tree and Google Site resulted in an improvement in the scores obtained through both formative testing (quiz scores and worked example submissions) and summative assessment (OSSE scores). More importantly, students reported that they had increased confidence when approaching the subject matter. Together, this demonstrates that students developed the necessary skills to *apply* their knowledge through the use of the decision tree and Google Site. These learning resources allowed the students to shift from surface learning to a deeper understanding of histology—they had developed from 'knows' to 'knows how' in Miller's Pyramid of competence (Miller 1990). This is particularly evident in Fig. 10.9 where progressive use of Worked Example 1 in successive cycles resulted in a decrease in the number of incorrect answers cycle by cycle, and a corresponding increase in the number of correct answers; students were no longer randomly selecting tissues but were applying their knowledge in a logical manner. Furthermore, the availability of resources outside of the practical setting encouraged the students to take responsibility for their own learning, promoting engagement inside and outside of the classroom, with students even requesting more quizzes.

10.6 Was This Project Successful?

In Sect. 10.1.4, the markers of quality and rigour in research were discussed. Here we will examine whether the data collected in this project meet these criteria.

10.6.1 The Data Can Be Generalised

The findings from this research project can be applied to other contexts, particularly disciplines that are content-heavy. Feedback from the students highlighted how this subject can be particularly overwhelming due to the volume of new content, and how the decision tree provided them with a logical process with which to approach the content. More generally, the provision of a toolkit to show students how to apply their knowledge to a new scenario proved popular amongst students and appeared to result in an improved understanding of the topic content. In addition, Cycles 2 and 2.5 involved the construction of a Google Site which contained Google Forms and Google Slides. All these creations could be used in alternative contexts. Indeed, on discussing the Google Site with a colleague they proceeded to create their own Site for use with their undergraduate students. In summary, the data from this action research project can be transferred to alternative contexts across the wider HE community.

10.6.2 The Data Are Reliable

In histology, the same tissues are examined every year, across all student groups and therefore the innovation can be used in subsequent years for different cohorts. This allows the project to be continuously developed, maintaining the cyclical nature of its development. Reliability is typically examined by investigating inter-rater reliability and triangulation. In terms of inter-rater reliability, the quantitative nature of much of the feedback in this project ensured that the interpretation was objective. Furthermore, the practical OSSE exam results provided feedback from three separate examiners and results were consistent across each academic. Multiple methods were used to collect data throughout the project, and in Cycles 2 and 2.5 feedback from the questionnaires was compared to results from the quizzes and worked examples to ensure reliability. The data from this project can be considered to be a reliable representation as to the context and the project outcomes.

10.6.3 The Results and Conclusions Are Objective

As the researcher and the educator involved in the development of the project, there is some potential for bias. This potential issue moves from an unconscious bias to a conscious bias which can therefore be accounted for. In addition, this is the basis for action research; the research takes place in the context in which the researcher is an educator.

The feedback from all cycles was obtained through anonymous online questionnaires. This removed any potential reluctance on the students' part to be as honest as possible when responding, due to the researcher acting as part of the research environment. Additional data was collected from the online quizzes and worked examples (Cycles 2 and 2.5). This was anonymous and provided an unbiased reflection of the students' use of the resource and their level of understanding of the content. The OSSE provided data on the scores obtained by the cohort in a histology practical exam. All scores were anonymous and averaged. The researcher examined one set of students (out of three potential sets) and therefore any impact the researcher may have had on this set of data is outweighed by the remaining two sets.

10.6.4 The Results and Conclusions Are Valid

When considering the validity of data obtained from a research project there are several generic markers that may be used such as credibility, transferability, dependability, and confirmability, amongst others. Here, the validity of the data will be considered in terms of the aims of action research. These aims, namely the form of validity which they assess, and the outcomes in this project are detailed here.

10.6.4.1 Generation of New Knowledge

The successful generation of new knowledge requires dialogic validity whereby work is reviewed or open to critical comment from a community of action researchers (Norton 2009; McNiff 2016). This project was discussed with the project supervisor and with peers in the format of an action learning set. Feedback from the action learning set helped to develop the project and provided an opportunity to discuss the implications and generalisability of the research. Such feedback included the recommendation of Google Forms as these can self-grade, and positive encouragement about the use of a toolkit (the decision tree) to help students to apply their knowledge.

Successful achievement of this aim also requires 'process validity' where problems are framed and solved in a way that allows ongoing learning (Norton 2009; McNiff 2016). This project developed through three cycles, one of which was unplanned and arose directly as a consequence of feedback from the previous cycle. Further data was obtained after the conclusion of the third cycle, and there is scope for further development of the innovation with future student cohorts.

10.6.4.2 Achievement of Action-Oriented Outcomes

For an action research project to achieve its intended outcome of improvement in the learning environment, it requires outcome validity where useful outcomes occur (Norton 2009; McNiff 2016). The data from this project indicate that the students perceived the changes introduced to be helpful. In addition, the researcher observed an increase in student engagement and understanding during the ethnographic aspect of the study. More objectively, the quiz scores improved over the subsequent cycles, and the OSSE scores improved on the previous cohort's results.

10.6.4.3 Education of Researcher and Participants

For a project to result in the successful education of both researchers and participants, it requires catalytic validity; motivation for those involved to think about the issue and initiate change (Lather 1991). At the end of this part of the project, the researcher now has a much greater understanding of what the students struggle with in this context. In addition, the students are aware of gaps in their understanding and have been prompted to engage with the learning process and motivated to undertake self-directed learning.

10.6.4.4 Results Are Relevant to the Local Setting

Democratic validity, whereby research is conducted in collaboration with others, ensures that the results obtained in the research project are relevant to the context to which they relate (Norton 2009; McNiff 2016). In this project, the opinions of staff were sought in an informal setting and provided insight for the initiation of the project and its development throughout the cycles. Students provided feedback on the context and the changes made throughout the project via anonymous questionnaires. The shift in student involvement from co-option in Cycle 1 to consultation in Cycles 2 and 2.5 highlights the active role participants played in the development of the project. In addition, input from other departments was obtained through the action learning sets.

10.6.4.5 Sound and Appropriate Research Methodology

Process validity ensures that the project involves appropriate methods to gather and analyse data. The inclusion of subjective data demands the maintenance of validity to ensure that subjectivity does not become prejudice (Norton 2009). As such, data was collected through a combination of anonymous questionnaires, test scores (quizzes, worked examples, and OSSEs), and informal observations. This provided a mixture of quantitative and qualitative data that allowed both objective and subjective conclusions to be drawn. The outcomes of each cycle directly informed the subsequent cycles ensuring alignment between feedback and action.

In summary, this project met all five aims of an action research project, and achieved successful dialogic, process, outcome, catalytic, and democratic validity. The conclusions drawn from the data therefore provide a valid representation of the context. Validity acts as a basis for legitimacy that allows the outcomes of an action research study to modify others' practice (Norton 2009) and is therefore a vital consideration in AR.

10.6.5 The Project Was Ethically Conducted

Ethical approval for the project was gained from the Keele Student Project Ethics Committee (SPEC) as this project was completed as part of the author's MA Learning and Teaching in HE. Furthermore, the principles of informed consent, maintenance of privacy and confidentiality, and protection from harm, were maintained throughout the project. In action research it is important to actively think ethically at all stages, rather than passively following the enforced ethics procedure (Hutchings 2002). Therefore, the project was considered ethically appropriate.

10.6.6 The Results Are Repeatable

When examining the markers for quality and rigour in research, repeatability can be considered to overlap with reliability. As the project was found to be reliable in Sect. 10.6.2, the project can therefore also be considered repeatable. Furthermore, sufficient detail has been provided here and in Supplementary File 10.1 for the project to be replicated outside of the original context.

10.6.7 Summary: This Was a Successful Project

After considering five markers for quality and rigour in research, it can be concluded that this project represents a good quality study that has been conducted in a rigorous manner. The project produced data that provides a valid, objective, and reliable representation of the context, which is repeatable, and transferable to different contexts, whilst being ethically sound.

10.7 Overall Discussion and Conclusions

This project has provided an invaluable opportunity to investigate how students can develop the skills necessary to apply their knowledge, and how feedback in histology can be improved.

The unique insider approach offered by action research allowed the author to question whether what the educator does in their practice has direct consequences on how students learn, and how awareness of this impact is essential for good practice. As the educator, the researcher was able to design, implement and test the efficacy of a novel learning resource within their own context. Using qualitative and quantitative methods it was possible to learn how students perceived the innovation, and directly observe how it affected their assessments.

The histology decision tree allowed the students to organise their knowledge and showed them a logical way in which to apply this knowledge to identify tissues. Student engagement, confidence, and exam scores improved following the introduction of the decision tree and the associated Google Site. The findings from this project regarding feedback and skill development are discussed below in relation to the literature.

10.7.1 Skill Development

Piagetian levels categorise learning into four stages: (1) Sensorimotor (up to 24 months) where the goal is object permanence, (2) Preoperational (up to 7 years old) with a goal of symbolic thought, (3) Concrete operational (up to 11 years) where the aim is logical thought, and (4) Formal operational (adolescence to adulthood) where individuals are capable of scientific reasoning (Piaget and Inhelder 2013). As educators in the tertiary sector, we expect all students to have progressed to the highest Piagetian level where they are able to explore abstract concepts and logically test hypotheses by the time they reach the HE setting (Yorke 2003). However, many students function at Blooms (1956) knowledge and comprehension levels, the lowest stages in the taxonomy of learning focused on simple information recall (knowledge) and summarising (comprehension), even when they leave University and enter the working world. HE has a responsibility to prepare students for the real world and employment, a responsibility that is increasing as the student fees rise and there is an increase in student debt (Qenani et al. 2014). Students must be equipped with skills that allow them to function in the twenty-first century; be able to critically evaluate large amounts of material and identify problems, create viable solutions to these problems, and identify and implement appropriate criteria for evaluation (Larson and Miller 2011). Embedding learning opportunities that develop these skills throughout the normal classroom environment allows students to transfer the logical thinking process required to novel situations in the real world. This skill development is advocated by the Partnership for twenty-first Century Skills (Larson and Miller 2011), and external pressure in the form of the Dearing report (NCIHE 1997) also demands that HE serves the national economy through the development of four key skills; communication, numeracy, use of Information Technology (IT), and understanding how to learn. What students can do with knowledge and how they apply what they learn in authentic contexts is, however, still highly undervalued in the HE curriculum. Inappropriate curriculum design, learning activities, and an emphasis on summative assessment means that students develop inert knowledge instead of what the real-world demands, namely transferable skills (McLoughlin and Luca 2002). HE has a responsibility to ensure that graduates are prepared for the working world, especially in the professional education sector. Learning through tasks allows student to develop their procedural knowledge, which is essential in a profession such as Medicine, and is necessary for lifelong professional learning (Eraut 1994). Furthermore, Gibbs (1992) stresses that a focus on processes rather than content is essential to promote active learning.

With the need for skill development established, the perception of what makes a competent professional needs to be discussed. Stephenson and Weil (1994) state that competence requires the ability to make satisfactory and effective decisions in a specific situation, and therefore students must encounter authentic contexts during their time in HE to foster the development of transferable skills rather than abstract ones.

This action research project explored a novel learning resource that was designed to encourage students to apply their knowledge. When students required more support to take this step up to 'knows how' (Miller 1990), they were provided with step-by-step guides in an online environment. This project therefore developed the skills acquisition aspect of the course, thus helping to prepare students for the real world (Eraut 1994; McLoughlin and Luca 2002; Larson and Miller 2011). Through this project, students developed a greater understanding of *how* they learn, moving towards the development of process knowledge and away from rote memorisation and propositional knowledge, thus meeting the needs of professional education (Eraut 1994). The decision tree also allowed students to critically evaluate large amounts of content, ask appropriate questions to produce criteria for evaluation and create viable solutions, and develop more generic twenty-first century skills (Larson and Miller 2011). There is also increasing demand for interactive learning resources (David et al. 1997) and these resources meet this demand as the Google Site was accessed by students in their own time.

Game-based learning has been shown to enhance motivation and increase student interest (Druckman 1995) and there is scope for this project to have a gaming aspect included. The tissue identification process and use of the decision tree could be designed as a game where progress is based on appropriate structure identification. In addition, group-based project work has been found to promote professional skills development (Klemm and Snell 1996; Collis 1998) and there is potential for the resource to have a collaborative element where groups of students generate their own decision tree.

10.7.2 Formative Assessment and Feedback

Feedback within histology teaching, and how it can be improved, was one of the research questions established at the start of this project. Prior to this project, outside of in-class clicker quizzes (Quinn 2017), no formative assessment was in place for histology teaching in the medical curriculum, with few opportunities for feedback, either formal or informal. Summative assessment determines the extent to which a student has achieved the objectives of the curriculum (Bloom 1971), and obviously this is important in HE—however, the significance of formative assessment is still largely undervalued in HE. Through formative assessment, the teacher plays the role as supporter of the learning whereas in summative assessment they are the assessor of achievement (Yorke 2003). Formative assessment, therefore, provides an invaluable learning opportunity for both student and teacher; the student identifies gaps in their knowledge and areas in which they can improve, and the teacher learns how they can more appropriately offer their students better support. Across the UK, the higher education setting has experienced a reduction in the proportion of formative assessment that is incorporated within the curriculum whilst the number of summative assessments are increased (Yorke 2003). Pressures to decrease formative assessment include increasing focus on the attainment of standards, increasing staff-to-student ratios, and demands placed on academic staff in addition to teaching such as increased pastoral responsibilities (Yorke 2003). As a result, this risks encouraging rote memorisation as assessment becomes *of* learning rather than *for* learning (Germany 2015). Furthermore, Shepard argues that whilst approaches to learning have moved towards constructivism, approaches to assessment have remained inappropriately focused on this style of testing (2000). Students place a high value on organised formative assessment (Carroll 1995; Rolfe and McPherson 1995; Vaz et al. 1996). This aligns with the finding that learning depends on the provision of feedback at a time that allows development (Bruner 1966; Yorke 2003) which means that summative assessment is often too late. According to Harlen and James (1997), feedback received is formative if, and only if, it has contributed to learning. For this to occur, the feedback needs to be *in*formative. Feedback should allow the students to appreciate the standards that are expected of them and to form accurate perceptions of their abilities (Mentkowski et al. 2000). The inherent risk with increased feedback, however, is that students may develop 'learned dependence' where they need the teacher to make decisions about what they know (Boud 1995), whereas the goal of feedback should always be to allow students to establish internal standards by which they assess their own work.

This action research project incorporated the benefits of both formative and summative assessments. The quizzes mimicked summative assessment (yet were repeatable), feedback was provided in a timely manner to allow self-development, and self-study was promoted. The feedback provided was a combination between informal and formal. Feedback on the quizzes was immediately provided through a mixture of scores and written feedback. The scores gave the learner an indication of their current level of knowledge, and the written feedback showed why the answer was correct or incorrect (Fig. 10.5). The online and anonymous nature of the feedback avoids the issue of embarrassment, which encourages students to participate in the assessment in an open way, and thus develop from the experience. As the teacher–researcher, the author also benefited from the experience as they were able to remotely monitor how students handled the content without the need for time-consuming marking of the submissions. This, combined with the field observations, gave an overview of what the students really struggled with. There is scope for this educational approach to benefit the educator in the long term; Swann and Ecclestone (1999) found that those who worked reflectively on the provision of more effective feedback saw improvements in their ability to grade work.

There are two key markers to determine if formative assessment is successful: (1) is the assessment the best that could have been done in the context and (2) did the formative assessment influence student behaviour (Yorke 2003). Firstly, with a cohort of 130 students it would be impossible for the educator to have individually marked each quiz and provided individual feedback. As such, the online feedback provided a practical way to provide appropriate feedback to students. Furthermore, the practical sessions provided an opportunity to provide real-time face-to-face feedback when required. Secondly, the OSSE exams provided an excellent opportunity to see first-hand how the project had changed student behaviour. In this setting, students shifted their focus from guessing the tissue identity to using a logical approach to analyse it.

Another issue for consideration is that a student's perception of their self-efficacy, their ability to achieve a task, has a direct impact on their actions (Bandura 1982). This perception is informed by their performance attainments, vicarious experience, verbal persuasion, and their physiological state (Bandura 1982). The worked examples contained within this project allowed modelling which facilitated vicarious learning through observation. Furthermore, the quizzes provided an authentic experience of mastery and therefore improved performance.

10.8 Future Plans

This project has addressed several questions regarding the author's own context and approach to teaching. As with any authentic action research project, however, this is not the end of the developmental process. This project has only begun to uncover some of the challenges regarding histology education, in particular, and medical education more broadly and has generated more research questions that need investigating. These questions have informed the author's future plans regarding their own educational context, and these are as follows:

1. Increasingly open the research up to the students as participants, thereby shifting from consultation where student opinions are sought but the researchers decide on action, to cooperation where both students and researcher work together to develop any changes (Stringer 2013). This is to ensure no assumptions are made about how the students learn best and what they would find more helpful in histology education.
2. Introduce the concept of the decision tree with students from their very first histology session, to act as a scaffold around which they can construct their knowledge. This plan is based on feedback from all three cycles where students reported that the structured framework of the tree would aid in their understanding of how the different tissues relate to each other.
3. Provide additional worked examples on the Google Site that are different to the tissues included in the quizzes. This would serve to investigate and determine whether the improved scores seen in the later cycles are due to repetition of content and repeated methods rather than from a greater understanding of how to apply the knowledge learned. These have been added to the Google Site since the project was conducted and can be seen by scanning the QR code in Fig. 10.6.
4. Assess students on different tissues in Quiz 1 and Quiz 2 on the Google Site. This is to investigate whether the improved scores seen in Quiz 2 are due to repetition of content or the newly learned skill of applying the decision tree to unknown tissues.
5. Investigate the possibility of a game-based approach to the use of the decision tree. This is in response to the success of game-based learning in the literature (Druckman 1995).
6. Consider development of the group-work aspect of the resource. This is in response to the success of group-work in developing skills (Klemm and Snell 1996; Collis 1998).

Acknowledgements This action research project would not have been possible without the support and guidance of so many people. Firstly, thanks must go to Jackie Potter for her enthusiasm about action research that stimulated this research by the author. Her guidance and support throughout the project have been invaluable. Rob Stannard provided expert advice regarding the project and was extremely helpful during the action learning set. Last but not least, my husband Leo and my daughter Sophia for their constant faith in my ability and for keeping my enthusiasm alive.

References

Bandura A (1982) Self-efficacy mechanism in human agency. Am Psychol 37(2):122

Bartlett S, Burton D (2006) Practitioner research or descriptions of classroom practice? A discussion of teachers investigating their classrooms. Educ Action Res 14(3):395–405

BERA Ethical Guidelines for Educational Research (2011). https://www.bera.ac.uk/wp-content/uploads/2014/02/BERA-Ethical-Guidelines-2011.pdf?noredirect=1. Accessed December 2016–July 2017

Bloodgood RA, Ogilvie RW (2006) Trends in histology laboratory teaching in United States medical schools. Anat Record Part B 289(5):169–175

Bloom, B.S., 1971. Handbook on formative and summative evaluation of student learning

Bloom BS, Englehart MD, Furst EJ, Hill WH, Krathwohl DR (1956) Taxonomy of educational objectives, handbook I: the cognitive domain. David McKay Co, New York

Boud D (1995) Assessment and learning: contradictory or complementary. Assess Learn High Educ:35–48

Bressers G, Brydges M, Paradis E (2020) Ethnography in health professions education: slowing down and thinking deeply. Med Educ 54(3):225–233

Brown S, Knight P (2012) Assessing learners in higher education. Routledge

Bruner JS (1966) Toward a theory of instruction, vol 59. Harvard University Press

Carr W, Kemmis S (1986) Becoming critical: education knowledge and action research. Routledge

Carroll M (1995) Formative assessment workshops: feedback sessions for large classes. Biochem Educ 23(2): 65–67

Cohen L, Manion L, Morrison K (2002) Research methods in education. Routledge

Collis B (1998) WWW-based environments for collaborative group work. Educ Inf Technol 3(3):231–245

David B, Werbin KC, Shaw SG (1997) Integrated development and production tools for building hypermedia courseware and interactive scenarios. In: Proceedings of ED-MEDIA/ED-TELECOM, vol 97, pp 241–246

Door V (2014) Developing creative and critical educational practitioners. Critical Publishing

Draper SW, Brown MI (2004) Increasing interactivity in lectures using an electronic voting system. J Comput Assist Learn 20(2):81–94

Druckman D (1995) The educational effectiveness of interactive games. In: Simulation and gaming across disciplines and cultures: ISAGA at a watershed. Sage, pp 178–187

Eraut M (1994) Developing professional knowledge and competence. Psychology Press

Fanghanel J (2007) Investigating university lecturers' pedagogical constructs in the working context. Higher Education Academy, York

Frechette J, Bitzas V, Aubry M, Kilpatrick K, Lavoie-Tremblay M (2020) Capturing lived experience: methodological considerations for interpretive phenomenological inquiry. Int J Qual Methods 19: 1609406920907254

Freeman D (1998) Doing teacher research: from inquiry to understanding. Heinle & Heinle, Boston

Germany D (2015) Blended Assessment-4-blended learning. In: ECEL2015-14th European conference on e-learning: ECEl2015. Academic Conferences and Publishing Limited, p 223

Gibbs G (1992) Improving the quality of student learning: based on the improving student learning. Project funded by the Council for National Academic Awards. Technical and Education Services, Bristol

Harlen W, James M (1997) Assessment and learning: differences and relationships between formative and summative assessment. Assess Educ 4(3):365–379

Heidger PM Jr, Dee F, Consoer D, Leaven T, Duncan J, Kreiter C (2002) Integrated approach to teaching and testing in histology with real and virtual imaging. Anat Record 269(2):107–112

Hutchings P (2002) Ethics of inquiry: issues in the scholarship of teaching and learning. Carnegie Publications, The Carnegie Foundation for the Advancement of Teaching

Jamieson S (2004) Likert scales: how to (ab) use them? Med Educ 38(12):1217–1218

Jick TD (1979) Mixing qualitative and quantitative methods: triangulation in action. Adm Sci Q 24(4): 602–611

JISC (2005) Innovative practice with e-learning. HEFCE

Johnson AP (2008) A short guide to action research. Allyn and Bacon

Kember D (1997) A reconceptualisation of the research into university academics' conceptions of teaching. Learn Instr 7(3):255–275

Kember D (2000) Action learning, action research: improving the quality of teaching and learning. Routledge

King A (1993) From sage on the stage to guide on the side. Coll Teach 41(1):30–35

Klemm WR, Snell JR (1996) Enriching computer-mediated group learning by coupling constructivism with collaborative learning. J Instr Sci Technol 1(2): 1–11

Kulasegaram KM, Martimianakis MA, Mylopoulos M, Whitehead CR, Woods NN (2013) Cognition before curriculum: rethinking the integration of basic science and clinical learning. Acad Med 88(10):1578–1585

Larson LC, Miller TN (2011) 21st century skills: prepare students for the future. Kappa Delta Pi Record 47(3): 121–123

Lather P (1991) Getting smart: feminist research and pedagogy within/in the postmodern. Routledge

Lisk K, Agur AM, Woods NN (2016) Exploring cognitive integration of basic science and its effect on diagnostic reasoning in novices. Perspectives Med Educ 5:147–153

McLoughlin C, Luca J (2002) A learner–centred approach to developing team skills through web–based learning and assessment. Br J Educ Technol 33(5):571–582

McNiff J (2016) You and your action research project. Routledge

Mentkowski M, Rogers G, Doherty A, Loacker G, Hart JR, Rickards W, O'Brien K, Riordan T, Sharkey S, Cromwell L, Diez M (2000) Learning that lasts: integrating learning, development, and performance in college and beyond. Jossey-Bass

Miller GE (1990) The assessment of clinical skills/competence/performance. Acad Med 65(9):S63–S67

Munn-Giddings C, Winter R (2013) A handbook for action research in health and social care. Routledge, London, pp 37–42

NCIHE (The National Committee of Inquiry into Higher Education) (GB) (1997) Higher education in the learning society: report of the National Committee. HM Stationery Office

Norton L (2009) Action research in teaching and learning: a practical guide to conducting pedagogical research in universities. Routledge

Oliver R, McLoughlin C (2000) Web-based learning and generic skills development. UniServe Sci News 15:3–7

Orne MT (2017) On the social psychology of the psychological experiment: with particular reference to demand characteristics and their implications. In: Sociological methods. Routledge, pp. 279–299

Piaget J, Inhelder B (2013) The growth of logical thinking from childhood to adolescence: an essay on the construction of formal operational structures, vol 84. Routledge

Polanyi M (2012) Personal knowledge. Routledge

Ponte P (2002) How teachers become action researchers and how teacher educators become their facilitators. Educ Action Res 10(3):399–422

Prince M (2004) Does active learning work? A review of the research. J Eng Educ 93(3):223–231

Qenani E, MacDougall N, Sexton C (2014) An empirical study of self-perceived employability: improving the prospects for student employment success in an uncertain environment. Act Learn High Educ 15(3):199–213

Quinn RE (2017) Clickers in the classroom: study into the use of interactive quizzes in a practical environment. J Acad Dev Educ 7:50–79

Rolfe I, McPherson J (1995) Formative assessment: how am I doing? Lancet 345(8953):837–839

Seider SN, Lemma P (2004) Perceived effects of action research on teachers' professional efficacy, inquiry mindsets and the support they received while conducting projects to intervene into student learning. Educ Action Res 12(2):219–238

Shepard LA (2000) The role of assessment in a learning culture. Educ Res 29(7):4–14

Sherman SC, Jue CK (2009) Pedagogical methods for teaching histology in anatomy and physiology courses. HAPS Educ 14:50–55

Steffe LP, Gale JE (eds) (1995) Constructivism in education. Psychology Press

Stephenson J, Weil S (1994) Quality in learning: a capability approach in higher education. Br J Educ Stud 42(1):86

Stringer ET (2013) Action research. Sage Publications

Swann J, Ecclestone K (1999) Improving lecturers' assessment practice in higher education: a problem-based approach. Educ Action Res 7(1):63–87

Vaz M, Avadhany ST, Rao BS (1996) Student perspectives on the role of formative assessment in physiology. Med Teach 18(4):324–326

Wahlstrom KL, Ponte P (2005) Examining teachers' beliefs through action research: guidance and counseling/pastoral care reflected in the cross-cultural mirror. Educ Action Res 13(4):543–562

Yorke M (2003) Formative assessment in higher education: moves towards theory and the enhancement of pedagogic practice. High Educ 45(4):477–501